Groundwater-surface water exchange in the proglacial zone of retreating glaciers in SE Iceland

Amir Levy

This thesis is submitted for the degree of Doctor of Philosophy

School of Geography, Geology, and the Environment

Keele University

June 2015

Abstract

Groundwater-surface water exchange significantly impacts proglacial hydrology and ecology. This study applies a multidisciplinary approach to investigate groundwater-surface water exchange in the proglacial zones of two retreating glaciers in SE Iceland. Mapping of decadal changes in the extent of proglacial groundwater seeps in the large outwash plain of Skeiðarársandur has shown a 97% decline, as well as substantial falls in groundwater levels. Field and laboratory measurements suggested high spatial variability in hydraulic conductivity at the Skaftafellsjökull foreland. The highest hydraulic conductivity was measured in areas underlain by glaciofluvial deposits whilst the lowest hydraulic conductivities were associated with glacial tills and lacustrine deposits.

Precipitation was identified as an important control on groundwater levels on various temporal scales. Automated monitoring of meltwater and groundwater levels also identified fluctuations in meltwater level as an important control on hydraulic heads, whose importance on groundwater levels has been observed during various flow regimes. The close connection between meltwater and groundwater levels suggest high meltwater-aquifer exchange. However, high meltwater-aquifer exchange is contested by significantly different geochemical and isotopic composition of groundwater and meltwater. Hydrogeological flux estimates suggest high spatial variability in groundwater seepage into the Instrumented Lake, which was attributed to the high variability in hydraulic conductivity around the lakeshores. These are also supported by high –resolution temperature mapping at the lake bed, which suggested that groundwater upwelling in the fine-grained lakeshore took place at discrete locations.

This study suggests climate and glacier margin fluctuations as primary controls on proglacial groundwater-surface water exchange. It also highlights the importance of groundwater contributions to water quality and ecology, with groundwater-fed bodies possibly sustaining important ecological niches. However, proglacial groundwater-fed

features are transient and are threatened by changes in precipitation and glacier retreat. Further declines in groundwater-fed hydrological systems are therefore projected to adversely impact proglacial groundwater-surface water interaction.

Acknowledgements

Intrinsically, a tremendous amount of work has gone into the production of this thesis, and it would not have been possible without the help of many people. I would like to start by thanking RANNIS (the Icelandic Research Authorities for granting research permissions) and several folks from Iceland, who have contributed tremendously towards the completion of this project: First of all, I would like to thank Regina Hreinsdóttir, Gudmundur Ogmundsson, and the rangers at the Skaftafell Visitor Centre of the Vatnajökull National Park for the permit to research in this wonderful location and for all the logistical support, which ranged from ladders to charging batteries to great parties. I would also like to thank Olafur Magnusson for his continuous help and infinite networking, which were a great help in obtaining fieldwork equipment for this research. I would also like to thank Gunnar Bjarki Rúnarsson (of Byko, Selfoss) for his excellent, innovative, and always pleasant service in providing and transporting field equipment.

I would also like to thank various people who have helped with fieldwork for this project, carrying long pipes and heavy sledge hammers across dusty outwash plains: Jack Beasley, Tom Utley, April Fitzgerald, and Ian Peachey. I would also like to thank the following members of Keele University's Department of Geography, Geology, and the Environment: Pete Gratbach and Dave Ward for their help with field equipment, Keith Mason for his help with the digitisation of the aerial images of Skeiðarársandur, Rich Burgess for all his help in anything IT related and for all the other banter, Andy Lawrence for his help with various printing tasks that formed a part of this project, and Dave Emley for his help with various components of the project. I would also like to thank Ian Wilshaw for his endless patience with the Dionex analysis and for his help and advice on obtaining fieldwork equipment. I would also like to thank Nigel Cassidy for his help with various technical components of this research such as the FO-DTS and laboratory permeameter. I would also like to thank Amy Cowles (Department of Chemistry, Keele University) for helping with cation analysis and for the staff at the Department of Geography at the University of Zurich, for helping with stable isotope analysis. I would also like to thank the administration staff of the Department and EPSAM for their help with various components of the project. I would like to thank my fellow post grads for their fun attitude and continuous support and laughter, particularly Liam Bullock and Adam Jeffrey, for all his help with helping me to get Word and Excel to behave. A special thanks is for John Weatherill, for all the advice and experience about aquifers, florescence, and drive pointing. I would also like to thank the financial support received for this project from Keele University's ACORN funding and the RI for the Environment, Physical Sciences, and

Applied Mathematics (EPSAM) and also to the Royal Geographic Society with the Institute of British Geographers (RGS-IBG) for their support for fieldwork through the 2012 Postgraduate Research Award, grant number PRA 26.12. I would also like to thank the Keele Postgraduate Association (KPA) for their travel grant to present at the DACA conference in Davos in July 2013. I would like to thank The Icelandic Glaciological Society (IGS) and the Icelandic Metrological Office (IMO) are for their kind provision of glaciological, meteorological, and hydrological data, which was a tremendous help for this project. Special thanks to Stefan Krause for his help with data analysis, feedback, and helping with field logistics. Special thanks also to Rich Waller and Zoe Robinson for the patience and all the feedback and help in the field and during the data analysis and write up, and for exposing me to amazing delicacies such as Arctic Caviar.

Various friends have helped, asked, prayed and generally supported me during this PhD, and I would like to therefore thank Andy Hayward, for always cheering me up and for the pints and cynicism, to Rob and Val Lowe and Kanchan Vahora, for the support, prayers, encouragement and feeding during the past four year, to Dave and Ione Newall for their support, coffee and feeding, to Rob Barnett and Mark Harding, Will Hunt and Chris and Kate Shack for their support and prayers. And to my lovely Kiwi, Hannah, who always showed support and asked how the project is going. Just before the end I would like to thank mum and dad for the support and love over the years. And last, I just thank God for being all along this long, challenging journey, and for the strength and perseverance that He has given me, even in hard times when things don’t work and everything seems to fall apart.

Table of Contents

List of Figures

List of Tables

List of Equations

1. Introduction

1.1. Scientific rationale

Groundwater provides an almost ubiquitous source of generally high quality fresh water which supports ecosystems and socioeconomic development in a variety of settings (e.g. Green *et al*., 2011; Taylor *et al*., 2013; Foster *et al*., 2013). Groundwater provides around 1/3 of global freshwater withdrawals, sourcing approximately 42%, 36%, and 27% of the water used for agricultural, domestic, and industrial uses, respectively (Döll *et al*., 2012; Taylor *et al*., 2013). Additionally, groundwater also provides critical water storage, which becomes especially important during times of low precipitation and drought (e.g. Alley, 2001; 2007; Vicuña *et al*., 2012; Andermann *et al*., 2012). Despite this importance, there is a paucity of research with regards to the impacts of climate change on groundwater systems (Arnell *et al*., 2001; Kundzewicz, 2007; Taylor *et al*., 2013). This uncertainty is particularly relevant in catchments dominated by snow and ice melt, where groundwater systems have received substantially less research than surface water systems (Piotrowski, 2007; Robinson *et al*., 2008; Crossman *et al*., 2011).

Glaciers significantly impact the hydrology (e.g. Braun *et al*., 2000; Favier *et al*., 2008; Crochet, 2013; La Frenierre and Mark, 2014), ecology (e.g. Milner *et al*., 2009), and geomorphology (e.g. Brardinoni and Hassan, 2006) of their catchments. Over 1/6 of the world's population rely on water which originates from snow and icemelt for their water supply (Barnett *et al*., 2005). Climate change is projected to enhance glacier retreat and substantially alter the magnitude and timing of precipitation events. These changes are projected to cause lower and earlier peak meltwater discharge (Lanke *et al*., 2007; Crochet, 2013). Catchments where glacial melt provides most streamflow during dry periods are especially vulnerable to the projected long term reduction in meltwater (Barnett *et al*., 2005; Tague and Grant, 2009; Langston *et al*., 2011; Vicuña *et al*., 2012;

Thorsteinsson *et al*., 2014). It is unclear whether glaciated basins contain sufficient storage capacity which will be able to buffer such changes, or whether these changes will lead to a reduction in effective water supply (Barnett *et al*., 2005; Langston *et al*., 2011; 2013). Some of this required storage can be provided by groundwater systems (e.g. Clow *et al*., 2003; Hood *et al*., 2006; Roy and Hayashi, 2008; 2009; Langston *et al*., 2011; 2013; Vicuña *et al*., 2012; Andermann *et al*., 2012).

Groundwater forms a key component of the hydrology of glaciated basins, with groundwater contributions significantly augmenting surface water runoff, especially during dry seasons or baseflow conditions (Mark and Seltzer, 2003; Jefferson *et al*., 2008; Roy and Hayashi 2008; 2009; Baraer *et al*., 2009; Andermann *et al*., 2012; Crochet, 2013). Groundwater discharge also significantly impacts the physicochemical parameters of surface water bodies, with greater groundwater contributions enhancing proglacial (the area in front of the glacier margin; Thomas and Goudie, 1991) ecology (e.g. Milner and Petts, 1994; Roy and Hayashi, 2008 and 2009; Milner *et al*., 2009; Gibert and Culver, 2009; Slemmons *et al*., 2013; Kurylyk *et al*., 2014a, b).

Hydrological exchange between groundwater and surface water significantly impacts instream water levels, physicochemical parameters (biogeochemistry), and the ecology of both systems. Additionally, this exchange also significantly impacts the zone where active mixing takes place, known as the hyporheic zone (e.g. Bencala, 1993; Hannah *et al*., 2009; Kløve *et al*., 2011a, b; Krause *et al*., 2009a, b; 2011; 2014). Therefore, groundwater and surface water form a single, integrated resource (e.g. Krause *et al*., 2009a). This integrated understanding of groundwater and surface water is crucial for the effective management of groundwater and surface water systems, compliance with regulatory frameworks (such as the Water Framework Directive), and to improve the resilience to projected changes in climate and land use (e.g. Hood *et al*., 2006; Roy and Hayashi, 2008; 2009; Krause *et al*., 2014). The increasingly interdisciplinary research on groundwater-surface water interaction significantly advanced the understanding of the

physical controls (e.g. Harvey and Bencala, 1993; Lewandowski *et al*., 2009; Sawyer *et al*., 2009; Krause *et al*., 2012; 2014) and the ecological (Milner and Petts, 1994; Brunke and Gonser, 1997; Boulton *et al*., 1998; Brown *et al*., 2007a, b; Roy *et al*., 2011) and biogeochemical (e.g. Ullah *et al*., 2014; Abnizova *et al*., 2014) importance of groundwater-surface water exchange. However, there is still a substantial paucity of research with regards to the temporal and spatial variability of groundwater-surface water exchange and the availability of freshwater downstream (e.g. Krause *et al*., 2014). This understating is particularly important in catchments dominated by snow and ice, where climate change and glacier retreat are projected to substantially alter the availability and timing of meltwater discharge, which will impact groundwater-surface water exchange (e.g. Hood *et al*., 2006; Gooseff *et al*., 2006; 2013; Rossi *et al*., 2012; Ala-aho *et al*., 2013; Drexler *et al*., 2013; Connon *et al*., 2014).

This project focuses on the proglacial zones of Skaftafellsjökull and western Skeiðarárjökull, two retreating glaciers in SE Iceland, where groundwater-fed lakes, seeps, and streams form important ecological niches. These niches sustain a variety of flora and fauna, in these otherwise relatively barren environments (e.g. Robinson *et al*., 2009a). This project has used a combination of field and laboratory techniques in order to investigate the controls on the spatial and temporal variability of, proglacial groundwater-surface water exchange.

This project addresses current gaps in research and adds to existing knowledge on:

- Decadal-scale changes in proglacial groundwater systems in an area of rapid glacial retreat. This includes mapping of changes in the extent of proglacial groundwater seeps and monitoring of changes in proglacial groundwater levels.
- The contribution of meltwater-derived groundwater to surface water bodies in the catchment.

- Improved process understanding with regards to the controls, temporal dynamics, and spatial variability of proglacial groundwater exchange with lakes and rivers.

1.2. Project aim

The aim of this project is to investigate the spatial and temporal variability and hydrological processes of groundwater-surface water exchange at the proglacial zones of Skeiðarárjökull and Skaftafellsjökull, two retreating glaciers in SE Iceland.

1.3. Specific objectives

i. To investigate the impact of glacier margin fluctuations on groundwater levels and on the spatial extent of proglacial groundwater-fed features in western Skeiðarársandur, which is impacted by rapid glacier retreat and high magnitude, low frequency events such as glacier surges and jökulhlaups (glacial outburst floods).

ii. To provide a hydrogeological framework for the Skaftafellsjökull foreland.

iii. To investigate the sources of groundwater and surface water recharge at the Skaftafellsjökull foreland.

iv. To investigate the spatial and temporal patterns and controls on proglacial hydrological exchange between the meltwater river and the aquifer at the Skaftafellsjökull foreland.

v. To investigate the spatial and temporal patterns and controls on proglacial hydrological exchange between the aquifer and lakes at the Skaftafellsjökull foreland.

1.4. Methods

This study applied remote sensing, hydrogeological, geochemical, isotopic, and geophysical methods in order to investigate proglacial groundwater-surface water exchange (Table 1.1). This approach follows the need in research on groundwater-surface exchange, which is becoming increasingly multi-disciplinary (e.g. Fleckenstein *et al*., 2010). The detailed methodologies for the respective techniques are found in Chapters 4-8. The structure of the thesis is described in

Table 1.2.

Table 1.1. The methods applied to address the specific objectives of the study

Objective		Methodology
i)	**Investigation of the impact of long term ice margin fluctuations on proglacial groundwater levels and on the extent of groundwater seeps.**	• Mapping of changes in the area and extent of groundwater seeps and lakes using aerial photographs (dated from 1986, 1997, and 2012). • Long term monitoring of proglacial groundwater levels (July 2000-August 2012). This dataset combines the results from Robinson *et al*. (2008) with measurements from the network that was installed in July 2011. The two networks were levelled to a common datum in 2012.
ii)	**Hydrogeological characterization of the Skaftafellsjökull foreland.**	• Determination of hydraulic conductivity from single well response (slug) tests for single piezometers and Particle Size Analysis (PSA). • Delineation of groundwater flow direction from the distribution of hydraulic heads in piezometers and piezometer nests. • Calculation of aquifer volume, groundwater discharge, and groundwater velocity using the results of the current study and values from the literature.
iii)	**To investigate the sources of recharge for proglacial groundwater and surface water.**	• Environmental tracing using major cation and anion geochemistry and water stable isotopes ($\delta^{18}O$ and δD).

iv) To investigate the spatial and temporal patterns and controls on proglacial hydrological exchange between the meltwater river and the aquifer.	• Automated and manual monitoring of proglacial meltwater and groundwater levels in piezometer nests and piezometers. • Environmental tracers (water temperature, electrical conductivity, geochemistry and stable isotopes).
v) To investigate the spatial and temporal patterns and controls on proglacial hydrological exchange between the aquifer and lakes.	• High resolution mapping of lakebed temperature anomalies using Fibre Optic Distributed Temperature Sensing (FO-DTS). • Quantification of groundwater seepage fluxes using Vertical Temperature Profiles (VTP) and hydrogeological measurements (Darcian fluxes).

Table 1.2. Structure of the thesis.

Chapter	Main contents
1. Introduction	• Aims and objectives • Scientific rationale • Field sites
2. Literature review	• Water sources in glaciated catchments • Proglacial groundwater flow • Groundwater-surface exchange
3. Methodology	• Monitoring infrastructures • Geochemistry and physicochemical parameters • Hydrogeology • Temperature tracing
4. Long term changes in proglacial hydrogeology	• Changes in the extent of groundwater seeps in western Skeiðarársandur • Changes in groundwater levels in western Skeiðarársandur
5. Hydrogeology	• Dominant geomorphic processes on proglacial hydrogeology • Spatial heterogeneity in hydrogeological parameters • Delineation of horizontal and vertical groundwater flow.
6. Geochemistry and stable isotopes	• Physicochemical parameters • Major anions and cations • Water stable isotope composition
7. River-aquifer exchange	• Horizontal groundwater flow direction • Vertical groundwater flow direction • The impact of low magnitude, high frequency processes (ablation and precipitation) on proglacial groundwater-surface water exchange • The impact of jökulhlaups on groundwater-surface water exchange

8. Lake-aquifer exchange	• Mapping of lakebed temperature anomalies • Quantification of seepage fluxes using pore-water temperatures and hydrogeological measurements
9. Proglacial groundwater-surface water exchange	• Conceptual model of the controls on proglacial groundwater-surface water exchange
10. Conclusions	• Summary of major findings • Wider implications • Further research

2. Literature review

2.1. Introduction

This chapter reviews the current literature on the research areas which are pivotal for this study and highlights gaps within the current state of knowledge. The literature review begins by describing the main water sources within glaciated catchments and the mechanisms of groundwater flow within these catchments. It then describes the importance of hydrological exchanges between groundwater and surface water and the factors which control them. The literature review also summarises projected impacts of climate change on the hydrology, groundwater flow, and groundwater-surface water exchange within glaciated catchments.

2.2. Water sources in glaciated catchments

This section describes the main water sources and hydrology of glaciated catchments, such as the storing of precipitation within snow and ice. The section also describes the projected impacts and implications of climate change and glacier retreat in catchments which are impacted by snow and ice melt. Glaciers cover approximately 10% of the earth's surface. The accumulation and melting of snow and ice exerts substantial controls on the water resources, natural hazards, sediment transport, geomorphology, and ecology of glaciated catchments (e.g. Gurnell *et al*., 1999). Meltwater from glaciers and ice sheets also exerts important control on sea-level changes (e.g. Frezzotti and Orombelli, 2014).

Glaciers are divided into an accumulation zone (where precipitation is stored) and ablation zone (where precipitation is released). The divide between the accumulation and ablation zones is known as the Equilibrium Line Altitude (ELA). Glacier mass balance shows the difference between accumulation and ablation. Hence, when accumulation exceeds

ablation, glaciers have a positive mass balance and advance, and vice versa. Globally, glaciers have generally been losing mass during the 1940-50s. Ice losses slowed until the 1970s, but then began to accelerate again (e.g. Zemp *et al*., 2009; Radić *et al*., 2013). However, there are some exceptions to this trend, with glacier advances in areas such as New Zealand, Scandinavia, and the Karakoram (Vaughan *et al*., 2013). These advances have been attributed to increases in precipitation (Lemke *et al*., 2007) and instabilities in glacial dynamics, such as surges (Quincey *et al*., 2011; Bolch *et al*., 2012). Hence, despite the advances in some areas, ice caps and glaciers in most regions, including Iceland, are generally retreating (e.g. Björnsson and Pálsson, 2008).

Glaciers store precipitation in the forms of snow, firn (snow that remained for at least one melt season), and ice (e.g. Jansson *et al*., 2003; de Woul *et al*., 2006). This storage forms an important control on the hydrology of glaciated catchments, and it also makes glaciers important natural water reservoirs. The storage and release of snow and ice leads to distinct diurnal, seasonal, and annual fluctuations in the discharge of meltwater-fed streams (e.g. Hubbard *et al*., 1995; Déry *et al*., 2009). Additionally, meltwater contributions increase discharge above the levels expected if streams were solely precipitation-fed (e.g. Barnett *et al*., 2005; Huss *et al*., 2008; Ruelland *et al*., 2011). The contributions to discharge from snow and ice melt are especially important in catchments with a distinct dry season, where meltwater sustains rivers during periods of low precipitation (e.g. Hannah *et al*., 1999; 2000; Mark and Seltzer, 2003; Favier *et al*., 2008; Juen *et al*., 2007; Baraer *et al*., 2009; 2012; Nolin *et al*., 2010; Condom *et al*., 2012). The significant impact of snow and icemelt on the hydrology of glaciated catchments is illustrated by the estimation that over 1/6 of the world's population relies on water which originates from snow packs and glaciers (Barnett *et al*., 2005).

In addition to the aforementioned impacts on meltwater generation, another striking outcome of the sustained glacial retreat is the global expansion in proglacial zones (Zemp *et al*., 2008; Cooper *et al*., 2011). The hydrology of proglacial zones is highly dynamic,

where the interaction between icemelt, snowmelt, precipitation and groundwater significantly impacts catchment hydrology, water quality, geomorphology, and ecology (e.g. Tockner *et al*., 1997; Ward *et al*., 1999; Robinson *et al*., 2008).

Groundwater is a key component of proglacial hydrology, which provides important water storage (Malard *et al*., 1999; Clow *et al*., 2003; Hood *et al*., 2006; Crossman *et al*., 2011; Rossi *et al*., 2012; Ala-aho, 2013). The main recharge sources of proglacial groundwater are precipitation, snow, and icemelt (e.g. Robinson *et al*., 2009b). Groundwater recharge is substantially impacted by geology and geomorphology (e.g. Meriano and Eyles, 2009; Blackport *et al*., 2014). Proglacial areas underlain by permeable deposits, such as alluvium, sustain significant aquifers (e.g. Tockner *et al*., 1997; Malard *et al*., 1999; Crossman *et al*., 2011: Bajc *et al*., 2014). Conversely, low permeability deposits and layers, such as permafrost and buried ice, which acts as aquitards, impede groundwater recharge and flow (e.g. Cooper *et al*., 2002; 2011; Langston *et al*., 2011; Magnusson *et al*., 2014). Additionally, groundwater recharge is also impacted by the availability of meltwater and its controls which include climate, altitude, latitude and aspect (e.g. Brown *et al*., 2006a, b; Jonsson *et al*., 2009). The spatial distribution of proglacial recharge components varies within the catchment, with the proportion of icemelt generally falling with distance from the glacier margin (e.g. Ward *et al*., 1999; Robinson *et al*., 2009a, Cauvy-Fraunié *et al*., 2014). The proportion of contribution of groundwater to surface runoff also varies temporally. The proportion of groundwater contribution to surface runoff is generally at its lowest during spring and summer, when snowmelt and icemelt dominate discharge. Groundwater contributions then increase during autumn and winter (Figure 2.1) (e.g. Malard *et al*., 1999; Ward *et al*., 1999; Marciniak *et al*., 2014).

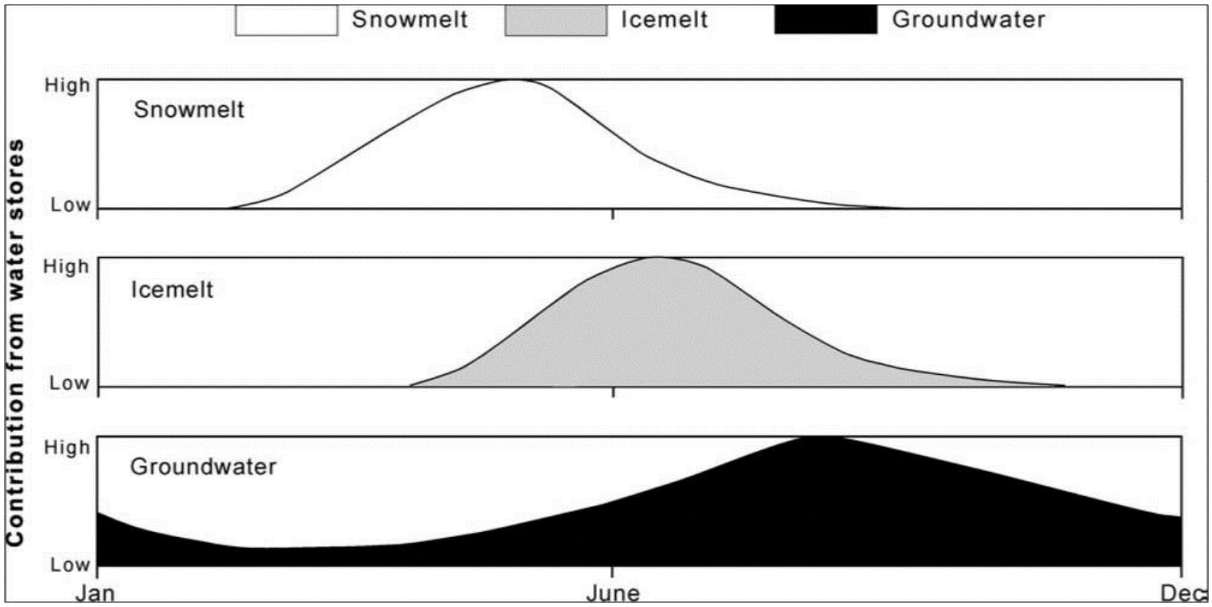

Figure 2.1. Temporal changes in the contributions of proglacial water sources.

The figure is adapted from (Brown *et al*., 2003).

Climate change is projected to impact all water sources within proglacial basins, with scenarios projecting substantial alterations in precipitation regimes, glacial extent and glacial mass balance (e.g. IPCC, 2007; Milner *et al*., 2009; Vaughan *et al*., 2013). Such changes have already been observed in the Andes (Mark *et al.*, 2005; Juen *et al*., 2007; Mark, 2008; Baraer *et al*., 2009), Himalayas (Hagg *et al*., 2007; Yong *et al*., 2010), China (Li *et al*., 2010; Liu *et al*., 2010; Wang *et al*., 2014), the Rockies (Clow *et al.*, 2003; St. Jacques *et al*., 2013), the Alps (Collins, 2006; Stott and Mount, 2007; Gremaud *et al.*, 2009; 2010; Finger *et al*., 2012; 2013), and Iceland (e.g. Björnsson and Pálsson, 2008; Crochet, 2013; Bradwell *et al*., 2013). Enhanced snowmelt and glacial melt will alter the amount of generated runoff and the timing of peak discharge, with discharge projected to fall during dry seasons (e.g. Barnett *et al*., 2005; Jefferson, 2008; Tague and Grant, 2009). These reductions will increase the vulnerability of water resources in catchments which are impacted by meltwater (IPCC, 2007; Adam *et al*., 2009; Huss *et al*., 2010; Taylor, 2013; Thorsteinsson *et al*., 2014). In contrast to these projections, studies from some glaciated basins have actually reported increasing discharges. However, this water originates from melting ice, which reduces non-renewable reserves (e.g. Huss *et al*.,

2008; Baraer *et al*., 2012; Bliss *et al*., 2014). Hence, after crossing a certain threshold, water supply is projected to decrease (Figure 2.2) (Jansson *et al*., 2003; Mark *et al*., 2005; Coudrain *et al*., 2005; Flowers *et al*., 2005; Aðalgeirsdóttir *et al*., 2006; Painter, 2007; Casassa *et al*., 2009; Cauvy-Fraunié *et al*., 2014).

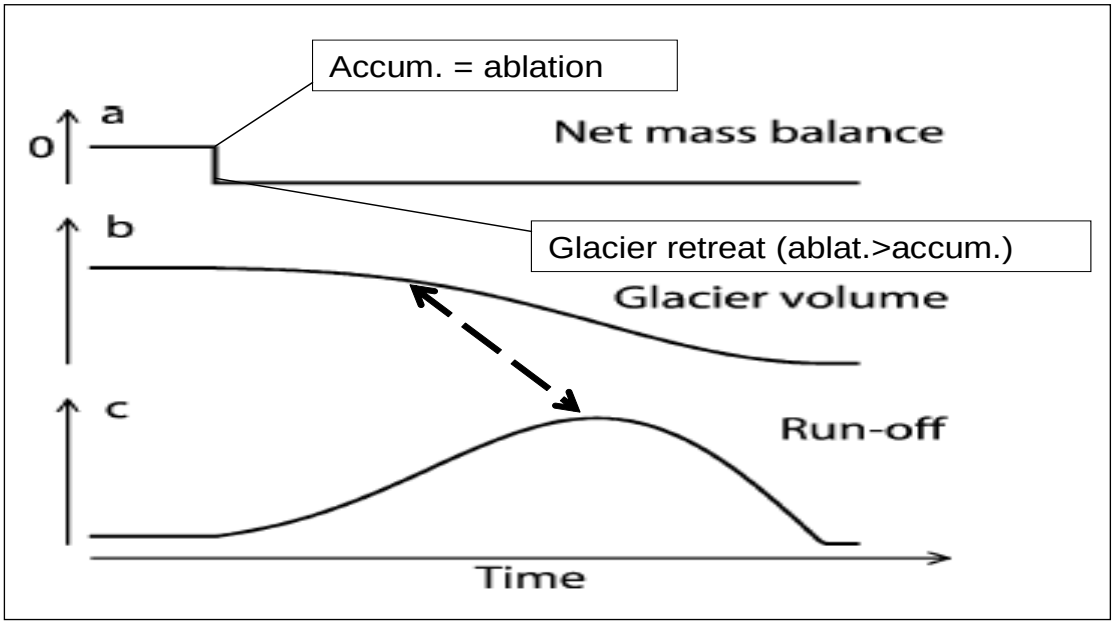

Figure 2.2. The relation between glacial mass balance, volume and runoff (Adapted from Jansson *et al*., 2003. p. 119)

The arrow denotes the threshold after which further reduction in glacial volume will cause runoff to decrease..

Groundwater in catchments which are impacted by snow and icemelt is also projected to alter following climate change and glacier retreat. However, the impact of climate change on groundwater has received much less research than surface water (e.g. Taylor *et al*., 2013). Due to the variety of water sources within proglacial environments, any assessment of changes in groundwater due to climate change needs to encompass the dynamic interactions between snowmelt, icemelt and groundwater contributions (Malard *et al*., 2006; Milner *et al*., 2009). Climate change models generally project an increase in air temperature and alteration in the magnitude and timing of precipitation events. These projections will alter the dynamics and distribution of snow, such as an increase in the rain/snow ratio (e.g. Adam, 2009; Okkonen *et al*., 2009; Crochet, 2013), which will affect recharge. The increase in temperatures, evapotranspiration, and the extent of dry periods

is projected to reduce groundwater levels during the summer (Mäkinen *et al*., 2008). Winter runoff and flooding are projected to increase due to the increase in rain/snow ratio (Adam *et al.*, 2009). However, the increase in runoff and the earlier peak in melt is projected to reduce spring recharge, which will subsequently lower summer baseflow (Tague *et al*., 2007; 2008; Okkonen and Kløve, 2010).

In summary, glaciated basins have unique hydrology, which is controlled by the temporal storage and release of snowmelt, icemelt, and groundwater. This storage substantially impacts the hydrology, ecology, geomorphology and socioeconomic activities of glaciated catchments. However, climate change and glacier retreat are projected to alter the timing of melt and reduce meltwater. These changes are projected to bring adverse outcomes in the long term to communities and ecosystems who rely on meltwater. The storage provided by proglacial groundwater systems can provide some mitigation to the fall in meltwater-dominated surface water discharge (e.g. Hood *et al*., 2006; Roy and Hayashi, 2008).

2.3. Groundwater flow in glaciated environments

2.3.1. Introduction

This section describes the processes and mechanisms that control groundwater flow and drainage in glaciated catchments. The section begins by describing the roles of geology, geomorphology, and glacier thermal regime on groundwater flow. It then describes groundwater flow during glaciations.

Alongside its importance in proglacial hydrology (e.g. Earman *et al.*, 2006), groundwater can also influence glacier movement (Boulton *et al*., 1993; 2001; Eyles, 2006; Piotrowski, 2007; Iverson and Person, 2012) and geomorphology (Boulton *et al*., 2007a, b; Robinson *et al*., 2008; Meriano and Eyles, 2009; Kehew *et al*., 2012). Groundwater in glacial

environments also influences water resources management (Meriano and Eyles, 2003; 2009; Person *et al*., 2007; Finger *et al*., 2013; Hublart *et al*., 2013; Khan *et al*., 2014), economic activities, such as mining (e.g. Melvold *et al*., 2003), and the disposal of nuclear waste (e.g. Normani and Sykes, 2012; Vidstrand *et al*., 2013; Hartley and Joyce, 2013). Groundwater contributions also substantially impact proglacial ecology (Milner and Petts, 1994; Gibert and Culver, 2009; Roy *et al*., 2011). However, despite its importance, groundwater in glacial environments has received much less research than surface water (e.g. Dragon and Marciniak, 2010; Radić and Hock, 2014).

2.3.2. Processes of groundwater flow in glaciated environments

The understanding that glaciers can flow over soft, deformable beds, rather than merely over hard bedrock, has only developed within the last three decades (Boulton, 1986). However, this paradigm shift is essential for the explanation of significant aquifers which are found in proglacial zones underlain by permeable deposits and in karst areas (e.g. Goldscheider and Gremaud, 2010). Groundwater flow underneath glaciers is generally controlled by similar mechanisms to the ones which control groundwater flow within confined aquifers in non-glaciated areas (e.g. Piotrowski, 2007). Water flow within a porous bed is governed by Darcy's Law (Equation 2.1)

$$Q = (KA)\left(\frac{dh}{dl}\right)$$

Equation 2.1. Darcy's Law of groundwater flow (1856)

With Q denoting groundwater flow flux (m^3/day), K the hydraulic conductivity, A the flow cross-sectional area, h the hydraulic head and l the flow length (Darcy, 1856). The hydraulic head *(h,* Equation 2.1) is a key parameter in hydrogeology. It is calculated as the

sum of the elevation head (the elevation of water level measured at the base of the piezometer above a datum) and the pressure head (the length of the water column) (e.g. Domenico and Schwartz, 1998). Groundwater flow is driven by the gradient between hydraulic heads $\left(\frac{dh}{dl}\right)$, with groundwater flowing from high to low hydraulic heads. The hydraulic gradient of unconfined groundwater flow systems in non-glaciated environments is generally determined by topography (e.g. Tóth, 1963; 2009; Freeze and Cherry, 1979). In contrast to that, the hydraulic gradient of subglacial groundwater is mainly determined by the ice-surface slope and the overburden ice pressure, with the subglacial groundwater flow lines mirror-imaging the ice sheet flow lines (Shreve, 1972; Fountain and Walder, 1998). Therefore, basal meltwaters will enter the substrate (forming groundwater recharge) if the pressure at the ice/bed interface exceeds the pressure at the glacial bed (Piotrowski, 2007; Lemieux *et al*., 2008a). The potentiometric surface of groundwater confined by a glacier stretches approximately parallel to the ice surface, with its height corresponding to the water pressure (Piotrowski, 2007). Using water pressures estimated from fine-grained sediments of overridden till, Piotrowski (1997a) calculated the potentiometric surface to equal roughly 72% of the ice thickness. Other observations from consolidated glacial sediments and current measurements of water pressure underneath the West Antarctica Ice Sheet have shown that hydraulic heads at the base of ice sheets were within 30% of the ice flotation value, with average heads being less than 7 m below flotation level (Iverson and Person, 2012). Conversely, at the glacier margin, the pressure within the aquifer becomes lower, which increases groundwater discharge. Additionally, the fall in pressure (exerted by the glacier) also alters the aquifer from confined to unconfined (Haldorsen *et al*., 2010; 2012).

Subglacial groundwater may include components of snow melt and the melt of supraglacial, englacial and subglacial ice, which are routed and joined at the glacier bed. Supraglacial and englacial ice melt are routed to the glacier bed through fractures,

crevasses, moulins, and cavities (Figure 2.3) (e.g. Nienow *et al*., 1998; Cowton *et al*., 2013). The efficiency of these drainage paths is significantly controlled by climatic conditions and the glacier's thermal regime (Röthlisberger and Lang, 1987; Richards *et al*., 1996; Bell, 2008; Gulley *et al*., 2009; Rutter *et al*., 2011; Irvine-Fynn *et al*., 2011; Chu, 2014; Hodgkins *et al*., 2013; Dahlke *et al*., 2014). In addition to the meltwater which has reached the glacier bed via the routes depicted in Figure 2.3, subglacial groundwater also consists of water which are generated at the glacier bed by ice deformation and ice melt which is caused by geothermal heat and basal friction (e.g. Piotrowski, 2007).

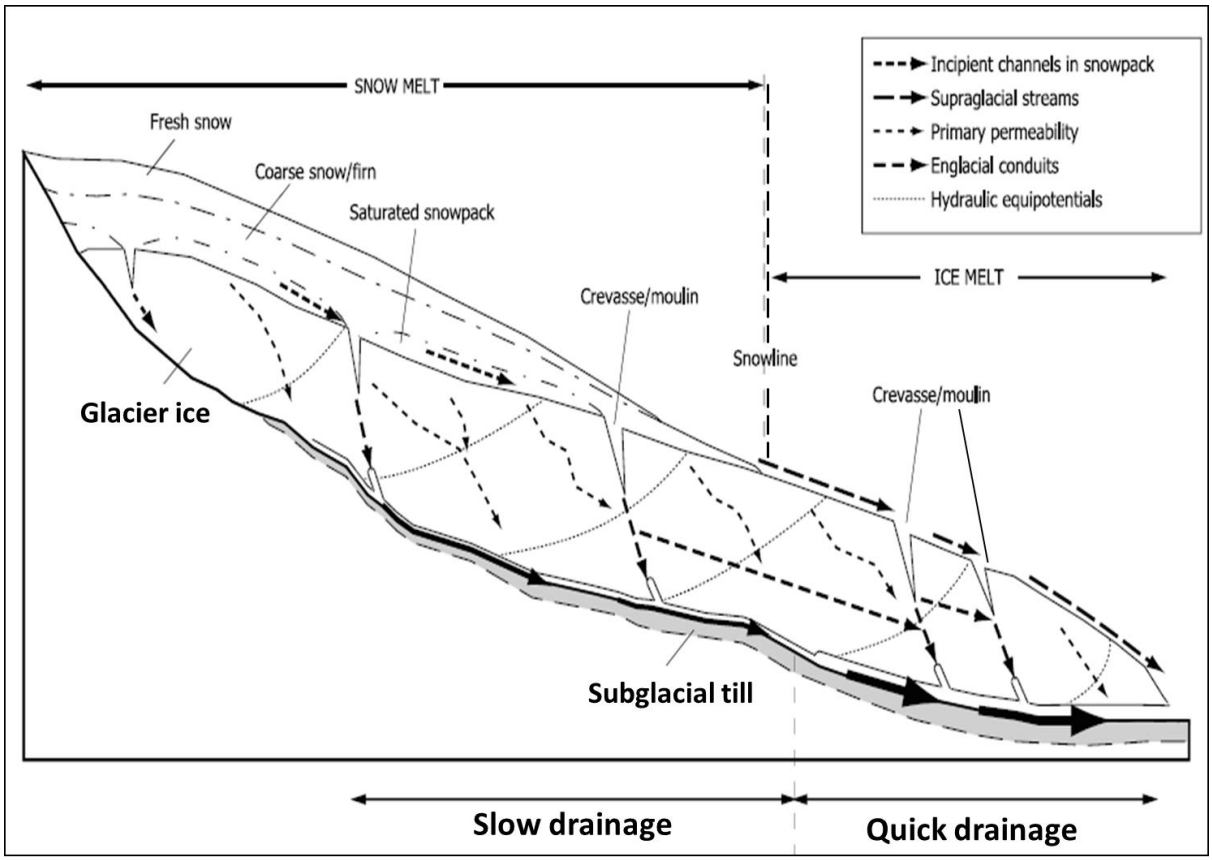

Figure 2.3. The supraglacial, englacial, and subglacial drainage routes by which snow and ice melt reach the glacier sole. Adapted from Irvine-Fynn *et al*. (2011)

The ability of the glacier bed to drain meltwater as groundwater is a key control on glacial motion and stability (e.g. Boulton and Zatsepin, 2006; Meierbachtol *et al*., 2013). The

drainage capacities of the glacier bed exert a key control on the effective pressure of the glacier bed, which is the difference between the overburden pressure and pore-water pressure. The effective pressure is controlled by the interaction between meltwater supply and the drainage capacity of the glacier bed. Failure to evacuate the meltwater increases pore water pressure, which can lower the effective pressure below the critical level for failure. This can cause decoupling between the bed and glacier, which reduces the strength of the subglacial sediments, which bears potential for shear sediment deformation and enhanced glacier movement (Kamb, 1987; Boulton *et al*., 2009; Hoffman and Price, 2014). In addition to drainage capacity, the temperature at the glacier bed also controls glacial stability, as an ice/bed interface which is at or above the Pressure Melting Point (PMP) temperature will generate water at the bed. This water must be drained in order to maintain glacial stability (e.g. Fountain and Walder, 1998).

Subglacial drainage systems are broadly divided into efficient (channelized) and inefficient (distributed) systems (e.g. Hubbard and Nienow, 1997; Fountain and Walder, 1998; Irvine-Fynn *et al*., 2011). An efficient drainage system is composed of subglacial tunnels that either arch up into the ice (R channels; Röthlisberger, 1972) or carve into the glacial bed (N channels; Nye, 1973). An efficient drainage system can effectively transfer large water fluxes from the bed to the glacier margin. Therefore, sudden changes in drainage efficiency, caused by rapid fluctuations in water supply or channel blockage, which takes place when meltwater encounter zones of low hydraulic conductivity or frozen beds, can reduce glacial stability. R channels can quickly adjust to fluctuating water fluxes, hence, they serve as important stabilising mechanisms for ice sheets (Boulton *et al*., 2009).

In contrast to the rapid meltwater flows within efficient drainage systems, a distributed (inefficient) glacial drainage system is characterized by low flow velocities. Water flow within a distributed system takes place through linked cavities on irregular bedrock (Kamb, 1987), a thin film (~1 mm) at the bed/ice interface, which is generated by regelation (Weertman, 1972), “canal” systems within soft subglacial sediments (Walder and Fowler,

1994) and groundwater flow through subglacial sediments (Boulton and Hindmarsh, 1987). The slow flow velocity within distributed systems raises the water pressure as the water flux rises, which can then approach the ice overburden pressure and lead to decoupling between the glacier and the bed (Boulton *et al*., 2007a). The seasonal evolution of the glacial drainage system has been studied extensively. Generally, an inefficient distributed drainage system operates at the start of the melt season, with drainage shifting into an efficient system as the melt season progresses. At the end of the melt season, the distributed drainage is resumed. These seasonal dynamics also impact groundwater flow, which is generally higher when the drainage system is efficient. Despite considerable variability, this general pattern has been reported from a variety of different glacial settings (e.g. Hodgkins *et al*., 1998; Nienow *et al*., 1998; Mernild, 2004; Chandler *et al*., 2013; Cowton *et al*., 2013).

2.3.3. Geological controls on subglacial and proglacial groundwater flow

Similar to non-glacial environments, geology exerts a significant control on subglacial and proglacial groundwater flow and recharge. The understanding that glaciers can be underlain by soft, deformable sediments and permeable beds, as opposed to solely hard bedrock (Boulton, 1986), implies that a portion of the subglacial meltwaters will enter the bed and be directed towards the margin as groundwater. Groundwater drainage is strongly controlled by the hydrogeological parameters of the glacier bed (e.g. Piotrowski, 1997a, b; Janszen *et al*., 2012; Atkinson *et al*., 2013). Therefore, substantial groundwater flow has been observed in glaciers underlain by permeable substrates (e.g. Rossi *et al*., 2012; Boulton *et al*., 2007a, b; Kehew *et al*., 2012;), karst systems (e.g. Gremaud and Goldscheider, 2009 Gremaud *et al*., 2010; Finger *et al*., 2013), and faults (e.g. Haldorsen and Heim, 1999). Significant groundwater systems have also been reported from proglacial zones which are underlain by coarse alluvial deposits, which sustain significant

aquifers (e.g. Ward *et al*., 1999; Crossman *et al*., 2011). These aquifers sustained groundwater flow through the summer months, and became particularly important during periods of low meltwater discharge (Malard *et al*., 1999). Conversely, groundwater flow in proglacial areas which are underlain by low permeability substrates, such as fine-grained deposits, permafrost, and buried ice is much lower (e.g. Boulton *et al*., 2007a; Haldorsen *et al*., 2010; Langston *et al*., 2011).

The hydrogeological parameters of sorted granular materials in glaciated environments are similar to those found in non-glacial conditions. However, glacial environments are impacted by an array of geomorphic processes, which include glacial, glaciofluvial, lacustrine, and aeolian processes (e.g. Freeze and Cherry, 1979; Bajc *et al*., 2014). Hence, the hydraulic conductivity of subglacial tills varies over several orders of magnitude, ranging between 10^{-1} and 10^{-7} m/s (Freeze and Cherry, 1979), with significant implications to groundwater fluxes (the *K* parameter, Equation 2.1).

The hydraulic conductivity of subglacial till is controlled by various sedimentological processes. For instance, compression and shear deformation lead to high anisotropic distribution of till properties (e.g. Boulton and Zatsepin, 2006). Laboratory experiments have shown that particle alignment causes horizontal hydraulic conductivity to exceed vertical hydraulic conductivity by up to two orders of magnitude (Murray and Dowdeswell, 1992). Pervasive deformation of till can advect significant amounts of groundwater towards the margin within the high-porosity deforming layer (Alley *et al*., 1986, 1987). Although such deformation may demolish the drainage paths within the ice/bed interface, it is hypothesised to enhance the drainage through the bed (Murray and Dowdeswell, 1992).

Despite the major gaps in knowledge with regards to the hydrogeological properties of glacial deposits, it is safe to conclude that they are subject to high spatial and temporal variability, imposed by the stresses applied by the overriding glaciers, source material,

and secondary processes (e.g. Domenico and Schwartz, 1998; Fischer and Clarke, 2001; Evans *et al*., 2006). This variability in the hydrogeological properties of glacial deposits is an important control on the spatial variability in proglacial groundwater flow (e.g. Robinson *et al*., 2008; Roy and Hayashi, 2008; Langston *et al*., 2013). In addition to the aforementioned processes, the field sites in southern Iceland are also substantially impacted by volcanic activity and jökulhlaups (e.g. Marren, 2005). This wide variability in geomorphic processes leads to high variability in depositional environments and hydrogeological parameters, which may significantly impact subglacial and proglacial groundwater flow (e.g. Bajc *et al*., 2014).

2.3.4. The impact of geomorphology on proglacial groundwater flow

Geomorphology also exerts an important control on proglacial groundwater flow. For instance, moraines have a complex, heterogeneous internal structure, which leads to various hydrogeological conditions, such as coarse-grained deposits, stepped and perched water tables (e.g. van Overmeeren, 1994; Robinson *et al*., 2008; Langston *et al*., 2011; Bajc *et al*., 2014). Fully or partially impermeable layers (buried ice, ground ice, and bedrock) can direct groundwater flow and focus it towards areas where water can infiltrate into the deeper flow system (Langston *et al*., 2011). Additionally, impermeable layers can also prevent groundwater recharge and lead to perched water tables (e.g. Robinson *et al*., 2008). The heterogeneous hydrogeology within moraines has been shown to generate different groundwater residence times, which impacts groundwater quality and groundwater-surface water exchange (Roy and Hayashi, 2008; 2009).

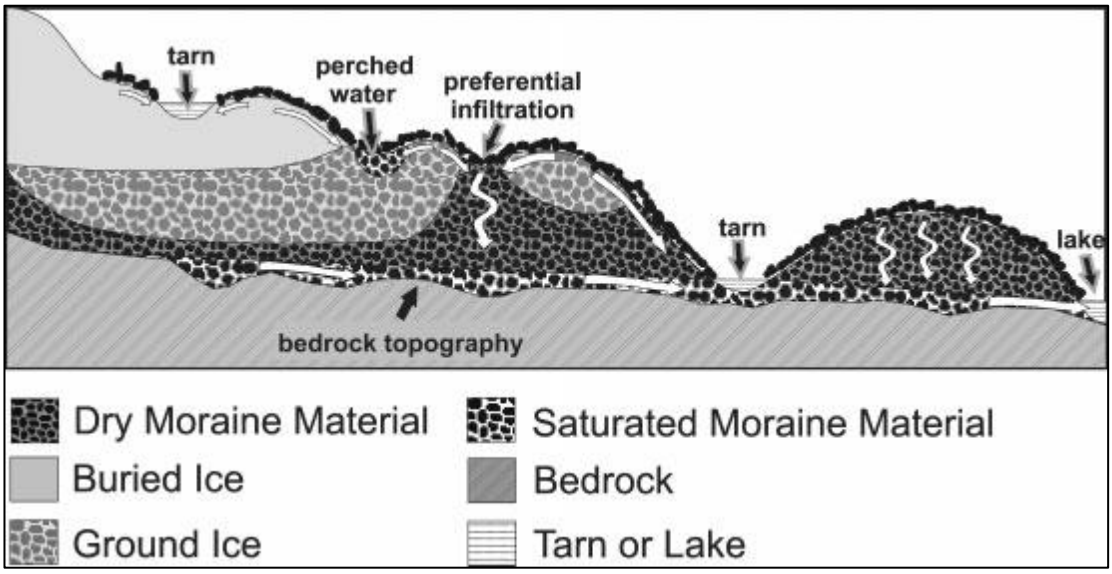

Figure 2.4. Schematic diagram of the internal structure and hydrology of the Opabin moraine, the Canadian Rockies (From Langston *et al*., 2011).

Coarse proglacial deposits, such as talus, also significantly impact groundwater flow and storage. Studies from the Colorado Rockies suggested that groundwater from talus deposits contributed over 60% (Liu *et al*., 2004) and 75% (Clow *et al*., 2003) of total streamflow between early summer and late fall. Furthermore, talus provided important storage for groundwater from snowmelt recharge, with groundwater contributions from the talus continuing even after the disappearing of snow (e.g. Muir *et al*., 2011). The impact of geomorphology on groundwater flow was also reported from the Cordillera Real in Bolivia, where experimental tracer studies have shown that groundwater flow through talus slopes exceeded groundwater flow through moraines by 24 hours (Caballero *et al*., 2002). In addition to talus slopes, eskers also contain highly permeable deposits, which sustain substantial aquifer systems. Studies of esker aquifers in Finland have shown significant exchange between groundwater and surface water, which substantially impacted surface water quality and levels (Rossi *et al*., 2012, Ala-aho *et al*., 2013).

In addition to the impact of high-permeability landforms on groundwater flow, the impact of low-permeability landforms and substrates also substantially impact proglacial groundwater systems. For instance, the low permeability of permafrost, which acts as an aquitard, substantially impedes groundwater recharge and discharge (e.g. Haldorsen and Heim, 1999; Lemieux *et al*., 2008a b; Bense *et al*., 2009; Scheidegger *et al*., 2012; 2014). However, seasonal shallow groundwater flow takes place in some catchments which contain permafrost. Shallow groundwater in such catchments is therefore strongly controlled by the seasonal development of the active layer (e.g. Carey *et al*., 2013). Although western Skeiðarársandur and the Skaftafellsjökull foreland are not underlain by permafrost, the sites are probably impacted by seasonally-frozen ground, which impedes groundwater recharge and increases runoff. However, such conditions were not observed during the fieldwork undertaken and are beyond the scope of this study.

The aforementioned studies illustrate the high variability in proglacial geomorphology, which substantially impacts proglacial groundwater systems. The field sites in Iceland also have high variety in depositional environments and geomorphology, which include glacial, glaciofluvial, and lacustrine landforms. It is therefore expected that the variability in proglacial hydrogeology and groundwater flow will be high.

2.3.5. The impact of glacial thermal regime on groundwater flow

Glacier thermal regime is a key control on subglacial groundwater recharge and flow. Glaciers are classified according to their thermal regime: Temperate (warm based), polythermal, and cold-based glaciers**.** Temperate glaciers contain ice whose temperature are near the Pressure Melting Point (PMP) throughout the glacier, with the exception of a thin surface layer which freezes during the winter, but is removed by melt in the following summer (Ahlmann, 1935, cited in Hodgkins, 1997). Temperate glaciers can be found in

various glacial environments between mid and sub-polar latitudes. These glaciers experience large mass transfers from the accumulation to the ablation zone. Temperate glaciers move by internal deformation, sediment deformation, and basal sliding. This sliding can lead to the fracturing of near surface ice and the formation of crevasses, which route meltwater to the glacier bed. In addition to that, the relatively high motion of temperate glaciers enhances meltwater generation at the glacier sole. Therefore, temperate glaciers which override permeable substrates generally have significant groundwater drainage systems (e.g. Piotrowski, 2007).

In contrast to temperate glaciers, the ice temperatures of cold-based glaciers are lower than the PMP. Hence, melt plays a minimal role in ablation, which mainly occurs by sublimation or calving. Meltwater penetration into the bed of cold-based glaciers is also low, due to the lack of englacial drainage routes. This paucity is a result of the slow rates of deformation of cold based glaciers, which reduces the formation of crevasses. Additionally, the formation of superimposed ice, which occurs on the glacier surface by the refreezing of meltwater also reduces englacial drainage (Hagen *et al*., 1991; Hodgkins, 1997; Gulley *et al*., 2009). Observations from Svalbard show that superimposed ice bears an important influence on drainage during the early melt season, as it serves as an aquitard, preventing water from entering the glacier, and causes it to form lakes within depressions The absence of meltwater lubrication causes cold glaciers to move slowly, mainly by internal creep, which significantly reduces their rates of movement and crevassing. This reduces both their impacts as geomorphic agents (Eyles, 2006) and hydrologically induced flow instabilities (Bingham *et al*., 2006). Groundwater underneath cold based glaciers is therefore suggested to be low (Haldorsen *et al*., 2010). .

Polythermal glaciers consist of ice with spatially heterogeneous temperature distribution. Generally, cold ice is found at the glacier margin and ice at the PMP upglacier from the margin. Warm-based ice may occur underneath thick sections of the glacier, due to the higher pressures and geothermal heat transfer. As glacial drainage is substantially

controlled by the basal thermal regime, the distribution of temperate ice within polythermal glaciers is an important control on groundwater drainage underneath polythermal glaciers (e.g. Haldorsen *et al*., 2010).

Glacier thermal regime also impacts subglacial and proglacial groundwater systems through its impact on permafrost formation. Permafrost distribution is significantly impacted by glaciation conditions, as ice sheets insulate the ground from lower surface temperatures, which prevents permafrost development. When an ice sheet develops over existing permafrost, it will insulate the permafrost from the low surface temperatures. This will gradually raise permafrost temperatures to the PMP, leading to permafrost migration along the periphery of the ice sheet margins (Lemieux *et al*., 2008). The glacier beds at Skeiðarársandur and Skaftafellsjökull are temperate and permafrost-free (Marren 2002; Robinson *et al*., 2008). Hence, further discussion about cold based, polythermal glaciers, and permafrost lies beyond the scope of this study.

2.3.6. Groundwater flow underneath past ice sheets

The development of ice sheets and glaciers over permeable substrates alters the groundwater systems within these substrates from being topographically-controlled, precipitation-fed systems to ones which are pressurized and recharged by the overlying ice (e.g. Haldorsen and Heim, 1999; Haldorsen *et al*., 2010). Additionally, changes in glacial conditions also alter the loading and relaxation stresses on the underlying sediments. These alterations lead to substantial changes in the direction, magnitude and composition of groundwater flow (Lemieux *et al*., 2008a,b; Person *et al*., 2007a b; Bense and Person, 2008; 2009; Lemieux and Sudicky, 2010; Normani and Sykes, 2012; Person *et al*., 2012; Provost *et al*., 2012; Grundl *et al*., 2013). Studies of groundwater flow underneath former ice sheets and glaciers have significantly contributed to the understanding of glacial movement and geomorphology, particularly the origins of tunnel valleys and eskers, which indicate areas with a surplus of basal meltwaters (Piotrowski,

2007; Boulton *et al*., 2007a, b; Boulton *et al*., 2009; Kehew *et al*., 2012). However, the attempts to quantify the amount of meltwater that discharged the major ice sheets during the last glaciation as groundwater have also caused many controversies in the literature.

Some models suggested that glaciers positioned over aquifers with sufficiently high hydraulic transmissivity were able to drain most meltwater as groundwater. For instance, Boulton and Dobbie (1993) suggested that during the Saalian glaciation, areas in the Netherlands were able to drain the entire meltwater supply as groundwater. Using a higher melting rate (25 mm/year) when modelling the groundwater flow along the transect from the Scandinavian ice divide to the periphery in the Netherlands, Boulton *et al*. (1995) also reached similar conclusions. However, their modelled aquifer only had one input of hydraulic conductivity (3.00×10^{-4} m/s), which corresponds to the conductivity of sand. However, this modelled homogenous aquifer clearly ignores the high variability of hydraulic conductivity which is found within glacial deposits (e.g. Freeze and Cherry, 1979; Meriano and Eyles, 2009).

The approach of a homogenous aquifer, suggested that substantial proportions of meltwater discharged as groundwater from the European ice sheets (e.g. Boulton and Dobbie, 1993; Boulton *et al*., 1995), have been contested by numerical models and field evidence from relict ice sheets in Europe and North America. For instance, a 3D groundwater flow model that did account for the heterogeneity of Quaternary sediments suggested that only ~25% of meltwater was evacuated as groundwater through the bed. The model also suggested that the remaining water drained through subglacial channels in spontaneous bursting episodes (Piotrowski, 1997b; Piotrowski *et al*., 2009). The relatively low proportion of groundwater drainage is also supported by field observations of tunnel valleys, some up to 80 metres deep, which were found at the study area (Piotrowski, 1994). Modelling of groundwater drainage from Nordfjord, Norway, suggested that initially, the entire basal meltwater drained as groundwater. However, as deglaciation progressed, only 14-38% of the basal meltwater drained as groundwater. The model

suggested that the addition of surface meltwater exhausted the capacity of groundwater drainage, which generated the formation of alternative drainage routes (Moeller *et al*., 2007). Estimations from North America also suggested that relatively small proportions of meltwater were discharged via the aquifer. Models of the Laurentide Ice Sheet hydrology, suggest that only around 5-10% of meltwaters drained as groundwater (Person *et al*., 2007a). Models of the Laurentide Ice Sheet's Lake Michigan Lobe have shown that even when the hydraulic conductivity of the entire bed is increased by two orders of magnitude, the aquifers were still not capable of draining the entire meltwater supply and maintain the pore-water pressure below the overburden pressure (Breemer *et al*., 2002). Modelling of the impact of the Wisconsian glaciation on groundwater flow in Canada suggested that 43% of the melt drained away as groundwater. However, these higher estimations were calculated using conservative melt rates (Lemieux *et al*., 2008a). Other research from Europe (Piotrowski and Kraus, 1997) and North America (Brown *et al*., 1987) also suggested that relatively small proportions of meltwaters were evacuated as groundwater. These studies suggest that significant proportions of meltwater would be transmitted to the proglacial zone as groundwater. However, overall, groundwater was not the main route of meltwater discharge.

2.3.7. Summary

Subglacial and proglacial groundwater flow is described by similar mechanisms to groundwater systems in non-glaciated systems. However, subglacial groundwater systems are driven by the pressure of the overburden ice rather than topography. The characteristics of the substrate exert key controls on groundwater flow, with thick coarse, unconsolidated substrates leading to substantial groundwater flow. Proglacial geomorphology is also an important control on proglacial groundwater flow, with landforms such as talus slopes, eskers, and moraines supporting extensive aquifer systems. However, the internal hydrology of these features can be highly heterogeneous.

The englacial and subglacial drainage systems, alongside glaciation conditions, which control basal thermal regime and the extent of permafrost, also exert key controls on subglacial and proglacial groundwater systems. The quantification of groundwater flow beneath past ice sheets has led to significant controversies. Some studies have suggested that substantial amounts of the overall melt discharged as groundwater, whilst others suggested much smaller proportions of melt were discharged in this way. Skeiðarársandur and Skaftafellsjökull are temperate glaciers, which are generally underlain by permeable beds, hence, contributions of glacial melt to groundwater flow is expected to be significant. However, the variability in hydrogeological parameters at the sites is also expected to be high. This section described the main mechanisms and controls on groundwater flow in glaciated environments. The following section builds on this knowledge to describe the controls and impact on proglacial groundwater-surface water exchange.

2.4. Groundwater-surface water exchange

2.4.1. Introduction

This section describes the importance, key concepts, and main controls of groundwater-surface water exchange. The interaction between groundwater and surface water substantially controls the physicochemical parameters and the cycling of energy, carbon, and nutrients between both systems (e.g. Brunke and Gonser, 1997; Bencala *et al*., 1993; Krause *et al*., 2009; Young *et al*., 2010). Additionally, this interface also impacts water quality and provides natural attenuation for certain pollutants by mixing, sorption, and biodegradation processes (e.g. Krause *et al*., 2009; Byrne *et al*., 2014; Neumann *et al*., 2013; Ullah *et al*., 2014; Weatherill *et al*., 2014; Chang and Yeh, 2014). The impact of proglacial groundwater-surface water exchange on water physicochemical parameters and ecology has also been studied in various proglacial settings (e.g. Brown *et al*., 2007a, b; Roy *et al*., 2010; Gooseff *et al*., 2013). However, the understanding that groundwater

and surface water are integrated, rather than separated components of the hydrological cycle has only increased significantly within the last three decades (e.g.; Winter and Rosenberry, 1995; Winter *et al*., 1998; Krause *et al*., 2009; 2014; Fleckenstein *et al*., 2010).

It is important to increase our understanding of groundwater-surface water interactions in order to improve the management of rivers and lakes, particularly in response to projected changes in climate and land use (e.g. Smerdon *et al*., 2005; 2012; Schmidt *et al*., 2010; Kidmose *et al*., 2013; Muellegger *et al*., 2013; Khan *et al*., 2014; Ullah *et al*. 2014;). Additionally, improved understanding of groundwater-surface water exchange will also help to implement legal directives such as the European Union's Water Framework Directive (WFD) (e.g. CEC 2000; EA 2009; Krause *et al*., 2014).

The mixing between groundwater and surface water takes place at the hyporheic zone (HZ), which forms the saturated zone between groundwater and surface water (Figure 2.5). The HZ derives its physicochemical and biogeochemical characteristics from the active mixing between groundwater and surface water, hence, it is characterised by sharp chemical gradients in Dissolved Oxygen (DO) and redox potential (Boulton *et al*., 1998), high biogeochemical activity (e.g. Gooseff *et al*., 2003), and highly specialised flora and fauna (Ward and Stanford, 1989; Brunke and Gonser, 1997; Kløve *et al*., 2011a, b).

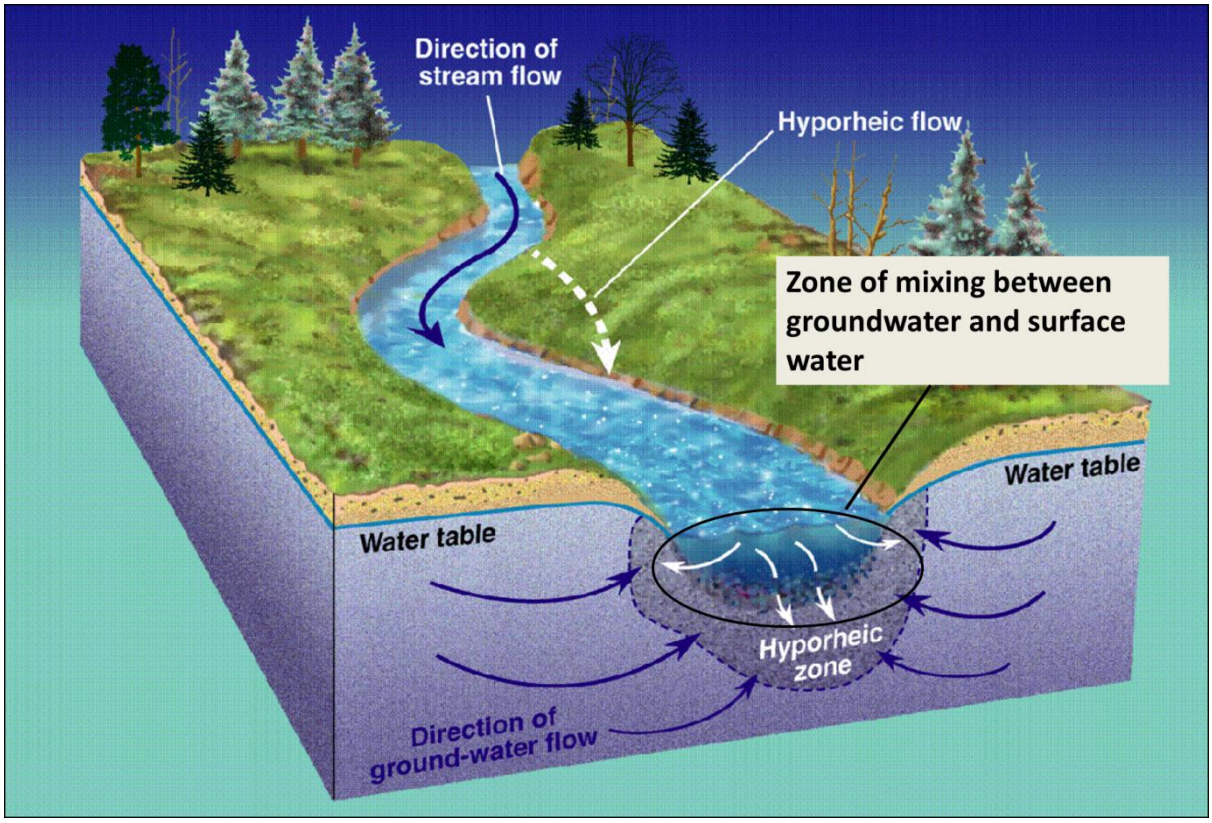

Figure 2.5 conceptual model of the Hyporheic Zone and groundwater-surface water exchange (Adapted from the EA, 2009).

Hydrological connectivity is an important concept in the study of groundwater-surface water exchange. Hydrological connectivity describes water-mediated transfer of energy, matter, and or organisms within or between different components of the hydrological cycle (Pringle, 2003). The concept of hydrological connectivity has been used extensively in riverine landscapes, including proglacial environments (e.g. Tockner *et al*., 1997). The interactive pathways within riverine landscapes occur along three spatial dimensions: vertical (river-groundwater), lateral (river-riparian zone-floodplain), and longitudinal (headwater-estuary) (e.g. Ward and Stanford, 1989). Complex patterns of hydrological connectivity have been reported from various proglacial environments (e.g. Tockner *et al*., 1997; Ward *et al*., 1999; Cooper *et al*., 2002; 2011; Crossman *et al*., 2011). For instance, studies from the Val Roseg catchment, a complex alluvial valley in the Swiss Alps, which is formed in glacial outwash, suggested that the valley contained various types of

channels, such as the main channel, side channels, intermittently-connected channels, mixed channels, groundwater channels, and tributaries. Hence, groundwater-surface water interaction at the catchment takes place on various spatial scales (Ward *et al*., 1999).

The temporal variability in groundwater-surface water exchange is mainly controlled by climatic/meteorological conditions (e.g. Fairchild *et al*., 1999b; Aragón *et al*., 2011; Ward *et al*., 2013; Kirillin *et al*., 2013). However, anthropogenic activities, such as the operation of dams, can also exert important controls on groundwater-surface exchange (e.g. Sawyer *et al*., 2009; Francis *et al*., 2010). Groundwater-surface water exchange within proglacial environments is mainly controlled by meltwater levels which vary on diurnal, seasonal, annual and decadal time scales (Hubbard *et al*., 1995; Brown *et al*., 2006; Cauvy-Fraunié *et al*., 2013). Additionally, low frequency, high magnitude events, such as floods and jökulhlaups can also impact proglacial groundwater-surface water exchange (Cooper *et al*., 2002; 2011; Kristiansen *et al*., 2013).

2.4.2. The impact of topography on proglacial groundwater-surface water exchange

Groundwater-surface water exchange is substantially impacted by topography and the position of surface water features within the landscape. Groundwater flow systems generally form a subdued replica of the surface (e.g. Hubbert, 1940; Freeze and Cherry, 1979). Groundwater flow systems in areas of irregular topography are divided into local, intermediate, and regional flow systems, which are nested in this ascending order (Tóth, 1963). Local groundwater systems flow to a nearby discharge location, such as streams and ponds. Regional groundwater flow systems travel longer distances than local ones, and discharge into the oceans, major rivers, or large lakes. Intermediate flow systems have one or more topographic high and low found between its recharge and discharge area. However, in contrast to the regional flow system, it does not contain both a major

topographic high and low (Tóth, 1963; 1999). The interaction between groundwater and streams, lakes, ponds, and wetlands is controlled by the position of these water bodies with respect to the groundwater systems. Local groundwater flow systems are generally found in areas of higher topographic relief, while intermediate and regional groundwater systems are generally found in areas of low relief. For instance, studies from Skeiðarársandur suggested that the regional groundwater flow system flows away from the glacier margin, towards the coast. The local groundwater systems at the site were found in areas of higher topography, and were generally located in moraine areas (Figure 2.6) (Robinson *et al*., 2008).

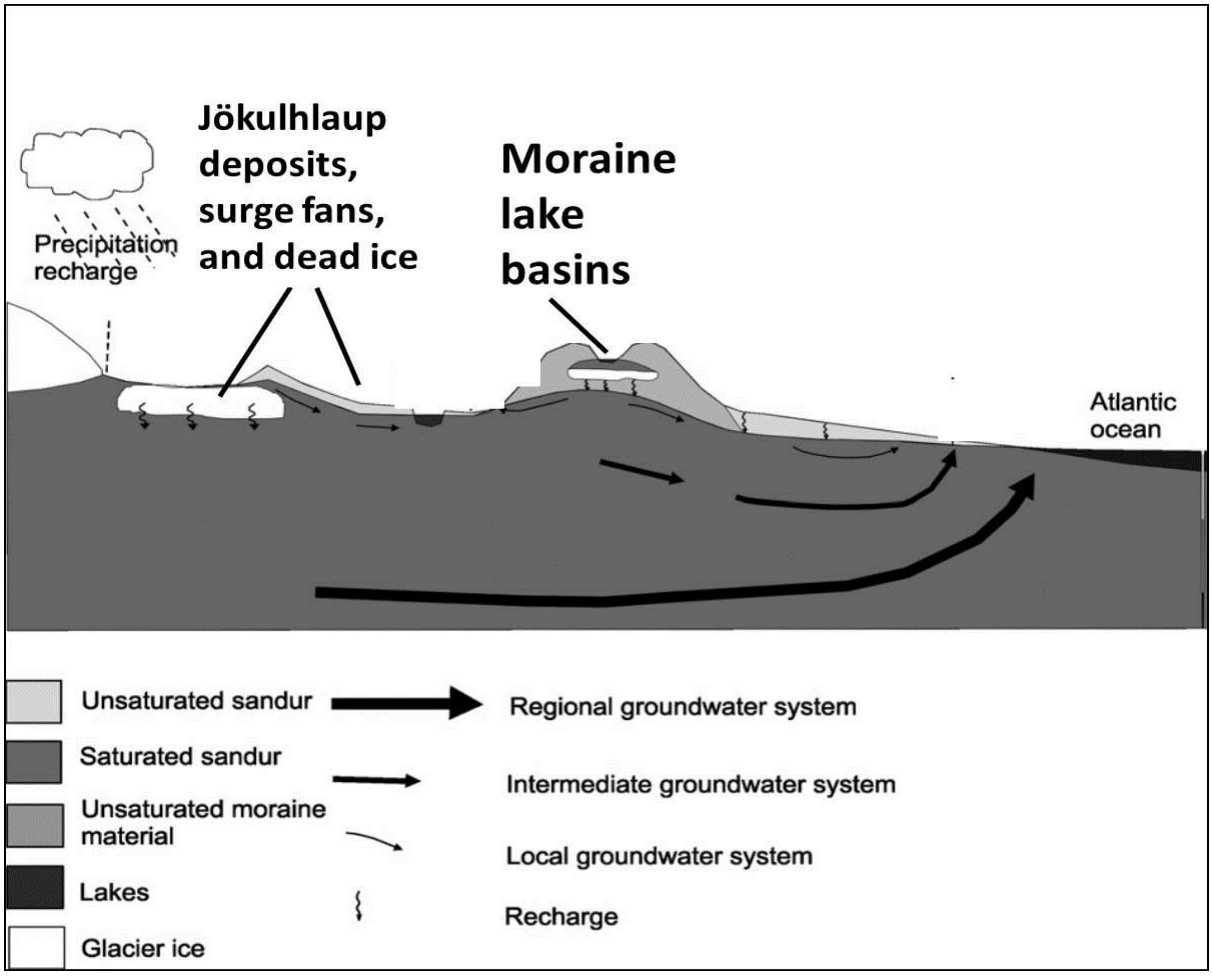

Figure 2.6. Conceptual model of the different scales of groundwater flow systems in western Skeiðarársandur.

In addition to high frequency, low magnitude accumulation and ablation processes, the area is also impacted by glacier surges and jökulhlaups. Adapted from Robinson *et al*. (2008).

The position of surface water systems within the landscape is an important control on groundwater-surface water exchange, with surface water bodies (e.g. lakes and ponds) connected to local groundwater flow systems reported to have lower exchange with the groundwater systems than surface water bodies connected to intermediate and regional groundwater flow systems (e.g. Campbell *et al*., 2004). These patterns have been reported from an array of hydrogeological settings, including boreal forests (Smerdon *et al*., 2005), alpine ridges (Campbell *et al*., 2004), esker aquifers (Ala-aho *et al*., 2013), and proglacial outwash plains (sandurs) (Bahr *et al*., 1997; Robinson *et al*., 2008). These differences in groundwater-surface water exchange also lead to substantial differences between the hydrology and biogeochemistry of lakes and ponds in topographically-high and topographically-low areas (e.g. Campbell *et al*., 2004).

The connectivity of lakes and ponds with groundwater systems is also an important control on their vulnerability to climate change, in situations where groundwater discharge increases surface water levels. Hence, lakes and ponds with lower connectivity to groundwater systems, which can buffer the projected falls in meltwater, are more vulnerable to projected changes in precipitation (e.g. Young *et al*., 2010; Ala-aho *et al*., 2013).

2.4.3. The impact of hydrogeology and geomorphology on proglacial groundwater-surface water exchange

Similar to their impact on groundwater flow, hydrogeology and geomorphology also exert important controls on groundwater-surface water exchange. Surface water features with low permeability beds generally have lower rates of exchange with the groundwater systems, as reported from an array of hydrogeological settings, including wetlands underlain by clay deposits (Ferone and Devito, 2004), lakes underlain by low-permeability beds (e.g. Roy and Hayashi, 2008; Shaw *et al*., 2013), and streambeds with high

proportion of fine-grained sediment (e.g. Conant, 2004). The hydraulic gradient between the surface water body and groundwater is also an important control on the interface between groundwater and rivers (e.g. Storey *et al*., 2003; Hannah *et al*., 2009; Krause *et al*., 2012), wetlands (Ferone and Devito, 2004), and lakes (e.g. Smerdon *et al*., 2005; Kirillin *et al*., 2013). Hydraulic gradients in proglacial environments are substantially impacted by meltwater levels, which vary on a diurnal, seasonal, annual and episodic basis (e.g. Cooper *et al*., 2002; Dragon *et al*., 2014). Proglacial groundwater-surface water exchange is also controlled by the prevalent high variability in hydrogeological parameters. This variability is caused by the array of geomorphic processes (e.g. Marren *et al*., 2005; Robinson *et al*., 2008; Bajc *et al*., 2014) and high sediment heterogeneity that is prevalent in these environments (e.g. Malard *et al.,* 1999; Hoehn and Meylan, 2009; Magnusson *et al*., 2014).

Geomorphic variability is also an important control on groundwater-surface water exchange (e.g. Kalbus *et al*., 2006; Norman and Cardenas, 2014). For instance, field observations have shown that coarse-grained landforms such as talus and moraines provided significant exchange between proglacial groundwater, lakes, and streams (e.g. Hood *et al*., 2006; Roy and Hayashi, 2008; 2009). Additionally, talus and rock glaciers also provided storage of groundwater recharge, some of which originated from snow and icemelt, which was then slowly released into streamflow (e.g. Clow *et al*., 2003; Liu *et al*., 2004).

In addition to the impact of large-scale landforms on groundwater flow, smaller scales of landforms are also important for groundwater-surface water exchange. For instance, a study from a losing stream in the Colorado Rockies has shown the impact of bed morphology on groundwater-surface water exchange, where stream water entered the alluvium and re-emerged after a short distance. Recharge and discharge took place at locations of transitions in bed slope, such as the transition between pools and steeper units (Harvey and Bencala, 1993). The impact of streambed topography on hyporheic

exchange has also been reported from a gravel-bed stream in Idaho (Gariglio *et al*., 2013). The impact of geomorphic features such as pools and riffles in lowland rivers, which impact river-aquifer exchange through their control on stream velocity, bed sedimentology and hydraulic conductivity, has also been reported (e.g. Käser *et al*., 2009).

Preferential Flow Paths (PFP) also exert important control on groundwater-surface water exchange. Soil pipes, which are made from connected subsurface macro pores are an important example of a PFP. These features were commonly observed in various settings of hill slope hydrology, including glaciated environments (Faeh, 1997; Uchida *et al*., 2001; Cozzetto *et al*., 2013). For instance, pipe flow at the boundary between frozen and unfrozen streambed sediments has served as a PFP in the hyporheic zone of a stream in Antarctica. The hyporheic exchange acted as a positive feedback, where the PFP enhanced hydrological connectivity and flow due to its impact on water viscosity and temperature (Cozzetto *et al*., 2013). The impact of PFP on subsurface water and solute storage and catchment biogeochemistry has also been reported from a field site in Alaska, where the flow paths were observed along the boundary between thawed ground and the permafrost (Koch *et al*., 2013). Water tracks are zones of high soil moisture which route water downslope over the ice table in polar environments, such as the Dry Valleys of Antarctica (Levy *et al*., 2011). These features were observed to transport water, energy, and nutrients between streams and lakes in Antarctica's Dry Valleys, which makes them important enhancers of hydrological connectivity. Although their magnitude is substantially smaller than that of meltwater discharge, the solute content of the water tracks is equal to or higher than that of streamflow. Hence, water tracks serve as important hydrological pathways, which substantially impact the geochemistry of streams and lakes (Levy *et al*., 2011).

2.4.4.The impact of climatic conditions on groundwater-surface water exchange

Climatic factors are also important controls on groundwater-surface exchange. Rainfall and evaporation are important controls on the levels of shallow groundwater and surface water bodies (e.g. Roy and Hayashi, 2008). These factors also affect the gradient between groundwater and surface water, which impacts hydrological exchange. For instance, rising river stage can reduce the hydraulic gradient between the river and aquifer, which can then reduce exchange (Karan *et al*. 2014). During substantial rainfall events this can also cause flow reversals with river stage rising so that it recharges groundwater, which can also alter the solute concentrations and biogeochemistry of the river and aquifer (e.g. Cooper *et al*., 2002; Bartsch *et al*., 2014). Evapotranspiration, which lowers shallow groundwater and surface water levels, hence impacting the gradient between groundwater and surface water, also exerts a control on groundwater-surface water exchange (e.g. Lewandowski *et al*., 2009). Within glacial environments, climate exerts a strong control on snow and ice melt, which are primary controls of groundwater and surface water exchange in proglacial environments through its impact on discharge levels (e.g. Brown *et al.,* 2006). Climate also controls evaporation and ice formation, which also impact groundwater-surface exchange, with the low permeability of ice limiting groundwater-lake exchange (e.g. Smerdon *et al*., 2005; Kirrillin *et al*., 2013; Blume *et al*., 2013).

2.4.5. Monitoring of groundwater-surface water exchange

The spatial patterns of groundwater-surface water exchange can vary on a scale of centimetres to meters in streams (Brunke and Gonser, 1997; Brunke *et al*., 2003; Kalbus *et al*., 2007; Roy *et al*., 2011; Krause *et al*., 2012) and lakes (Kidmose *et al*., 2011; 2013; Blume *et al*., 2013). Additionally, groundwater-surface water exchange also exhibits

substantial temporal variability (e.g. Hubbard *et al*,. 1995; Smerdon *et al*., 2005; Kirillin *et al*., 2013). It is therefore important to have methods that can accurately, simply, and unobtrusively characterize this fine scale spatial variability in groundwater-surface water exchange. The chosen methods also need to be appropriate for the respective aims of the investigation (e.g. Kalbus *et al*., 2006; Schmidt *et al*., 2007). The main methods which are covered in this literature review are based on direct measurements, environmental tracers, and hydrogeological measurements. However, this literature review only provides a general description of the methods. Further information can be found in individual research articles and in general (e.g. Kalbus *et al*., 2006) and method-specific (e.g. Anderson, 2005b; Rau *et al.,*, 2014) literature reviews and special issues of publications (e.g. Krause *et al*., 2009a, b; 2014; Fleckenstein *et al*., 2010).

Direct measurements of water fluxes between groundwater and surface water are usually performed using seepage meters, composed of a bottomless cylinder, which is inserted into the sediment, and a deflated bag, which collects water fluxes between the aquifer and surface water. Water fluxes can then be calculated from the cross section area of the cylinder, collected volume, and the time taken to fill the bag (e.g. Lee, 1977; Kalbus *et al*., 2006). This method has been used extensively in streams (Murdoch and Kelly, 2003), lakes (e.g. Rautio and Korkka-Niemi, 2011; Ala-aho *et al*., 2013), and wetlands (e.g. Hunt *et al*., 1996). Seepage meters provide direct measurements at relatively low cost. However, seepage meters only provide point measurements and may not reflect substrate heterogeneity effectively (e.g. Kalbus *et al*., 2006). Additionally, seepage meters are also subjected to uncertainties such as bag distortion, folding, and other technical difficulties. However, some of these uncertainties can be overcome by technological advances, such as automated seepage meters (e.g. Krupa *et al*., 1998; Paulsen *et al*., 2001; Sholkovitz *et al*., 2003).

Environmental tracers investigate groundwater-surface water exchange assuming significant differences between end-members (e.g. Rossi *et al*., 2012). The main

environmental tracers which are used to study groundwater-surface water exchange are temperature, Electrical Conductivity (EC), water stable isotopes ($\delta^{18}O$ and δD), and solute concentrations. Temperature has been used increasingly as a tracer for groundwater-surface water exchange, exploiting the relative stability of groundwater temperatures, in comparison to the higher variability of surface water temperature (e.g. Anderson, 2005b). Significant temperature differences between groundwater and surface water can therefore be used to identify the general behaviour of a reach (whether it is impacted by groundwater upwelling or downwelling), with gaining reaches characterised by relatively stable pore-water and surface water temperatures (e.g. Winter *et al*., 1998; Krause *et al*., 2012). Conversely, losing reaches are characterized by high variability in pore-water and surface water temperatures (Constantz, 1998; Constantz and Stonestrom, 2003; Kalbus *et al*., 2006). The significant differences between groundwater and meltwater temperatures, therefore make temperature an especially useful tracer for proglacial groundwater-surface water exchange (e.g. Schneider *et al*., 2011; Ala-aho *et al*, 2013; Tristram *et al*., 2015). The use of temperature in investigating groundwater-surface water exchange has substantially increased in the last two decades. This increase has been stimulated by the increasing availability of robust, inexpensive, and simple heat sensors and technologies such as Fibre Optic Distributed Temperature Sensing (FO-DTS), which provide temperature monitoring at very high spatial and temporal resolutions (e.g. Selker *et al*., 2006a, b).

Temperature profiles from the sediment-water interface and the lake/stream bed can be used in various ways to infer and quantify groundwater discharge into streams and lakes. For instance, temperature profiles are used to solve the heat transport equation, which is analogous to the advection-dispersion equation of solute transport in groundwater (e.g. Suzuki, 1960; Hatch *et al*., 2006). Temperature measurements which are taken in high spatial and temporal resolution from a stream/lakebed can also be used to investigate groundwater-surface water exchange. This approach assumes that the measured

temperature variations can be attributed to spatial, rather than temporal, variations in groundwater-surface water exchange (e.g. Conant, 2004; Schmidt *et al*., 2006; 2007). Another approach which uses temperature to investigate groundwater-surface water exchange applies a heat balance equation, where surface water temperatures are a function of groundwater discharge, the differences between groundwater and surface water temperatures, and additional heat fluxes through the stream surface (Becker *et al*., 2004).

Geochemistry and water stable isotopes, notably $\delta^{18}O$ and δD, have also been used as environmental tracers in various proglacial environments (e.g. Roy and Hayashi, 2008; 2009; Robinson *et al*., 2009 b; Flaim *et al*., 2013). These methods are based on the different geochemical and isotopic composition between different recharge sources, which result from the different controls and hydrological processes which impact the different end-members (e.g. Tranter *et al*., 1993; Robinson *et al*., 2009a, b). These distinct compositions have been previously used to investigate various hydrological issues such as sources of recharge (e.g. Fairchild *et al*., 1999b), hydrological flow paths (e.g. Gooseff *et al*., 2013), hydrological pathways and residence time (e.g. Boucher and Carey, 2010), hydrograph separation (Williams *et al*., 2006), and groundwater-surface water exchange (e.g. Roy and Hayashi, 2009). Radon (^{222}Rn), which is used to measure the residence time of groundwater, has also been increasingly used as a tracer for groundwater-surface water exchange (e.g. Dugan *et al*., 2012; Kluge *et al*., 2012; Diova *et al*., 2013; Magnusson *et al*.,2014). Geochemistry and stable isotopes provide simple, relatively inexpensive measurements. However, these methods only provide point measurements, which can lower the spatial resolution (e.g. Yde *et al*., 2008; Hindshaw *et al*., 2011). Additionally, investigating groundwater geochemistry and stable isotopes requires infrastructure for the collection of water samples, which may be difficult in remote and protected areas (e.g. Cooper *et al*., 2011).

Groundwater-surface water exchange can also be investigated using surface water levels and hydraulic heads. These measurements can be used to map horizontal and vertical groundwater flow direction which can then be used to infer groundwater-surface water interaction (e.g. Drexler *et al*., 1999; Magnusson *et al*., 2014). Additionally, such measurements, in addition to the hydraulic conductivity, can also be used to calculate groundwater seepage (Darcian) fluxes (e.g. LaBaugh *et al*., 1997). The advantage of these methods are the accuracy and relative simplicity of the measurements of hydraulic heads (e.g. Brassington, 2008). However, these methods rely on an accurate determination of hydraulic conductivity, which is highly variable within proglacial environments (e.g. Robinson *et al*., 2008; Langston *et al*., 2013). Additionally, the logistics and intrusive nature of hydrogeological monitoring networks can be problematic, particularly in protected and remote areas (e.g. Cooper *et al*., 2011).

2.4.6. Summary

There is an increasing understanding with regards to the integration between groundwater and surface water systems. Groundwater-surface water exchange substantially impacts the hydrology, ecology, and biogeochemistry of both systems and the hyporheic zone. Groundwater-surface water exchange is controlled by topography, geology, and climatic conditions. However, groundwater-surface water exchange is subjected to substantial temporal and spatial variability. This is particularly true for proglacial environments, which have high spatial heterogeneity in substrate characteristics, and high temporal variability in discharge and recharge characteristics. There is a wide array of methods to investigate groundwater-surface water exchange such as direct measurements, hydrogeological methods, and environmental and temperature tracing. However, despite the increase of research on groundwater-surface water exchange, there is still a significant paucity of research with regards to the temporal and spatial variability in proglacial groundwater-surface water exchange. The high heterogeneity in meltwater discharge and

hydrogeological parameters at the Skaftafellsjökull foreland and Skeiðarársandur therefore suggests that proglacial groundwater-surface water exchange will be highly variable.

2.5. The impact of groundwater on proglacial habitats

This section describes the impact of groundwater on the conditions of proglacial surface water habitats. This section also describes the projected impacts of climate change and glacier retreat on proglacial hydrology and ecology. Proglacial ecosystems are substantially impacted by climatic variability, diverse water sources , and the hydrological connectivity between these water sources, which lead to high variability in small-scale habitats (Ward *et al*., 1999; Füreder *et al*., 2001; Malard *et al*., 2001; Finn *et al*., 2013). The interactions between the different water sources create variable hydrological, physiochemical and geomorphic conditions, which significantly control the structure, distribution and function of stream ecosystems (e.g. Milner and Petts, 1994; Malard *et al*., 2006; Jacobsen *et al*., 2012; 2014).

2.5.1. The impact of water source on water physicochemical parameters in glaciated catchments

The hydrology of proglacial catchments is highly variable, with icemelt, snowmelt, rainfall and groundwater contributing most runoff. Streams within alpine catchments were traditionally divided according to their contributing water source: glacial (kryal), snowmelt (rhithral) or krenal (groundwater) streams (Milner and Petts, 1994). The distinction between stream types according to this classification was almost solely based on stream temperature. Later classification categorised streams were then based on the relative contributions of each water source (Brown *et al*., 2003).

Glaciated and recently deglaciated catchments are characterised by harsh ecological conditions, caused by the prevalent high sediment mobility, strong winds, and lack of fertile soils (Jumpponen *et al.,* 1999; Marteinsdóttir *et al.,* 2010; 2013). Krenal (icemelt-fed) and rhithral (snowmelt-fed) streams are characterised by high and variable discharge, high suspended sediment concentrations, and high concentrations of dissolved oxygen. The environmental conditions in these streams are harsh due to the cold temperatures, low nutrients, high turbidity, and high variability in discharge leading to low channel stability (e.g. Milner and Petts, 1994; Tockner *et al*., 1997; 2002; Gooseff *et al*., 2003; Slemmons *et al*., 2013; Brown *et al*., 2007a; Cauvy-Fraunié *et al*., 2013; 2014). Conversely, groundwater-fed (krenal) streams in glacial environments generally have higher temperatures, nutrient concentrations and channel stability. These streams also have lower turbidity and variability in discharge (e.g. Milner and Petts, 1994; Malard *et al*., 1999; 2000; 2001; Ward *et al*., 1999; Roy *et al*., 2011; Brown *et al*., 2007a, b, Crossman *et al*., 2011; Jacobsen *et al*., 2012). The distance from the glacier margin is an important control on water physicochemical parameters within glaciated basins. Temperatures and nutrient concentrations generally increase with distance from the glacier margin due to increasing contributions from groundwater, rainfall, and snowmelt (e.g. Brown *et al*., 2006a). Algal biomass also increases with distance from the glacier margin (e.g. Uehlinger *et al*., 2010). Hence, the variability in water temperature, chemistry, and ecology increases with distance from the glacier margin (e.g. Füreder *et al*., 2001; Milner *et al*., 2009; Cauvy-Fraunié *et al*. 2013; Slemmons *et al*., 2013).

Water temperature critically influences the growth, development, emergence, reproduction, and distribution of aquatic fauna (Ward and Stanford, 1982; Brown and Hannah, 2008; Kurylyk *et al*., 2014a, b). Crossing critical temperature thresholds can increase disease vectors, metabolic stress, and impede fish migration, which adversely affects organisms and ecosystems (Acuña and Tockner, 2009). The temperatures of

meltwater and groundwater-fed streams within proglacial environments are controlled by an array of factors including water source, proximity to the glacier margin, climate, basin and channel characteristics, riparian conditions, and hyporheic exchanges (Webb and Zhang, 1999; Brown *et al*., 2005; Brown and Hannah, 2008; Acuña and Tockner, 2009; Cauvy-Fraunié *et al*., 2013). Glacial coverage significantly reduces stream temperatures, with a 10% increase in catchment glaciation equating to a cooling of stream temperature by 1-2 °C in July/August and 0.6 °C in September (Moore, 2006). In contrast to surface water temperatures in proglacial environments, groundwater temperatures are mainly determined by the mean annual, rather than the prevailing, air temperature (e.g. Bonan, 2008). Therefore, groundwater temperatures are generally higher and less variable than those of meltwater (e.g. Füreder *et al*., 2001). For instance, studies from the Val Roseg have shown that hyporheic temperatures exceeded meltwater temperatures by 12.1°C in the summer and 2.7°C during winter (Malard *et al*., 2001; Acuña and Tockner, 2009). Higher groundwater temperatures than meltwater temperatures have also been reported from glaciated catchments in the Alps (e.g. Lafont and Malard, 2001; Malard *et al*., 2001), the Pyrénées (e.g. Brown *et al*., 2006; 2007b), the Andes (e.g. Jacobsen *et al*., 2010; 2012), New Zealand (Datry *et al*., 2007), Iceland (Gíslason *et al*., 2000; Tristram *et al*., 2014), and Svalbard (e.g. Blaen *et al*., 2013). In addition to buffering the variability in stream temperatures, groundwater discharge can also provide thermal refugia, which increases the heterogeneity of river thermal regime and enables the survival of fauna in river reaches that would not be suitable otherwise (e.g. Sutton *et al*., 2007; Kurylyk *et al*., 2014). Groundwater contributions to streams therefore increase stream temperature and thermal stability, which also significantly impacts stream ecology. Higher biodiversity has generally been observed in streams with high groundwater contributions (e.g. Milner and Petts, 1994; Ward *et al*., 1999; Brown *et al*., 2007a, b; Crossman *et al*., 2011; 2013).

Water source in glaciated catchments also substantially impacts water chemistry, which impacts nutrient levels. Groundwater-fed streams and lakes generally have higher solute

concentrations than snow and glacial fed streams, due to longer residence time, hence interaction, of groundwater with the substrate (Füreder *et al*., 2001; Malard *et al*., 2001; Gooseff *et al*., 2003; 2006; Wimpenny *et al*., 2010; Fortner *et al*., 2011). However, groundwater chemistry can vary within and between catchments due to the different residence times and lithology with which groundwater interacts (e.g. Cooper *et al*., 2002; Dragon and Marciniak, 2010; Hindshaw *et al*., 2011; Gooseff *et al*., 2013). In addition to geology, water chemistry is also controlled by the distance from the glacier margin. Observations from the Val Roseg catchment showed that streams near the glacier margin contained only a limited amount of allochotonous organic matter, which was attributed to sparse vegetation. Nutrient and organic matter concentrations then increased with distance from the glacier terminus (e.g. Zah and Uehlinger, 2001; Milner *et al*., 2009; Slemmons *et al*., 2013).

Stream water source also substantially impacts biogeochemistry. Within the various stream sources in the Val Roseg catchment, groundwater was observed to have the highest concentrations of dissolved organic carbon (DOC) (Tockner *et al*., 2002). Observations of low flow conditions during winter from SE Alaska also report an increase in DOC concentrations during winter, due to an increase in the baseflow contribution of DOC-rich groundwater (Hood and Berner, 2009). Glacial meltwater are also reported to have substantially higher nitrate concentrations than those of snowmelt water (Robinson and Kawecka, 2005; Hood and Scott, 2008; Slemmons and Saros, 2012; Slemmons *et al*., 2013). In addition to the studies from streams in glacial environments, the impact of water source on aquatic biogeochemistry and ecology has also been reported in other proglacial water bodies. For instance, substantial differences in water physicochemical parameters have been observed in kettle holes at Skeiðarársandur, Iceland, where icemelt-fed kettle holes had lower EC and higher turbidity. Conversely, kettle holes which are hypothesized to be groundwater-fed had higher EC and low turbidity. Additionally, the kettle holes had distinct sulphide oxidation reactions, which were hypothesised to be bacterially-mediated.

These reactions and field observations of algal mats and invertebrates suggest that the groundwater-fed kettle holes serve as important ecological niches (Robinson *et al*., 2009a). The ecological impacts of shallow groundwater systems have also been reported from the McMurdo Dry Valleys in Antarctica, where solute transport through water tracks and the hyporheic zone of streams enhanced solute mobilisation and improved habitat conditions for microbial and invertebrate communities (Gooseff *et al*., 2013).

Water source within glaciated environments also substantially impacts water turbidity. Turbidity is high in glacial-fed streams due to the high suspended sediment concentrations, which reduces water clarity (Hallet *et al*., 1996; Malard *et al*., 2006; Hood and Berner, 2009; Moore *et al*., 2009). Conversely, groundwater-fed streams have lower concentrations of suspended sediment concentration, hence lower turbidity (e.g. Brown *et al*., 2007a; Milner *et al*., 2009). Turbidity can substantially impact aquatic ecology. For instance, observations from lakes that receive significant glacial melt inputs have shown that the high turbidity can attenuate 20-25% of photosynthetically active radiation and ultraviolet radiation (Hylander *et al*., 2011). This attenuation of radiation impacts the distribution and behaviour of fauna, with possible implication for aquatic food webs (Utne-Palm, 1999; Jönsson *et al*., 2011; Hylander *et al*., 2011). Therefore, the low turbidity of groundwater-fed streams is hypothesised to enhance aquatic biodiversity (e.g. Milner *et al*., 2009).

2.5.2. Projected impacts of climate change on proglacial hydrology and ecology

Climate change is projected to enhance glacial retreat and substantially alter the magnitude and timing of snow and icemelt. These changes are projected to alter the hydrology of glaciated basins, reducing streamflow meltwater contributions and increasing rainfall and groundwater contributions (e.g. Milner *et al*., 2009; Blaen *et al*., 2013; 2014). These changes are projected to impact water physicochemical parameters, such as

temperature. For instance, a decrease of 10% in catchment glaciation was modelled to have a similar impact to an increase of 1.6 °C in stream Mean Weekly Annual Temperature (MWAT), which is an important indicator of thermal suitability for fish species (Nelitz *et al*., 2008).

These changes are also projected to substantially impact the ecology of glaciated basins (e.g. Milner *et al*., 2009; Slemmons *et al*., 2013; Blaen *et al*., 2013; 2014). The biodiversity of aquatic fauna is assessed using various biological indices which focus on the site (α), inter-streams (β) and regional (γ) scales (Brown *et al*., 2007b). Models project complex reactions of ecosystems to a reduction in meltwater input. The mollification of the harsh conditions associated with glacial streams due to increased proportions of groundwater is projected to increase α biodiversity (e.g. Milner *et al*., 2009). However, the reduction in snow, ice melt, and groundwater recharge can lead to a loss of habitat heterogeneity, which will reduce the β biodiversity. Alongside the reduction in meltwater input, the steepening of the temperature gradient, due to glacier retreat, is also projected to have detrimental effects on the biodiversity of these environments (e.g. Milner *et al*., 2009; Finn *et al*., 2010). The implications of shifting water sources within glaciated basins can be illustrated by the disappearance of highly endemic species which are adapted to the unique conditions found in glacial meltwater, such as high variability in discharge (e.g. Cauvy-Fraunié *et al*. 2013), low water temperatures and channel stability (e.g. Milner *et al*., 2001; Rossaro *et al*., 2006), and high turbidity (e.g. Hylander *et al*., 2011). These extinctions are also projected to reduce γ biodiversity (Brown *et al*., 2007b; Hannah *et al*., 2007; Milner *et al*., 2009). These projections are supported by observations and modelling from various proglacial settings. For instance, a comparison between the biodiversity indices of glaciated and deglaciated catchments in the Pyrénées has shown that the gamma indices of the former were significantly lower than the latter (Finn *et al*., 2014). Observations from the Apennines in Italy suggest the disappearance of chironomid species which are endemic to glacial snouts following the disappearance of the glaciers

(Rossaro *et al*., 2006). The impact of falling meltwater discharge due to glacial retreat has also been investigated in Antisana, in the Ecuadorian Andes. Models suggest that glacier retreat will lead to a significant reduction in habitats which are impacted by high hydraulic stress (caused by the high variability in meltwater discharge). The models therefore project a reduction in the abundance of macroinvertebrate species adapted to living in such habitats (Cauvy-Fraunié *et al*., 2014). These studies suggest that the projected changes in the contributions of icemelt, snowmelt and groundwater to proglacial streams following glacial retreat, will significantly impact proglacial biodiversity (e.g. Blaen *et al*., 2013; 2014).

2.5.3. Summary

The main water sources within proglacial environments are icemelt, snowmelt, and groundwater. The relative contribution of each source significantly impacts water physicochemical parameters, biogeochemistry, and ecology. Meltwater generally has very low temperatures and nutrient concentrations and high variability in discharge. Conversely, groundwater temperatures and nutrient concentrations are higher, while the variability in discharge is smaller. These favoured conditions in groundwater substantially impact proglacial ecology, with higher biodiversity generally reported from water bodies with higher groundwater contributions. Climate change and glacier retreat are projected to alter the amount of timing of melting, which will alter the contributions of icemelt, snowmelt and groundwater within proglacial streams. These changes are projected to have mixed impacts on proglacial biodiversity. On one hand, the mollification of the harsh conditions associated with meltwater is projected to increase site biodiversity. Conversely, inter-stream and regional biodiversity are projected to fall due to the reduction in abundance, and possible extinction, of highly endemic species following the decline in habitat heterogeneity.

2.6. Conclusions

This chapter has summarised current research on: 1) the unique hydrological characteristics of glaciated basins, 2) The dominant processes and controls on groundwater flow within glacial environments, 3) the importance and controls on groundwater-surface water exchange, 4) the impact of groundwater contributions to proglacial ecology. Additionally, the projected impacts of climate change on proglacial groundwater hydrology and groundwater-surface water exchange have also been summarised. This literature review highlights the paucity of research with regards to proglacial groundwater systems and groundwater-surface water exchange. The literature review also highlights the following research priorities:

- The need for long term monitoring of proglacial groundwater levels and the extent of groundwater-fed surface water features.
- Determination of the spatial variability of hydrogeological parameters within proglacial settings using field and laboratory methods in order to understand the patterns of proglacial groundwater flow at the site and to develop a hydrogeological framework for the individual site margins.
- Quantitative analysis of hydrological exchange between meltwater, lakes, and groundwater in order to improve the understanding with regards to proglacial groundwater-surface water exchange.

These highlighted issues will be addressed in this study using a combination of geographical, hydrogeological, and geochemical techniques. These results will improve the understanding of the spatial and temporal variability of groundwater-surface exchange at the proglacial zones of two retreating glaciers in SE Iceland.

3. Field sites

3.1. Introduction

This chapter describes the field sites where research has taken place. Fieldwork for this project was undertaken during three campaigns: 10 July-15 August 2011, 15 June-01 August 2012, and 23-31 August 2012. Fieldwork took place at the proglacial zone of Skaftafellsjökull and the proglacial outwash plain (sandur) of western Skeiðarársandur, which are located in SE Iceland (Figure 3.1, Figure 3.2). These sites were chosen for the following reasons:

- The groundwater table at the sites is relatively shallow (approximately 1.5 m below ground). Hence a simple, shallow piezometer network is sufficient for the effective monitoring and sampling of proglacial groundwater and for the investigation of groundwater-surface water exchange.
- The proglacial outwash plain of Skeiðarársandur was chosen due to the extensive background data on aquifer properties, hydrogeology (e.g. Bahr, 1997; Fairchild *et al*., 1999a; Guðmundsson, 2002; Robinson *et al*., 2008; 2009a, b) and geomorphology (e.g. Marren 2002a; 2005; Russell *et al*., 2006; Robinson *et al*., 2008; Mountney and Russell, 2009). This data includes records of groundwater levels which spans from July 2000 to August 2012. The background data also includes aerial photographs of western Skeiðarársandur from the years 1986, 1997, and 2012, which were used to map changes in the extent of groundwater seeps. These data sets were used to investigate the impact of glacier retreat on proglacial groundwater levels and the extent of groundwater seeps over time (objective i).
- The proglacial flow regimes at the field sites are impacted by a wide array of processes which provide opportunities to investigate groundwater-surface water

exchange at various temporal and spatial scales, including episodic low frequency, high discharge events (floods and jökulhlaups) (objective iv).

- The importance of groundwater to the proglacial ecology. Relatively high abundance of flora and fauna has been observed around groundwater seeps and groundwater-fed streams and lakes, which suggests that these features provide important ecological niches in the otherwise barren proglacial environments. However, groundwater-fed hydrological systems are likely to be impacted by glacier retreat and changes in precipitation. Therefore, an enhanced understanding of proglacial groundwater-surface water exchange will help to increase the understanding with regards to the resilience of these systems to the projected adverse impacts of climate change.
- The proximity of the sites to Route no. 1 and the Skaftafell camp site eased accessibility and simplified the logistics of the project.

Section 3.2 briefly describes the hydrogeological and hydrological setting of Iceland. Sections 3.3 and 3.4 describe the field sites at western Skeiðarársandur and Skaftafellsjökull, respectively. Section 3.5 describes the design of the piezometers which were used for groundwater monitoring at the sites and monitoring procedures.

3.2. Icelandic hydrology and hydrogeology

Iceland is located along the North Atlantic mid-ocean ridge, which runs through the island in a SW to NE direction. The geology of Iceland is composed of volcanic rocks, of mainly basaltic composition (80-85%). The remaining 15-20% are composed of basaltic sediments and andesitic intrusions (Johannesson and Saemundsson, 1989; Óskarsdóttir *et al*., 2011). Due to crustal accretion, the age of rocks increases with distance from the volcanic rift zones, hence, Iceland's oldest geology is located in the East and West Fjords [Figure 3.1] (Oskarsson *et al*., 1982).

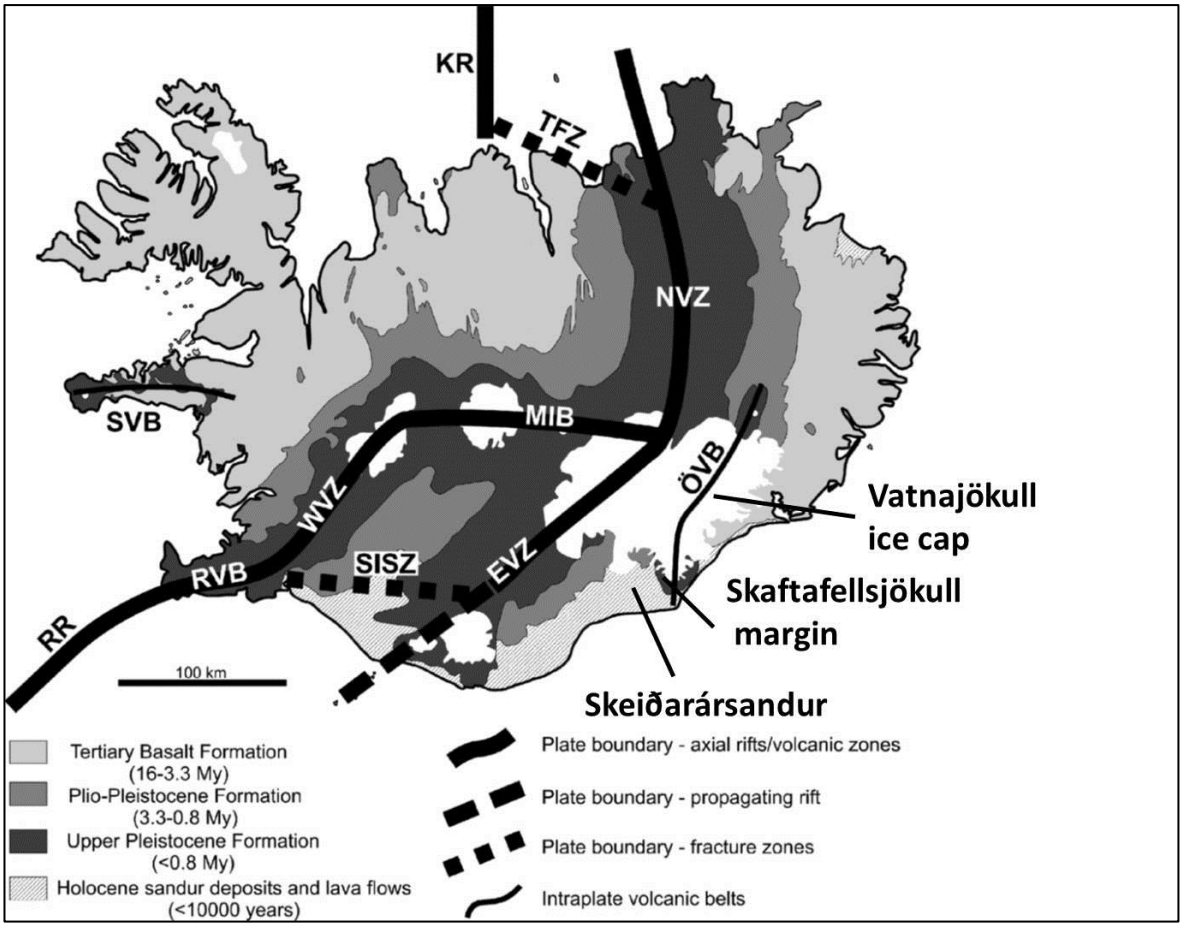

Figure 3.1. The principal components of the geology of Iceland, including the main fault structures, volcanic zones, and field sites.

The abbreviations are as follows: RR-Reykjanes Ridge; RVB-Reykjanes Volcanic Belt; SISZ-South Iceland Seismic Zone; WVZ-West Volcanic Zone; MIB-Mid-Iceland Belt; EVZ-East Volcanic Zone; NVZ-North Volcanic Zone; TFZ-Tjörnes Fracture Zone; KR-Kolbeinsey Ridge; ÖVB, Öræfi Volcanic Belt; SVB, Snæfellsnes Volcanic Belt. Adapted from Thordarson and Larsen (2007).

Icelandic hydrology and hydrogeology are strongly influenced by the interaction between volcanism, glaciers, seasonal snow cover and groundwater (Sigurðsson, 1990; 1993; Björnsson and Pálsson, 2008; Óskarsdóttir *et al*., 2011). Geology forms an important control on Icelandic hydrology and hydrogeology, with surface runoff dominating the Tertiary and Quaternary formations. Conversely, the fissure swarms and lava fields found in the younger volcanic zones have high permeability and hydraulic conductivity, which enhances infiltration and the formation of springs and spring-fed streams. Therefore, surface runoff is less dominant in these regions (e.g. Hjartarson, 1994; Gíslason *et al*.,

1996; Sigurðsson and Einarsson, 1988; Sigurðsson 1990; 1993; Jónsdóttir, 2008 Einarsson and Jónsson, 2010a, b). Additionally, substantial aquifers can also be found within proglacial outwash plains (sandurs) whose thickness can reach several hundred metres (Bahr, 1997; Robinson *et al*., 2008).

Glaciers and seasonal snow cover, which store and delay runoff on various temporal scales, also exert important controls on Icelandic hydrology and hydrogeology (e.g. Björnsson and Pálsson, 2008; Crochet, 2013). Icelandic glaciers store the equivalent of 15-20 years of mean annual precipitation (Jóhannesson *et al*., 2006). Icelandic rivers are usually divided according to their source: precipitation (snow and rainfall), glacial rivers, and groundwater-fed rivers (e.g. Kjartansson, 1945; Óskarsdóttir *et al*., 2011). Although precipitation contributes the highest proportion to runoff, glacial and groundwater-fed rivers also contribute substantial amounts (e.g. Jónsdóttir, 2008; Robinson *et al*., 2009a, b; Einarsson and Jónsson, 2010a, b). Glacial runoff usually has higher Suspended Sediment Concentration (SSC) and lower Total Dissolved Solutes (TDS) than non-glacial rivers (Anderson *et al*., 2000; Wimpenny, 2010). However, the SSC in glacial-fed rivers is related to discharge, and highest during summer and early autumn. Spring-fed rivers in Iceland have low variability in temperature, discharge, and chemical content, and low SSC (Sigurðsson and Einarsson, 1988; Sigurðsson, 1990; Gíslason, 2008). The mean runoff for Iceland is approximately 1500-1600 mm/year (Tómasson 1981, 1982; Jónsdóttir, 2008). Simulations suggest an increase of 25% in runoff, due to climate change and enhanced glacial melt, between 2071 and 2100 (Jónsdóttir, 2008).

Glaciers cover around 11% of Iceland's land surface, and receive about 20% of its precipitation (Jóhannesson *et al*., 2006; Björnsson and Pálsson, 2008). Icelandic glaciers are temperate, hence, they are dynamic and actively respond to changes in climatic conditions. Despite several exceptions, Icelandic glaciers have generally been retreating since the 1890s, with ice surface elevation within the ablation zone dropping by dozens of metres. Some glacier margins are retreating at nearly 100 m/year (Björnsson and

Pálsson, 2008; Bradwell *et al*., 2013; IGS 2013). The modelled changes in snowmelt and glacier mass balance project substantial changes in the magnitude and timing of glacial runoff. These changes impose significant challenges, particularly to the hydroelectric power industry (e.g. Thorsteinsson and Björnsson, 2011). Changes in runoff are also projected to impact river and coastal sedimentation, ocean salinity, and currents (Einarsson and Jónsdóttir, 2008). Glacier retreat is also projected to cause substantial shifts in drainage routes (Flowers *et al*., 2003; 2005) and to enhance the formation of ice contact lakes, with repercussions to proglacial hydrology (Schomacker, 2010; Marren and Toomath, 2013).

Iceland is located in a climatically important region within the North Atlantic, at the interface between the mid-latitude and polar atmospheric circulation cells and ocean currents. Its location between warm and cold ocean currents also increases its sensitivity to changes in oceanic circulation (Flowers *et al*., 2005; Björnsson and Pálsson, 2008). Most climate change projections for Iceland suggest that over the 21st century temperatures will increase at around 0.2-0.3°C/decade, with higher increases during winter. Precipitation is also projected to increase around 0.5-1.8 % per decade (Nawri and Björnsson, 2010).

Modelling the impact of climate change on the Icelandic ice caps project glacier retreat and changes in meltwater runoff. The loss of glacier volume is projected to increase runoff from the icecaps until around 2060, when runoff will begin to decrease (Guðmundsson *et al*., 2009). Jóhannesson *et al*. (2006) modelled projected changes in temperature and precipitation on the mass balance and runoff of Langjökull, Hofsjökull and southern Vatnajökull. Their results suggest that the glaciers with the largest mass balance turnover and longest ablation season had the highest static sensitivity (change in mass balance due to a rise of 1°C). Such changes, along with diurnal and seasonal alterations in meltwater generation (de Woul *et al*., 2006), are projected to significantly impact water resources in Iceland (Jóhannesson *et al*., 2006). Climate change models for Langjökull

and Hofsjökull also project substantial changes in the ice caps' extent within 100-200 years (Guðmundsson *et al*., 2009). Hofsjökull is approximately 300 m higher, with its ice thickness exceeding that of Langjökull by approximately 100-200 m. These differences substantially impact the ice caps' response to warming, as Langjökull is projected to disappear within approximately 145 years. Conversely, the highest peaks of Hofsjökull are projected to remain ice-covered after 200 years (Guðmundsson *et al*., 2009).

The field sites for this study are located in the proglacial zones of Skeiðarárjökull and Skaftafellsjökull, which are outlet glaciers of the Vatnajökull ice cap, the largest icecap in Europe. The impacts of climate change on the Vatnajökull ice cap have also initiated various studies due to its extent and geometry, which control groundwater and surface water discharge, jökulhlaup generation, and ice divides (e.g. Flowers *et al*., 2003; 2005; Aðalgeirsdóttir *et al*., 2006). The majority of Vatnajökull's mass is stored in low elevations, which increases the sensitivity of its geometry to small changes in air temperature (Flowers *et al*., 2003). Vatnajökull's volume has decreased by about 300 km^3 (10%) since 1890, with major outlets retreating by 2 to 5 km (Björnsson and Pálsson, 2008; IGS, 2013). Climate warming is projected to significantly impact the hydrology of Vatnajökull and its surroundings. Following retreat, the southern outlets are projected to experience a substantial reduction in runoff (Flowers *et al.*, 2005). Models also project that changes in glacial extent will dramatically reduce discharge and shift drainage patterns. An extensive retreat of Skeiðarárjökull is also projected to disturb the frequency and routing of jökulhlaups (Flowers *et al.*, 2005). Glacier retreat is also projected to increase the influence of topography on river routing, diverting waters between basins. The reorganisation of drainage following glacier retreat can therefore isolate catchments in southern Vatnajökull from glacial runoff (Flowers *et al*., 2005).

Figure 3.2. Skeiðarársandur and southern Vatnajökull.

A. Location of the Vatnajökull ice cap in Iceland. The red box denotes the extent of image B. B. The outlet glaciers of Southern Vatnajökull. The field sites are outlined in black. Images are taken from Google Earth (2013).

3.3. Western Skeiðarársandur

Skeiðarársandur forms the proglacial outwash plain of Skeiðarárjökull (latitude 63°57' N, longitude 17°21' W), a retreating temperate piedmont glacier in SE Iceland that is a southern outlet glacier of the Vatnajökull ice cap (Figure 3.2). Skeiðarársandur is reputed to be the world's largest active sandur (~1,000 km^2) (Marren, 2002a). It extends across the ~23 km wide glacier margin of Skeiðarárjökull and ~20 km from the glacier margin to the Atlantic coast (Figure 3.3). Several active volcanic centres, including Grímsvötn, which last erupted in May 2011, are located beneath Vatnajökull (Figure 3.2) and are the source of periodic glacial outburst floods (jökulhlaups) which impact Skeiðarársandur. Skeiðarársandur is drained by three major meltwater rivers: The Skeiðará, Gígjukvísl and

Súla, located in the eastern, central and, western parts of Skeiðarársandur, respectively (Guðmundsson *et al*., 2002) (Figure 3.3). Substantial changes in sandur drainage occurred in 2009 when ongoing glacier retreat led to a rerouting of the majority of meltwater from the Skeiðará into the Gígjukvísl river system. Skeiðarársandur is also impacted by jökulhlaups in the Súla river system from Lake Grænalón, which is located to the north west of the sandur (Figure 3.2).

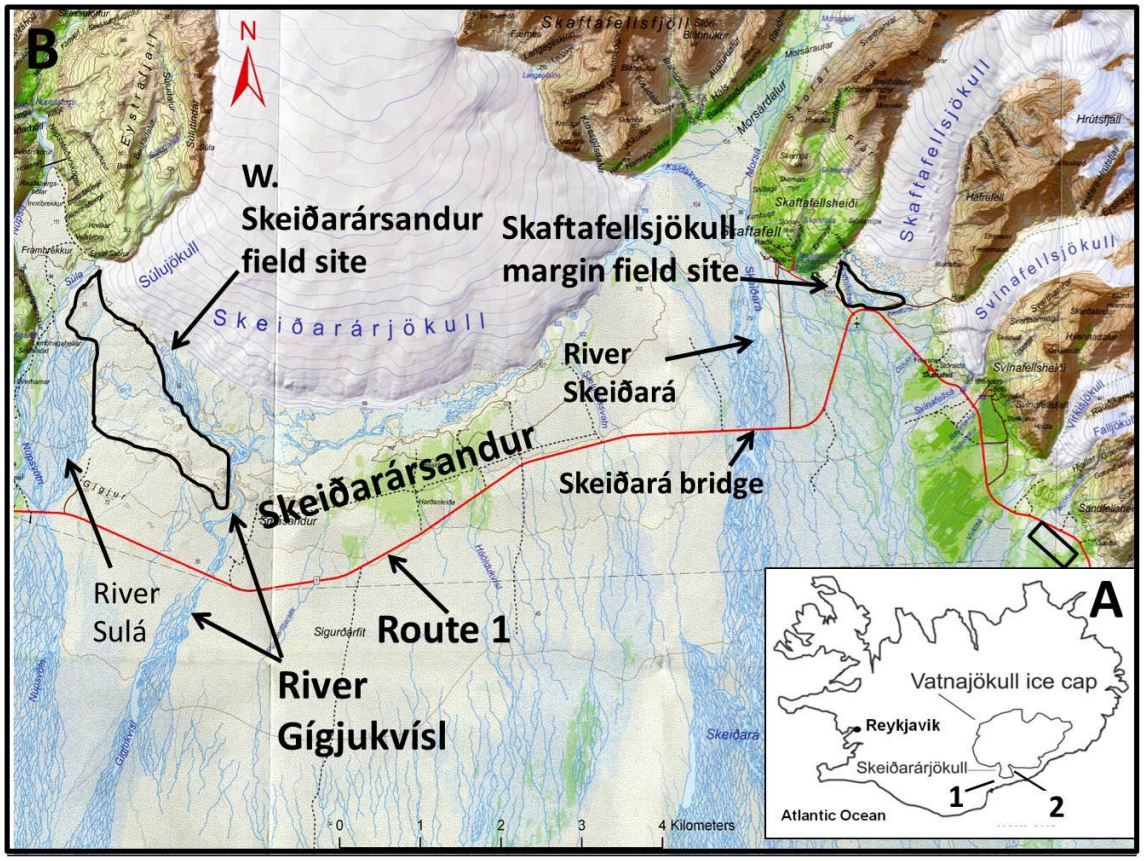

Figure 3.3. The field sites at Skeiðarársandur and the Skaftafellsjökull foreland.

A. Site location in Iceland showing the field sites at western Skeiðarársandur (1) and the Skaftafellsjökull foreland (2). B. General field site map (the map is from Skaftafell Sérkort 5 hiking map, 2009)

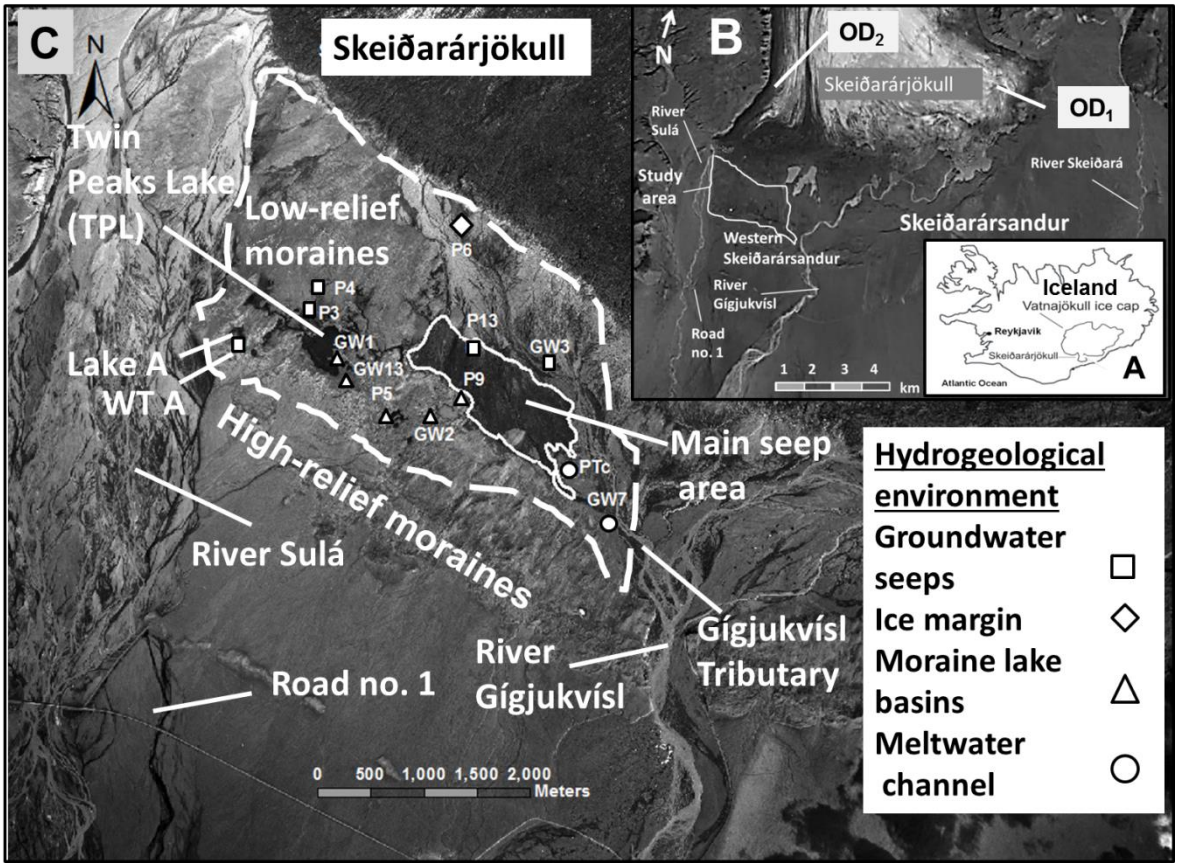

Figure 3.4. A view of the field site in western Skeiðarársandur.

A. Location map of Skeiðarárjökull in Iceland. B. The Skeiðarársandur outwash plain and the study area (denoted in solid white line) in western Skeiðarársandur (from Google Earth, 2013). OD1 and OD2 show the locations of overdeepenings in eastern/central and western Skeiðarárjökull, respectively. These locations are based on Björnsson *et al*. (1999). C. The field site in western Skeiðarársandur (the Icelandic Geodetic Service, Landmælinger Íslands [LMÍ], 1997). The study area is denoted by the dashed white line. Shallow piezometers are denoted in white with the different shapes denoting the different hydrogeological environments in which the piezometers were installed (see legend). The solid white line denotes the main area of groundwater seeps in 1997.

The Skeiðarárjökull geomorphic landsystem has been classified using the landsystem model of Evans and Twigg (2002) as a temperate, actively-receding glacier margin that also experiences periodic surge events. The main depositional domains are marginal moraines, incised and terraced glaciofluvial forms, and subglacial landforms (Robinson *et al.,* 2008). The geomorphology and hydrology of Skeiðarársandur are impacted by the interaction between high frequency, low magnitude processes (i.e. seasonal and annual accumulation and ablation) and low frequency, high magnitude events (i.e. glacial surges

and jökulhlaups) (Marren, 2005). The mean annual precipitation between 1978-2012 was 1712±218 mm (Figure 3.5, Table 3.1). The mean air temperature was 4.81± 0.64 °C (Icelandic Meteorological Office [IMO, 2013]). The mean annual and seasonal air temperature and precipitation in western Skeiðarársandur and Skaftafell are shown in Table 3.1.

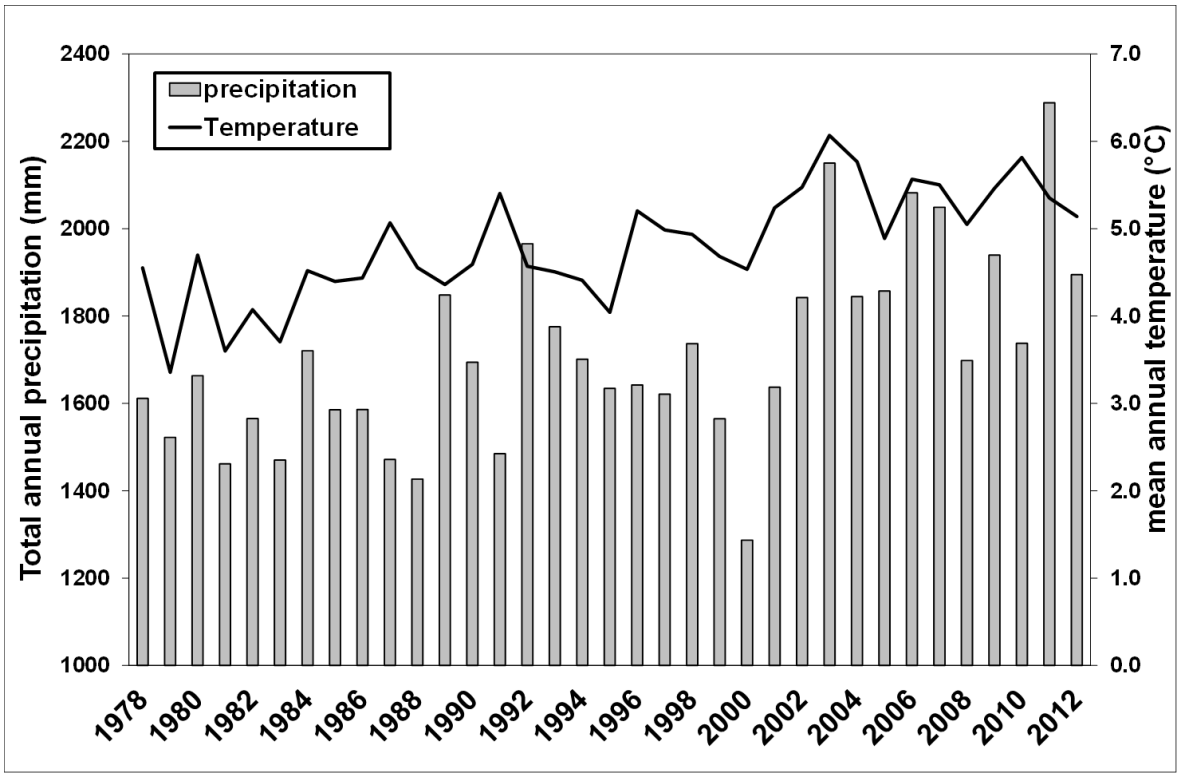

Figure 3.5. Total annual precipitation and mean annual air temperature for western Skeiðarársandur (1978-2012).

The data was obtained from the Kirkjubæjarklaustur meteorological station (IMO, 2013).

Table 3.1. Annual and seasonal mean air temperature and total precipitation at the Skeiðarársandur and Skaftafellsjökull field sites.

The data was obtained from the IMO meteorological stations in Kirkjubæjarklaustur (A) and Skaftafell (B) (IMO, 2013).

Mean Variable	Temperature (°C)	Precipitation (mm)
A. Western Skeiðarársandur		
Annual		
Winter (December-February)	0.08 ± 0.88	491 ± 125
Spring (March-May)	3.62 ± 1.06	360 ± 91
Summer (June-August)	10.78 ± 0.58	388 ± 91
Autumn (September-November)	4.82 ± 0.87	484 ± 146
B. Skaftafellsjökull foreland		
Annual	5.15 ± 0.38	1595 ± 302
Winter (December-February)	2.38 ± 0.11	497 ± 184
Spring (March-May)	4.36 ± 2.65	329 ± 132
Summer (June-August)	10.23 ± 0.58	313 ± 116
Autumn (September-November)	5.05 ± 3.07	470 ± 142

The margin of western Skeiðarárjökull has been retreating since the end of the 19th Century, the Little Ice Age (LIA) maxima in Iceland (Björnsson and Pálsson, 2008). Western Skeiðarárjökull has retreated a net distance of approximately 3.5 km beyond its position since monitoring began in 1932 (The Icelandic Glaciological Society [IGS], 2013). However, this distance excludes advances in the years 1946, 1965-6, 1973-5, and 1985-6 and the 1991 surge event (Figure 3.6). From 1978 to 2012, the glacier margin retreated ~2 km, at a mean rate of 30 m/year. However, this distance was offset by advances during the mid 1980s and the 1991 surge. Consequently, the net retreat of the glacial margin between 1978 and 2012 was approximately 1 km. Following the 1991 surge, western Skeiðarárjökull has retreated continuously. The distance of retreat between 1997 and

2012 was approximately 1.5 km. The mean annual rate of retreat during this period has increased by a threefold (from 31 m/a to 95 m/a). The rates of retreat which were measured in western Skeiðarárjökull are 2-4 times higher than those reported from smaller retreating outlet glaciers of southern Vatnajökull (Bradwell *et al*., 2013; IGS, 2013; Marren and Toomath, 2013).

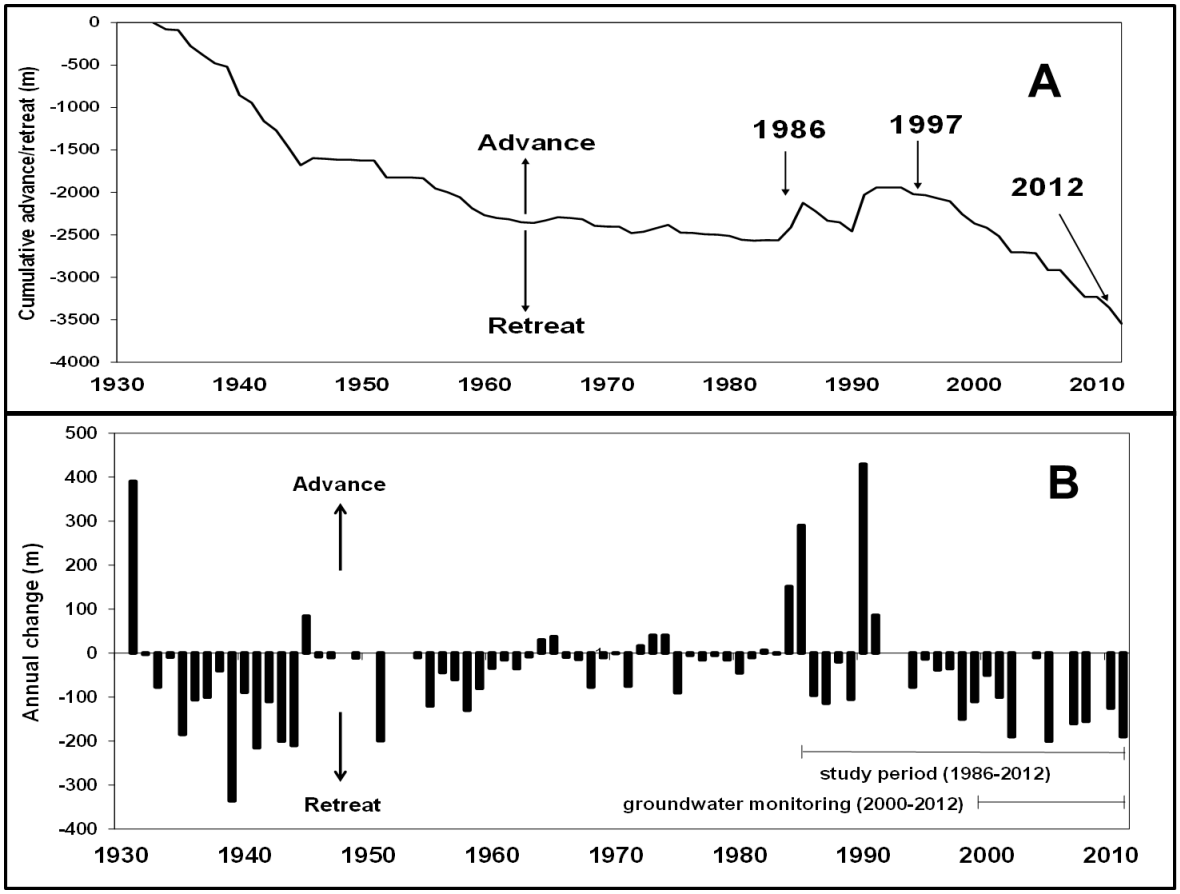

Figure 3.6. Fluctuations in the position of the glacier margin of western Skeiðarárjökull (1932-2012).

A. The cumulative retreat distance of western Skeiðarárjökull from 1932 to 2012 (IGS, 2013). The arrows show the years of the aerial images (Chapter 4). 2B. Annual changes in the position of the glacial margin of Western Skeiðarárjökull (1932-2012). The full length of the mapping of groundwater seeps (1986-2012) and the period of groundwater monitoring are marked. The data was obtained from the database of the IGS, 2013. The figure was taken from Levy *et al*. (2015).

Western Skeiðarársandur is also substantially impacted by glacial surges, which lead to significant advances of the glacier margin. These events are coupled with a shift of the

subglacial drainage from an efficient, channelized drainage system, into an inefficient, linked-cavity system (Kamb *et al.,* 1985; Björnsson, 1998). Such changes to the subglacial drainage system are likely to impact the spatial distribution and amount of water transmission into the glacier bed, which will impact subglacial groundwater recharge (Boulton *et al*., 2001a, b; Boulton and Zatsepin, 2006).

Skeiðarárjökull has experienced glacial surges in 1929 and 1991. During the 1991 surge, the western glacier margin advanced up to one km between September-November 1991, advancing at ~9.4 m/day. The surge increased the glacier surface area by ~10 km^2 (Pálsson *et al*., 1992; Waller *et al*., 2008). The extent of surging during the 1991 event varied across the Skeiðarárjökull margin, with a significant advance in the west (~1 km) and only minor advance in the east (Waller *et al*., 2008). This study focuses on the ice-marginal zone of the more dynamic western area of the glacier (Figure 3.4B). The geomorphic impacts of surges in western Skeiðarársandur include the formation of push moraines, deposition of outwash fans adjacent to the glacier, and changes in the routing of meltwater drainage (Russell *et al*., 2001; Van Dijk and Sigurðsson, 2002; Waller *et al*., 2008). Surges also impact proglacial hydrology and hydrogeology by steepening the ice surface slope and the hydraulic gradient (Wiśniewski *et al*., 1997; Russell *et al*., 2001; Robinson *et al*., 2008). The steeper hydraulic gradient is expected to increase groundwater flow (Haldorsen and Heim, 1999).

The geomorphology and hydrology of Skeiðarársandur are also substantially impacted by the interaction between Vatnajökull and its subglacial volcanoes, which include Grímsvötn and Gjalp. The subglacial Grímsvötn volcano is located about 40 kilometres to the north of Skeiðarársandur (Figure 3.2). It is Iceland's most active volcano in historic times, with an eruption frequency of 7 eruptions/100 years (Óladóttir *et al*., 2011). Recent eruptions of Grímsvötn took place in 1996, 1998, 2004 and May 2011 (Jude-Eton *et al*., 2012). The activity of the Vatnajökull's subglacial volcanoes substantially impacts Skeiðarársandur

through the generation of subglacial jökulhlaups (e.g. Russell *et al*., 2006) and, to a lesser extent, ash fall.

The main impact of glacier-volcanic interaction is the generation of jökulhlaups, which originate from glacio-volcanic interactions with the subglacial volcanic centres beneath Vatnajökull. In addition to the small jökulhlaups which occur regularly, substantial jökulhlaups with peak discharges between 25,000-53,000 m^3/sec took place in 1934, 1938, and November 1996 (Guðmundsson *et al.,* 1995; Magilligan *et al*., 2002). Major jökulhlaup events are associated with substantial hydrogeological and geomorphic impacts. These include rearrangement of the subglacial and proglacial drainage, the likely pressurisation of the groundwater system, and extensive sediment erosion and deposition. The latter processes can change the depth to the water table, which also alters the response of groundwater to precipitation. Jökulhlaup deposition and erosion also alters the distribution and extent of aquifer properties, which will also impact groundwater flow. The highest and most variable values of hydraulic conductivity in Skeiðarársandur were measured in the shallow subsurface zones that were inundated by the November 1996 jökulhlaup (Robinson *et al*., 2008). This event also resulted in an extensive formation of kettle holes, which originate from the melting of grounded ice blocks that were carried during jökulhlaups (Fay, 2002). Groundwater-filled kettle holes can provide important, yet transient, ecological niches (Robinson *et al*., 2009a).

The hydrogeology of Skeiðarársandur is significantly impacted by the wide variability of geomorphic processes (glacial, glaciofluvial, volcanic, and aeolian) which occur on Skeiðarársandur and leads to significant heterogeneity in hydrogeological parameters (Robinson *et al.,* 2008). The sandur stratigraphy forms an extensive unconfined aquifer where thickness varies from 80-100 m near the glacier margin to ~250 m near the coast (Guðmundsson *et al*., 2002). The main sources of groundwater recharge are local precipitation and glacial melt, which originates from several different sources including basal melt; subglacially-routed, supraglacial, and englacial melt; and the melting of buried

stagnant ice. Stable isotopes (δD and $\delta^{18}O$) have shown that the influence of glacial melt on groundwater decreases rapidly with distance from the margin (Robinson *et al*., 2009b). However, this pattern can be complicated due to hydrological exchange between groundwater and meltwater rivers. Skeiðarársandur is also locally underlain by buried ice (Everest and Bradwell, 2003), which can strongly impact groundwater recharge, dynamics and routing (Robinson *et al*., 2008).

The regional groundwater system generally flows from north to south. However, local, perched groundwater systems, which are imposed on the regional groundwater flow system (Tóth, 1963), have also been identified. These perched groundwater systems were mainly found within moraine areas (Robinson *et al*., 2008). The groundwater table across most of the sandur is shallow, typically 2-3 m below ground level. The proximal sandur is generally dominated by groundwater recharge, while the distal sandur is dominated by groundwater discharge, with water table depths reducing to a few centimetres near the coast (Bahr, 1997; Robinson *et al*., 2008). The spring lines are generally parallel to the Skeiðarárjökull margin, which suggests that the position of the glacier margin, rather than the lateral rivers, controls their distribution. The calculated regional groundwater discharge is ~2.5 m^3/sec, with mean regional groundwater velocity of 0.15 m/day (Robinson *et al*., 2008). High sediment mobility, strong winds, and the lack of fertile soils create harsh ecological conditions in Skeiðarársandur (Marteinsdóttir *et al.,* 2013). Field observations report relatively high abundance of flora and fauna near groundwater-fed seeps, which possibly form important ecological microsites where growth conditions are more favourable (Figure 3.7).

Figure 3.7. The impact of groundwater seeps on proglacial ecology.

Relative abundance of vegetation around a groundwater seep in western Skeiðarársandur. The relative abundance suggests that these sites serve as important ecological niches. In addition to volcanic and glaciofluvial processes, aeolian activity (in the background) is also prevalent in this harsh proglacial landscape.

The field site in western Skeiðarársandur is located between the Súla and Gígjukvísl river systems (Figure 3.8) and is characterised by a range of contrasting landsystems. The western boundary of the study site is defined by an active braid plain of the River Súla. This river system drains subglacially from Lake Grænalón, an ice-dammed lake located alongside Skeiðarárjökull's extreme western margin, approximately 20 km north of the field site (Figure 3.2). As well as discharging glacial meltwater, this river system also includes non-glacial contributions from the surrounding valley sides. The northern limit of the study area is characterised by a distinct moraine ridge bordered by stagnant ice and hummocky moraine on its ice proximal side and fine-grained outwash fans on its distal side. This landform assemblage marks the limit of the 1991 surge event (Russell *et al.,*

2001). The southern limit of the area is associated with a broader zone of higher-relief moraines that comprises part of a larger moraine system that is a distinctive feature of this part of Skeiðarársandur. This high-relief moraine complex has similarly been related to an earlier surge event (Russell *et al.,* 2001). Whilst parts of this complex feature clear moraine ridges, other parts, including the area located immediately south of a lake basin referred to as Twin Peaks Lake (TPL), are characterised by relict meltwater channels and pitted outwash surfaces indicating the influence of former jökulhlaups. The proximal boundary of the high-relief moraines is characterised by a prominent ice-contact slope. Finally, the eastern border of the field site is marked by the meltwater channel of the Gígjukvísl tributary.

The Twin Peaks Lake area is a prominent feature of the western part of the study area, located at the foot of the ice-contact slope and is characterised by a series of enclosed depressions that feature prominent cracks with sharp edges that are suggestive of the presence and gradual melt-out of buried ice. The presence of ice on the proximal side of the high-relief moraines is consistent with the observation of buried ice in a large moraine section exposed on the western bank of the River Gígjukvísl (Everest and Bradwell, 2003). To the north of this area, the topography is characterised by a large area of low-relief moraines. The occurrence of small moraine ridges and possible crevasse-fill ridges suggest that this is a former subglacial surface (Waller *et al*., 2008).

The eastern part of the study area is characterised by a braid plain formed by a combination of supraglacial and subglacial drainage that resulted from advance during the 1991 surge. This braid plain was also active during the subsequent November 1996 outburst flood (e.g. Russell *et al.,* 2006). Progressive glacier recession and down wasting following the 1991 surge has resulted in a decrease in the extent of fluvial activity in this area. The distal part of this braid plain forms one of the lowest parts of the study area and is the main area of active seeps. An extensive monitoring network was emplaced in this area in 2000 and 2001 (Robinson *et al*., 2008). However, following glacier retreat,

groundwater levels have continued to fall below the intake of most piezometers. The monitoring infrastructure was therefore augmented in July 2011.

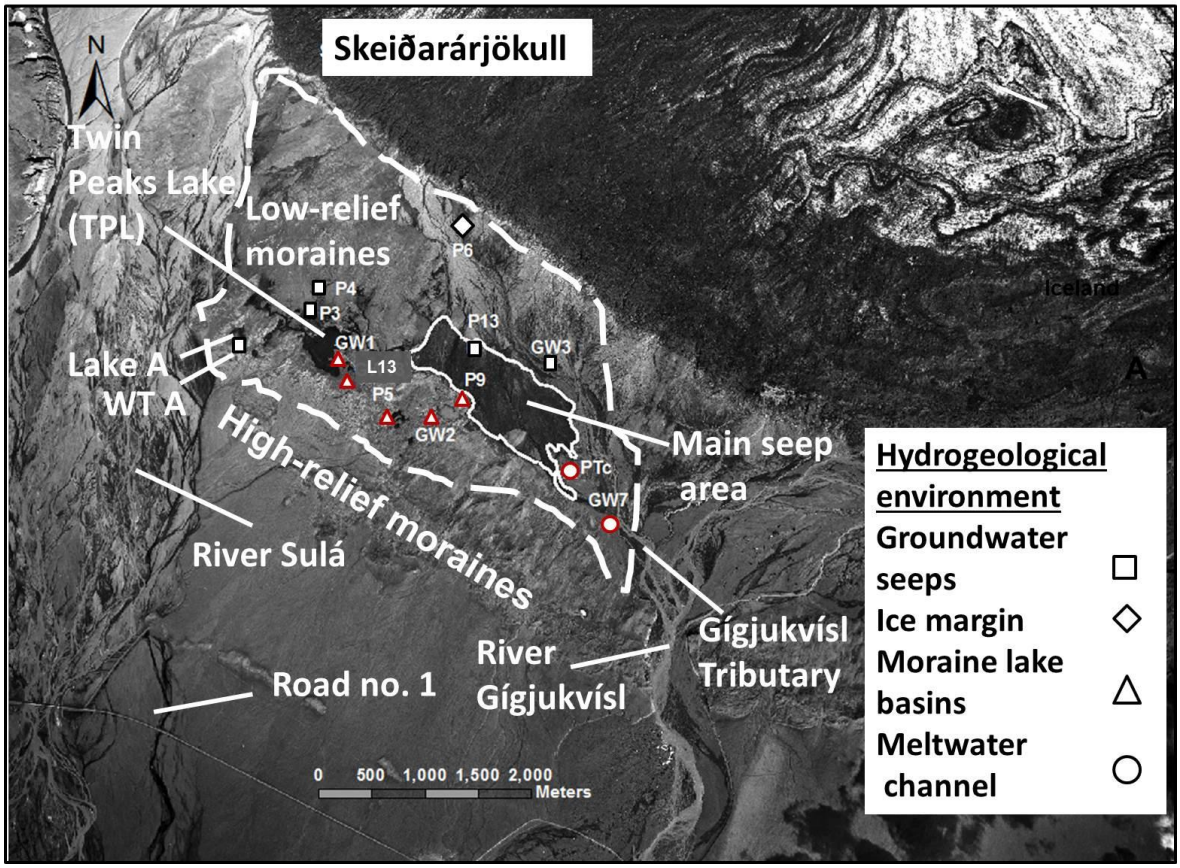

Figure 3.8. The field site in western Skeiðarársandur (the Icelandic Geodetic Service, Landmælinger Íslands [LMÍ], 1997).

The study area is denoted by the dashed white line. Shallow piezometers are denoted in white with the different shapes denoting the different hydrogeological environments in which the piezometers were installed (see legend). The solid white line denotes the main area of groundwater seeps. Piezometers which were installed in 2011 are outlined in red.

3.4. The Skaftafellsjökull foreland field site

Skaftafellsjökull (64°00'42.84''N, 16°54'20.77''W) is a temperate valley glacier, located in SE Iceland . The glacier sources most of its ice from the Vatnajökull ice cap, with a minor component in the east that originates from Öræfajökull (Figure 3.2) (Tweed *et al.*, 2005; Cook *et al.*, 2010). The glacier margin is approximately 120 m above sea level, and is part of the extensive low lying coastal plain sandur, which stretches from Skeiðarárjökull to

Öræfajökull. The Skaftafellsjökull glacier margin is approximately three km wide, and is drained by the meltwater river Skaftafellsá (Figure 3.9) (Marren, 2002b).

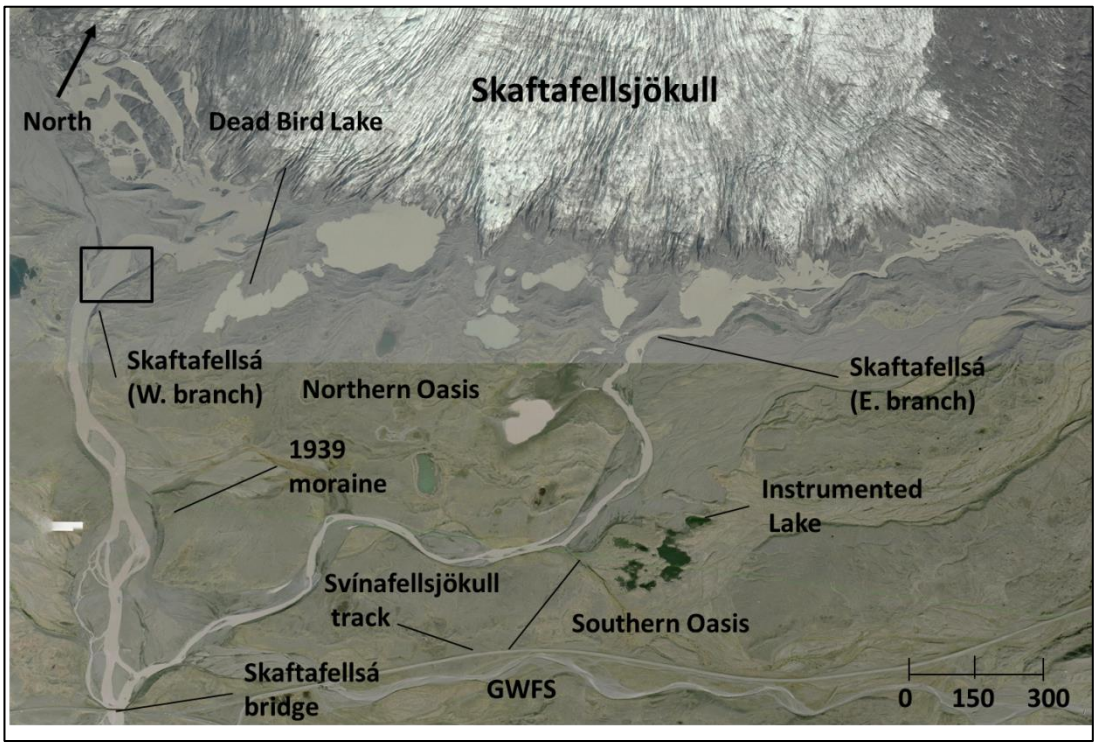

Figure 3.9. Study area of the Skaftafellsjökull foreland (Vatnajökull National Park, 2007).

The main changes between the photo and the study (2012) are the expansion of the ice contact lake at the Skaftafellsjökull foreland, the shrinking of Dead Bird Lake, and the diversion and drying out of the western branch of the Skaftafellsá. The black rectangle shows the approximate location for Figure 3.11.

Figure 3.10 shows the fluctuations in the position of the Skaftafellsjökull glacier margin, which has been monitored at the present site since 1942 (Thorarinsson 1943, 1956; Thompson 1988; Sigurðsson, 1998). The glacier reached its LIA maximum extent between 1870 and 1904. Up until 1935, Skaftafellsjökull and the adjacent glacier Svínafellsjökull (Figure 3.3) were joined, forming a single piedmont lobe (Thorarinsson, 1943). Skaftafellsjökull retreated steadily between 1904 and 1970. However, some advances took place in 1951-2, 1957 and 1968. The mean rate of retreat between 1942 and 1970 was 72 m/a. The glacier generally advanced between 1971 and 1988, with a total advance of 96 m. This placed the margin in similar position to its location during the mid 1960s. Following these advances, the glacier retreated 136 m between 1989 and 1995. This retreat was followed by an advance between 1996 and 1998 (Figure 3.10A).

The glacier has been retreating continuously since 1999, during which it has retreated approximately 600 m (Figure 3.10B) (Marren and Toomath, 2013; IGS, 2013).

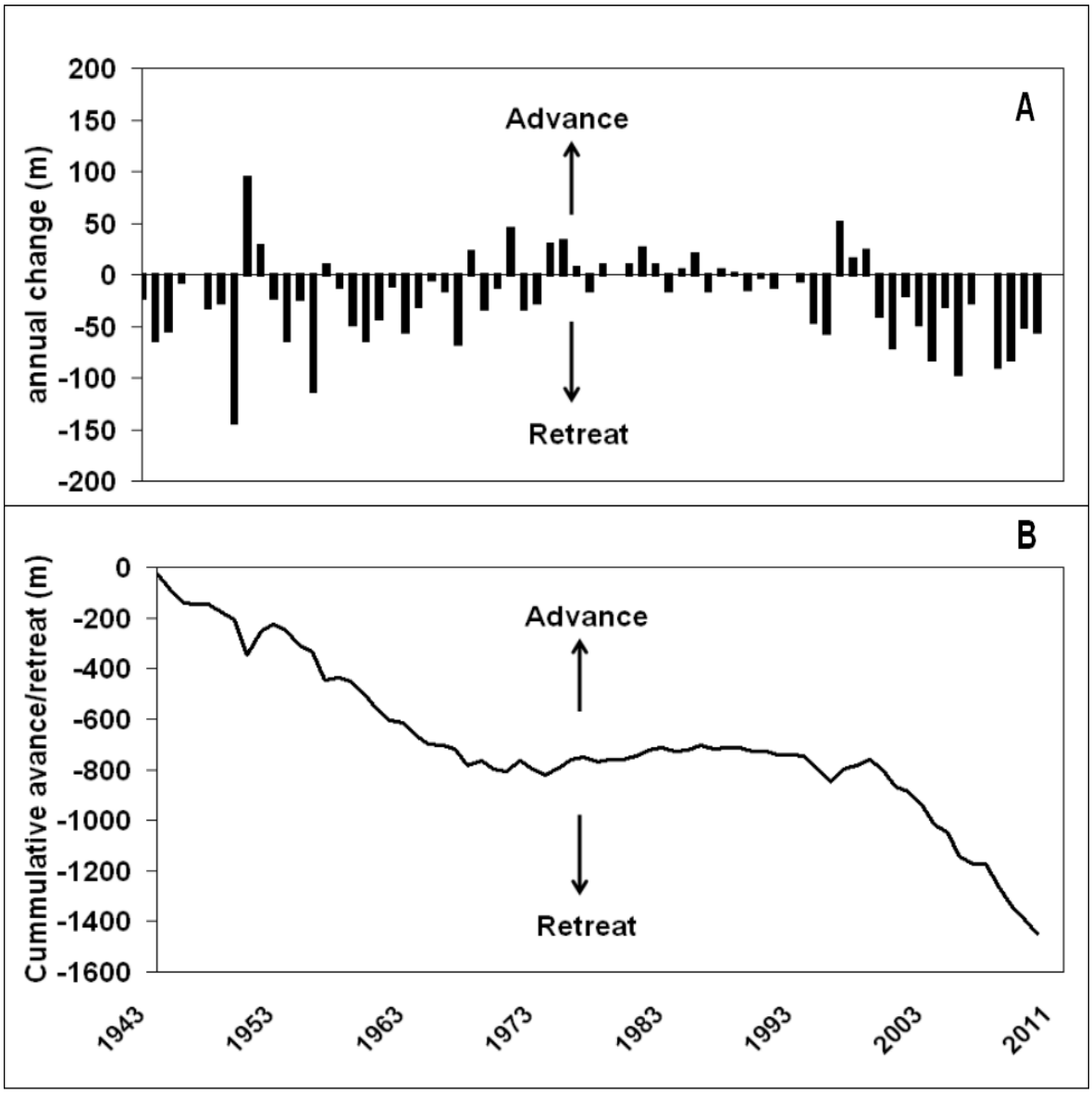

Figure 3.10. Fluctuations in the position of the Skaftafellsjökull foreland.

A. Annual glacier margin fluctuations for Skaftafellsjökull (1943-2012). B. Cumulative glacier margin fluctuations (1943-2012). Data was kindly donated by the Icelandic Glaciological Society.

The retreat of the glacier margin from the LIA maximum left a series of parallel moraine ridges, which are separated by a relict sandur (Thompson, 1988; Marren and Toomath, 2012). The moraines confine the two branches of the meltwater channel within the

proximal proglacial zone. The channels then merge behind a large moraine ridge, which dates back to 1939 (Figure 3.9). Past the moraine belt, the Skaftafellsá forms an unconfined sandur plain, which stretches to the coast (Thompson, 1988, Marren, 2002; Marren and Toomath, 2012). Similar to other outlet glaciers of Vatnajökull, an over-deepened basin has also been detected beneath Skaftafellsjökull (Tweed *et al*., 2005). The overdeepening significantly impacts sediment entrainment, the formation of ice by glaciohydraulic supercooling, and the expansion of the ice-contact lake (Tweed, 2005; Cook *et al.*, 2010; Cook and Swift, 2012).

Glacier retreat has substantially impacted the proglacial hydrology and geomorphology of the Skaftafellsjökull foreland (Marren and Toomath, 2013; 2014). The recent retreat of Skaftafellsjökull into the overdeepening has substantially increased the size of the ice-contact lake (Figure 3.11) (Schomacker, 2010; Marren and Toomath, 2013). This expansion intercepted the eastern meltwater outlet and made it topographically lower. This lowering diverted meltwater from the western outlet, which was abandoned in late 2010. The area between the two outlets contains several moraine lake basins (The Northern Oasis, Figure 3.9), which are underlain by fine-grained sediment. Field observations have shown substantial decreases in the extent of these lakes between July 2011 and August 2012 (Figure 3.11).

Figure 3.11. Aerial view of the Skaftafellsjökull glacier margin (August, 2012).

Note the expansion of the ice-contact lake and the desiccation of Dead Bird Lake. The relict meltwater channels of the Skaftafellsá can be seen in the foreground (Photo courtesy of Z. Robinson).

Annual and seasonal meteorological data for the site has been obtained from the IMO [Veðurstofa Íslands] (2013) station near the Skaftafell Visitor Centre, where available meteorological records date back to 1995 (Figure 3.12). The mean annual precipitation (1995-2012) was 1595 mm/year. The mean annual temperature was 5.15°C (IMO, 2013). The highest precipitation falls in winter and autumn. However, the seasonal distribution of precipitation is fairly even (

Table 3.1B) [IMO, 2013].

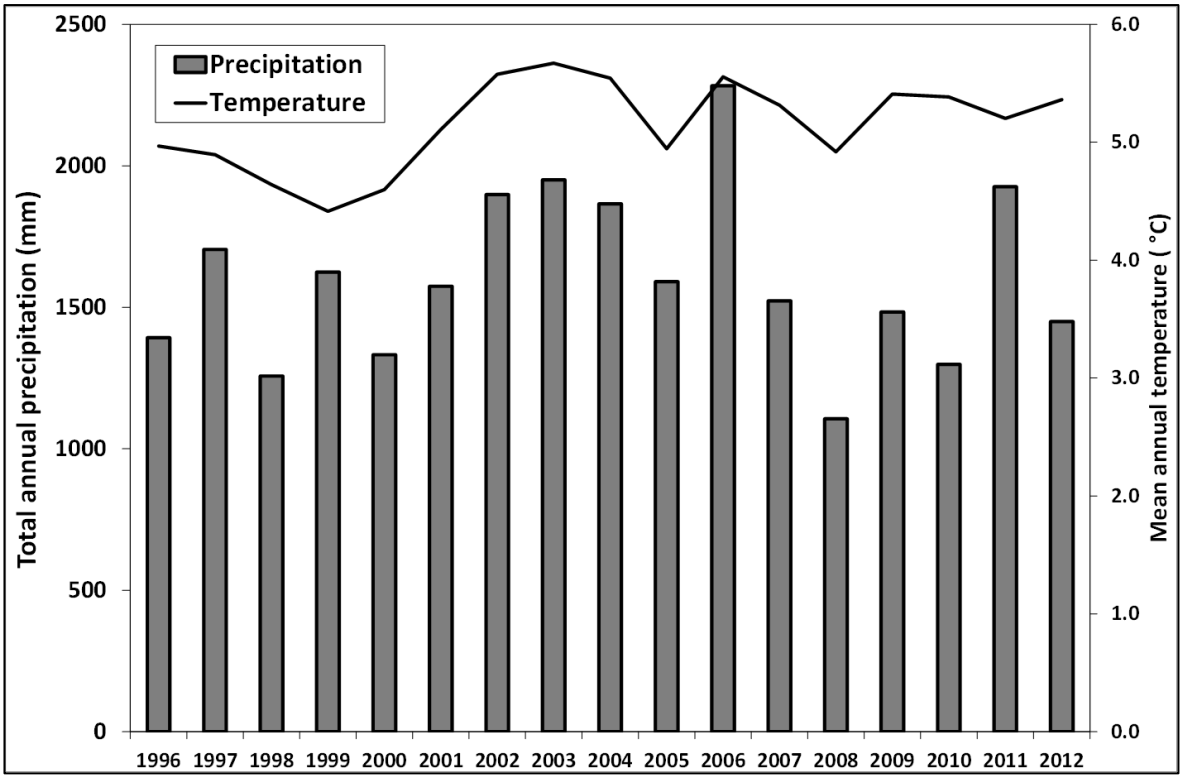

Figure 3.12. Total annual precipitation and mean annual temperature at the IMO Skaftafell meteorological station (IMO, 2013).

The geomorphology of the Skaftafellsjökull foreland reflects the combined influence of proglacial, subglacial, glaciofluvial and glaciolacustrine processes (e.g. Marren 2002b). The influence of subglacial and proglacial processes are predominant in the areas of higher topography and are responsible for the development of undulating surfaces and a prominent series of recessional moraines. Whilst they are only 1-2 m in elevation, the recessional moraines are laterally extensive and describe a saw-tooth pattern that illustrates both the ongoing recession of the glacier margin and its crevassed and lobate nature. These areas associated with subglacial and proglacial deposition are generally underlain by fine-grained tills that can reach a few metres in thickness. Glaciofluvial processes are represented by the formation of a series of braid plains composed of outwash sands and gravels. The braid plain adjacent to the Eastern branch of the Skaftafellsá (Figure 3.9) is the only one that is currently active and there are a series of higher elevation braid plains that have become inactive as a result of ongoing glacier

recession. These inactive braid plains often occur as distinct corridors of outwash (e.g. to the east of the “Instrumented Lake”), which illustrate the influence of proglacial topography on the routing of proglacial drainage. The active and inactive braid plains are also often separated by prominent terraces that reflect progressive incision and a lowering in the elevation of the key drainage routes over time. Finally, the proglacial area also features a series of lakes and lake basins. These are particularly prominent along the current ice margin as a result of the recession of the ice margin into a subglacial overdeepening (Marren and Toomath, 2013). In more distal areas, the foreland features lakes that are impacted by glacial meltwater, characterised by high suspended sediment loads, which appear light grey in the imagery. Conversely, lakes which appear darker (Figure 3.9) are fed primarily by groundwater and precipitation, hence the lower suspended sediment loads (e.g. Crossman *et al.*, 2012).

The main monitoring area at the Skaftafellsjökull foreland is located between the eastern meltwater channel of the Skaftafellsá and the Svínafellsjökull track (Figure 3.9). This area, termed “the Southern Oasis”, sits mainly within a relict braid plain extending from east to west that was originally fed by meltwater from the adjacent glacier Svínafellsjökull (Figure 3.3). The Southern Oasis contains several freshwater lakes and a groundwater-fed stream, which are significant to the local ecology, supporting birds, fish, and a wide range of invertebrates. A small moraine ridge, which runs from north to south, bounds the area from the west (Figure 3.13).

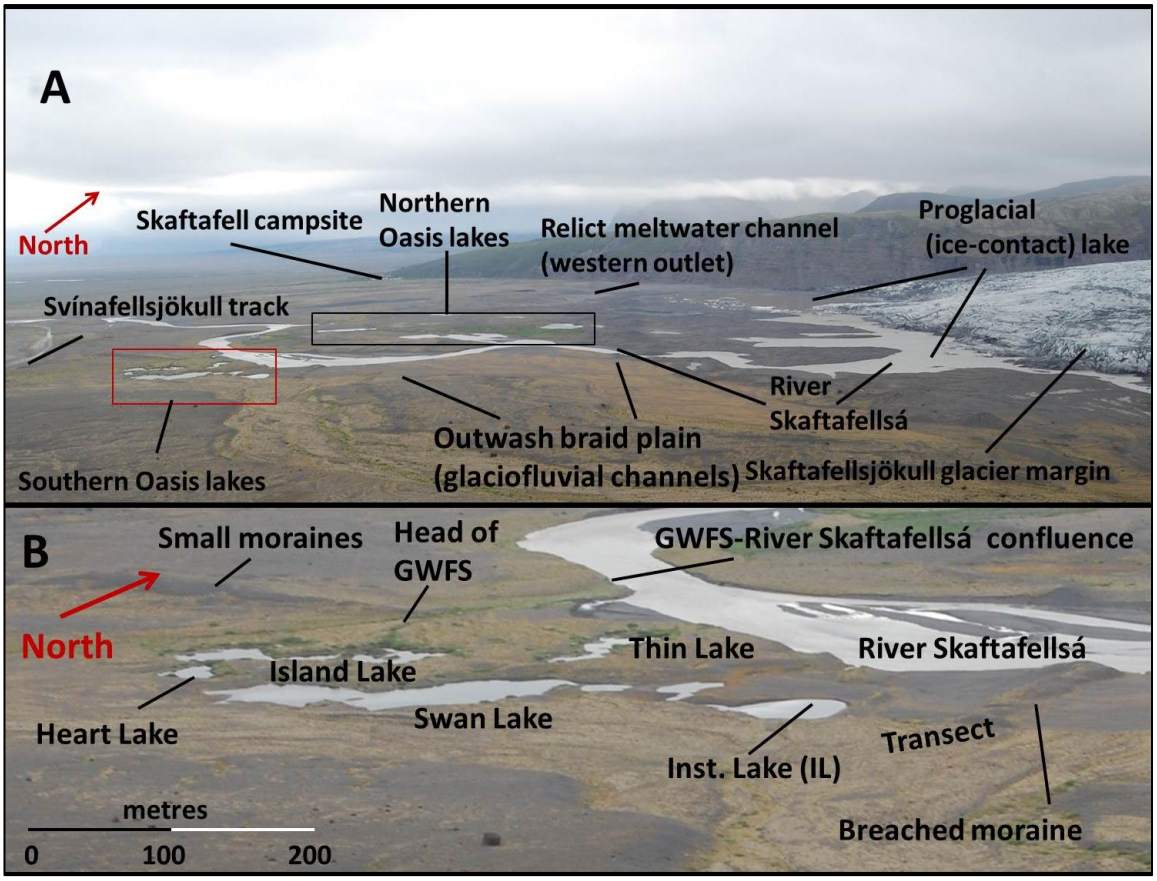

Figure 3.13. An oblique view of the Skaftafellsjökull foreland, July 2012.

A. The main features within the Skaftafellsjökull foreland study area (looking west). The Southern Oasis is denoted by the red box. The black box shows the approximate boundaries of the Northern Oasis. B. The main hydrological and geomorphic features of the Southern Oasis lakes field site. The transect (piezometers T1-T3) is located between the Skaftafellsá and Swan Lake, where pressure transducers monitored groundwater levels in order to investigate river-aquifer-lake exchange.

The meteorological conditions at the Skaftafellsjökull foreland were obtained from the IMO meteorological station, which is located approximately 5 km northwest of the fieldsite. The mean monthly precipitation and temperature are based on the measurements of the aforementioned station between 1995 and 2013 (Table 3.1, Figure 3.12). The mean hourly air temperature and total daily precipitation during the 2012 field season are presented in Figure 3.14. Rainfall was the only form of precipitation during the field season. The total amount of rainfall during the field season was 142 mm. The highest daily rainfall was 33.3 mm, which was recorded on the 23/07/2012. Apart from this event,

only three days within the season had rainfall in excess of 10 mm, (11/08, 21/08, and 24/08) (IMO, 2013). The mean air temperature during the field season was 11.17±3.75 °C. The maximum temperature was 22.40 °C, which was measured at 1300 hours on 08/07/2012. The minimum temperature was 0.90 °C, measured at 0700 hours on 30/08/2012 (IMO, 2013).

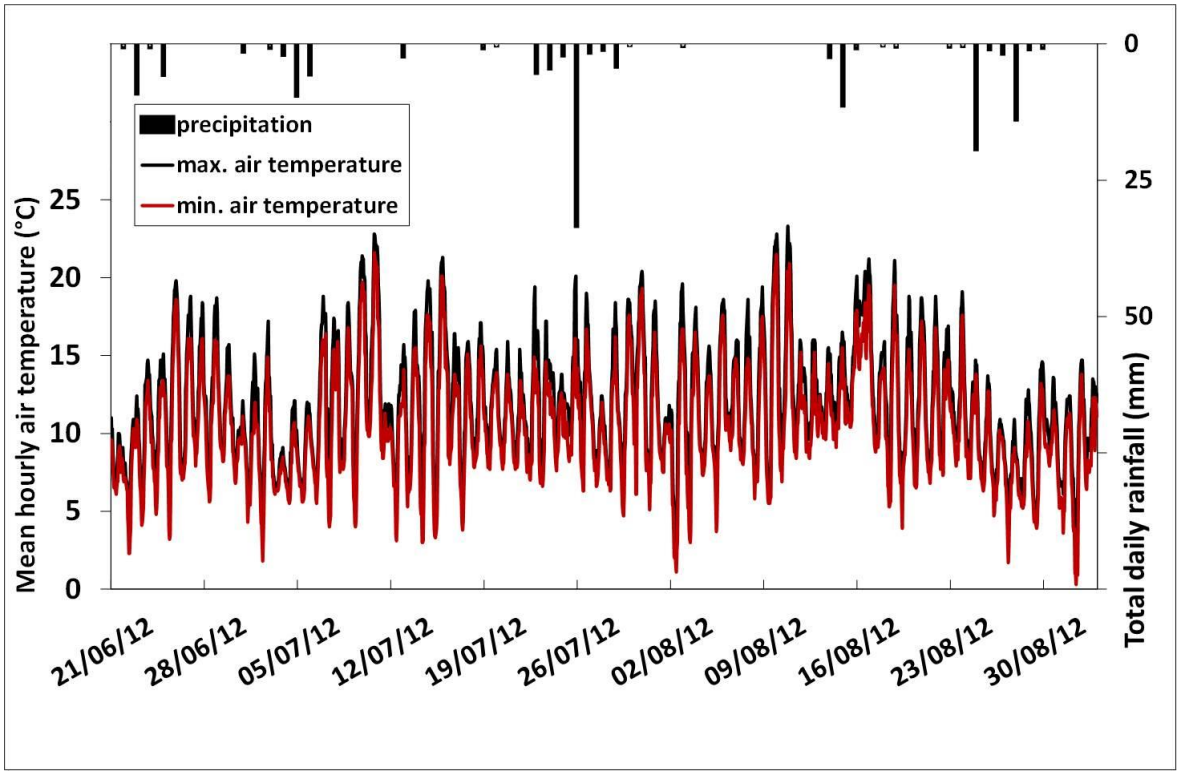

Figure 3.14. Meteorological conditions at the Skaftafellsjökull foreland during the 2012 field season (IMO, 2013).

The figure shows total daily rainfall and the minimum and maximum hourly air temperature at the Skaftafell IMO meteorological station.

The comparison between the total monthly precipitation during the years of the study (2011-2013) and the mean monthly precipitation at the IMO Skaftafell meteorological station (Figure 3.15) shows that the precipitation regime at the Skaftafellsjökull foreland is highly variable. During the autumn and winter of 2011-2012 (October 2011-March 2012), the total monthly precipitation in each month (except December 2011) exceeded the long term mean total monthly precipitation by approximately 120 mm. In contrast, the total

monthly precipitation between April-December 2012 was ~50-150 mm lower than the long term monthly mean (Figure 3.15). It is hypothesised that the low precipitation between April-June 2012 had a substantial impact on the decline in lake levels at the field site.

The precipitation regime in 2013 was very different to that of 2012. Precipitation substantially exceeded the long term monthly mean in January and February 2013, with unusually high precipitation levels measured in February 2013, when the total monthly mean was exceeded by 350 mm. The high precipitation in February included unusually large precipitation events of 70.2 (09-10/02/2013) and 307.5 mm (25-26/02/2013) [IMO, 2013], which led to substantial runoff and flooding (Ogmundsson 2013, personal communication). In contrast to these high rainfall events, precipitation in March-June 2013 was either substantially below (March, April) or only slightly above (May, June) the mean monthly precipitation (Figure 3.15).

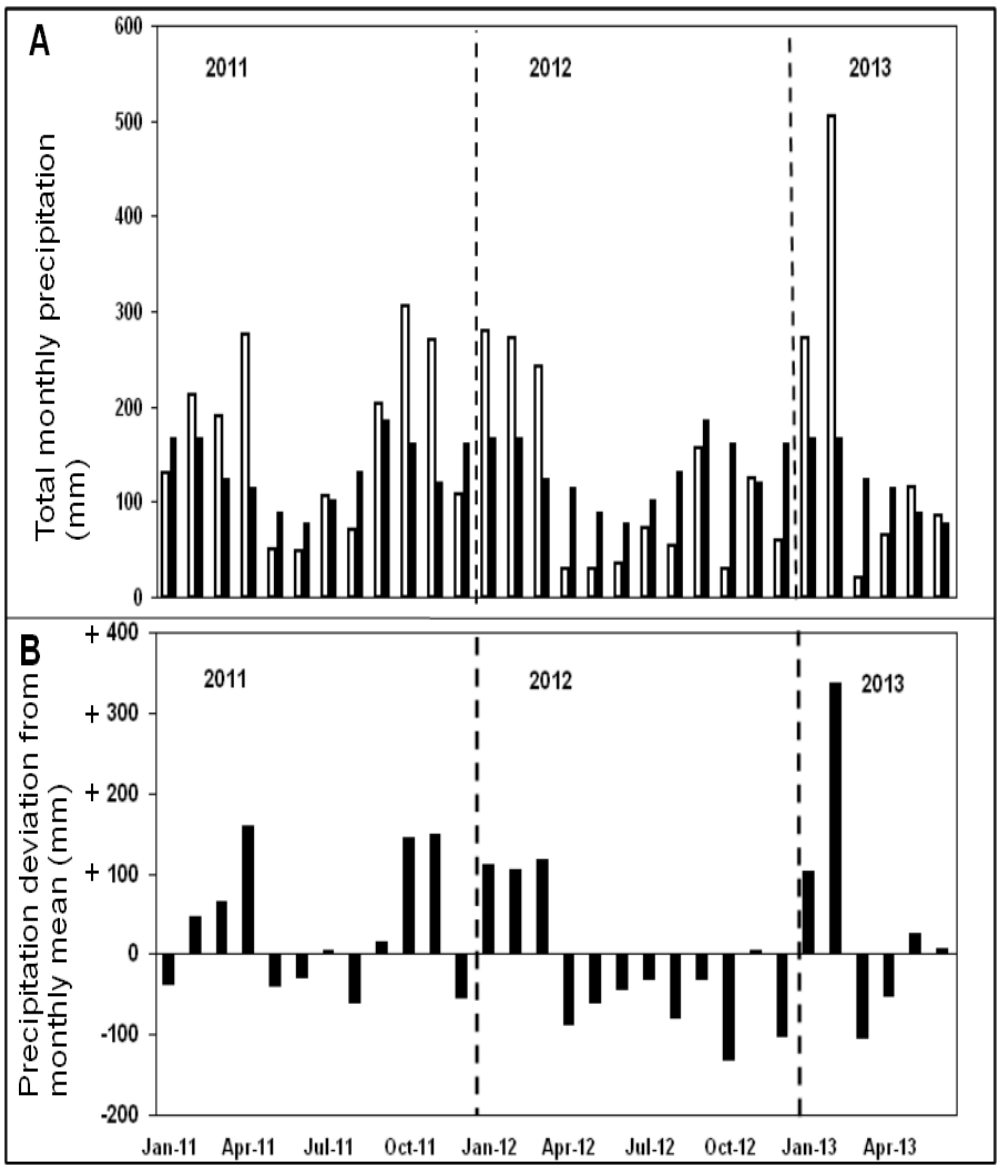

Figure 3.15. Comparison between total monthly precipitation in January 2011 to June 2013 and the mean monthly precipitation.

A. Mean monthly precipitation at Skaftafell (black bars) and the recorded monthly precipitation between January 2011 to June 2013 (white bars). B. Deviation of monthly precipitation between January 2011 and June 2013 from the mean monthly precipitation. The figure is based on data from the IMO (2013).

The comparison between mean monthly air temperature during the years of the study (2011-2013) and the mean monthly air temperature at the IMO Skaftafell metrological station (Figure 3.16) shows that the air temperature at the Skaftafellsjökull foreland is highly variable. Alongside the high precipitation rates during the winter of 2012,

temperatures were also ~2°C warmer than average during February and March 2012. In contrast, spring temperatures (April-June) in 2012 were slightly lower than the long-term monthly mean. The temperatures in July and August 2012 were ~ 1°C above the monthly mean. Similar to the winter of 2012, temperatures in January and February 2013 were also warmer than average, exceeding the mean monthly temperatures by ~2.5 and ~3°C respectively. In contrast to that, temperatures in March-May 2013 were between 0.5 and 2°C lower than average. Temperatures in June exceeded the monthly mean by ~ 0.3°C. Hence, the winter of 2013 was warmer and spring colder, than the mean temperatures (Figure 3.16).

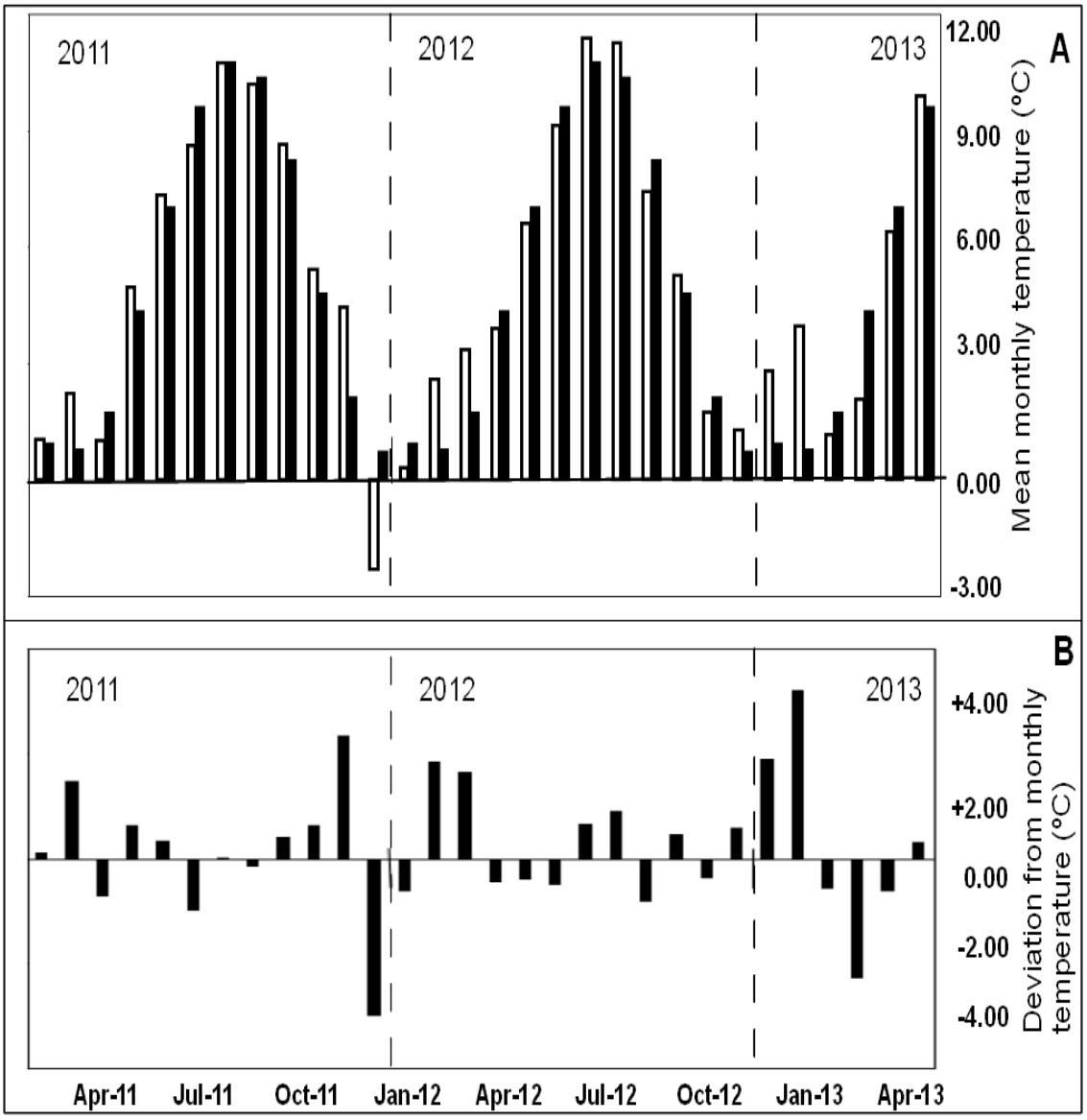

Figure 3.16. Comparison between measured monthly air temperature during the study and mean monthly air temperature.

A. **Mean monthly air temperature at Skaftafell (black bars) and the measured mean monthly mean air temperature between January 2011 to June 2013 (white bars). B. Deviation of monthly air temperature between January 2011 and June 2013 from the mean monthly precipitation. The figure is based on data from the IMO (2013).**

3.5. Monitoring of proglacial groundwater systems

3.5.1. Piezometer design and installation

Groundwater levels were monitored in this study in order to investigate the impact of fluctuations in the position of the glacier margin on proglacial groundwater levels (objective i) and for the investigation of proglacial river-aquifer and lake-aquifer exchange (objectives iv and v). The monitoring of proglacial groundwater in western Skeiðarársandur and the Skaftafellsjökull foreland were done using drive-point piezometers, whose design and installation were modified from Krause *et al*. (2011b). Two types of piezometers were installed (using their notation):

GW - 40 mm (28 mm inner) diameter plastic pipes. The full length of the piezometer was 2.00 m. The screen length is 0.60 m long, with the holes (0.08 cm diameter) drilled 0.10 m apart. The screened section was then covered in fine cloth mesh, in order to prevent sediment from entering the piezometer. In order to assist the driving of the piezometers into the ground and to prevent sediment entrance from the bottom, each piezometer was equipped with a sharp metal end, which was driven into the ground using a sledge hammer (Figure 3.17). These piezometers were used for sampling and automated measurements of groundwater levels (using pressure transducers) and for performing slug tests to measure hydraulic conductivity. Additionally, a stilling well, which was constructed in a similar manner to the GW piezometers (although the screen section was not covered with mesh) was installed in the Skaftafellsá to monitor river levels. Lake levels at the Instrumented Lake (IL) were measured manually every day using a stage board.

L_x (if located around the Instrumented Lake at the Skaftafellsjökull foreland). The full length of the piezometer is 2.00 m. The inner diameter is 12 mm. The screen length is approximately 0.40 m long, and consisted of 5-7 holes (0.08 cm diameter), which were 0.07 m apart. These piezometers were used for sampling and manual measurements of

groundwater levels. The bottom of these piezometers was sealed with a wall plug and a washer, which was also used to drive the piezometer into the ground. In some instances a pit, into which the piezometers were inserted, was dug prior to the driving of the piezometer into the ground. The 12 mm piezometers were initially emplaced within a wider tube, which was then driven into the ground. When reaching the desired depth, the outer tube was pulled out, leaving the piezometer in the ground.

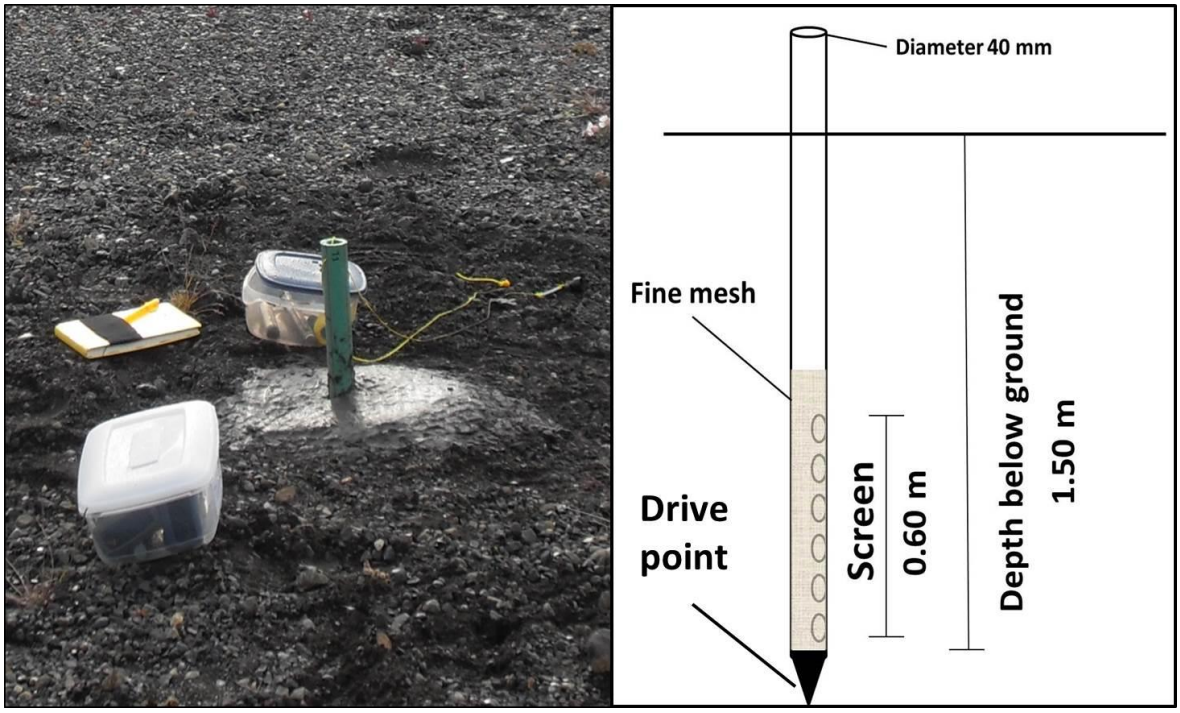

Figure 3.17. Shallow piezometers for the monitoring of proglacial groundwater.

A sketch of the 40 mm (GW) piezometers is shown on the right. The image on the left shows T2 piezometer, located between the Skaftafellsá meltwater channel and the Instrumented Lake.

The underlying substrate exerted an important control on the location of the piezometers, with difficulties in installing piezometers in substrates with high proportion of clay or boulders. For instance, it was intended to install piezometers near the Skaftafellsjökull margin. However, this plan was abandoned due to difficulties in inserting piezometers into the coarse substrate of the glaciofluvial channels in the relict sandur near the Skaftafellsjökull margin (Figure 3.9). The author is aware of the bias in the understanding

of site hydrogeology which was introduced due to the instalment of piezometers mainly in coarse-grained areas. However, despite these limitations, the drive point method still provided a simple, cost-effective, and efficient monitoring network. Once emplaced, the piezometers were left for several days in order to equilibrate with the aquifer (Brassington, 2007).

The instrumentation emplaced in the Skaftafellsjökull foreland in June 2012 covered a relatively small area (Figure 3.18). The infrastructure design was intended to investigate groundwater exchange with the meltwater river (objective iv) and the lakes (objective v). Groundwater-meltwater river exchange was investigated at the GW5, GW9; and T1-T3 piezometers. Groundwater exchange with lakes was investigated at the Instrumented Lake (IL) using piezometers L1-L8, which were emplaced around the lake perimeter. In addition to the piezometers around the IL, two piezometer nests were installed in the eastern (fine-grained) and western (coarse-grained) ends of the IL. These nests consisted of piezometers which were less than 1 metre apart, but were installed at different depths: 1.50, 1.00 and 0.50 m below the lake bed. The nests were used to measure the direction of vertical groundwater flow around the IL. In addition to the instrumentation around the IL, several piezometers (GW10-12) were also emplaced in the coarse outwash deposits, north of the IL (Figure 3.18) in order to provide an understanding of the regional groundwater flow direction at the Skaftafellsjökull foreland (Chapter 7). The configuration of groundwater flow and river-aquifer exchange at the Skaftafellsjökull foreland is described in Chapter 7. The investigation of aquifer-lake exchange is described in Chapter 8.

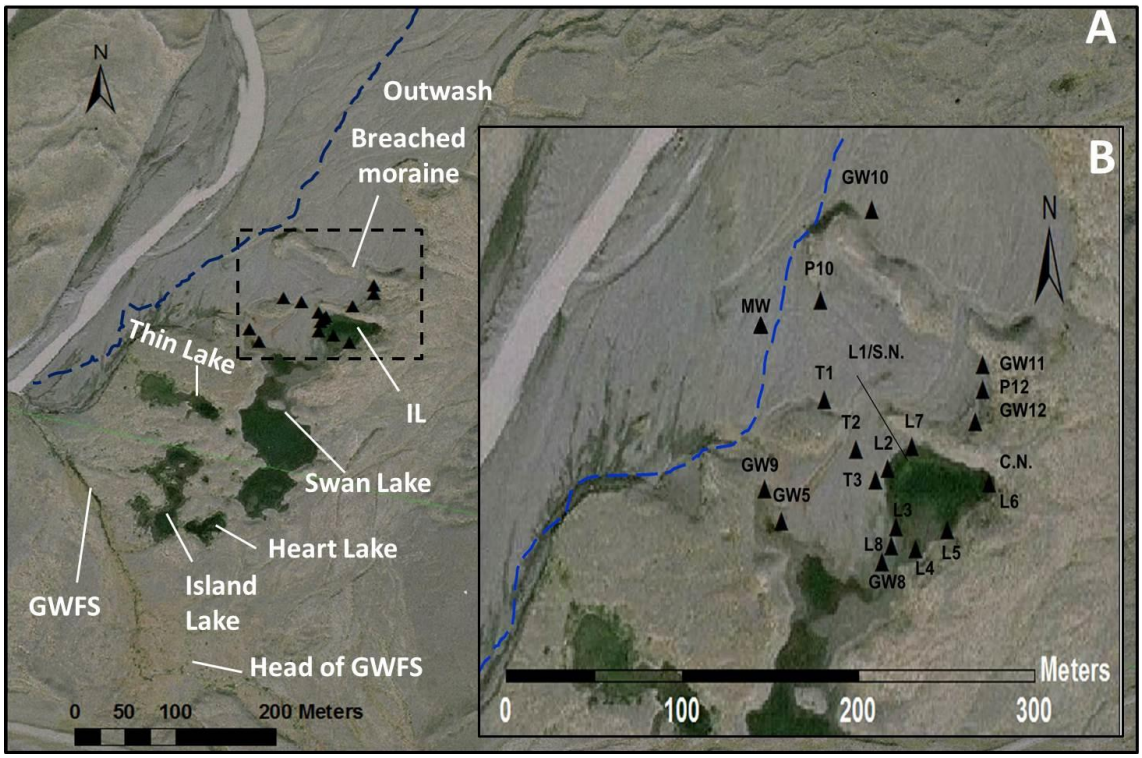

Figure 3.18. Instrumentation at the Skaftafellsjökull field site.

A. The main hydrological features of the Southern Oasis. B. The piezometers installed at the Southern Oasis. Note that the Skaftafellsá channel has migrated east since the date of the image (2007). The position of the river (meltwater) channel during the monitoring in June-August 2012 is marked by the dashed blue line. The figure also shows the location of the stilling well (MW) in the meltwater channel.

The majority of the monitoring infrastructure in the Skaftafellsjökull foreland was concentrated at the Instrumented Lake (the IL) (64°00'42.84''N, 16°54'20.77''W) (Figure 3.19). This lake is surrounded to the north, south and east by small moraines (~3 m high). The lake length is ~30 m and width is ~50 m. The circumference is ~150-160 m. Lakebed sedimentology varies substantially between the eastern and western lake shores. The eastern section of the lake is underlain by ~0.5 m of fine-grained deposits and boulders, with coarser substrate below that depth. Conversely, the western section is underlain by sands and gravels, which suggests glaciofluvial origin.

The investigation of aquifer-lake exchange at the IL (objective v) was executed using hydrogeological and temperature measurements. The hydrogeological measurements were obtained from the piezometers around the IL. The temperature measurements were obtained using Fibre Optic Distributed Temperature Sensing (FO-DTS) and three Vertical Temperature Profiles (Figure 3.19) (Chapter 8).

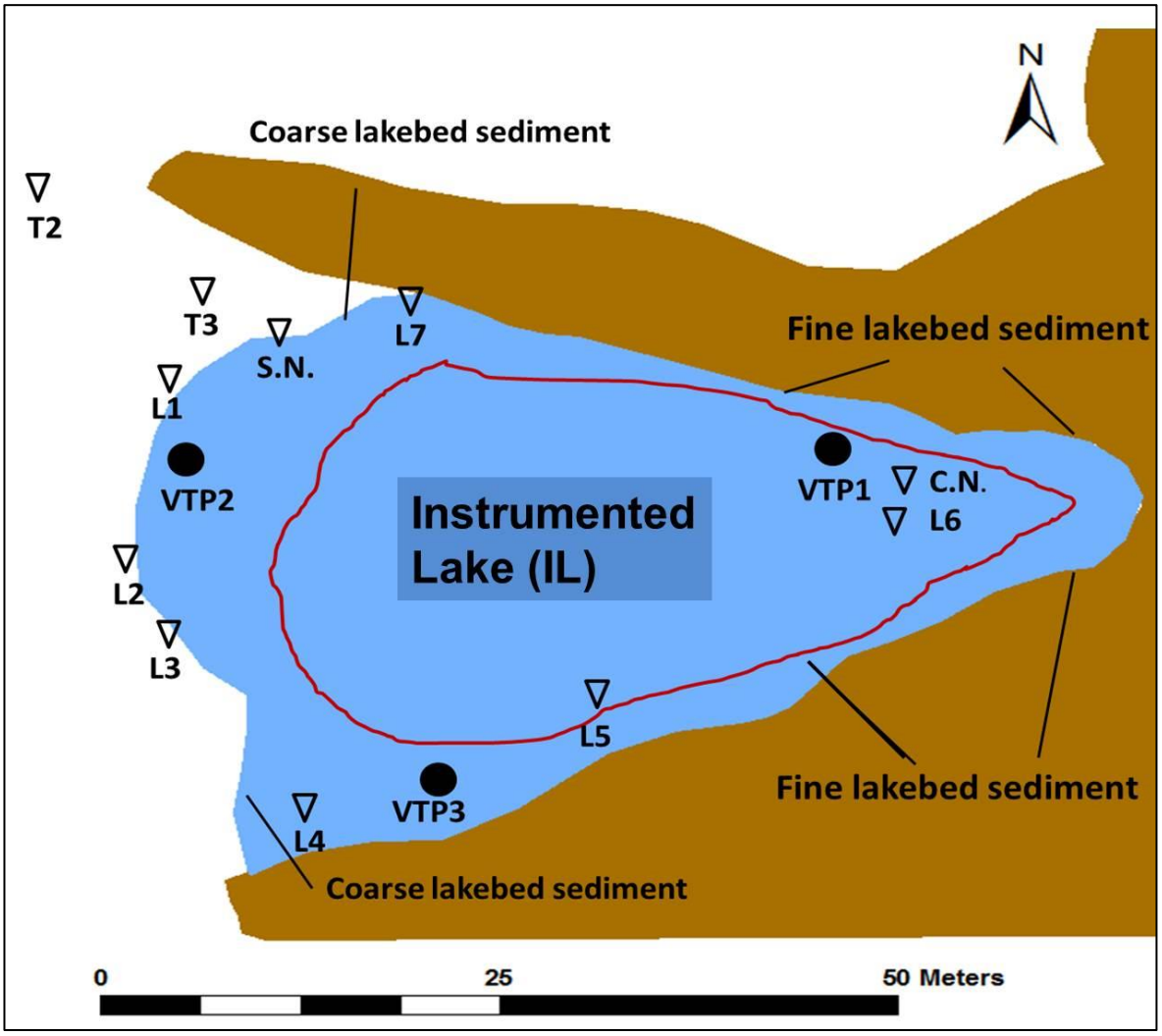

Figure 3.19. Instrumentation around the Instrumented Lake.

L1-L7 are 12 mm piezometers. The deployment of the FO-DTS cable is denoted in red. The locations of the Vertical Temperature Profiles are also shown. Moraines are shown in brown. The figure also illustrates the differences in lakebed sedimentology.

3.5.2. Topographic surveying of the piezometers

The piezometers in western Skeiðarársandur and the Skaftafellsjökull foreland were levelled to a single datum in August 2012, using a Leica Geosystems TCRP1205 Total Station (TS). It was used with a 360° prism. The accuracy is ±2-5mm (Leica user manual, 2004). In the Skaftafellsjökull foreland, the wells were levelled to an arbitrary datum (which was assigned to be 100 m), chosen by the line of sight to the maximum number of wells. When possible, the levelling was done to the top of the wells. In instances when this was not possible, the distance from the ground to the top of the well was measured, and then added in order to calculate the height of the well. When the wells were not visible from the datum, the TS was placed at an intermediate high point which enabled sight of the desired wells and levelled back to the datum. Similar procedures were followed during the topographic levelling of the wells at western Skeiðarársandur, although more intermediate points were required due to the size of the sandur. Back sightings were then taken to the former location of the TS. When setting up, maximum efforts were made to place the TS as close as possible to the location where the staff was previously. The differences between the back sights and fore sights were generally below 2 cm. The elevation of the piezometers are found in Appendix 1).

3.5.3. Monitoring of groundwater levels

Groundwater levels at the Skaftafellsjökull foreland were monitored both manually and automatically. Manual groundwater level monitoring was performed using a Solinst acoustic dip meter, which emits a sound when the sensor touches water. This then allows the measurement of the height of the pressure head (e.g. Brassington, 2007). In order to ensure accuracy and precision, measurements were taken by two people, until a

consensus within 0.5 cm was reached (Robinson *et al*., 2008). The monitoring of groundwater levels at the Skaftafellsjökull foreland was usually done twice a day.

Automated monitoring of groundwater levels, temperatures and EC at the Skaftafellsjökull foreland were performed using two types of Solinst automated pressure transducers: The Solinst model 3001 Level Temperature Conductivity (LTC) Levelogger Junior measures (accuracy in brackets) groundwater levels (0.1% Full Scale), temperature (±0.1°C), and Electrical Conductivity (2% or 20µS/cm). The Solinst Levelogger Junior Edge measures groundwater Level (0.1% FS) and Temperature (±0.1°C). Additionally, a Solinst model 3001 Barologger Edge was used to measure air pressure during the two field seasons. These measurements are needed to separate between actual changes in groundwater levels from those which reflect changes in air pressure (Brassington, 2007). The accuracy of the barologger is (±0.05 kPa). The Barologger was emplaced above the water table at GW12 (Figure 3.18).

The pressure transducers were emplaced at the transect, (T1-T3) and in a stilling well (MW) at the Skaftafellsá meltwater river (Figure 3.18) in order to investigate meltwater river-groundwater exchange. Groundwater levels, river levels; temperature and EC were recorded hourly between 20/06/2012 to the 31/08/2012, including during three weeks in which the field site was unmanned (31/07-23/08/2012). The data was measured hourly in order to be synchronised with the measurements from the IMO. The data was then compensated for fluctuations in atmospheric pressure using the Solinst Levelogger 4.0 software. Hydraulic heads were calculated by adding the pressure heads (obtained from the pressure transducers) and the elevation (section 3.3.2).

4. Long-term variability of proglacial groundwater-fed hydrological systems in Skeiðarársandur

4.1. Introduction

The aim of this chapter is to investigate the long term impacts of fluctuations in the position of the glacier margin on proglacial groundwater systems (objective i). The chapter maps long term changes (between 1986 to 2012) in the spatial extent of proglacial groundwater seeps and groundwater levels (monitored between 2000 and 2012) in western Skeiðarársandur, which is impacted by rapid glacial retreat, glacial surges, and jökulhlaups (section 3.3). In spite of the importance of proglacial groundwater systems and the likelihood that they will be impacted by climatically-driven changes, there is a severe lack of research into the potential impacts of climate change and glacier retreat on the extent and distribution of proglacial groundwater-fed hydrological systems. The specific objectives for this chapter are:

1. To map the spatial distribution and extent of groundwater seeps in western Skeiðarársandur during different time periods (1986, 1997, 2007).

2. To monitor long term (2000-2012) changes in groundwater levels in western Skeiðarársandur.

3. To determine the controls and drivers on the extent of proglacial groundwater seeps and levels.

4.2. Methods of monitoring long term changes in proglacial groundwater levels and the extent of groundwater seeps

The impact of long term changes in the position of the glacier margin on proglacial groundwater hydrological systems and groundwater levels (objective i) was investigated in western Skeiðarársandur (Figure 3.4). The changes in the extent of groundwater seeps in western Skeiðarársandur were mapped from historical aerial imagery (dating from 1986, 1997, and 2012) using ArcMap© 9.3.1. The photographs were georectified using Ground Control Points (GCP) as described by Bennett *et al*. (2010). Groundwater seeps and groundwater-fed streams were then mapped in the three images based on water colour and shading. Water colour, and hence black and white shading, is determined by the interaction between the upwelling light reflectance of suspended inorganic and organic compounds and the downwelling of solar irradiance. When black and white images are used, the high turbidity and reflectance of meltwater make them appear lighter than groundwater. When colour images are used, the high turbidity of meltwater streams makes them appear brown. Conversely, the low turbidity of groundwater-dominated bodies makes them appear green-brown (Jerome *et al*., 1994a, b). These differences were therefore used to map groundwater seeps and meltwater streams. The likelihood of the mapped areas in western Skeiðarársandur to be impacted by groundwater has been ground-truthed. A similar approach was previously used in the western USA to map changes in the extent of groundwater-fed fens following changes in snowmelt (Drexler *et al*., 2013).

Groundwater levels in western Skeiðarársandur were monitored since July 2000 by Robinson (2003) and Robinson *et al*. (2008). Their piezometers were emplaced in a transect which projected away from the glacier margin for ~1.5 km, around moraine lake basins, and in areas of groundwater seeps (Figure 3.8). However, following the

continuous retreat of the Skeiðarárjökull margin (Figure 3.6), groundwater levels at western Skeiðarársandur have declined substantially and fell below the intake of many piezometers. Therefore, new piezometers were installed in July 2011 in order to augment the network and continue the long term monitoring of proglacial groundwater levels in Skeiðarársandur. The new piezometers were emplaced near moraine lakes, near the remains of groundwater seeps, and near a small meltwater channel (Figure 3.8). The design of the piezometers installed in 2011 is similar to the piezometers which were installed at the Skaftafellsjökull margin (section 3.5.1). Groundwater levels in western Skeiðarársandur area were monitored using the same methods and device (Solinst dip meter) which were used at the Skaftafellsjökull foreland (section 3.5.3). The topographic levelling of the piezometers in western Skeiðarársandur was performed with the same instrument as the levelling in Skaftafellsjökull. However, in order to extend the existing records, the 2011 piezometers were tied into the 2000 datum using relative heights from a 2000 piezometer baseline ($P3_{1m}$, whose top is at the height of 82.78 m). The top of the pipe was used, as this height is less likely to change than the distance between the top of pipe and the ground following sediment erosion and deposition.

4.3. Temporal changes in the extent of groundwater seeps

4.3.1. 1986 aerial photograph

The extent of groundwater seeps and lakes in 1986 (the Icelandic Geodetic Survey (Landmælinger Íslands [LMÍ]), 1986) is shown in Figure 4.1. The glacier margin retreated a net distance of ~2.5 km between the start of monitoring in 1932 and the time of this image. Groundwater seeps in this image have the largest areal extent, ~ 2,767,200 m^2 of the three time slices (Table 4.1). The main area of groundwater seeps is bordered to the north and east by a large meltwater and groundwater-fed braided channel (“the Gígjukvísl

tributary"); to the west by an area of low-relief moraines and stagnant ice that is located to the north of Twin Peaks Lake (TPL); and to the south by the high-relief moraine belt. In 1986, groundwater seeps covered the entire area between the Gígjukvísl tributary and the eastern limit of the low-relief moraines. The main seeps area was connected to the seeps east of TPL by an active groundwater-fed channel. Additional areas of groundwater seeps existed east of the Gígjukvísl tributary and to the north of TPL and Lake A (Figure 4.1).

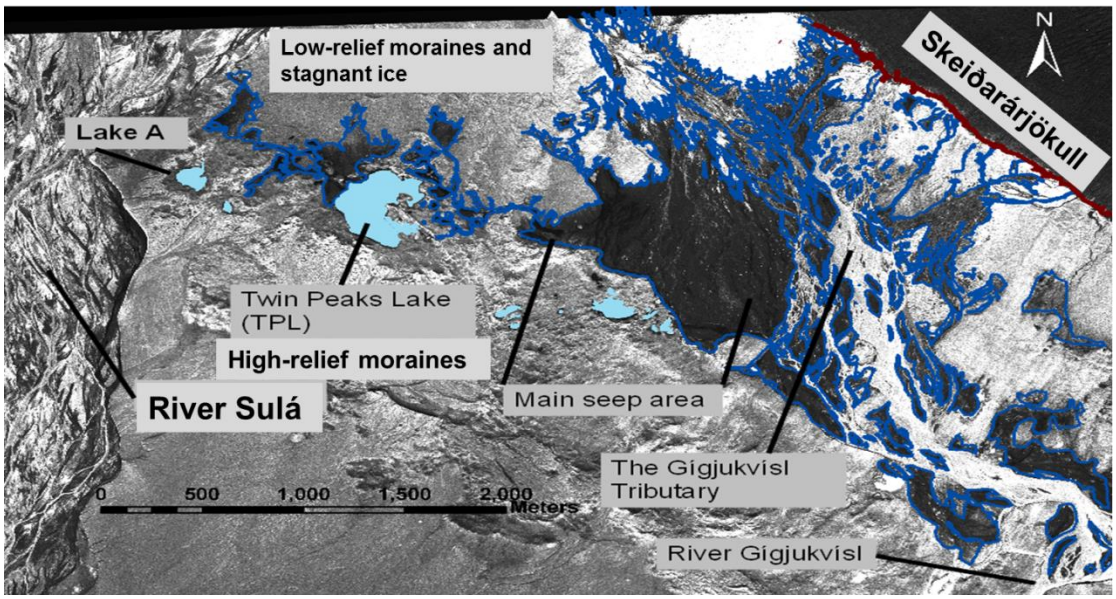

Figure 4.1. The extent of groundwater seeps in western Skeiðarársandur in 1986 (LMÍ, 1986).

Groundwater seeps are outlined in blue. Lakes are denoted in turquoise. The position of the glacier margin (red line) is only an approximation, due to the extensive amounts of buried ice in this area.

4.3.2. 1997 aerial photograph

The extent of groundwater seeps in 1997 and the impacts of the November 1996 jökulhlaup (LMÍ, 1997) are shown in Figure 4.2. Following the advances during the mid 1980s and the 1991 surge, the glacier margin has advanced by ~ 420 m relative to its position in 1978 (Figure 4.2). The area of groundwater seeps has declined by ~20% since 1978 (Table 4.1). The main declines took place around the main jökulhlaup route, near jökulhlaup outlets at the glacier margin, and to the north west of TPL. Approximately

430,000 m^2 (~18%) of the groundwater seeps that were mapped in 1978 were buried by jökulhlaup deposits. Following the jökulhlaup, the main seep area has shrunk and moved southwards, away from the margin. However, it has also expanded to the east, with seeps replacing areas that contained braided channels in 1986 (Figure 4.1).

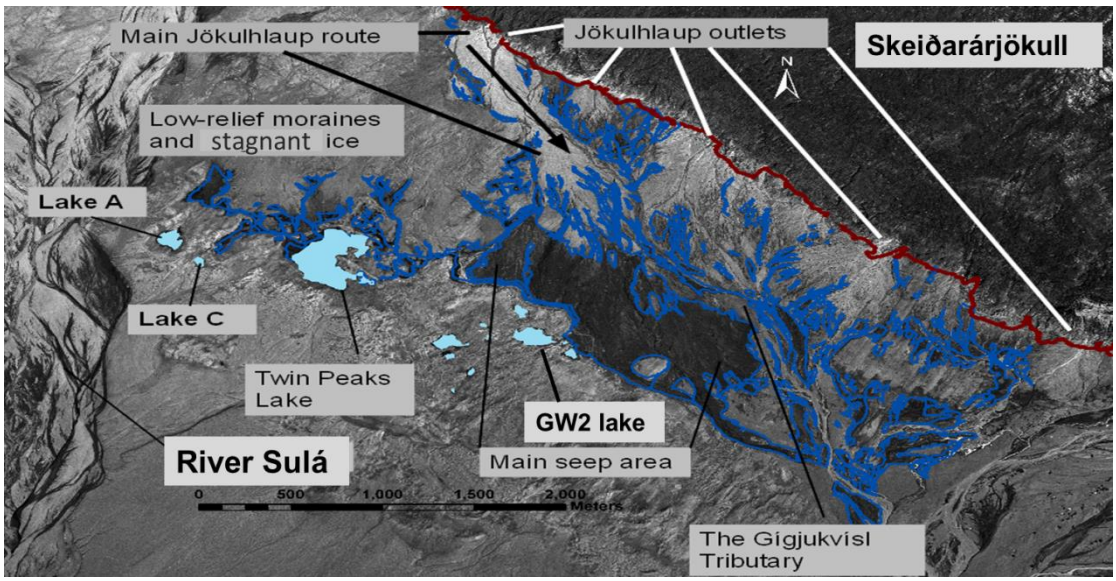

Figure 4.2. The extent of groundwater seeps in western Skeiðarársandur in 1997 (LMÍ, 1997).

Groundwater seeps are outlined in blue. Lakes are denoted in turquoise. The figure also shows the main route (denoted by the black arrow) and outlets of the November 1996 jökulhlaup. The position of the glacier margin is only an approximation, due to the extensive amounts of buried ice in this area.

4.3.3. 2012 aerial photograph

The extent of groundwater seeps in 2012 is presented in Figure 4.3 (Google Earth, 2013). The figure illustrates the continued recession of western Skeiðarárjökull, which retreated 845 m beyond its position in 1997. The mean annual rate of glacier retreat has also substantially increased during this period (Figure 3.6). During this period of retreat there has also been a substantial decline in the area of groundwater seeps and lakes (Figure 4.4, Table 4.1).

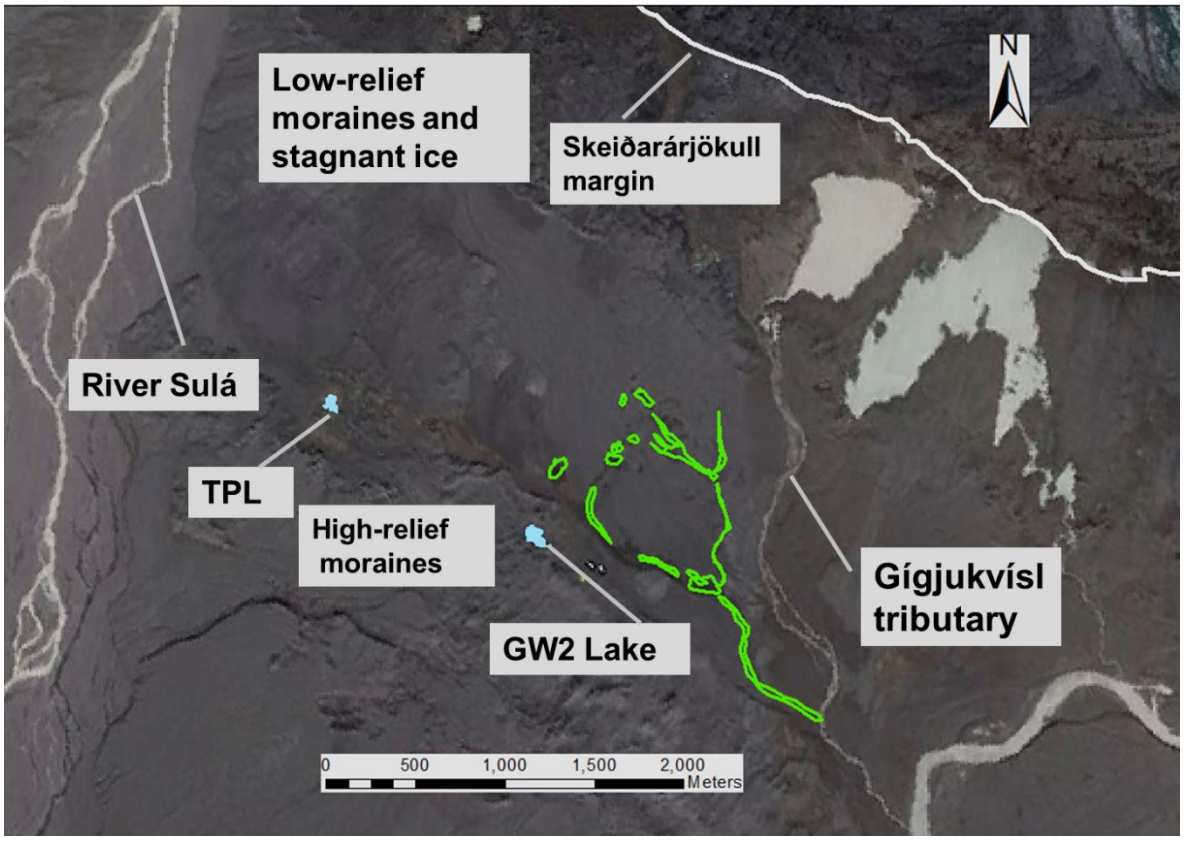

Figure 4.3. The extent of groundwater seeps in western Skeiðarársandur in 2012 (Google Earth, 2013).

Groundwater seeps are outlined in green. The lakes are denoted in turquoise. The position of the glacier margin is only an approximation, due to the extensive amounts of buried ice in this area.

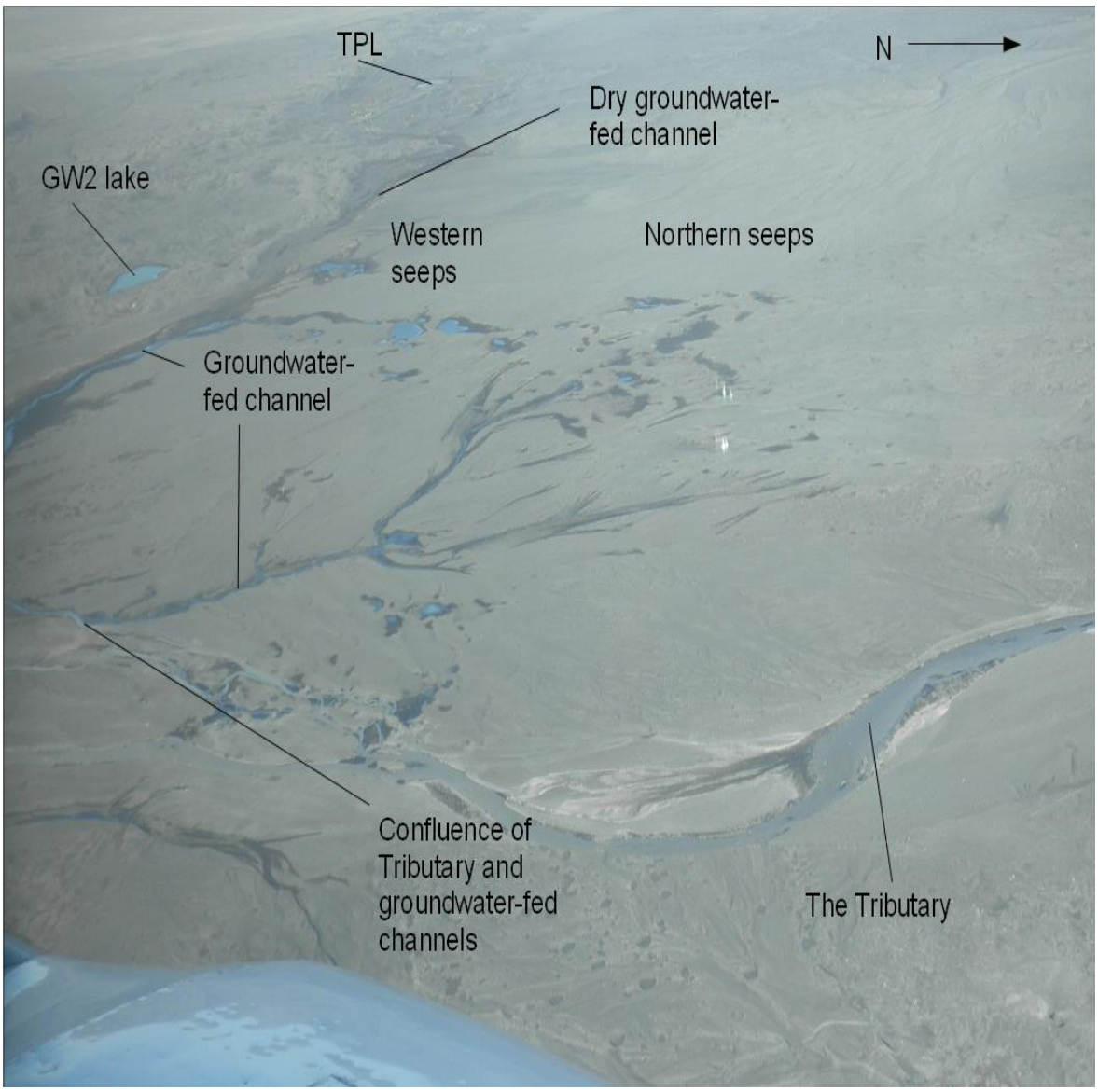

Figure 4.4. Oblique aerial view of the remains of the main groundwater seep area in western Skeiðarársandur (August 2012)

The area of groundwater seeps has declined by ~97% between 1986 and 2012, with only small springs remaining within the main groundwater seep area (Figure 4.4). The surface area and perimeters of lakes also declined substantially between 1986 and 2012, with the areas of TPL and GW2 Lake declining by 95% and 44%, respectively. Many of the smaller lakes have substantially shrunk or completely dried out, including Lake A (Figure 4.5, Table 4.1).

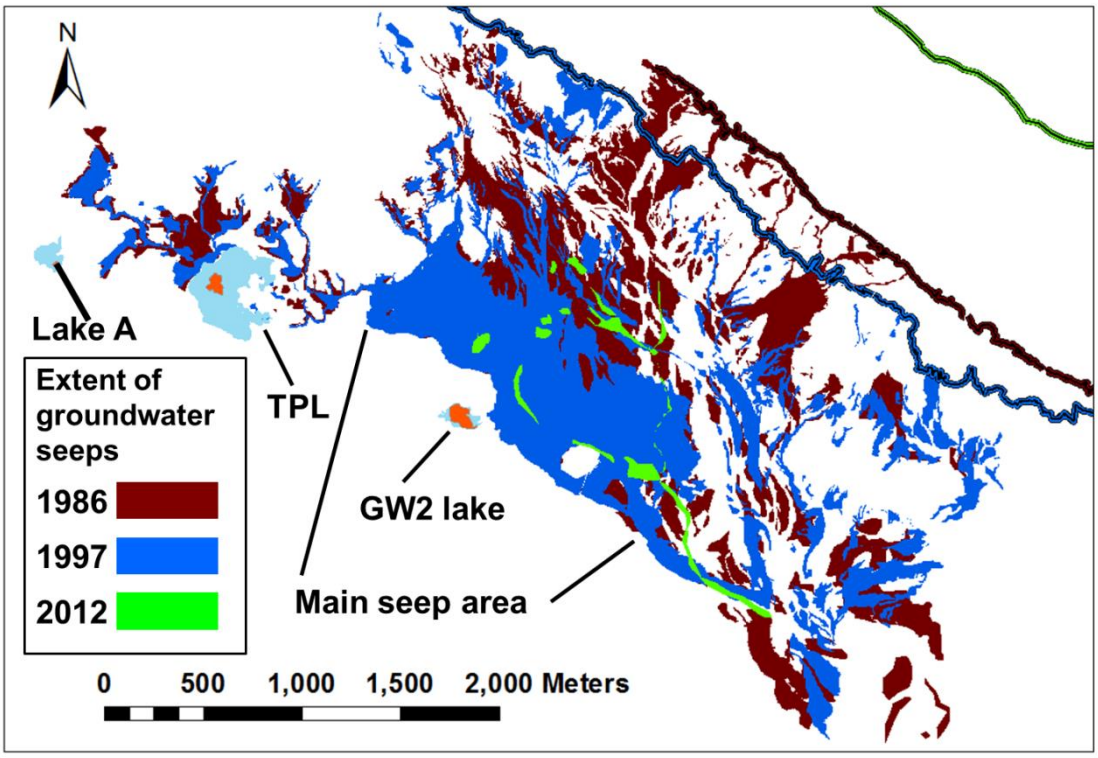

Figure 4.5. Changes in the extent of groundwater seeps and lakes in western Skeiðarársandur (1986-2012).

The figure shows the extent of groundwater seeps in 1986 (red), 1997 (blue) and 2012 (green). The position of the glacier margin is shown by the solid lines of the respective colours. The area of Twin Peak Lake is illustrated for the following years: 1986 (turquoise), 2012 (orange). The 1997 extent of Twin Peaks Lake was very similar to that in 1986 and was therefore omitted to improve clarity. The image was taken from Levy *et al*. (2015)

Table 4.1. Changes in the area and perimeter of proglacial groundwater seeps and lakes in western Skeiðarársandur (1986-2012).

	1986	1997	2012	% change (1986-1997)	% change (1986-2012)
Area (m^2)					
Seeps	2,767,200	2,195,800	90,600	-21	-97
TPL	119,000	106,500	5,900	-10	-95
Lake A	15,600	12,800	0	-18	-100
GW2 lake	16,600	18,800	9,200	13	-44
Perimeter (m)					
Seeps	110,200	121,000	9,300	-10	-91
TPL	2,900	2,400	300	-18	-88
Lake A	650	525	0	-19	-100
GW2 lake	740	746	500	-1	-33

4.4. Changes in groundwater levels in western Skeiðarársandur

This section describes changes in proglacial groundwater levels between July 2000 and August 2012 (objective 2) (Table 4.2). Proglacial groundwater levels were monitored regularly over a ~6 week period in the summers of 2000, 2001 and 2011. Additionally, spot measurements were taken in March 2001, October 2001, August 2009, April 2011, and the summer of 2012. Groundwater levels at the study site declined substantially between July 2000 and 2012 (Figure 4.6). These declines were observed over both decadal (2000-2012) and annual (2011-2012) time scales, and have shown a considerable spatial variability. Groundwater levels have fallen below the bottom of the borehole screened section (intake) in most piezometers at the site, meaning that only *minimum* amounts of water table decline can be measured. Such declines were already observed at P4, P6 and WT A by August 2009 (Figure 4.6). The largest measured declines between 2000 and 2009 were >1.97 m near the glacial margin (borehole P6) and >1.77 m in an area of dried groundwater seeps north of TPL (borehole P3) (Table 4.2). Groundwater levels at P13, located near the remains of the main groundwater seep area (Figure 3.8) fell by ~1.55 m between 2000 and 2012. However, this area contained the

only piezometer in the 2000 network where groundwater levels have not fallen below the intake. Groundwater levels in the piezometers installed in 2011 have also declined between August 2011 and August 2012 (Table 4.2).

Table 4.2. Changes in proglacial groundwater levels at the different hydrogeological environments of western Skeiðarársandur (July 2000-August 2012).

Piezometers in italics were installed in July 2011. Water table elevation with < show the elevation of the bottom of the piezometer, meaning that groundwater fell below this level. Values of change with > means that groundwater levels have dropped below the borehole intake, hence only the minimum levels of decline are shown.

Piez.	August 2000	August 2001	August 2009	April 2011	August 2011	August 2012	Change (m)
Water table elevation (m)							
Groundwater seeps							
$P13_2m$	78.577	78.385	76.890			77.025	-1.552
$P4_2m$	85.993	85.828	<84.975	<84.975			->1.063
$P3_2m$	82.283	82.227	81.270	81.275		<80.510	->1.773
GW3					77.771	77.506	-0.265
Near margin							
$P6_2m$	91.486	91.178	<89.820	<89.820			->1.971
Moraine lakes							
WT A	81.161	80.951	<80.235				->0.926
GW1					78.948	<78.575	->0.373
GW2					75.582	75.592	-0.100
P5					76.317	<75.71	->0.606
GW13					78.662	<78.147	>0.515
Meltwater channels							
GW7 (5 m from the channel)					69.680	69.610	-0.070
PT_A (40 m from the channel)					69.923	68.777	-1.146
PT_C (70 m away from channel)					70.139	68.847	-1.292

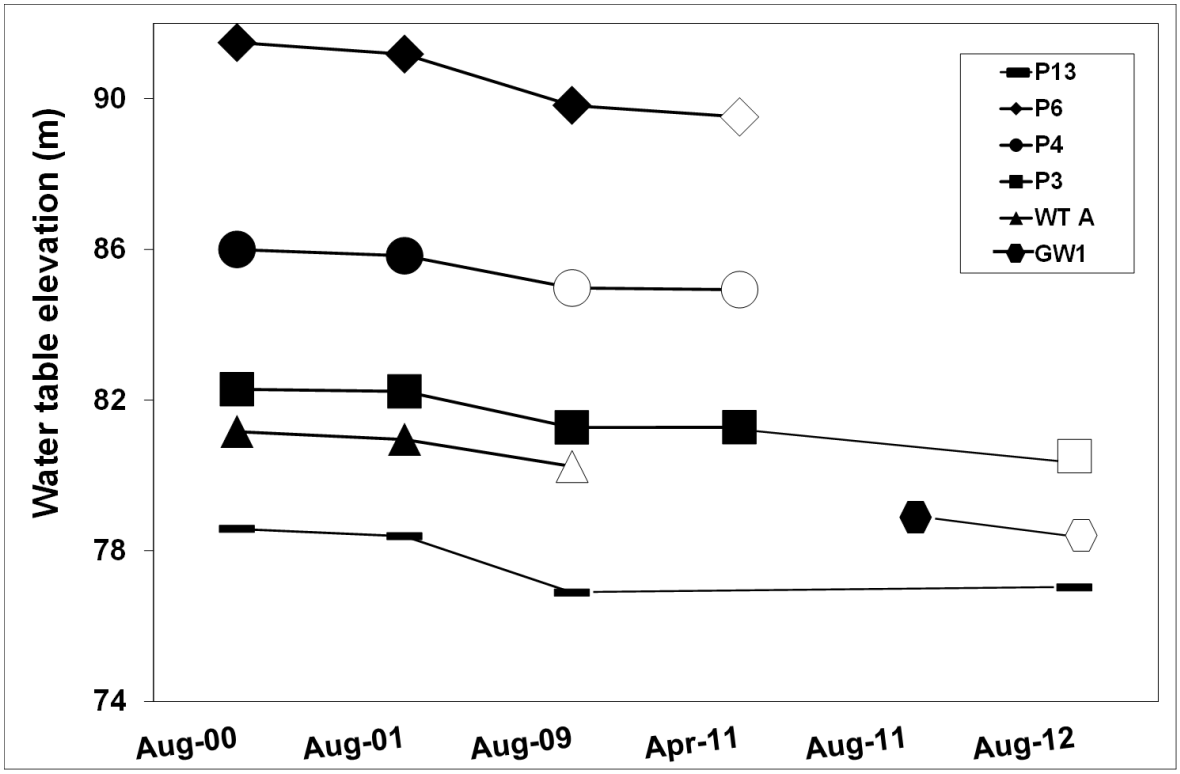

Figure 4.6. Time series of changes in proglacial groundwater levels in western Skeiðarársandur (August 2000 to August 2012).

Open shapes denote piezometers where groundwater levels have fallen below the intake. For the location of the piezometers please refer to Figure 3.8. The image was taken from Levy *et al*. (2015)

4.5. Changes in proglacial water budget

Changes in water budget (precipitation minus Potential Evaporation) can impact groundwater levels and the extent of groundwater seeps. Therefore, the annual and seasonal water budgets in western Skeiðarársandur were calculated in order to determine their roles in the changes in proglacial groundwater seeps and groundwater levels (objective 3). Temperature and precipitation data were obtained from the Icelandic Meteorological Office (IMO) station at Kirkjubæjarklaustur, located ~35 km west of the site. This station was chosen because it is the closest one whose records span through the whole study period (1986-2012). The meteorological data was smoothed using Order 3 Moving Average (MA), which was chosen in order to minimize the losses of time periods

at the end of the time series, which is a major drawback associated with higher orders of MA (Makridakis *et al*., 1998).

Potential Evaporation (PE) was calculated from the meteorological data using the Thornthwaite (1948) equation [Equation 4.1]. This method previously provided broadly comparable results to the more data-intensive Bowen Ratio Energy Budget (BREB) methods, and has been ranked 6th out of 14 equations in a study comparing different equations for determining PE (Rosenberry and LaBaugh, 2008). It was therefore chosen for this study due to its previous successful uses and low data requirements, as it only requires mean monthly temperatures.

$$E = \left(1.6 \times \left(\frac{10 T_a}{I} \right)^{6.75\times10^{-7} I^3 - 7.71\times10^{-5} I^2 + 1.79\times10^{-2} I + 0.49} \right) \left(\frac{10}{d} \right)$$

Equation 4.1. Calculation of Potential Evapotranspiration (Thornthwaite, 1948)

,

Where E is evaporation (mm/day), T_a is the mean monthly air temperature (°C), and I is the Annual Heat Index (AHI), which is calculated as $I=\sum i$, where $i = (T_a/5)^{1.514}$, and *d* is the number of days in each month. Due to the sparse vegetation at the field site, transpiration was omitted from the calculations. Water budget was then calculated by subtracting PE from precipitation.

The mean annual temperature at the Kirkjubæjarklaustur meteorological station during the study period (1986 to 2012) was 5.02 ± 0.52 °C. The mean annual precipitation was 1753 ± 229 mm (IMO, 2013). Precipitation was approximately three times higher than PE during the study period, resulting in a constantly positive annual water budget which ranged between 1076 and 1589 mm (Figure 4.7). The annual and most of the seasonal mean air temperature and water budgets have increased during the study period. However,

seasonal variability in water budget was observed, with the highest seasonal water budgets occurring in winter and autumn and the lowest in summer. During the full study period (1986-2012), winter and autumn water budgets increased by 117 and 284 mm respectively. Conversely, the increases in spring and summer water balance were much smaller (Table 4.3).

The changes in annual and seasonal water budget during the main period of decline in the extent of groundwater seeps (1997-2012) showed a mixed trend, which differs from the general increases which were measured during the full study period (Table 4.3). The annual and autumn water budgets have increased substantially (350-430 mm), while winter and spring water budgets have increased by ~100 mm. Conversely, summer water budget declined by 110 mm. This is mainly due to lower summer precipitation rather than higher PE. However, despite these declines, the summer water budget still remained positive (Table 4.3).

Table 4.3. Changes in the Moving Average (MA) of annual and seasonal temperature, precipitation, Potential Evaporation (PE), and water budget in the study area from 1986-2012 and 1997-2012 (IMO, 2013).

The seasonal distribution is as follow: Winter (Dec.-Feb.), Spring (March-May), Summer (June-Aug.), Autumn (Sept.-Nov).

	1986-2012			1997-2012		
	Start of period	**End of period**	**Change**	**Start of period**	**End of period**	**change**
	Temperature			**Temperature**		
Annual	4.63	5.71	1.08	5.04	5.62	0.58
Winter	0.23	1.22	0.99	0.49	1.05	0.57
Spring	3.59	5.27	1.68	4.02	4.77	0.75
Summer	10.43	11.31	0.88	10.83	11.40	0.57
Autumn	4.29	5.36	1.07	4.83	5.66	0.83
	Precipitation(mm)			**Precipitation (mm)**		
Annual	1548	1967	419	1667	2126	460
Winter	448	598	150	468	714	246
Spring	337	402	65	314	397	83
Summer	324	369	45	453	346	-106
Autumn	439	707	268	432	743	311
	PE (mm)			**PE (mm)**		
Annual	412	453	41	422	446	24
Winter	8	21	13	15	21	6
Spring	87	113	26	92	111	19
Summer	208	210	2	205	207	2
Autumn	99	102	3	110	107	-3
	Water budget (mm)			**Water budget (mm)**		

Annual	1082	1460	378	1221	1654	433
Winter	440	556	117	458	575	117
Spring	250	287	36	229	332	102
Summer	136	179	42	245	135	-110
Autumn	340	624	284	320	672	351

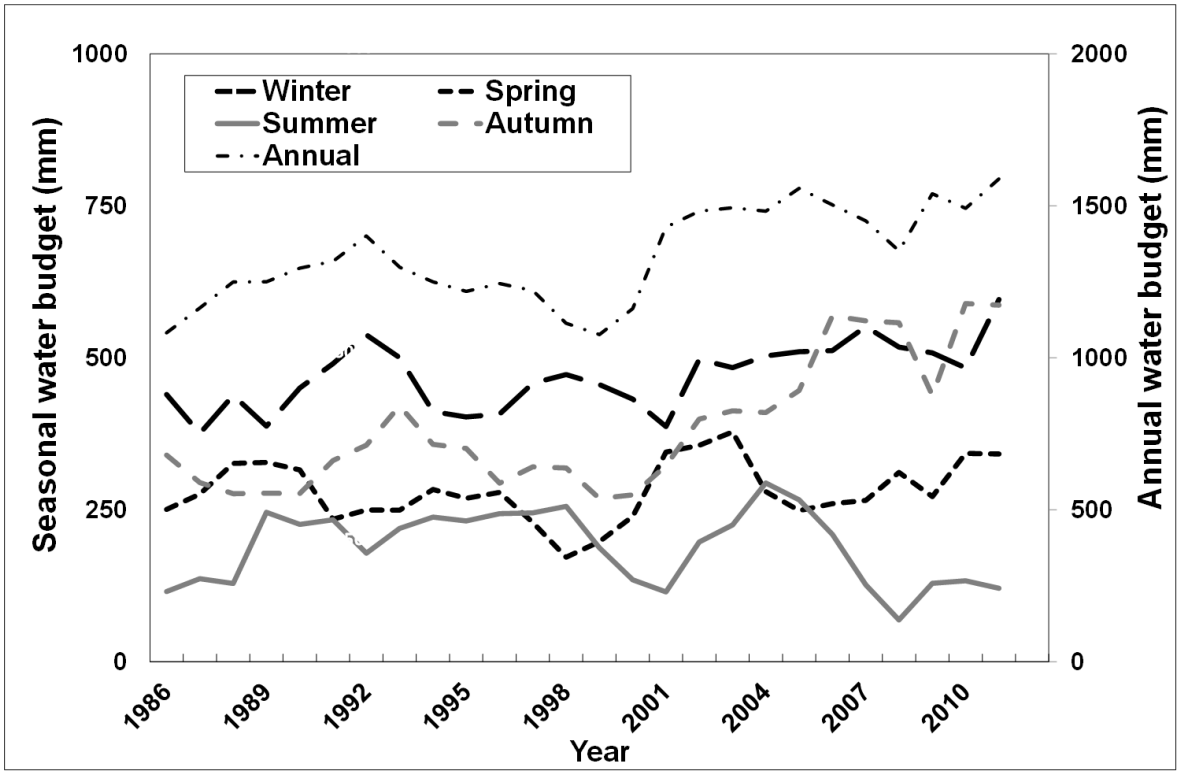

Figure 4.7. Moving Average (MA) of annual and seasonal water budget in western Skeiðarársandur (IMO, 2013).

4.6. Interpretation and discussion

This section describes the spatial distribution in the changes of proglacial groundwater levels and then discusses various hypotheses for the observed declines in proglacial groundwater levels and the extent of groundwater seeps.

4.6.1. The spatial distribution of changes in groundwater levels

Groundwater levels in western Skeiðarársandur have declined between 2000 and 2012, with groundwater levels falling below the intake in most piezometers. However, these declines showed a considerable spatial variability (Table 4.2). The largest decline in groundwater levels between 2000 and 2009 was measured at P6, located near the Skeiðarárjökull margin, adjacent to an area of ice-cored moraines and stagnant ice (Table 4.2, Figure 3.8). This fall in groundwater levels is accompanied by a reduction in the extent of the main groundwater seeps area (Figure 4.1-4.3). The importance of ice melt as a source for groundwater recharge increases with proximity to the glacial margin, as evidenced by $\delta^{18}O$ and δD compositions (Robinson *et al*., 2009b). Therefore, the fall in groundwater levels at P6 could be indicative of declining recharge from glacial melt sources. Groundwater levels near the glacier margin previously showed large declines in autumn and early spring, seasons during which ablation is low (Robinson *et al*., 2008). This suggests that only a small component of the groundwater at these sites originates from subglacial melt, as such melt should not be significantly impacted by seasonal ablation (Flowers *et al*., 2003; Robinson *et al*., 2008). This suggests that the zone of dead and stagnant ice near the margin is the likely source of groundwater recharge during the summer months. The only location from the 2000 monitoring network where groundwater levels did not fall below the borehole intake is located near the remains of the main groundwater seep area (Table 4.2). The smallest annual (Figure 4.6) and seasonal variability in groundwater levels were also measured in this environment (Robinson, 2003). The relatively small variability is also supported by observations of groundwater discharge in the form of seep areas, which suggest that the seeps are fed by a local groundwater flow system that is imposed on the regional one (Tóth, 1963; Robinson *et al*., 2008). This small variability in groundwater level illustrates the relatively consistent water

supply which groundwater-fed systems provide (e.g. Tague and Grant, 2009; Muir *et al.,* 2011).

Groundwater levels near lakes have generally declined, with levels falling below the borehole intake in many locations. These falls were coupled with substantial declines in lakes surface areas. The decline of groundwater levels near lakes has also shown considerable spatial variability. Lake A shrank continuously during the study period, and then completely dried out after 2007. Groundwater levels near Lake A also declined substantially (Table 4.1). Observations suggest that the area of Lake A consists of either a perched aquifer or an impermeable lake bed, underlain by either clay or buried ice (Robinson *et al*., 2008). This hypothesis is supported by observations of buried ice in Skeiðarársandur (Everest and Bradwell, 2003) and the complex and heterogeneous internal hydrology of moraines (Roy and Hayashi, 2009; Langston *et al*., 2011). It is suggested that the lake may have drained due to the failure of the underlying ice layer (Robinson *et al*., 2008). Groundwater levels in other piezometers near lakes, which were installed in 2011, have also fallen below the borehole intake (Table 4.2).

Conversely, groundwater levels near GW2 Lake have shown different dynamics. The area of this lake declined by 44% since 1986 (Table 4.1). However, there is a much smaller fall in groundwater levels, with only a 0.1 m decline between August 2011 and 2012 (Table 4.2). These differences illustrate the spatial variability in the patterns of decline in groundwater levels around lakes and in moraine basins in western Skeiðarársandur.

4.6.2. Possible causes for the declines in groundwater levels and seeps

This section suggests various hypotheses for the substantial declines in groundwater levels and in the extent of groundwater seeps in western Skeiðarársandur (objective 3).

The first suggested hypothesis for these observed declines is changes in proglacial water budget. Figure 4.7 and Table 4.3 show that the annual and most of the seasonal water budgets have increased over the study period, especially during winter and autumn. Conversely, summer water budgets have fallen by ~100 mm since 1997. The fall in summer water budget may partially explain the declines in groundwater seeps and levels (which have been measured in summer). However, this fall may be expected to be offset by the increases in winter and autumn precipitation. Higher rainfall can also increase groundwater recharge indirectly by enhancing glacial ablation (Wolfe and English, 1995), with rainfall becoming especially effective in debris-covered glaciers such as Skeiðarárjökull (e.g. Nield *et al*., 2013). The increase in autumn and winter precipitation may therefore be expected to increase groundwater recharge and storage. This suggests that changes in water balance are important but not the sole factors in the decline of groundwater levels and groundwater seeps.

Glacier retreat is projected to substantially alter the hydrology of Vatnajökull, reducing runoff and diverting river routes. Such changes are also projected to impact subglacial groundwater systems (Flowers *et al*., 2003; 2005). Glacier retreat can lower the ice overburden pressure and hydraulic gradient, which will reduce groundwater flow (Haldorsen and Heim, 1999; Piotrowski, 2007). Such changes could be an important cause for the declines depicted in Figure 4.1-4.3. However, at present the effect of the glacially-induced hydraulic gradient on the proglacial zone is not fully understood.

Changes in proglacial groundwater flow may also be caused by the lowering of the glacier bed and river outlets. Sandur development models suggest that glacier retreat leads to an upstream lowering of river equilibrium profile, which encourages fluvial incision and the formation of alluvial terraces (Thompson and Jones, 1986; Thompson, 1988). The lowering of the equilibrium profile would then direct flow into the lowest channel (e.g. Thompson, 1988). The impact of the lowering of the equilibrium profile can be augmented when glaciers retreat into subglacial overdeepenings. Such retreat can increase the

sensitivity of the proglacial zone to glacial margin fluctuations, where relatively small fluctuations in the position of the glacier margin cause fairly large changes in the upstream long profile of proglacial rivers (Marren and Toomath, 2013).

The lowering of river outlets due to an overdeepening is a possible cause for the observed declines in groundwater seep extent and levels. Radio echo soundings have identified two principal overdeepenings associated with Skeiðarárjökull. The larger overdeepening extends from the glacier's centreline to the eastern margin. The second one is located towards the western extremity of the margin (Figure 3.4B), associated with the drainage of the river Súla (Björnsson *et al.,* 1999). However, neither of these overdeepenings impact the immediate study area. Therefore, whilst over-deepened basins are clearly influential in some parts of the glacier margin, it is unlikely that this specific part of the margin is significantly impacted by an overdeepening, and therefore the decline in groundwater levels are unlikely to be affected by this phenomenon.

Groundwater recharge from meltwater rivers, through river-aquifer exchange, is an important control on proglacial groundwater levels (Cooper *et al*., 2002; Magnusson *et al*., 2014). The location of meltwater rivers exerts an important control on such exchange; hence a reduction in river-aquifer exchange, due to changes in the position of meltwater rivers, provides another possible explanation for the observed changes in the proglacial groundwater systems. However, the location of the main Gígjukvísl and Súla river channels did not change considerably during the study period, which suggests that river-aquifer exchange should not have decreased. Additionally, the recent drainage changes in Skeiðarársandur have substantially increased the discharge in the Gígjukvísl. These changes are expected to augment, rather than reduce, groundwater recharge through river-aquifer exchange. Therefore, although river-aquifer exchange has not been measured directly, its decrease is probably not the main cause for the declines depicted in Figure 4.1-4.3.

Deglaciation and isostatic uplift have been previously shown to impact topography, hydrology, hydrogeology, and ecology (Glaser *et al*., 2004; Solberg *et al*., 2008). The rates of vertical glacio-isostatic uplift in response to glacial retreat around southern Vatnajökull range between 9-25 mm/year (Pagli *et al*, 2007). These rates suggest that the study area has risen by 0.23 to 0.65 m during the study period (1986-2012) and between ~0.14 m to 0.38 m during the main decline in groundwater seeps and levels (1997 to 2012). However, even when the higher rates of these estimations are used, the uplift rates remain below the observed declines in most piezometers (Table 4.2). Hence, although glacio-isostatic uplift may have contributed to the decline in groundwater levels and seeps, it is probably not its main cause.

The deposition of volcanic tephra buries groundwater seeps and deepens the distance between the water table and the surface, which reduces the aquifer's responsiveness to precipitation. These processes may also explain some of the declines in groundwater levels and seeps in western Skeiðarársandur. Grímsvötn, situated under the Vatnajökull ice cap, ~40 km north of the site (Figure 3.2) is Iceland's most active volcanic system in historical times (Thordarson and Larsen, 2007). During the study period, it has erupted in 1996, 1998, 2004, and May 2011 (Jude-Eton *et al*., 2012). The eruption in May 2011 released 0.6-0.8 km^3 of tephra (Guðmundsson *et al*., 2012). Tephra deposits buried many groundwater-fed channels and seeps. Measurements taken at western Skeiðarársandur in August 2011 showed a wide spatial variability in the depths of tephra deposits. The mean depth of tephra deposits near piezometers was 0.055 (±0.031) m. The depth of tephra deposits near groundwater-fed channels and seeps exceeded 0.40 m. However, these measurements were obtained three months after the eruption, during which the tephra has been subjected to extensive fluvial and aeolian entrainment and deposition. In addition to the fairly transient nature of tephra deposition, groundwater levels have declined between August 2011 and August 2012 (Table 4.2), during which there was no volcanic activity. Therefore, although burial by tephra deposits can clearly have a localised

impact on groundwater seeps, it was not a major cause for the declines depicted in Figure 4.1-4.3.

4.6.3. Implications of the declines in groundwater seeps and levels

This study observes substantial declines in the extent of proglacial groundwater seeps in an area of rapid glacial retreat. It is suggested that the major declines in proglacial groundwater levels and groundwater seeps have had major impacts on the terrestrial and aquatic ecology of Skeiðarársandur. This hypothesis is supported by field observations showing higher densities of vegetation associated with groundwater seep areas (Figure 3.7) and highlighted the important ecological niches provided by groundwater-fed kettle holes (Robinson *et al*., 2009a). In addition, there is a wealth of literature highlighting the importance of groundwater contributions to increased aquatic diversity in proglacial areas (e.g. Milner and Petts, 1994; Crossman *et al*., 2011). This suggests that groundwater seeps form important microsites, which enhance terrestrial ecological establishment and provide ameliorated conditions from the frequent high sediment mobility, strong winds, and lack of fertile soils which often prevail in recently-deglaciated areas (Jumpponen *et al.,* 1999; Marteinsdóttir *et al.,* 2010; 2013).

As proglacial groundwater flow, spring discharge, and groundwater contributions to runoff and storage are projected to alter due to glacial retreat (Haldorsen *et al.,* 2010; Rutter *et al.,* 2011; Blaen *et al*., 2014), these changes are projected to adversely impact proglacial ecosystems and possibly lead to the redistribution and extinction of endemic species (Brown *et al.,* 2007a, b; Milner *et al*., 2009; Jacobsen *et al*., 2012; Blaen *et al*., 2013). Therefore, due to the importance of groundwater to proglacial ecology, it is suggested that further decline in groundwater levels and in the extent of groundwater seeps in Skeiðarársandur will adversely impact available water sources and sandur ecology. The

hypotheses for the controls and implications of long term glacier retreat on proglacial groundwater-surface water exchange are summarised by a conceptual model (Figure 4.8).

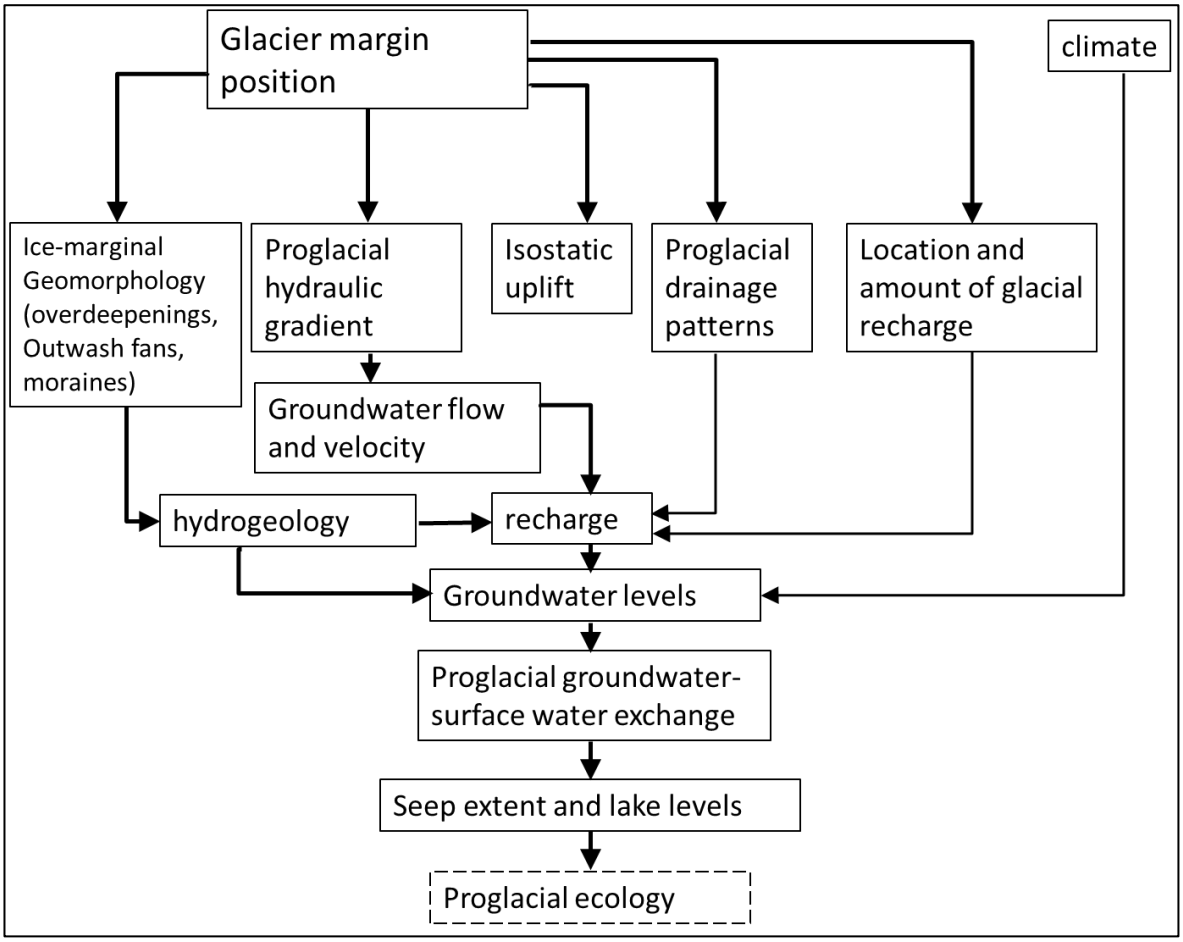

Figure 4.8. A conceptual model of the controls and implications of long term glacier fluctuations on proglacial groundwater-surface water exchange (from Levy *et al*., 2015).

The dashed box shows suggested implications, which were not directly investigated in this study.

4.7. Conclusions

Western Skeiðarárjökull has retreated approximately 1 km during the study period (1986-2012). This retreat was coupled with a decline of ~97% in the areas of groundwater seeps and many of the lakes at the site. Most of these declines took place after 1997, when the

rate of glacial retreat has increased by a threefold. Groundwater levels at the study area have also fallen substantially between 2000 and 2012, although the magnitude of these declines varies spatially. The largest declines were observed near the glacier margin. The smallest declines in groundwater levels were observed near current groundwater seeps. The annual water budget has increased substantially between 1986 and 2012. Seasonal water budgets have also increased in every season except summer, where it has declined.

The geomorphology, hydrology and groundwater systems of Skeiðarársandur are substantially impacted by glacial fluctuations, surges, and jökulhlaups. The 1991 surge steepened the topography and transformed surface and subsurface drainage at Skeiðarársandur. The November 1996 jökulhlaup led to the formation of kettle holes and extensive erosion and deposition of sediment. Jökulhlaup deposits buried ~18% of the area of groundwater seeps that were mapped in 1986.

It is suggested that the combination of jökulhlaups and changes in water budget and in the hydraulic gradient caused by glacier retreat, alongside vertical glacio-isostatic uplift is probably the cause for the observed declines in groundwater seeps and levels. However, further research is needed in order to verify and quantify the contribution of the different factors. Groundwater seeps support important ecological microsites in this harsh proglacial environment. A continuous decline in groundwater levels and seeps is therefore suggested to adversely impact Skeiðarársandur's proglacial ecology (Levy *et al*., 2015).

5. Proglacial Hydrogeology

5.1. Introduction

The aim of this chapter is to describe the hydrogeological characteristics of the proglacial zones of Skaftafellsjökull and Skeiðarársandur such as hydraulic conductivity, aquifer volume, and groundwater discharge and velocity. These parameters are necessary for the understanding of horizontal and vertical groundwater flow and groundwater-surface water exchange. However, an extensive hydrogeological framework for Skeiðarársandur has already been provided (e.g. Bahr, 1997; Robinson, 2003; Robinson *et al*., 2008). Therefore, this study focuses on the aquifer characterisation the Skaftafellsjökull foreland.

The hydrogeology of contemporary proglacial aquifers, such as the Skaftafellsjökull foreland (Figure 3.13) and Skeiðarársandur (Figure 3.4), is impacted by a variety of geomorphic and sedimentological processes. Glaciofluvial deposition associated with both ablation-driven and jökulhlaup-related discharge fluctuations are clearly of central importance, although glacial, glaciolacustrine and aeolian processes are also influential (Maizels, 1995; Marren, 2002a ; Robinson *et al*., 2008; Mountney and Russell, 2009). These primary depositional processes usually impact proglacial aquifers more than secondary processes such as compaction, cementation and dissolution. The hydrogeological characterisation described in this chapter is based on two approaches: (1) large-scale overview of the site's hydrogeology based on the various geomorphic and sedimentological processes which impact the field site, and (2) a small-scale hydrogeological characterisation based on field and laboratory techniques.

The main hydrogeological property that was investigated at this study was hydraulic conductivity, which describes the ease with which a medium transmits fluids (Freeze and Cherry, 1979). An accurate measurement of hydraulic conductivity is essential for the understanding of groundwater behaviour. However, despite its importance, the

measurement of hydraulic conductivity is a significant challenge in hydrogeology (e.g. Brassington, 2007). This challenge is enhanced in proglacial settings, due to the highly varied nature of depositional processes and associated sedimentary sequences which lead to high variability in hydrogeological parameters (e.g. Caballero *et al*., 2002; Robinson *et al*., 2008; Gremaud *et al*., 2009; Gremaud and Goldscheider, 2010; Magnusson *et al*., 2014; Cabj *et al*. 2014). This chapter compares between laboratory (Particle Size Analysis [PSA] and constant head permeameter) and field measurements (falling head [slug] tests) of hydraulic conductivity. The results were then used to compare the hydrogeology of Skaftafellsjökull with that of Skeiðarársandur and other proglacial environments.

The specific objectives for this chapter are:

1. To measure the spatial heterogeneity in hydraulic conductivity at the Skaftafellsjökull foreland using laboratory and field measurements.

2. To compare between the different methods for determining hydraulic conductivity.

3. To calculate the hydrogeological properties of the Skaftafellsjökull foreland: groundwater discharge, aquifer volume and groundwater velocity.

5.2. Dominant geomorphic processes and hydrological environments at the Skaftafellsjökull foreland

This section describes the dominant geomorphic processes at the Skaftafellsjökull foreland, notably glaciofluvial and glacial processes. These varied processes are the main cause for the high spatial variability in hydraulic conductivity at the site. In contrast to Skeiðarársandur, the Skaftafellsjökull foreland is mainly impacted by glacial processes,

such as moraine development, glaciofluvial processes (Marren, 2002b) rather than glacial surges and jökulhlaups.

5.2.1. Glaciofluvial deposits

Glaciofluvial deposits are deposited by meltwater streams which originate at the glacier margin. These deposits are generally composed of coarse sand and gravel size, which then becomes finer downstream (e.g. Anderson, 1989). Glaciofluvial deposits have high hydraulic conductivity, of around $1.00x10^{0}$ to $1.00x10^{2}$ m/day (Brassington, 2007). Therefore, coarse-grained glaciofluvial sediments form extensive aquifers in areas that were previously glaciated in North America (e.g. Burns *et al*., 2010; Bajc *et al*., 2014) and Europe (e.g. Bayer *et al*., 2011).

The largest extent of glaciofluvial deposits at the Skaftafellsjökull foreland is associated with the active braid plain of the Skaftafellsá. This area consists of outwash and is characterised by active and relict braided channels, that reflect the lateral migration of the Skaftafellsá (Figure 5.1). The majority of the glaciofluvial deposits at the Skaftafellsjökull foreland originated from low-magnitude, high-frequency events, which are mainly controlled by ablation (e.g. Marren, 2002b). This is in stark contrast to Skeiðarársandur, where high magnitude, low frequency events play a major role in the deposition of sandur glaciofluvial deposits (e.g. Robinson *et al*., 2008). Fluctuations of the glacier margin are an important control on channel development and spacing at both Skeiðarársandur (Robinson *et al*., 2008) and the Skaftafellsjökull foreland, with drainage patterns and channel positions continuously changing in response to advances and retreats of the margin (Marren, 2002b; Marren and Toomath, 2013; 2014). For instance, the ongoing retreat of Skaftafellsjökull has resulted in the abandonment of the western branch of the Skaftafellsá such that the eastern channel is the only active river draining the ice margin (Figure 5.1).

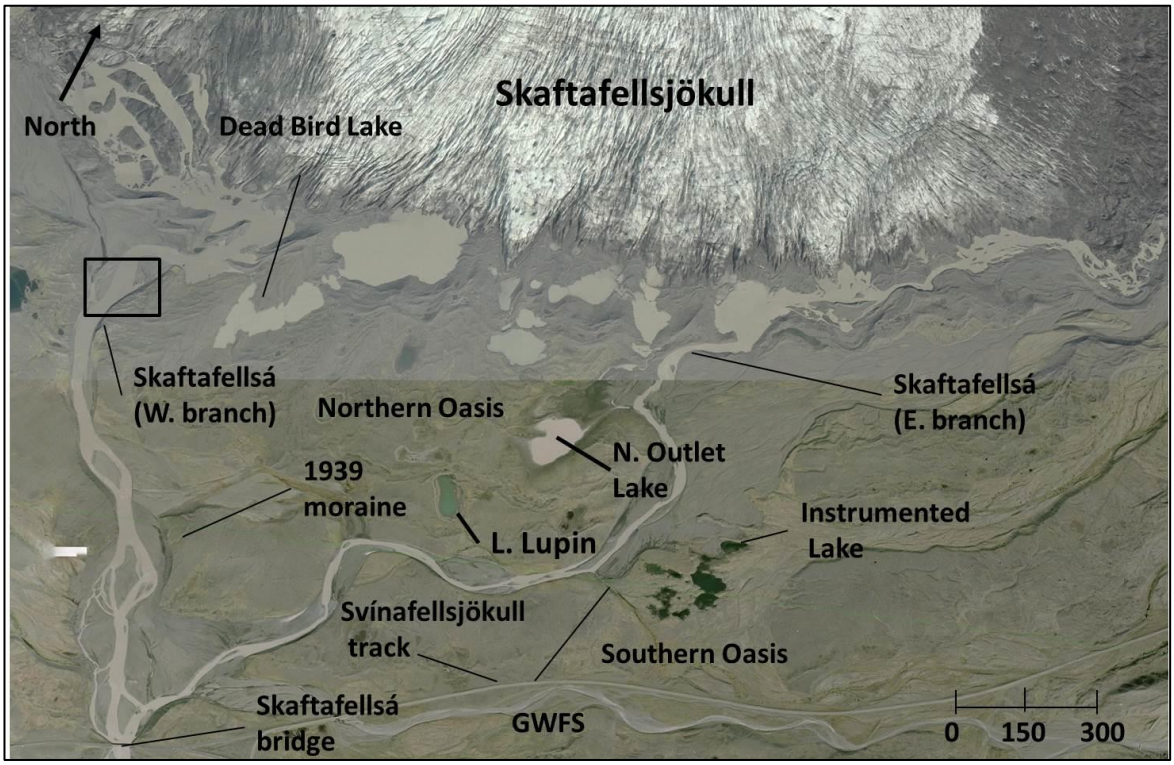

Figure 5.1. The Skaftafellsjökull foreland fieldsite (Vatnajökull National Park, 2007).

Significant drainage changes have taken place since the image was taken. The main ones are the expansion and merging of the ice-contact lakes and drainage diversion causing the drying of the western branch of the Skaftafellsá. The black box shows the approximate location of Figure 3.11, which shows the dry branch of the Skaftafellsá.

5.2.2. Glacial deposits

Till is a sediment that has been entrained and deposited by glacial ice, with little or no sorting by water (e.g. Shaw, 1985). Till deposits are complex and can be highly heterogeneous, containing deposits with varied hydraulic properties (e.g. Anderson, 1989; Meriano and Eyles, 2009). The hydraulic conductivity of till can vary over seven orders of magnitude (Freeze and Cherry, 1979). The origin and secondary processes which impact till are important determinants of its hydraulic conductivity (e.g. Hendry, 1982; Stephenson *et al*., 1988). Till deposits can also contain extensive layers of fine grained material, which can form extensive aquitards (e.g. Meriano and Eyles, 2009). The dominant glacial landform at the Skaftafellsjökull foreland is moraines, which surround many of the lakes at the Northern and Southern Oasis. The internal hydrology of moraines is complex, and can include layers of low permeability (e.g. Langston *et al*., 2013), which can impact

groundwater flow and lake formation. Therefore, it is hypothesised that the groundwater flow through moraines will be highly variable. Field observations suggest that the main till deposits at the Skaftafellsjökull foreland are found in the Northern Oasis (Figure 5.2).

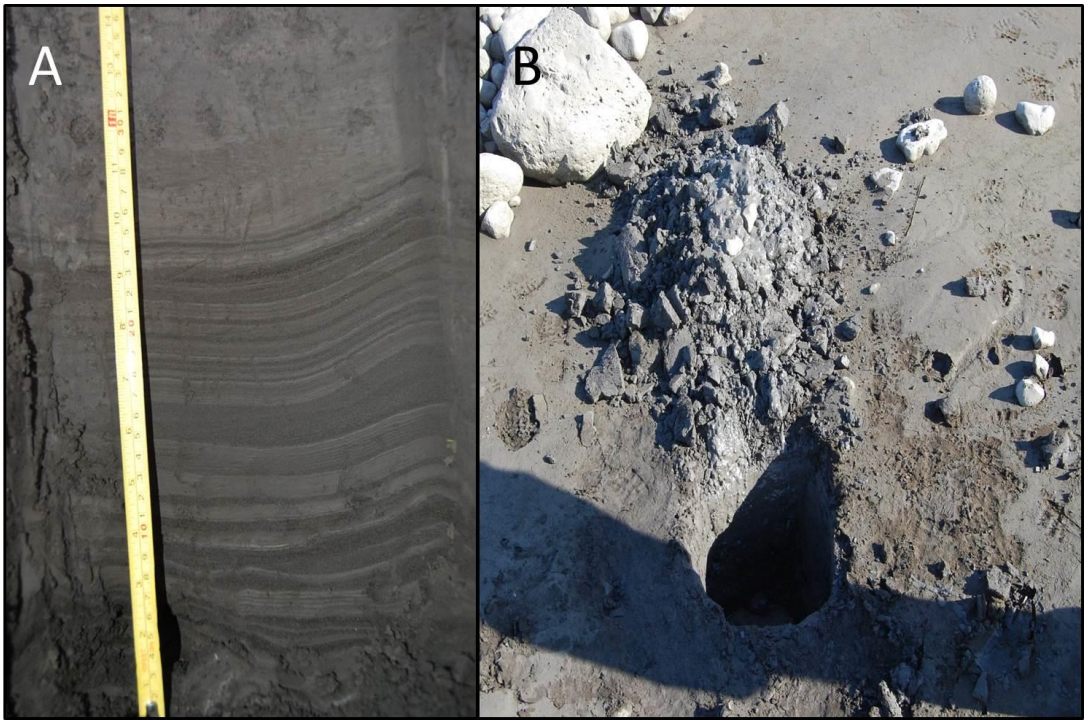

Figure 5.2. Fine-grained deposits at the Northern Oasis.

A. Sequence of fine-grained clay layers near Lake Lupin (Figure 5.1). B. An attempt to emplace piezometers at the Northern Oasis lakes. Notice the poor sorting of the deposits, which consist of fine sediments and boulders. The pit is located approximately 50 m from the lakeshore of Lake Lupin.

5.2.3. Lacustrine processes

Lacustrine deposits are generally fine grained and have low permeability (e.g. Domenico and Schwartz, 1998). These layers of fine sediment are likely to significantly impact the hydraulic conductivity of the lakes and impact lake-aquifer exchange (e.g. Blume *et al*., 2013). Conversely, significant groundwater-lake exchange has been observed in lakeshores with coarse deposits, such as talus slopes (e.g. Hood *et al*., 2006; Roy and Hayashi, 2008).

Lakes and lake basins of various sizes are common features of glacier forelands, including the Skaftafellsjökull foreland (Figure 3.13). Confined topographic basins in which lakes can form can be created by a number of glacial processes including the erosion of overdeepenings (e.g. Marren and Toomath, 2013) and the melt-out of buried ice. They can also form with inter-moraine basins (e.g. Robinson *et al*., 2008). Glacial lakes connected with proglacial meltwater systems with high sediments loads are associated with relatively rapid sedimentation rates. Seasonal variations in meltwater discharge and sediment delivery to glacial lake basins can result in the formation of varves that are characteristic of glaciolacustrine sequences (e.g. Marren, 2002a). These typically comprise alternating layers of clay and silt-sand representing annual cycles. Lake basins that are not connected to surface meltwater rivers and that are in contrast fed by rainfall and groundwater are characterised by much lower turbidity and sedimentation rates.

Lakeshores which are underlain by fine-grained deposits at the Skaftafellsjökull foreland are located in the Northern Oasis (Figure 5.1), in drying lakebeds at the western part of the Southern Oasis, and at the eastern shore of the Instrumented Lake (IL). Conversely, the western lakeshore of the IL is underlain by coarse glaciofluvial deposits. These differences suggest high variability in the hydraulic conductivity of lakeshores at the Skaftafellsjökull margin. In addition to the lakes in the Southern and Northern Oasis, the foreland of Skaftafellsjökull is also dominated by the ice-contact lake, which has been expanding substantially following the retreat of Skaftafellsjökull into an overdeepened basin (Marren and Toomath, 2013).

5.2.4. Summary of depositional environments at the Skaftafellsjökull foreland

The retreating of the Skaftafellsjökull foreland generates complex glaciofluvial, glacial, and lacustrine processes (Marren, 2002a). In contrast to Skeiðarársandur, the dominant fluvial regime at the Skaftafellsjökull foreland is generally controlled by ablation. Furthermore,

the Skaftafellsjökull foreland is not impacted by jökulhlaups and glacial surges. Most of the deposits at the Skaftafellsjökull foreland originate from glaciofluvial processes, till deposition, and lacustrine deposits (Marren and Toomath, 2013). This high variability in proglacial geomorphology is therefore expected to lead to a high variability in hydrogeological parameters.

This overview provides a good understanding for the geomorphic processes and their associated environments which impact the Skaftafellsjökull foreland and the related deposits which are characteristic to these environments. In addition to the description of the dominant depositional and geomorphic processes the current study also took field and laboratory hydrogeological measurements to determine small-scale aquifer parameters. These results are important for the hydrogeological classification of the field site (objective ii) and for the understanding of groundwater exchange with rivers (objective iv) and lakes (objective v).

5.3. Methods for determining hydraulic conductivity

Hydraulic conductivity (*K*) describes the ability of a porous medium to transmit fluid through interconnected voids. Therefore, it represents the ease with which fluid flows through porous media (e.g. Freeze and Cherry, 1979). Hydraulic conductivity is a key hydrogeological parameter, and its accurate estimation is necessary for accurate calculations of groundwater flow, the assessment of groundwater-surface water interactions and baseflow (e.g. Soulsby *et al*., 2007; Song *et al*., 2009; Krause *et al*., 2011a, b), and for understanding the transport of contaminants (e.g. Weatherill *et al*., 2014). This study focuses on measuring hydraulic conductivity (objective ii) in order to delineate proglacial groundwater-surface water interaction, particularly the exchange between groundwater and rivers (objective iv) and lakes (objective v).

Within proglacial environments, hydraulic conductivity is impacted by large scale geological and geomorphic processes, such as glacier margin fluctuations and jökulhlaups (e.g. Robinson *et al*., 2008; Bajc *et al*., 2014). However, hydraulic conductivity is also controlled by the development and occurrence of smaller-scale features and processes such as fractures (Hendry, 1982, 1988) sand layers (Bradbury and Muldoon, 1990), and till oxidation (Hiscock and Najafi, 2011). For instance, observations from Alberta, Canada, have shown that fracture flow within a glacial till matrix with very low hydraulic conductivity (10^{-10} m/sec) can increase groundwater flow velocities by one to three orders of magnitude (Hendry, 1982). Within proglacial settings, hydraulic conductivity can be substantially reduced by low permeability features such as clay deposits and buried ice (e.g. Langston *et al*., 2011; Muir *et al*., 2011).

However, despite the importance of hydraulic conductivity, its measurement in the field and the laboratory is complicated. Various methods exist for it, each with its merits and limitations [Table 5.1] (e.g. Freeze and Cherry, 1979; Odong, 2007).

Table 5.1. Methods for determining hydraulic conductivity. Note that the scale of test increases down the table

Method	Advantages	Disadvantages
Particle Size Analysis (PSA)	• Low cost • Ease of repeatability • Different formulas relate to different grain sizes • Easy collection of samples • Relatively low environmental impact	• High variability within the results, which are strongly dependant on the material and formula used. • The small scale of the test does not address preferential flow paths and aquifer heterogeneity. • Difficulty in obtaining representative samples of aquifer materials.
Laboratory permeameter tests	• Relative ease of obtaining samples.	• High variability of results • packing and drainage along the side of the device can impact the results
Single well response (slug) tests	• Testing is done within the aquifer itself. • Simple performance and analysis • Relatively inexpensive	• Only a small area is tested • Requires data loggers and piezometers that will fit them. • The injection of the ‘slug’ can impact well water • Difficult to implement in wells with high hydraulic conductivity
Pumping tests	• Integrates aquifer heterogeneities over larger scales	• High costs • Time consuming • Requires piezometers • Difficult to implement in remote/sensitive areas.

The development of a good understanding of the hydrogeological framework for the Skaftafellsjökull foreland was a key goal for the current study (objective ii). However, the logistical requirements and costs associated with pumping tests ruled out this method. Due to their relative simplicity, low costs, and previous successful uses in proglacial environments, it was decided to use PSA (Robinson *et al*., 2008) slug tests (Cooper *et al*., 2002; 2011), and laboratory permeameter (e.g. Mohanty *et al*., 1994) for the determination of hydraulic conductivity at the Skaftafellsjökull foreland. However, due to the relatively small area which slug tests impact and the difficulties in obtaining a representative sample for PSA and permeameter measurements, it was decided to use all methods and compare the results where applicable. The results of the slug tests were therefore compared with PSA results from "proxy locations" near the piezometers (section 5.4.3).

5.3.1. Falling head (slug) tests

Falling head tests are based on the addition of a volume of water ("slug") into the well and the analysis of the dissipation of the change in head. This method has been previously used to determine the hydraulic conductivity of a proglacial outwash plain in Svalbard (Cooper *et al*., 2002; 2011). The slug tests for the current study were performed in the 0.28 mm piezometers (GW, Figure 3.18), where pressure transducers fit. The procedures for the slug tests followed those recommended by Brassington (2007). Initially, groundwater level in the piezometer was measured manually. After the groundwater level was stable, a pressure transducer was then emplaced inside the piezometer, and suspended from the top. Approximately 1-2 litres of water were then added quickly, which instantly raised the water level and then began to dissipate. In order to ensure that the change in hydraulic head caused by the slug had dissipated completely and that groundwater returned to the level prior to the injection, groundwater levels were measured manually before the pressure transducer was taken out.

In addition to the general limitations of slug tests (Table 5.1), an additional problem at the Skaftafellsjökull foreland was the high hydraulic conductivities of the coarse-grained outwash deposits, in which groundwater levels returned very quickly to the levels prior to the slug injection. The quick recovery of groundwater levels made the calculation of the 0.37 time lag a crude estimate (Brassington, 2007). In order to overcome this challenge, the tests were performed at least twice in each borehole.

The analysis of the slug tests was based on the formula suggested by Hvorslev (1951), which was revised by Domenico and Schwartz (1998). Hydraulic conductivity was calculated from the results of the slug tests using Equation 5.1, found in Domenico and Schwartz (1998).

$$K = \frac{r^2 \ln(L/r)}{2LT_0}$$

Equation 5.1. Slug test analysis for calculating hydraulic conductivity (modified from Hvorslev, 1951)

K is hydraulic conductivity (m/day), r is the radius of the borehole (cm), L is the length of the screened section (m) and T_0 is the basic time lag where the head ratio is 0.37 (Hvorslev, 1951). T_0 is determined by h/h_0, where h_0 is the maximum height of the slug and h is the head at the aquifer at time t. T_0 was analysed by plotting time against head ratio on a semi-log paper, and finding the time which corresponded with the 0.37 of the head ratio. As suggested by Brassington (2007), an additional line, parallel to the original, was drawn when the origin did not go through the origin. The head ratio was than determined using the parallel line. Another important assumption of the Hvorslev (1951) method is that the screen is completely below the water table. In order to determine that,

the depth below water table in this study was compared with the height of the top of the screen. It was found that all the top of the screen was below the water table in all the observations at this study, hence, the usage of Equation 5.1 was valid.

5.3.2. Particle Size Analysis (PSA)

Particle Size Analysis (PSA) is based on the important relationship between particle size distribution and the hydraulic conductivity of a hydrogeological unit, which generally increases with coarser particles (e.g. Shepherd, 1989). PSA equations are usually based on a threshold grain size, of which a certain percentage of the sample is finer (Hazen, 1892). For instance, the d_{10}, the particle size at which 10% of the sample is finer, serves as the key input parameter in many PSA empirical relationships (e.g. Hazen, 1892; Krumbein and Monk, 1943; Carrier, 2003). Other equations which use a single parameter are based on the percentage of clay (Puckett *et al*., 1985) or sand and clay particles within a sample (e.g. Rawls and Brakensiek, 1989). However, the latter method is only applicable to soils with maximum 70% of sand. Hence, it is possibly not applicable to coarse-grained glaciofluvial sediments.

The main advantages of PSA are its relatively easy and inexpensive sample collection and analysis. Additionally, the environmental impact of PSA is lower than that of methods which require piezometers (i.e. pumping tests, slug tests) (Table 5.1). However, PSA also has various limitations such as high variability in results, small scale representation of aquifer parameters, and strong dependence on the formula that is used (e.g. Brassington, 2007; Ronayne *et al*., 2012). However, despite these limitations, PSA has been widely used in a variety of hydrogeological settings including fluvial environments (e.g. Song *et al*., 2009), desert alluvium (e.g. Alyamani and Sen, 1993) and proglacial outwash plains (e.g. Robinson *et al*., 2008).

PSA at the Skaftafellsjökull foreland was determined from sediment samples collected as close as possible to the water table (~0.60 m below ground). The samples were collected from lakeshores, relict glaciofluvial channels, the transect area, and from near the piezometers within the monitored area (Figure 3.13). PSA was obtained by a Coulter® LS230 laser Grain Size Analyser (GSA), which provides the volume percentage finer than the following grain sizes: 2, 1, 0.5, 0.25, 0.125, 0.063, 0.003, 0.001, 0.0005, 0.00025, 0.000125, and 0.0000625 mm. However, some of the coarser samples were too angular to be analysed on the GSA. Therefore, the PSA for these samples were obtained by wet sieving, using mesh sizes of 2, 1, 0.5, 0.25, 0.125 and 0.063 mm. These samples contained a very small amount of material below 0.063 mm. Hence, analysis of finer particle sizes was not taken on these samples.

This study compared between three PSA equations, which focus on different particle sizes: Hazen (1892), Puckett (1985), and Alyamani and San (1993). The Hazen (1892) method has been extensively used to estimate the hydraulic conductivity of clean sands, including those from glacial environments (e.g. Hazen, 1892; Robinson *et al*., 2008). The Hazen method estimates hydraulic conductivity based on Equation 5.2:

$$\boldsymbol{K = C(d_{10})^2}$$

Equation 5.2 The Hazen equation (1892)

Where K is hydraulic conductivity (m/day), C is a coefficient based on both grain size and sorting, and d_{10} is the particle size diameter (mm) of which 10% of the sample is finer. When comparing various PSA equations, Bradbury and Muldoon (1990) observed that the Hazen method consistently underestimated field-obtained results by one-two orders of magnitude. However, it also provided the closest results to laboratory measured values, despite a consistent overestimation by one order of magnitude. Additionally, Goodman

(1999) has also reported that the Hazen method predicted lower values and was more consistent than other methods which consider sorting, such as Krumbein and Monk (1943). In addition to its reported relative consistency, the Hazen method was also used in this study because of its previous usage in proglacial environments (e.g. Robinson *et al*., 2008).

In addition to the d_{10}, the Hazen equation also includes an empirical coefficient (C), which is related to sediment grain size and sorting (Brassington, 2007). It has also been suggested that the C parameter is influenced by sediment compaction, with higher Hazen coefficient assigned to looser material (Uma *et al*., 1989). Although it is usually assumed that the coefficient is equal to 100, a review has shown that cited Hazen coefficients can range between 1 and 1000 (Carrier, 2003). However, values as high as 1300 have also been suggested (Brassington, 2007). The C coefficients which were used in the current study were 350 (lowest value suggested) for fine-grained sediments and 1000 for coarse-grained sediments (Brassington, 2007).

The Alyamani and Sen (A&S) (1993) equation was developed in order to overcome the bias problems associated with PSA equations that only use a single parameter. A&S have suggested that finer particles carry a higher physical impact on hydraulic conductivity, hence, the central tendency chosen in a one parameter equation is usually biased toward fine grain sizes. They also suggested that one parameter fails to fully represent the whole grain-size distribution curve. Therefore, a single parameter does not yield consistent results with respect to actual values of hydraulic conductivity (Alyamani and Sen, 1993). In order to overcome these limitations, they developed an alternative approach, which is based on a portion of the curve, using its slope, intercept and the difference between the d_{50} and d_{10} particles (Equation 5.3) (Alyamani and Sen, 1993).

$$K = 1300\,[I_0 + 0.025(d_{50} - d_{10})]^2$$

Equation 5.3. The Alyamani and Sen (A&S) equation (1993).

K denotes hydraulic conductivity (m/day), d_{50} and d_{10} are the grain sizes which are 10% and 50% coarser than the remaining of the sample, respectively. I_0 (mm) is the grain size diameter where the d_{10} and d_{50} values intersect the horizontal axis (Figure 5.3).

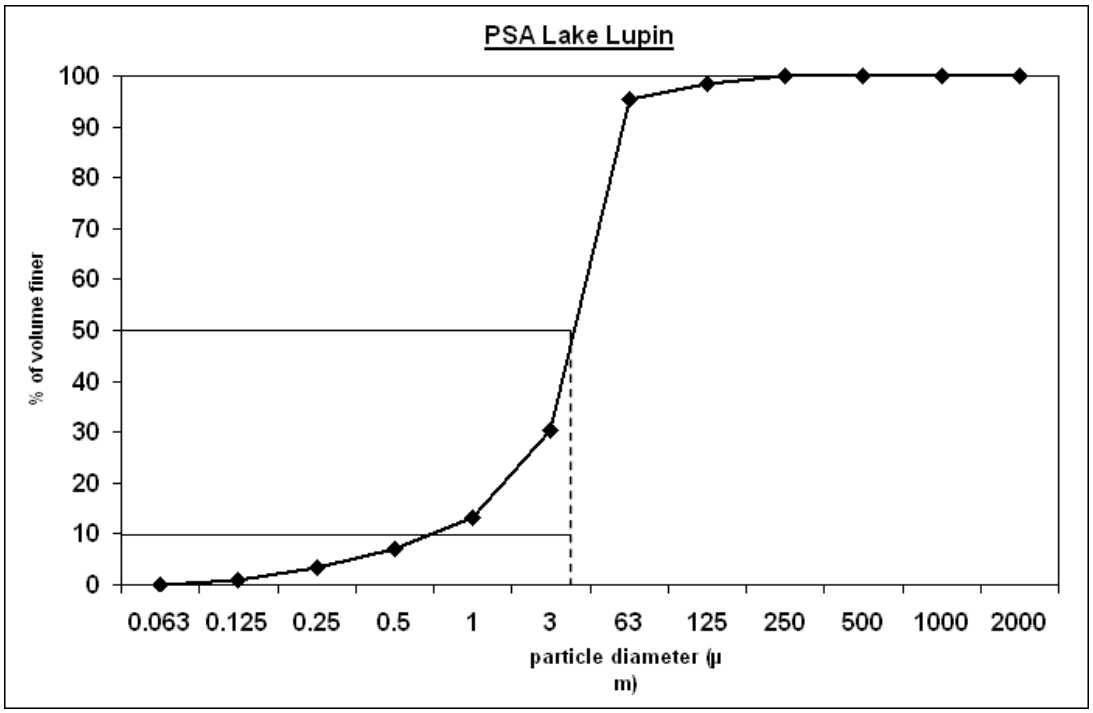

Figure 5.3. Determination of the I_0 (the particle diameter which corresponds to the intersection of d_{10} and d_{50}) from PSA data.

The I_0 is located where the dotted line crosses the x axis.

The third equation for measuring hydraulic conductivity which was tested in this study has been developed by Puckett *et al*. (1985) (Equation 5.4).

$$\boldsymbol{K = \left(4.36 \times 10^{-5}\right) \times e^{(-0.1975 \times \%cl)}}$$

Equation 5.4. The Puckett *et al*. equation (1985)

K is hydraulic conductivity (m/sec) and *% cl* is the percentage of the total sample that is finer than 0.002 mm. The obtained values from this equation were later converted to m/day. This method is specifically designed for sediment with high clay contents. It was chosen due to the high proportion of fine-grained sediment at the Northern Oasis and the eastern lakeshore of the Instrumented Lake.

Sorting was calculated according to Equation 5.5 **(**Folk, 1986).

$$\frac{\sigma_1 = \Phi_{84} - \Phi_{16}}{4} + \frac{\Phi_{95} + \Phi_5}{6.6}$$

Equation 5.5. Calculation of sediment sorting coefficient (after Folk, 1986).

σ_1 is the sorting coefficient and $\Phi_{84}, \Phi_{16}, \Phi_{95}, \Phi_5$ are the phi values at the respective 84, 16, 95, and 5 percentiles. These coefficients are accompanied by a verbal description of the sorting (Table 5.3, Appendix 3).

5.3.3. Constant head permeameter

Hydraulic conductivity for three samples from each hydrogeological environment (Northern Oasis, IL, Southern Oasis lakes, and the Outwash) were tested using a constant head permeameter following British Standard 1377 (1990). Each sample was emplaced in a glass chamber, where water saturated the sample from the top. Pipes connected to manometers were connected above and below the sample, in order to determine the difference in head. However, due to the low availability of samples, the sediment in the chamber was only ~1 cm thick, with gravel filling the rest of the chamber. Water fluxes through the chamber were then measured. These fluxes and head

differences then allowed Darcy's Law to be used to calculate hydraulic conductivity (Equation 5.6).

$$K = \left(\frac{\left(\frac{V}{t}\right) \times l}{(h \times A)} \right)$$

Equation 5.6. Calculation of hydraulic conductivity (*K*) using constant head permeameter

Where K is hydraulic conductivity (cm/sec), v is the volume of water (mL), t is time (sec), l is the length of the sample (cm), h is the difference in head (cm), and A the cross sectional area (cm^2). The results were then converted to m/day.

5.4. Results for the determination of hydraulic conductivity

5.4.1. Spatial variability in grain size

30 sediment samples for PSA were collected from the different hydrogeological environments at the Skaftafellsjökull foreland (Figure 5.4, Appendix 2): The Northern Oasis, the Southern Oasis lakes, the outwash, and the Instrumented Lake (IL). The Northern Oasis consists of the area between the two main channels of the Skaftafellsá meltwater river (Figure 5.1). This area contains several large lakes, which are receding (Figure 3.11), and large moraine complexes. It is mainly underlain by poorly sorted sediment, which consist of fine-grained deposits, cobbles, and boulders (Figure 5.2). The Southern Oasis contains five main lakes, located south of the Skaftafellsá meltwater channel (Figure 5.1). These lakes are generally underlain by pebbles and coarse sands. However, some lakeshores are underlain by finer sediments. These lakes support large amount of flora and fauna. The IL is the northernmost lake within the Southern Oasis. It is

located in a depression, and is surrounded by moraines from the north, south and east. The lakeshores of the IL show a considerable variability in grain size (Tristram *et al*., 2015). The eastern end is underlain by approximately 0.5 m of fine-grained deposits. The western lakeshore is underlain by similar deposits to those of the outwash, hence, it was included in the outwash. The outwash consists of active and relict glaciofluvial channels, underlain by coarse sand and cobbles deposits, which drained the retreating glacier margin of Skaftafellsjökull (Figure 5.1).

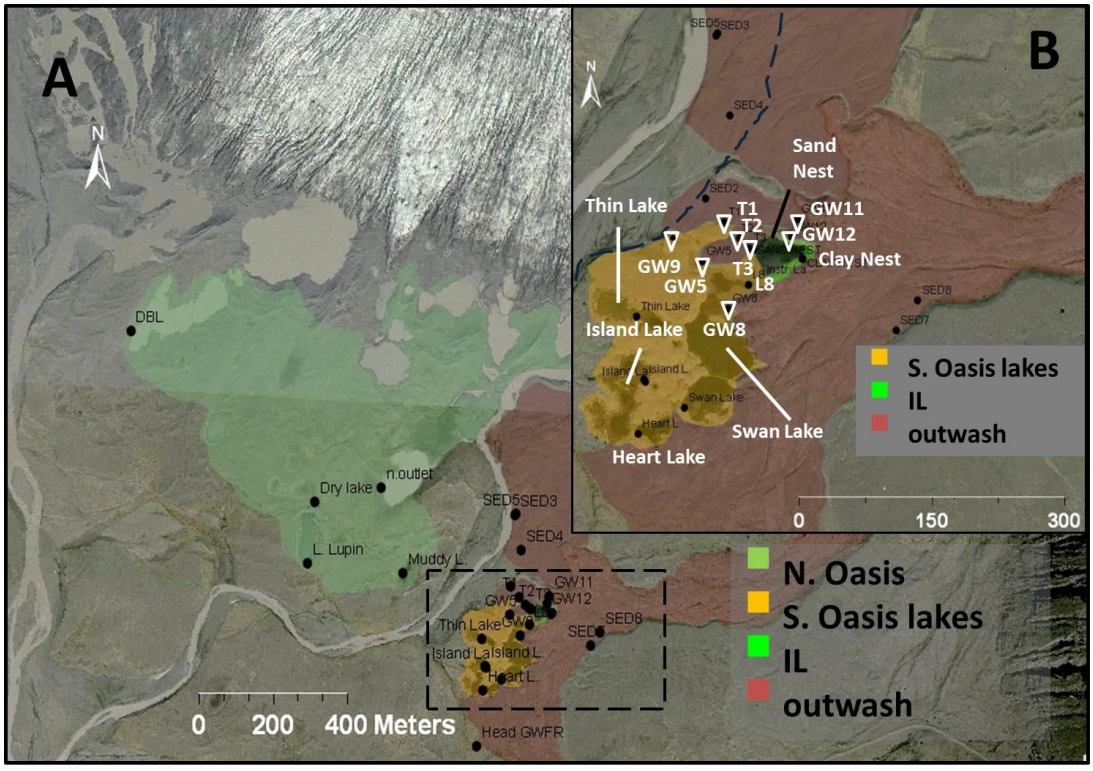

Figure 5.4. Hydrogeological environments and the locations for PSA samples and slug tests at the Skaftafellsjökull foreland.

PSA samples are denoted by black dots. Piezometers in which slug tests were performed are denoted with white triangles. The box in black dashed lines shows the approximate area of Insert B, which zooms in on the Southern Oasis area. The position of the Skaftafellsá channel has shifted since the image was taken. The position of the channel during the field season (June-August 2012) is denoted by the dashed blue line in B. The image was taken from Vatnajökull National Park, 2007.

The procedures for the PSA are described in section 5.3.2. The PSA results show a high heterogeneity in grain size distribution at the Skaftafellsjökull foreland (Figure 5.5). The

samples from the Northern Oasis and the fine-grained lakeshore of the IL have narrow particle size distributions, which consist of very high proportion of fine grain size (<0.063 mm). This is also illustrated by the narrow difference in particle size (0.060 mm) between their d_{10} (0.001-0.015 mm) and d_{90} (0.063 mm) particles (Table 5.2). Although only five samples were collected from the Northern Oasis, excavations suggest that extensive areas of this area site are underlain by poorly sorted deposits of fine-grained sediment and boulders (till) (Figure 5.2).

In contrast to the fine-grained sediments at the Northern Oasis and the IL, the samples from the Southern Oasis lakes and the outwash were much coarser. For instance, the d_{10} for the Southern Oasis lakes and the outwash are 0.070 mm and 0.30 mm, respectively (Figure 5.5). The coarsest grain size in the Southern Oasis lakes and outwash (~2 mm) are also substantially coarser than those from the IL and Northern Oasis (0.063 mm). Additionally, the range of the particle size distributions for these two environments was much wider (~1.7 mm) than that of the Northern Oasis and the fine-grained lakeshore of the IL (Table 5.2). These differences highlight the high sediment heterogeneity at the Skaftafellsjökull foreland.

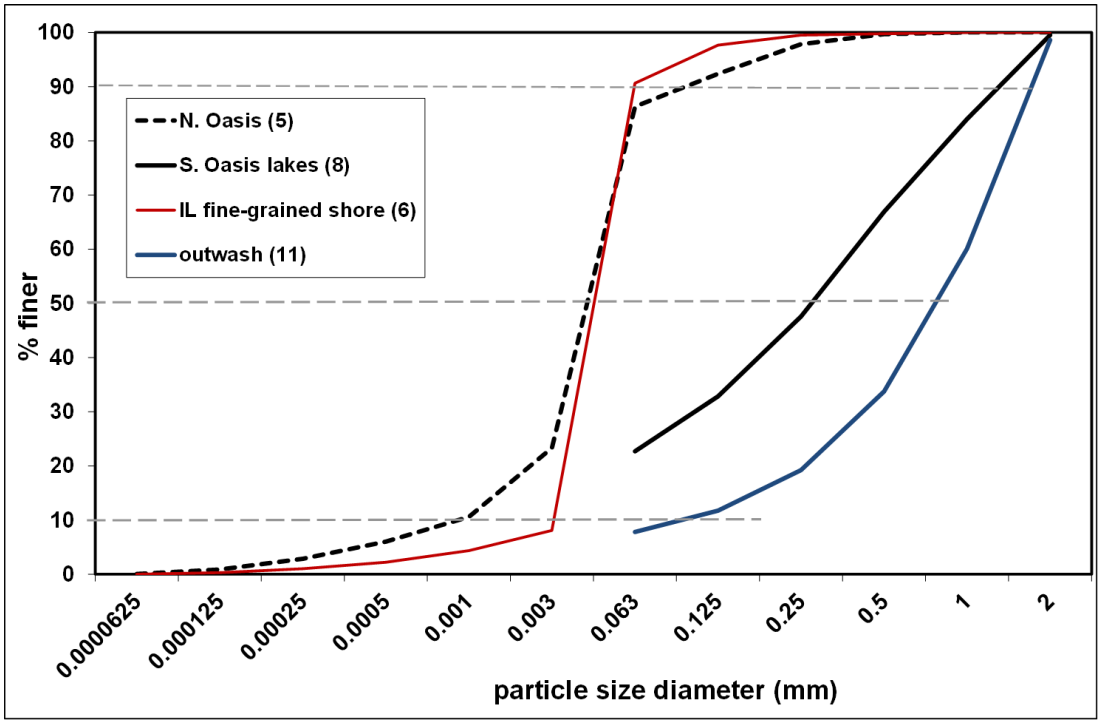

Figure 5.5. Cumulative plot of Particle Size Analysis for the different hydrogeological environments at the Skaftafellsjökull foreland.

The horizontal dashed grey lines show the corresponding d_{10}, d_{50}, and d_{90} for each environment. Note that only wet sieving was done on the S. Oasis lakes and Outwash samples, hence the lowest diameter is 0.063 mm. The brackets in the legend show the number of samples in each environment.

Table 5.2. Mean grain size (mm) and standard deviation for the different hydrogeological environments at the Skaftafellsjökull foreland.

The figures are based on the cumulative PSA distribution. The number of samples in each environment is in brackets.

Grain size (mm)	d_{10}	d_{50}	d_{90}
S. oasis lakes (8)	0.061±0.045	0.311±0.169	1.202±0.558
N. Oasis (5)	0.001±0.001	0.016±0.018	0.081±0.088
IL (6)	0.004±0.001	0.022±0.001	0.063±0.009
Outwash (11)	0.190±0.127	0.834±0.322	1.720±0.236

Sorting was calculated from the PSA results following the method of Folk (1986) (Equation 5.5). The results for the sorting showed that all samples were between very well sorted to moderately well sorted (Table 5.3). The samples with high proportion of fine particles (Northern Oasis and the IL) were very well sorted. However, it is important to note that the values from the Northern Oasis did not include large clasts, which are prevalent in this till-

dominated environment. Based on individual samples and the standard deviation, the highest variability in sorting was found in the Southern Oasis lakes (Table 5.3).

Table 5.3. Mean sorting coefficients and standard deviation in different hydrogeological environments at the Skaftafellsjökull foreland.

Spatial variability in sorting		
Hydrogeological environment	Mean sorting coefficient	Sorting description
N. Oasis	0.041±0.038	Very well sorted
S. Oasis lakes	0.421±0.198	Well sorted
Fine-grained lakeshore of the IL	0.208±0.005	Very well sorted
Outwash	0.584±0.041	Moderately well sorted

.

5.4.2. Comparison of hydraulic conductivity between the PSA equations

The comparison of hydraulic conductivity estimations which were obtained from the three PSA equations and the slug tests is presented in Figure 5.6 and Table 5.4. The Alyamani and Sen (A&S) method obtained the highest mean hydraulic conductivity values ($4.47x10^2$ m/day) and highest standard deviation ($6.86x10^2$ m/day), which exceeded the other methods by one to two orders of magnitude. The Puckett method had the lowest mean and standard deviation ($1.29x10^0$±1.28 m/day), which were one and two orders of magnitude lower than those obtained from the Hazen and A&S equations, respectively. The mean and standard deviation for the Hazen method and the slug tests were within the same order of magnitude ($2.0x10^1$ m/day).

Table 5.4. Mean and standard deviation of hydraulic conductivity from the different methods. The full data set is found in Appendix 4.

Method	Mean hydraulic conductivity (m/day)
Hazen (30)	20.05±38.23
Puckett (18)	1.29±1.28
A&S (30)	447.36±686.79
Slug tests (18)	19.26±19.64
Constant head permeameter (12)	11.15±5.89

The results for all the PSA samples and the falling head tests are presented in Figure 5.6. This shows that both the A&S and Hazen results had very high variability, which ranged over six and seven orders of magnitude, respectively. The slug tests and Puckett estimations ranged over three and four orders of magnitude, respectively. Conversely, the results from the permeameter testing only varied over two orders of magnitude (Figure 5.6). The slug tests had the highest minimum value (8.65×10^{-2} m/day), which exceeds the lowest minimum value estimated by the Hazen equation (1.14×10^{-4} m/day) by two orders of magnitude. The high minimum values obtained by the slug tests are probably explained by the coarse-grained substrates underlain by the piezometers in which slug tests were performed (Figure 5.4). The minimum Puckett and A&S estimations were within the same order of magnitude (1×10^{-2} m/day).

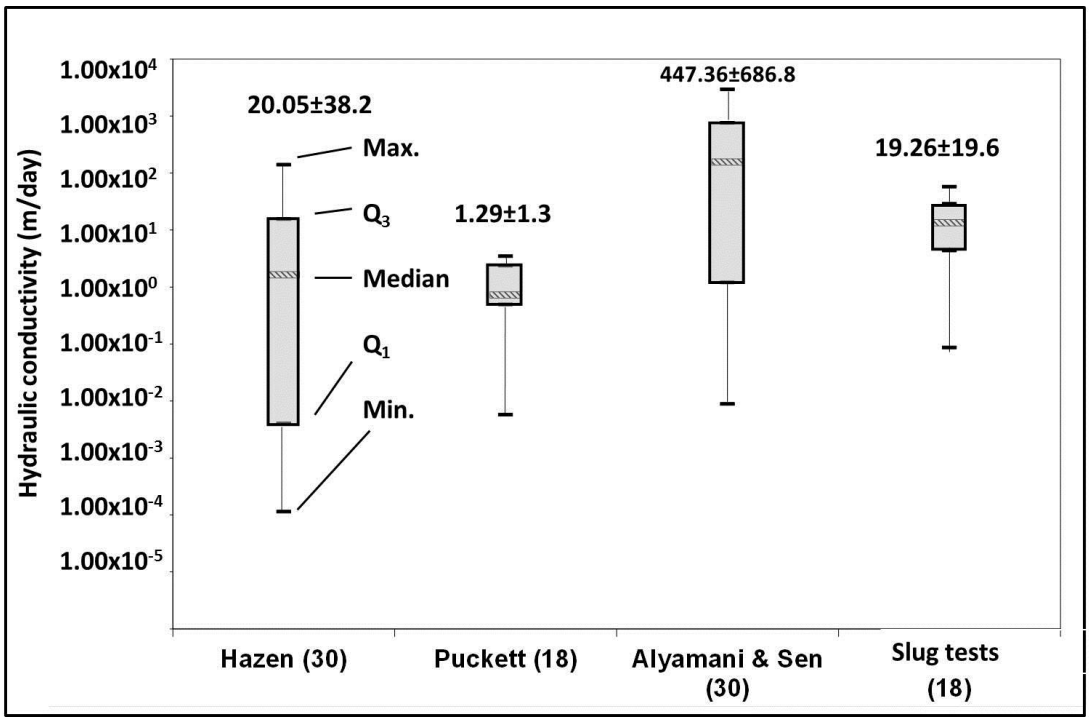

Figure 5.6. Hydraulic conductivity estimations from the three PSA equations and slug tests.

This figure contains all samples. Please note the logarithmic scale. The results from the permeameter tests only varied over two orders of magnitude and, due to the logarithmic scale of the figure, have been omitted for clarity. The numbers of samples for each method are in brackets. The numbers above the box plots denote the mean and standard deviation of each method (m/day).

The hydraulic conductivity values that were obtained from all of the samples are presented in Figure 5.6. However, some samples were not analysed by the Puckett method and slug tests. These omissions were due to the limited amount of piezometers where pressure transducers fit (slug tests) and to the very small proportion of sediment <2 µm (Puckett method) in some environments, particularly in the outwash and Southern Oasis lakes. Therefore, in order to overcome this methodological challenge, and perform a more direct comparison, the results from samples where all three PSA methods were used ("direct comparison") are presented in Figure 5.7.

Similar to the results from all the samples (Figure 5.6), the direct comparisons between the methods also suggest a high variability in hydraulic conductivity between the different methods (Figure 5.7). The hydraulic conductivity values obtained from the direct comparison samples stretched over 3-6 orders of magnitude. The Puckett method had the

lowest mean and standard deviation ($1.29x10^{0}$ m/day), which were one and two orders of magnitude below those of Hazen and A&S, respectively. The mean hydraulic conductivity of each equation for the direct comparison (Figure 5.7) was within the same order of magnitude as that of the total number of samples (Figure 5.6).

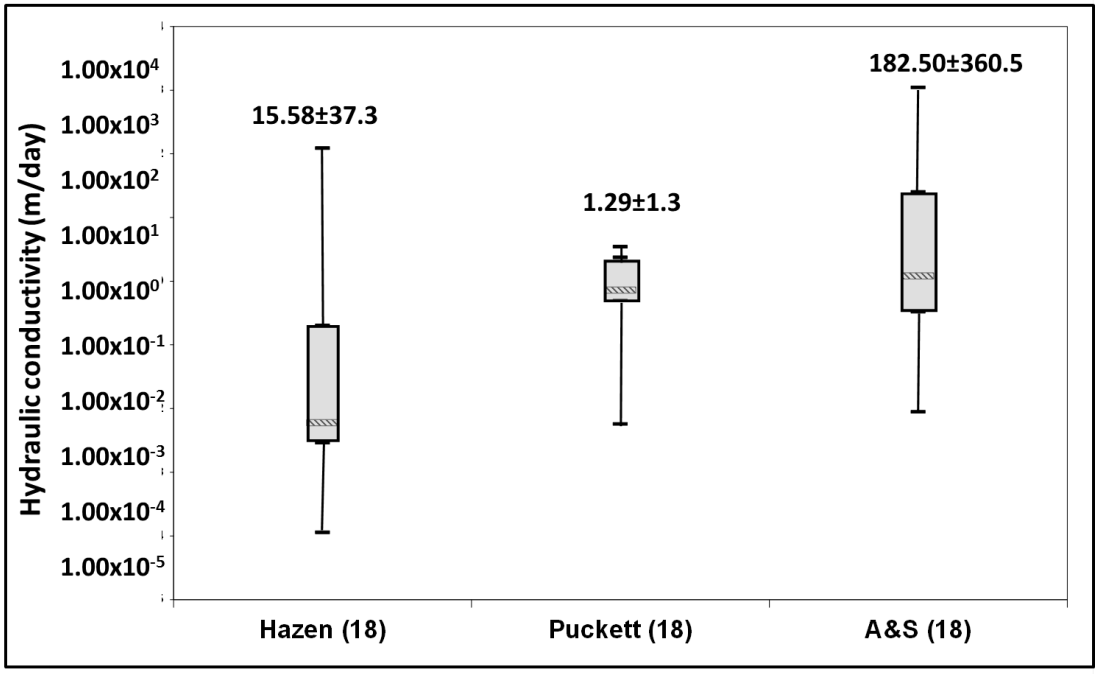

Figure 5.7. Direct comparison of hydraulic conductivity (m/day) for the three PSA equations. The numbers of samples for each method are in brackets. The numbers above the box plots denote the mean and standard deviation (m/day). Note the logarithmic scale.

5.4.3. Slug tests

Hydraulic conductivity estimations from the slug tests spanned over three orders of magnitude ($1.12x10^{-1}$- $4.02x10^{1}$ m/day) (Figure 5.6). The lowest hydraulic conductivity was estimated at GW8 ($1.12x10^{-1}$ m/day), located in relatively fine-grained deposits near the IL. These estimates were very close to the Hazen PSA estimations from this area ($1.00x10^{-1}$ m/day). The relatively low hydraulic conductivity in this area is due to the high proportion of fine-grained deposits in this location, which gets periodically inundated by lake water. These inundations probably increase the deposition of fine- grained sediment, which reduce the hydraulic conductivity.

The hydraulic conductivity in the transect varied around two orders of magnitude ($1x10^0$-$1x10^1$ m/day). The slug tests have shown that hydraulic conductivity increased away from the river, with the highest values estimated at T3 [Figure 5.4] ($4.02x10^1$ m/day). Hydraulic conductivity at the closest borehole to the river (T1) was an order of magnitude lower than at T3 ($4.70x10^0$ m/day). These values and spatial patterns are similar to those reported from other proglacial settings (e.g. Cooper *et al*., 2002; Magnusson *et al*., 2014). For instance, the hydraulic conductivity of the well located next to a meltwater channel in Svalbard was estimated at $3.81x10^0$, and it increased with distance away from the channel (Cooper *et al*., 2002). Similar results were also reported from the forefield of the Damma Gletscher (Swiss Alps), where slug tests estimated hydraulic conductivity to vary between $5.4x10^0$ – $4.23x10^1$ m/day (Magnusson *et al*., 2014).

GW11 and GW12 are located between two moraines, in an area underlain by coarse glaciofluvial deposits and relict channels (Figure 5.1). The substrate where these piezometers are located is similar to that of the transect, albeit being located further from the river. The hydraulic conductivity at GW11 and GW12 was very similar ($1.5x10^1$ m/day). These results are also within the same order of magnitude as the hydraulic conductivity of T3, located in a coarse-grained substrate near the IL. The hydraulic conductivity at GW5, located in coarse-grained glaciofluvial deposits 38 m away from the Skaftafellsá, was $1.51x10^0$ m/day. Although this was the lowest hydraulic conductivity in the outwash, these results are within the same order of magnitude as the estimated hydraulic conductivity for T1 and T2 (Table 5.5). Additionally, the results of the slug test for T3 were within the same order of magnitude as the mean Hazen hydraulic conductivity for the outwash. In summary, the results of the slug tests were generally within the same order of magnitude as those obtained from the Hazen equation.

Table 5.5. Mean hydraulic conductivity and standard deviation for the slug tests.

The brackets denote the number of samples. The table also presents comparison of PSA results from areas which were near the piezometers where slug tests were performed.

Borehole	**Mean slug test hydraulic conductivity (m/day)**		
GW8 (2) (relatively fine-grained lacustrine deposits)	0.11±0.04		
GW5 (2) (glaciofluvial deposits)	1.51±0.3		
GW11 (1) (glaciofluvial deposits)	15.72		
GW12 (1) (glaciofluvial deposits)	14.42		
T1 (3) (glaciofluvial deposits)	4.70±0.4		
T2 (2) (glaciofluvial deposits)	9.06±4.7		
T3 (7) (glaciofluvial deposits)	40.16±14.3		
Hydraulic conductivity (m/day)	**Hazen**	**Puckett**	**A&S**
GW8 (1)	0.10	1.52	8.55
Mean S.N. (3) (glaciofluvial deposits)	92.58	3.44	915.89
Mean outwash (4)	61.01		1148.72

5.4.4. Constant head permeameter

Hydraulic conductivity estimations from the permeameter ranged between $4.97x10^{0}$ and $2.45x10^{1}$ m/day. The mean *K* estimations from the permeameter was $1.15x10^{1}$±5.89 m/day, which lies within the same order of magnitude of the slug tests and Hazen estimations (Table 5.5). However, in contrast to the PSA, where substantial differences between the hydrogeological environments were observed, the results of the permeameter only stretched over two orders of magnitude (Figure 5.8).

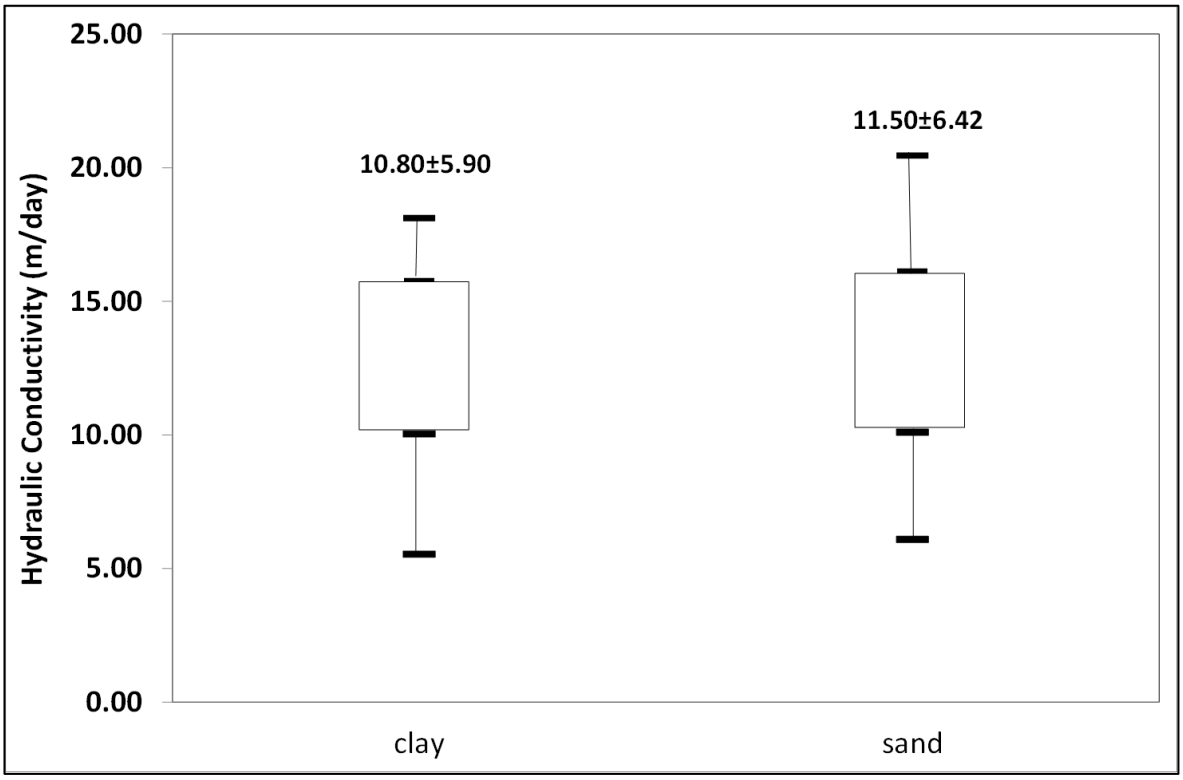

Figure 5.8. Hydraulic conductivity estimates (m/day) obtained from constant head permeameter laboratory tests.

The numbers above the box plots denote the mean and standard deviation of each method (m/day). Both sand and clay contained 6 samples.

5.4.5. Choice of preferred method for estimating hydraulic conductivity

The direct comparisons of the results shows that the mean hydraulic conductivity for the Puckett and A&S equations were generally the lowest and highest, respectively. The Hazen estimations were in the middle, with mean hydraulic conductivity an order of magnitude higher and lower than the Puckett and A&S estimations, respectively (Figure 5.7). The estimations of hydraulic conductivity from the slug tests and permeameter were generally closest to the Hazen estimations (Table 5.5). However, the slug tests were only conducted in relatively coarse-grained areas. Conversely, the results from the Puckett and A&S were generally at least an order of magnitude lower and higher, respectively (Table 5.4When choosing the most appropriate method for the estimation of hydraulic conductivity, the main limitation of the A&S equation was its high estimations and

variability (Figure 5.6). The main limitation of the Puckett method is its unsuitability for areas containing low proportion of fine-grained sediments. The main limitation of the slug tests was its limited spatial coverage. Although the permeameter included samples from all hydrogeological environments, the differences between the different environments were small, failing to capture the expected heterogeneity in hydraulic conductivity of proglacial sediments that has been displayed by the PSA (Figure 5.6). It is suggested that this is due to limitations with the method, such as the need to emplace the sample on top of gravel layers, which leads to preferential flow paths, which increase the flow. In light of these limitations, it was therefore decided to use the hydraulic conductivity estimations which were obtained from the Hazen equation due to its past usage in similar environments (e.g. Robinson *et al*., 2008) and its nearest agreement to the falling-head tests.

5.5. Spatial variability in hydraulic conductivity at the Skaftafellsjökull foreland

This section describes the spatial variability in hydraulic conductivity at the Skaftafellsjökull foreland. These results are based on the Hazen PSA estimations of hydraulic conductivity. Similar to other studies from proglacial environments (e.g. Robinson *et al*., 2008; Bajc *et al*., 2014), the hydraulic conductivity at the Skaftafellsjökull margin has also shown wide spatial variability.

The hydraulic conductivity estimations at the Skaftafellsjökull foreland varied over seven orders of magnitude ($1x10^{-4}$ – $1x10^{2}$ m/day), with large differences between the Northern and Southern Oasis (Figure 5.9). The lowest hydraulic conductivity was estimated in areas underlain by high proportion of fine-grained sediment such as the Northern Oasis lakes and the eastern lakeshore of the IL (Figure 5.9). The lowest mean hydraulic conductivity was measured in the Northern Oasis (approximately $7.28x10^{-3}$ m/day). These estimations were two orders of magnitude lower than the mean hydraulic conductivity for

the fine-grained lakeshore of the IL. The Northern Oasis also had the smallest variability in hydraulic conductivity.

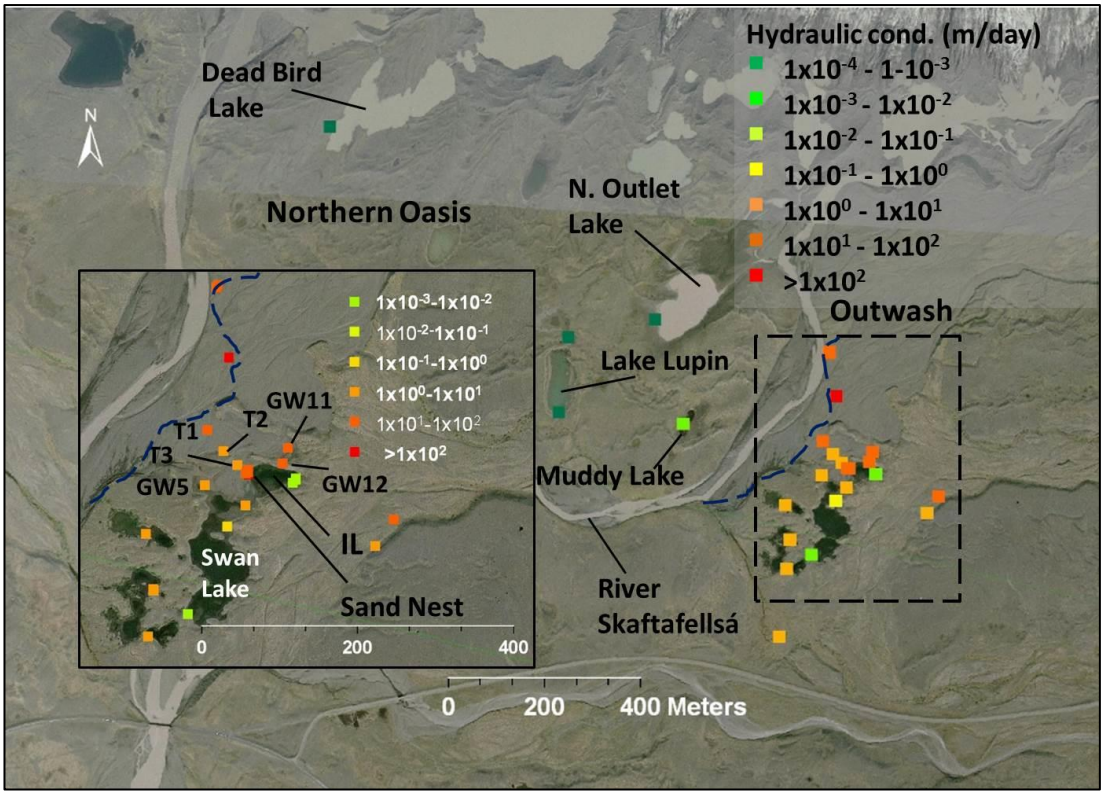

Figure 5.9. The spatial distribution in hydraulic conductivity (m/day) at the Skaftafellsjökull foreland.

Note the logarithmic scale. These results are based on the results from the Hazen equation. The hydraulic conductivity of the Southern Oasis (dashed box) is shown in more detail within the black box. The position of the Skaftafellsá channel has shifted since the image was taken. The position of the channel during the field season (June-August 2012) is denoted by the blue dashed line. The image was taken from Vatnajökull National Park, 2007.

The hydraulic conductivity estimations from the IL (7.28×10^{-3} m/day) and the Northern Oasis (3.79×10^{-4} m/day) exceeded the values suggested by Brassington (2007) for glacial clay by one and two orders of magnitude, respectively (Figure 5.9). Slug tests estimated that the hydraulic conductivity of till from the Burroughs Glacier in Alaska to be around 1×10^{-2} m/day (Simpkins and Mickleson, 1990). However, these samples contained a high proportion of sand, which probably explains the hydraulic conductivity estimations being one-two orders of magnitude higher than those measured in the Skaftafellsjökull foreland. In contrast to the relatively high hydraulic conductivity of till reported from the Burroughs

Glacier, the hydraulic conductivity of clay-rich Quaternary glacial till deposits from East Anglia ($3.46x10^{-4}$-$4.23x10^{-6}$ m/day) were lower than those from the Skaftafellsjökull foreland (Hiscock and Tabatabi Najafi, 2011). Observations of glacial till from Shropshire were also lower than those from the Skaftafellsjökull foreland, with median hydraulic conductivity of approximately $1.73x10^{-5}$ m/day (Cuthbert *et al*., 2010). These estimates are between one and three orders of magnitude lower than the estimations from the IL and up to two orders of magnitude lower than the Northern Oasis (Figure 5.9).

The hydraulic conductivity of till can vary over a very wide range, typically between $8.64x10^{-3}$-$8.64x10^{3}$ m/day (Freeze and Cherry, 1979). Another summary has estimated an even higher variability, where hydraulic conductivity ranges between $6.91x10^{-7}$-$1.73x10^{3}$ m/day (Piotrowski, 2007). The hydraulic conductivity of the IL is ranked at either the lower end of the ranges suggested by Freeze and Cherry (1979) or at the lower-mid range for that of Piotrowski (2007). The Northern Oasis estimations are an order of magnitude lower than the till estimates of Freeze and Cherry's (1979) range and at the low-mid range of Piotrowski (2007). However, the low hydraulic conductivity of till from the Skaftafellsjökull foreland can be possibly attributed to its relatively young age, in which the impact of secondary processes (such as oxidation) is lower (e.g. Hiscock and Tabatabi Najafi, 2011). These low hydraulic conductivity estimations and observations from the Northern Oasis (Figure 5.2) suggest that it is underlain by fine-grained sediments of low hydraulic conductivity. Furthermore, it is hypothesised that these lakes are perched above the regional groundwater system.

The (geometric) mean hydraulic conductivity in the Southern Oasis is $1.21x10^{0}$ m/day. The variability of hydraulic conductivity in the Southern Oasis ranges over seven orders of magnitude (Figure 5.9). This high variability in hydraulic conductivity can be illustrated at the IL, where hydraulic conductivity varied over five orders of magnitude ($3.9x10^{-3}$-$9.26x10^{1}$ m/day). However, intermediate hydraulic conductivities were estimated at GW8 and L8. These locations have relatively high proportions of silt-sized sediment, which

possibly originated from temporary inundation by the lake. The hydraulic conductivity of lakeshores in the Southern Oasis are generally in the range of $1.00x10^{0}$ to $1.00x10^{1}$ m/day. These areas are situated further away from the Skaftafellsá, and are also surrounded by moraines, which possibly shelter them from diurnal and seasonal fluctuations in meltwater discharge, which control sediment entrainment and deposition. *K* estimations for the Southern Oasis lakes were within the same order of magnitude as those for moraine lake basins from Skeiðarársandur [Table 5.6] (Robinson *et al*., 2008).

The highest hydraulic conductivity at the Skaftafellsjökull foreland was estimated at the outwash areas, where hydraulic conductivity ranged between $1x10^{1}$-$1x10^{2}$ m/day. The mean hydraulic conductivity for the outwash was $1.76x10^{1}$ m/day (Table 5.6). This environment is mainly underlain by active and relict braided glaciofluvial channels, where the coarsest grain sizes (mean d_{10} of 0.19 mm) were measured (Figure 5.5). The estimates of hydraulic conductivity from the outwash are within the same order of magnitude for glacial sands and gravels (Brassington, 2007). These estimates are also very close to estimates from the outwash areas of Skeiðarársandur ($4.50x10^{1}$ m/day) and are within the same order of magnitude as the hydraulic conductivity of proglacial channels at Skeiðarársandur ($2.80x10^{1}$ m/day) (Robinson *et al*., 2008). The hydraulic conductivity at the forefield of the Damma Gletscher forefield in Switzerland (Magnusson *et al.,* 2014) is also within the same orders of magnitude as the current study (Table 5.6). Conversely, the hydraulic conductivity estimations of most samples from the Skaftafellsjökull outwash are higher by an order of magnitude than those of sandur deposits from Svalbard ($5.19x10^{0}$ m/day) (Cooper *et al*., 2002; 2011).

In summary, this section described the spatial variability in hydraulic conductivity at the different hydrogeological environments of the Skaftafellsjökull foreland. The results illustrate the high heterogeneity of hydraulic conductivity at the Skaftafellsjökull foreland, which was observed even on small spatial scales (e.g. between the lakeshores of the IL). These observations support previous studies which highlighted the high heterogeneity of

glacial deposits (e.g. Anderson, 1989; Bajc *et al*., 2014). This high variability also reiterates the importance of the sampling location and methodology for the determination of hydraulic conductivity (e.g. Ronayne *et al*., 2012). The estimations of hydraulic conductivity for the fine-grained areas from this site were either within the middle to low position in the range suggested by Piotrowski (2007) or slightly lower than the range suggested by Freeze and Cherry (1979). The hydraulic conductivity estimations for coarse-grained locations at the Skaftafellsjökull foreland are within the same order of magnitude as those reported from Skeiðarársandur (Robinson *et al*., 2008), the Swiss Alps (Magnusson *et al*., 2014) and the values suggested by Brassington (2007) [Table 5.6].

Table 5.6. Comparison of hydraulic conductivity from glaciated and deglaciated catchments

Study	**Hydraulic conductivity (m/day)**
Skaftafellsjökull foreland (geometric mean)	
N. Oasis (5)	0.00038±0.001
S. Oasis lakes (8)	1.42±2.54
IL (6)	0.0073±0.01
Outwash (11)	17.57±50.56
Total Southern Oasis (25)	1.21±40.62
Brassington (2007)	
Glacial sands and gravel	10-100s
Glacial clay, till and varved clay	0.864
Skeiðarársandur (Robinson *et al*., 2008)	
Moraines	11.6 (combined)
Moraine relief	14.2
Moraine seeps	7.1
Moraine lake basins	16.8
Proglacial basin, inundated by 1996 jökulhlaup, >0.5 km from the margin	33.9
Proglacial river channels	26.6
Svalbard (Cooper *et al*., 2002; 2011)	
Well 1, sandur fluvial sed. Fine and silt on channel floodplain, 5 m from channel	3.81
Well 3, poorly sorted gravely sand moraine, 118m from channel	38.02
Sandur sediment	5.19
Moraine complex sediment	35.25
Burroughs Glacier, Alaska (Simpkins and Mickleson (1990) Till. 57% sand, 36% silt, 7% clay	0.086
Clay rich Quaternary deposits, East Anglia (Hiscock and Najafi, 2011)	$3.46X10^{-4}$-$4.23x10^{-6}$m/day $1.73x10^{-5}$
Damma Gletscher forefield (Swiss Alps) (Magnusson *et al*., 2014) Alpine proglacial channel, generally coarse (sand-cobbles)	5.4-42.3m/day
Proglacial moraine material, Canadian Rockies (Langston *et al*., 2013)	$(8.64x10^{1)}$

5.6. Calculations of hydrogeological parameters for the Skaftafellsjökull foreland aquifer

5.6.1. Equations for the calculations of aquifer parameters

This section builds on the results from previous sections and other studies to calculate the aquifer volume, groundwater discharge, and groundwater velocity of the Skaftafellsjökull foreland aquifer. These parameters are important for understanding the regional proglacial groundwater flow systems.

Groundwater discharge is governed by Darcy's (1856) Law (Equation 5.7):

$$Q = KA\left(\frac{dh}{dl}\right)$$

Equation 5.7. The calculation of groundwater discharge fluxes (Darcy, 1856).

Where Q denotes groundwater flow flux (m^3/day), *K* is the hydraulic conductivity (m/day) , *A* the flow cross-sectional area (m^2), and *dh/dl* (unitless) the hydraulic gradient (Darcy, 1856).

Matrix properties are fundamentally important in determining groundwater flow. Porosity is the void space within the matrix, and is expressed as a percentage of the void volume over the total volume. Porosity is affected by both the initial depositional environment and secondary processes such as compaction, fracturing, and dissolution. Effective porosity is a key hydrogeological parameter, which describes the percentage of pores that are interconnected. Permeability describes the ease with which fluid can flow through a porous substrate. When fluid transport is considered, effective porosity serves as a better surrogate for permeability than total porosity (Domenico and Schwartz, 1998).

Groundwater flow equations usually address permeability by the hydraulic conductivity term, which is a function of both fluid properties (such as density and viscosity) and the substrate permeability. The *dh/dl* term (Equation 5.7) is the difference in hydraulic head over a distance, also known as the hydraulic gradient. The hydraulic gradient is derived from the total head (*dh*) (the sum of elevation head, pressure head and velocity head) over the distance between the measuring points (*dl*).

The calculations of aquifer key parameters (objective 3) such as aquifer groundwater discharge (Equation 5.7), the volume of water in the aquifer (Equation 5.8), and groundwater velocity (Equation 5.9) can be made when the hydraulic conductivity, hydraulic gradient, porosity and aquifer dimensions are known or well estimated. The volume of groundwater within the aquifer is calculated by Equation 5.8:

$$V = T \times W \times L \times S$$

Equation 5.8. Calculation of aquifer volume

V is the volume of groundwater in the aquifer (m^3), *T* is aquifer thickness (m), W is aquifer width (m), *L* is aquifer length (m), and S is the specific yield (%), which is the amount of water that is drained from the aquifer in response to a drop in the groundwater table (e.g. Freeze and Cherry, 1979). Groundwater velocity is calculated by Equation 5.9:

$$v = \left(\frac{K}{\frac{h}{\alpha l}} \right)$$

Equation 5.9. Calculation of groundwater velocity.

Where *v* is groundwater velocity (m/day), *K* is hydraulic conductivity (m/day), α is effective porosity (%) and *dh/dl* is the hydraulic gradient (unitless).

5.6.2. Choice of input parameters for the calculation of aquifer properties

This section describes the rationale for choosing the input parameter for the calculations of hydraulic conductivity, hydraulic gradient, and aquifer thickness of the Skaftafellsjökull foreland (Equations 5.6-5.8). The chosen parameters for Equations 5.7-5.9 are summarised in Table 5.7. The chosen hydraulic conductivity (*K*) inputs were the mean Hazen from the Southern Oasis. In order to account for the variability of hydrogeological parameters at the site, all measurements from the Southern Oasis were used (outwash, lakes and IL), including those from the areas underlain by fine-grained areas (Figure 5.9). The calculations using Darcy's Law also assumed that the aquifer is isotropic and homogenous (Freeze and Cherry, 1979).

The difference in hydraulic head (*dh)* was mapped from the patterns of groundwater horizontal flow at the site, with groundwater flowing from high to low hydraulic heads. Similar to other proglacial environments (e.g. Bahr, 1997; Robinson *et al*., 2008), the regional groundwater flow at the Skaftafellsjökull foreland also flows away from the margin. Hence, groundwater generally flows from north to south. Additionally, a local groundwater system has been identified at the transect, between the River Skaftafellsá and the IL (Figure 5.1). The detailed description of groundwater levels and flow paths are given in Chapter 7. Having measurements of hydraulic head from near the glacier margin would of provided a better understanding of the hydraulic gradient at the site. However, this was not possible due to the difficulties in installing piezometers closer to the glacier

margin. Therefore, considering the north-south direction of the regional groundwater flow, the head difference (*dh*) component of the hydraulic gradient (*dh/dl*) was the mean difference in heads between the most northerly (GW10) and most southerly piezometers (GW8). The distance between these piezometers (*dh*) is 150 m (Figure 3.18).

The estimation of aquifer thickness is one of the key parameters for calculating groundwater fluxes (Equation 5.7) and aquifer volumes (Equation 5.8) (e.g. Domenico and Schwartz, 1998). However, this study did not benefit from measurements of aquifer thickness which have been obtained from seismic geophysics (Guðmundsson *et al*., 2002; Robinson *et al*., 2008) or active layer depth in aquifers underlain by permafrost (Cooper *et al*., 2002; 2011). Previous geophysical measurements from the areas near the snouts of Skeiðarársandur and Svínafellsjökull suggested sediment depths of approximately 70-80 m. Sediment depths then increase with distance from the margin, reaching between 200-250 m at the coast (Guðmundsson *et al*., 2002). Other estimates from Svínafellsjökull also suggested similar depths to bedrock (Ó Dochartaigh, 2012, personal communication). Seismic data suggested that sediment depths to the southwest of the Skaftafellsjökull foreland, close to the Skeiðará bridge (Figure 3.2), are approximately 160-200 m (Guðmundsson *et al*., 2002). However, this location is further away from the glacier margin than the current field site, hence, these reported depths are possibly thicker. As the Skaftafellsjökull proglacial area is substantially smaller than Skeiðarársandur, and is not underlain by thick jökulhlaup deposits, it is assumed that the depth to bedrock at the Skaftafellsjökull foreland will be shallower. Since the geomorphic setting of Svínafellsjökull is similar to that of Skaftafellsjökull, it was decided to use 75 m for the aquifer thickness, as it is the middle value between the approximations of sediment depths reported from near the margin of Svínafellsjökull (Guðmundsson *et al*., 2002). The specific yield and porosity values for the current calculations were the same as used for Skeiðarársandur (Bahr, 1997; Robinson, 2003). These values were chosen because the hydraulic

conductivity at the Skaftafellsjökull foreland and Skeiðarársandur was within the same order of magnitude (Table 5.6).

Table 5.7. Chosen parameters for the calculation of the hydrogeological properties of the Skaftafellsjökull foreland aquifer.

Symbol	Parameter	Value	source
K	Mean(geometric) hydraulic conductivity (m/day)	1.211	This study
W	Aquifer width (m)	1300	This study
L	Aquifer length (m)	2500	This study
T	Aquifer thickness (m)	75	This study
A	Cross sectional area [length x depth] (m^2)	97500	This study
h	Mean head difference (unitless)	0.544	This study
l	Length of head difference (m)	150	This study
S	Specific yield (%)	25	Brassington (2007)
α	Effective porosity (%)	45	Bahr (1997)

5.6.3. Aquifer parameters of the Skaftafellsjökull foreland

The results for the calculations of hydrogeological parameters are provided in Table 5.8. Groundwater velocity for the Southern Oasis (0.033 m/day) was an order of magnitude lower than that of Skeiðarársandur (0.21 m/day; Robinson, 2003). The groundwater discharge for the Skaftafellsjökull foreland (0.0496 m^3/sec) was an order of magnitude lower than that calculated for Hoffelsandur, SE Iceland (Hjulström, 1955). Groundwater discharge estimates for Skeiðarársandur (3.7 $m^{3/}$sec; Robinson, 2003) exceeded that of those from the current study by three orders of magnitude. The hydraulic conductivity used for Skeiðarársandur was within the same order of magnitude as this study. However, the aquifer volume for the Skaftafellsjökull foreland was three orders of magnitude lower than that of Skeiðarársandur ($2.3x10^{10}$ m^3; Robinson, 2003) (Table 5.8). The lower

estimations for the Skaftafellsjökull foreland are due to its substantially smaller aquifer size and narrower sediment layers, which are mainly due to the lack of jökulhlaups and the smaller sandur area. With regards to the contribution of groundwater discharge to catchment water balance, measurements from Skeiðarársandur suggest that the discharge of the glacial melt rivers (Churski, 1973) exceed the groundwater discharge by two orders of magnitude (Robinson, 2003). Small groundwater contributions to catchment water balance have also been reported from a sandur in Svalbard, where calculated subsurface fluxes accounted for only around 1% (11 mm) of the total annual water flux (Cooper *et al*., 2011). However, this catchment is underlain by permafrost, which substantially reduces the aquifer thickness and hydraulic conductivity, which subsequently reduces aquifer volume (Equation 5.8) and groundwater discharge (Equation 5.7).

The main sources of uncertainty in these calculations are those associated with the determination of hydraulic conductivity and the estimation of aquifer thickness and specific yield at the Skaftafellsjökull foreland site. Due to these uncertainties, and the high spatial heterogeneity which was found at the Skaftafellsjökull foreland, the obtained groundwater discharge, velocity, and aquifer volume (Table 5.8) can only remain as plausible estimations.

Table 5.8. Calculated aquifer parameters for the Southern Oasis.

Regional groundwater discharge (Q)	4.28×10^{2} m^3/day = 4.96×10^{-3} m^3/sec = 1.56×10^{6} m^3/annum
Volume of water stored in aquifer (V)	6.09×10^{7} m^3
Regional velocity (arithmetic)	0.033 m/day

5.7 Chapter conclusions

This chapter provided a hydrogeological framework for the Skaftafellsjökull foreland field site (objective ii). This framework was based on both field and laboratory measurements and an evaluation of the relict and active depositional environments which impact the site. The hydraulic conductivity at the site was estimated from field (slug tests) and laboratory (PSA equations) techniques. The results suggested high variability in estimated values, with Hazen's equation generally providing the lowest and least varied estimations. The results of the slug tests and permeameter were generally within the same order of magnitude as the Hazen estimations for coarse-grained samples. However, the permeameter failed to capture the substantial differences in hydraulic conductivity between the fine and coarse-grained samples. Due to these limitations, the Hazen results were chosen for the estimation of hydraulic conductivity.

This study highlighted the high spatial heterogeneity in the hydrogeology of the Skaftafellsjökull foreland, with hydraulic conductivity ranging over seven orders of magnitude. This variability was especially pronounced between the Northern and Southern Oasis areas. The Northern Oasis is underlain by layers of fine-grained deposits, with low hydraulic conductivity (~$1x10^{-4}$ m/d). Conversely, the Southern Oasis is much more heterogeneous, and contains areas of fine and coarse-grained sediments. The mean hydraulic conductivity for the Southern Oasis was $1.21x10^{0}$ m/d. The outwash area had the highest hydraulic conductivity, impacted by the entrainment and deposition of coarse-grained sediment in the relict and active meltwater channels. However, areas of low hydraulic conductivity were also observed in the Southern Oasis, particularly around the IL. The calculated hydraulic conductivity reported in this chapter is generally similar to that reported from Skeiðarársandur and the Swiss Alps.

The groundwater discharge, velocity, and aquifer volume were lower than Skeiðarársandur (Robinson *et al*., 2008). However, despite the lower groundwater discharge and smaller aquifer at Skaftafellsjökull, the aquifer does store and transports substantial amount of groundwater. Understanding these hydrogeological parameters is important for the understanding of regional groundwater systems and dynamics, geochemical fluxes and groundwater-surface water exchange processes. The hydrogeological framework provided in this chapter provides a foundation for the understanding of groundwater dynamics and groundwater exchange with meltwater (objective iv) and lakes (objective v).

6. The Geochemistry and isotopic (δH and $\delta^{18}O$) composition of groundwater and surface water at the Skaftafellsjökull foreland

6.1. Introduction

This chapter describes the spatial and temporal variability in groundwater and surface water quality (sections 6.3 and 6.4) and stable isotope (δD and $\delta^{18}O$) composition (section 6.5) at the Skaftafellsjökull foreland. Groundwater and surface water quality and isotopic composition are usually substantially different within catchments which are dominated by snow and icemelt (e.g. Robinson *et al*., 2009a, b). These differences have been previously used to investigate the configuration and seasonal evolution of the subglacial drainage system (e.g. Collins, 1978; Sharp, 1991; Tranter *et al*., 1993; 1996; Brown, 2002; Hindshaw *et al*., 2011), sources of groundwater recharge (e.g. Roy and Hayashi, 2008; 2009; Robinson *et al*., 2009b), hydrological pathways (Boucher and Carey, 2010; Dragon and Marciniak, 2010; Carey *et al*., 2013; Marciniak *et al*., 2014), quantifying proglacial weathering, and identifying solute sources (Tranter *et al*., 1993; 1997 Fairchild *et al*., 1999a, b; Wadham *et al*., 2001; Pogge van Strandmann *et al*., 2006; 2008; Wimpenny *et al*., 2010, 2011). Water geochemistry and stable isotopes were also used to assess the impacts of climate change and glacier retreat on groundwater and surface water quality in regions dominated by ice and snow melt (Dragon and Marciniak, 2010; Fortner *et al*., 2011; Okkonen and Kløve, 2012), and to investigate proglacial groundwater-surface water exchange (e.g. Ward *et al*.,1999; Brown *et al*., 2007a; Roy and Hayashi, 2008; 2009; Gooseff *et al*., 2013). Water quality and isotopic composition were therefore employed in this study in order to investigate the hydrological exchange between groundwater and

meltwater (objective iv) and groundwater and lakes (objective v) at the Skaftafellsjökull foreland. Water stable isotopes were used in this study to investigate the sources of recharge for groundwater and surface water at the Skaftafellsjökull foreland (objective iii).

6.1.1. The mechanisms of proglacial geochemical weathering

Glaciated catchments have high rates of chemical denudation, which are maintained by the rapid flow and large supply of meltwater, ample supply of fine-grained reactive material, and reactive mineral surfaces (Tranter, 1982; Tranter *et al*., 1993; Wadham *et al*., 2001; Cooper *et al*., 2002; Wolff-Boenisch *et al*., 2009; Wimpenny *et al*., 2010). These high rates are maintained despite the generally low temperatures, short residence time of liquid water and thin vegetation and soil cover commonly found in glaciated catchments (Tranter, 1982; Wongfun *et al*., 2013). The input of solutes from the chemical weathering of rock material into the proglacial zone leads to a sharp enrichment in solute fluxes over relatively short distances (e.g. Brown, 2002; Hindshaw *et al*., 2011). For instance, observations from Finsterwalderbreen, SW Svalbard, have reported a 30-47% increase in solute fluxes between the glacier margin and the catchment outlet, a distance of approximately 2.5 km (Wadham *et al*., 2001). Meltwater chemistry is dominated by low water contact times and highly incongruent weathering, which involves the formation of alteration products (Wadham *et al*., 2001; Cooper *et al*., 2002; Robinson *et al*., 2009b). The main cations in meltwaters are Ca^{2+}, Na^{+}, Mg^{2+}, and K^{+}. The main anions are SO_4^{2-} and HCO_3^{-} (e.g. Tranter *et al*., 1993). Meltwater solute concentrations are generally substantially lower than groundwater solute concentrations (e.g. Tranter *et al*., 1993; 2002; Wadham *et al*., 2007). The greater solute concentrations in groundwater has been attributed to the longer residence time of groundwater, and high rock/water contact time and ratio (Tranter *et al*., 1993; Malard *et al*., 2001; Gooseff *et al*., 2003; 2006). Groundwater only contributes small amounts to the water balance of glaciated

catchments, with meltwater providing the most water (Cartwright and Harris, 1981; Fairchild *et al*., 1999a, b; Hodgkins *et al*., 2004; Cooper *et al*., 2011; Hindshaw *et al*., 2011). However, due to its high solute concentrations, even small groundwater contributions substantially impact proglacial geochemistry and solute fluxes (Hodgkins *et al*., 1998; Harris *et al*., 2007; Levy *et al*., 2011; Gooseff *et al*., 2003; 2013).

Chemical weathering in proglacial environments is dominated by several major processes. The initial reactions when snow and ice melt interact with glacial flour are carbonate (Equation 6.1.) and silicate hydrolysis (Equation 6.2).

$$CaCO_{3(s)} + H_2O_{(l)} + CO_{2(aq)} \leftrightarrow Ca^{2+}_{(aq)} + 2HCO^{-}_{3(aq)}$$

Equation 6.1. Carbonate hydrolysis

$$CaAl_2Si_2O_{8(s)} + 2CO_{2(aq)} + 2H_2O_{(l)} \leftrightarrow Ca^{2+}_{(aq)} + 2HCO^{-}_{3(aq)} + H_2Al_2Si_2O_{8(s)}$$

Equation 6.2. Silicate hydrolysis

$$4FeS_2(s) + 16CaCO_3(s) + 15O_2(g) + 14H_2O(l) \leftrightarrow 16Ca^{2+}(aq) + 16HCO^{-}_3(aq) + 8SO^{2-}_4(aq) + 4Fe(OH)_3(s)$$

Equation 6.3. Coupled sulphide oxidation and carbonate dissolution

The rates of kinetic dissolution for carbonates greatly exceed those of silicates. Field evidence from Haut Glacier d'Arolla (Swiss Alps) shows that, although the bedrock contained only trace amounts of carbonates and sulphides, the dissolution ratio of carbonate to silicates was around 5:1 (Tranter *et al*., 2002a, b). The coupling of carbonate dissolution and sulphide oxidation provides protons to solution, which then drive further carbonate dissolution and weathering (Equation 6.3) (e.g. Fairchild *et al*., 1999; Wadham *et al*., 2001; Tranter *et al*., 1996; Hodson *et al*., 2002; Tranter, 2003; Robinson *et al*., 2009b). Coupled carbonate dissolution-sulphide oxidation was found to be the dominant

weathering mechanism in young proglacial sediments, even in catchments where carbonates and sulphides only occur in trace amounts (Cooper *et al*., 2002; Hindshaw *et al*., 2011). Therefore, coupled carbonate dissolution and sulphide oxidation (Equation 6.3) significantly impacts meltwater chemistry, even in catchments where carbonates are only found in trace concentrations (e.g. Raiswell and Thomas, 1984; Tranter *et al*., 2002; Hindshaw *et al*., 2011). When the reactive sulphide minerals are exhausted, silicate dissolution becomes the dominant process (Anderson *et al*., 2000; Wadham *et al*., 2001). However, this trend becomes less pronounced in catchments with high spatial variability in the availability of exposed sulphide minerals, such as those dominated by frequent glacier margin fluctuations and jökulhlaups (Robinson *et al*., 2009b). Although some of the factors that contribute to the high denudation rates are common in most proglacial settings, there is a significant spatial variability in proglacial geochemistry. This heterogeneity is attributed to differences in catchment geology (e.g. Hindshaw *et al*. 2011), age of substrate (e.g. Anderson *et al*., 2000), glacier thermal regime (e.g. Hodgkins *et al*., 1998), drainage patterns and hydrological connectivity (e.g. Boucher and Carey, 2010), and meteorological factors such as the amount of precipitation and evaporation (e.g. Cooper *et al*., 2002) .

Proglacial solute concentrations in meltwaters have high temporal variability, which is strongly linked to the efficiency of the glacial drainage system. Solute concentrations are usually high at the start of the melting season, probably due to preferential leaching of solutes from the edges of snow crystals (e.g. Yde *et al*., 2008) and to the distributed configuration of the subglacial drainage system (e.g. Tranter *et al*., 1993). As the ablation season progresses, solute concentrations begin to fall due to the exhaustion of snowmelt and to the increasing efficiency of the glacial drainage, which reduces water/rock contact and solute acquisition. At the end of the melt season, solute concentrations increase, as distributed drainage and long water/rock contract becomes dominant again (Clow *et al*., 2003; Gabet *et al*., 2010; Hindshaw *et al*., 2011; Kristiansen *et al*., 2013).

The mean chemical and physical denudation rate in Iceland is 37 t/km^2/yr, which exceeds the mean continental rate by approximately 11 t/km^2/yr (Berner and Berner, 1996; Gíslason, 2005). These high weathering rates are attributed to the combination of high relief, high runoff, abundance of reactive substrate and a lack of sedimentary traps (Gíslason, 2008). The chemistry of Icelandic rivers is controlled by variations in water source and discharge, chemical weathering, geothermal activity, atmospheric deposition, and vegetation (Gíslason and Arnorsson, 1993; Gíslason, 2005; Gíslason and Torssander, 2006; Flaathen and Gíslason, 2007; Eiriksdóttir *et al*., 2008; Sigfusson *et al*., 2008; Óskarsdóttir *et al*., 2011). Volcanic eruptions also impact the chemistry of Icelandic groundwater and surface water, particularly by the deposition and dissolution of tephra (Flaathen *et al*., 2009; Olsson *et al*., 2013; Galeczka *et al*., 2014).

Catchment lithology plays an important control on proglacial geochemistry, with high weathering rates occurring in catchments with reactive minerals (e.g. Rutter *et al*., 2011). The weathering rates of young rocks in Iceland exceed those of older ones (Louvat *et al*., 2008). Skaftafellsjökull is located within the catchment of Öræfajökull, an ice-covered stratovolcano, which is located in the young neovolcanic zone in SE Iceland (Björnsson and Einarsson, 1990). The rock suite is mainly composed of subglacial pillow lava and hyaloclastite tuff, whose composition ranges from basalt to rhyolite. The rock suite of Öræfajökull contains high amounts of glassy basalt, which has been preferentially formed during subglacial eruptions (Prestvik, 1980; Selbekk and Trønnes, 2007). The weathering and dissolution rates of basaltic glass substantially exceed those of crystalline basalt, hence providing high solute fluxes to the catchment (Gíslason and Eugster, 1987, Gíslason *et al*., 2006; Pogge van Strandmann, 2008, Robinson *et al*., 2009b; Hindshaw *et al*., 2013).

6.1.2. The use of stable water isotopes ($\delta^{18}O$ and δD) in hydrology

Water stable isotopes ($\delta^{18}O$ and δD) have been used extensively in glaciated catchments for the tracing of hydrological pathways and sources of recharge (e.g. Theakstone and Knudsen, 1996; Chiogna *et al*., 2014), to perform hydrograph separation (e.g. Fairchild *et al*., 1999b; Klaus and McDonnell, 2013), and in studies of paleohydrogeology (e.g. Hendry *et al*., 2013). The composition of water stable isotopes is determined by the atomic weight of the hydrogen and oxygen molecules, which sums the amount of protons and neutrons of each element. However, a small percentage of the molecules have higher atomic weight, due to higher number of neutrons ($\delta^{18}O$ and δD). These differences in isotopic composition lead to different rates of reaction between the molecules, where the reactions of the heavy molecules (^{18}O, ^{2}H) are slower than those of the light ones (^{16}O and ^{1}H). These different rates of reaction lead to isotopic fractionation, which takes place as the lighter isotopes are preferentially removed into the vapour mass during evaporation from a water source. Conversely, the heavier isotopes are preferentially removed from the vapour phase during condensation and precipitation, which progressively depletes the vapour mass of its heavier isotopes as it moves further from its source of origin (Clark and Fritz, 1997) (Figure 6.1). The global distribution of water stable isotopes is based on the predictable relationship between δD and $\delta^{18}O$ in precipitation, which is described by the Global Meteoric Water Line (GMWL) (Craig, 1961a, b). The GMWL is calculated using Figure 6.1. The increasing depletion of isotopic composition with increasing continentality and altitude (from Robinson, 2003).

$$: \delta D = 8\,(\delta^{18}O) + 10‰$$

Equation 6.4. The Global Meteoric Water Line (GMWL).

Isotopic fractionation is strongly dependent on climatic factors such as humidity and temperature. Fractionation generally increases at low humidity and high temperature (Dansgaard, 1964; Rozanski *et al*., 1993; Clark and Fritz, 1997). Elevation impacts isotopic composition due to its impact on the formation of orographic precipitation, lower evaporation, and lower snow melt. Hence, the isotopic composition of precipitation generally becomes lighter with increasing elevation (Clark and Fritz, 1997; Jonsson *et al*., 2009; Ohlanders *et al*., 2013; Flaim *et al*., 2014). The source of moisture for precipitation exerts an important control on the seasonal variability in isotopic composition, with multiple precipitation sources leading to higher variability in the isotopic composition of precipitation (Jeelani *et al*., 2010). Due to these aforementioned factors, the isotopic composition of precipitation becomes more depleted with increasing latitude, continentality and altitude (Figure 6.1) (e.g. Jeelani *et al*., 2010; Gooseff *et al*., 2013).

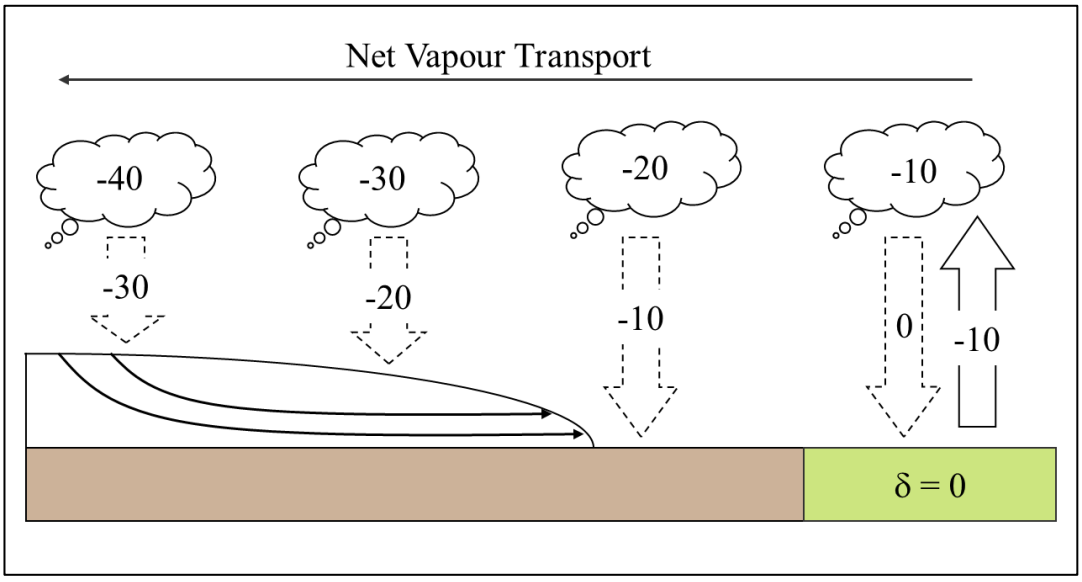

Figure 6.1. The increasing depletion of isotopic composition with increasing continentality and altitude (from Robinson, 2003).

The Local Meteoric Water Line (LMWL) is the line of best fit for the isotopic composition of precipitation at any given location (Gat *et al*., 2001). The LMWL provides a better

representation for the isotopic composition of the precipitation that feeds the catchment than the GMWL because of the importance of local factors. Hence, it is useful in understanding the regional variability in the GMWL (e.g. Clark and Fritz, 1997). In middle and high latitudes, a seasonal variation along the LMWL is driven by temperature, with winter precipitation being more isotopically-depleted than during summer (e.g. Robinson *et al*., 2009a; Yang *et al*., 2013). Samples along the LMWL which plot on a slope lower than that of the GMWL can suggest isotopic enrichment due to post-condensation evaporation, which can occur when rain falls through a dry air column (Clark and Fritz, 1997, Mayr *et al*., 2007). However, the LMWL can be sensitive to local disturbances and precipitation events.(e.g. Chiogna *et al*., 2014).

The isotopic composition of groundwater (Kortelainen and Karhu, 2004; Jeelani *et al*., 2010), streams (e.g. Burgman *et al*., 1987; Jeelani *et al*., 2010; Dahlke *et al*., 2014; Kong *et al*., 2014), and lakes (e.g. Roy and Hayashi, 2009; Jonsson *et al*., 2009; Gao *et al*., 2014) in cold environments is substantially impacted by seasonality. Isotopic composition is generally more depleted in spring and summer, due to greater inputs from snow and icemelt, and becomes more isotopically heavier in autumn and winter, following increasing contributions from precipitation and baseflow. The seasonal isotopic variability of groundwater is generally less than that of surface water (e.g. Yang *et al*., 2013; Chiogna *et al*., 2014). The temporal variability in the isotopic composition of lakes is impacted by meteorological variability and by hydrological parameters such as lake morphometry, water residence times, storage capacity, drainage efficiency, groundwater contributions, and evaporation (Gonfiantini, 1986; Rozanski *et al*., 1993; Gat, 1996; Vitvar and Balderer, 1997; Hammarlund *et al*., 2002; Darling, 2004; Edwards *et al*., 2004; Kortelainen and Karhu, 2004; Henderson and Shuman 2009; 2010; Zhou *et al*., 2008; 2013; Flaim *et al*., 2014). The isotopic composition of lakes in cold regions is also substantially impacted by the degree of mixing within the water column, and the ice cover (Saulnier-Talbot *et al*., 2007; Jonsson *et al*., 2009).

The Deuterium Excess (*d-excess*) measures the relative proportions of δD and $\delta^{18}O$ within the water molecule (Equation 6.5), which represent an index of deviation from the GMWL, where *d-excess* is 10‰ (Dansgaard, 1964). The *d-excess* has been previously used to delineate sources of precipitation and to investigate the prominence of evaporation and melt-freeze cycles (e.g. Williams *et al*., 2006; Gooseff *et al*., 2006; Kristiansen *et al*., 2012).

$$\boldsymbol{d - excess}\ (‰) = \boldsymbol{\delta D - 8 \times \left(\delta^{18} O\right)}$$

Equation 6.5. Determination of Deuterium Excess (d-excess)

The *d-excess* is controlled by physical conditions (air and sea surface temperature and humidity) at the ocean where precipitation originates (Merlivat and Jouzel, 1979). Hence, it reflects the prevailing conditions during the evolution and mixing which takes place as air masses travel to the site of precipitation (Merlivat and Jouzel, 1979; Froehlich *et al*., 2002). In addition to the history of the air mass, the *d-excess* is strongly impacted by seasonality, changes in moisture sources, and kinetic effects (Fisher, 1991; Clark and Fritz, 1997; Froehlich *et al*., 2002; Kristiansen *et al*., 2012). Therefore, *d-excess* is higher in winter, due to the higher contrasts between sea surface and air temperature, which occur in winter, and lead to stronger kinetic effects during evaporation from local source regions. Conversely, *d-excess* is lower during summer due to the larger influence from warmer seas, which reduces the kinetic fractionation in which vapour is formed (Gat, 1996; Clark and Fritz, 1997).

The overall aim of this chapter is to identify the sources of recharge for the groundwater and surface water systems at the Skaftafellsjökull foreland (objective iii). The specific objectives of this chapter are:

1. To describe the spatial and temporal variability in groundwater and surface water geochemistry in the different hydro(geo)logical environments of the Skaftafellsjökull foreland.

2. To describe the spatial variability of $\delta^{18}O$ and δD composition of groundwater and surface water in the different hydro(geo)logical environments of the Skaftafellsjökull foreland.

3. To identify the sources of groundwater and surface water recharge at the Skaftafellsjökull foreland using geochemical and stable isotope evidence.

4. To investigate proglacial groundwater-surface exchange processes and mechanisms using water geochemistry and water stable isotopes.

6.2. Methods

6.2.1. Analysis of groundwater and surface water quality

Temperature and Electrical Conductivity (EC) are important environmental parameters, which are monitored with relative ease and low cost (e.g. Hayashi, 2004). Temperature and EC can therefore be used to investigate groundwater-surface water exchange in proglacial environments (e.g. Crossman *et al*., 2011). Groundwater was extracted from the piezometers using a hand pump. Prior to sampling, three well volumes were purged, in order to ensure a representative sample (Brassington, 2007). In order to check that this amount was sufficient, groundwater EC was checked every 150 ml, until EC was stable (e.g. Brassington, 2007). These tests have shown that groundwater EC stabilised before three well volumes were purged (Figure 6.2). Hence, purging three well volumes was sufficient for obtaining a representative sample.

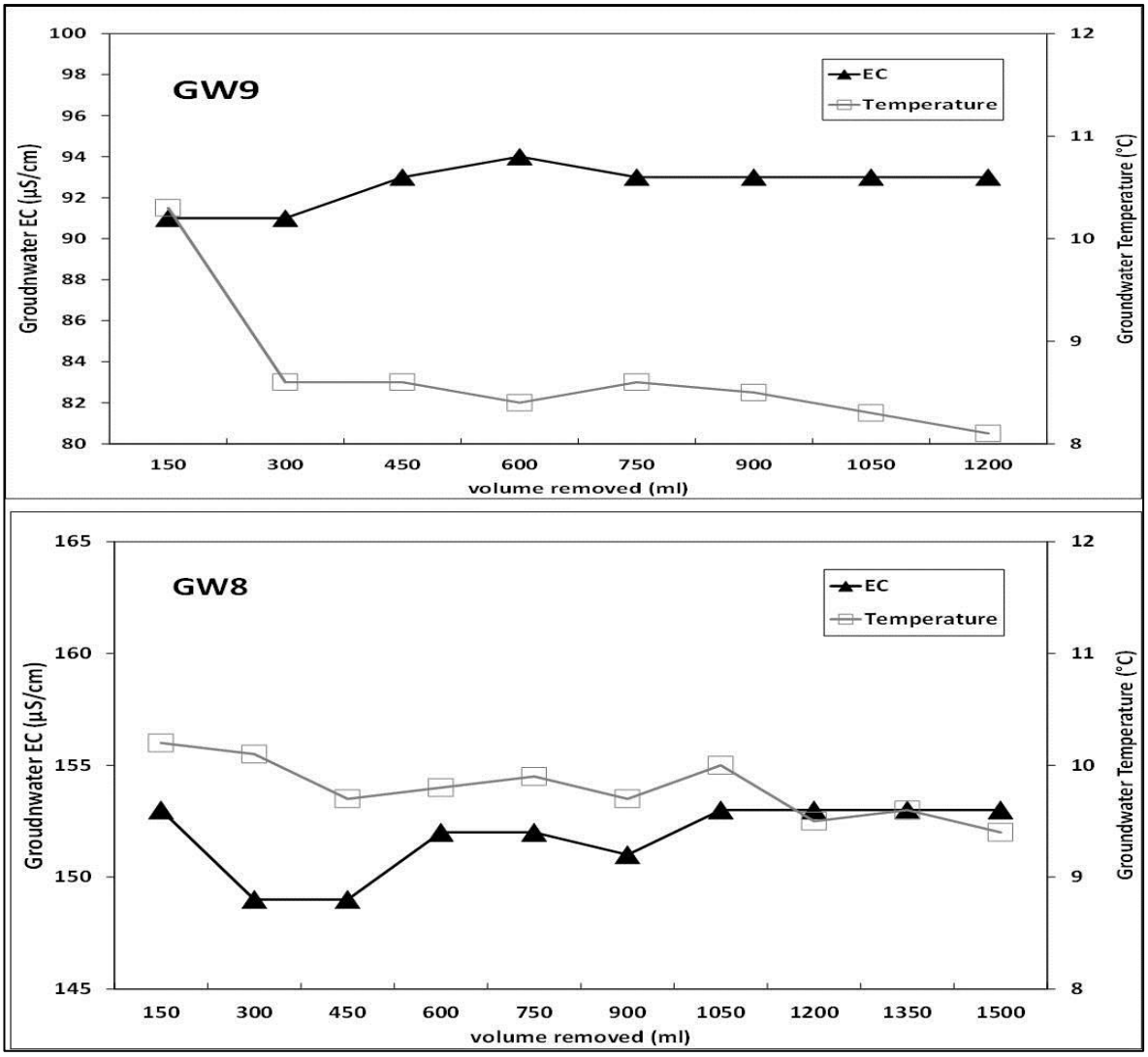

Figure 6.2. Purging experiments to determine the volume of groundwater needed to attain representative samples.

These results were obtained from GW9 and GW8, where the required three well volumes were 1.14 L and 1.61 L, respectively.

The samples were filtered in the field using a Fisher® filter kit, with filter paper pore size of 0.47 µm. The filter paper was replaced after each sample. In order to prevent cross-contamination between sites, all sampling apparatus were rinsed at least three times with representative sample water prior to sampling. The samples were then placed in new 30 ml Fisher® HDPE Nalgene bottles, which were pre-contaminated with sample water and then filled to a positive meniscus. The bottles were sealed with Parafilm® and stored away from direct sunlight between two to six weeks. Upon returning to the laboratory, the

samples were refrigerated at 4°C. In order to prevent the adsorption of cations onto the bottle, samples intended for cation analysis were pre-acidified with 0.1 ml of 5% nitric acid (Brassington, 2007). The samples were analysed within four weeks upon their return to the laboratory.

EC and temperature at this study were monitored using a handheld WTW Multiline P4 EC/Temperature probe. The meter was calibrated with standard 1431 µS/cm solution prior to the start of the field season. The accuracy is within ±1 % of the measured value (WTW manual).

Since most samples at the Skaftafellsjökull foreland were below 300 µS/cm, the accuracy can be approximated to be around 2 µS/cm. The accuracy for the temperature measurements are 0.1°C. In addition to the manual measurements, groundwater temperature (±0.1°C) and EC (±20µS/cm) at T1-T3 and the Skaftafellsá were monitored using pressure transducers (Table 6.1). In order to prevent cross contamination between samples, all probes were also rinsed at least three times with representative sample water prior to measurements.

Table 6.1. Analytical equipment, accuracy of equipment, and frequency of measurements taken in this study.

Parameter	Equipment	Accuracy	Frequency of monitoring
GW levels (automatic)	Solinst Leveloggers	±0.001 m	hourly
Water temperature	Solinst Leveloggers	±0.1 °C	hourly
Water EC	Solinst Levelogger	±20 µS/cm	hourly
GW levels (manual)	Solinst dip meter	±0.003 m	Twice a day
GW temperature	WTW Multiline P4 probe	0.1 °C	Every time samples were obtained for geochemical analysis
GW EC	WTW Multiline P4 probe	2 µS/cm	Every time samples were obtained for geochemical analysis
δD composition	Cavity Ring-Down Spectroscope-Picarro L1102-i liquid analyzer	±0.5 ‰	
$\delta^{18}O$ composition	Cavity Ring-Down Spectroscope-Picarro L1102-i liquid analyzer	±0.1 ‰	

6.2.2. Analysis of major anions and cations

Major cations (Ca^{2+}, K^{+}, Mg^{2+}, Na^{+}) were analysed on an Varian Vista MPX Inductive Coupled Plasma-Optical Emission Spectrometer (ICP-OES) at Keele University. The standards used were 10 and 100 mg/l. Major anions were analysed on an Ion chromatography DIONEX, using standards for 1, 5 and 10 mg/l for Cl^{-}, NO_3^{-}, F^{-} and PO_4^{2-} and 2, 10 and 20 mg/l for SO_4^{2-}. PO_4^{2-},F^{-}, NO_3^{-} concentrations were below the limit of

detection (Table 6.2). The Limit of Detection (LoD) for cations and anions (Table 6.2) was determined by the mean concentration in the blanks ± standard deviations.

Table 6.2. Limit of Detection and precision for major anions and cations.

The detection limits and precision were obtained from analysis of blanks for all ions except for Na^+, which was obtained from the manufacturer's website.

Anion	Precision (%)	Detection Limit (mg/l)
Cl^-	1.52	0.09
SO_4^{2-}	3.71	0.20
Cations		
Ca^{2+}	0.77	0.42
Mg^{2+}	3.15	0.16
Na^+	2.95	0.2 (Varian, 2014)
K^+	2.32	0.74

Four field blanks were collected in order to determine the potential for contamination during sampling, storage and analysis. These blanks consisted of deionised water which was filtered and emplaced in bottles following the same procedures that were used for sampling groundwater and surface water. The blanks were then analysed for major cations and anions. Cation concentrations in all the blanks were below the detection limits. With the exception of one blank (0.27 mg/l), SO_4^{2-} concentrations in all blanks were below the LoD. However, the field blanks had between 0.17-0.50 mg/l of Cl^-. This indicates some contamination during sampling, storage or analysis. Drift was determined by analysing a sample at the start, middle and end of a batch (48 samples for the anions, 40 samples for the cations). The drift for all anions and cations were below 2%. "Hangover" effects during the analysis were checked by emplacing vials containing deionised water after some samples. Cation concentrations in the deionised water were below detection limit. The mean Cl^- concentration was 0.14±0.01 mg/l. This shows some "hangover" effects in the analysis of Cl^- and SO_4^{2-}.

6.2.3. Water stable isotopes (δD and $\delta^{18}O$)

Samples for water stable isotopes (n=31) were collected from groundwater, lakes, and the meltwater river (section 6.5) on the 24-25/08/2012. The collected 20 ml water samples were analyzed for their δD and $\delta^{18}O$ composition at the Isotope laboratory at the Hydrology and Climate Unit, the Department of Geography, University of Zurich. In addition to the filtration in the field, all isotope samples were filtered prior to analysis with a 0.45 µm filter (25 mm PTFE Syringe Filter, Simplepure™ USA) from which 1 ml was pipetted in a vial (1.5 ml 32×11.6 mm screw neck vials with cap and PTFE/silicone/PTFE septa). Samples were analyzed with a Cavity Ring-Down Spectroscope-Picarro L1102-i Liquid Analyser 1st generation analyzer, following the analyzing scheme of Penna *et al*. (2010). The precision of the instrument is <0.5 ‰ for $\delta^{2}H$ and < 0.1 ‰ for $\delta^{18}O$ (Picarro Inc., 2008). Values are reported as δ-values in parts per thousand (‰) relative to Vienna Standard Mean Ocean Water (V-SMOW). The deviation of isotope ratios from the V-SMOW standard (δ) was calculated using Equation 6.6 (Craig, 1961a).

$$\delta = \left(\frac{R_{sample} - R_{standard}}{R_{standard}}\right) \times 1000$$

Equation 6.6. Deviation of isotope ratio from the V-SMOW standard.

R is the isotope ratio ($^{2}H/^{1}H$ and $^{18}O/^{16}O$) in the sample and the standard (V-SMOW).

6.3. Spatial and temporal variability in groundwater quality

Manual measurements of groundwater physicochemical parameters (section 6.2.1) and samples for geochemical analysis (section 6.2.2) were obtained from piezometers. The samples were collected during three sampling intervals, which took place around the 10/07/2012, 26/07/2012, and 31/08/2012, with each interval lasting between one and two days (Figure 6.4). Water physicochemical parameters (Temperature and Electrical Conductivity [EC]) were measured during the same time as samples were collected for geochemical analysis.

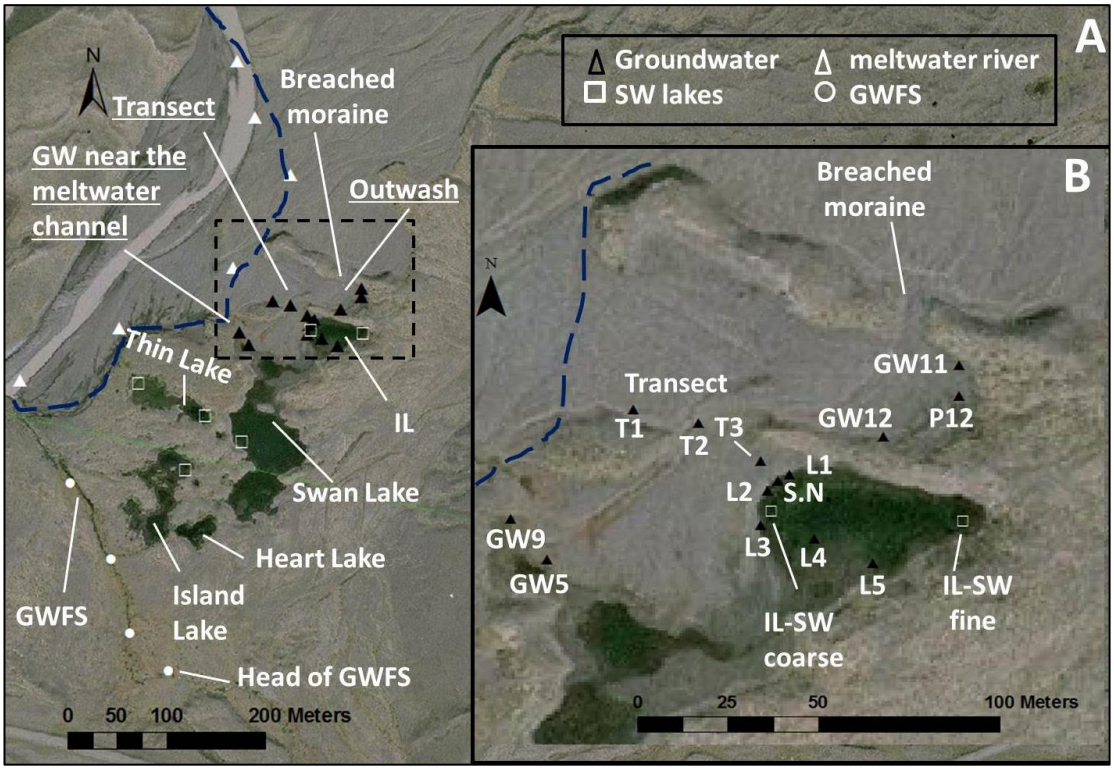

Figure 6.3. The field site and sampling points at the Skaftafellsjökull foreland.

A. The hydro(geo)logical environments at the Skaftafellsjökull foreland. Groundwater samples are denoted in black and surface water sampling points are denoted in white. B. The piezometers where groundwater samples were collected (black triangles). The area of inset B is denoted by the black box in inset A. The position of the meltwater channel has shifted eastwards since the time of the image (Vatnajökull National Park, 2007). The position of the meltwater channel during the study (August 2012) is denoted by the dashed blue line.

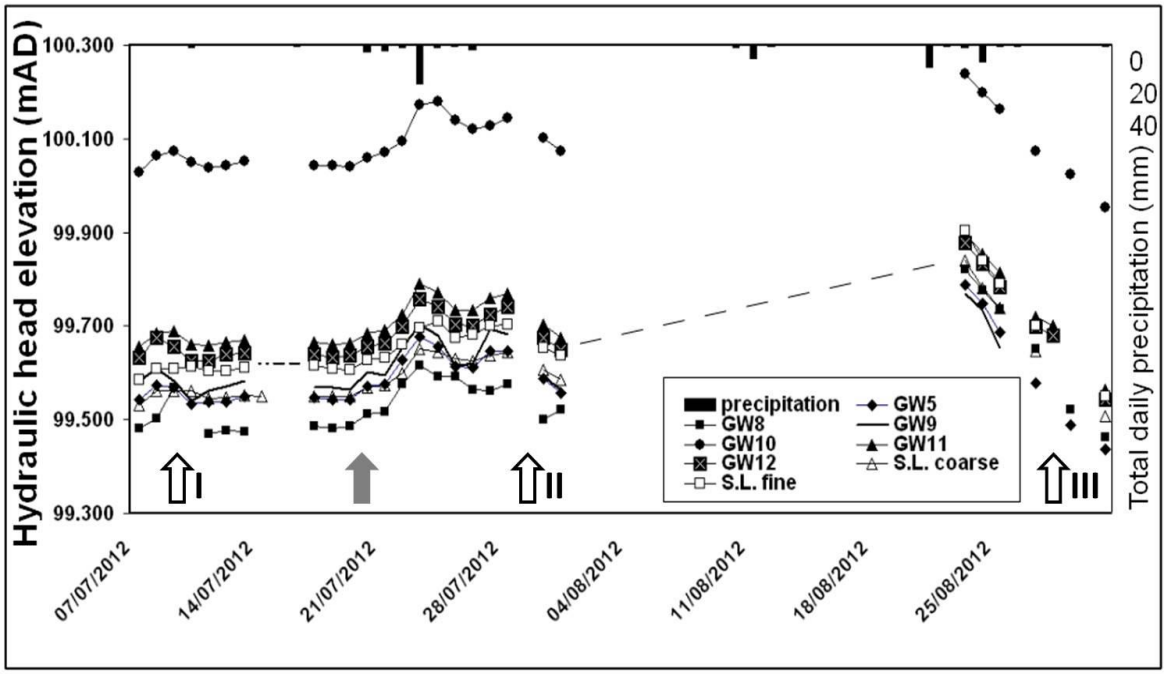

Figure 6.4. Total daily precipitation (IMO, 2013), hydraulic heads at the Skaftafellsjökull foreland, and the sampling intervals for groundwater (white arrows) and surface water.

The number of the intervals are marked. Surface water were sampled four times, with the extra interval (grey arrow) taking place on the 21/07/2012.

6.3.1. Groundwater physicochemical parameters

This section describes the temporal and spatial variability in groundwater temperature and EC. Temperature is an effective environmental tracer for groundwater-surface water exchange due to its relatively simple, economic, and robust measurements (e.g. Westhoff *et al.,* 2007; Hannah *et al,* 2009). Temperature tracing is especially effective when significant temperature differences exist between groundwater and surface water (e.g. Rossi *et al*., 2012). Such conditions were reported from various proglacial environments (e.g. Kristiansen *et al*., 2013), including the current study (Figure 6.5). In addition to the manual monitoring, groundwater and meltwater temperatures and EC at the transect (piezometers T1-T3) were also monitored automatically alongside hydraulic heads. The

current chapter only discusses the manual monitoring. The results from the automated monitoring from T1-T3 and the Skaftafellsá are discussed in Chapter 7.

The spatial and temporal variability in groundwater and surface water temperature at the Skaftafellsjökull foreland is presented in Figure 6.6. The mean surface water temperature was higher than groundwater temperature by 3°C. However, surface water temperatures also had higher variability (Figure 6.5). The lowest groundwater temperatures were measured in the GW9 piezometer (depth of 1.45 m below ground), located 20 m away from the Skaftafellsá meltwater channel. The highest groundwater temperatures were measured in the piezometers around the Instrumented Lake (IL). However, groundwater temperatures were lower during sampling interval III (30/08/2012), particularly in piezometers which are located in the fine-grained lakeshores of the IL. Conversely, groundwater temperature near the Skaftafellsá (GW5 and GW9) during interval III were substantially higher than during previous intervals (Figure 6.6).

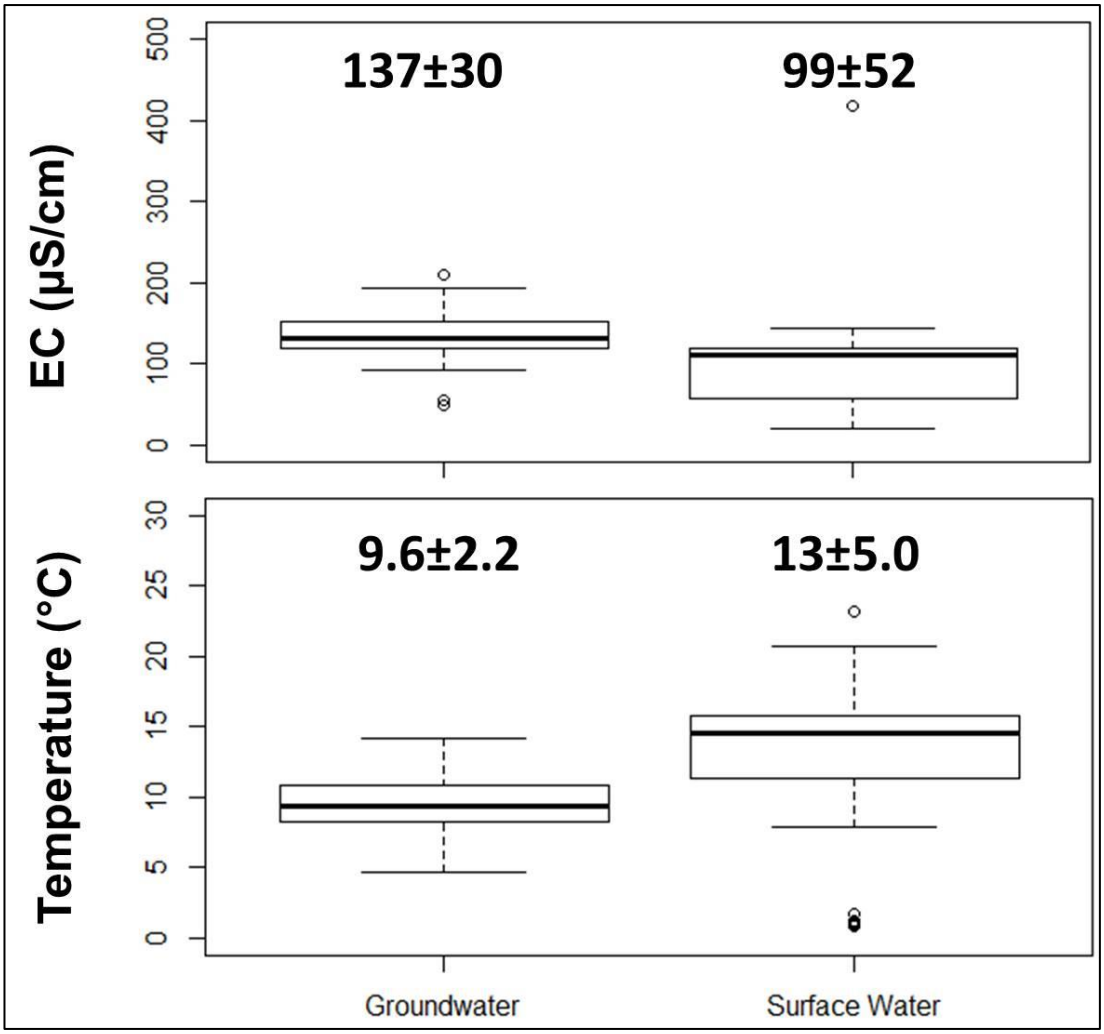

Figure 6.5. Boxplot of groundwater and surface water temperature (°C) and Electrical Conductivity (EC) [µS/cm].

The comparison includes all groundwater (n=57) and surface water samples (n=78). The horizontal lines denote the minimum, Q1, Q3, and the maximum. The thick black line denotes the median. The mean and standard deviation are presented above each box. The dots denote outliers in the data. The full data set is found in Appendix 5.

EC has also been previously used alongside temperature in the investigation of proglacial groundwater-surface water exchange. Similar to temperature, EC is also particularly effective for investigating proglacial groundwater-surface water exchange due to the significant differences between the end-members (Cirpka *et al*., 2007; Vogt *et al*., 2010; Hayashi *et al*., 2012; Schmidt *et al*, 2012). Groundwater and surface water EC at the Skaftafellsjökull foreland ranged between 20-210 µS/cm, with groundwater EC generally exceeding that of surface water (Figure 6.5). The spatial variability in groundwater and

surface water EC is presented in Figure 6.6. The lowest groundwater EC was measured at GW9 (~ 50 µS/cm). The highest EC was measured in the transect (~180 µS/cm at T1) and at GW5 (~210 µS/cm). The EC of most groundwater samples from the IL and the outwash ranged between 100-150 µS/cm. The temporal fluctuations in groundwater EC were generally below 10 µS/cm, except at the transect and GW9, where concentrations increased by ~30-40 µS/cm in August (Figure 6.6).

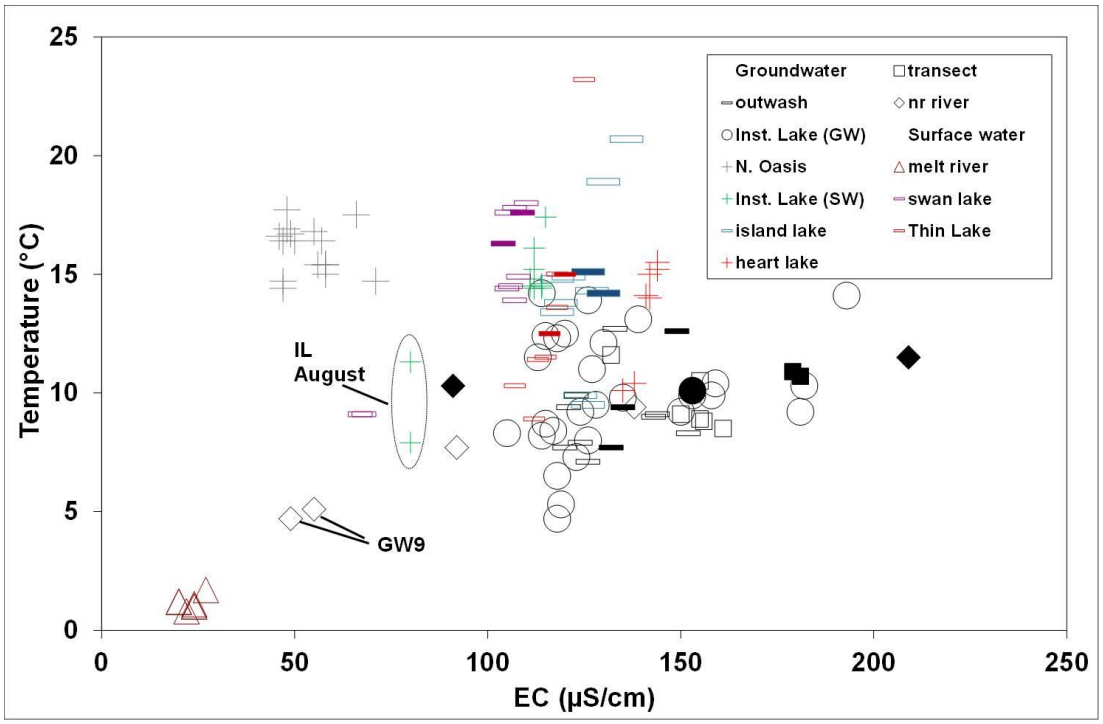

Figure 6.6. Temperature and EC in the different hydrological environments of the Skaftafellsjökull foreland.

Groundwater samples are denoted in black. Surface water samples are denoted in colour. The filled shapes mark measurements during interval III (31/08/2012).

6.3.2. Spatial and temporal variability in groundwater solute concentrations

This section describes the spatial and temporal variability in groundwater solute concentrations at the different hydrological environments of the Skaftafellsjökull foreland: near the meltwater river; groundwater from around the lakeshores of the Instrumented

Lake (IL); the transect, and the outwash (Figure 6.3). Substantial differences were measured between the geochemistry of groundwater and surface water, with solute concentrations in groundwater generally exceeding those in surface water (Figure 6.7). Ca^{2+} and Na^{+} were the dominant cations in both groundwater and surface water. The mean SO_4^{2-} concentrations in groundwater exceeded those of Cl^{-}. The mean Cl^{-} concentrations in surface water exceeded those in groundwater (Table 6.3). The concentrations of the divalent (Ca^{2+} and Mg^{2+}) and monovalent (Na^{+} and K^{+}) were presented together, following the approach of other studies of proglacial geochemistry (e.g. Cooper *et al*., 2002). The concentrations of F^{-}, NO_3^{-} and PO_4^{2-} were generally below detection limit in most samples, and are not presented. Due to logistical constraints, HCO_3^{-} was not measured at this study, although it is likely to be the dominant anion (e.g. Brown, 2003). Similar to other studies which have looked at geochemical aspects of proglacial groundwater-surface water interaction (e.g. Cooper *et al*., 2002) the data in the current study was not compensated for marine aerosols.

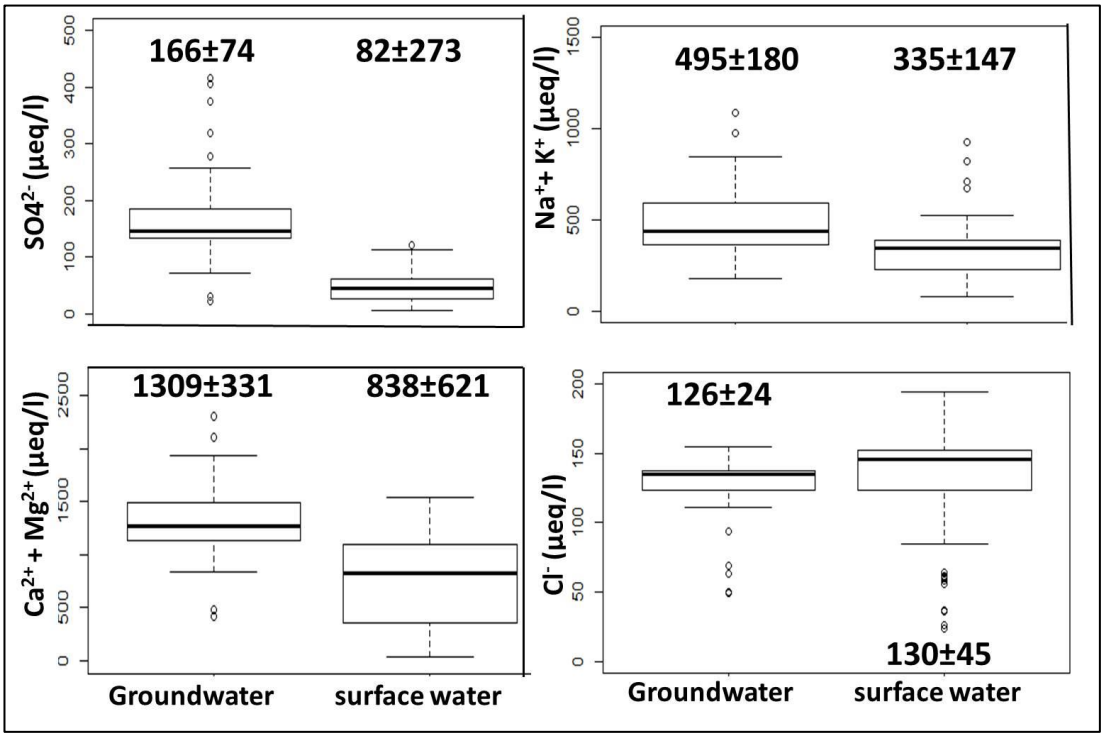

Figure 6.7. Boxplot comparison of Ca^{2+} + Mg^{2+}, SO_4^{2-}, Cl^{-}, and Na^{+} + K^{+} concentrations (µeq/l) between groundwater and surface water.

This comparison includes all groundwater (n=57) and surface water (n=78) samples. More detailed descriptions of solute concentrations in the different hydrological environments are provided later in the chapter. The horizontal lines of the boxes denote the minimum, Q1, Q3, and the maximum. The thick black line denotes the median. The dots show outliers in the data. The mean and standard deviation (µeq/l) are presented above each box.

The spatial variability in solute concentrations within the different hydrological environments is presented in Figure 6.8-6.10. Similar to the spatial distribution in EC, the lowest groundwater solute concentrations were also measured at GW9, located 20 m away from the Skaftafellsá meltwater channel (Figure 6.3). The highest solute concentrations were generally measured in the piezometers of the transect (T1-T3), which stretches between the Skaftafellsá and the IL (Figure 6.3). Statistical t-tests (one tail test, 2.5% Significance Level [SL]) have shown that SO_4^{2-}, Ca^{2+}+ Mg^{2+}, and Na^{+}+ K^{+} concentrations in groundwater were significantly higher (*p=<0.001*) than the concentrations in surface water. Conversely, Cl^{-} concentrations in groundwater were not significantly higher than those in surface water (*p=0.831*).

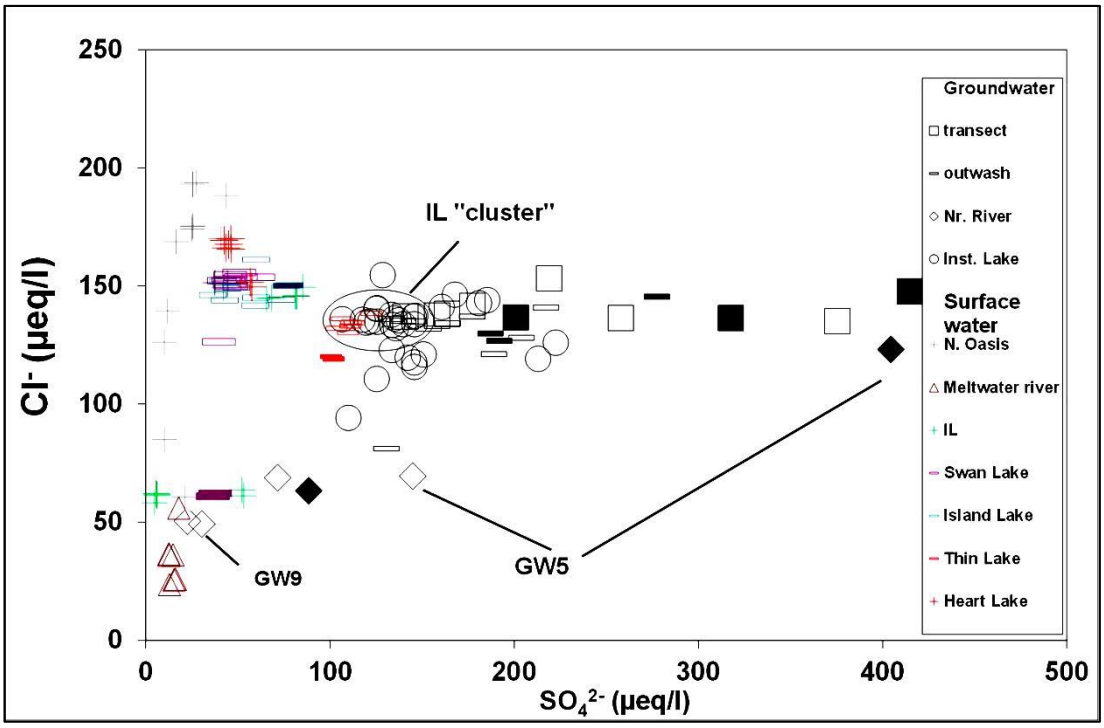

Figure 6.8. SO_4^{2-} and Cl^{-} concentrations (µeq/l) in groundwater and surface water at the Skaftafellsjökull foreland.

Black markers denote groundwater samples. Coloured markers denote surface water samples. The filled shapes mark solute concentrations during interval III (31/08/2012).

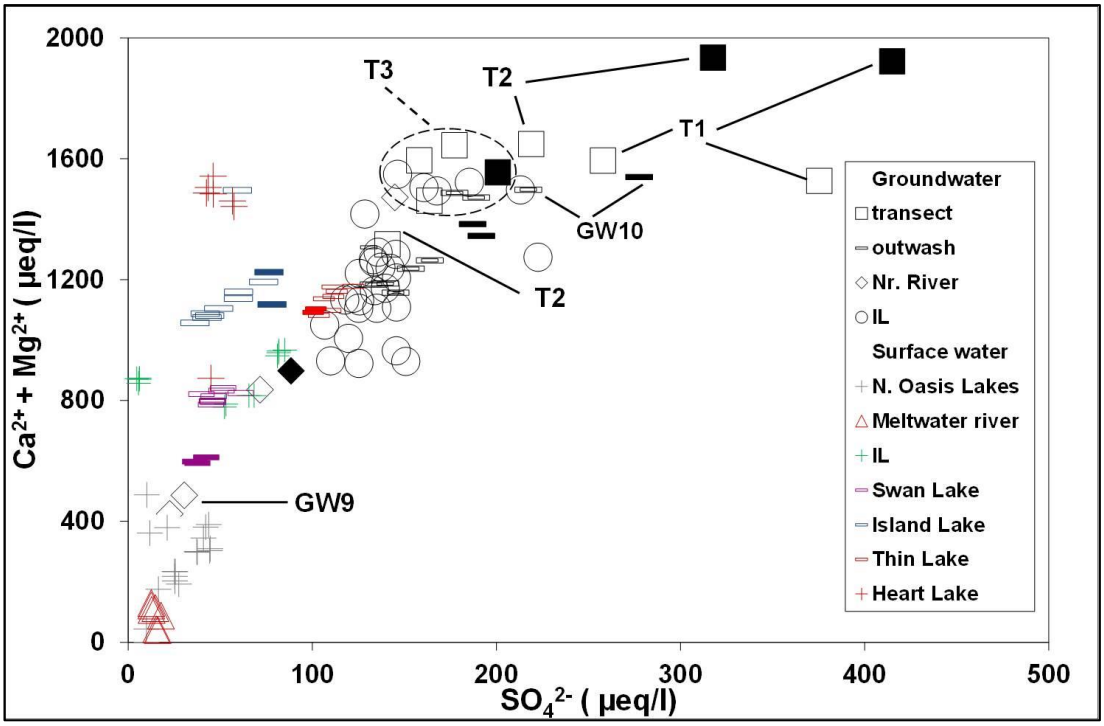

Figure 6.9. SO_4^{2-} and Ca^{2+}+ Mg^{2+} concentrations (µeq/l) in groundwater and surface water at the Skaftafellsjökull foreland.

Groundwater samples are denoted in black. Surface water samples are denoted in colour. The filled shapes mark solute concentrations during interval III (31/08/2012). The samples from T3 are within the dashed circle.

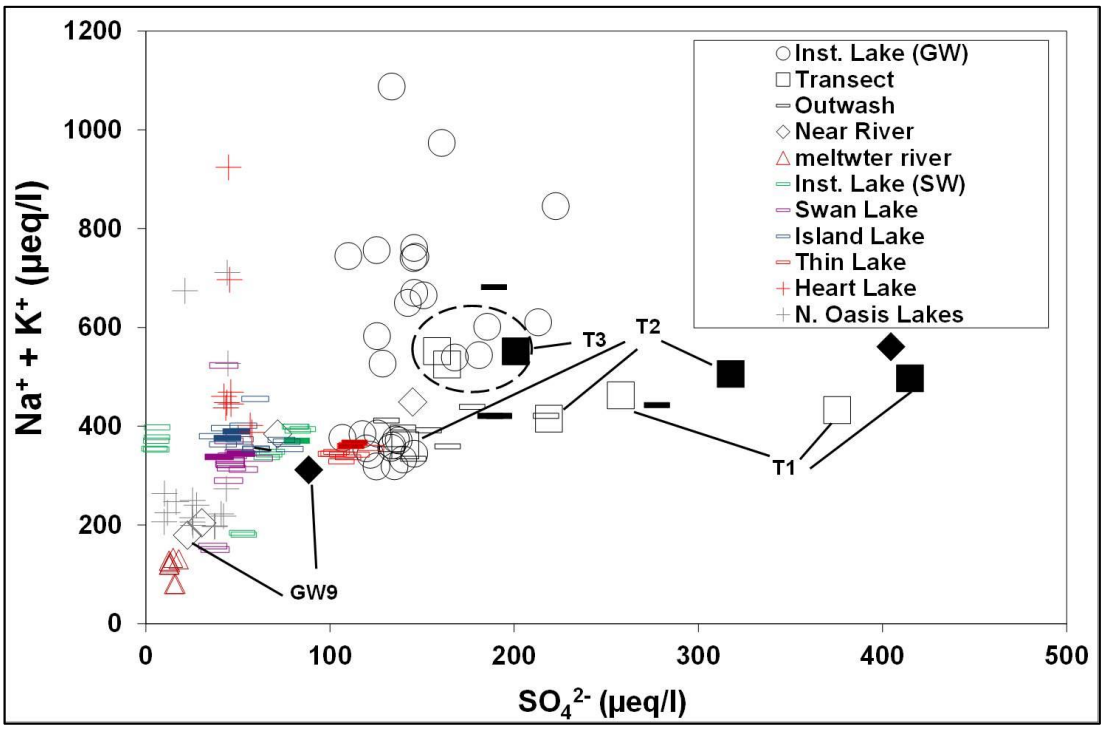

Figure 6.10. SO_4^{2-} and Na^++ K^+ concentrations (µeq/l) in groundwater and surface water from the Skaftafellsjökull foreland.

Groundwater samples are denoted in black. Surface water samples are denoted in colour. The filled shapes mark solute concentrations during interval III (31/08/2012). The samples from T3 are within the dashed circle.

Table 6.3. Mean and standard deviation of solute concentrations, EC, and temperature of groundwater and surface water at the Skaftafellsjökull foreland.

The numbers in brackets denote the number of samples within each environment. A fuller description of the surface water solute concentrations and physicochemical parameters is provided in section 6.4.

Solute concentration (µeq/l)	SO_4^{2-}	Cl^-	$Ca^{2+}+Mg^{2+}$	$Na^+ + K^+$	EC (µS/cm)	Temperature (°C)
Groundwater						
Transect (10)	243±96	140±6	1620±190	490±72	159±14	10.0±1.1
Outwash (11)	176±42	130±17	1338±136	423±89	134±11	9.2±1.8
Near river (6)	127±143	71±27	1070±711	348±147	125±72	8.1±2.8
Inst. Lake (30)	144±27	132±12	1241±245	555±212	134±23	10.0±2.5
Surface water						
River Skaftafellsá (7)	15±2	34±11	91±37	113±23	23±3	1±0.3
N. Oasis lakes (17)	29±12	153±36	285±105	298±167	55±10	16±1
S. Oasis lakes (65)	62±27	138±21	1063±246	382±79	118±16	14±1

Groundwater levels and geochemistry near the Skaftafellsá were investigated at GW9 and GW5, which are located 20 and 38 m away from the meltwater channel, respectively. The piezometers are located south of the transect, between the river Skaftafellsá and Swan Lake (perpendicular to the river meltwater channel) (Figure 6.3). The piezometers are underlain by coarse-grained deposits. The riverbank near GW9 is shallow (0.35 m high) and meltwater overspill was regularly observed during the field season. However, the frequency of such overflows fell in late August 2012, following a substantial decline in meltwater levels.

Groundwater Cl^-, $Ca^{2+}+ Mg^{2+}$, and $Na^+ + K^+$ concentrations near the Skaftafellsá were significantly higher (1 tail t test, 2.5% S.L., $p=<0.001$ to 0.011) than meltwater concentrations of these solutes (Figure 6.8-6.10). Conversely, groundwater SO_4^{2-} concentrations were not significantly greater than meltwater concentrations ($p=0.056$). Despite the short distance between GW9 and GW5, substantial differences in groundwater solute concentrations were observed between these two piezometers. Groundwater from GW9 had the lowest EC, which ranged between 40-90 µS/cm (Figure

6.6) and solute concentrations. These values varied between 50-70 µeq/l Cl^-, 20-63 µeq/l SO_4^{2-} (Figure 6.8), 424-898 µeq/l Ca^{2+}+Mg^{2+} (Figure 6.9), and 179-312 µeq/l Na^++ K^+ (Figure 6.10). In contrast to the low solute concentrations at GW9, solute concentrations at GW5 were much higher, with most solute concentrations (except Cl^-) approaching those measured at T3 and the more solute-rich groundwater from around the IL (Figure 6.9, 6.10). However, Cl^- concentrations at GW5 were lower than those measured in other groundwater environments (Figure 6.8).

Groundwater solute concentrations near the river generally increased during the field season (Figure 6.11). Solute concentrations at GW9 increased slightly between intervals I and II. However, the changes in solute concentrations between intervals II and III (end of August 2012) were much larger, with solute concentrations increasing by 1.5 - 3 times. In contrast to the moderate increases between Intervals I and II at GW9, solute concentrations at GW5 have shown substantial and continuous increase during all three intervals (with the exception of Cl^- concentrations between intervals I and II). However, the larger increases took place between intervals II and III. These increases in solute concentrations were followed by a substantial drop in river and groundwater levels which began around the 20/08/2012 (Figure 6.4). The SO_4^{2-} (400 µeq/l) and Ca^{2+}+Mg^{2+} (2300 µeq/l) concentrations which were measured at GW5 in August were abnormally high.

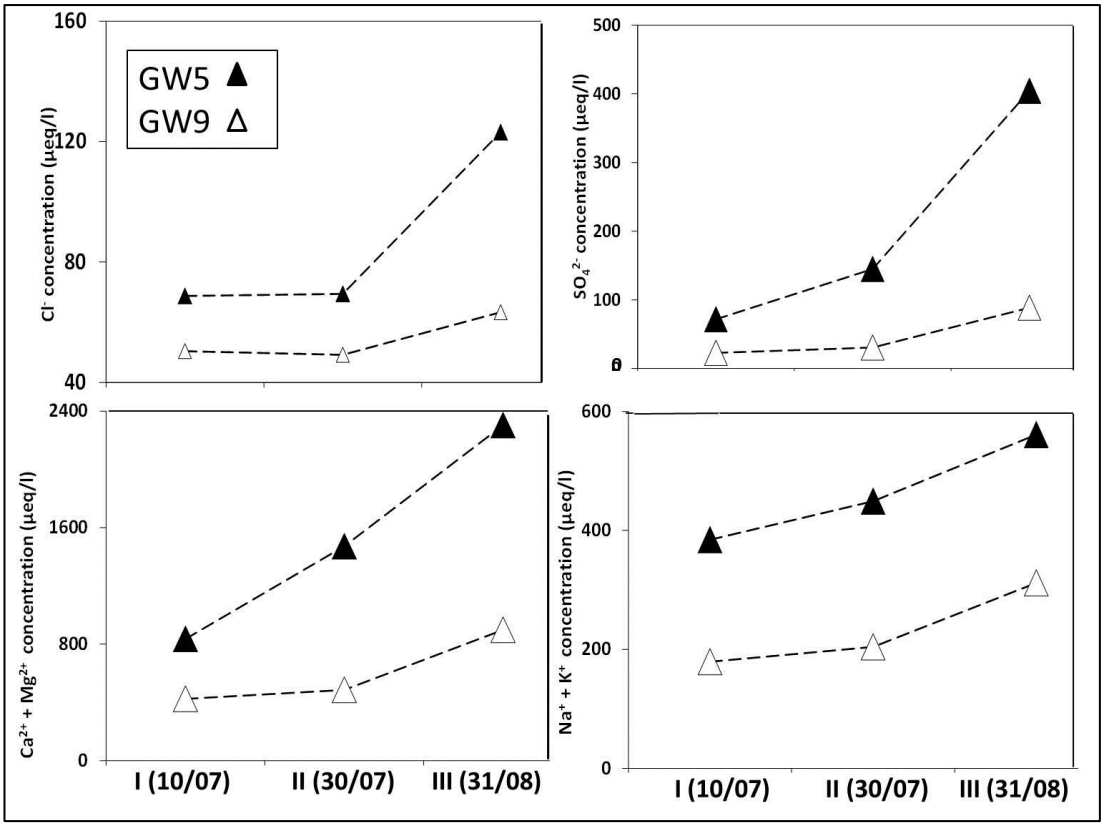

Figure 6.11. Temporal variability of solute concentrations in the piezometers near the meltwater channel (GW5 and GW9) between July-August 2012.

The transect is located between the meltwater channel and the IL and is underlain by coarse glaciofluvial sediments (Figure 6.3). The depth of the three piezometers (T1-T3) varies between 1.6-1.8 m below ground. Groundwater solute concentrations in the transect were high. However, a considerable spatial variability between the three piezometers was observed, with high groundwater solute concentrations at T1 (27 m away from the Skaftafellsá channel) and T2 (54 m away from the channel) and lower concentrations at T3 (69 m away from the channel).

The highest SO_4^{2-} concentrations were measured at T1, where concentrations varied between 260 and 415 µeq/l. SO_4^{2-} concentrations at T2 varied between 140-318 µeq/l. In contrast to the high SO_4^{2-} concentrations at T1 and T2, the concentrations and range at T3 (158-200 µeq/l SO_4^{2-}) were substantially lower (Figure 6.8). Cl^- concentrations at the transect exceeded most groundwater concentrations in the outwash area and around the

IL, with mean Cl^- concentrations of approximately 140 µeq/l in all three piezometers. Groundwater Ca^{2+} + Mg^{2+} concentrations in the transect were amongst the highest measured in this study, exceeding those from the outwash and around the IL. The highest mean concentrations of Ca^{2+}+ Mg^{2+} were measured at T1 (1681 µeq/l), followed by T2 (1633 µeq/l) and T3 (1564 µeq/l) (Figure 6.9). The mean groundwater Na^++ K^+ concentrations in the transect (490 µeq/l) were also amongst the highest in the field site. However, the range and standard deviation at the transect were the smallest (Table 6.3). In contrast to SO_4^{2-} and Ca^{2+}+ Mg^{2+}, the highest mean Na^++ K^+ concentrations were measured at T3 (556 µeq/l), where mean concentrations exceeded those at T1 and T2 by approximately 100 µeq/l (Figure 6.10).

Groundwater solute concentrations at the transect generally increased between sampling intervals I and II. Ca^{2+}+ Mg^{2+} concentrations increased in all three piezometers, with the highest overall increase (~300 µeq/l) measured at T2. The temporal variability in SO_4^{2-} concentrations during this period was mixed. SO_4^{2-} concentrations fell by approximately 120 µeq/l at T1. Conversely, concentrations at T2 rose by approximately 80 µeq/l. Na^++ K^+ concentrations in all three piezometers have also increased slightly. Groundwater solute concentrations increased between Interval II and III at T1 and T2. Groundwater concentrations at T1 and T2 have increased by ~300 µeq/l Ca^{2+}+ Mg^{2+}, approximately 120 µeq/l SO_4^{2-} and, ~60 µeq/l Na^++ K^+, respectively. Conversely, the changes in solute concentrations at T3 were substantially smaller (Figure 6.12).

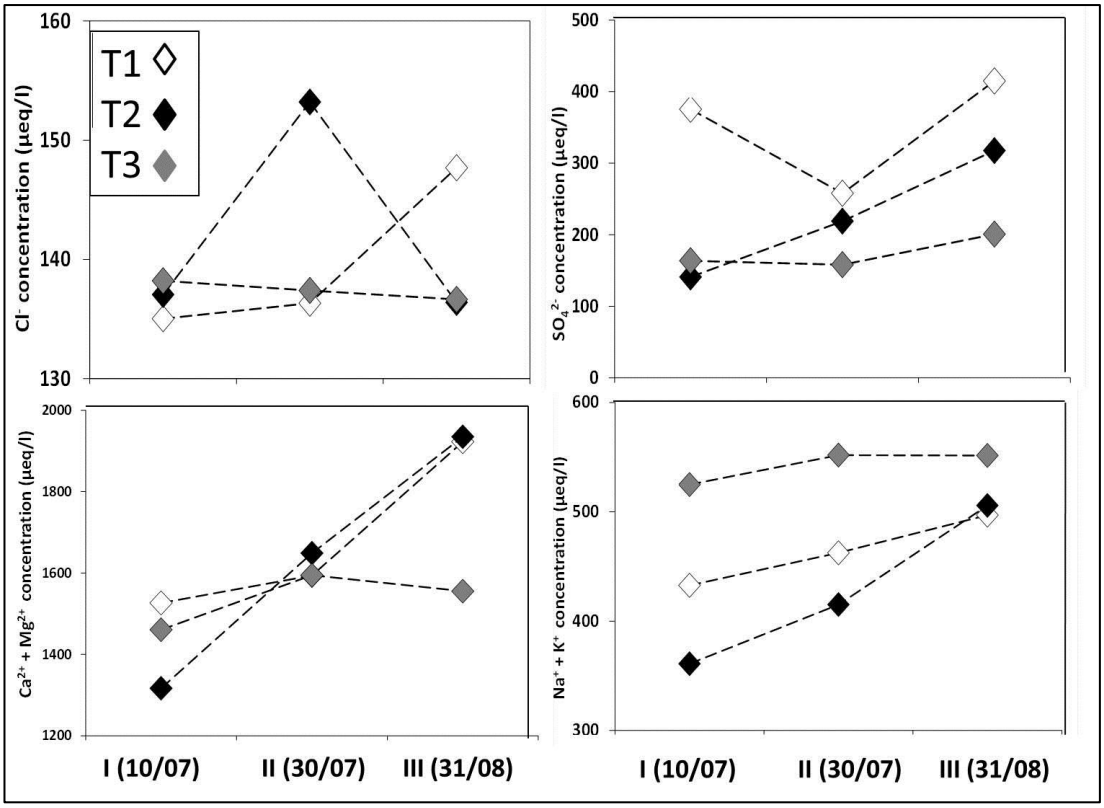

Figure 6.12. Temporal variability in groundwater solute concentrations at the transect (T1-T3) in July-August 2012.

A considerable spatial variability in groundwater geochemistry has been observed between the fine and coarse-grained lakeshores of the Instrumented Lake (IL). Cl^- and SO_4^{2-} concentrations ranged between 95-155 and 110-223 µeq/l, respectively. Generally, groundwater SO_4^{2-} concentrations at the coarse-grained lakeshore [L1-4, L7, and the Sand Nest (S.N.)] exceeded groundwater SO_4^{2-} concentrations at the fine-grained lakeshore (L5, 6, Clay Nest [C.N.]). The highest concentrations of Cl^- and SO_4^{2-} were measured at L1, which is located in coarse-grained sediment. In contrast to the transect and the piezometers near the Skaftafellsá, the variability in Cl^- concentrations around the IL generally exceeded that of SO_4^{2-}. Most Cl^- and SO_4^{2-} IL groundwater concentrations are "clustered" together, with concentrations of ~130-140 µeq/l Cl^- and 100-135 µeq/l SO_4^{2-}. However, Cl^- and SO_4^{2-} concentrations in some piezometers from the coarse-grained area

(L1, L2) and the fine-grained area (L7) exceeded the concentrations measured in the "cluster" (Figure 6.8).

The Ca^{2+}+ Mg^{2+} concentrations of IL groundwater varied between 930-1550 µeq/l. In contrast to the distinct "cluster" of Cl^- and SO_4^{2-} concentrations (Figure 6.8), the Ca^{2+}+ Mg^{2+} concentrations were more scattered (Figure 6.9). The lowest Ca^{2+}+ Mg^{2+} concentrations were measured at L4, L6, and the Sand Nest (SN). Similar to the Cl^- and SO_4^{2-} concentrations, the highest Ca^{2+}+ Mg^{2+} concentrations were also measured at L1. The highest mean and standard deviation of Na^++ K^+ concentrations at this study were measured in the IL groundwater, where concentrations varied between 300-1100 µeq/l. This contrasts other solutes, where maximum concentrations were generally measured in the transect (Table 6.3). Groundwater concentrations of all solutes around the IL were significantly higher (one tail t test, 2.5%, p=<*0.001*) than the concentrations in the lake's surface water (Figure 6.8-6.10).

The temporal variability in groundwater solute concentrations around the IL has shown that Cl^- concentrations generally fell during the season, with the lowest concentrations measured at interval III (end of August 2012). The declines in groundwater Cl^- concentrations in the fine-grained lakeshore generally exceeded that of the coarse-grained lakeshore. Conversely, groundwater SO_4^{2-} concentrations around the IL generally rose during the season, with the highest concentrations measured in interval III. The highest increases in SO_4^{2-} concentrations were measured at L1. The SO_4^{2-} concentrations and temporal variability of the piezometers located in the fine-grained lakeshore were similar (Figure 6.13). Groundwater Ca^{2+}+ Mg^{2+} concentrations in most of the piezometers around the IL increased by approximately 50 µeq/l between intervals I and II. However, groundwater concentrations in most piezometers fell by approximately 140 µeq/l during Interval III (Figure 6.14). These falls in Ca^{2+}+ Mg^{2+}concentrations contrasted the temporal dynamics which were observed in the transect and near the Skaftafellsá, where Ca^{2+}+ Mg^{2+} concentrations during interval III exceeded concentrations during interval II (Figure

6.11, 6.12). Groundwater Na^++ K^+ concentrations in some of the piezometers located in the coarse-grained lakeshore increased between interval I and II. Conversely, concentrations in piezometers emplaced in the fine-grained lakeshore remained similar. However, Na^++ K^+ concentrations in IL groundwater increased during Interval III, with concentrations rising by approximately 300 µeq/l and concentrations in many piezometers nearly doubling those measured during Interval II (Figure 6.14). These large increases contrast with the smaller increases (100 µeq/l) which were observed in the outwash (Figure 6.15), near the Skaftafellsá (Figure 6.11), and the transect (Figure 6.14). The Na^++ K^+ concentrations at the IL groundwater and surface water were similar (around 400 µeq/l) before interval III. However, while groundwater Na^++ K^+ concentration increased during interval III, Na^++ K^+ concentrations in IL surface water fell by approximately 50% (Figure 6.16~~)~~

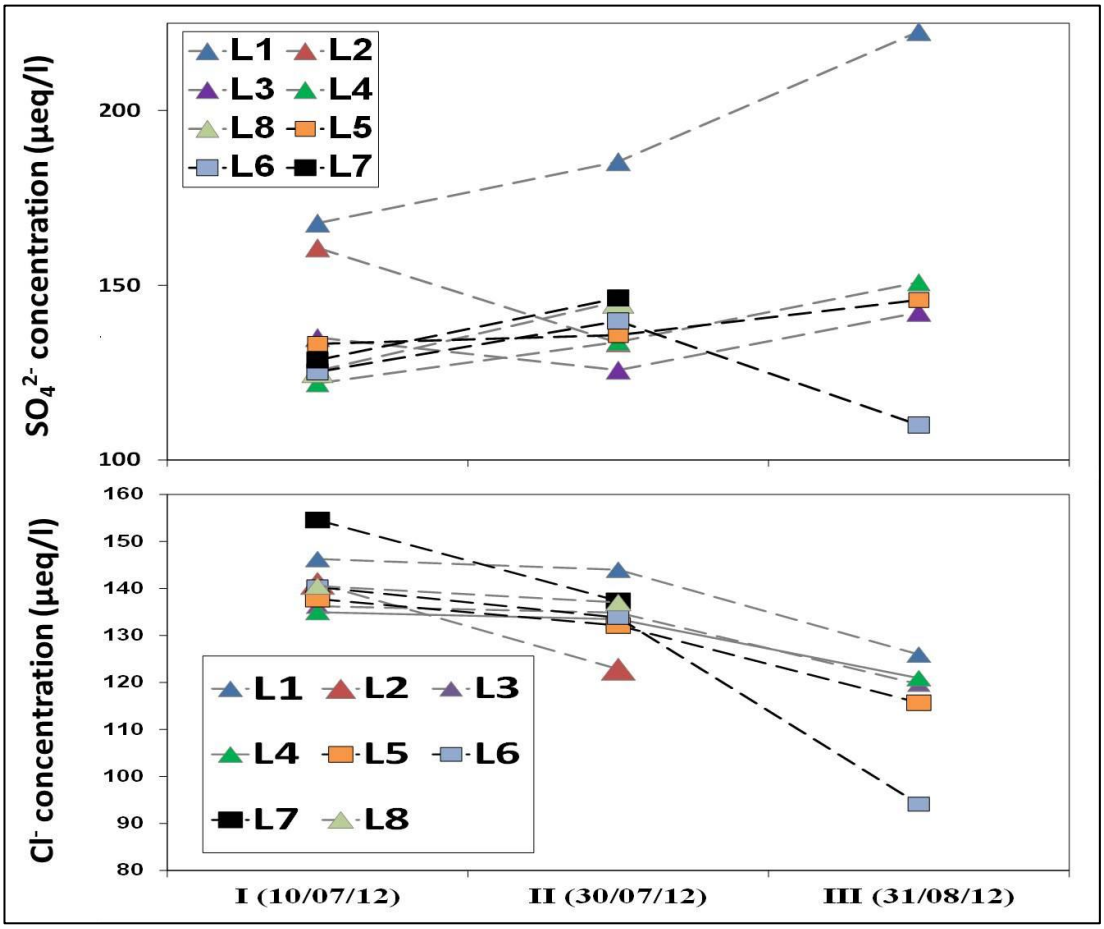

Figure 6.13. Temporal variability in Cl^- and SO_4^{2-} in IL groundwater (July-August 2012).

The fine-grained lakeshore is denoted with square and black lines. The coarse-grained lakeshore is denoted by triangles and grey lines.

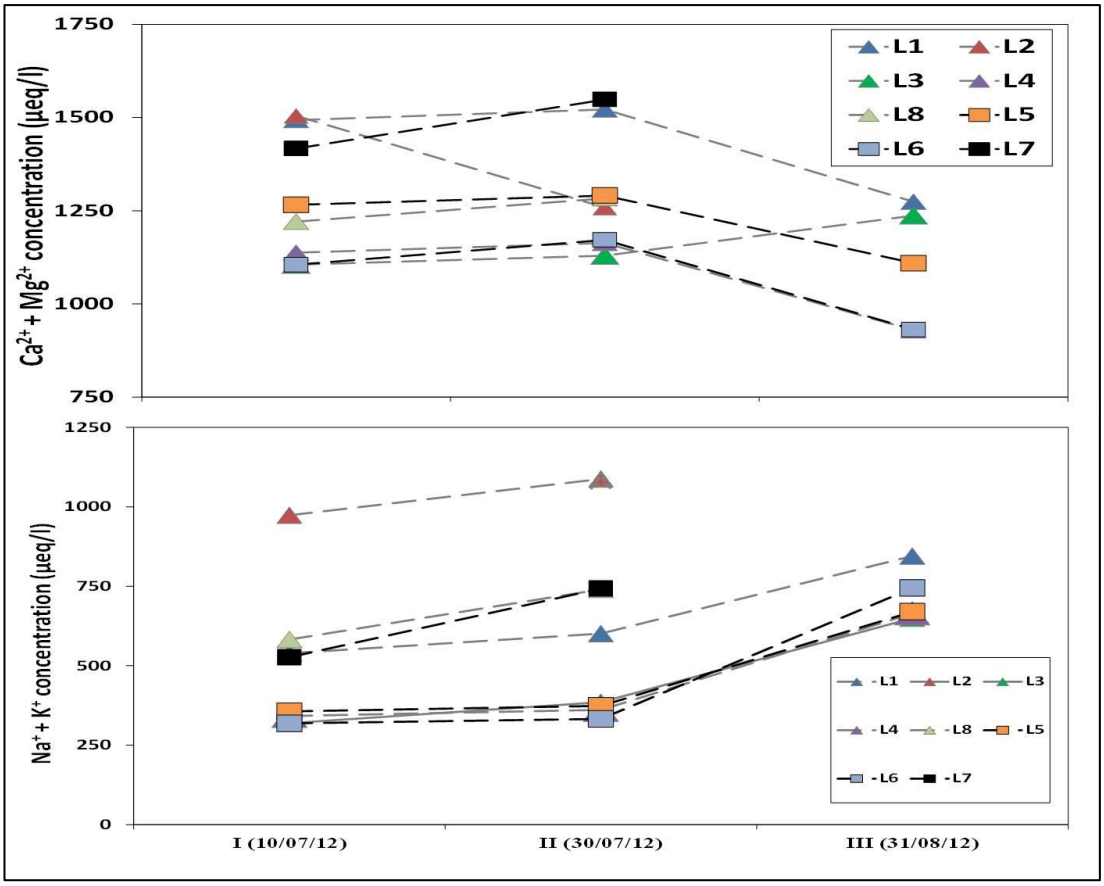

Figure 6.14. Fluctuations in IL groundwater concentrations of Ca^{2+}+ Mg^{2+} and Na^{+}+ K^{+}.

The fine-grained lakeshore is denoted with squares and black lines. The coarse-grained lakeshore is denoted by triangles and grey lines.

The outwash area is the closest hydrological environment to the Skaftafellsjökull glacier margin (~900 m). It is bordered by moraines to the north, east and south and by the Skaftafellsá channel in the west (Figure 6.3). The outwash area is underlain by coarse glaciofluvial deposits, with hydraulic conductivity of ~$1.16x10^{1}$ m/day (Figure 5.9). Four piezometers were installed in the outwash, open at depths of 1.36-1.80 m below ground level. GW10 is located north of the western section of the breached moraine, close to the river channel. The remaining three piezometers (GW11, GW12, and P12) are located between the breached moraine and the moraine located north of the IL (Figure 6.3).

Groundwater Ca^{2+}+ Mg^{2+} and SO_4^{2-} concentrations in the outwash were lower than the transect, but exceeded groundwater concentrations from the IL and near the Skaftafellsá (Figure 6.9). Groundwater Cl^- concentrations in the outwash were similar to those from the IL and the transect (Figure 6.8). Na^++ K^+ concentrations in the outwash were similar to those of IL groundwater (Figure 6.10). The highest SO_4^{2-}, Ca^{2+}+ Mg^{2+}, and Cl^- concentrations in the outwash were measured at GW10 (Figure 6.8, 6.9). Conversely, Na^++ K^+ concentrations at GW10 did not substantially exceed those at GW11 and GW12 (Figure 6.10).

During interval I, groundwater Ca^{2+}+ Mg^{2+}, Cl^-, and SO_4^{2-} concentrations in the outwash were close to those of the IL “cluster” and lower than solute concentrations in the transect. Concentrations then rose slightly during interval II. Similar to the transect and the piezometers near the river, hydraulic heads at the outwash area also fell by 0.06-0.20 m between intervals II and III. However, in contrast to the large increase in groundwater solute concentrations at these environments, the increases in the outwash were smaller. The largest increases were Ca^{2+}+ Mg^{2+} at GW11 and GW12 and Na^++ K^+ at P12. This pattern (a fall in Cl^- and rise in SO_4^{2-}) is similar to the patterns observed at the IL “cluster”. However, the increases in SO_4^{2-} and Ca^{2+}+ Mg^{2+} concentrations at the outwash have extended the differences in groundwater concentrations between the two environments.

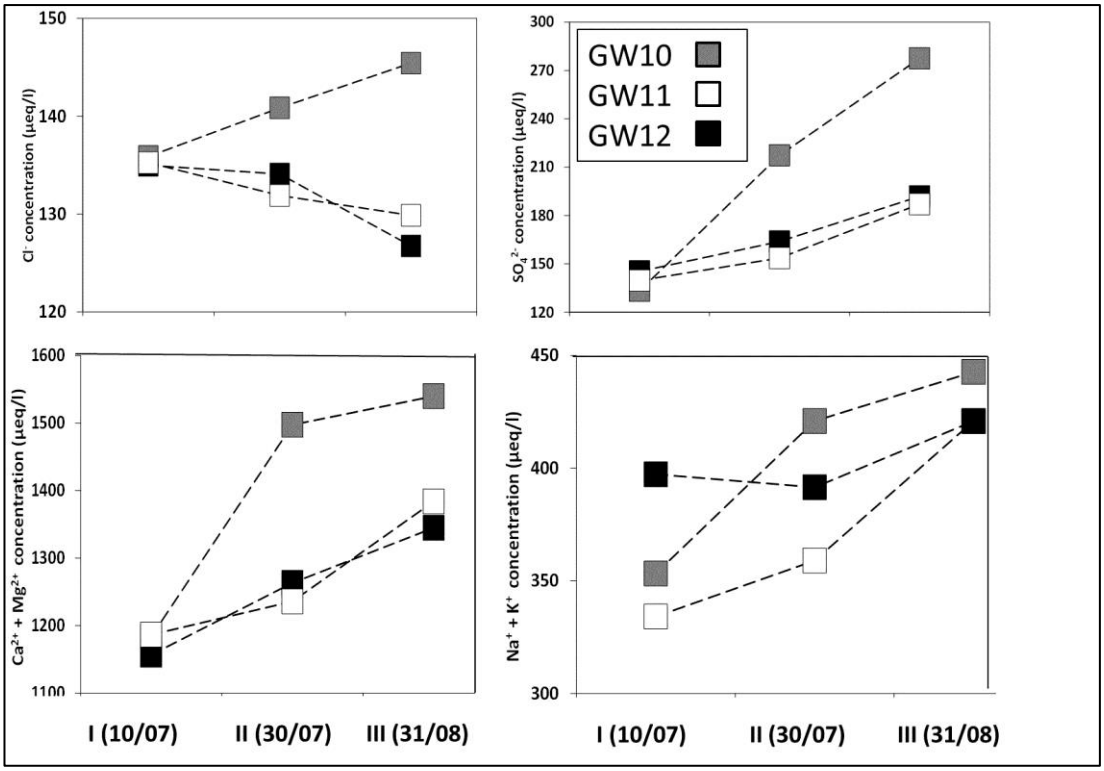

Figure 6.15. Groundwater solute concentrations in the outwash.

6.3.3. Summary

The lowest groundwater temperatures and EC were measured at GW9, located 20 m from the Skaftafellsá channel. The highest groundwater EC was measured at the transect (T1, located closest to the river) and GW5. Groundwater solute concentrations substantially exceeded those in the lakes and the meltwater river. The highest groundwater solute concentrations (Ca^{2+}+ Mg^{2+} and SO_4^{2-}) were generally measured in the transect. However, a considerable spatial variability was also observed in this area, with the lowest solute concentrations (and smallest temporal variability) found in T3 and highest at T1 (furthest and nearest the river, respectively). The highest Na^{+}+ K^{+} at the study were measured at the IL groundwater and T3.

6.4. Spatial and temporal variability in surface water quality and geochemistry

This section describes the spatial and temporal variability in surface water physicochemical parameters and solute concentrations. Surface water samples were collected from the Skaftafellsá, Northern Oasis lakes, and Southern Oasis lakes (Figure 6.3). The samples were collected during four sampling intervals, which took place around the 10/07/2012, 21/07/2012, 30/07/2012, and 25/08/2012 (Figure 6.4). The mean surface water concentrations of SO_4^{2-} , Ca^{2+}+ Mg^{2+}, and Na^{+}+ K^{+} were generally lower than groundwater concentrations. Conversely, Cl^{-} concentrations was higher than mean groundwater concentrations (Figure 6.7)

Considerable spatial variability in surface water quality and solute concentrations has been observed between the different hydrological environments of the Skaftafellsjökull foreland. The lowest temperature and variability (~1°C) in surface water were measured in the meltwater river Skaftafellsá. The highest surface water temperatures were measured in the Northern Oasis lakes (14.4-17.7°C). During the last measurement campaign (end of August 2012), temperatures in the Southern Oasis lakes substantially fell by 3-10 °C. The lowest surface water EC was measured in the Skaftafellsá (~30 µS/cm) and the Northern Oasis lakes (~50-70 µS/cm). The EC in the Southern Oasis lakes ranged between ~100-150 µS/cm. Within the Southern Oasis lakes, the highest temporal variability in EC was observed at the IL and Swan Lake, where EC fell by approximately 30 µS/cm in August (Figure 6.6)

The lowest mean Cl^{-} (34 µeq/l), SO_4^{2-} (15 µeq/l), Ca^{2+}+ Mg^{2+} (91 µeq/l) and Na^{+}+ K^{+} (120 µeq/l) concentrations and variability were also measured in the Skaftafellsá. After the Skaftafellsá, the Northern Oasis lakes had the lowest SO_4^{2-} (<30 µeq/l), Ca^{2+}+ Mg^{2+} (<500 µeq/l), and Na^{+}+ K^{+} (<250 µeq/l) concentrations. However, Cl^{-} concentrations in the Northern Oasis lakes were significantly higher than in the Southern Oasis lakes (one tail t

test, 2.5% S.L. *p=0.999*). Conversely, SO_4^{2-}, Ca^{2+}+ Mg^{2+}, and Na^{+}+ K^{+} concentrations in the Southern Oasis were significantly higher (1 tail t test, 2.5% SL, *p=<0.*001) than the concentrations in the Northern Oasis lakes (Figure 6.8-6.10).

The highest solute concentrations and variability in surface water geochemistry were measured at the Southern Oasis lakes. The highest SO_4^{2-} surface water concentrations (~100-120 µeq/l) were measured at Thin Lake, where Cl^{-} and SO_4^{2-} concentrations approached groundwater concentrations from the fine-grained (L5, L6, CN) lakeshore of the IL (Figure 6.8). Similar to the decline in groundwater Cl^{-} and SO_4^{2-} around the IL in August, the concentrations of these solutes also fell at Thin Lake (Figure 6.16). The highest Ca^{2+}+ Mg^{2+} (~1550 µeq/l), Cl^{-} (~170 µeq/l), and Na^{+}+ K^{+} (~ 430 µeq/l) concentrations in the Southern Oasis were measured at Heart Lake. Cl^{-} concentrations at Heart Lake exceeded those measured in most groundwater samples (Figure 6.8). The variability in Cl^{-} and SO_4^{2-} concentrations at the IL and Swan Lake generally exceeded that of Heart, Thin and Island Lakes (Figure 6.16). The Cl^{-} and SO_4^{2-} concentrations at Swan Lake ranged between 60-155 µeq/l and 36-61 µeq/l, respectively. The Na^{+}+ K^{+} concentrations at the IL were ~400 µeq/l. These concentrations were similar to those in Thin and Island Lakes, and are slightly higher than those in Swan Lake (Figure 6.10). Ca^{2+}+ Mg^{2+} concentration in the Southern Oasis lakes showed high spatial variability (Figure 6.9). The highest Ca^{2+}+ Mg^{2+} concentrations (~1500 µeq/l) were measured at Heart Lake, followed by Thin and Island Lakes (~1000-1200 µeq/l). These lakes also had smaller variability in Cl^{-} and SO_4^{2-} concentrations (Figure 6.8). Conversely, Ca^{2+}+ Mg^{2+} concentrations at the IL and Swan Lake were much lower (~600-900 µeq/l) (Table 6.4).

Table 6.4. Mean solute concentrations and physicochemical parameters in different surface water bodies at the Skaftafellsjökull foreland.

The numbers in brackets denote the number of samples within each environment (Figure 6.3).

	SO_4^{2-} (µeq/l)	Cl^- (µeq/l)	Ca^{2+}+ Mg^{2+} (µeq/l)	Na^+ + K^+ (µeq/l)	EC (µS/cm)	Temperature (°C)
River Skaftafellsá (7)	15±2	34±11	91±37	113±23	23±3	1±0
N. Oasis lakes (17)	29±12	153±36	285±105	298±167	55±10	16±1
Southern Oasis lakes						
Instrumented Lake (12)	49±34	104±44	875±69	341±77	107±13	14±3
Swan lake (12)	46±7	135±35	759±97	315±95	101±16	15±3
Island Lake (11)	57±15	148±5	1157±124	378±29	125±6	15±3
Thin Lake (9)	109±7	131±7	1130±37	349±12	116±5	13±4
Heart Lake (7)	48±6	163±9	1399±234	503±188	141±3	13±2
GWFS (3)	897±1344	161±28	2519±1887	529±253	231±162	12±2

The temporal variability in surface water solute concentrations is presented in Figure 6.16, Figure 6.17. A considerable variability was observed in surface water concentrations of different solutes between intervals I and II (10/07-21/07/2012). Cl^- and SO_4^{2-} concentrations generally fell in all lakes, with the highest falls (84 µeq/l Cl^- and 61 µeq/l SO_4^{2-}) measured at the IL. The changes in Ca^{2+}+ Mg^{2+} concentrations varied, with a fall in Ca^{2+}+ Mg^{2+} concentrations at Swan (51 µeq/l) and Thin Lakes (67 µeq/l) and a rise at the IL (52 µeq/l), Island Lake (82 µeq/l), and the Skaftafellsá (30 µeq/l). Na^++ K^+ concentrations have also increased in all lakes except Thin Lake (Figure 6.16, 6.17).

During interval II, hydraulic heads and lake levels at the site rose by ~0.10 m between the 21/07 to the 30/07, coinciding with the season's highest rainfall event (33 mm on the 23/07/2012). Ca^{2+}+ Mg^{2+} concentrations in the IL, Swan and Thin Lakes increased by ~90 µeq/l. Conversely, concentrations fell substantially at Island (-97 µeq/l) and Heart (-284 µeq/l) Lakes. Cl^- and SO_4^{2-} concentrations at the IL have also increased. Na^++ K^+ concentrations at Heart Lake substantially increased by 250 µeq/l. Na^++ K^+ concentrations

at Thin Lake and the IL have increased by 20 µeq/l. Conversely, concentrations at Swan and Island Lakes fell by ~30 µeq/l Na^++ K^+ (Figure 6.16, 6.17).

The field site was unmanned between 31/07/2012 and 23/08/2012. When monitoring was resumed, an increase of ~0.010-0.020 m was measured in groundwater and lake levels. The pressure transducers measured a substantial flood on the 13-14/08/2012, during which meltwater and hydraulic heads increased by approximately 0.50 m in 10-14 hours. In addition to the flood, two rainfall events of 20 mm (21/08/2012) and 12 mm (25/08/2012) also took place during this period. However, despite the flood and rainfall events, groundwater and lake levels quickly declined at the end of August. The changes in solute concentrations following these events has shown a considerable spatial variability. Solute concentrations at the IL and Swan Lake have fallen between intervals III and IV (Figure 6.16, 6.17). Smaller declines also took place at Thin Lake. Conversely, Ca^{2+}+ Mg^{2+} concentrations at Island and Heart Lake have increased by 64 µeq/l and 244 µeq/l, respectively. SO_4^{2-} concentrations have also increased in these lakes. Na^++ K^+ concentrations at Heart Lake declined by 302 µeq/l (Figure 6.17)

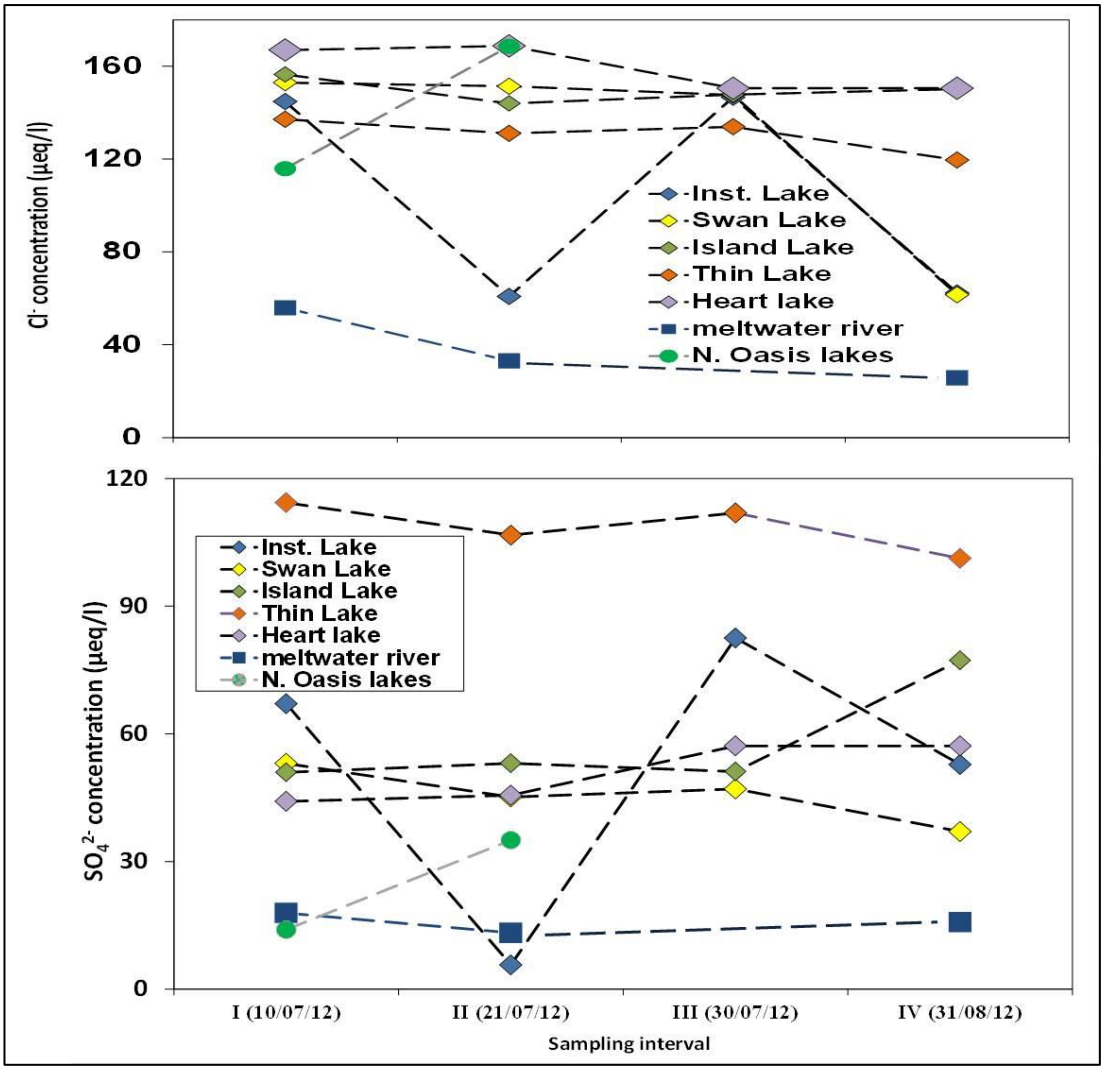

Figure 6.16. Fluctuations in surface water Cl^- and SO_4^{2-} concentrations.

Please note the notation for the different hydrological environments: The Southern Oases lakes (diamonds), Northern Oasis lakes (circles), and the meltwater river Skaftafellsá (squares). Note that the measurements for the Northern Oasis lakes were only taken during sampling intervals I and II. The figure shows the mean concentration during each interval.

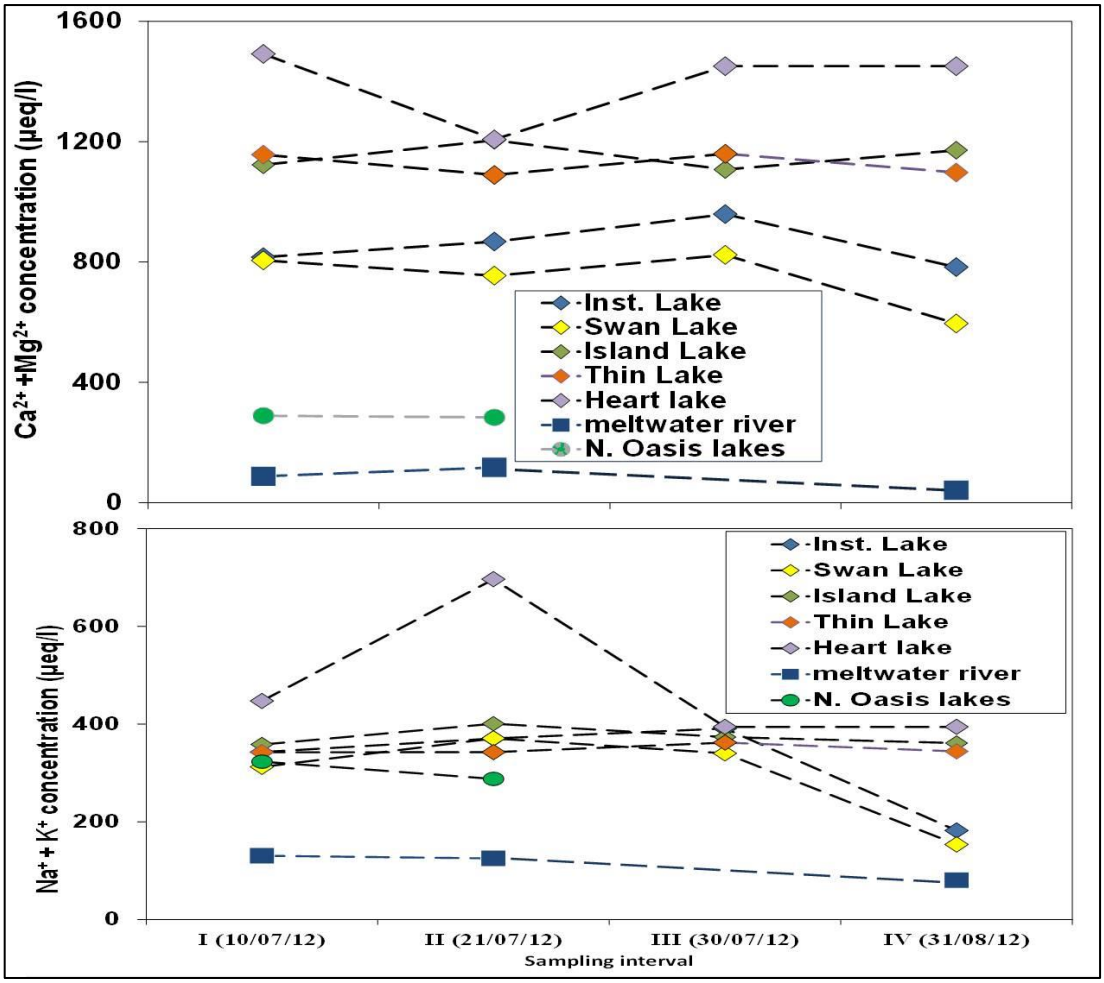

Figure 6.17. Fluctuations in surface water Ca^{2+}+ Mg^{2+} and Na^{+}+ K^{+} concentrations.

Please note the notation for the different hydrological environments: the Southern Oasis lakes (diamonds), Northern Oasis lakes (circles), and the meltwater river Skaftafellsá (squares). Note that the measurements for the Northern Oasis lakes were only taken during sampling intervals I and II. The figure shows the mean concentration during each interval.

In summary, this section described the spatial and temporal variability in surface water quality and geochemistry at the Skaftafellsjökull foreland. A considerable spatial variability has been observed between the river Skaftafellsá, the Northern Oasis lakes and the Southern Oasis lakes. The river Skaftafellsá had the lowest temperature, EC, and solute concentrations. The EC and solute concentrations at the Northern Oasis lakes was lower and less variable than that of the Southern Oasis lakes. However, Cl^{-} concentrations were higher in the Northern Oasis lakes. The highest surface water concentrations of SO_4^{2-} were measured at Thin Lake. The highest Cl^{-}, Ca^{2+}+ Mg^{2+}, and Na^{+}+ K^{+} were measured at

Heart Lake. Substantial declines in lake water temperature, EC, and solute concentrations were observed at the IL and Swan Lake during the sampling interval at the end of August. Conversely, these parameters have increased in the other lakes at the Southern Oasis.

6.5. The $\delta^{18}O$ and δD composition of groundwater and surface water at the Skaftafellsjökull foreland

6.5.1. Introduction

This section describes the spatial variability in the stable isotope composition of meltwater, groundwater, surface water, and precipitation. A total of 31 stable isotope samples were obtained from various groundwater and surface water locations at the field site: Skaftafellsá (n =6), Southern Oasis lakes (IL=2, Swan Lake=1, Thin Lake=2, Island Lake=2), the Ground Water Fed Stream (n =4) (GWFS), and piezometers (n =15). The piezometers which were sampled are: T1-T3 (transect), GW5 and GW9 (near the river channel), L1-L5 and the piezometer nests (the IL), and GW11, GW12, and P12 (the outwash). The samples were collected on the 24-25/08/2012, hence, after the flood of the Skaftafellsá (Chapter 7). The mean isotopic composition for the different hydrological environments in the Skaftafellsjökull foreland is presented in Table 6.5. The isotopic composition of precipitation, groundwater and surface water at the Skaftafellsjökull foreland is presented in Figure 6.18. The glacial melt end member is composed of the mean $\delta^{18}O$ and δD composition for the Skaftafellsá (current study) and the isotopic composition of glacial ice from Skaftafellsjökull (n=4), which were obtained from Cook *et al*. (2010). The precipitation data was obtained from Robinson (2003). The rationale for using this data set is provided in section 6.5.2.

The Local Meteoric Water Line (LMWL) at the Skaftafellsjökull foreland plots below the Global Meteoric Water Line (GMWL), but with a slightly steeper slope. The slopes of the

groundwater (6.87) and lakes (6.49) samples are much lower than that of the GMWL. Most of the groundwater, lakes, and the GWFS samples plot on the LMWL, with the isotopic composition ranging between -7.7 to -8.6 $\delta^{18}O$ and -41.0 to -59.0 δD. However, several groundwater (GW9, GW5, L2) and surface water samples from the IL and Swan Lake plot further down the LMWL, having a lighter isotopic composition. Conversely, the isotopic composition of the head of the GWFS and Island Lake plots below the LMWL. The glacial melt end-member and samples plot very close to the GMWL (Figure 6.18). Groundwater, lakes and the GWFS samples are significantly more isotopically heavy than those of glacial melt (1 tail t test, 2.5% SL, *p*=<*0.001*).

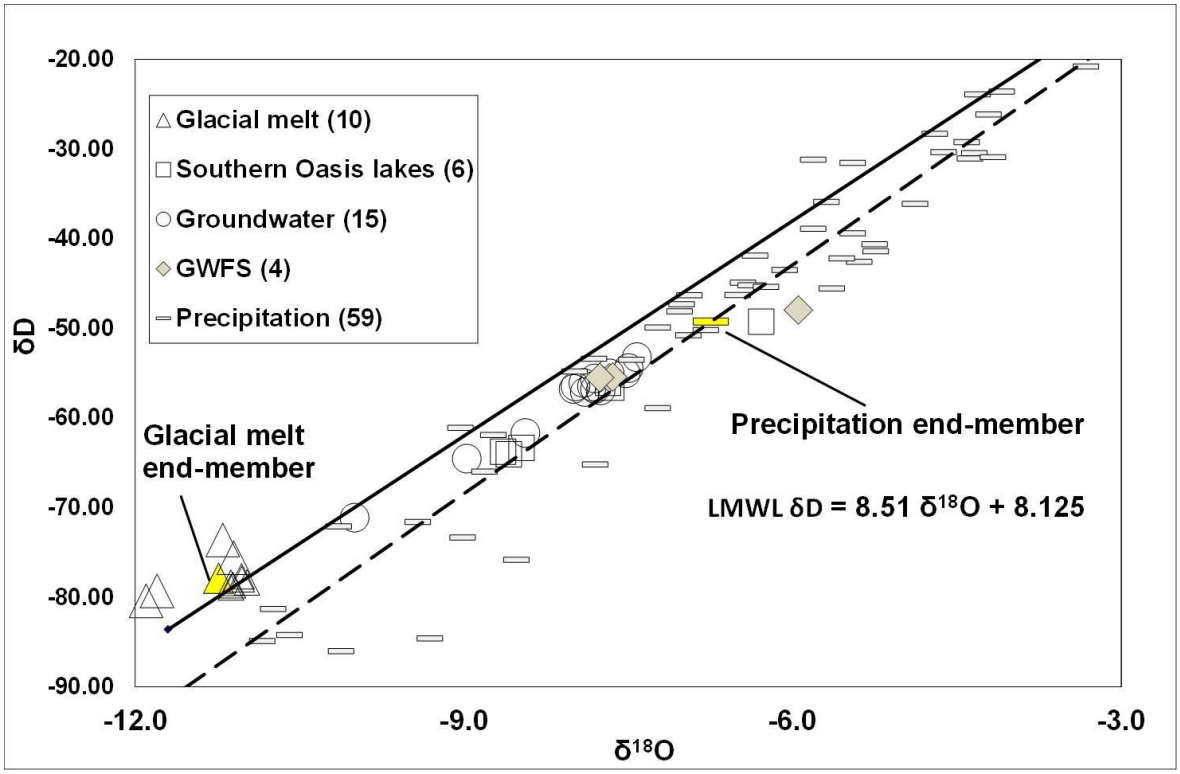

Figure 6.18. δD vs $\delta^{18}O$ composition of groundwater and surface water at the Skaftafellsjökull foreland.

The GMWL is denoted by the solid black line. The LMWL (dashed line) was calculated from the trend line of the isotopic composition of precipitation (equation shown). The end-member for the isotopic composition precipitation and glacial melt are denoted in yellow.

Table 6.5. Mean isotopic composition of the different hydrological environments at the Skaftafellsjökull foreland.

The number of samples in each environment is in brackets. Full data set is found in Appendix 6.

	$\delta^{18}O$ (‰)	δD (‰)
Glacial melt (10)	-11.24±0.33	-77.9±2.0
Lake surface water (6)	-7.89±0.90	-58.9±5.9
Groundwater(15)	-8.03±0.67	-57.8±4.6
GWFS (4)	-7.25±0.87	-53.6±3.8
Precipitation (59)	-6.74±2.80	-49.2±24.3

6.5.2. The isotopic composition of precipitation

The reliable determination of the isotopic composition of precipitation and a LMWL requires precipitation samples that span over at least one year (Clark and Fritz, 1997). However, due to logistical constraints, stable isotope samples from local precipitation were not collected during this study. Therefore, in order to define the isotopic composition for precipitation, this study compared the isotopic composition of summer (June-August) precipitation from Skeiðarársandur (Robinson, 2003) with that of summer precipitation from the International Atomic Energy Agency (IAEA) station in Reykjavik, which forms part of the Global Network of Isotopes in Precipitation (GNIP). The isotopic composition of precipitation in Skeiðarársandur was determined from samples that were collected from several field stations during 1998, 2000, and 2001. The stations are located up to 20 km to the NW of the Skaftafellsjökull foreland field site. The IAEA data set contains the mean monthly isotopic composition of precipitation in Reykjavik from the years 1961-1976, 1992-1999, 2000-2006, 2008, and 2009 (IAEA/WMO, 2014).

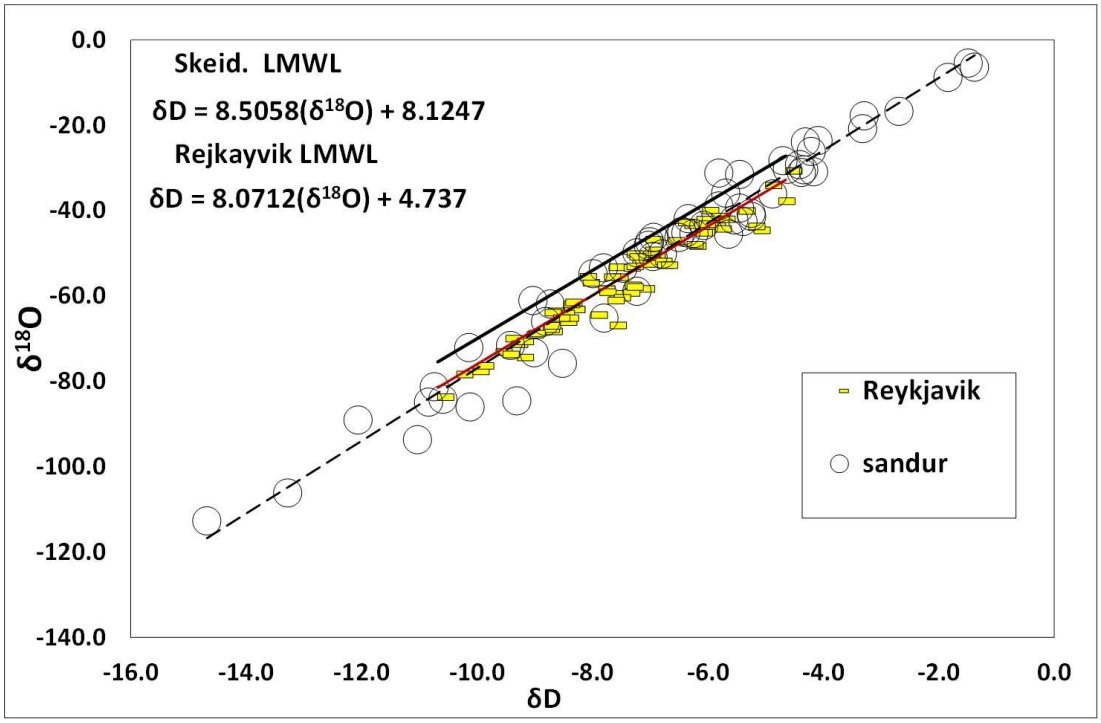

Figure 6.19. The isotopic composition of summer precipitation from Skeiðarársandur (Robinson 2003) and Reykjavik (IAEA/WMO, 2014).

The figure also shows the LMWL for Reykjavik isotopic composition (red line), the GMWL (bold black line) and the LMWL (black dashed line) for Skeiðarársandur.

The isotopic composition of precipitation from the two data sets is presented in Figure 6.19. The slope of the Reykjavik precipitation LMWL was slightly lower than that of Skeiðarársandur. The intercept of the Reykjavik LMWL was much lower than that of Skeiðarársandur. The LMWL for both Skeiðarársandur and the Reykjavik data deviate from the GMWL along a slightly steeper slope below the GMWL. Table 6.5 shows that the mean isotopic composition for Skeiðarársandur precipitation (-6.74±2.80‰ $\delta^{18}O$ and -49.24± 24.27‰ δD) was more isotopically enriched than the Reykjavik precipitation (-7.60±1.35‰ $\delta^{18}O$ and -56.57±11.31‰ δD). However, despite the smaller number of samples and shorter data set, the standard deviation and range for the Skeiðarársandur data is higher than the Reykjavik data (Table 6.5). This suggests that precipitation at the two sites is impacted by different sources (Clark and Fritz, 1997). The high variability in the isotopic composition of precipitation in Skeiðarársandur can also be attributed to the data being collected from field stations, where following all of the IAEA collecting protocols

was not always possible, making modifications by evaporation and contamination are more likely.

Table 6.6. Summary of the isotopic composition of summer precipitation from Skeiðarársandur (Robinson, 2003) and Reykjavik (IAEA/WMO, 2014).

Note that the Reykjavik data shows the mean monthly isotopic composition.

	$\delta^{18}O$ (‰)	**δD (‰)**
Skeiðarársandur summer (59)	-6.74± 2.80	-49.24± 24.27
Reykjavik summer (77)	-7.60± 1.35	-56.57± 11.31
	Trend line of the LMWL	
Slope	8.51	8.07
Intercept	8.12	4.74
R^2	0.964	0.933

Each data set has its merits and limitations for being used for the determination of an end-member isotopic composition for precipitation. The data from Skeiðarársandur provides a better representation for local precipitation at the study site. However, this data is 15 years old and more limited in number. This can be problematic, especially with regards to the high temporal variability of the isotopic composition of precipitation from Skeiðarársandur (Robinson, 2003). On the other hand, the Reykjavik data is more recent (up to 2009) and covers a much longer period than the Skeiðarársandur data. Quality control measures for the Reykjavik data are also assumed to be tighter. However, this data was collected ~350 km from the field site. Additionally, the data from Skeiðarársandur was collected from individual precipitation events, whilst the Reykjavik data shows the mean monthly isotopic composition, which can mask finer temporal variability. Therefore, due to the proximity to the site, and the inclusion of individual events, rather than monthly mean isotopic composition, the isotopic composition of precipitation from Skeiðarársandur (Robinson, 2003) was used in the current study.

6.5.3. Groundwater isotopic composition

The spatial distribution of groundwater $\delta^{18}O$ at the Skaftafellsjökull foreland is presented in Figure 6.20. The isotopic composition of groundwater at the Skaftafellsjökull foreland ranged between -10.00‰ to -7.42‰ $\delta^{18}O$ and -71.1‰ to -53.2‰ δD (Table 6.5). The isotopically lightest groundwater was measured in the piezometers near the river (GW9 and GW5). GW9, which is located 20 m from the Skaftafellsá meltwater channel, has the lightest groundwater isotopic composition, with -10.0‰ $\delta^{18}O$ and -71.1‰ δD. The isotopic composition of GW5, located 38 m away from the meltwater channel was slightly heavier (-8.97‰ $\delta^{18}O$ and -64.5‰ δD). However, it was still isotopically lighter than other groundwater samples in the catchment. Groundwater isotopic composition from the IL ranged between -7.5‰ to -8.4‰ $\delta^{18}O$ and -55.0‰ to -61.7‰ δD. The heaviest isotopic composition was measured in L1, which is located in the coarse-grained lakeshore of the IL (-7.52 $\delta^{18}O$ and -55.0 δD‰). The lightest isotopic composition from the IL groundwater was measured in L2, which is also located in the coarse-grained lakeshore (-8.44 $\delta^{18}O$‰ and -61.7 δD‰). However, apart from the L1 and L2, the isotopic composition of groundwater from the remaining piezometers was very similar (approximately -7.9 $\delta^{18}O$ ‰ and -56.1 δD ‰). The spatial variability of groundwater isotopic composition in the outwash was smaller than the IL groundwater, with a very narrow range of 0.2 ‰ $\delta^{18}O$ and 1.6 ‰ δD. Groundwater isotopic composition in the transect ranged between -7.4 to -8.0 ‰ $\delta^{18}O$ and -53.2 to -56.5 ‰ δD. The lightest isotopic composition in the transect was measured at T2. The heaviest isotopic composition was measured at T1, which is closest to the river (27 m) (Figure 6.20).

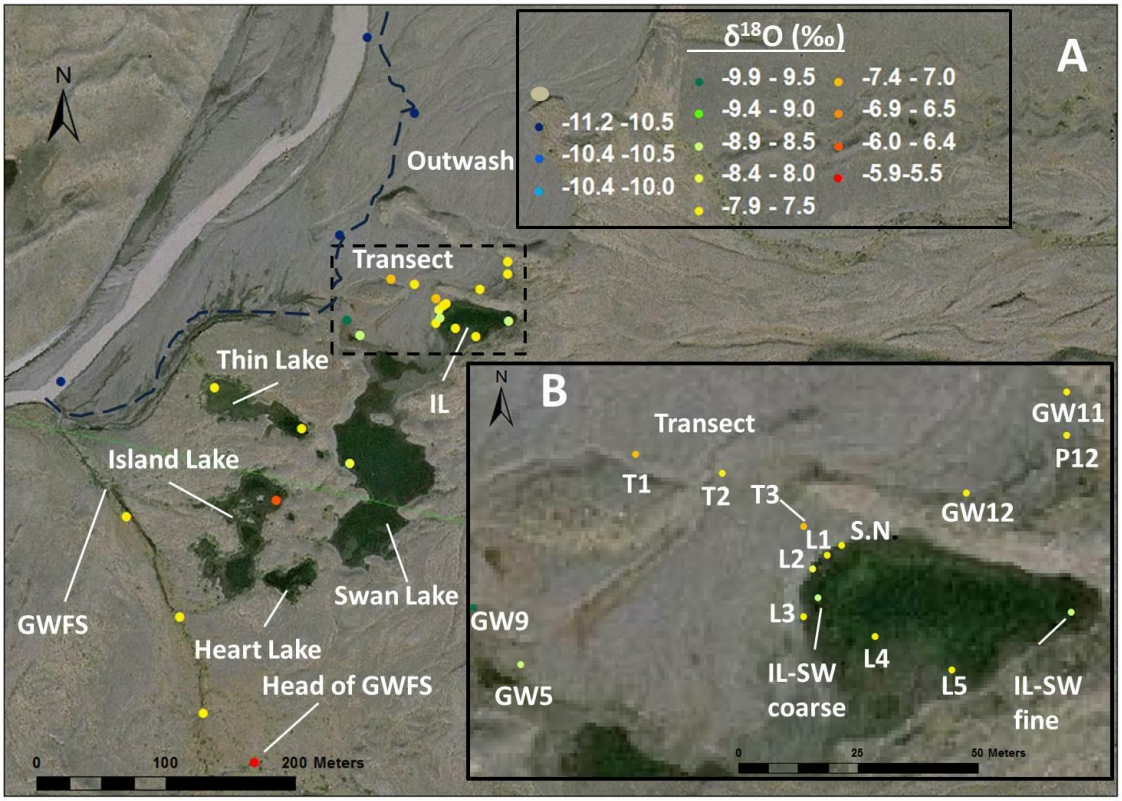

Figure 6.20. Spatial variability of $\delta^{18}O$ in groundwater and surface water at the Skaftafellsjökull foreland.

The sampling locations around the IL are included in detail in inset B (black dashed box). The image was taken from Vatnajökull National Park (2007). The Skaftafellsá meltwater channel has changed its location since the image was taken. The location of the meltwater channel when the samples were collected (August 2012) is denoted by the dashed blue line.

6.5.4. The isotopic composition of surface water

Substantial heterogeneity has been observed in the isotopic composition of surface water at the Skaftafellsjökull foreland (Figure 6.20, 6.21). The isotopic composition of surface water ranged between -5.9 to -11.9‰ ± 1.44‰ $\delta^{18}O$ and -48.0 to -80.4± 9.40‰ δD. The river Skaftafellsá (n=6) had the most depleted isotopic composition (-11.06 ± 0.06 $\delta^{18}O$ and -78.3 ± 0.4 δD‰) and the lowest standard deviation. The isotopic composition of lake surface water (n=6) ranged between -8.64 and -6.28‰ $\delta^{18}O$ and -64.1 to -49.3‰ δD. The mean $\delta^{18}O$ and δD for lake surface water was similar to that of groundwater (-8.00±0.90 ‰ $\delta^{18}O$ and -58.5±5.9 ‰ δD). However, the standard deviation for groundwater was lower

(Table 6.5). The lightest isotopic composition of lake water was measured in the IL and Swan Lake (approximately -8.5‰ $\delta^{18}O$ and -64‰ δD). The heaviest lake water isotopic composition was measured at Island Lake (-6.3‰ $\delta^{18}O$ and -49.3‰ δD). The isotopic composition of Thin Lake lay between the compositions of Island Lake and the IL (Figure 6.20)

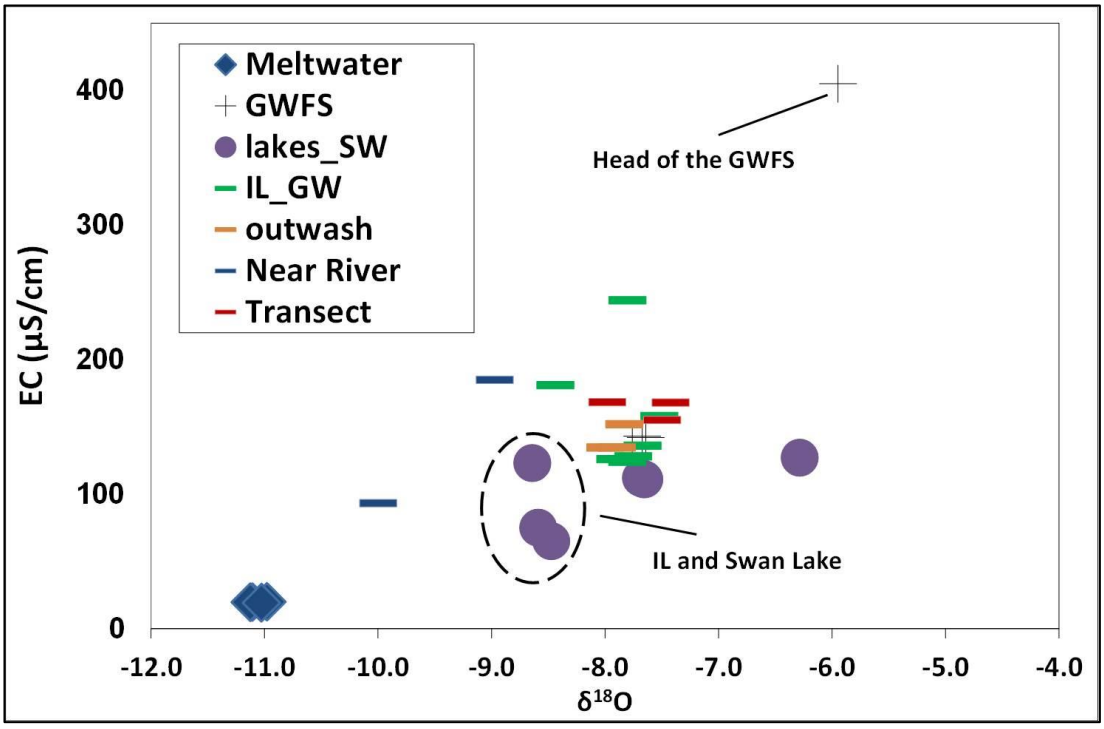

Figure 6.21. Groundwater and surface water EC vs. δ18O composition (after Lambs, 2004). Groundwater samples are denoted by the different rectangles.

6.5.5. Spatial variability in Deuterium Excess (*d-excess*)

The *d-excess* of groundwater and surface water at the Skaftafellsjökull foreland ranged between -0.39 and +10.60 ‰ (Figure 6.22). The highest values and lowest standard deviation of *d-excess* were measured in the Skaftafellsá, where values ranged between +9.5 to +10.6 ‰. Groundwater *d-excess* was generally higher than that of the lakes. However, high variability was measured in groundwater *d-excess*, where values ranged between +5.1 (L5) to +8.8 ‰ (GW9). Relatively high *d-excess*, of approximately +7.0‰

was measured in some piezometers in the transect (T2), outwash (GW11), IL (L4), and near the river (GW5). However, the *d-excess* in other piezometers within these environments were lower (+5.1 to +6.0‰).

The *d-excess* values of surface water in the Southern Oasis lakes and GWFS (excluding the head of the GWFS) were generally lower (+4.4 to +5.4 ‰) than groundwater *d-excess*. However, the *d-excess* from the middle of the GWFS was +6.6‰. The lowest *d-excess* values were obtained from Island Lake (+1.0‰) and the head of the GWFS (-0.4‰) (Figure 6.22).

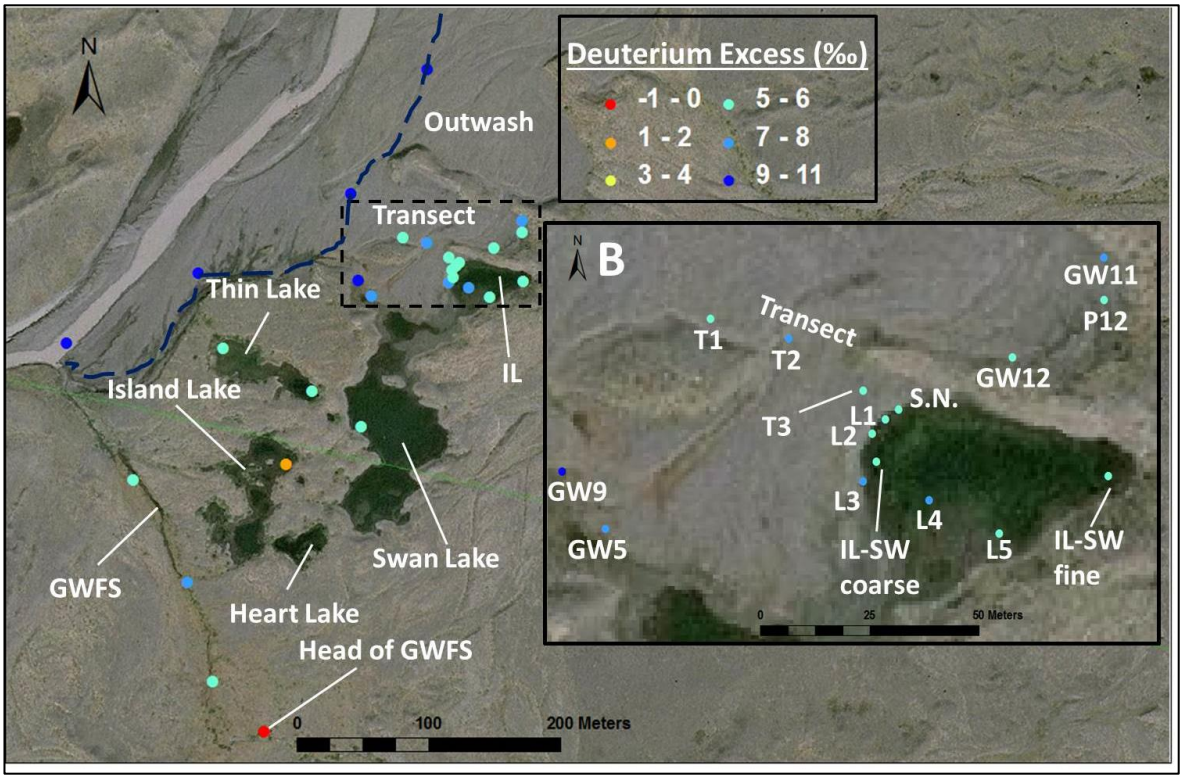

Figure 6.22. The spatial variability of Deuterium Excess (‰) in groundwater and surface water at the Skaftafellsjökull foreland.

The sampling locations from around the IL are included in detail in inset B, whose area is denoted by the black dashed box. The image was taken from LMI (2007). The Skaftafellsá meltwater channel has changed its location since the image was taken. The location of the meltwater channel when the samples were collected (August 2012) is denoted by the dashed blue line.

6.5.6. Summary

The isotopic composition of groundwater at the Skaftafellsjökull foreland ranged between -10.00‰ to -7.42‰ $\delta^{18}O$ and -71.1‰ to -53.2‰ δD. However, considerable spatial variability was observed in the isotopic composition of groundwater in the different hydrological environments. The isotopically lightest groundwater and highest *d-excess* was measured near the Skaftafellsá (GW9 and GW5). The isotopic composition of groundwater at GW9 was located on the GMWL while groundwater at GW5 was located further down the LMWL than most groundwater samples. The isotopic compositions of groundwater in the outwash, around the IL, and the transect were heavier than that of groundwater near the Skaftafellsá, with most samples located on the LMWL. A considerable variability was also observed in the isotopic composition of surface water. The Skaftafellsá had the most isotopically light composition and highest *d-excess*. From the Southern Oasis lakes, the IL and Swan Lake had more depleted isotopic compositions than Thin Lake and Island Lake. The head of the GWFS had the most isotopically heavy composition and lowest *d-excess*. However, apart from the head of the GWFS, the other samples from the GWFS had similar isotopic composition to that of the groundwater around the IL and the surface water of Thin Lake (Figure 6.18).

6.6. Interpretation and discussion

6.6.1. Sources of recharge at the Skaftafellsjökull foreland

Water stable isotopes were used in this study to identify the sources of recharge for groundwater and surface water at the Skaftafellsjökull foreland. Using stable isotopes, local precipitation and glacial melt were previously identified as the main sources of groundwater recharge in Skeiðarársandur, where the impact of glacial melt diminished

with distance away from the glacier margin. However, this pattern was complicated by exchange between groundwater and meltwater rivers (Robinson *et al*., 2009b). The isotopic composition of groundwater, lakes and the GWFS at the Skaftafellsjökull foreland was significantly heavier than that of glacial melt (one tail t test, 2.5% S.L., p=<*0.001*). Additionally, the isotopic compositions of most groundwater and lake water samples were located on the LMWL (Figure 6.18). This suggests that local precipitation is the main source of recharge at the areas studied at the Skaftafellsjökull foreland (Clark and Fritz, 1997; Jonsson *et al*., 2009). Island Lake and the head of the GWFS had the heaviest isotopic composition and lowest *d-excess*, which suggests that evaporation is significant at these sites. Conversely, the groundwater at GW9 and GW5, located near the Skaftafellsá, had lighter isotopic composition, close to that of glacial melt (Figure 6.20). This relatively light isotopic composition suggests higher proportions of meltwater at GW5 and GW9 (Malard *et al*., 1999; Chiogna *et al*., 2014). The isotopic composition of groundwater and meltwater from the Skaftafellsjökull foreland was close to the isotopic composition in Skeiðarársandur (Robinson *et al*., 2009b). This is probably due to the similar sources of precipitation which impact both areas. The isotopic composition of both sites is generally more enriched than those reported from the Alps (Hindshaw *et al*., 2011), Alaska (Crossman *et al*., 2011), Arctic Sweden (Dahlke *et al*., 2014), Greenland (Kristiansen *et al*., 2012), Antarctica (Gooseff *et al*., 2006; 2013), and the Andes (e.g. Ohlanders *et al*., 2013), where the latitude, altitude and continentality effects are more dominant than in the lowland sandurs of SE Iceland (e.g. Clark and Fritz, 1997).

6.6.2. Controls on groundwater and surface waters geochemistry at the Skaftafellsjökull foreland

This section investigates the major controls on groundwater and surface water geochemistry at the Skaftafellsjökull foreland. Similar to studies from other glacial environments, solute concentrations in groundwater at the Skaftafellsjökull foreland also

generally exceeded those in meltwater (Table 6.7, 6.8). Groundwater solute concentrations in the Skaftafellsjökull foreland generally exceeded those reported from Alaska (Anderson *et al*., 2000) and the Alps (Tranter *et al*., 2002; Hindshaw *et al*., 2011). This can be explained by the wide availability of reactive glassy basalts (e.g. Gíslason and Eugster, 1987) in the Skaftafellsjökull foreland in comparison to that in the Alps (Fairchild *et al*., 1999a, b; Hindshaw *et al*., 2011). Conversely, groundwater solute concentrations at the Skaftafellsjökull foreland are substantially lower than those reported from Svalbard and Antarctica (Table 6.7). The elevated solute concentrations in these catchments have been attributed to the formation, by evapoconcentration, and dissolution during the melt period, of efflorescent salts (e.g. Wadham *et al*., 2001). However, these processes do not appear to be significant in SE Iceland, due to the milder temperatures and high and frequent precipitation events (Robinson *et al*., 2009a).

Volcanic and geothermal activity can also impact groundwater and surface water chemistry at the field sites. Skeiðarársandur is impacted by volcanic eruptions from the subglacial volcanoes beneath Vatnajökull. In addition to their hydrological and geomorphic impacts (e.g. Russell *et al*., 2006), such as jökulhlaups, these eruptions and associated geothermal systems may also have impacted the geochemistry of groundwater and surface water. For instance, the high concentrations and standard deviation of solute concentrations in eastern Skeiðarársandur groundwater (Table 6.7) and in the River Skeiðará (Table 6.8) suggest that this area is episodically impacted by geothermal water (Robinson *et al*., 2009a). Additionally, the deposition and subsequent dissolution of volcanic tephra, which weathers very quickly, can also increase solute concentrations in groundwater and surface water (e.g. Galeczka *et al*., 2014). In contrast to the aforementioned results from areas which are impacted by geothermal activity (e.g. Gíslason and Eugster, 1987b; Kristmannsdóttir *et al*., 2004), the EC, temperature and most solute concentrations of groundwater and surface water at the Skaftafellsjökull foreland are substantially lower (Table 6.7) . Hence, it is suggested that mixing with

geothermal water is probably not an important control on the proglacial geochemistry of groundwater and surface water at the Skaftafellsjökull foreland.

Table 6.7. Solute concentrations in groundwater from various proglacial environments. The numbers in brackets shows the number of samples.

Groundwater solute concentration (µeq/l)	Cl^-	SO_4^{2-}	Na^+	K^+	Mg^{2+}	Ca^{2+}
Skaftafellsjökull groundwater[1] (59)	126±24	166±73	482±169	17±18	153±63	1182±332
Skeiðarársandur groundwater (West)[2]	82±40	63±26	224±56*			388±137
Skeiðarársandur groundwater (East)[2]	116±52	300±197	481±134*			1873±1056*
Lower Skeiðarársandur groundwater[2]	339±193	114±57	536±144*			1031±389*
W. Skeiðarár. GW[1] (2011-12) (20)	153±74	319±573	336±137	8±5	144±163	408±274
Groundwater seeps W. Skeiðarársandur (2011/12)[1]	86±29	54±42	258±41	2±2	132±32	403±80
Damma Glacier, Swiss Alps[3] (12)	98±251	13±7	17±7	25±12	21±15	85±58
Haut Glacier d'Arolla, Swiss Alps[4] (17)	7±7	249±160	19±15	24±14	66±37	607±322
Bench glacier, Alaska[5] (1)	4	374	21	76	42	1054
Mittivakkat Gletscher, SE Greenland[6] (4)	296±103	316±117	358±327	43±11	177±60	241±113
Finsterwalderbreen Glacier, Svalbard[7] (60)	200±99	7500±3600	220±91	76±52	3200±1300	6000±2200
Finsterwalderbreen Glacier, Svalbard[8] (40)	ND	9890±4390	ND	ND	3980±4360	7109±2650
Ebba Valley, Central Spitsbergen[9] (33)	407±190	5501±4081	337±207	56±27	2160±868	7990±3440
Rieperbreen-Foxfonna catchment, Svalbard[10] (2)	232±18	5423±463	5428±975	102±0	1444±64	2738±385
Hornsund fjord region, south Spitsbergen, Svalbard[11] (7)	1573±1310	781±1114	1693±1532	62±41	1000±905	1122±1081
Waterloo moraine, Canada[12] (11)	3361±3172	6355±6163	1888±1031	55±20	3584±2289	7300±4009
Taylor Valley, Antarctica[13] (5)	4577±3140	1616±1172	3198±1515	537±257	1773±1066	2933±1561

Sources and hydrological setting: 1. Current study Skaftafellsjökull, SE Iceland 2. Robinson *et al*. (2009) 3. Hindshaw *et al*. (2011) 4. Tranter *et al*. (2002) Subglacial piezometers, Haut Glacier d'Arolla, Swiss Alps. 5. Anderson *et al*. (2005a) proglacial groundwater, 1.3 km from the glacier snout. 6. Kristiansen *et al*. (2012) Proglacial groundwater, Mittivakkat Gletscher, SE Greenland. 7. Wadham *et al*. (2001) Active Layer (AL) groundwater, Finsterwalderbreen Glacier, Svalbard. 8. Wadham *et al*. (2007) Active Layer (AL) groundwater, Finsterwalderbreen Glacier, Svalbard. 9. Dragon and Marciniak (2010). 10. Rutter *et al*. (2011) springs at the Rieperbreen-Foxfonna catchment, Svalbard. 11. Olichwer *et al*. (2013) Permafrost groundwater in the Hornsund fjord region, south Spitsbergen, Svalbard. 12. Stotler *et al*. 2010. 13. Harris *et al*. (2007).

Table 6.8. Solute concentrations in meltwater from different proglacial settings.

The numbers in brackets show the number of samples. However, this was not always available.

Meltwater solute concentration (µeq/l)	Cl^-	SO_4^{2-}	Na^+	K^+	Mg^{2+}	Ca^{2+}
World average[1]	160	170	220	33	280	670
River Súla*[2] (11)	54±12	43±9	275±55			340±67
River Gígjukvísl*[2] (n=8)	39±14	76±51	172±43			322±100
Skeiðará*[2] (13)	86±36	155±128	565±345			1199±±739
Skaftafellsá[3] (7)	34±11	15±2	113±23	0±1	3±4	89±35
River Virkisá (Iceland)[4]	166	ND	117	13	30	56
River Fjallsárlón (S. Iceland)[4]	164	105	66	4	33	320
Mittivakkat Gletscher meltwater, SE Greenland[5] (16)	40±5	42±6	43±6	7±1	32±6	48±12
Finsterwalderbreen glacier, Svalbard[6] (40)		319±90	ND	ND	225±42	521±70
Scott Turnerbreen Svalbard[7]	390	240	430	12	210	221
Rieperbreen- Foxfonna, Svalbard[8] (7)	54±24	3682±3768	657±333	71±56	905±1200	2224±2182
Kangerlussuaq region, W. Greenland[9] Glacial rivers Non-glacial rivers	4±1 248±217	30±9 161±209	26±12 261±185	18±5 58±55	23±4 508±590	72±13 531±456
Kuannersuit, Disko Island, Greenland[10]	25	9	120	2	73	160
Longyearbreen, Greenland[11] (183)	29-510	350-14900	130-2750	11-66	230-6290	210-6710
Glacier de Tsanfleuron, Switzerland[12]	5	118	5	6	91	640
Alps Damma Gletscher, Swiss Alps[13] (39)	3±1	12±6	10±7	10±6	6±4	31±15
Haut Glacier d'Arolla, Swiss Alps[14] (220)	5±4	135±53	16±4	13±4	37±9	375±65
Elliott Glacier meltwater Oregon[15] (10)	11±0	52±3	39±4	5±0	43±2	87±4
Meltwater in the Peruvian Andes Cordillera Blanca[18] Cordillera Negra tribuaries[18]. Rio Santa[18]	 154±248 179±144 445±290	 742±896 631±692 817±673	 248±287 809±361 648±187	 41±28 72±54 92±18	 214±239 626±807 346±165	 695±410 1380±955 1475±460
Taylor Valley, Antarctica[16] (5)	459±411	325±363	387±263	131±81	274±214	919±709
Gangotri glacier, Himalayas, India[17]	233±228	674±155	48±17	44±22	1314±620	620±265
Kennicott Glacier, Alaska[19] 1999 (60) 2000 (93)	 36 68	 262 268	 63 87	 14 17	 160 176	 932 1002
rock glacier outflow, Colorado Rockies[20]	ND	1829	40	ND	329	1487

Sources and hydrological settings 1. Brown *et al*. (2002). 2. Robinson *et al*. (2009)* Na^+ and K^+ and Ca2+ and Mg2+ are presented as Na^++K^+ and Ca^{2+}+Mg^{2+}, respectively.3. Current study 4. Pogge von Strandmann *et al*. (2008). 5. Kristiansen *et al*. (2013) 6. Wadham *et al*. (2007) Active Layer meltwater, Finsterwalderbreen glacier, Svalbard 7. Hodgkins *et al*. (1997) proglacial stream, Scott Turnerbreen glacier, Svalbard 8. Rutter *et al*. (2011) proglacial streams, Rieperbreen- Foxfonna catchment, Svalbard 9. Wimpenny *et al*. (2010) Glacial and non-glacial river (rives are defined as rivers that are not directly linked to the ice sheet), Kangerlussuaq region, west Greenland. 10. Yde *et al*. (2005) Subglacial outlet of a surging glacier, Kuannersuit, Disko Island, Greenland. 11. Yde *et al*. (2008). Bulk meltwater runoff from the entire melt season in 2004 (only range is given), Longyearbreen, Greenland. 12. Fairchild *et al*. (1994). 13. Hindshaw *et al*. (2011) 14. Tranter *et al*. (2002). 15. Fortner *et al*. (2009). 16. Harris *et al*. (2007). Proglacial streams Taylor Valley, Antarctica 17. Kumar *et al*. (2009). 18. Mark *et al*. (2008). 19. Anderson *et al*. (2003). 20. Williams *et al*. (2006).

6.6.3. Spatial and temporal variability in river-aquifer exchange

This section uses the spatial and temporal variability in groundwater and surface geochemistry and stable isotopes to infer proglacial river-aquifer exchange at the Skaftafellsjökull foreland (objective iv). In addition to the monitoring of groundwater and river levels (Chapter 7), river-aquifer exchange can also be investigated using water geochemistry and stable isotopes, with significant differences between groundwater and surface water suggesting low river-aquifer exchange (e.g. Roy and Hayashi, 2009; Dragon *et al*., 2010). Conversely, rivers and aquifers where high exchange takes place are expected to have similar geochemical and isotopic compositions (Hood and Berner, 2009; Wimpenny *et al*., 2010; Hindshaw *et al*., 2011). For instance, the recharge of groundwater by significant fluxes of diluted meltwater will lower groundwater solute concentrations (e.g. Anderson *et al.*, 2003; Okkonen and Kløve, 2012; Carey *et al*., 2013). The current study used the fluctuations in groundwater and meltwater levels alongside geochemistry and stable isotopes in order to investigate river-aquifer exchange. The measured high variability in groundwater solute concentrations (sections 6.3, 6.4) and stable isotope composition (section 6.5) suggest that high variability in river-aquifer exchange at the Skaftafellsjökull foreland.

The configuration of hydraulic heads and fluctuations at the Skaftafellsá and the transect suggest that groundwater flows away from the river, and that the river is recharging the

groundwater at the transect (i.e. a losing river stretch) (Chapter 7). However, groundwater and meltwater geochemistry and stable isotope compositions do not support this hypothesis. The solute concentrations and isotopic composition of transect groundwater were significantly different than those of the Skaftafellsá. Solute concentrations at the transect were high, particularly at T1, which is located closest to the meltwater channel (Figure 6.8-6.10). Additionally, groundwater at the transect also had heavy isotopic composition (Figure 6.20), which was close to the LMWL (Figure 6.18). The significant differences between groundwater and meltwater geochemistry and isotopic composition do not suggest high levels of exchange between meltwater and groundwater (e.g. Marciniak *et al*., 2014). Furthermore, the heavy groundwater isotopic composition at the transect (Figure 6.21) suggests that precipitation, rather than glacial melt, is the main source of groundwater recharge at the transect (e.g. Robinson *et al*., 2009b; Kristiansen *et al*., 2013).

In contrast to the inferred low river-aquifer exchange at the transect, the water quality and stable isotopes suggest higher river-aquifer exchange at the piezometers located between the Skaftafellsá and Swan Lake (GW9 and GW5). Groundwater at GW9 had low EC (Figure 6.6), low solute concentrations (Figure 6.8-6.10), relatively light isotopic composition (Figure 6.20), and relatively high *d-excess* (Figure 6.22). These observations suggest that groundwater-meltwater exchange takes place in this piezometer.

Groundwater solute concentrations at GW9 increased substantially in August (Figure 6.11), which coincided with a decline in groundwater and meltwater levels (Chapter 7). This inverse relationship between meltwater levels and groundwater solute concentrations suggests that river stage is an important control on river-aquifer exchange, hence, an increase in river level is expected to lower groundwater solute concentrations due to increased exchange from the river to groundwater, and vice versa. Similar relationships between meltwater levels and solute concentrations have also been reported from various proglacial environments (e.g. Anderson *et al*., 2003; León and Pedrozo, 2014). Therefore,

the substantial increase in groundwater solute concentrations at GW9 in August (Figure 6.11) which coincided with a fall in river and groundwater levels, suggest a fall in meltwater-aquifer exchange at this site.

Groundwater isotopic composition at GW5, which is located 38 from the Skaftafellsá channel (Figure 6.3), was heavier than GW9, but lighter than the other groundwater samples at the site (Figure 6.20). This suggests that, although GW5 is influenced by meltwater, river-aquifer exchange dampens with distance from the channel (Cooper *et al*., 2002; 2011). However, in contrast to the low solute concentrations at GW9, groundwater at GW5 had high solute concentrations and EC, particularly in August (Figure 6.6, 6.11). These high solute concentrations at GW5 appear to contradict the hypothesis of exchange with meltwater which is suggested by the stable isotope composition. However, these high solute concentrations could have been possibly caused by local contamination from wildlife or sheep which have been observed near the borehole on numerous occasions. Hence, the isotopic composition of GW5 still supports the hypothesis of meltwater-aquifer exchange at GW5.

The reasons for the spatial variability in meltwater-groundwater exchange between the transect and at GW9 are not clear. The groundwater quality and stable isotope composition at GW9 suggests relatively high proportions of meltwater recharge. However, it is not clear how much of this is due to flooding and localised recharge from overbank flow of meltwater, which is facilitated at this location by the relatively shallow riverbank (0.35 m). Conversely, the river bank at the transect is approximately 1.0 m high, which reduces overland meltwater flow during normal ablation-controlled flow regime. The spatial variability in groundwater-surface water exchange can be investigated further using chemical tracers (e.g. Ward *et al*., 2013), which can be used to delineate the hydrological pathways of river-aquifer exchange at the site.

6.6.4. Lake-aquifer exchange

In addition to river-aquifer exchange, groundwater and surface water geochemistry was also used to investigate lake-aquifer exchange at the Skaftafellsjökull foreland (objective v). The significant differences in solute concentrations between the lakes in the Northern and Southern Oasis suggest substantial differences in lake-aquifer exchange between the two areas. SO_4^{2-}, Ca^{2+}+ Mg^{2+}, and Na^{+}+ K^{+} concentrations in the Northern Oasis lakes were significantly lower than concentrations in the Southern Oasis (Figure 6.9, 6.10). Conversely, Cl^{-} concentrations in the Northern Oasis lakes exceeded those in the Southern Oasis (Figure 6.8). It is suggested that these differences in lake solute concentrations are caused by the contrasting water sources of the lakes, which are controlled by the contrasting hydrogeology between the Northern and Southern Oasis lakes. The hydraulic conductivity of the Northern Oasis lakes is several orders of magnitude lower than that of the Southern Oasis (Figure 5.9). This impedes the connectivity between the Northern Oasis lakes and the aquifer and limits the discharge of solute-rich groundwater into the lakes (Kattlemann and Elder, 1991; Shaw *et al*., 2013).

In addition to groundwater-surface water exchange, the geochemistry and isotope data also highlighted differences in the hydrological connectivity between the lakes in the Southern Oasis and the Skaftafellsá. Hydrological connectivity describes linkages between and within different components of the hydrological system (e.g. Pringle, 2003; Egozi and Lekach, 2014). The variability in hydrological connectivity at the site was demonstrated by the contrasting impacts of the August flood (13-14/08/2012) on lake water quality in the Southern Oasis. Measurements of lake water physicochemical parameters and solute concentrations which were taken 10 days after the flood have shown a substantial increase in lake turbidity and a fall in lake temperature, EC, and solute concentrations at the IL and Swan Lake (Figure 6.6,6.16, 6.17). Observations also suggest that fish numbers at the IL have declined after the flood, probably due to the

impact of meltwater on habitat conditions (e.g. Brown *et al*., 2007a) at the IL. In contrast to the aforementioned impacts of the flood on the IL and Swan Lake, lake temperature, EC, and solute concentrations at Thin, Island, and Heart Lakes either did not change or have risen after the flood (Figure 6.6, 6.16, 6.17). It is hypothesised that the observed changes in water quality at the IL and Swan Lake were probably due to the influx of meltwater during the flood. This hypothesis is also supported by the lighter isotopic composition of the IL and Swan Lake, which were sampled about 12 days after the flood (Figure 6.20). These observations in lake water quality and geochemistry between the IL and Swan Lake and the other lakes suggest that the flood has not impacted the latter lakes. Furthermore, it also suggests that the hydrological connectivity between the river and the IL and Swan Lake is higher than the connectivity between the river and the other lakes.

6.7. Conclusions

This chapter used water quality and stable water isotopes in order to delineate the sources of groundwater and surface water recharge at the Skaftafellsjökull foreland (objective iii). These techniques were also used to investigate the spatial and temporal dynamics of proglacial groundwater-surface water exchange at the site (objective iv and v).

Similar to other proglacial environments, groundwater solute concentrations at the Skaftafellsjökull foreland generally exceeded those in surface water. The main control on solute concentrations at the Skaftafellsjökull foreland is catchment lithology, which is composed of highly soluble basaltic glass. The quick weathering of this lithology at the Skaftafellsjökull foreland contributes to higher groundwater solute concentrations than those reported from some proglacial catchments. However, due to the lack of formation and dissolution of efflorescent salts at the Skaftafellsjökull foreland, groundwater solute concentrations at this catchment were substantially lower than those reported from polar glacial environments. In contrast to eastern Skeiðarársandur, geothermal activity does not

appear to significantly impact groundwater and surface water geochemistry at the Skaftafellsjökull foreland. Using stable isotopes, precipitation was identified as the main source of recharge to groundwater in the catchment. However, recharge from meltwater was also identified in some locations.

Substantial spatial and temporal heterogeneity in groundwater and surface water solute concentrations and stable isotope composition has been observed in the catchment. The high solute concentrations and relatively enriched isotopic composition suggest that river-aquifer exchange at the transect is low. In contrast to the observations from the transect, low solute concentrations and light groundwater isotopic composition near the river (GW9) suggest higher proportions of meltwater, which diminishes with distance from the channel. However, it is not clear whether this meltwater originates from surface recharge during small overbank spills of the river.

The spatial variability in aquifer-lake exchange at the Skaftafellsjökull foreland has been illustrated by the differences in water quality between the Northern and Southern Oasis lakes, with solute concentrations at the Southern Oasis significantly exceeding concentrations in the Northern Oasis lakes. These differences were attributed to the differences in aquifer-lake exchange, which are controlled by the contrasting hydrogeology between the two areas. It is suggested that the low hydraulic conductivity at the Northern Oasis impedes lake-aquifer exchange and the discharge of solute-rich groundwater into the lakes, leading to the lower solute concentrations in this area. In addition to groundwater-surface water exchange, this chapter also suggested high spatial variability in hydrological connectivity, illustrated by the differences in water quality and geochemistry between the Southern Oasis lakes following the Skaftafellsá flood.

7. River-aquifer exchange

7.1. Introduction

This chapter investigates the spatial and temporal variability and controls of proglacial river-aquifer exchange. Hydrological exchange between rivers and groundwater substantially impacts water levels, physicochemical parameters, biogeochemistry, water quality, and ecology (e.g. Brunke and Gonser, 1997; Krause *et al*., 2009; Hoehn and Maylan, 2009; Roy *et al*., 2011; Blaen *et al*., 2013). River-aquifer exchange can exhibit high spatial heterogeneity due to high variability in sediment properties and morphology (e.g. Hannah *et al*., 2009; Sawyer and Cardenas, 2009; Schmidt *et al*., 2012; Norman and Cardenas, 2014). These heterogeneities lead to high variability in hydraulic conductivity (e.g. Robinson *et al*, 2008, MacDonald *et al*., 2012; Langston *et al*, 2013), pressure gradients (Stonedahl *et al*., 2010), and hydrological connectivity (Ward *et al*., 1999; Storey *et al*,. 2003). The temporal variability in proglacial river-aquifer exchange is impacted by diurnal and seasonal variations in meltwater discharge (e.g. Cooper *et al*., 2002; Smerdon *et al*., 2005) and high magnitude, low frequency events such as floods and jökulhlaups (e.g. Cooper *et al*., 2002; Vogt *et al*., 2010)

Previous studies of proglacial river-aquifer exchange have focused on groundwater and meltwater hydrochemistry (e.g. Dragon and Marciniak, 2010), catchment hydrology (e.g. Marciniak *et al*., 2014), and the impact of different water sources on proglacial ecology and biodiversity (e.g. Milner and Petts, 1994; Ward *et al*., 1999; Tockner *et al*., 2002; Brown *et al*., 2006; 2007a, b). However, the processes that control proglacial groundwater flow, storage and exchange with surface water are still not well understood (e.g. Cooper *et al*., 2002; Crossman *et al*., 2011; Langston *et al*., 2011; McClymont *et al*., 2012).

This chapter aims to investigate the controls on the spatial and temporal variability of proglacial river-aquifer exchange. Section 7.2 describes the spatial and temporal variability in hydraulic heads at the Skaftafellsjökull margin, which were monitored

between 25/06-31/08/2012. The configuration of hydraulic heads was then used to delineate the proglacial groundwater flow systems at the Skaftafellsjökull foreland, with groundwater flowing from high to low heads (e.g. Freeze and Cherry, 1979). These results are added to the configuration of groundwater flow in Skeiðarársandur (Robinson *et al*. 2008). Section 7.3 investigates the impacts of high frequency, low magnitude processes (precipitation and ablation) on river-aquifer exchange. This section is based on time series of meltwater and groundwater levels, temperature, and EC, which were measured at the Skaftafellsjökull foreland during the 2012 field season. Section 7.4 investigates the impacts of low frequency, high magnitude events (jökulhlaups) on proglacial river-aquifer exchange. This section is based on automated measurements of groundwater and meltwater levels, temperature, and EC, which were taken in western Skeiðarársandur during the 2011 field season (08/07-15/08/2011). The time series of meltwater and groundwater levels and physicochemical parameters from the two sites were then used alongside water geochemistry and stable isotopes composition (Chapter 6) to investigate the controls on proglacial river-aquifer exchange.

The specific objectives for the chapter are:

1. To delineate the horizontal and vertical groundwater flow directions at the Skaftafellsjökull foreland.

2. To analyse the spatial and temporal patterns of proglacial river-aquifer exchange.

3. To analyse the control of low magnitude, high frequency events (precipitation, ablation) on proglacial river-aquifer exchange.

4. To analyse the control of episodic (glacial outburst floods) events on proglacial river-aquifer exchange.

7.2. Groundwater flow at the Skaftafellsjökull foreland

This section describes the groundwater flow directions and the groundwater flow systems at the Skaftafellsjökull foreland. Groundwater flow systems can form a nested hierarchy,

with local groundwater flow systems imposed on regional ones (e.g. Tóth, 1963). Observations of nested groundwater flow systems have also been reported from proglacial environments such as Skeiðarársandur (Robinson *et al*., 2008). The configuration of groundwater systems at the Skaftafellsjökull foreland was derived from the hydraulic heads which were monitored during the 2012 field season (25/06-31/08/2012). Hydraulic heads were calculated from combining the elevation of the piezometer with groundwater levels, which were monitored daily in piezometers in the Southern Oasis (Figure 7.1) using a Solinst acoustic dip meter (accuracy of +0.005 m, section 3.5.3). The spatial distribution of hydraulic heads were then used to delineate groundwater flow system at the site, with groundwater flowing from high to low hydraulic heads (Freeze and Cherry, 1979). This section describes the fluctuations in hydraulic heads in the various hydrological environments at the Skaftafellsjökull foreland, which include the Instrumented Lake (IL) lakeshore, the outwash, and near the Skaftafellsá meltwater channel (GW5 and GW9). The results from the automated monitoring of meltwater and groundwater levels in the transect are presented in section 7.3.

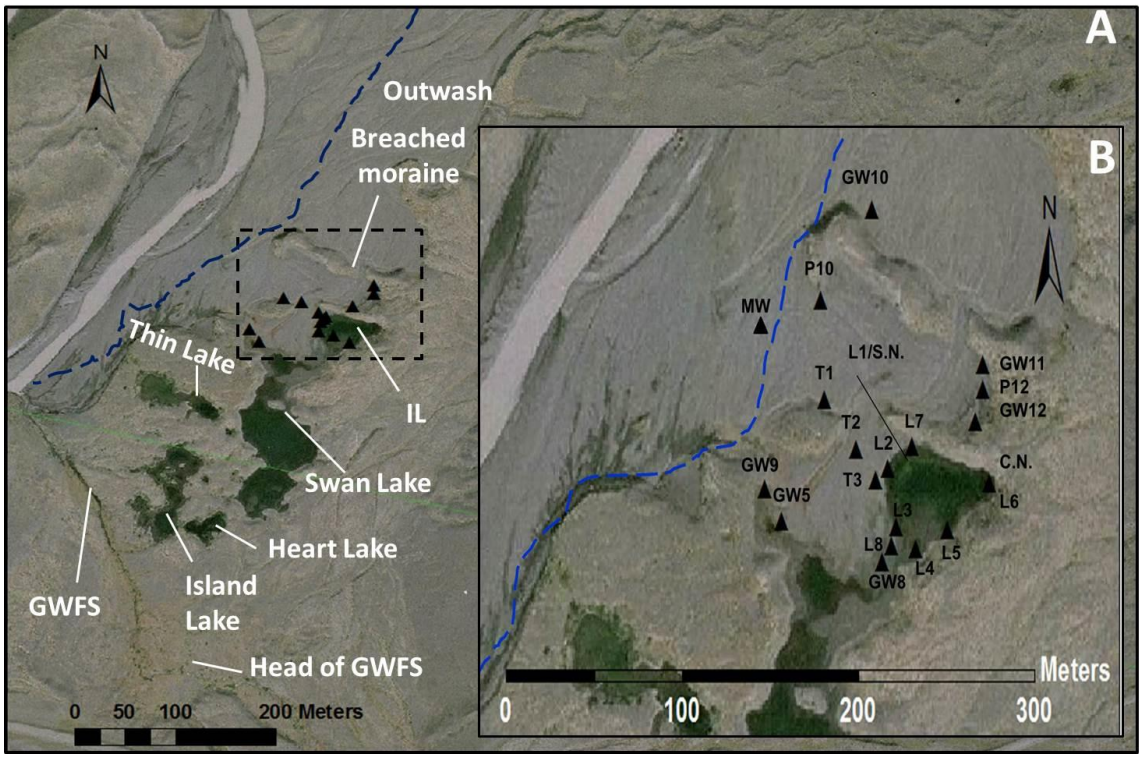

Figure 7.1. Groundwater monitoring infrastructure at the Southern Oasis (Vatnajökull National Park, 2007).

Piezometers (emplaced~1.6-1.8 m below ground surface) are denoted by black triangles. Note that the Skaftafellsá channel has migrated east since the date of the image (2007). The position of the river (meltwater) channel during the monitoring in June-August 2012 is marked by the dashed blue line. The figure also shows the location of the stilling well (MW) in the meltwater channel and the transect (piezometers T1-T3), where meltwater and groundwater levels, temperature, and EC were automatically monitored (section 7.3).

7.2.1. Hydraulic heads at the Skaftafellsjökull foreland

The fluctuations in hydraulic heads at the Skaftafellsjökull margin during the 2012 field season are presented in Figure 7.2. The fluctuation in hydraulic heads generally followed similar spatial trends across the observation network. Hydraulic heads were stable between 99.50 and 99.70 mAD until the 20/07/2012, when levels rose by approximately 0.05 m. The rise in hydraulic heads followed several small (< 10 mm) precipitation events and an increase of ~0.15 m in river levels (Figure 7.3). Groundwater levels then rose by 0.1-0.15 m in less than 24 hours after the largest precipitation event of the season on the 22/07 (33.3 mm). Following this rainfall event, groundwater levels slowly declined. Manual

monitoring of groundwater levels was not performed between 31/07–23/08/2012. However, a flood was recorded on the 13-14/08/2012, during which groundwater levels have also substantially increased (Figure 7.3). When manual monitoring was resumed on the 23/08/2012, groundwater levels were at their highest levels. Despite minor rainfall events (<10 mm), groundwater levels declined continuously following the flood, reaching similar levels to those measured at the start of the monitoring period. Using the division of hydrogeological environments at the site (Figure 5.4), the remainder of this section describes the spatial and temporal distribution of fluctuations in hydraulic heads at different hydrogeological environments at the Skaftafellsjökull foreland: the outwash, the IL, and near the meltwater channel.

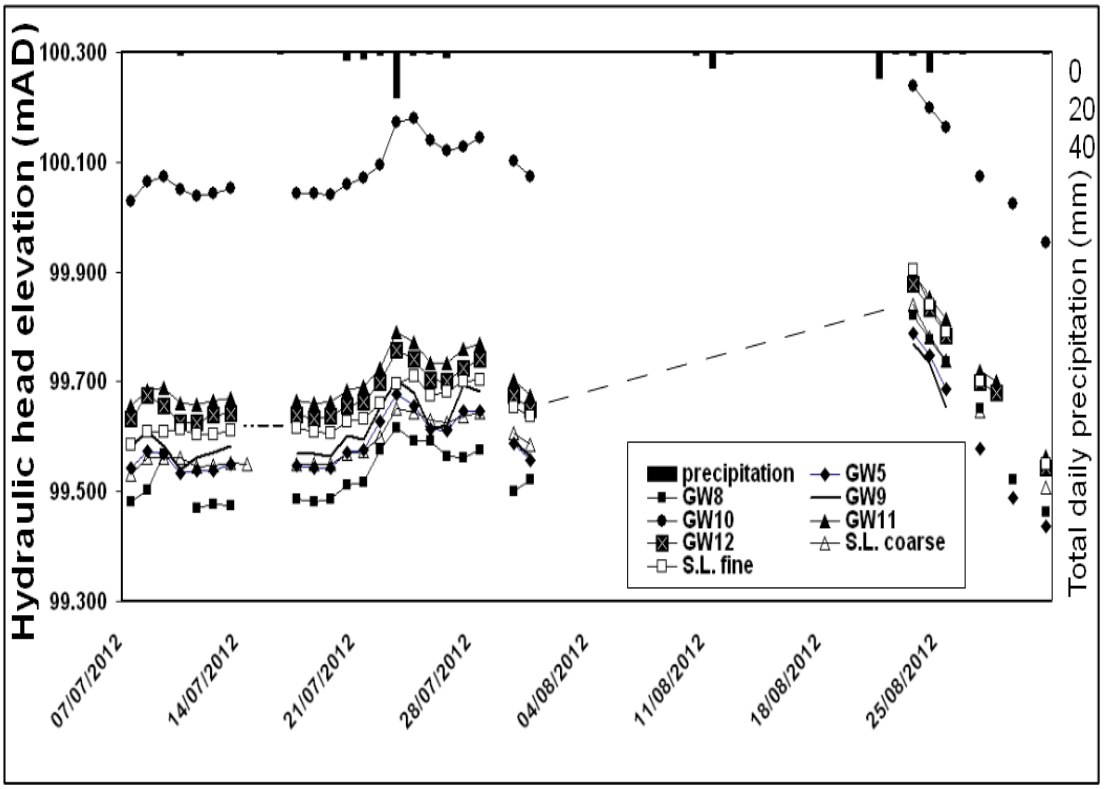

Figure 7.2. Total daily precipitation (IMO, 2013) and elevation of hydraulic heads at the field site.

For clarity, only the mean hydraulic heads are shown for the piezometers located in the coarse (L1-4, L8) and fine shores (L5-L7) of the Instrumented Lake (IL). Dashed lines denote days when measurements were not taken.

The outwash is composed of coarse-grained glaciofluvial deposits, with mean hydraulic conductivity of $6.1x10^{1}$ m/day. However, some areas of the outwash are underlain by finer sediment, such as GW8, which is located in an area of relatively fine lacustrine deposits between the IL and Swan Lake, with hydraulic conductivity of $1.00x10^{-1}$ m/day. The fluctuations in hydraulic heads in the outwash ranged between 99.45 and 100.24 mAD (Figure 7.3). The highest hydraulic heads at the Skaftafellsjökull foreland were measured at GW10, which is the most northern borehole, located closest to the glacier margin (Figure 7.1). Hydraulic heads at GW10 ranged between 100.00 and 100.24 mAD, persistently exceeding heads in other piezometers by ~0.40-0.50 m. The lowest hydraulic heads, ranging between 99.48 m and 99.60 m, were measured at GW8. Intermediate levels of hydraulic heads were observed at GW11, GW12 and P12, where levels ranged between 99.60 and 99.90 m. GW11 and GW12 displayed very similar dynamics, with levels in GW11 exceeding GW12 by ~0.05 m. However, different dynamics were observed at P12, which is located between GW11 and GW12. For instance, the rise in hydraulic heads at P12 following the rainfall events around the 20/07/2012 was earlier and steeper than the rises in hydraulic heads in other piezometers. Groundwater levels at P12 then declined, and the response of groundwater in this piezometer to rainfall lags behind the main rainfall event and rise in river levels by approximately three days. Additionally, in contrast to the declines which were measured in other piezometers, groundwater levels at P12 also rose by ~0.17 m around 30/07/2012 (Figure 7.3)

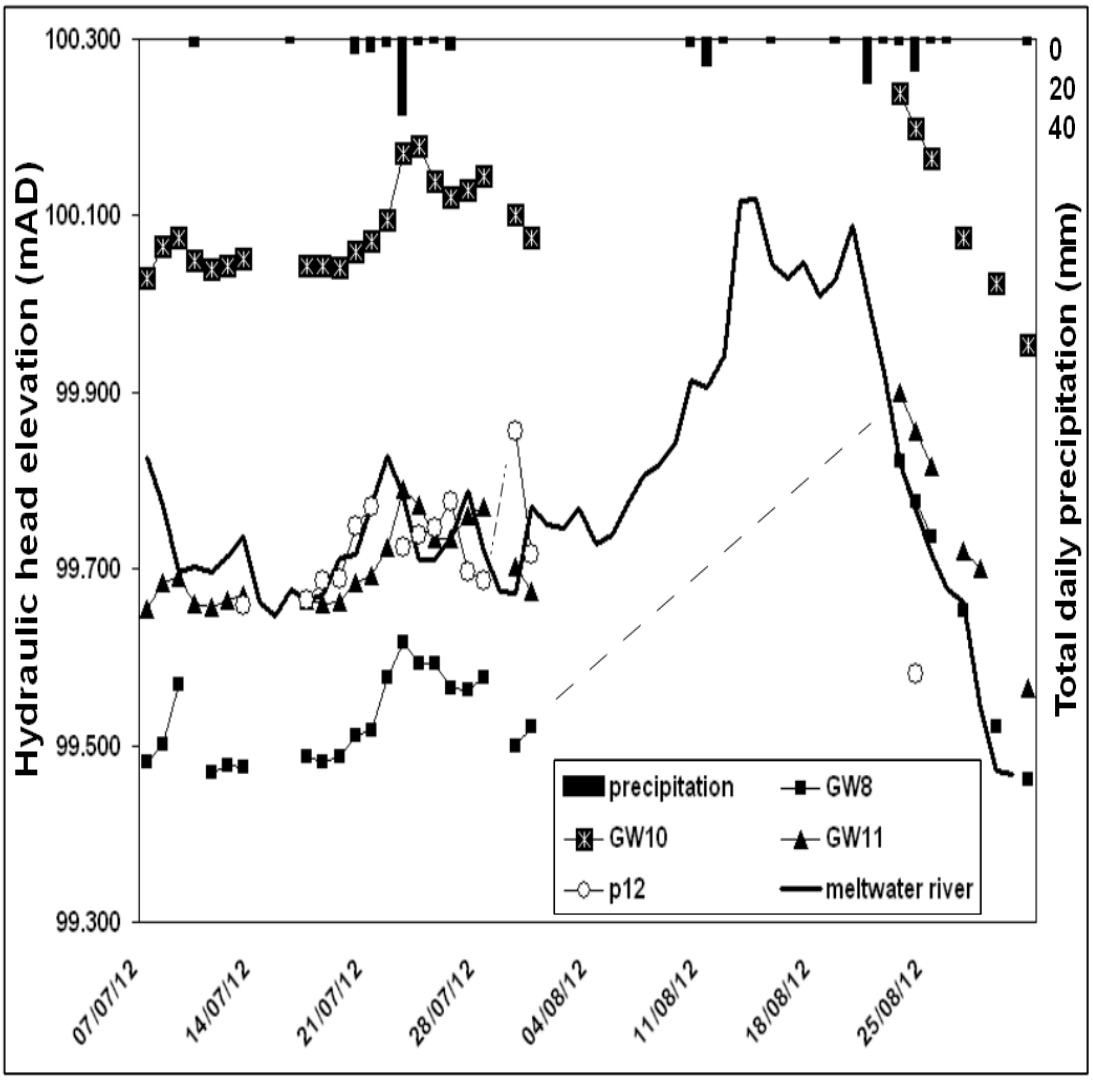

Figure 7.3. Total daily precipitation, hydraulic heads at the outwash and mean daily levels of the meltwater river Skaftafellsá.

The data for GW12 was very close to that of GW11(see text). Hence, it was omitted for clarity. The river levels are based the daily mean levels, which were monitored automatically (section 7.3).

Figure 7.4 shows the temporal and spatial distribution of hydraulic heads around the IL, which were monitored in the L1-L8 piezometers. The fluctuations in hydraulic heads around the IL (Figure 7.4) generally followed similar patterns to the rest of the site (Figure 7.2). However, spatial heterogeneity was observed around the lake, with hydraulic heads at the fine-grained lakeshore (L5-L7) persistently exceeding hydraulic heads at the coarse-grained (L1-L4, L8) lakeshore by approximately 0.15 m. Hydraulic heads around

the IL ranged between 99.48 and 99.65 mAD until the end of July. The fluctuations in hydraulic heads in all the piezometers were around 0.10 m, with higher fluctuations measured in the fine-grained lakeshore. Hydraulic heads rose gradually following the small rainfall events between 17-22/07/2012. However, the increase in groundwater levels at the fine-grained shore was sharper than the observed rise at the coarse-grained lakeshore (Figure 7.4). Hydraulic heads rose by approximately 0.10 m in less than 24 hours after the rainfall event on the 23/07/2012 (33 mm), with the latest peaks measured in L6 and L7. Hydraulic heads then declined after the rainfall event. Following the small rainfall events (<5 mm) on the 25-27/07/2012, hydraulic heads in the fine-grained shore rose by approximately 0.05 m. Conversely, hydraulic heads at the coarse-grained shore remained at similar levels. Groundwater levels then declined until the end of 31/07/2012, when manual monitoring ceased for approximately three weeks. When manual monitoring was resumed on the 23/08/2012, hydraulic heads were at their highest levels, approximately 0.20 m higher than the measurements prior to the break in monitoring. However, despite a total of 38.3 mm of rainfall during the second monitoring period (23-31/08) hydraulic heads around the IL declined rapidly (Figure 7.4), following the same trends as the rest of the piezometers at the site (Figure 7.2). By the end of the monitoring (31/08/2012), hydraulic heads around the IL have reached similar levels to those measured at the start of the season (Figure 7.4).

.

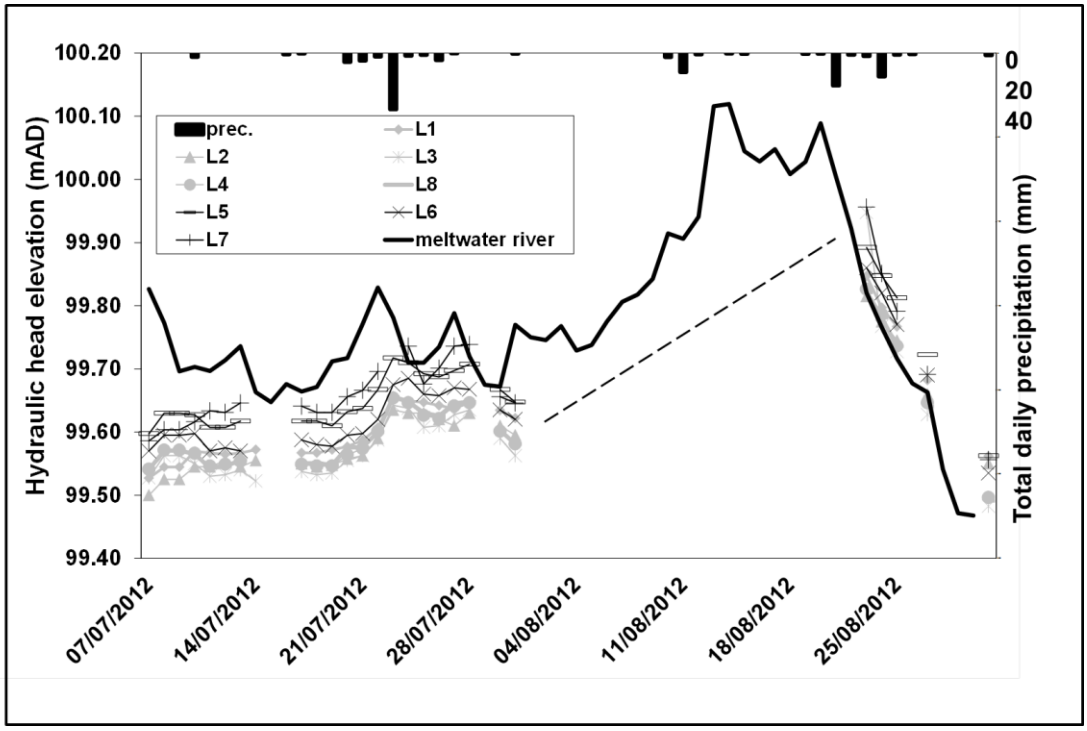

Figure 7.4. Total daily precipitation (IMO, 2013), hydraulic heads around the IL and the mean daily level of the river Skaftafellsá.

Mean meltwater levels were obtained from the automated measurements. Piezometers denoted in grey are located in the coarse-grained lakeshore. Piezometers denoted in black are located in the fine-grained lakeshore.

Hydraulic heads were also monitored near the Skaftafellsá meltwater channel, at piezometers GW5 and GW9 (Figure 7.5), which are located 20 m (GW9) and 38 m (GW5) away from the channel (Figure 7.1). The hydraulic heads near the Skaftafellsá channel generally followed similar dynamics to those in the outwash and around the IL (Figure 7.2). Hydraulic heads near the Skaftafellsá were around 99.60 mAD until the 22/07/2012. Following the rainfall between 20-23/07/2012, hydraulic heads then rose by approximately 0.15 m. Hydraulic heads then declined by ~0.10 m around the 31/07/2012. When manual monitoring was resumed on the 23/08/2012, hydraulic heads at GW5 and GW9 were approximately 0.20 m higher than the levels at the end of July. The hydraulic heads at GW9 were generally 0.02-0.04 m higher than those at GW5, which suggests that groundwater flows away from the river. Figure 7.5 shows that groundwater levels followed the fluctuations in meltwater levels, albeit with a time lag. This suggests groundwater

recharge by meltwater. This hypothesis is also supported by the low groundwater water temperature, EC, and solute concentrations (Figure 6.6, 6.8-6.10) , and relatively depleted δD and δ^{18}O isotopic composition (Figure 6.20). However, the entrance of meltwater into the aquifer can also be caused by overbank flow from the river (which has been observed during the season). Furthermore, disturbance of substrate near the piezometer can possibly serve as a preferential flow path for groundwater recharge.

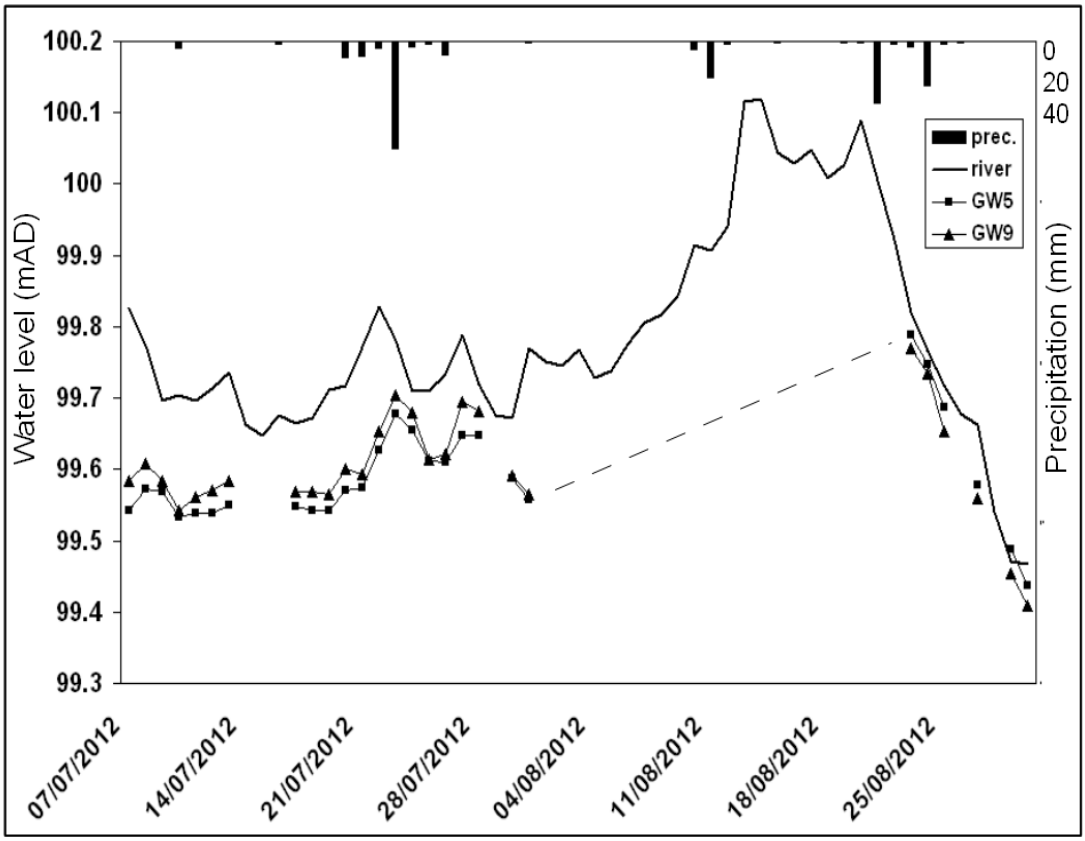

Figure 7.5. Daily mean river level and hydraulic heads (mAD) near the meltwater channel (GW5 and GW9).

The daily mean river levels were calculated from the automated river level data. Dashed lines denote days when manual measurements were not taken.

7.2.2. Vertical groundwater flow

The direction of vertical groundwater flow determines whether groundwater is discharging (upward flow) or recharging (downward flow), which is important when investigating groundwater-surface water exchange. Vertical groundwater flow can be inferred from hydraulic heads in piezometer nests in which the piezometers are open to the aquifer at different depths. A zone of groundwater discharge (upward groundwater flow) is defined where hydraulic head increases with depth. Conversely, a recharge zone (downward groundwater flow) is defined where hydraulic head decreases with depth. When the difference in water levels was less than two centimetres, a horizontal flow direction was inferred, in order to compensate for measurement errors (Drexler *et al*., 1999). Similar configurations and classifications have been used previously in various hydrogeological investigations, including proglacial environments (Robinson *et al*., 2008).

Vertical groundwater flow at the Skaftafellsjökull foreland was determined from hydraulic heads in piezometer nests, which are open to the aquifer at different depths (0.50, 1.00, and 1.50 m below ground). The two piezometer nests were located in the fine-grained (CN) lakeshore and the coarse (SN) lakeshore of the IL (Figure 7.1). Hydraulic heads in the piezometer nests were measured during the same time intervals as the other manual measurements of hydraulic heads.

The mean hydraulic heads at each piezometer were then used to infer the vertical groundwater flow direction in each nest. The results show groundwater discharge at all depths at the coarse-grained shore. In contrast, the results from the clay nest show downward groundwater flow in the deeper piezometers (100 and 150 cm) and groundwater discharge in the shallower piezometers (100 and 50 cm) (Figure 7.6).

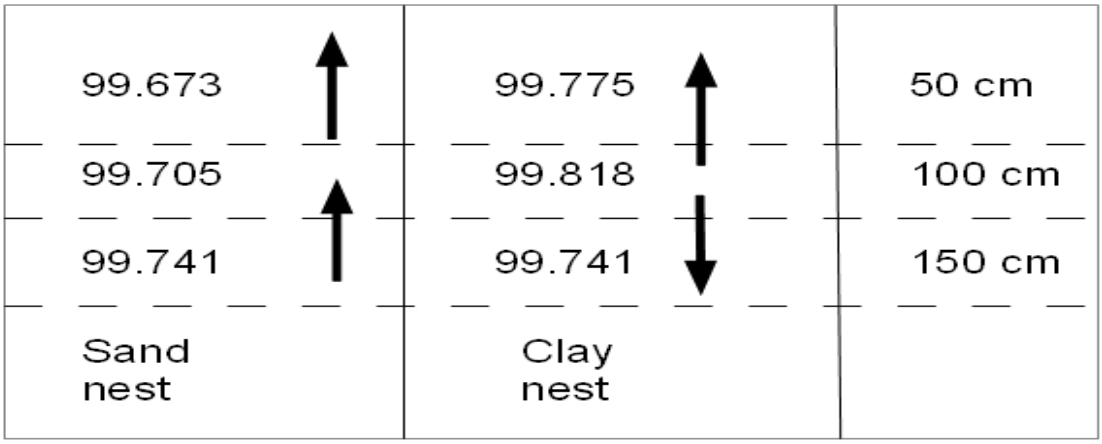

Figure 7.6. Vertical groundwater flow direction at the Skaftafellsjökull foreland.

The data is based on the distribution of vertical hydraulic heads at the sand and clay nests. The column on the right shows the depth of piezometer openings underneath the lakebed. The measurements are based on the mean hydraulic head (mAD) which were measured in each piezometer during the 2012 monitoring season.

7.2.3. Configuration of proglacial groundwater flow at the Skaftafellsjökull foreland

Groundwater flow systems can be divided into regional, intermediate, and local flow systems. Regional groundwater flow systems generally discharge into large water bodies such as the ocean and major river and lakes. Conversely, local groundwater systems flow to a nearby discharge location, such as lakes and streams (e.g. Tóth, 1963). The patterns and configuration of proglacial groundwater flow at the Skaftafellsjökull foreland (Figure 7.7) was inferred from the spatial distribution in hydraulic heads with groundwater flowing from high to low hydraulic heads (e.g. Freeze and Cherry, 1979).

The highest hydraulic heads were observed at GW10, which is the most northern piezometer in the monitoring network. Therefore, groundwater at the site flow from north to south, away from the glacier margin (Figure 7.7A). Similar patterns of groundwater flow away from the glacier margin have also been reported from alpine glaciers (e.g. Gremaud and Goldscheider, 2010) and proglacial outwash plains (Bahr, 1997; Robinson *et al*., 2008). However, the hydraulic gradient at the site is shallow, as the difference in hydraulic

head between GW10 and GW8 is only 0.59 mAD (Figure 7.7). In addition to the regional groundwater flow, a local groundwater flow system, which is imposed on the regional groundwater flow system, has also been identified (e.g. Tóth, 1963; Robinson *et al*., 2008). This system was identified at the transect, where groundwater flow from the Skaftafellsá towards the IL (west-east) (Figure 7.7B). The system seems to be controlled by river-groundwater interactions and moraines, which have been reported to impact groundwater-surface water exchange in various proglacial settings (e.g. Clow *et al*., 2003; Roy and Hayashi 2008; 2009; Cooper *et al*., 2011).

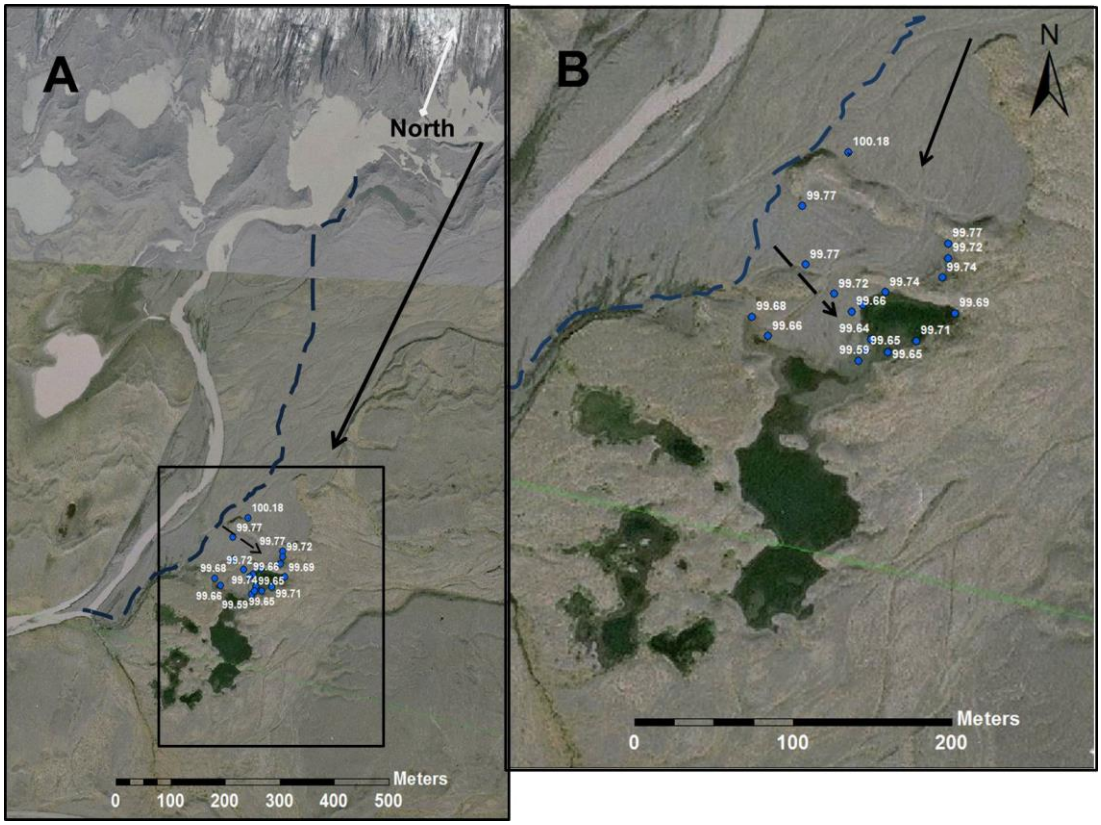

Figure 7.7. Regional groundwater flow systems at the Skaftafellsjökull foreland.

Hydraulic heads (mAD) are denoted in white. Regional groundwater flow is denoted by the solid black arrow. Local groundwater flow systems are denoted by the dashed black arrows. Note that the Skaftafellsá channel has migrated east since the date of the image (2007). The position of the channel during the monitoring in June-August 2012 is marked by the dashed blue line. The image was taken from Vatnajökull National Park (2007).

7.2.4. Summary

Hydraulic heads generally followed similar patterns across the site. Hydraulic heads responded to precipitation, with heads increasing following the highest rainfall event during the field season (33 mm) on the 23/07/2012. Most hydraulic heads were at their highest levels when monitoring was resumed on the 23/08/2012. However, hydraulic heads quickly declined between the resuming and the end of monitoring (31/08/2012) (Figure 7.2). Vertical groundwater flow at the site was investigated in two piezometer nests, which were located in the eastern (fine-grained) and western (coarse-grained) lakeshore of the IL. The nest in the coarse-grained shore has shown upward flow in all depths. The nest in the fine-grained has shown upward flow at the shallower depths (0.50-1.00 m) and downward flow at the deeper depths (1.00-1.50 m) (Figure 7.6). The regional groundwater flow system at the site is from north to south, away from the glacier margin. This configuration is consistent with observations from various proglacial settings. However, a local groundwater flow system, which flows between the Skaftafellsá and the IL, has also been identified (Figure 7.7).

7.3. The impact of high frequency, low magnitude processes on proglacial river-aquifer exchange

This section investigates the impact of high frequency, low magnitude events (precipitation and ablation) on proglacial river-aquifer exchange. These impacts were investigated using time series of hourly meltwater (section 7.2.1) and groundwater levels (section 7.2.2.), temperature (section 7.2.3), and EC (section 7.2.4.), which were automatically monitored at the transect (T1-T3) between 18/06/2012-31/08/2012. The piezometers' depths were between 1.6-1.8 m below ground level, in an area underlain by coarse glaciofluvial deposits. T1 is located closest to the meltwater channel (27 m) while

T3 is the furthest (69 m). Meltwater level, temperature, and EC were monitored in a stilling well, which is located approximately 20 m downstream of the western section of the breached moraine (Figure 7.1). The mean level, temperature, and EC for groundwater and meltwater are presented in .

Table 7.1. Mean groundwater and meltwater levels, temperature and EC at the Skaftafellsjökull foreland and western Skeiðarársandur.

	Level (mAD)	Temperature (°C)	EC (µS/cm)
Skaftafellsjökull foreland			
T1	99.74±0.12	8.05±0.88	135±14
T2	99.70±0.13	8.74±0.53	112±12
T3	99.65±0.14	7.18±0.51	140±28
Skaftafellsá	99.76±0.15	0.53±0.24	4±2
Skeiðarársandur			
GW4	57.31±0.07	5.16±0.53	175±30
Súla-Núpsvötn (from the IMO, 2013)	58.91±0.34	1.87±1.24	39±14

7.3.1. Temporal variability in meltwater levels

Groundwater-surface water exchange between the Skaftafellsá meltwater river and the aquifer was investigated by automated monitoring of meltwater levels and hydraulic heads in a transect of piezometers (T1-T3) (Figure 7.1). Similar configurations for the monitoring of proglacial river-aquifer exchange have been previously used in other proglacial environments (e.g. Cooper *et al*., 2002; Magnusson *et al*., 2014). The fluctuation in meltwater levels and hydraulic heads at the transect during the 2012 field season is shown in Figure 7.8, where the time series was divided into four intervals (I-1 to I-4).

I-1- This interval was mainly dominated by high frequency, low magnitude ablation-controlled diurnal variability, in which the Skaftafellsá levels displayed clear diurnal oscillations in response to changes in ablation. The river stage is increasing during the

first few days of monitoring, following small rainfall events of approximately 10 mm. meltwater levels then stabilised around 99.62 mAD on the 01/07/2012.

I-2- This interval began with rising river levels on the 04/07/2012, during which meltwater levels rose by approximately 0.25 m. Air temperatures during this increase, rising from approximately 10 °C to 16 °C. River levels continued to rise by 0.12 m, reaching peak levels of 99.86 mAD on the 09/07/2012. The latter peak was followed by further increase of ~4 °C in air temperature, reaching 21.5 °C. However, no rainfall was measured during the rise in meltwater levels that took place between the 03-09/07/2012 (Figure 7.8). River levels stabilised and then fell to approximately 99.50 mAD on the 16/07/2012. The remainder of this interval was dominated by ablation-controlled diurnal flow regime, although an increase of approximately 0.15 m in river levels is observed around the 23/07/2012. This increase coincided with 40 mm of rainfall, which fell between 19-23/07/2012, including the season's highest event (33 mm on the 23/07/2012). River levels then fell by approximately 0.10 m and then rose by the same level between 25-30/07/2012. The river then followed an ablation-controlled flow regime between 30/07-06/08/2012. Meltwater levels then increase continuously, with the initial increases in meltwater levels on the 06-08/08/2012 associated with an increase of approximately 4.0 °C in air temperatures. However, meltwater levels continued to rise until the end of the interval despite a fall in air temperature. Meltwater levels were at 99.91 mAD at the end of the interval (Figure 7.8).

I-3- This interval was marked by a substantial flood event, which starts on 1300 hours, 13/08/2012 and peaked on 1700 hours,14/08/2012. River levels rose by approximately 0.35 m in 34 hours during this event, peaking at 100.162 mAD. Meltwater levels declined by approximately 0.10 m after the flood, and then fluctuated diurnally until the 21/08/2012. The flood was not associated with major rainfall events nor abnormally high air temperature (maximum of 19 °C) (Figure 7.8).

I-4- This interval was dominated by a quick, continuous recession in river levels from the 21/08/2012 until the end of the monitoring period (31/08/2012). The decline in river levels was also supported by field observations of falling meltwater levels and the exposure of a gravel bar in the channel. During interval 4, river levels declined by approximately 0.65 m, reaching a minimum of 99.40 mAD at the end of the monitoring season (Figure 7.8)

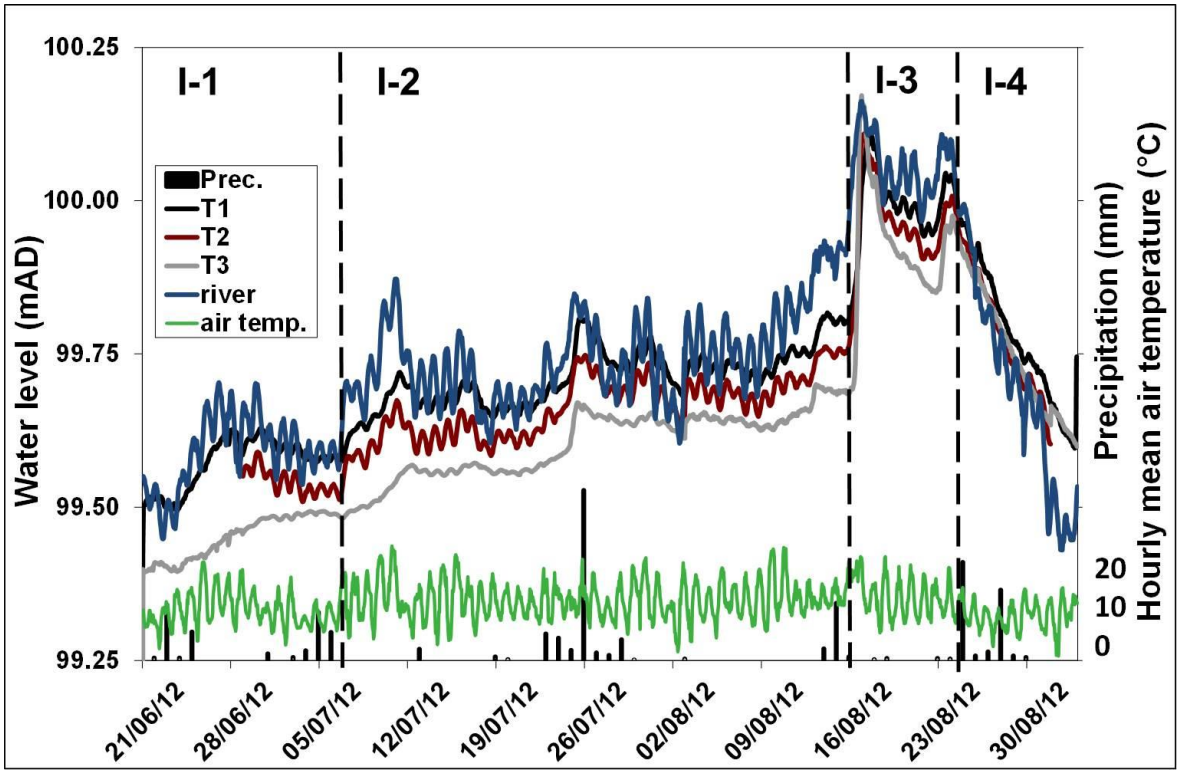

Figure 7.8. Hourly mean meltwater, river levels and hydraulic heads for the transect.

The Figure also shows total daily precipitation and mean air temperature during the study period (IMO, 2013). I1-I4 denote the four intervals to which the time series was divided (see text). The increase in meltwater levels around the 01/08/2012 is possibly due to the changing of the pressure transducer.

7.3.2. Temporal variability in hydraulic heads at the transect

The fluctuations in hydraulic heads at the transect are presented in Figure 7.8. With the exception of approximately 10 hours during the flood event (interval 3, Figure 7.8), hydraulic heads at T1 were the highest, followed by T2 and T3. Figure 7.8 shows that hydraulic heads respond closely to fluctuations in meltwater levels, with hydraulic heads

generally showing a dampened pattern of the fluctuations in meltwater levels during intervals 1 and 2. Hydraulic heads gradually rose from approximately 99.35 mAD (T3) and 99.50 mAD (T1) to 99.55 mAD (T3) and 99.75 mAD (T1) at the end of interval 2. Groundwater and river levels rose substantially during the flood in Interval 3, with hydraulic heads rising by 0.40 m in approximately 27 hours. However, the rise in hydraulic heads lagged behind the rise in river levels by approximately 15-20 hours (Figure 7.8). The differences in hydraulic heads between the piezometers reduced to less than 0.05 m during the flood and the initial hours of recession. This included a brief period of groundwater flow reversal, where groundwater was flowing from T3 towards the river. Following the flood, river and groundwater levels have fallen by approximately 0.20 m until the end of Interval 3 on the 20/08/2012. Groundwater rose by approximately 0.15 m in the beginning of interval 4, following a similar rise in river levels. However, after this short increase meltwater and groundwater levels have declined continuously, with hydraulic heads falling by approximately 0.50 m since the start of interval 4. The head difference between the piezometers reduced to less than 0.02 m, although hydraulic heads at T1 remained the highest (Figure 7.8).

The fluctuations in hydraulic heads T1-T3 followed the general patterns of meltwater levels, albeit with a time lag, with the signal of meltwater fluctuations generally dampening with distance from the river channel (Figure 7.8). However, considerable spatial variability of the dampening of the meltwater signal has been observed between the three piezometers. Although T2 is located further (54 m) from the meltwater channel than T1 (27 m), the dampening of meltwater signal at T2 was smaller than at T1. The largest attenuation of the meltwater level signal was observed was T3, 69 m away from the river channel. Additionally, the longest lag time between meltwater and hydraulic heads and the smallest diurnal fluctuations were also observed at T3 (Figure 7.8). These observations suggest that meltwater levels are an important control on hydraulic heads in the transect.

The attenuation of the meltwater signal was investigated using Cross Correlation Function (CCF) analysis, which were calculated using the program R. The CCF shows the interrelationship between the input and output series, where the delay between the maximum CCF and the time lag when the lag equal 0 shows the stress transfer velocity of the system. This can then be used to determine the lag time between two time series (Lee and Lee, 2000). CCF have been previously used in various hydrological environments for the analysis of hydrological time series (e.g. Panagopoulos and Lambrakis, 2006; Hannah *et al*., 2009; Krause *et al*., 2011b; Zhang *et al*., 2013). The CCF was used in the current study to show the lag time between meltwater levels and hydraulic heads in the transect. The different lag times between meltwater levels and hydraulic heads in each borehole (Table 7.2) also support the hypothesis of spatial heterogeneity in the coupling between river levels and hydraulic heads (Figure 7.8), with the lowest and highest lag time between meltwater levels and hydraulic heads measured at T2 and T3, respectively.

Table 7.2. Lag time (in hours) between meltwater river levels and hydraulic head at the transect.

Variables	**Lag time of hydraulic heads from meltwater levels (hours)**
T1 hydraulic heads (27 m away from channel)	-6
T2 hydraulic heads	-4
T3 hydraulic heads (54 m)	-10

7.3.3. Fluctuations in groundwater and meltwater temperature

Groundwater and meltwater temperatures were automatically monitored in the same time intervals as water levels in the Skaftafellsá and the transect (Figure 7.9). The lowest and least variable water temperatures were measured in the river Skaftafellsá, which is mainly fed by icemelt from the Skaftafellsjökull glacier (Figure 7.1). The mean river temperature

during the study was 0.53±0.24°C. The diurnal fluctuations in meltwater temperatures were around 0.2-0.4°C. The highest mean groundwater temperatures were observed at T2, with the lowest mean temperatures and standard deviation measured at T3 (Table 7.1). However, the maximum groundwater temperatures were also measured at T3, during the flood. Groundwater temperatures in all three piezometers generally increased during the 2012 field season, with the highest temperatures generally measured during Interval 4 (Figure 7.9).

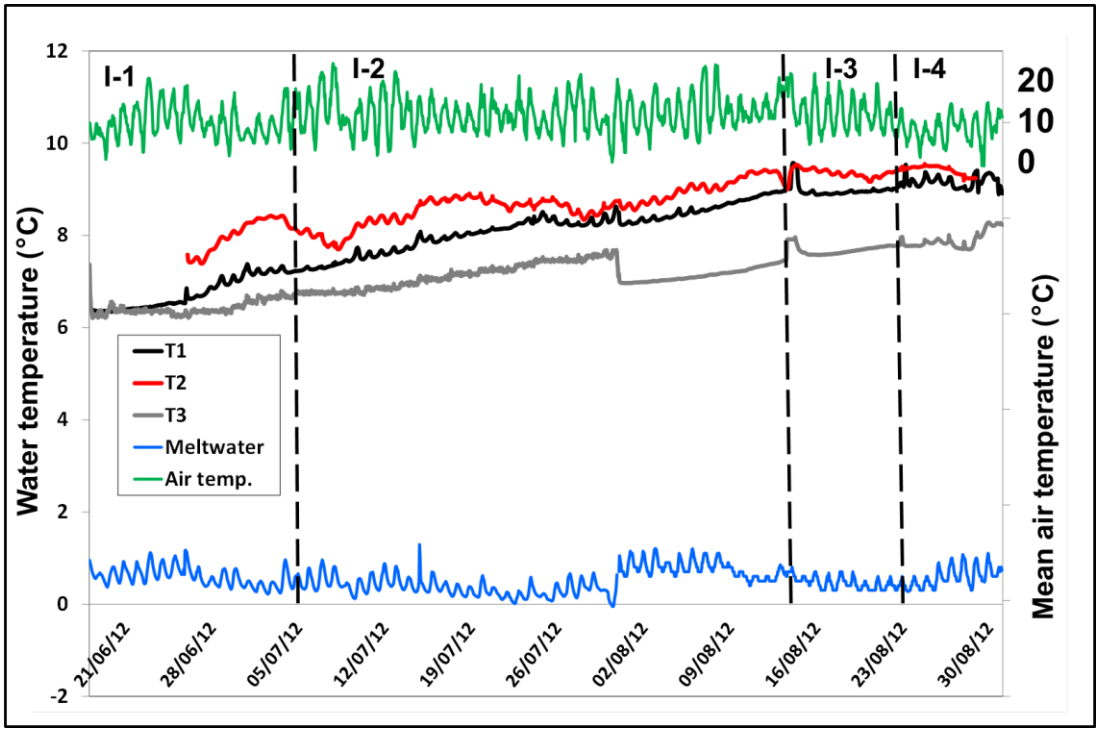

Figure 7.9. Mean hourly meltwater, groundwater (T1-T3), and air temperature 21/06-31/08/2012.

Note that the time series for T2 starts on the 26/06/12. Note also the different scale for air temperature. Air temperatures was obtained from the Skaftafell met. Station (IMO, 2013).

Groundwater temperature at T1 varied between 6.8 and 9.3 °C, with temperatures rising during the field season (Figure 7.10). Hydraulic heads at T1 generally followed the oscillations in meltwater levels between 25/06-01/07/2012 (Figure 7.8). However, the fluctuations in groundwater temperatures during this period were negligible. Following the small falls in river and groundwater levels (02/07-08/07/2012), groundwater temperatures

slowly rose by approximately 1.0 °C. Groundwater temperatures generally showed inverse dynamics to the oscillations in river levels, with groundwater temperatures rising (falling) when river levels fall (rise) (Figure 7.10). Groundwater temperatures rose from 7.5 to 9.0 °C during interval 2. The oscillations in groundwater temperatures at T1 became negligible when river and groundwater levels rose after 06/08/2012. Groundwater temperatures were highest during the flood (~9.6°C), which was followed by a fall of 0.8°C after the flood (interval 3, Figure 7.10). Groundwater temperatures remained around 8.8 °C between the end of the flood and the end of interval 3 (14/08-20/08/2012). Groundwater temperatures varied between 9.0-9.4 °C during interval 4, following the recession in meltwater and groundwater levels. Apart from the short increase in groundwater temperature during the flood, the highest groundwater temperatures at T1 were measured during interval 4 (Figure 7.10).

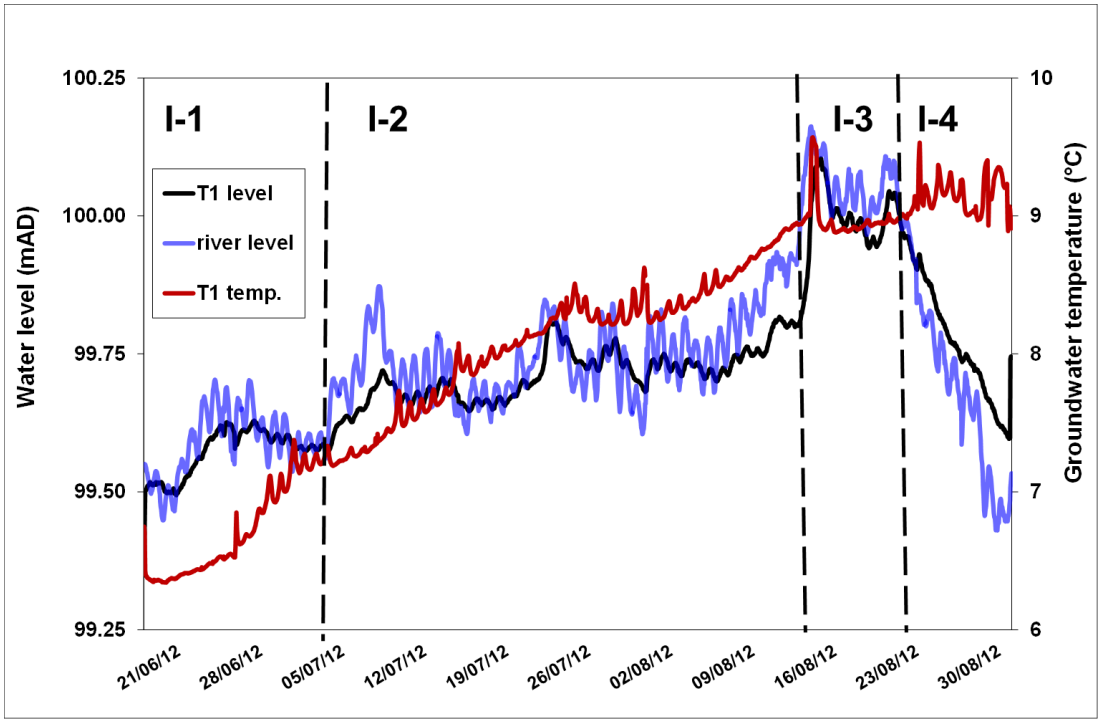

Figure 7.10. Mean hourly meltwater river level and groundwater levels and temperature at T1 during the 2012 field season.

Groundwater temperatures at T2 rose from 7.5°C at the start of monitoring to 9.2 °C at the end of the monitoring. Groundwater temperatures at T2 were opposite to the fluctuations

in meltwater and groundwater levels, with fall (rise) in water level followed by a rise (fall) in groundwater temperatures (Figure 7.11). Groundwater temperatures at T2 rose by approximately 1.0 °C at the start of interval 1. Groundwater temperatures then fell by approximately 0.65 °C at the beginning of interval 2, following the increase in meltwater and hydraulic heads. Groundwater temperatures then rose back to 8.3 °C following the fall in water levels. T2 was the only piezometer where groundwater temperatures fell during the flood, with temperatures decreasing by 0.3°C (Figure 7.11). Groundwater temperatures recovered within 16 hours after the flood. Groundwater temperatures at T2 oscillated around 9.5 °C after the flood. However, the oscillations in groundwater temperature at T2 during Interval 4 were smaller than those observed prior to the flood (Figure 7.11)

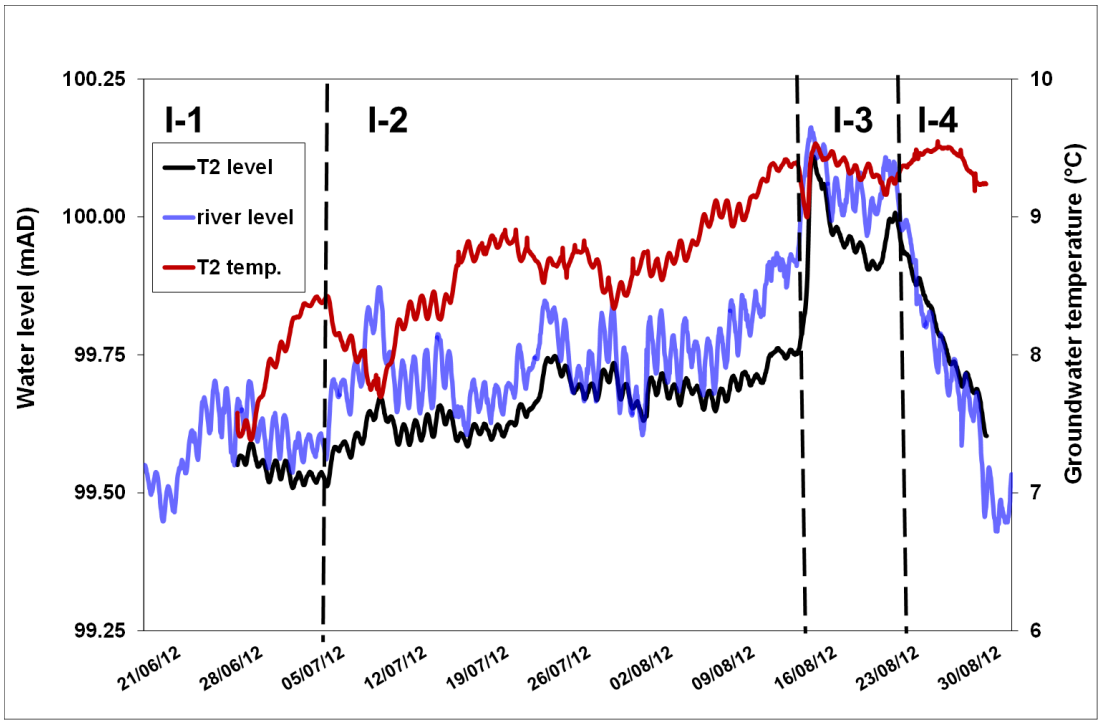

Figure 7.11. Mean hourly meltwater river level and groundwater levels and temperature at T2 during the 2012 field season.

The smallest variability and lowest groundwater temperatures were measured at T3 (Figure 7.9). However, outliers of maximum temperatures have been recorded in this

piezometer during the flood (Figure 7.10). Similar to T1, groundwater temperatures at T3 also increased over the season. However, in contrast to the notable fluctuations of groundwater temperatures and levels at T1 and T2, the coupling between fluctuations in groundwater temperatures and levels at T3 was very small (Figure 7.12). Groundwater temperatures at T3 were approximately 6.3 °C at the start of interval 1. Temperatures then gradually increased, which coincided with a fall in meltwater levels, around the 29/06/2012, reaching 6.75 °C by the end of the interval. Groundwater temperatures at T3 rose by approximately 1.0°C between the start of interval 2 and the 30/07/2012, when temperature fell by approximately 0.65 °C when the pressure transducer was exchanged with the transducer in the Skaftafellsá. Following this drop in temperature, groundwater temperatures gradually rose, reaching 7.43 °C during the flood. Temperatures then dropped after approximately 20 hours from the start of the flood. Groundwater temperatures remained around 7.61 °C until the end of interval 3. During interval 4, the oscillations in groundwater temperature increase towards the end of measurements (Figure 7.12).

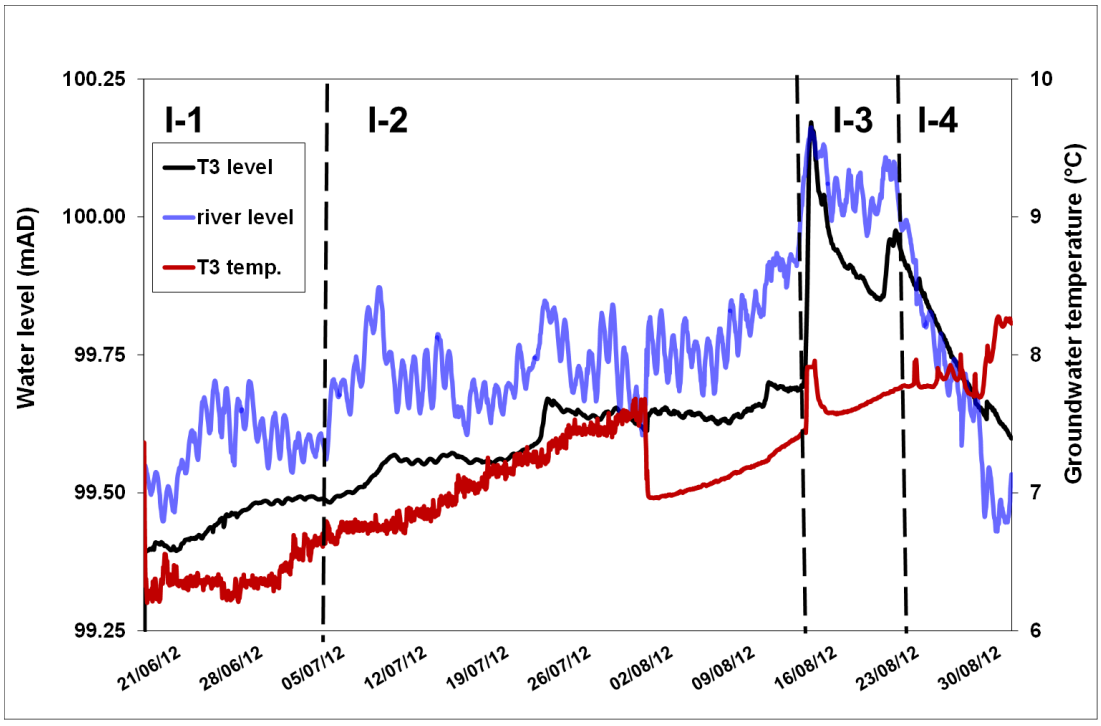

Figure 7.12 Mean hourly meltwater river level and groundwater levels and temperature at T3 during the 2012 field season.

7.3.4. Fluctuations in groundwater and meltwater EC

The fluctuations in groundwater and meltwater EC during the 2012 field season are presented in Figure 7.13. The mean groundwater EC in all three piezometers is significantly different (5% confidence level, 2 tail test, *p*=<*0.001*) than the mean EC of meltwater. Similar to observations from other proglacial environments (e.g. Robinson *et al*., 2009a), meltwater EC at the Skaftafellsá was also the lowest and least varied. Meltwater EC fluctuated between 1 and 8 µS/cm, with no notable impact of fluctuations in river levels on EC. However, the meltwater EC time series ends on the 30/07/2012, when the pressure transducer at the stilling well was exchanged with the transducer at T3 (hence the start of the EC measurements at T3 on that date). The pressure transducer which was used in the Skaftafellsá from 30/07/2012 only measured water level and temperature, hence, the impact of the flood in August on meltwater EC is unknown.

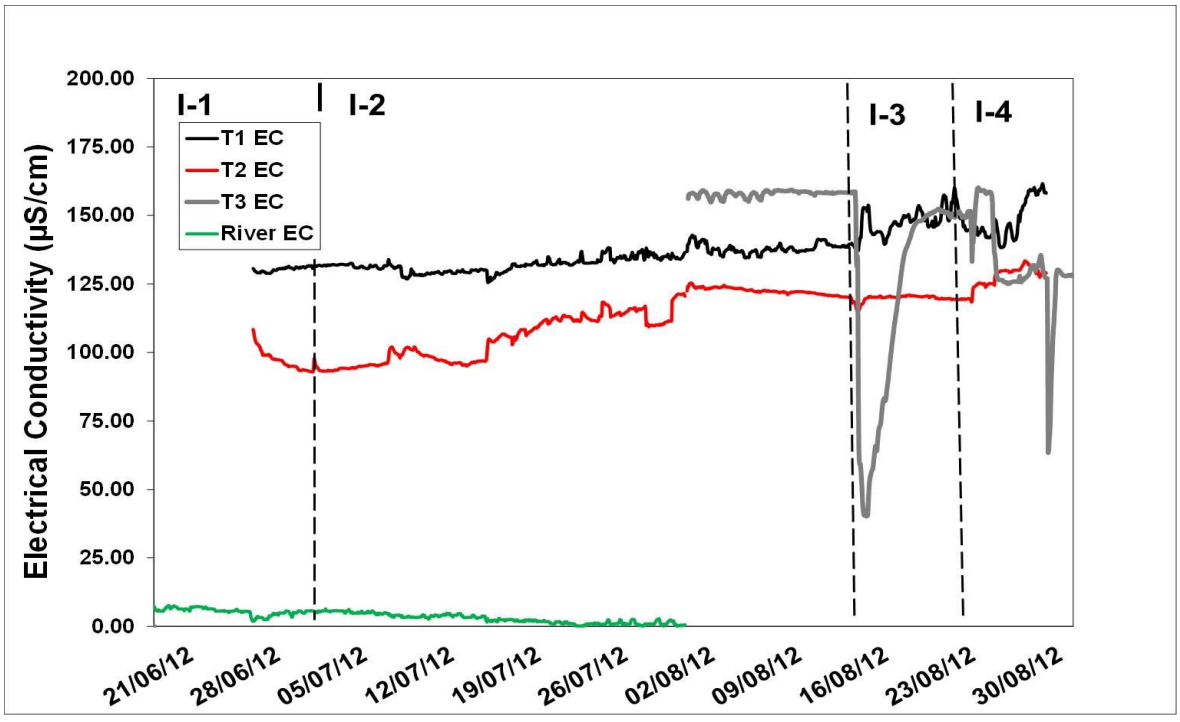

Figure 7.13. Meltwater and groundwater EC at the Skaftafellsá and the transect.

EC was monitored hourly between 28/06-29/08/2012. Meltwater EC was only measured between 26/06-30/07/2012. EC at T3 was only measured between 30/07-29/08/2012.

Groundwater EC was only measured at T1 and T2 before the 30/07/2012. During this time, EC at T1 exceeded EC at T2 by approximately 30 µS/cm. However, groundwater EC at T3 were the highest, exceeding groundwater EC at T1 by approximately 25 µS/cm between 30/07/2012 and the end of Interval 2 (Figure 7.13. Groundwater EC at T1 was approximately 130 µS/cm during intervals 1 and 2, with fluctuations of up to15 µS/cm (Figure 7.14). EC at T1 was around 140 µS/cm at the beginning of interval 3. During the flood, EC has risen to 155 µS/cm in 14 hours. However, EC fell back to 140 µS/cm within 30 hours. Following the flood, EC rose by approximately 10 µS/cm, peaking at 158 µS/cm at the end of interval 3. During interval 4, EC fell by approximately 15 µS/cm on the 26/08/2012 and then rose back to 160 µS/cm (Figure 7.14).

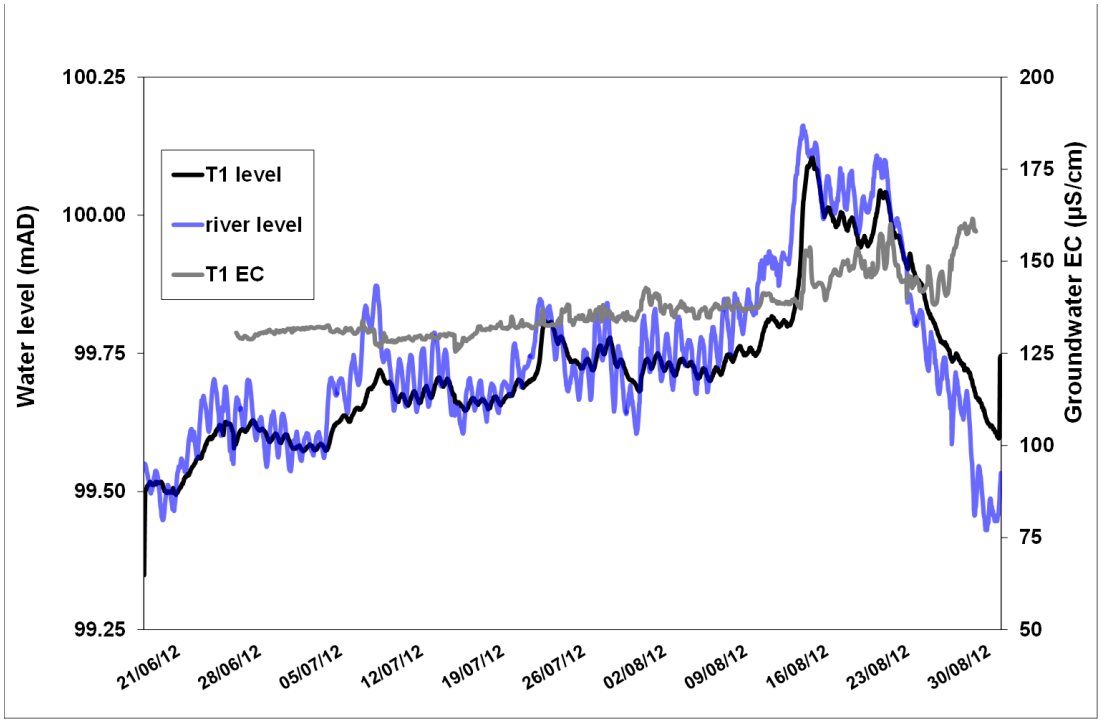

Figure 7.14. Meltwater river level, hydraulic head, and groundwater EC at T1.

Groundwater EC at T2 fluctuated between 95 and 130 µS/cm (Figure 7.15). The lowest mean and smallest variability in groundwater EC were measured at T2 (Table 7.1). Groundwater EC fell by about 10 µS/cm between the start of measurements and the end

of interval 1. EC gradually rose during interval 2, reaching 125 µS/cm around the 02/08/2012. However, the fluctuations in EC were inverse to those in meltwater levels and hydraulic heads, with EC rising (falling) during fall (rise) in meltwater levels (Figure 7.15). During the gradual rise in meltwater levels at the end of interval 2, EC remained around 125 µS/cm. The impact of the flood during interval 3 on groundwater EC at T2 was negligible. Following the flood, groundwater EC at T2 remained around 120 µS/cm until the end of interval 3. Groundwater EC at T2 rose during interval 4, reaching 133 µS/cm by the end of the monitoring period (Figure 7.15).

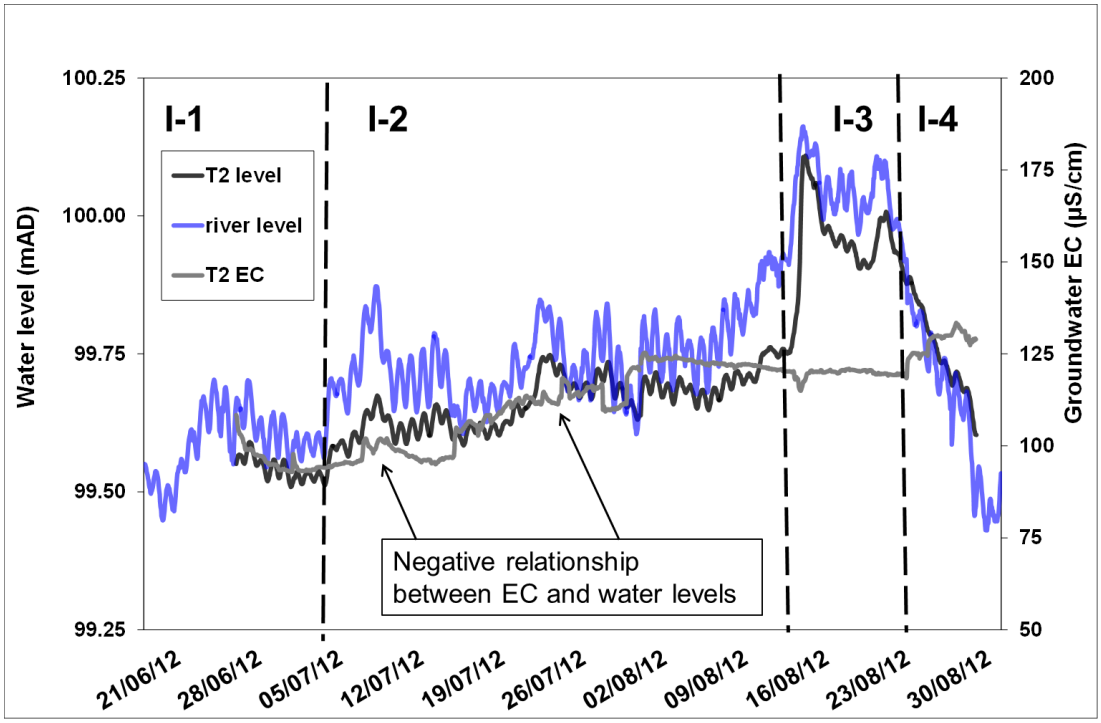

Figure 7.15. Meltwater river levels, hydraulic heads, and groundwater EC at T2.

Groundwater EC at T3 was only measured between 30/07-31/08/2012. Groundwater EC at T3 was the highest (approximately 150 µS/cm) during the ablation-controlled flow regime of interval 2 (Figure 7.16). EC at T3 also had the highest mean and standard deviation (Table 7.1). However, in contrast to the small changes in groundwater EC that were observed at T1 (Figure 7.14) and T2 during the flood (Figure 7.15), groundwater EC at T3 declined substantially during the flood, falling from 160 to 40 µS/cm in 24 hours. Following the flood, groundwater EC at T3 rose back to 150 µS/cm in around 100 hours,

where it remained until the end of interval 3. During interval 4, EC rose to 160 µS/cm around the 23/08/2012 and then fell to 130 µS/cm. An abrupt fall and recovery in groundwater EC at T3 (from 130 to 60 µS/cm in 24 hours) was also measured near the end of the monitoring period (Figure 7.16).

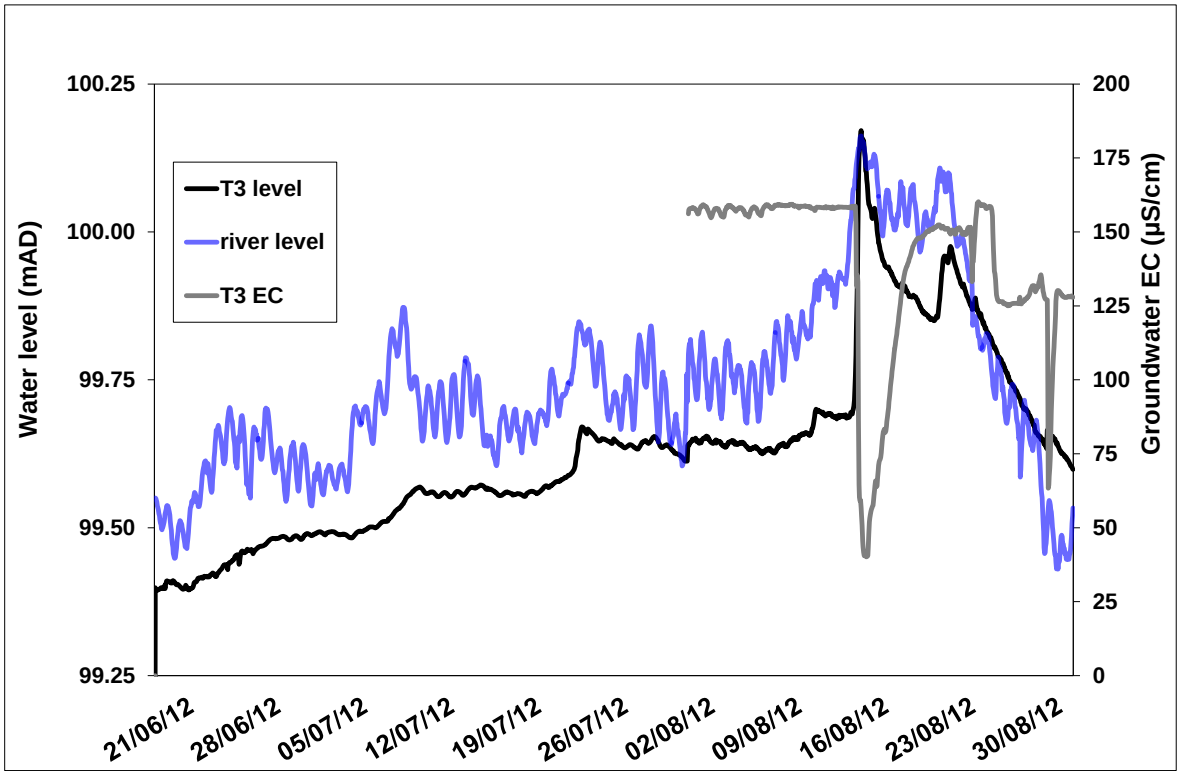

Figure 7.16. Meltwater levels, hydraulic heads, and groundwater EC at T3.

7.3.5. Interpretation

Fluctuations in the levels of hydraulic heads and river-aquifer exchange can be caused by groundwater mounding, water table depression, variability in regional recharge, climatic variability, changes in transpiration, and changes in groundwater and surface water levels (e.g. Drexler *et al*,. 1999; Käser *et al*., 2009). Within proglacial environments, changes in ablation also exert important control on groundwater levels and river-aquifer exchange (e.g. Magnusson *et al*., 2014).

The highest hydraulic heads at the transect were measured at T1, followed by T2 and T3 (Figure 7.8). This shows that groundwater flows away from the Skaftafellsá. Additionally, the west-east groundwater flow direction suggests that this area has a local groundwater flow system which is imposed on the north-south flowing regional groundwater system (Figure 7.7), in accordance with the model of Tóth (1963).

The close response between hydraulic heads at the transect and fluctuations in meltwater levels shows that meltwater levels are an important control on groundwater levels. The response of hydraulic heads to fluctuations in meltwater levels has been observed in all three piezometers. However, the strength in the signals of hydraulic heads and meltwater levels generally diminished with distance away from the meltwater channel. The largest attenuation of the signal of meltwater level fluctuations was observed T3, located furthest piezometer from the channel (Figure 7.8). However, the smallest dampening has been observed at T2, located further away from the channel than T1. These observations are also supported by the CCF analysis, which showed that the longest lag time was at T3 and the shortest at T2 (Table 7.2). This spatial variability suggests that distance from the channel is not the sole control on the dampening of the meltwater signal. Similar patterns of attenuation in river levels signal with distance away from the channel have been previously reported from catchments underlain by permafrost (Cooper *et al*., 2002; 2011), a proglacial forefield in the Swiss Alps (Magnusson *et al*., 2014), snowmelt-dominated catchments (Loheide and Lundquist, 2009), lowland floodplains (e.g. Jung *et al.*, 2004; Vidon, 2012), and regulated rivers (e.g. Sawyer *et al*., 2009).

The close response of hydraulic heads to fluctuations in meltwater level (Figure 7.8) possibly suggests that large fluxes of meltwater are entering the aquifer, leading to high groundwater-meltwater exchange at the transect. However, an alternative hypothesis is that the coupling between hydraulic heads and meltwater levels is caused by the propagation of a kinematic pressure wave, which impacts groundwater levels and dampens with distance from the channel (e.g. Sawyer *et al*., 2009; Magnusson *et al*.,

2014). Close coupling of groundwater levels with fluctuations in surface water following the propagation of a pressure wave have been previously described from various hydrological settings, including the proglacial forefield of an Alpine valley glacier (Magnusson *et al*, 2014), snow-dominated catchments (e.g. Loheide and Lundquist, 2009), and lowland flood plains (e.g. Vidon, 2012).

The extent of meltwater-groundwater exchange is pivotal for this study, as proglacial recharge sources exert an important control on groundwater levels, physicochemical parameters, and ecology (e.g. Brown *et al*., 2006a, b; Roy and Hayashi, 2008; 2009). The close dynamics between hydraulic heads and meltwater levels (Figure 7.8) suggest high levels of meltwater-aquifer exchange at the transect. However, there are contrasting reports in the literature with regards to the fluxes of groundwater-surface water exchange in sites where groundwater levels show close response to fluctuations in surface water. Some studies have suggested high level of river-aquifer exchange (e.g. Cooper *et al*., 2002; Fritz and Arntzen, 2007; Loeheide and Lundquist, 2009). Conversely, other studies suggested negligible amount of exchange, suggesting that the coupling was caused by the propagation of a pressure wave, rather than actual surface water entering the aquifer (e.g. Magnusson *et al*., 2014). These controversies suggest that additional methods should be used in addition to fluctuations in groundwater and surface water levels (e.g. Käser *et al*., 2009; Welch *et al*., 2013; 2014). Therefore, in order to test the hypotheses of the causes for the coupling between groundwater and meltwater levels, the current study also used groundwater and meltwater physicochemical parameters (Figure 7.9, 7.13), geochemistry (Figure 6.8-6.10), and stable isotopes (Figure 6.18) in addition to the water levels data. Similar water quality and isotopic composition will suggest high level of mixing between groundwater and meltwater. Conversely, significantly different water quality and isotopic composition will suggest that mixing is low (e.g. Roy and Hayashi, 2009).

Groundwater and meltwater temperature and EC at the Skaftafellsjökull foreland were significantly different, with groundwater temperature and EC higher than that of meltwater

(Table 7.1, Figure 7.9, 7.13). These observations are consistent with those reported from many proglacial settings (e.g. Robinson *et al*., 2009b; Brown *et al*., 2007a; Kristiansen *et al*., 2013). The fluctuations in groundwater temperature has shown coupling with groundwater and meltwater levels, particularly at T2, where groundwater temperatures fell (rose) in response to a rise (fall) in meltwater and groundwater levels. Additionally, T2 was also the only borehole where groundwater temperature have fallen during the flood (Figure 7.11). Conversely, groundwater temperatures at T1 and T3 generally rose during the season, alongside the increase in meltwater levels (Figure 7.11. This suggests low exchange between the Skaftafellsá and T1 and T3. The fluctuations in EC also do not support high exchange between meltwater and groundwater, as groundwater EC was approximately 100-150 µS/cm higher than meltwater (Figure 7.13.). Additionally, EC fluctuations at T1 and T2 were fairly small and at times rose alongside groundwater and meltwater levels (Figure 7.14, 7.15), which does not suggest significant meltwater-groundwater exchange. Conversely, T3 has shown different dynamics, particularly during the flood, where EC fell substantially (Figure 7.16). Substantial drops in EC following a large input of low EC meltwater following outburst floods have also been reported from Greenland (Kristiansen *et al*., 2013). The decline in EC at T3 during the flood therefore suggests higher mixing between meltwater and groundwater at T3 than at T1 and T2. However, since EC at T1 and T2 did not fall during the flood, it is suggested that the flood did not flow across the transect.

In addition to temperature and EC, groundwater and meltwater solute concentrations and stable isotopes (Chapter 6) were also used to infer groundwater-meltwater exchange at the transect. Similar to water physicochemical parameters, similar solute concentrations and isotopic composition of meltwater and groundwater also suggest high meltwater-groundwater exchange (e.g. Cooper *et al*., 2002). However, groundwater SO_4^{2-}, Ca^{2+}+ Mg^{2+}, and Na^{+}+ K^{+} concentrations were significantly higher than meltwater solute concentrations, particularly at T1 and T2 (Figure 6.8-6.9). Additionally, groundwater

isotopic composition at the transect was significantly heavier than that of meltwater, suggesting recharge from precipitation rather than meltwater (Figure 6.18). High recharge of groundwater by meltwater is expected to result in groundwater with low solute concentrations and light isotopic composition (e.g. Hodgkins *et al*., 1998; Wadham *et al*., 2001). However, groundwater solute concentrations and isotopic composition at the transect were significantly different than those of meltwater. It is therefore suggested that meltwater-aquifer exchange at the transect is low, and that the close response of hydraulic heads to fluctuations in meltwater levels is caused by other mechanisms, possibly the propagation of a kinematic pressure wave, rather than significant recharge of the aquifer by meltwater.

In addition to the impact of meltwater levels on groundwater levels, precipitation also impacted groundwater levels. The impact of seasonal and inter-annual variability of precipitation on groundwater and surface water levels at the Skaftafellsjökull foreland is illustrated by the substantial changes in lake levels. Following an unusually dry spring and summer in 2012, lake levels at the Skaftafellsjökull foreland were very low. However, precipitation in the winter of 2013 was substantially higher than the monthly mean (Figure 3.15). Observations taken during a brief visit to the field site in July 2013 have shown that lake levels were substantially higher than in 2012 (Figure 7.17). Hydraulic heads at the outwash and near the river were higher by approximately 0.25 m than in August 2012. Although the coarse temporal resolution of these observations (1 year) masks finer fluctuations in groundwater and surface water levels, it is suggested that precipitation is an important control on groundwater levels at the Skaftafellsjökull foreland.

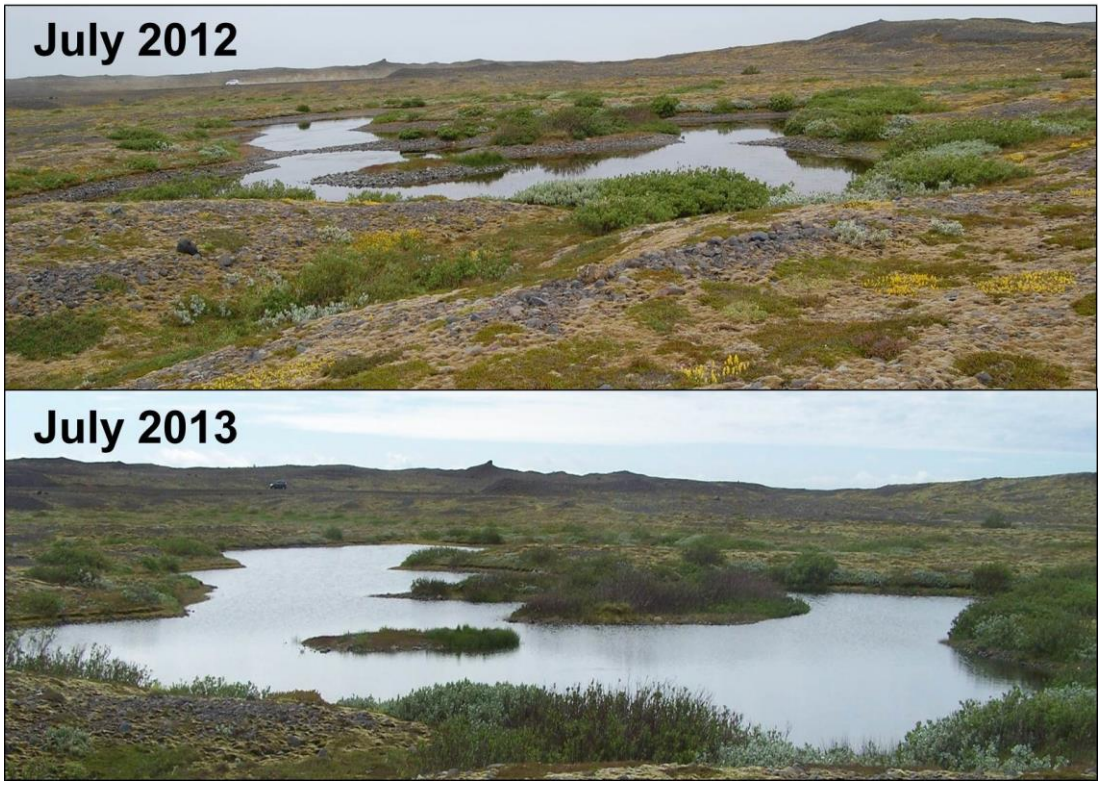

Figure 7.17. Inter-annual changes in lake levels at Island Lake.

In addition to the impact of precipitation on inter-annual variability in groundwater levels, the impact of precipitation on daily and weekly fluctuations in hydraulic heads was also observed. Hydraulic heads at the site generally rose after rainfall events (Figure 7.2). However, spatial variability in the response of hydraulic heads to precipitation was also observed, which is suggested to be strongly impacted by the high variability in hydraulic conductivity (K) at the field site (Figure 5.9). For instance, hydraulic heads at GW8, which is located in an area of fine lacustrine deposits (K= 0.14 m/day) had steeper rises and slower recession following rainfall events than hydraulic heads which are located in coarser deposits (Figure 7.2). These observations are also supported by studies from glaciated (Robinson *et al*., 2008; Magnusson *et al*., 2014) and deglaciated catchments (e.g. Rains, 2011) who reported similar responses of groundwater levels in areas of lower hydraulic conductivity to precipitation events.

The flood which took place on the 13-14/08/2012 was the main hydrological event during the 2012 field season, substantially impacting groundwater levels (Figure 7.8), physicochemical parameters (Figure 7.9, 7.13), and solute concentrations (Chapter 6). In addition to the impacts on groundwater at the transect, the flood also impacted water quality at the IL and Swan Lake, where turbidity increased and lake temperature and EC fell after the flood (Figure 6.6, 7.18). These observations show that in addition to precipitation, high discharge events are also important controls on proglacial groundwater-surface water exchange. However, since the flood took place during the break in monitoring (13-14/08/2012), the investigation of its route had to be inferred from the automated measurements of hydraulic heads, groundwater temperatures and EC at the transect.

Hydraulic heads in all three piezometers in the transect increased during the flood. However, the impact of the flood on groundwater temperature and EC varied substantially between the piezometers. Groundwater EC at T1 has risen by approximately 30 µS/cm and temperature increased by 0.5 °C during the flood. Conversely, groundwater temperature at T2 have fallen by 0.3 °C while EC declined negligibly. The largest impact of the flood on groundwater EC was observed at T3, where EC substantially fell by 110 µS/cm (Figure 7.13). Conversely, groundwater temperatures at T3 have risen by approximately 0.4 °C during the flood. The differences in the impact of the flood on groundwater physicochemical parameters suggest that the flood possibly followed various flow paths. The relatively small impacts on groundwater physicochemical parameters at T1 suggest that the flood did not flow from west to east across the transect, as a quick rise in groundwater or overland flow in such manner is expected to have reduced the EC and temperature at T1 and T2. As the highest impacts were observed at T3, it is suggested that T3 was impacted by either overland flow or enhanced groundwater flow from the north, which possibly travelled preferentially through the breached moraine (Figure 7.18).

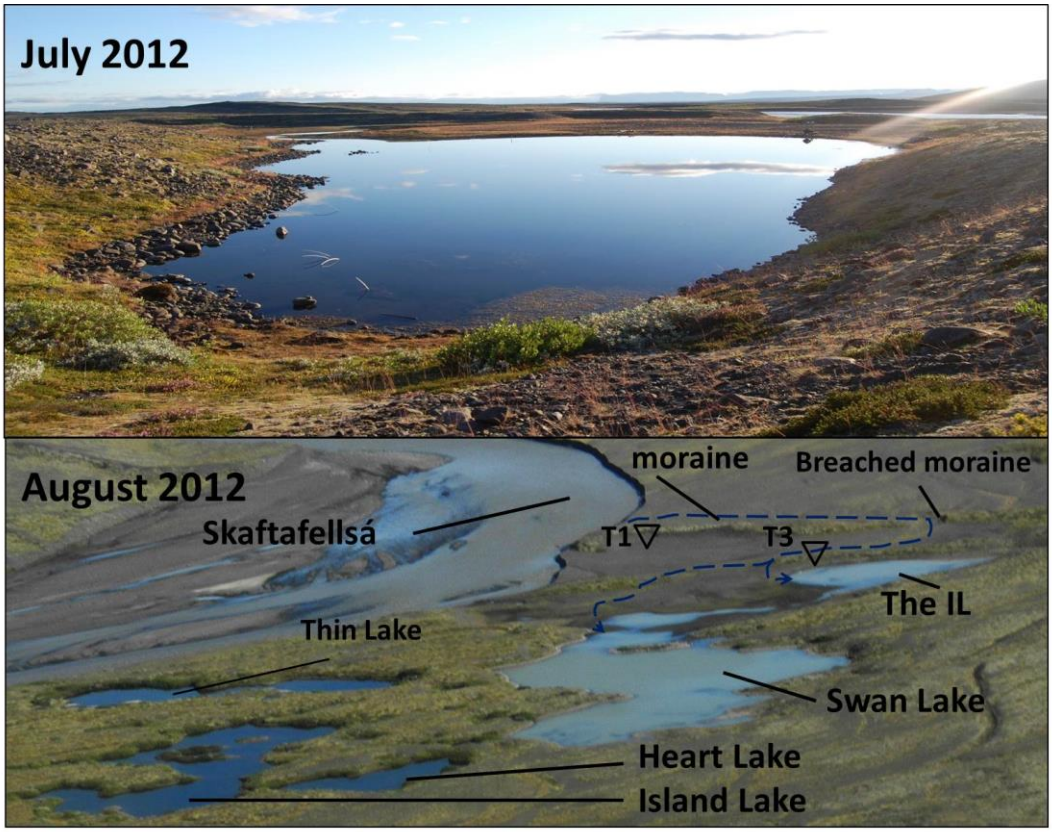

Figure 7.18. The impacts of the flood in August 2012 flood on lake water quality at the IL and Swan Lake.

The figure shows the differences in lake turbidity in the IL before (July 2012) and after (August 2012) the flood. The dashed blue lines suggest the route of the flood, based on the differences in EC at T1 and T3.

7.3.6. summary

Meltwater and groundwater levels have risen at the beginning and middle of interval 2, following rainfall and an increase in air temperature. The main event during the field season was the flood on the 13-14/08/2012, during which groundwater and meltwater rose by approximately 0.5 m in 24 hours. Water levels then quickly receded following the flood. Hydraulic heads in the transect have shown close responsiveness to fluctuations in meltwater levels, which dampened with distance from the channel. The dampening of river levels signal with distance from the channel has been previously observed in various proglacial and non-glacial settings. However, despite the apparent coupling between

groundwater and meltwater levels, the geochemistry and isotopic composition of groundwater and meltwater were significantly different. It is therefore suggested that meltwater-aquifer exchange at the transect is low and that the coupling in levels is possibly caused by the propagation of a pressure wave rather than the actual exchange between groundwater and meltwater. The impacts of the flood have shown considerable spatial variability, with the highest impacts observed at T3. This suggests that the flood possibly travelled as overland flow from the north rather than in a west-east direction across the transect. The impact of precipitation on groundwater and surface water levels was illustrated on various time scales. The short term impacts of precipitation are illustrated by the rising in hydraulic heads following rainfall events. The inter-annual impacts of precipitation were illustrated by the changes in groundwater and lake levels between August 2012 and July 2013.

7.4. The impact of jökulhlaup events on proglacial river-aquifer exchange

This section investigates the impact of jökulhlaups (glacial outburst floods) on proglacial river-aquifer exchange. This was investigated at the river Núpsvötn-Súla, western Skeiðarársandur, where several small jökulhlaups were detected in July-August 2011. The Núpsvötn-Súla is formed by the confluence of the meltwater river Súla, which drains western Skeiðarárjökull and the river Núpsvötn, which is mainly fed by precipitation and snowmelt (Figure 7.19) (Churski, 1973; Guðmundsson *et al*., 2002). The river Súla is occasionally impacted by jökulhlaups which originate from Lake Grænalón, an ice marginal lake located to the west of Skeiðarárjökull, approximately 20 km to the north of the monitoring site (Figure 7.19) (Roberts *et al*., 2005). The lake is located in a subaerial valley, whose eastern end is dammed by the Skeiðarárjökull glacier. The glaciological conditions at Skeiðarárjökull therefore control the drainage and jökulhlaup generation from

Lake Grænalón (Roberts *et al*., 2005). The source of the outlet for jökulhlaups and their routing (subglacial or subaerial) has fluctuated over the years, which substantially altered jökulhlaup frequency. Drainage occurs approximately every 9 years when drained via the ice dam. Conversely, drainage occurs approximately once a year when drained via an ice buttress. Jökulhlaup frequency increased substantially during 2002-3, when five events occurred at approximately 30 day intervals (in 2002) and four jökulhlaup events occurred at approximately 40 day intervals (in 2003). The magnitude of these more frequent jökulhlaups, are substantially smaller than those controlled by the ice buttress (Roberts *et al*., 2005).

The impact of jökulhlaups on river-aquifer exchange was investigated using time series of groundwater and meltwater levels, temperature, and EC. These variables were automatically monitored between 08/07-15/08/2011. The monitoring took place at the GW4 piezometer, located near the Route No. 1 bridge, and at the river Súla (IMO, 2013). GW4 was chosen to assess river-aquifer exchange at this site due to its proximity (~200 m) to the Núpsvötn-Súla's IMO gauging station (Figure 7.19). The hourly measurements of river levels, temperature and EC in this chapter were kindly provided by the IMO (2013). This site was also chosen due to its accessibility and the ease of installing shallow piezometers in the coarse-grained sandur deposits.

Figure 7.19. Location of the river Núpsvötn-Súla and the GW4 borehole.

The map was taken from Skaftafell Sérkort 5 hiking map (2009). Published by Mál og menning/Forlagið

7.4.1. Temporal variability in meltwater and groundwater levels

Meltwater levels at the Súla generally fluctuated diurnally in response to changes in ablation. However, three low frequency, high magnitude episodic events, hypothesised to be small jökulhlaups, have also been detected. These jökulhlaups substantially impacted meltwater and groundwater levels. Hydraulic heads at GW4 varied between 57.20 and 57.40 mAD. Initially, groundwater levels slowly declined, falling to 57.23 mAD on

11/07/2011 at 1000 hours. During event 1, the Súla levels rose by 1.20 m in 17 hours, from 58.77 mAD (11/07/2011 at 0800 hours) to 59.97 m on 12/07/2011 at 0100 hours. In comparison, the diurnal fluctuations at the Súla were approximately 0.15 m (Figure 7.20). Groundwater levels rose sharply during event 1, until levels stabilised at 57.38 mAD on 1200 hours at 12/07/2011, approximately 10 hours after peak discharge in the Súla. Hydraulic heads have increased by 0.16 m over 26 hours during this event.

Groundwater remained at the same levels until 16/07/2011, when levels began to decline. River levels fell by 0.88 m, reaching 59.09 mAD on 12/07/2011 at 1700 hours. River levels then fluctuated until returning to the levels prior to the event (58.78 mAD) at 1000 hours, 15/07/2011. Meltwater fluctuations following the jökulhlaup were around 0.5 m. No significant rainfall was measured during this period (Figure 7.20). Water levels at the Súla then returned to an ablation-controlled flow regime, with diurnal fluctuations of approximately 0.15 m. hydraulic heads at GW4 declined gradually, although several minor increases (<0.05 m) were also observed. Groundwater levels reached a low of 57.22 m on 29/07/2011. A small increase in river levels was observed between 1100 hours on 26/07/2011 to 2200 hours on 27/07/2011, where river levels have risen by 0.35 m. Groundwater levels have risen by approximately 0.07 m in response to this event (Figure 7.20).

Event 2 began at 0700 hours on 29/07/2011, when meltwater levels rose from 58.67 to 60.03 mAD on 0100 hours on 30/07/2011. Following the jökulhlaup, groundwater levels rose from 57.22 mAD on 0800 hours on 29/07/2011 to 57.39 mAD on 0700 hours on 30/07/2011. Meltwater levels have risen by 3.0 m in 10 hours during this event, which was the largest one recorded during the monitoring season. Groundwater levels have risen by 0.17 m in 23 hours in response to this event. During this event, the increase in groundwater levels lagged beyond the river levels by approximately one hour. Following the second event, river levels have returned to an ablation-controlled regime (Figure 7.20).

Event 3 began on the 04/08/2011. This event included three short episodes of rapid rise and fall in meltwater levels, during which the overall increase in meltwater levels was 1.19 m (Figure 7.20). The second and third rises during event 3 were smaller in magnitude than the first. In contrast to Events 1 and 2, Event 3 did not have a significant impact on groundwater levels at GW4, as groundwater levels remained around 57.39 mAD, with a small recession (0.05 m) during the first increase of Event 3. After the third increase during Event 3, meltwater levels have returned to ablation-controlled flow regime, under which it remained until monitoring ended on the 12/08/2011. Groundwater levels have steadily declined after Event 3, reaching levels of 57.20 mAD by the end of the monitoring period (Figure 7.20). However, it is possible that the relatively stable groundwater levels between 29/07-10/08/2011 were due to a technical problem with the pressure transducer. Apart from the sharp increases in response to the jökulhlaups, it is also noticeable that, in contrast to the groundwater dynamics at the Skaftafellsjökull foreland (Figure 7.8), the groundwater level at GW4 does not show significant response to oscillations in river levels when the latter is under ablation-controlled flow regime.

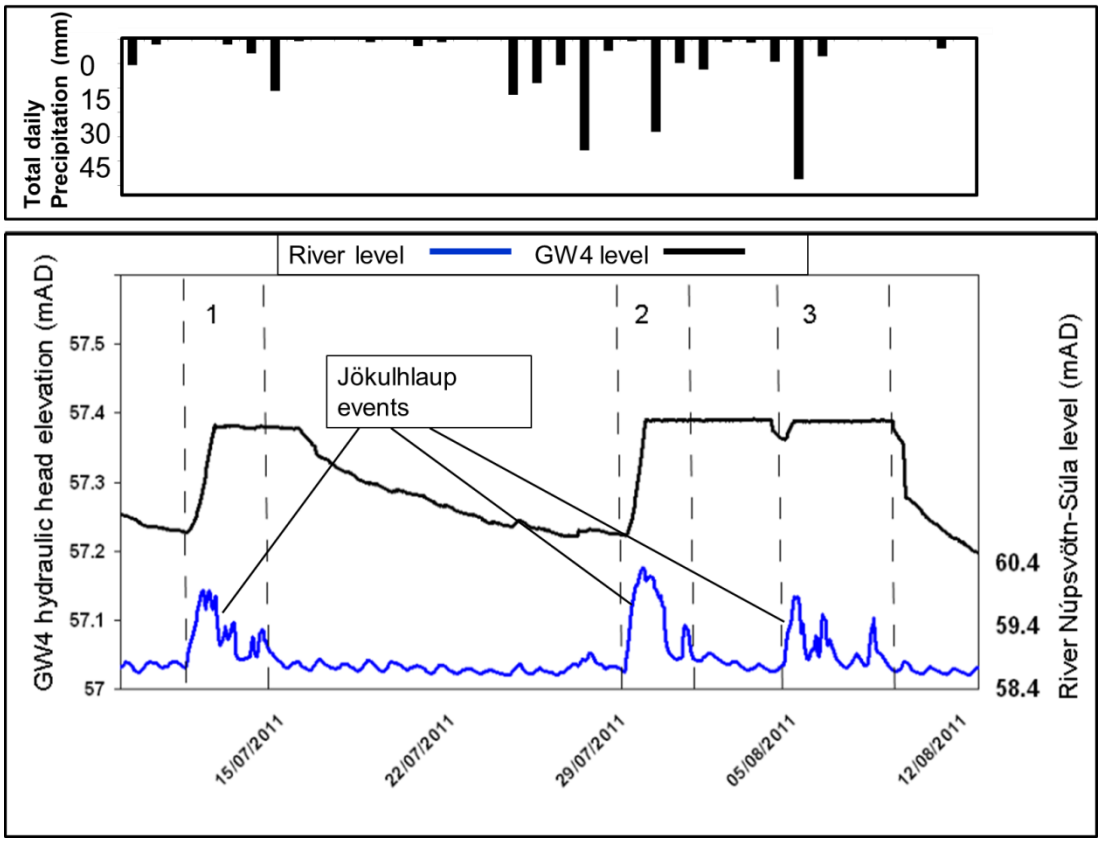

Figure 7.20. River levels at the Núpsvötn-Súla (IMO, 2013), hydraulic heads at GW4, and total daily precipitation at Kirkjubæjarklaustur IMO (2013) station.

The Figure also highlights the two different controls on the river flow regime: ablation-controlled flow regime and the three small jökulhlaups events (see text).

7.4.2. Temporal variability in groundwater and meltwater temperature

Similar to the approach used at the Skaftafellsjökull foreland, river and groundwater temperature were used in addition to meltwater and hydraulic heads for the investigation of river-aquifer exchange in western Skeiðarársandur. The mean groundwater temperature at GW4 exceeded river temperature by approximately 3.3°C. Furthermore, in contrast to the small variability in meltwater temperature at the Skaftafellsá (Figure 7.9), water temperatures at the Súla were more variable than groundwater temperatures at GW4. The Súla temperatures were higher and more variable than the Skaftafellsá (Table 7.1). However, despite the higher variability in Súla temperature, groundwater

temperatures at GW4 were lower than groundwater temperatures at the Skaftafellsjökull foreland (Table 7.1). The closest groundwater temperatures at the Skaftafellsjökull foreland to the temperatures at GW4 were those at GW9, where groundwater isotopic composition suggests recharge of meltwater recharge (Figure 6.20).

Similar to the observations from the Skaftafellsjökull foreland (Figure 7.9), groundwater temperatures at GW4 also increased during the season. Groundwater temperature at GW4 at the start of the season was 4.20°C, with temperatures reaching 6.09°C by the end of the season. However, the daily oscillations in groundwater temperature at GW4 were substantially smaller (Figure 7.21) than groundwater temperature oscillations at the Skaftafellsjökull foreland (Figure 7.9).

The increase in groundwater temperature at GW4 over the monitoring season has been very gradual. The main exceptions for this trend were after Event 1, when groundwater temperature rose by 0.15°C and following the increase in groundwater levels after Event 2, when groundwater temperature rose by 0.6°C. In contrast to the dynamics of groundwater levels, which declined after the jökulhlaups (Figure 7.20), groundwater temperatures continued to rise, and did not return to the pre-jökulhlaup values (Figure 7.21).

The large fluctuations in meltwater temperature in the Núpsvötn-Súla were very different from the sustained, gradual increase in groundwater temperature during the season (Figure 7.21). Meltwater temperature showed an inverse relationship to the oscillations in river levels, with river temperature falling (rising) with rising (falling) river levels. These dynamics are also supported by the negative correlation coefficient ($r = -0.437$) between river level and temperature. The jökulhlaup events substantially lowered stream temperature, which fell by 2.58 °C after Event 1 and 4.42°C after Event 2 (Figure 7.21). In contrast, meltwater temperature oscillations under ablation-controlled conditions (i.e. between Events 1 and 2) were smaller (1.5-2°C). However, these oscillations were

substantially larger than those measured in the Skaftafellsá, which were approximately 0.5°C (Figure 7.9).

In contrast to the rapid response between jökulhlaups and hydraulic heads (Figure 7.20), the impact of oscillations in meltwater levels on groundwater temperatures was much smaller. Meltwater temperatures in the Súla were substantially lower than groundwater temperatures, particularly during jökulhlaups (Figure 7.21). Hence, an infiltration of large fluxes of meltwater is expected to lower groundwater temperature (e.g. Kristiansen *et al*., 2013). However, groundwater temperature at GW4 actually rose between 0.2-0.6 °C after the jökulhlaups (Figure 7.21). The correlation between meltwater levels and groundwater temperatures at GW4 was weakly negative (r = -0.196).

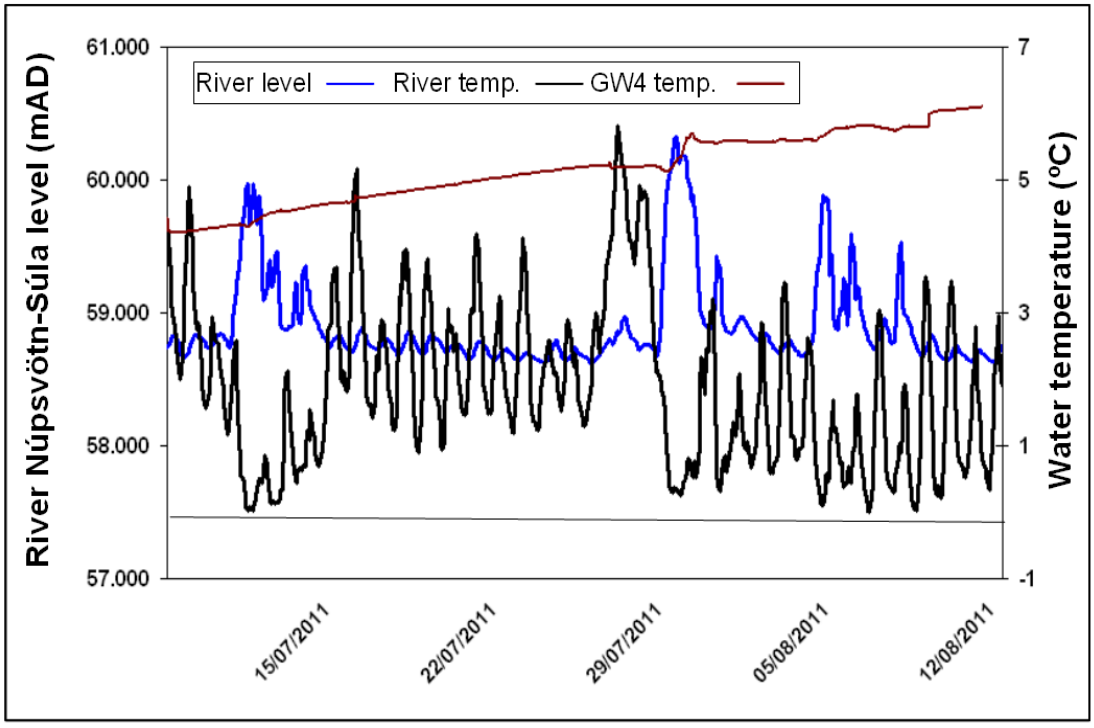

Figure 7.21. Meltwater levels and temperature at the Núpsvötn-Súla (IMO, 2013) and groundwater temperature at GW4.

7.4.3. Temporal variability in groundwater and meltwater EC

Meltwater and groundwater EC in the river Súla and GW4 was higher than groundwater and meltwater EC at the Skaftafellsjökull foreland (Table 7.1). Groundwater EC at GW4 was approximately 150 µS/cm during the start of the monitoring season. EC then rose sharply following Event 1 and the rise in groundwater levels, peaking to 204 µS/cm. During the ablation-controlled period, groundwater EC fluctuated around 160 µS/cm. Following Event 2, EC has risen by approximately 100 µS/cm, reaching 262 µS/cm. However, after event 2 EC declined rapidly. EC then rose again, although it did not reach the same values that were reached during the initial rise (Figure 7.22).

Groundwater EC increased to 265 µS/cm following Event 2, and then rapidly fell to 195 µS/cm. Groundwater EC fluctuated between 200 and 230 µS/cm between Events 2 and 3. However, in contrast to Events 1 and 2, where groundwater EC rose following the jökulhlaups, groundwater EC during Event 3 fell when meltwater levels rose. Groundwater EC declined by 80 µS/cm when the Súla returned to ablation-controlled flow regime after Event 3 (Figure 7.22). The correlation between groundwater levels and groundwater EC was strongly positive (r= +0.733). The correlation between meltwater levels and groundwater EC was also positive, though weaker (r= +0.257).

Meltwater EC at the Súla was substantially lower than groundwater EC (Table 7.1), similar to the findings of previous research from Skeiðarársandur and other proglacial environments (e.g. Robinson *et al*., 2009b). Meltwater EC ranged between 25 to 35 µS/cm during ablation-controlled flow regime, where EC rose (fell) when meltwater levels fell (rose). However, meltwater EC was also substantially impacted by the jökulhlaups, with meltwater EC increasing by approximately 50 µS/cm during Event 1 and by approximately 30 µS/cm during events 2 and 3 (Figure 7.22). The correlation between meltwater levels and EC was strongly positive (r= +0.816). Similar to groundwater temperature, meltwater

EC at the Súla (Figure 7.22) were also substantially higher and more variable than those observed in the Skaftafellsá in 2012 (Figure 7.13.).

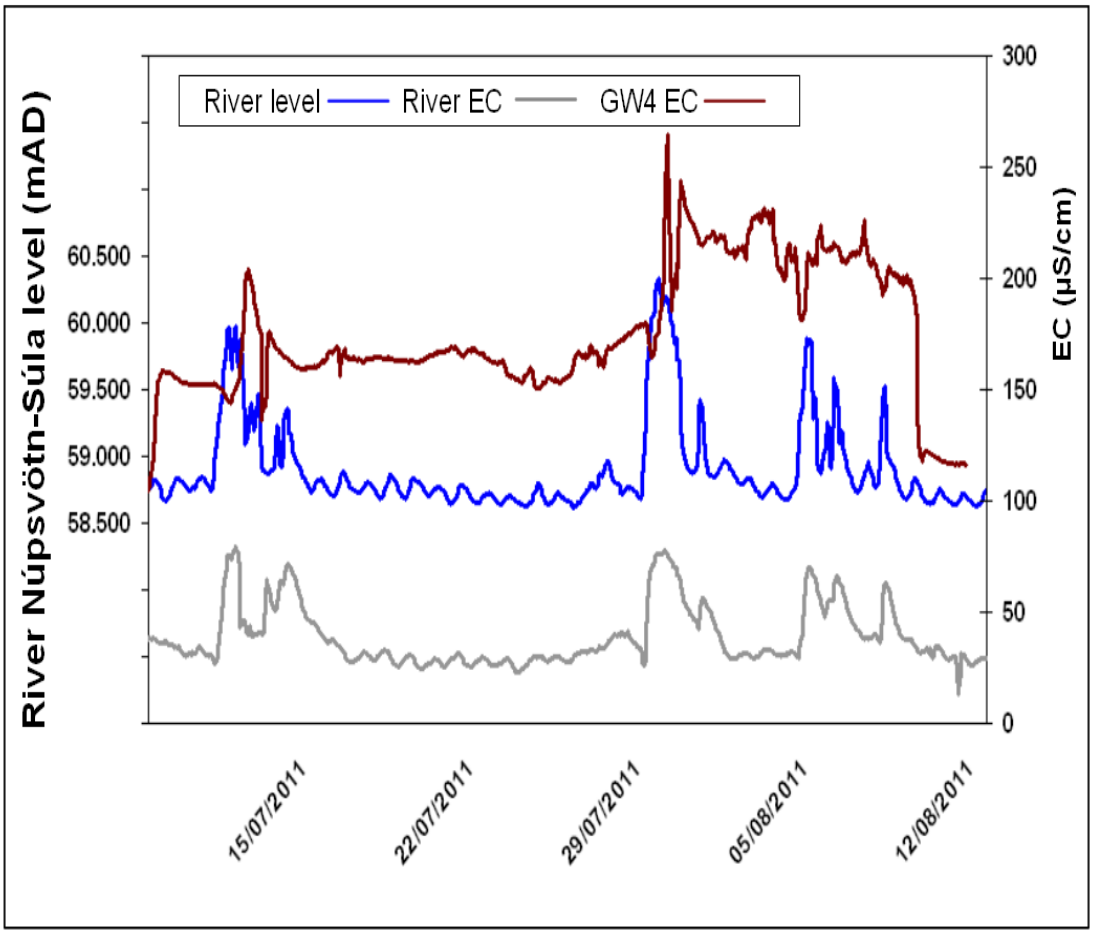

Figure 7.22. Meltwater levels and EC at the river Núpsvötn-Súla (IMO 2013) and groundwater EC at GW4.

7.4.4. Interpretation

Various studies have looked at the hydrological, sedimentological, geomorphic and natural hazards implications of jökulhlaups (e.g. Russell *et al*., 2006; Robinson *et al*., 2008; Emer and Vilímek, 2013**).** However**,** the impact of jökulhlaups on groundwater systems has not been well studied. The main impact of jökulhlaups on groundwater which was observed at this study was the quick increases in groundwater levels by approximately 0.20 m immediately following jökulhlaups (Figure 7.20). However, despite

these increases, the actual extent of river-aquifer exchange at GW4 is not clear. Similar to the observations from the Skaftafellsjökull foreland (Figure 7.8), close response between groundwater levels and fluctuations in meltwater levels during high discharge events has also been observed at GW4 (Figure 7.19). However, the substantial differences between meltwater and groundwater EC and temperature do not suggest significant meltwater-groundwater exchange at GW4.

Substantial differences were identified between groundwater and meltwater temperature at the Skaftafellsjökull foreland and in western Skeiðarársandur. However, the variability in meltwater temperatures at the Súla was higher than that of the Skaftafellsá (Table 7.1). Additionally, temperatures at the Súla fell substantially during the jökulhlaups (Figure 7.21), which was not observed at the Skaftafellsá during high discharge conditions (Figure 7.9). The higher temperatures at the Súla are possibly due to the larger distance from the glacier margin and the mixing with the rain/snow-fed river Núpsvötn (Guðmundsson *et al*., 2002). However, despite the contrasting temperature dynamics and geomorphic processes between the Súla and the Skaftafellsá, fluctuations in meltwater levels were observed to be an important control on proglacial groundwater levels at both sites.

Similar to the observations from the Skaftafellsjökull foreland, high river-aquifer exchange, which is suggested by the quick response of hydraulic heads to fluctuations in meltwater, is contested because of significantly different groundwater and meltwater EC and temperature at GW4.The propagation of substantial meltwater fluxes into the aquifer is expected to substantially reduce groundwater temperatures and EC (e.g. Roy and Hayashi, 2009). However, groundwater temperatures and EC at GW4 rise by 0.3-0.6 °C and 50-100 µS/cm, respectively, rather than fall, during the jökulhlaup events (Figure 7.21). However, river EC is still lower by approximately 100 µS/cm than groundwater EC (Figure 7.22), which does not support high river-aquifer exchange at the site.

A possible hypothesis for the controversies between observed increases in groundwater levels and the changes in groundwater temperature and EC following jökulhlaups is the propagation of a kinematic pressure wave (e.g. Jung *et al*., 2004). Another hypothesis is the distance from the channel. GW4 is located approximately 200-250 m from the Súla channel, which is nearly three times the distance between the Skaftafellsá and the furthest borehole T3 (67 m). Studies from a sandur in Svalbard showed that the impacts of meltwater infiltration on groundwater geochemistry were substantially dampened in a well located 118 m from the meltwater channel (Cooper *et al*., 2002). It is therefore possible that, due to the distance from the channel, the only parameter which can be detected during jökulhlaups is the increase in hydraulic heads. However, changes in groundwater temperature and EC, which suggest the entrance of meltwater into the aquifer, might be detected closer to the channel.

The increases in groundwater temperature and EC at GW4 during jökulhlaups can also be possibly attributed to piston flow (e.g. Geyh *et al*., 2000), where groundwater flows as a single parcel. This hypothesis suggests that groundwater, with relatively high EC and temperature, has been pushed horizontally towards GW4 by the jökulhlaups. However, there is insufficient evidence at this stage to define the cause for the changes in groundwater EC and temperature at GW4 following jökulhlaups.

These preliminary results have highlighted the connection between jökulhlaups and groundwater levels. The impacts of jökulhlaups on groundwater levels which were highlighted in this study are important for the understanding of jökulhlaup processes and impacts and for the modelling and planning of mitigation strategies against their adverse impacts (Emmer and Vilimek, 2013).

7.4.5. Summary

This section investigated the impact of low frequency, high magnitude events (jökulhlaups) on groundwater levels, physicochemical parameters, and hydrological

exchange between the aquifer and the meltwater river Súla. Fluctuations in river level are generally ablation-controlled. However, the ablation-controlled flow regime was episodically interrupted by three distinct jökulhlaup events. These events have led to substantial increases in meltwater levels and EC and substantial falls in river temperatures. Hydraulic heads at GW4 also increased substantially following the jökulhlaups. Conversely, groundwater temperatures and EC have risen. The increase in hydraulic heads suggest high river-aquifer exchange at the site. However, penetration of meltwater into the aquifer is expected to have reduced groundwater temperatures and EC. It is therefore suggested that the increases in hydraulic heads were not caused by the entry of large fluxes of meltwater into the aquifer. Possible hypotheses for the observed changes in groundwater physicochemical parameters are the propagation of a pressure wave and piston flow. However, further work is needed in order to test these hypotheses.

7.5. Discussion

The observations from the Skaftafellsjökull foreland and the river Súla in western Skeiðarársandur have shown that fluctuations in meltwater levels are an important control on hydraulic heads. However, despite the close response of hydraulic heads to fluctuations in meltwater levels, groundwater temperature, EC, solute concentrations, and isotopic composition were significantly different than that of meltwater. This suggests that groundwater-meltwater exchange at the transect is low. Previous studies from Skeidararansudr, which have used stable isotopes, identified ice melt and local precipitation as the main sources of groundwater recharge (Robinson *et al*., 2009a). The stable isotope composition of groundwater and surface water at the Skaftafellsjökull foreland suggest that precipitation is the dominant source for groundwater recharge (Figure 6.18). Precipitation was also identified as an important control on groundwater levels at the Skaftafellsjökull foreland (Figure 7.2). These observations have significant implications with regards to the impacts of climate change and glacier retreat on proglacial river-aquifer exchange, with the observations from this study suggesting that groundwater

recharge at this site will be more sensitive to changes in precipitation than to changes in meltwater caused by glacier retreat. Additionally, this chapter has also highlighted the impact of fluctuations in meltwater levels following high discharge events on proglacial groundwater levels. These impacts have been observed at both study sites, in spite of their different geomorphology and hydrology, suggesting that fluctuations in meltwater levels are an important control on proglacial groundwater levels and flow direction. The results of this chapter are summarised in a conceptual model of proglacial river-aquifer exchange (Figure 7.23).

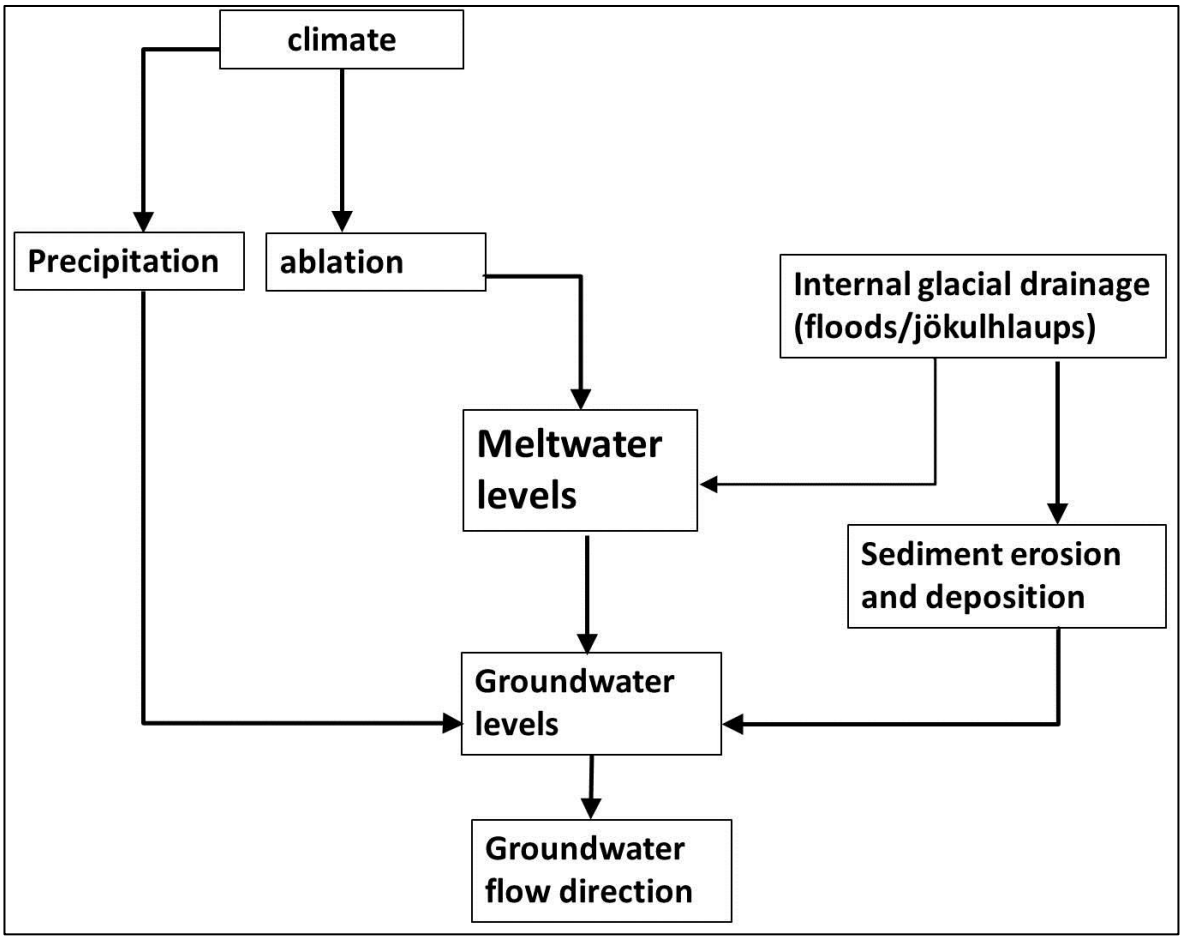

Figure 7.23. Conceptual model of the controls and impacts of proglacial river/aquifer exchange.

7.6. Conclusions

This chapter investigated groundwater flow direction and river-aquifer exchange at the Skaftafellsjökull foreland. The configuration of proglacial groundwater flow was inferred from the distribution in hydraulic heads. The regional groundwater flow system generally flows from North to South, away from the glacier margin. However, a local west-east groundwater flow system, which is superimposed on the regional groundwater flow system, has been identified at the transect. The general groundwater flow patterns are consistent with observations from other proglacial settings. Hydraulic heads at the Skaftafellsjökull foreland were responsive to rainfall events.

Time series of meltwater and groundwater levels, temperature, and EC were used to investigate the controls of high frequency, low magnitude (precipitation and ablation) and episodic events (jökulhlaups) on proglacial river-aquifer exchange. Hydraulic heads followed the fluctuations in meltwater levels, albeit with a lag of 6-10 hours. The lag generally increased with distance from the channel. A large flood event in August 2012 was the main hydrological event during the monitoring period, during which meltwater and groundwater levels rose by approximately 0.5 m. The meltwater flow regime was dominated by ablation, with meltwater levels rising (falling) with increasing (falling) air temperature. However, this relation was not straightforward, as some rises in meltwater levels, notably the flood in mid-August 2012, were not associated with a large rise in air temperature or large precipitation events. The close coupling between the fluctuations in meltwater and groundwater levels shows the impact of fluctuations in meltwater levels on groundwater levels and groundwater flow direction, suggesting high river-aquifer exchange. However, groundwater physicochemical parameters, solute concentrations, and isotopic composition contest this suggestion. It is hypothesised that the fluctuations in groundwater levels are caused by other processes, such as the propagation of a pressure

wave, rather than meltwater recharge of the aquifer. It is therefore suggested that meltwater-groundwater exchange at the transect is low. In contrast to the transect, solute concentrations and the isotopic composition of GW9 suggests proportions of meltwater in the groundwater. However, it is not clear whether this water originated from overbank flow. This chapter also highlighted the importance of precipitation to groundwater levels, particularly the impacts of spatial variability in hydrogeology on the response of groundwater levels to rainfall. The impacts of precipitation were observed at both short (daily-sub seasonal) and longer (inter-annual) time scales.

This chapter also investigated the impact of low frequency, high impact events (jökulhlaups) on river-aquifer exchange. The results have shown that groundwater levels ~200-250 m away from the channel quickly rose by approximately 0.20 m following small jökulhlaup events. However, the temperature and EC data do not suggest that these increases were caused by meltwater recharge. It is therefore suggested that the observed increase in groundwater levels has been caused by other mechanisms such as the propagation of a kinematic pressure wave or piston flow. Hence, the exchange between meltwater and groundwater at the river Súla field site is low. However, the impact of fluctuations in meltwater levels on groundwater levels was reported from both sites, showing the important control of fluctuations in meltwater on proglacial groundwater levels.

8. Thermal and hydrogeological tracing of aquifer-lake exchange

8.1. Introduction

Groundwater contributions to lakes substantially impact the hydrology, ecology, and biogeochemistry of lakes (e.g. Winter, 1999; Hieber *et al*., 2001; Hood *et al*., 2006; Roy and Hayashi, 2009; Ala-aho *et al*., 2013; Neumann *et al*., 2013). Therefore, understanding and quantifying the exchange between groundwater and lakes is necessary for understanding nutrient fluxes into lakes (e.g. Sebok *et al*., 2013; Shaw *et al*., 2013), the impact of anthropogenic activities on water quality (e.g. Schmidt *et al*., 2010; Smerdon *et al*., 2012; Muellegger *et al*., 2013), and to improve catchment and water resources management, particularly in light of projected changes in climate and land use (e.g. Meinikmann *et al*., 2013).

Proglacial aquifer-lake exchange is subjected to high spatial and temporal variability. The spatial variability in aquifer-lake exchange is strongly controlled by the heterogeneity in proglacial geomorphology and geology, which has been reported from an array of proglacial settings (e.g. Hannah and Gurnell, 2000; Smith *et al*., 2001), including the Skaftafellsjökull foreland (Chapter 5). In addition to geology and geomorphology, spatial variability in lake-aquifer exchange is also controlled by the degree of connectivity of the lake system to local and regional groundwater flow systems (Tóth, 1963; Winter 1999), topography, and position within the landscape (e.g. Campbell *et al*., 2004; Abnizova and Young, 2008; Ala-aho *et al*., 2013), lake stage (Smerdon *et al*., 2005), lakebed morphology and sedimentology (e.g. Rautio and Korkka-Niemi, 2011), the drainage area/lake area ratio (Schmidt *et al*., 2010), and climatic conditions (e.g. Roy and Hayashi, 2008). Temporal heterogeneities in groundwater-lake exchange are mainly controlled by meteorological variability and water levels (e.g. Kirillin *et al*., 2013; Rosenberry *et al*.,

2013). However, within proglacial settings, this variability is enhanced by the high diurnal, seasonal and annual variability of snowmelt, icemelt, and frozen ground (e.g. Hannah *et al*., 1999; 2000).

Although the importance of groundwater-lake exchange is well recognised (e.g. Winter, 2001; Krause *et al*., 2014), there have not been many studies which directly investigated groundwater-lake exchange in catchments which are dominated by snow and ice melt (Hood *et al*., 2006). Furthermore, there are controversies with regards to the magnitude of groundwater-lake exchange, with some studies suggesting aquifer-lake exchange to be negligible (Kattlemann and Elder, 1991; Michel *et al.*, 2002; Winter, 2003). Conversely, other studies suggested groundwater-lake exchange to be significant. For instance, it has been suggested that groundwater contributed between 30-74% of water inflow into Lake O'Hara in the Canadian Rockies (Hood *et al*., 2006). Another study from the same watershed suggested that groundwater contributed at least 35-39% of inflow into Lake Hungabee (Roy and Hayashi, 2008). Significant groundwater contributions were also reported from Williams Lake, Minnesota, where groundwater seepage was calculated to contribute approximately 74% of the annual water input to the lake (LaBaugh *et al*., 1997). Other studies have also suggested groundwater-lake exchange to be significant although groundwater-lake exchange was not directly quantified (Campbell *et al.,* 2004; Gurrieri and Furniss, 2004).

Aquifer-lake exchange has been traditionally investigated using methods based on hydrological observations, such as seepage meters (e.g. Lee, 1977; Kalbus *et al*., 2006). However, the variability in hydrogeological parameters and logistical difficulties found in proglacial settings can limit the applicability of such methods (e.g. Langston *et al*., 2013). In order to overcome some of the challenges associated with these methods, temperature (heat) tracing has been extensively used in order to investigate groundwater-surface water exchange in rivers (e.g. Schneider *et al*., 2011) and lakes (e.g. Sebok *et al*., 2013).

This usage has increased substantially following the falling costs and improvements in the robustness of reliable temperature sensors.

Heat transfer within sediment pore-water can take place by four methods: conduction, advection, convection, and radiation (e.g. Krause *et al.,* 2012). Heat conduction involves the transfer of thermal energy by diffusive molecular motion. Conversely, both heat advection and convection involve the movement of the water itself. Heat transfer by radiation occurs when solar heat energy is adsorbed by the water column which propagates into the sediment pore-water (Constantz*,* 2008). The tracing of groundwater-surface water exchange using heat is based on temperature anomalies at the river or lake bed, which may suggest areas of enhanced groundwater-surface water exchange. Hence, water temperature is an effective tracer for groundwater-surface water exchange in stream and lakebeds with substantial differences between groundwater and surface water temperatures. Such conditions are common in proglacial environments (e.g. Ward *et al*., 1999; Kristiansen *et al*., 2013), including the Skaftafellsjökull foreland, where groundwater and surface temperature are significantly different (2 tails t test, 5% Significant Level (S.L.); p=<0.001) [Table 7.1]. The merits of temperature tracing are its ubiquity, robust and relatively inexpensive measurements (e.g. Keery *et al.,* 2007), and the lack of possible contamination that is associated with chemical tracers (e.g. Constantz, 2008). Additionally, the thermal properties of sediment, which provide key inputs to the analytical solutions of heat transport equations, are much more narrowly constrained than the high variability that is associated with hydrogeological properties such as hydraulic conductivity (Lautz, 2010). Heat tracing can be used to investigate the direction (e.g. Anderson, 2005b; Anibas *et al.,* 2009) and magnitude of groundwater-surface water exchange (e.g. Westhoff *et al.,* 2007; Briggs *et al*., 2012; Kidmose *et al*., 2013).

Proglacial lake-aquifer exchange at the Skaftafellsjökull foreland was investigated at the Instrumented Lake [IL] (Figure 3.19). This lake was chosen due to the substantial differences in hydrogeological parameters between its eastern (fine-grained) and western

(coarse-grained) lakeshores (Figure 5.9), which will increase the understanding of the controls of hydrogeological heterogeneity on aquifer-lake exchange.

This study employed two techniques of temperature tracing: High spatial and temporal resolution mapping of lakebed temperatures at the IL was achieved using Fibre Optic-Distributed Temperature Sensing (FO-DTS). Temperature anomalies at the lakebed were then used to infer the spatial and temporal patterns of aquifer-lake exchange. In addition to the FO-DTS, groundwater seepage into the lake was calculated from hourly measurements of pore-water temperatures which were obtained from three Vertical Temperature Profiles (VTP) around the IL (Tristram *et al*, 2015). However, due to the high variability in groundwater-surface water exchange, previous studies have recommended to use more than one method (e.g. LaBaugh, 1997; Hunt *et al*., 1996; McCallum *et al*., 2014). Therefore, in addition to the VTP, groundwater seepage fluxes obtained from traditional hydrogeological measurements (Darcian fluxes) were also used to investigate proglacial aquifer-lake exchange at the Skaftafellsjökull foreland.

This chapter aims to investigate the spatial and temporal patterns of hydrological exchange between groundwater and the IL. The specific objectives for this chapter are:

1. To map lakebed temperatures and use temperature anomalies to investigate the spatial and temporal variability of aquifer-lake exchange at the IL.

2. To quantify groundwater discharge to the IL using temperature tracing methods and Darcian fluxes.

3. To compare between the temperature methods and hydrogeological methods of quantifying aquifer-lake exchange.

4. To delineate the spatial variability of aquifer-lake exchange at the IL.

8.2. Methods for investigating proglacial-aquifer lake exchange

8.2.1. Mapping of lakebed temperatures

Temperature tracing requires monitoring of pore-water temperatures at high temporal and spatial resolutions, which is able to reveal temperature anomalies at the stream/lake bed (e.g. Malcolm *et al.,* 2002). Such anomalies can then be used to infer the spatial and temporal dynamics of groundwater discharge into the lake/stream bed (e.g. Krause *et al*., 2012). Lakebed temperatures at the IL were mapped using FO-DTS. This method uses Raman-backscatter of 10 nanosecond FO-DTS pulses laser beams, which originate from the absorption and re-emission of light energy at different wavelengths. The beams are sent along a fibre-optic cable and then get reflected back towards the sensor, located at the beginning of the cable. Using the speed of light and the time taken for the laser to return, the distance from where the laser has been reflected can then be calculated. The majority of the reflected light remains at the same wavelength. However, some of the light is reflected back at shorter (Anti-Stokes) and longer (Stokes) wavelengths than that of the original. The Anti-Stokes backscatter is linearly affected by temperature whereas the Stokes backscatter is negligibly affected by temperature. Therefore, the Stokes/Anti-Stokes ratio can be used to measure temperature at any point along the cable. FO-DTS allows for both temporal and spatial temperature measurements to be recorded with resolutions of up to 0.01°C for every metre along the cable for up to 10,000 m (Selker *et al.,* 2006 a). This technique has been increasingly used in various hydrological settings (Selker *et al.,* 2006 a, b; Lowry *et al*, 2007; Tyler *et al.,* 2009; Westhoff *et al.,* 2011; Tristram *et al*., 2015).

The current study applied a Sensornet Halo FO-DTS which measures temperature at high precision (0.05 °C) at 30 second intervals and a sampling resolution of 2 m (Sensornet 2009). The survey deployed a 500 m long 2-channel fibre-optic cable (BruOutdoor, Brugg/CH). The FO-DTS setup used alternating single-ended measurements in clockwise

and anti-clockwise directions that were combined in a 2-way single ended averaging mode, as described by Krause and Blume (2013). The dynamic temperature calibration was performed using a calibration bath (water obtained from meltwater river), where temperatures were continuously monitored in the same time intervals as the FO-DTS measurements.

The fibre-optic cable in the current study was installed at two depths: The upper cable was laid directly on the lakebed, while the other cable was buried manually at approximately 0.10-0.15 m within the lakebed sediment. This design allowed a direct comparison between sediment temperatures within the lakebed (buried cable) and lakebed (upper cable) temperatures, which are potentially more influenced by surface water column temperatures. The fibre-optic cables were deployed around the circumference of the lake, at ~2 m distance from the lake shore (Figure 3.19). The buried cable was pushed into the sediment and spot checks indicated that the deployment depth remained constant during the course of the experiment. The FO-DTS monitoring of lakebed temperatures took place from 1200 hours on 24/06/2012 to 1300 hours on 25/06/2012.

8.2.2. Calculation of groundwater fluxes from pore-water temperatures

Groundwater fluxes into the IL were quantified using pore-water temperatures which were obtained from Vertical Temperature Profiles (VTP) (Figure 3.19). This technique has been previously used to investigate the interaction between streams (e.g. Hatch *et al*., 2006; Lautz, 2010; Briggs *et al*., 2012; 2013) and lakes (Kidmose *et al*., 2011; 2013). Pore-water temperatures at the lakebed were monitored between 1800 hours 20/06/2012 to 1400 hours 28/07/2012 using automatic HOBO thermistors, with an accuracy of ±0.025 °C (Krause *et al*., 2011b). The thermistors were emplaced within perforated metal tubes, which provided protection and allowed groundwater infiltration and direct contact with the temperature sensor at specified depths. Each VTP location included three thermistors,

which were emplaced at 10 cm, 25 cm and 40 cm below the lakebed, following similar configuration to Krause *et al*. (2011b). Substantial sediment heterogeneity was observed between the three VTP locations. The northern (VTP_1), eastern, and southern (VTP_3) lakeshores are underlain by fine sediment, while the western side (VTP_2) is underlain by coarse sands and gravels.

Groundwater fluxes were calculated from pore-water temperatures using a 1-D model of vertical seepage fluxes (Equation 8.1) which has been previously used to investigate groundwater interaction with streams (e.g. Hatch *et al*., 2006; Lautz, 2010; Briggs *et al*., 2012; 2013) and lakes (Kidmose *et al*., 2011; 2013; Tristram *et al*., 2015). The model is based on sinusoidal diurnal temperature oscillations within the sediment, where the dampening of the amplitude and phase shift with depth forms the basis for calculating the temperature variation as a function of time and depth (Stallman, 1965). These inputs can then be used to calculate groundwater seepage rates (Hatch *et al.,* 2006; Lautz, 2010; Tristram *et al*., 2015). A particular advantage of this method is the need for knowing solely the vertical distance between the temperature sensors, rather than their absolute depth. This advantage removes complications that occur from changes in bed conditions due to scouring and sedimentation. The model is based on the assumptions of purely vertical flow, sinusoidal temperature fluctuations, and no thermal gradient at the lakebed (Hatch *et al.,* 2006, Lautz, 2010). Intrinsically, these assumptions will be violated under non-ideal field conditions. However, this method was found robust to some of the violations of the assumptions particularly when groundwater flow is vertical (Lautz, 2010).

The One-dimensional heat transport model (Equation 8.1) for quantifying groundwater fluxes (e.g. Hatch *et al*. 2006) is based on conduction, advection and dispersion.

$$\frac{\partial T}{\partial t} = \kappa_e \frac{\partial^2 T}{\partial z^2} - \frac{q}{\gamma}\frac{\partial T}{\partial z}$$

Equation 8.1. The 1-D heat transport model

T is temperature (°C), which is a variant of time (t, in sec) and depth (z, in m), κ_e is effective thermal diffusivity (m^2/s), q is vertical seepage flux (m/s), and γ the ratio of heat capacity of the sediment matrix in the lakebed to the water heat capacity (Lautz 2010).

Groundwater fluxes (q) (m/s) (Lautz, 2010) were calculated using Equation 8.2.

$$q = \frac{\rho c}{\rho c_w}\sqrt{\alpha - 2\frac{\Delta\phi 4\pi\kappa_e^{\,2}}{P\Delta z}}$$

Equation 8.2. Quantification of groundwater fluxes

ρc and ρc_w denote heat capacity of sediment water matrix and water, respectively ($J/(m^3$ °C), Δz is the difference in depth between two thermistors at the lakebed (m), κ_e is the effective thermal diffusivity (m^2/s), P is the period of temperature signal (sec), and Δϕ is the lag time (hours) between the maximum correlation of temperature between the uppermost and lower temperature sensors. The lag time was calculated by using the Cross Correlation Function (CCF) between the different temperature sensors (Hannah *et al*. 2009, Krause *et al*. 2011a, b). The CCF was calculated using R version 3.0.1. The α perimeter was calculated using Equation 8.3.

$$\alpha = \sqrt{v^4 + \left(\frac{8\pi\kappa_e}{P}\right)^2}$$

Equation 8.3. The alpha perimeter for quantifying heat fluxes

V is the velocity of the thermal front (m/s), calculated using the 'speed = distance/time' equation, where distance is the depth to the logger sensor (m) and time is the lag time (hours) obtained by the CCF, following the analytical procedures of Tristram *et al*. (2015). The effective thermal diffusivity (κ_e) was calculated using Equation 8.4.

$$\kappa_e = \frac{\lambda_e}{\rho c}$$

Equation 8.4. Effective thermal diffusivity

Table 8.1. The parameters used in equations 1-4 (Hillel, 2004, Lautz, 2010) for the calculation of seepage fluxes. The table shows calculations using parameters for fine (a) and coarse (b) sediments.

Sediment property	Units	Value used in the equation
Effective thermal conductivity λ_e (Lautz, 2010)	(J/(s m °C))	$0.84^{(a)}$ $1.67^{(b)}$
Heat capacity of saturated sediment-fluid system (ρC) (Lapham, 1989)	(J/(m^3 °C))	$3.6\text{x}10^{6\,(a)}$ $3.1\text{x}10^{6\,(b)}$
Heat capacity of water (ρC_W) (Lautz, 2010)	(J/(m^3 °C))	$4.2\text{x}10^6$
Effective thermal diffusivity (κ_e) (Lapham, 1989, Lautz, 2010)	(m^2 /s)	$2\text{x}10^{-7\,(a)}$ $5\text{x}10^{-7\,(b)}$

λ_e is the effective thermal conductivity (J/(s m), and ρc is the heat capacity of the saturated sediment water matrix (J/(m^3 °C) (Hatch *et al*. 2006). λ_e was obtained from stream studies concerning finer and coarser sediment (Lautz 2010) and ρc was obtained from Lapham

(1989). The parameters which were used in the equations are found in Table 8.1. The different grain size for each VTP, which was used in Equation 8.4, are presented in Table 8.2.

Table 8.2. Grain size variability for the different VTP locations.

Sediment properties at the locations of the Vertical Temperature Profiles			
Grain size (μm)	**VTP 1**	**VTP 2**	**VTP 3**
d_{10}	4.93	15.37	5.12
d_{50}	21.91	175.70	22.43
d_{90}	54.58	1021.00	57.28

8.2.3. Calculation of groundwater fluxes from hydrogeological measurements

In addition to the temperature tracing, groundwater fluxes were also quantified using hydrogeological-based methods (Darcian fluxes). This method has been previously used to investigate groundwater-surface interaction in streams (e.g. Kennedy *et al*., 2010; Binley *et al*., 2013), wetlands (LaBaugh *et al*., 1997), and lakes (Blume *et al*., 2013). Darcian fluxes were calculated using hydraulic heads and hydraulic conductivity (Equation 8.5).

$$\boldsymbol{q = \left(\frac{\Delta h}{\Delta l}\right) \times K}$$

Equation 8.5. Calculation of Darcian fluxes

q is the Darcian flux of groundwater discharge (m/day), $\left(\frac{\Delta h}{\Delta l}\right)$ is the Vertical Hydraulic Gradient (VHG), and K is the saturated hydraulic conductivity (m/day). The hydraulic conductivity was determined by Particle Size Analysis of sediment samples using the Hazen method (section 5.4).

The Vertical Hydraulic Gradient (VHG) describes the ratio of the difference between the hydraulic head (mAD) in the piezometer and the lake stage (in mAD) [Δh] and the vertical distance between the lakebed and the midpoint of the screened section of the piezometer (m) [Δl]. The VHG shows the strength and direction of groundwater-surface water exchange. Positive VHG suggest that piezometric heads are higher than lake stage, implying groundwater discharge. Conversely, negative VHG suggests that the subsurface head is lower than the stage at the surface water, suggesting groundwater downwelling (e.g. Käser *et al*., 2009). VHG were previously used to investigate the interaction between groundwater and streams (e.g. Arntzen *et al*., 2006) and lakes (Rautio and Korkka-Niemi, 2011). VHG at this study were calculated using hydraulic head measurements from the piezometer nests, installed at 0.50, 1.00 and 1.50 m below the lakebed at the fine-grained (Clay Nest [C.N.] and coarse-grained (Sand Nest [S.N.] lakeshores. The Sand Nest is located approximately 20 m from VTP 2 and the Clay Nest was located approximately 40 m from VTP 1(Figure 3.19). The Darcian fluxes from the nests were then compared to the fluxes calculated from the VTP (objective 3). In order to provide a more comprehensive comparison between the methods, Darcian fluxes were also calculated from the piezometers located nearest [proxy locations] to VTP_1 (C.N., L6), VTP_2 (S.N.), and VTP_3 (L4, L5). The hydraulic conductivity for the proxy locations was calculated from the PSA of the respective VTP (Table 8.3).

Table 8.3. Hydraulic conductivity (m/day) for the VTP locations and proxies

VTP	**Piezometers used as proxy location for each VTP**	**Hydr. conductivity (m/day)**
VTP 1	Sand Nest150	$9.77x10^{1}$
	Clay Nest 50	$5.4x10^{-3}$
	Clay Nest 100	$3.5x10^{-3}$
	Clay Nest 150	$3.4x10^{-3}$
	L6	$8.5x10^{-3}$
VTP 2	Sand Nest 50	$1.23x10^{2}$
	Sand Nest 100	$5.64x10^{1}$
VTP 3	L4	$4.7x10^{-2}$
	L5	$4.7x10^{-2}$

8.3. FO-DTS monitoring of lakebed temperature

The FO-DTS mapping of lakebed temperatures at the lakebed (the upper cable) and at 0.10 m within the lakebed sediments (the buried cable) of the IL are presented in Figure 8.1 and 8.2. The maps are separated into six 4-hour averaged data groups, which show clear diurnal patterns of temperature oscillations at both the lakebed and at 0.10 m within the lakebed. Temperatures at 0.10 m below the lakebed were colder, particularly between 0400 and 0800 hours. The general dynamics of the mean temperature are similar, with a rise in mean temperature between 1200 and 2200 hours and a decline between 2200 and 0400 hours. Temperatures were fairly stable between 0400-0800 hours, which was followed by a rise in temperatures until the end of the measurements (Figure 8.1, 8.2). The range of averaged spatial temperatures at the lakebed (11.5-21°C, range of 9.5 °C) and at 0.10 m depth (~11-20 °C, range of 9 °C) were similar. However, the variability in temperatures at the lakebed was larger than at 0.10 m below the lakebed. This was especially pronounced during the temperature decline between 22:00 - 08:00 hours, when average temperatures at the lakebed varied by up to 2.5°C (Figure 8.1). Conversely, the temperature variability at 0.10 m depth within the lakebed was less than 1 °C (Figure 8.2). The higher variability in temperatures at the upper cable is illustrated by the difference between the 5^{th} and 95^{th} percentile for each cable and by the smaller oscillations in mean temperature at the buried cable, particularly during the fall in temperatures between 2200 and 0400 hours (Figure 8.3). These general similarities in the temperature dynamics between the two depths suggests some propagation of the surface water temperature signal into the sediment. However, the lower temperatures and variability at the buried cable suggest that the thermal patterns from the surface are dampened with depth.

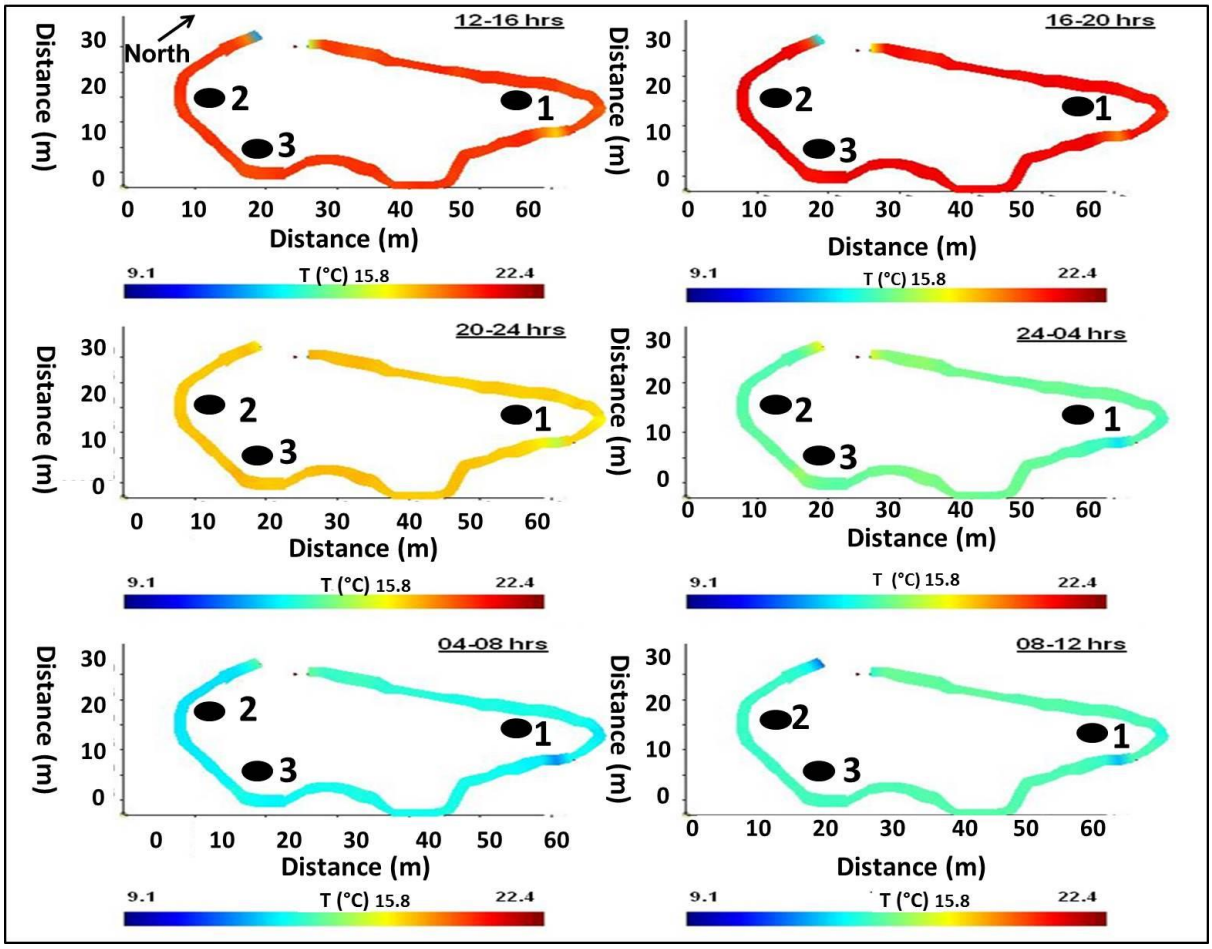

Figure 8.1 FO-DTS monitored temperatures measured on top of the lakebed sediments (upper cable).

The figure (from Tristram *et al*., 2015) shows 4 hour averages from 12:00 hours (24/06/2012) – 12:00 (25/06/2012). The 1, 2, 3 mark the respective locations of the Vertical Temperature Profiles (VTP).

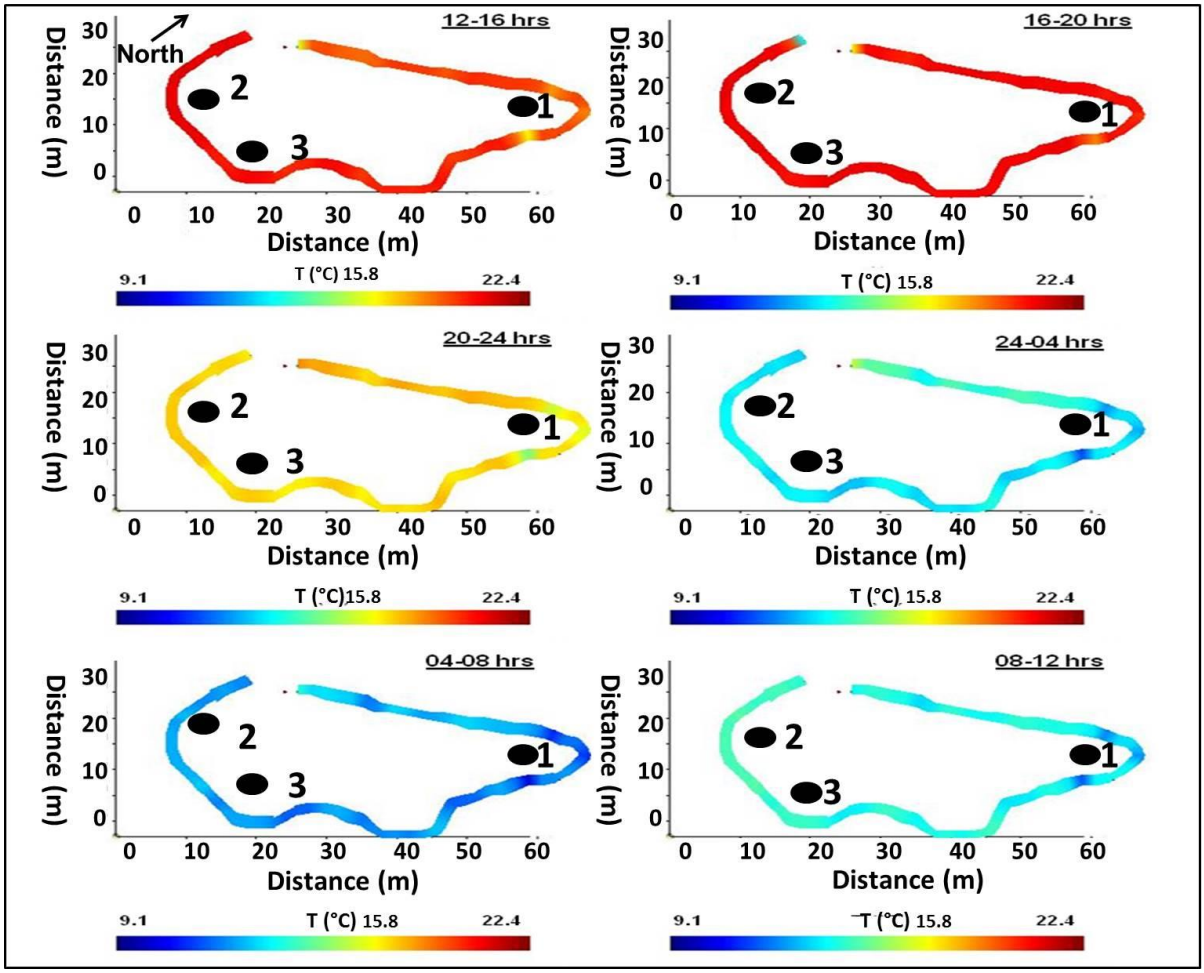

Figure 8.2. FO-DTS monitored temperatures measured at 0.10 m depth within the lakebed sediments (buried cable).

The figure (from Tristram *et al*., 2015) shows 4 hour averages from 12:00 hours (24/06/2012) – 12:00 (25/06/2012). The 1, 2, 3 mark the respective locations of the Vertical Temperature Profiles (VTP).

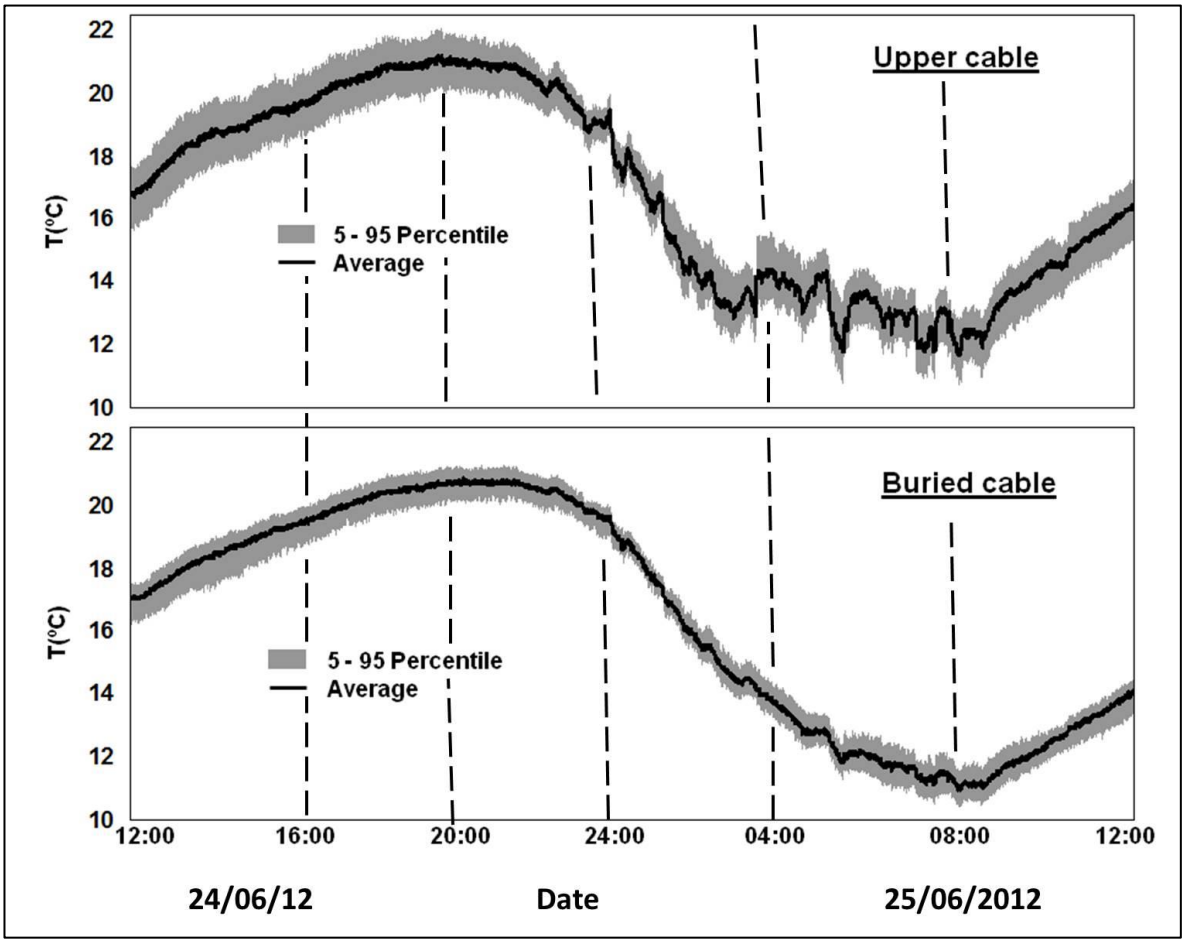

Figure 8.3. Mean, 5th and 95th Percentile of the FO-DTS surveys temperatures for lakebed sediments (upper cable) and 0.10 m depth within the lakebed sediments (buried cable).

The surveys were conducted between 24/06/2012 12:00 to 25/06/2012 12:00 hrs (from Tristram *et al*., 2015).

Figure 8.4 shows the spatial distribution of temperature deviation from the mean cable temperature at the upper and buried cables. These deviations are based on the mean temperature deviation of the full FO-DTS monitoring survey. This mapping shows substantial differences in the magnitude and spatial distribution of deviation from the mean temperature between the two depths (Figure 8.4). The range in the deviation of lakebed temperatures (the upper cable) from the spatial mean was approximately 0.3-0.6 °C. However, the survey showed a discrete location (cold spot) in the eastern side of the lake where temperatures were approximately 1.8°C cooler than the spatial mean (Figure

8.4). In contrast to the narrow range of deviations from the mean at the lakebed, the temperature deviations at the buried cable were larger. The deviation from the spatial mean at the fine-grained lakeshore were highly variable, and varied between -1.3 to +0.3 °C. Conversely, the deviations in the coarse-grained (western) lakeshore were more homogenous, and exceeded the mean temperature by approximately 0.4 °C. In addition to those broad patterns, Figure 8.4 also highlights two discrete cold spots at the buried cable, situated to the north and east of VTP_1, where temperatures were approximately 1.7 °C lower than the spatial mean (Figure 8.4).

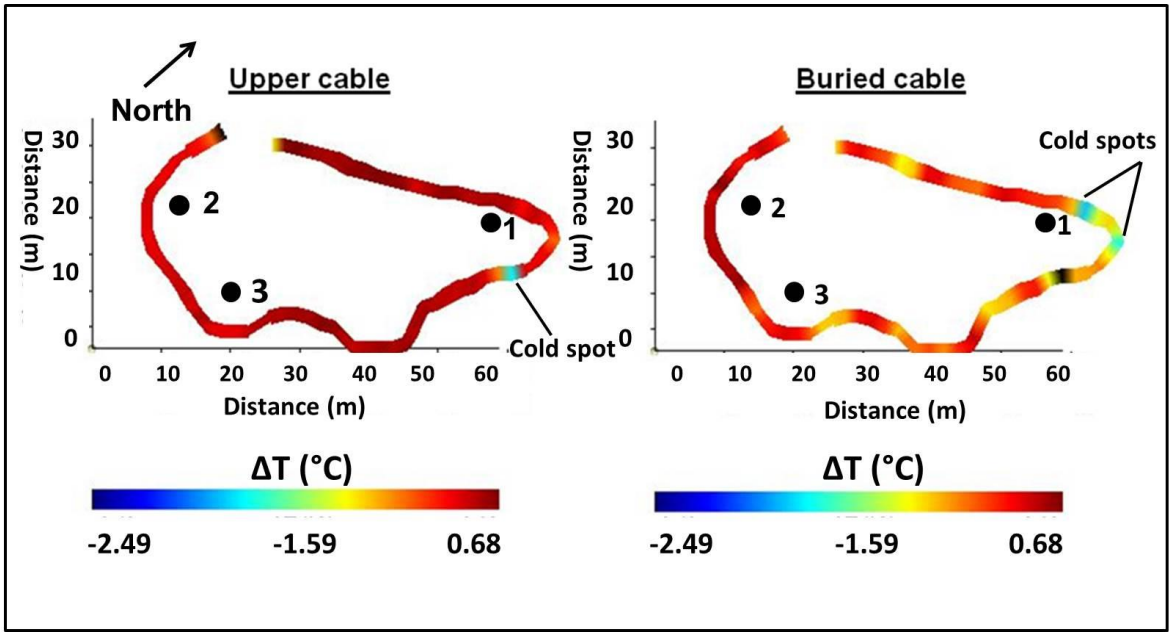

Figure 8.4. The averaged deviation from the mean temperature along the lakebed (upper cable) and at 0.10 m below the lakebed (buried cable).

The data is based on the FO-DTS monitoring between 24/06-25/06/2012.

8.4. Pore-water temperature dynamics at the IL

Pore-water temperatures were monitored using HOBO temperature loggers which were arranged in three Vertical Temperature Profiles (VTP) (Figure 3.19). Each VTP consisted of three temperature probes which were inserted at three depths (0.10 m, 0.25 m, and 0.40 m) below the lakebed. Strong diurnal oscillations in pore-water temperatures were observed in all three VTP locations. The largest temperature oscillations were observed at

0.10 m depth whilst oscillations at 0.40 m depth were negligible. This indicates that pore-water thermal stability increases with depth (e.g. Krause *et al.*, 2011b; Tristram *et al.*, 2015). The largest diurnal oscillations were observed at VTP_2. The smallest differences in mean pore-water temperature between 0.10 m and 0.25 m (0.25 °C) and 0.25 m to 0.40 m depth (1.12 °C) were also measured at VTP_2. The lowest diurnal oscillations were measured at VTP_3 where absolute temperatures were generally higher than at VTP_1 and VTP_2. The mean diurnal oscillation of pore-water temperatures at 0.10 m depth at VTP_1 was 1.06°C. It then attenuated with depth to ~ 0.49°C at 0.25 m depth and ~0.23°C at 0.40 m depth (Figure 8.5).

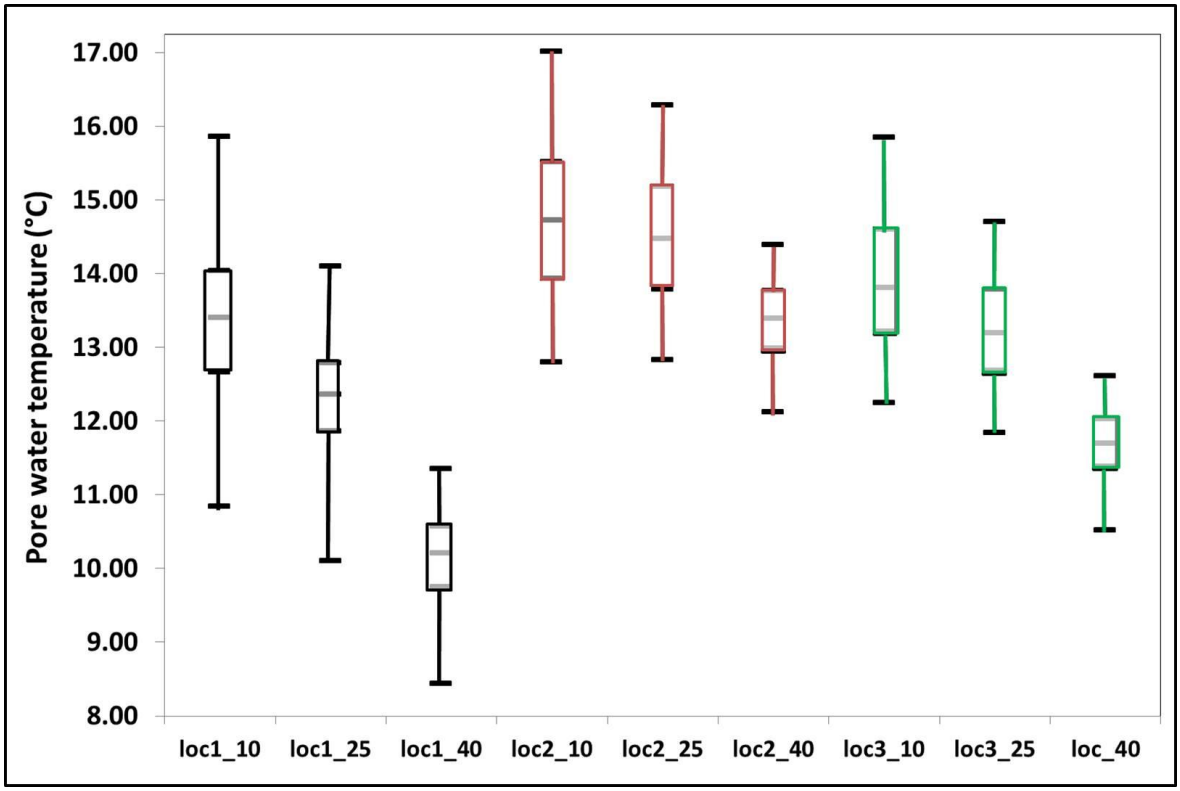

Figure 8.5. Box plots of temperature at the three VTP.

The horizontal lines denote the minimum, Q1, Q3, and the maximum. The thick grey line denotes the median. The figure shows the three depths (10, 25, 40 cm) in each VTP.

Pore-water temperatures have corresponded to changes in air temperature (Figure 8.6). The response of pore-water temperatures at 0.10 m was the closest, followed by 0.25 m and 0.40 m. However, the 0.40 m below the lakebed showed a very damped response to

changes in air temperature. The differences in pore-water temperatures between 0.10 m and 0.25 m were more pronounced when air temperature was high. This is illustrated by the differences between pore-water temperature at 0.10 m and 0.25 m on the 21/06/2012 (when air temperature rises) and the 30/06/2012, when air temperature falls (Figure 8.6).

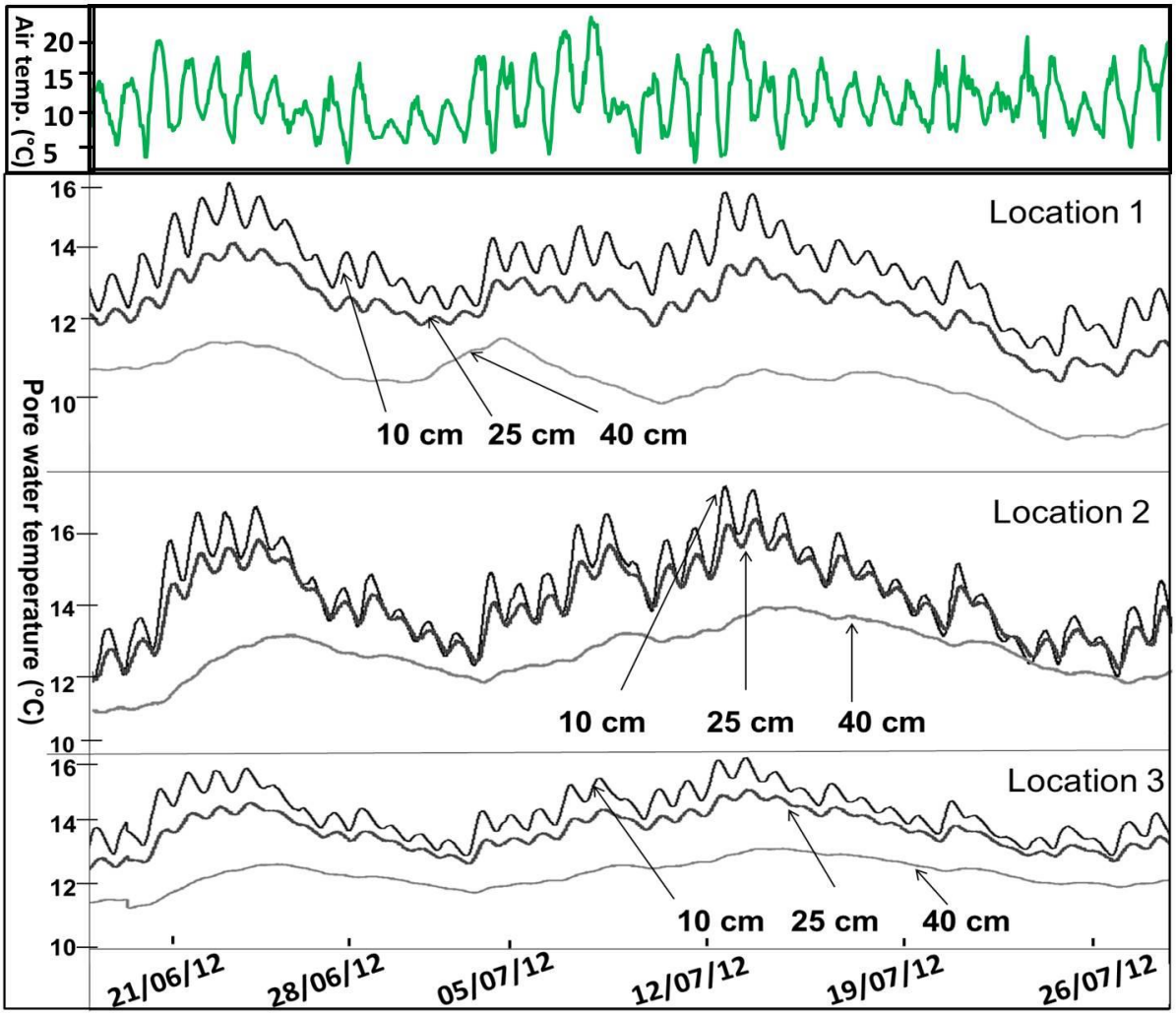

Figure 8.6. Mean hourly air temperature at the field site (green line) and pore-water temperatures at VTP 1-3.

Air temperature was measured at the Skaftafell IMO (2013) station (situated approximately 5 km from the fieldsite. The locations for each VTP are shown in Figure 3.15.

8.5. Quantification of groundwater fluxes

8.5.1. Groundwater fluxes (temperature-based) obtained from VTP

The daily groundwater fluxes (Figure 8.7) were calculated from each VTP using the methods of Tristram *et al*. (2015). Daily groundwater fluxes varied between 0.33 to 6.10 m/day. The highest mean groundwater fluxes were calculated at VTP_3 (). The mean fluxes at VTP_2 exceeded those at VTP_1 by 0.16 m/day. However, the standard deviation of groundwater fluxes at VTP_2 was approximately 0.55 m/day lower than VTP_1 and VTP_3. The inputs for sediment thermal properties which were used in Equation 8.2-8.4 were adjusted in order to address the substantial differences in sediment grain size at the three locations (Table 8.1). However, despite the significant difference in grain size between the VTP locations, the calculated VTP fluxes in all three VTP were generally within the same order of magnitude (1x 10^0 m/day). Furthermore, an ANOVA analysis (at 5% confidence level, *p=0.17*) has shown that the mean seepage fluxes between the three VTP were not significantly different from each other.

Table 8.4. Groundwater fluxes calculated from the VTP

Groundwater flux (m/day)	**VTP_1 (fine)**	**VTP_2 (coarse)**	**VTP_3 (fine)**
Mean	3.60±1.88	3.77±1.38	4.34±1.93
Max.	6.10	5.31	6.10
Min.	1.02	1.33	0.33

The results of the VTP from the IL are compared against reported rates of groundwater fluxes which were obtained from pore-water temperatures in lakes located within deglaciated areas in Denmark and Finland. The groundwater fluxes which were calculated from the VTP in the IL were within the same orders of magnitude as the mean groundwater discharge fluxes which were calculated from temperature profiles in Lake Væng in Denmark (1.4x10^{-1} to 1.21x10^0 m/day), which is connected to an unconfined,

medium-coarse sands and gravels aquifer (Sebok *et al*., 2013). The mean groundwater fluxes based on temperature profiles in another study from Lake Væng were also within the same order of magnitude ($1.5x10^{-1}$ m/day) (Kidmose *et al*., 2013). Groundwater discharge at this site has also showed clear seasonal variability, with winter fluxes (mean of $1.21x10^{0}$ m/day) exceeding summer fluxes ($1.6x10^{-1}$ m/day) by an order of magnitude (Sebok *et al*., 2013).

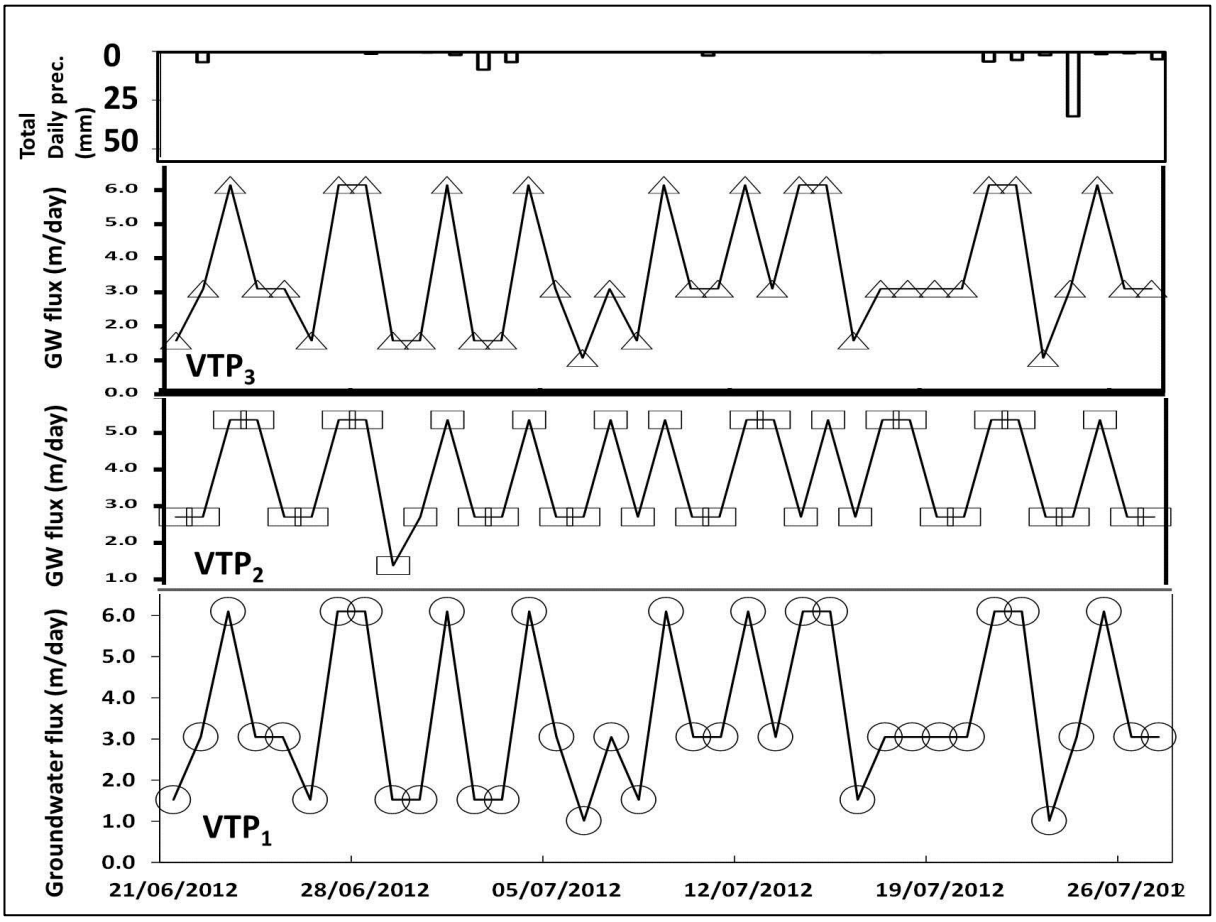

Figure 8.7. Groundwater fluxes (m/day) from VTP_1-VTP_3.

VTP_1 and VTP_3 are located in fine-grained sediment. Location VTP_2 is located in coarse-grained lakeshore.

8.5.2. Groundwater (Darcian) fluxes from hydrogeological measurements

The Vertical Hydraulic Gradient (VHG) at the IL varied between +0.011 to +0.632 (unitless). With the exception of L4 and L6 on the 31/08/2012, all the VHG during this study were positive. This implies continuous groundwater discharge into the lake (e.g. Rautio and Korkka-Niemi, 2011). The Darcian groundwater fluxes varied between $1.52x10^{-4}$ and $1.7x10^{1}$ m/day (Figure 8.8). In contrast to the relatively small variability (one order of magnitude) in the VTP fluxes (Figure 8.7), the Darcian fluxes showed substantial differences in groundwater discharge between the coarse (SN) and fine (CN, L4-6) grained lakeshores. Seepage fluxes at the coarse-grained lakeshore varied between $2.56x10^{0}$ and $7.08x10^{0}$ ±2.59 m/day. The fluxes from the fine-grained lake shore varied between $1.52x10^{-4}$ and $3.02x10^{-2}$ ±0.002 m/day. Groundwater fluxes from the coarse-grained lakeshore exceeded those from the fine-grained by approximately four to five orders of magnitude (Figure 8.8). The fluxes at the coarse-grained lakeshore were significantly higher (one tail t test, 2.5% significant level, p=<0.001) than those from the fine-grained lakeshore. In addition to these general patterns, the mean groundwater fluxes at the proxies for VTP_3 (L4 and L5) were significantly different (two tails t test, 2.5% S.L. p=<0.001) and higher by an order to two orders of magnitude than the fluxes obtained from the proxies for VTP_1 (Clay Nest and L6) (Table 8.5). Furthermore, groundwater fluxes at L4 and L5 were also more responsive to changes in lake levels showing a greater increase in flux with an increase in lake stage (Figure 8.8).

Table 8.5. Comparison between the Darcian and VTP groundwater fluxes

The table compares the mean fluxes calculated from the VTP (in brackets) with the Darcian fluxes of the proxy location for each VTP. Note that the data for the piezometer nests is the mean flux from the three different depths. All locations had 17 samples.

	VTP 1 (3.60x10^{0} ±1.88)	VTP 1 (3.60 x10^{0}±1.88)	VTP 2 (3.77x10^{0}±1.38)	VTP3 (4.34 x10^{0}±1.93)	VTP3 (4.34 x10^{0}±1.93)
Proxy location	Clay Nest	L6	Sand Nest	L4	L5
Mean Darcian Fluxes for the proxy (m/day)	6.71x10^{-4}± 3.87x10^{-4}	5.58x10^{-4}± 4.37x10^{-4}	7.08x10^{0}± 2.59x10^{0}	3.48.259x10^{-3}± 8.62x10^{-3}	3.24x10^{-3}± 4.70x10^{-3}

The temporal variability of the Darcian fluxes has shown that these fluxes generally followed the changes in lake levels, notably the increase in lake levels around the 24/07/2012, the increase in lake levels at the beginning of the second monitoring period (23/08/2012) and the decline in lake levels at the end of August (Figure 8.8). In summary, the seepage fluxes for the VTP were significantly higher than the Darcian fluxes calculated from the proxy locations for the VTP (Table 8.5). However, the variability in the Darcian fluxes was much higher than the VTP fluxes, with groundwater fluxes at the coarse-grained lakeshore substantially exceeding those from the fine-grained lakeshores (Figure 8.8).

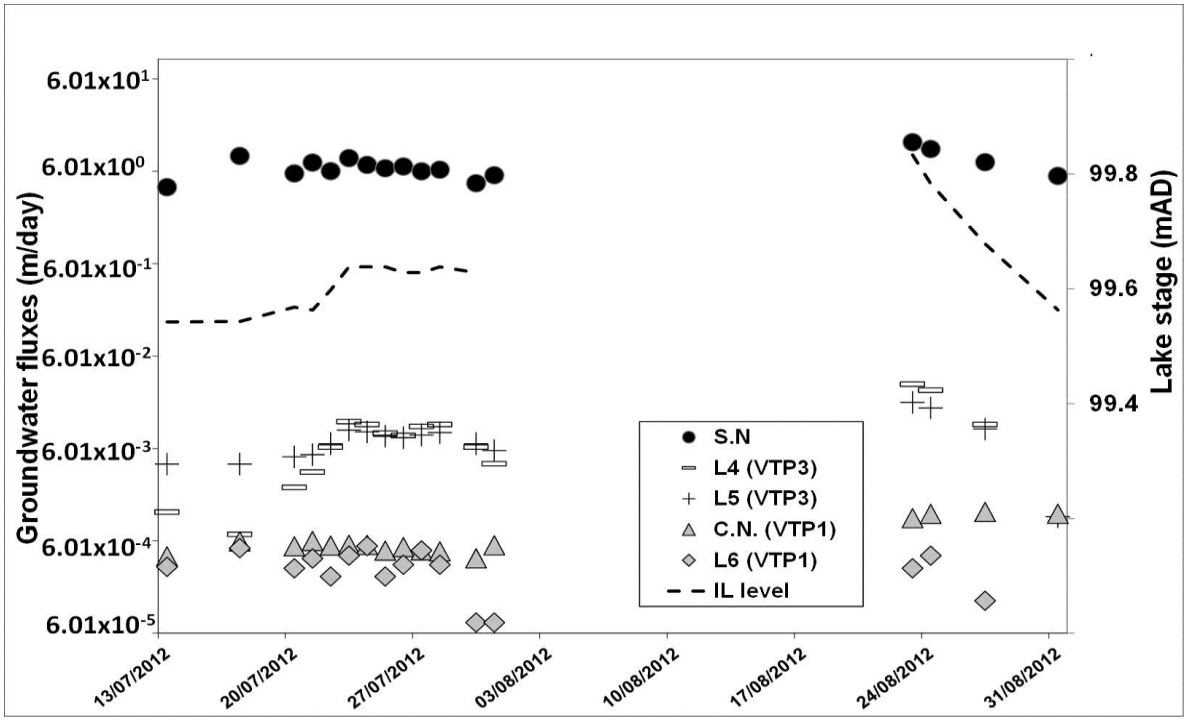

Figure 8.8. Comparison of Darcian groundwater fluxes from the coarse-grained (filled black shapes) and fine-grained (grey shapes) lakeshores. Note the logarithmic scale.

The different piezometers where the VHG were determined also served as proxy locations for fluxes obtained with VTP (see legend). The Figure also shows the temporal variability in groundwater fluxes, presented against the level of the IL. The gap between the 30/07/2012 and the 24/08/2012 is due to the lack of manual measurements of lake levels during the period in which the field site was not manned.

8.6. Discussion

8.6.1. Method comparison between VTP and Darcian fluxes

The current study combined temperature tracing of lakebed and lake pore-water temperatures with hydrogeological measurements for the investigation of the spatial and temporal dynamics of aquifer-lake exchange at the Instrumented Lake. Darcian fluxes, which are based on VHG, have been previously combined with seepage meters (e.g. Smerdon *et al*., 2005) and FO-DTS in order to investigate groundwater-lake exchange in rivers (Krause *et al*., 2012) and lakes (Blume *et al*., 2013). However, VHG in many of

these studies were only used as indicators for the direction of groundwater flow (e.g. Rautio and Korkka-Niemi, 2011; Kidmose *et al*., 2011). The only known study, to date, that has quantified groundwater fluxes using both VTP and Darcian fluxes obtained from VHG was done by Blume *et al*. (2013).

The seepage fluxes which were calculated from the VTP temperature data were not significantly different between the three locations. This lack of significant differences is despite of the different sedimentology in each location (Table 8.2). Conversely, the groundwater fluxes which were calculated from hydrogeological measurements (Darcian fluxes) for the coarse-grained lake shore exceeded the fluxes from the fine-grained lakeshore by four orders of magnitude and were significantly different (Figure 8.8). Similar patterns, in which groundwater fluxes obtained from hydrogeological measurements are generally lower and more variable than fluxes obtained from temperature profiling, were also reported in the literature. A study from Lake Væng, Denmark, has shown that seepage meters and temperature tracing have yielded similar mean and maximum summer fluxes (1.6-6.2x10^{-1} m/day). However, the minimum fluxes for the seepage meters were lower than fluxes calculated from the temperature profiles by two orders of magnitude (2.7x10^{-3} m/day) (Sebok *et al*., 2013). Relatively high spatial variability in groundwater fluxes which were obtained from seepage meters has also been reported from Lake Pyhäjärvi, located in an esker aquifer in SW Finland, where groundwater fluxes varied over three orders of magnitude (4.05 x10^{-2} to 4.15 x10^{0} m/day) (Rautio and Korkka-Niemi, 2011). A study of hydrological exchange between groundwater and wetlands in SW Wisconsin has also shown that groundwater fluxes calculated using Darcy's law were an order of magnitude lower (2.00x10^{-4} to 3.00x10^{-3} m/day) than fluxes estimated from temperature profiles and water balance modelling (1.00x10^{-3} to 1.10x10^{-2} m/day) (Hunt *et al*., 1996). Studies of river-aquifer exchange also reported substantial differences between fluxes obtained from hydrogeological methods and temperature tracing. For instance, investigations of river-aquifer exchange from the Munsan stream, Paju-si, South Korea,

where streambed hydraulic conductivity varied between four orders of magnitude ($1.82x10^{-3}$ to $4.20x10^{0}$ m/day), have shown that estimations based on Darcy's Law were approximately three orders of magnitude lower than those based on temperature profiles (Hyun *et al*., 2011). However, contrasting results to the discrepancy between Darcian and temperature-based fluxes have also been reported. For instance, a different study from Lake Væng in Denmark reported that groundwater fluxes obtained from temperature profiles were very close to those obtained from seepage meters ($3.00x10^{-3}$ to $7.45x10^{0}$ m/day) (Kidmose *et al*. 2013).

The significant differences between the Darcian and the VTP fluxes suggest that the VTP fluxes were less sensitive to the substantial differences in sediment properties between the three locations (Table 8.2). These observations support previous research which reported that the range of sediment thermal properties (Equation 8.2-8.4) is much narrower and more confined than the range of hydrogeological parameters (e.g. Stonestrom and Constantz, 2003; Lautz, 2010). It is therefore suggested that the substantial differences between the Darcian fluxes are attributed to the high spatial variability in hydraulic conductivity around the IL (Figure 5.9), which is common within proglacial environments (e.g. Robinson *et al*., 2008).

In addition to the results from the Skaftafellsjökull foreland, the impact of spatial variability in lakebed hydrogeology on aquifer-lake exchange has also been reported from Lake Opabin in the Canadian Rockies, where sections of the lake underlain by low permeability material were suggested as unlikely to contribute significant groundwater fluxes. Conversely, field evidence suggested that a large moraine served as the main source of groundwater to and from the lake (Roy and Hayashi, 2008). Studies from Lake Georgetown, a high elevation lake in Montana, reported substantial spatial variability in groundwater-lake exchange, which was attributed to the spatial differences in geology and sedimentology. Groundwater discharge into the lake took place in an area of fractured limestone. Conversely, no groundwater discharge was detected in areas underlain by

metasedimentary bedrock. These spatial differences in aquifer-lake exchange have also significantly impacted lake biogeochemistry and water quality (Shaw *et al*., 2013). The impact of spatial heterogeneity in hydrogeological parameters has also been reported from riverbeds. For instance, The spatial variability in Darcian fluxes from a streambed in Ontario which is underlain by sand and clay deposits, where hydraulic conductivity varied by four orders of magnitude, were up to five orders of magnitude (Conant, 2004). Therefore, the significant differences in groundwater fluxes at the IL (Figure 8.8) provide further evidence of the impact of high hydrogeological heterogeneity on the spatial variability in groundwater-surface water exchange. It is therefore suggested that the differences in the Darcian fluxes have been attributed to the differences in hydrogeological parameters around the IL (Figure 5.9). Furthermore, the small differences between the temperature-based fluxes suggest that, despite the adjustment of the perimeters in Equation 8.2 (Table 8.1), this method is not sensitive for the variability in lakebed sedimentology which occurs at the IL. This suggestion is also supported by numerical modelling of the impact of sediment heterogeneity on groundwater fluxes obtained from temperature data, which suggested that simple methods that analytically solve the heat flow equation fail to provide reliable exchange fluxes in areas of high sediment heterogeneity and significant contrasts in hydraulic conductivity (Schornberg *et al*., 2010).

The discrepancy between the calculated fluxes from the VTP and the Darcian fluxes has significant implications on the interpretation of the dynamics of groundwater exchange with the IL. The fluxes obtained using VTP suggest that groundwater discharge around the lake is fairly homogenous (Figure 8.7), regardless of lakebed sediment characteristics (Table 8.2). Conversely, the Darcian fluxes suggest that groundwater discharge at the coarse-grained lakeshore is significantly higher than the fine-grained lakeshore (Figure 8.8). Due to the control of hydraulic conductivity on aquifer-lake exchange (e.g. Roy and Hayashi) and in light of the high heterogeneity in hydrogeological parameters around the IL (Figure 5.9), it is suggested that the Darcian fluxes give a more accurate representation

of groundwater-lake exchange at the IL than the temperature-based fluxes, which do not reflect the variability in lakebed sedimentology. The heterogeneity in groundwater discharge is also supported by the FO-DTS survey, which suggests that enhanced groundwater discharge at the fine-grained lakeshore takes place through discrete zones, which were identified by the cold spots (Figure 8.4). The results obtained by the Darcian fluxes were therefore used for describing the spatial patterns of lake-aquifer exchange at the IL.

8.6.2. Spatial patterns of proglacial aquifer-lake exchange

The high resolution mapping of lakebed temperatures using FO-DTS and the quantification of groundwater seepage fluxes were used to delineate proglacial aquifer-lake exchange at the IL. The FO-DTS mapping of lakebed and sediment temperatures highlighted distinct cold spots, which were located in the northern and eastern lakeshores (Figure 8.4). Groundwater temperatures at the site were significantly lower than lake temperatures (Table 6.3, 6.4). Hence, it is suggested that these cold-spots can be attributed to enhanced groundwater upwelling (Rautio and Korkka-Niemi, 2011; Sebok *et al*., 2013). As this area of the lake is underlain by approximately 0.50 m of fine-grained sediment with low hydraulic conductivity (Chapter 5), this detected upwelling possibly takes place through preferential flow paths within the confining clay layer (e.g. Conant, 2004) or due to cracks in the fine-grained layer which were caused during the installation of the FO-DTS cable (e.g. Rosenberry *et al*., 2010; Blume *et al*., 2013). In addition to the cold spots below the lakebed in the eastern lakeshore, a cold spot which was also identified on the lakebed (the upper FO-DTS cable) has also been detected (Figure 8.4). However, this cold spot did not propagate underneath the lakebed, suggesting the lack of groundwater upwelling at this location. It is suggested that the colder temperature at this spot is possibly due to vegetation cover and a deeper lakebed (Tristram *et al*., 2015).

Groundwater and surface water geochemistry and stable isotope composition suggest that precipitation, rather than meltwater, is the dominant source of groundwater at the site (Chapter 6). Despite the small proportion of groundwater recharge from meltwater, the configuration of hydraulic heads in the transect has shown that groundwater flows towards the IL (Figure 7.8). This area has been identified as a local groundwater system, which is imposed on the regional groundwater flow system (Figure 7.7). The significantly-higher groundwater fluxes at the western (coarse-grained) lakeshore and the west-east flow direction of the local groundwater flow system suggest that this system feeds most of the groundwater discharge into the lake (Figure 8.9). The low seepage fluxes at the fine-grained lakeshore (VTP_1 and VTP_3) suggest that the confining layer on that side impedes groundwater discharge into the lake in this area. The small fluxes at the fine-grained (eastern) lakeshore suggest that the small moraines that surround the IL from the North, East, and West do not contribute significant groundwater fluxes to the IL. This hypothesis is supported by observations of the complex internal hydrology of moraines (e.g. Langston *et al*., 2013; Bajc *et al*., 2014). However, further investigation is needed in order to determine the contribution of the moraines to lake hydrology. A conceptual model of the controls and impacts of proglacial aquifer/lake exchange is presented in Figure 8.10.

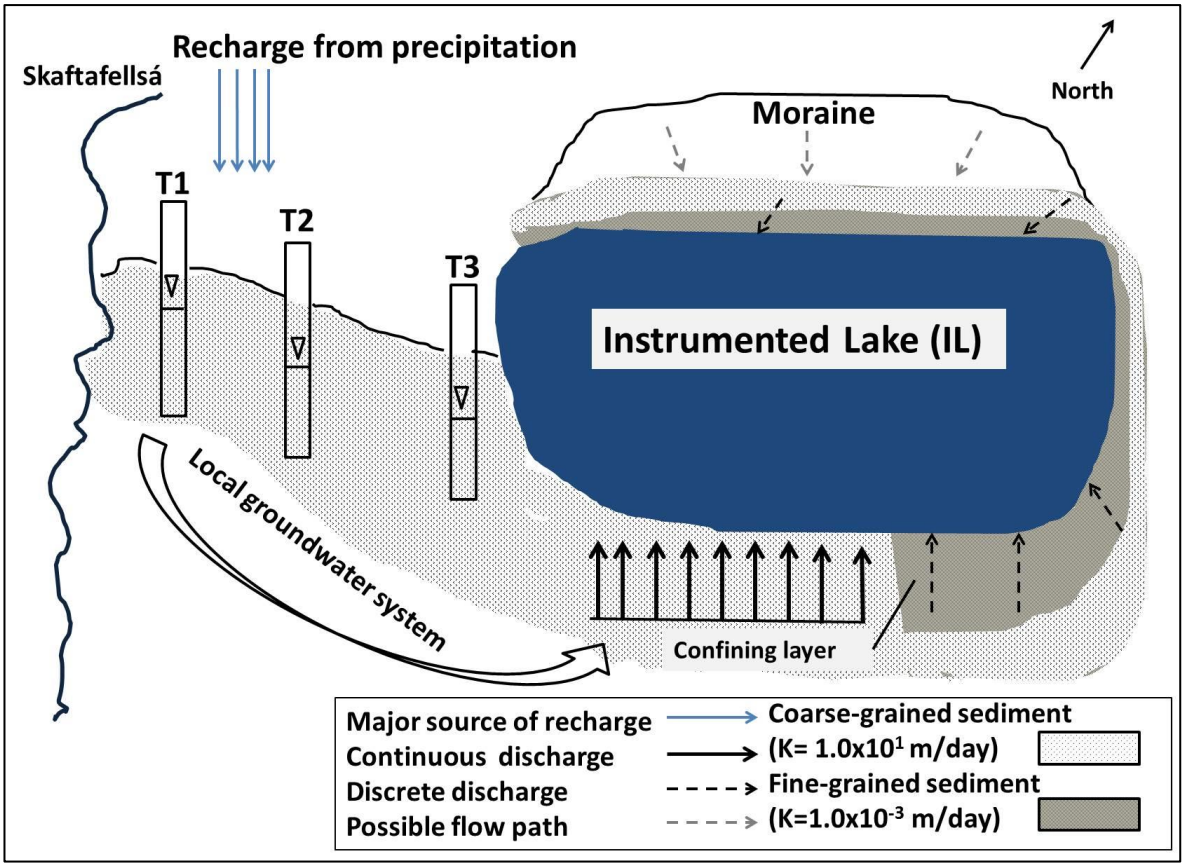

Figure 8.9. Schematic representation of recharge and aquifer-lake exchange at the IL. The model is not drawn to scale.

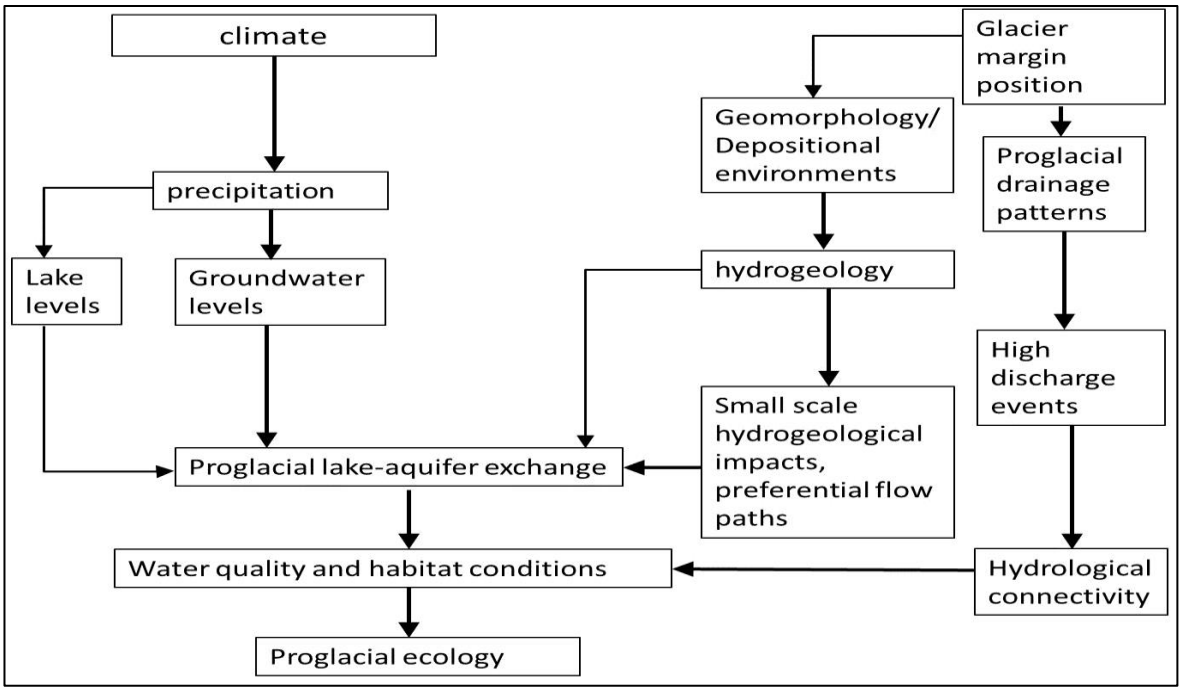

Figure 8.10. A conceptual model of the controls and impacts of proglacial aquifer/lake exchange

8.7. Conclusions

This study combined hydrogeological measurements (Darcian fluxes) with environmental temperature tracing techniques (FO-DTS and VTP) in order to delineate the spatial and temporal variability of aquifer-lake exchange and to quantify this exchange. Despite significant differences in hydraulic conductivity between the VTP locations, their mean groundwater fluxes were all within one order of magnitude, and not significantly different. Conversely, the Darcian fluxes from the coarse-grained lakeshore exceeded those from the fine-grained lakeshore by four orders of magnitude. These results support previous studies that reported similar discrepancies between groundwater fluxes obtained from temperature and hydrogeological measurements. The Darcian fluxes were therefore used to construct a conceptual model of river-aquifer-lake exchange at the Skaftafellsjökull margin.

Groundwater discharge from the local groundwater flow system which flows from west to east (Chapter 7) appears to be the main source of groundwater for the IL. Aquifer-lake exchange at this lakeshore is relatively high. Conversely, the exchange at the fine-grained lakeshore is lower by several orders of magnitude. The temperature mapping of the lakebed suggests that groundwater-lake exchange at that lakeshore occurs in discrete locations, possibly through preferential flow paths.

9. Conclusions

9.1. Summary of main findings

This study investigated groundwater-surface water exchange in the proglacial zone of two retreating glaciers in SE Iceland. The findings of this study are important in light of the observed impact of groundwater-surface water exchange on proglacial hydrology, geomorphology and water quality. Furthermore, this study has also shown the importance of precipitation and glacier margin fluctuations, which are projected to alter due to climate change and glacier retreat.

The first part of this study investigated the impact of fluctuations in glacier margin position on proglacial groundwater levels and the spatial extent of groundwater seeps (objective i). The western Skeiðarárjökull margin has retreated approximately 1 km between during the study period (1986-2012). Changes in the extent of groundwater seeps were mapped from aerial photographs, which showed a 97% decline in seep extent. The extent of seeps was also impacted by the November 1996 jökulhlaup, whose deposits buried 18% of the area of groundwater seeps at the site. Proglacial groundwater levels also substantially declined between 2000 and 2012, with observed declines exceeding 1.5 m in many locations, with groundwater levels in most piezometers falling below the intake. However, the decline in groundwater levels has shown considerable spatial variability.

The regional groundwater flow at the Skaftafellsjökull margin is from north to south, away from the glacier margin. However, deviations from this pattern have also been identified. The main local groundwater system flows from west to east toward the Instrumented Lake (IL), perpendicular to the river Skaftafellsá. The PSA and slug tests results showed high variability in hydrogeological characteristics, caused by the different geomorphic processes which are active at this environment. The hydraulic conductivity (K) at the Skaftafellsjökull foreland varied over seven orders of magnitude. This high variability in

hydraulic conductivity has led to substantial heterogeneity in proglacial groundwater-surface water exchange.

Substantial differences in hydrogeology and water quality were observed between the Northern and Southern Oasis. The hydraulic conductivity at the Southern Oasis exceeded that of the Northern Oasis by five orders of magnitude. The solute concentrations at the Northern Oasis are significantly lower than that of the Southern Oasis. It is therefore hypothesised that the Northern Oasis is perched and mainly precipitation-fed. Hence, aquifer-lake exchange at the Northern Oasis is low.

Conversely, the Southern Oasis is generally underlain by glaciofluvial sediments, with mean hydraulic conductivity of ~$2.51x10^{1}$ m/day. It is suggested that the higher hydraulic conductivity led to substantial groundwater-lake exchange at the Southern Oasis lakes. However, high variability in hydrogeological parameters was also observed at the Southern Oasis, with some areas of the IL underlain by fine-grained deposits.

The third part of this study investigated the sources of groundwater recharge (objective iii) and the temporal and spatial dynamics of hydrological exchange between meltwater, groundwater, and lakes (objectives iv and v). Groundwater levels at the transect, have shown high response to fluctuations in meltwater levels, with the response generally dampened with increasing distance from the river. These dynamics suggest high levels of exchange between the meltwater river and the aquifer.

However, this hypothesis is contested by the substantial differences in water quality and stable isotope composition between transect groundwater and meltwater. Groundwater solute concentrations and isotopic composition at the transect were significantly higher and heavier, respectively. These significant suggest relatively low rates of aquifer-meltwater exchange. It is therefore hypothesised that the coupling between the response in hydraulic heads and meltwater levels is due to other factors, such as the propagation of pressure waves, rather than actual entrance of water into the aquifer.

Similar dynamics of high response between hydraulic heads and fluctuations in meltwater levels alongside significantly different water quality were also observed at the river Súla in western Skeiðarársandur during small jökulhlaups. This suggests that, despite the different geomorphology of the two proglacial zones, fluctuations in meltwater levels are an important control on hydraulic heads during high discharge events. These processes have been observed at the Skaftafellsjökull foreland during both ablation-controlled meltwater flow regime and episodic floods. Conversely, the fluctuations in hydraulic heads at the river Súla were only observed during the small jökulhlaups. However, the lack of fluctuation in hydraulic heads between during ablation-controlled flow regime can possibly attributed to the distance of GW4 from the Súla channel (~ 250 m), which is larger than the distance at the Skaftafellsjökull foreland (69 m away for the furthest piezometer).

Groundwater recharge sources were investigated using water stable isotopes (objective iii). Groundwater isotopic composition was generally heavier than that of meltwater, and located close to the composition of the LMWL. This suggests that precipitation is the main source for groundwater recharge at the Skaftafellsjökull foreland. The importance of precipitation in groundwater and surface water recharge has also been supported by the substantial differences in lake levels between the different precipitation levels in 2012 (dry) and 2013 (very wet).

The spatial variability in proglacial aquifer-lake exchange was investigated at the IL using temperature tracing and hydrogeological methods (objective v). The FO-DTS mapping revealed discrete points of colder-than-average temperatures. Due to the significant differences between groundwater and surface water temperatures, these spots were inferred as discrete locations of cold groundwater upwelling into the IL. The FO-DTS has also highlighted the differences between the eastern (fine-grained) and western (coarse-grained) lakeshores. The temperatures at the coarse-grained lakeshores were relatively homogenous, suggesting a relatively uniform groundwater discharge. Conversely, the FO-DTS detected two locations of which were approximately 1.8 °C cooler than the mean

temperature. It is suggested that these cold spots are discrete locations of enhanced groundwater upwelling, in contrast to the low upwelling in the rest of the fine-grained (eastern) lakeshore.

Groundwater seepage into the IL was quantified using a temperature-based method (VTP) and hydrogeological measurements. Despite substantial differences in lakebed sedimentology between the three VTP locations, groundwater fluxes from all three VTP were within the same order of magnitude. Conversely, the Darcian fluxes from the coarse-grained location exceeded those from the fine-grained locations by three orders of magnitude. These differences were attributed to the substantial heterogeneity in hydrogeological parameters around the IL. It is hypothesised that most groundwater in the lake originate from a local groundwater flow system. These observations highlight the relatively high exchange between the aquifer and the IL.

9.2. Wider implications

9.2.1. Spatial heterogeneity in proglacial hydrogeology

This study highlighted the high spatial variability in proglacial hydrogeology. The variability in proglacial hydrogeology at the Skaftafellsjökull margin has been attributed to the range of glacial, glaciofluvial, and lacustrine processes operating (e.g. Marren 2002a, b; Marren and Toomath, 2013). In addition to the aforementioned processes, the hydrogeology and geomorphology of western Skeiðarársandur are also impacted by glacial surges, jökulhlaups and aeolian processes (e.g. Russell *et al*., 2006). This observed variability leads to high heterogeneity in proglacial groundwater-surface water exchange.

The widely observed heterogeneity in hydrogeological parameters also imposes significant challenges for the numerical modelling of proglacial groundwater flow systems. Many groundwater flow models treat proglacial groundwater systems as homogenous

(e.g. Boulton and Dobbie 1993). However, the complexities and heterogeneities which have been reported from various proglacial settings, including the current study, suggest that these assumptions are usually violated. Furthermore, due to this heterogeneity, obtaining accurate data on groundwater flow rates and the hydraulic properties of proglacial deposits is a substantial challenge (Tague and Grant, 2009; Person *et al*., 2012; Langston *et al*., 2013). The hydrogeological parameters which were obtained at this study (Chapter 5), can therefore be used as boundary conditions and input parameters for numerical models of proglacial groundwater flow and groundwater-surface water exchange.

9.2.2. Implications of climate change and glacier retreat on proglacial groundwater-surface water exchange

Climate change models project a general increase in air temperatures and glacier retreat in regions dominated by snow and icemelt. These changes are projected to substantially impact the hydrology of such catchments (e.g. Barnett *et al*., 2005). Glacier retreat is projected to alter the composition of proglacial discharge, with increasing contributions from snowmelt, rainfall, and groundwater at the expense of icemelt (e.g. Blaen *et al*., 2013; 2014). These changes are projected to have significant impacts on proglacial hydrology, biogeochemistry, physicochemical parameters and ecology (e.g. Cauvy-Fraunié *et al*., 2013). Most climate models for Iceland also project an increase in precipitation and temperatures over the 21st century, with the highest increases during winter (e.g. Nawri and Björnsson, 2010). These changes are also projected to increase glacier retreat (e.g. Jóhannesson *et al*., 2006). In addition to its impact on the extent of the Icelandic icecaps, glacier retreat is also projected to alter proglacial hydrology (Flowers *et al*., 2003; 2005), hydrogeology (e.g. Robinson *et al*., 2008), and geomorphology (Marren and Toomath, 2013). Despite an initial increase, the falls in glacier volume and ice slope,

caused by glacier retreat, are expected to reduce meltwater generation (e.g. Flowers *et al*., 2005) and groundwater flow, caused by the shallower hydraulic gradient (e.g. Haldorsen and Heim, 1999; Haldorsen *et al*., 2010; 2012). A reduction in groundwater flow following glacial retreat has been hypothesised to be a major cause for the substantial decrease in the extent of groundwater seeps and groundwater levels in western Skeiðarársandur (Levy *et al*., 2015).

In addition to glacier retreat, climate change projections also suggest an alteration in precipitation patterns and timing. These projections include an increase in the rain/snow ratio, which will increase winter runoff and reduce snow storage, and cause earlier snowmelt, which will lead to an earlier peak in runoff (e.g. Adam *et al*., 2009; Stewart *et al*., 2009). These impacts are projected to substantially alter surface water quality and the timing, magnitude and quality of groundwater recharge (e.g. Okkonen and Kløve, 2009; 2010; 2012; Fortner *et al*., 2011).

Precipitation has been identified as the main source of groundwater recharge at the Skaftafellsjökull foreland (section 6.5.1). In addition to the impacts on lake water balance, fluctuating lake levels, which are caused by fluctuations in precipitation, can also lead to small scale changes in lake hydrogeology. For instance, the dry conditions in 2012 led to a fall in lake levels, which exposed significant sections of the lakeshores. These exposures can lead to the desiccation of confining clay layers, with the newly forming cracks possibly forming preferential flow paths for groundwater upwelling (such as the cold spots at the IL [Figure 8.4]). The discharge of cold, nutrient-rich groundwater into the lake via such flow paths can impact lake physicochemical parameters and ecology (e.g. Roy *et al*., 2011).

9.2.3. Methodological implications

Groundwater and surface water temperatures, geochemistry and stable isotopes provided effective, relatively low cost techniques to investigate various hydrological topics in an array of settings (e.g. Robinson *et al*, 2009a, b). This study has combined these methods with traditional hydrogeological methods and novel temperature tracing techniques in order to investigate the temporal and spatial dynamics of proglacial river-aquifer and lake-aquifer exchange. These methods also showed spatial and temporal heterogeneities in the exchange between groundwater, rivers, and lakes and highlighted small scale variability such as preferential flow paths. However, this study has also highlighted the importance of using multiple methods when investigating groundwater-surface water exchange (Hunt *et al*., 1996; Blume *et al*., 2013). This was illustrated by the contrasting observations between the hydraulic heads (Chapter 7) and the geochemistry and isotopic data (Chapter 6) with regards to the level of aquifer-meltwater exchange. The importance of combining several methods has also been highlighted when investigating groundwater discharge around the IL, where temperature tracing and the hydrogeological methods provided contrasting results. In summary, the methods used in this study helped to unmask processes and increase the understanding of the complex temporal and spatial heterogeneity of proglacial groundwater-surface water exchange. However, hydrogeological methods should be corroborated by other methods, such as geochemical or temperature tracing.

9.3. Further research

This research has highlighted the controls and the high spatial and temporal heterogeneity of proglacial groundwater-surface water exchange. Additionally, it has also highlighted the importance of groundwater discharge to surface water bodies and the relatively transient

nature of proglacial groundwater-fed bodies. This study can be advanced further by pursuing further research:

- The installation of deeper piezometers, especially closer to the glacier margin at Skaftafellsjökull, in order to improve the understanding with regards to the impact of glacier margin position on proglacial groundwater flow. Monitoring over longer time periods, particularly winter and spring, will also help to investigate groundwater dynamics during baseflow conditions and the impact of snowmelt on proglacial groundwater-surface water exchange.
- Improved understanding of the hydrogeology of the site, particularly delineating the internal structures of proglacial landforms, such as moraines, and their impact on proglacial groundwater flow. This can be done using various geophysical techniques (e.g. Muir *et al*., 2011).
- Further investigation of river-aquifer exchange. This can be done using tracers such as radon, in order to calculate groundwater residence times (e.g. Magnusson *et al*., 2014) and to improve the understanding with regards to the contribution of meltwater to groundwater and the lakes at the Skaftafellsjökull foreland.
- Ecological survey of flora and fauna of the Skaftafellsjökull foreland. Due to the differences in aquifer-lake exchange between the Northern (inferred low aquifer-lake exchange) and Southern Oasis lakes (inferred relatively high aquifer-lake exchange), an ecological survey will help to assess the impacts of the difference in groundwater contributions to the ecology of each site.
- Numerical modelling of the impact of climate change and glacier retreat on proglacial groundwater-surface water exchange.

References

Abnizova A, Young KL, Lafreniere, MJ. 2014. Pond hydrology and dissolved carbon dynamics at Polar Bear Pass wetland, Bathurst Island, Nunavut, Canada. *Ecohydrology* **7**: 73-90 DOI: 10.1002/eco.1323 .

Abnizova A, Young KL. 2008. Hillslope hydrological linkages: importance to ponds within a polar desert High Arctic wetland. HYDROLOGY RESEARCH Volume: 39 Pages: 309-321 DOI: 10.2166/nh.2008.007.

Acuña V, Tockner K. 2009. Surface–subsurface water exchange rates along alluvial river reaches control the thermal patterns in an Alpine river network. *Freshwater Biology* **54**: 306–320. DOI: 10.1111/j.1365-2427.2008.02109.x

Aðalgeirsdóttir G. Jóhannesson T, Björnsson H, Pálsson F, Sigurðsson O. 2006. Response of Hofsjökull and southern Vatnajökull, Iceland, to climate change. Journal of Geophysical Research **111**: F03001. DOI:10.1029/2005JF000388

Adam JC, Hamlet AF, Lettenmaier DP. 2009. Implications of global climate change for snowmelt hydrology in the twenty-first century. *Hydrological processes* **23:** 962-972. DOI: 10.1002/hyp.7201

Ala-aho P, Rossi PM, Kløve B. 2013. Interaction of esker groundwater with headwater lakes and streams. *Journal of Hydrology* **500**: 144-156. DOI: 10.1016/j.jhydrol.2013.07.014.

Alley RB, Blankenship DD, Bentley CR, Rooney ST. 1986. Deformation of till beneath ice stream B, West Antarctica. *Nature* **322**: 57-59.

Alley RB, Blankenship DD, Bentley CR, Rooney ST. 1987. Till beneath Ice Stream B, 3. Till deformation: evidence and implications. *Journal of Geophysical Research Solid Earth and Planets* **92**: 8921-8928.

Alley WM. 2001. Ground water and climate. *Ground Water* **39**: 161 DOI: 10.1111/j.1745-6584.2001.tb02295.x

Alley WM. 2007. Flow and storage in groundwater systems. *Science* **296**: 1985–1990.

Alyamani MS, Sen Z. 1993. Determination of hydraulic conductivity from complete grain-size distribution curves. *Ground Water* **31**: 551-555.

Andermann C, Longuevergne L, Bonnet S, Crave A, Davy P, Gloaguen R. 2012. Impact of transient groundwater storage on the discharge of Himalayan rivers. *Nature Geoscience* **5**: 127–132. DOI:10.1038/ngeo1356

Anderson MP. 1989. Hydrogeological facies models to delineate large-scale spatial trends in glacial and glaciofluvial sediments. *Geological Society of America Bulletin* **101**: 501-511.

Anderson MP. 2005a. Heat as a ground water tracer. *Ground Water* **43**: 951-968.

Anderson SP. 2005b. Glaciers show direct linkage between erosion rate and chemical weathering rate. *Geomorphology* **67**: 147-157. DOI: 10.1016/j.geomorph.2004.07.010

References

Anderson SP, Drever JI, Frost CD, Holden P. 2000. Chemical weathering in the foreland of a retreating glacier. *Geochemica et Cosmochimica Acta* **64**: 1173-1189.

Anderson SP, Longacre SA., Kraal ER. 2003. Patterns of water chemistry and discharge in the glacier-fed Kennicott River, Alaska: evidence for subglacial water storage cycles. *Chemical Geology* **202**: 297-312. DOI: 10.1016/j.chemgeo.2003.01.001

Anibas C, Fleckenstein JH, Volze N, Buis K, Verhoeven R, Meire P, Batelaan O. 2009. Transient or steady-state? Using vertical temperature profiles to quantify groundwater–surface water exchange. Hydrological Processes **23**:2165–2177. DOI: 10.1002/hyp.7289

Aragón R, Jobbágy EG, Viglizzo EF. 2011. Surface and groundwater dynamics in the sedimentary plains of the Western Pampas (Argentina). *Ecohydrology* **4**: 433–447. doi: 10.1002/eco.149

Arnell NW *et al.* in *Climate Change 2001: Impacts, Adaptation and Vulnerability* (eds McCarthy, J. J. *et al.*) Ch. 4 (Cambridge Univ. Press, 2003).

Arntzen EV, Geist DR, Dresel PE. 2006. Effects of fluctuating river flow on groundwater/surface water mixing in the hyporheic zone of a regulated, large cobble bed river. *River Research and Applications*, 22: 937–946. DOI: 10.1002/rra.947

Atkinson N, Andriashek LD, Slattery SR. 2013. Morphological analysis and evolution of buried tunnel valleys in northeast Alberta, Canada. *Quaternary Science Reviews* **65**: 53-72 DOI: 10.1016/j.quascirev.2012.11.031

Bahr, T., 1997. *Hydrogeologische Untersuchungen im Skeiðarársandur (Südisland)*. Müncher Geologische Hefte Reihe B, 3, xiv.

Bajc AF, Russell HAJ, Sharpe DR. 2014. A three-dimensional hydrostratigraphic model of the Waterloo Moraine area, southern Ontario, Canada. *Canadian Water Resources Journal* **39**: 95-119. DOI: 10.1080/07011784.2014.914794

Baraer M, McKenzie JM, Mark BG, Bury J, Knox S. 2009. Characterizing contributions of glacier melt and groundwater during the dry season in a poorly gauged catchment of the Cordillera Blanca (Peru). Advances in Geosciences **22**:41-49. DOI:10.5194/adgeo-22-41-

Barnett TP, Adam JC, Lettenmaier DP. 2005. Potential impacts of a warming climate on water availability in snow-dominated regions. Nature **438**: 303–309. DOI:10.1038/nature04141.

Bartsch S, Frei S, Ruidisch M, Shope CL, Peiffer S, Kim B, Fleckenstein JH. 2014. River-aquifer exchange fluxes under monsoonal climate conditions. *Journal of Hydrology* **509**: 601-614. DOI: 10.1016/j.jhydrol.2013.12.005

Bayer P, Huggenberger P, Renard P, Comunian. 2011. Three-dimensional high resolution fluvio-glacial aquifer analogue: part 1: field study. *Journal of Hydrology* **405**: 1-9. DOI: 10.1016/j.jhydrol.2011.03.038

Becker MW, Georgian T, Ambrose H, Siniscalchi J, Fredrick K. 2004. Estimating flow and flux of ground water discharge using water temperature and velocity. *Journal of Hydrology* **296**: 221-233. DOI: 10.1016/j.jhydrol.2004.03.025

Bell RE. 2008. The role of subglacial water in ice-sheet mass balance. *Nature Geoscience* **1**: 297-304. doi:10.1038/ngeo186

References

Bennett GL, Evans DJA, Carbonneau P, Twigg DR. 2010. Evolution of a debris-charged glacier landsystem, Kvíárjökull, Iceland. *Journal of maps*: 40-67. DOI: 10.4113/jom.2010.1114

Bense VF, Ferguson G, Kooi H. 2009. Evolution of shallow groundwater flow systems in areas of degrading permafrost. *Geophysical Research Letters* **36**: L22401 DOI:10.1029/2009GL039225.

Bense VF, Person MA. 2008. Transient hydrodynamics within intercratonic sedimentary basins during glacial cycles*, Journal of Geophysical Research* **113***: F04005 doi:*10.1029/2007JF000969

Berner EK, Berner RA. 1996. *Global Environment: Air, Water and Geochemical Cycles*. New Jersey.

Bingham RG, Nienow PW, Sharp MJ, Copland L. 2006. Hydrology and dynamics of a polythermal (mostly cold) High Arctic Glacier. *Earth Surface Processes and Landforms* **31**: 1463-1479.

Binley A, Ullah S, Heathwaite AL, Heppell C, Byrne P, Lansdown K, Trimmer M, Zhang H. 2013. Revealing the spatial variability of water fluxes at the groundwater-surface water interface. *Water Resources Research* **49**: 3978–3992 doi:10.1002/wrcr.20214.

Björnsson H, Einarsson, P. 1990. Volcanoes beneath Vatnajökull, Iceland: evidence from radio echo-sounding, earthquakes and jökulhlaups. *Jökull* **40**: 147-167.

Björnsson H, Pálsson F, Magnusson E. 1999. Skeiðarárjökull: Lansdlag og rennslisleðir vants undir spirði. *Raunvisindastofnun Haskolans*: 10-20.

Björnsson H, Pálsson F. 2008. Icelandic Glaciers. *Jökull* **58:** 365-386.

Björnsson H. 1998. Hydrological characteristics of the drainage system beneath a surging glacier. *Nature* **395:** 771–774 DOI: 10.1038/27384

Blackport RJ, Meyer PA, Martin PJ. 2014. Towards an understanding of the Waterloo Moraine hydrogeology. *Canadian Water Resources Journal* **39**: 120-135. DOI: 10.1080/07011784.2014.914795

Blaen PJ, Hannah DM, Brown LE, Milner AM. 2013. Water temperature dynamics in High Arctic river basins. *Hydrological Processes* **27**: 2958-2972. DOI: 10.1002/hyp.9431

Blaen PJ, Brown LE, Hannah DM, Milner AM. 2014. Environmental drivers of macroinvertebrate communities in high Arctic rivers (Svalbard). *Freshwater Biology* **59**: 378-391. DOI: 10.1111/fwb.12271

Bliss A, Hock R, Radić V. 2014. Global response of glacier runoff to twenty-first century climate change. *Journal of Geophysical Research Earth Surface* **119**: 717–730. DOI:10.1002/2013JF002931.

Blume T, Krause S, Meinikmann K, Lewandowski J. 2013. Upscaling lacustrine groundwater discharge rates by fiber-optic distributed temperature sensing. *Water Resources Research* **49**: 7929–7944 doi:10.1002/2012WR013215.

Bolch T, Kulkarni A, Kääb A, Huggel C, Paul F, Cogley JG, Frey H, Kargel JS, Fujita K, Scheel M, Bajracharya S, Stoffel M. 2012. The State and Fate of Himalayan Glaciers. *Science **336***: 310-314*.* DOI:10.1126/science.1215828

Bonan G. 2008. *Ecological Climatology*, Cambridge Univ. Press, Cambridge, U. K.

References

Boucher JL, Carey SK. 2010. Exploring runoff processes using chemical, isotopic and hydrometric data in a discontinuous permafrost catchment. *Hydrology Research* **41**:508–519. doi:10.2166/nh.2010.146

Boulton GS .1986. Geophysics- a paradigm shift in glaciology. *Nature* **322**: 18.

Boulton GS, Hindmarsh RCA. 1987. Sediment deformation beneath glaciers: rheology and geological consequences. *Journal of Geophysical Research* **92**: 9059-9082.

Boulton GS, Dobbie KE. 1993. Consolidation of sediments by glaciers: relations between sediment geotechnics, soft-bed glacier dynamics and subglacial ground-water flow. *Journal of Glaciology,* vol. 39, p. 26-44.

Boulton GS, Zatsepin S. 2006. Hydraulic impacts of glacier advance over a sediment bed. *Journal of Glaciology* **52:** 497-527. DOI: 10.3189/172756506781828403

Boulton GS, Slot T, Blessing K, Glasbergen P, Leijnse T, van Gijssel, K. 1993. Deep circulation of groundwater in overpressured subglacial aquifers and its geological consequences. *Quaternary Science Reviews*. **12**: 739-745.

Boulton GS, Caban PE, van Gijssel, K. 1995. Groundwater flow beneath ice sheets: part I large scale patterns. *Quaternary Science Reviews* **14**: 545-562.

Boulton AJ, Findlay S, Marmonier P, Stanley EH, Valett HM. 1998. The Functional Significance of the Hyporheic Zone in Streams and Rivers. *Annual Review of Ecology and Systematics* **29**: 59-81. DOI: 10.1146/annurev.ecolsys.29.1.59.

Boulton GS, Dobbie KE, Zatsepin, S. 2001a. Sediment deformation beneath glaciers and its coupling to the subglacial hydraulic system. *Quaternary International* **86:** 3–28. DOI: 10.1016/S1040-6182(01)00048-9

Boulton GS, Zatsepin S, Maillot B. 2001b. Analysis of groundwater flow beneath ice sheets. SKA Technical Report TR-01-06, 53 pp.

Boulton GS, Lunn R, Vidstrand P, Zatsepin S. 2007a. Subglacial drainage by groundwater-channel coupling, and the origin of esker systems: Part I- glaciological observations. *Quaternary Science Reviews* **26**: 1067-1090.

Boulton GS, Lunn R, Vidstrand P, Zatsepin S. 2007b. Subglacial drainage by groundwater-channel coupling, and the origin of esker systems: Part II- theory and simulation of a modern system. *Quaternary Science Reviews* **26**: 1091-1105.

Boulton GS, Hagdorn M, Maillot PB, Zatsepin S. 2009. Drainage beneath ice sheets: groundwater-channel coupling, and the origin of esker systems from former ice sheets. *Quaternary Science Reviews* **28**: 621-638.

Bradbury KR, Muldoon MA. 1990. Hydraulic conductivity determinations in unlithified glacial and fluvial materials. *In:* Nielsen, D.M. and Johnson, A.I. (Eds.) *Ground Water and Vadose Zone monitoring*, ASTM STP 1053, American Society for Testing Materials, Philadelphia.

Bradwell T*,* Sigurðsson O*,* Everest J. 2013. Recent, very rapid retreat of a temperate glacier in SE Iceland*. Boreas* **42**: 959-973. DOI: 10.1111/bor.12014

Brardinoni F Hassan MA. 2006. Glacial erosion, evolution of river long profiles, and the organization of process domains in mountain drainage basins of coastal British Columbia*, Journal of Geophysical Research* **111** *F01013, DOI:*10.1029/2005JF000358*.*

References

Brassington, R. (2007). *Field Hydrogeology*. 3rd edition. Wiley, Chichester.

Braun LN, Weber M, Schulz M. 2000. Consequences of climate change for runoff from Alpine regions. *Annals of Glaciology* **31**: 19-25.

Breemer CW, Clark PU, and Haggerty R. 2002. Modelling the subglacial hydrology of the late Pleistocene Lake Michigan Lobe, Laurentide Ice Sheet. *Geological Society of America Bulletin* **114**: 665-674.

Briggs MA, Lautz LK, McKenzie JM, Gordon RP, Hare DK. 2012. Using high-resolution distributed temperature sensing to quantify spatial and temporal variability in vertical hyporheic flux. *Water Resources Research* **48**: W02527. DOI:10.1029/2011WR011227.

Briggs MA, Lautz LK, Hare DK, González-Pinzón R. 2013. Relating hyporheic fluxes, residence times, and redox-sensitive biogeochemical processes upstream of beaver dams. *Freshwater science* **32**: 622-641. DOI: http://dx.doi.org/10.1899/12-110.1

British Standard (BS) 1377. 1990. Methods of test for soils for civil engineering purposes. Part 5. Comressibility, permeability, and durability tests. Pages 10-14.

Brown GH. 2002. Glacier meltwater hydrochemistry. *Applied Geochemistry* **17**: 855-883.

Brown NE, Hallet B, Booth DB. 1987. Rapid soft bed sliding of the Puget Glacial Lobe. *Journal of Geophysical Research* **92**: 8985-8997.

Brown LE, Hannah DM, Milner AM. 2003. Alpine stream habitat classification: An alternative approach incorporating the role of dynamic water source contributions. *Arctic, Antarctic, and Alpine Research* **35:** 313-322. DOI: 10.1657/1523-0430(2003)035[0313:ASHCAA]2.0.CO;2

Brown LE., Hannah DM, Milner AM. 2005. Spatial and temporal water column and streambed temperature dynamics within an alpine catchment: implications for benthic communities. *Hydrological Processes* **19**: 1585-1610.

Brown LE, Milner AM, Hannah DM, Soulsby C, Hodson A, Brewer MJ. 2006a. Water source dynamics in an alpine glacierized river basin (Taillon-Gabiétous, French Pyrénées). *Water Resources Research* **42**: W08404. DOI: 10.1029/2005WR004268

Brown LE, Hannah DM, Milner AM. 2006b. Hydroclimatological influences on water column and streambed temperature dynamics in an alpine river system. *Journal of Hydrology* **325**: 1–20.

Brown LE, Milner AM, Hannah DM. 2007a. Groundwater influence on alpine stream ecosystems. *Freshwater Biology* **52**: 878-890. DOI: 10.1111/j.1365-2427.2007.01739.x

Brown LE, Hannah DM, Milner AM. 2007b. Vulnerability of Alpine stream biodiversity to shrinking glaciers and snowpacks. Global Change Biology **13**: 958-966. DOI: 10.1111/j.1365-2486.2007.01341.x

Brown LE, Hannah DM. 2008. Spatial heterogeneity of water temperature across an alpine river basin. *Hydrological Processes* **22**: 954–967. DOI: 10.1002/hyp.6982.

Brunke M, Gonser T. 1997. The ecological significance of exchange processes between rivers and groundwater. *Freshwater Biology* **37**: 1–33.

Brunke M, Hoehn E, Gonser T. 2003. Patchiness of river–groundwater interactions within two floodplain landscapes and diversity of aquatic invertebrate communities. *Ecosystems* **6**: 707–722.

References

Burgman JO, Calles B, Westman F. 1987. Conclusions from a ten year study of Oxygen-18 in precipitation and runoff in Sweden. In: Proceedings of an International symposium on the use of isotope techniques in Water Resources Development. Vienna, International Atomic Energy Agency, pp. 579–590.

Burns ER, Bentley LR, Hayashi M, Grasby SE, Hamblin AP, Smith DG, Wozniak PRJ. 2010. Hydrogeological implications of paleo-fluvial architecture for the Paskapoo Formation, SW Alberta, Canada: a stochastic analysis. *Hydrogeology Journal* **18**: 1375-1390. 10.1007/s10040-010-0608-y

Byrne P, Binley A, Heathwaite AL, Ullah S, Heppell CM, Lansdown K, Zhang H, Trimmer M, Keenan P. 2014. Control of river stage on the reactive chemistry of the hyporheic zone. *Hydrological Processes* **28**: 4766-4779 DOI: 10.1002/hyp.9981

Caballero Y, Jomelli V, Chevallier P, Ribstein P. 2002. Hydrological characteristics of slope depostis in high tropical mountains (Cordillera Real, Bolivia). *Catena* **47**: 101-116.

Campbell DH, Muths E, Turk JT, Corn PS. 2004. Sensitivity to acidification of subalpine ponds and lakes in north-western Colorado. Hydrological Processes **18**: 2817– 2834. DOI: 10.1002/hyp.1496.

Carey SK, Boucher JL, Duarte CM. 2013.Inferring groundwater contributions and pathways to streamflow during snowmelt over multiple years in a discontinuous permafrost subarctic environment (Yukon, Canada). *Hydrogeology Journal* **21**: 67-77. DOI 10.1007/s10040-012-0920-9

Carrier WD. 2003. Goodbye, Hazen; hello, Kozeny-Carman. *Journal of Geotechnical and Geoenvironmental Engineering* **129**: 1054-1056. **DOI:** 10.1061/~ASCE!1090-0241~2003!129:11~1054!

Cartwright K, Harris HJH. 1981. Hydrogeology of the Dry Valley Region, Antarctica. In: McGinnis L (ed) Dry Valley Drilling project. Antarctic Research Series, AGU, Washington, DC, pp 193–214

Casassa G, López P, Pouyaud B, Escobar F. 2009. Detection of changes in glacial run-off in alpine basins: examples from North America, the Alps, central Asia and the Andes. Hydrological processes **23**: 31–41. DOI: 10.1002/hyp.7194.

Cauvy-Fraunié S, Condom T, Rabatel A, Villacis M, Jacobsen D, Dangles O. 2013. Technical Note: Glacial influence in tropical mountain hydrosystems evidenced by the diurnal cycle in water levels. *Hydrology and Earth System Sciences* **17**: 4803-4816. doi:10.5194/hess-17-4803-2013.

Cauvy-Fraunié S., Andino P., Espinosa R., Calvez R., Anthelme F., Jacobsen D, Dangles O. 2014. Glacial flood pulse effects on benthic fauna in equatorial high-Andean streams. Hydrological Processes **28**: 3008–3017.DOI: 10.1002/hyp.9866

Chandler DM, Wadham JL, Lis GP, Cowton T, Sole A, Bartholomew I, Telling J, Nienow P, Bagshaw EB, Mair D, Vinen S, Hubbard A. 2013. Evolution of the subglacial drainage system beneath the Greenland Ice Sheet revealed by tracers. *Nature Geoscience* **6**: 195–198, 2013. DOI:10.1038/ngeo1737.

Chang C-M, Yeh H-D. 2014. Uncertainty estimation in one dimensional heat trasnsport model for heterogeneous porous medium. *Groundwater* **52**: 326-331. doi: 10.1111/gwat.12088.

References

Chiogna G, Santoni E, Camin F, Tonon A, Majone B, Trenti A, Bellin A. 2014. Stable isotope characterization of the Vermigliana catchment, *Journal of Hydrology* **509**: 295-305. DOI: 10.1016/j.jhydrol.2013.11.052

Chu VW. 2014. Greenland ice sheet hydrology: a review. *Progress in Physical Geography* **38**: 19-54. DOI: 10.1177/0309133313507075

Churski Z. 1973. Hydrographic features of the proglacial area of Skeiðarárjökull. *Geographica Polonica*, 26, 209-254.

Cirpka OA,, Fienen MN, Hofer M, Hoehn E, Tessarini A, Kipfer R, Kitanidis PK. 2007. Analyzing bank filtration by deconvoluting time series of electric conductivity. *Ground Water* **45**: 318–328, DOI:10.1111/j.1745-6584.2006.00293.x

Clark ID, Fritz P. 1997. Environmental Isotopes in Hydrogeology. Lewis, Boca Raton, FL. pp. 328.

Clow DW, Schrott L, Webb R, Campbell DH, Torizzo A, Dornblaser M. 2003. Ground Water Occurrence and Contributions to Streamflow in an Alpine Catchment, Colorado Front Range. Ground Water **41**: 937-950. DOI: 10.1111/j.1745-6584.2003.tb02436.x.

Collins DN. 1978. Hydrology of an alpine glacier as indicated by the chemical composition of meltwater. *Zeitschrift f˙ur Gletscherkunde und Glazialgeologie* **13**: 219–238.

Collins DN. 2006. Climatic variation and runoff in mountain basins with differing proportions of glacier cover. *Nordic Hydrology* **37**: 315-326.

Conant BJ. 2004. Delineating and quantifying ground water discharge zones using streambed temperature. *Ground Water* **42**: 243–257.

Condom T, Escobar M, Purkey D, Pouget JC, Suarez W, Ramos C, Apaestegui J, Tacsi A, Gomez J. 2012. Simulating the implications of glaciers' retreat for water management: a case study in the Rio Santa basin, Peru. *Water International* **37**: 442-459. **DOI:** 10.1080/02508060.2012.706773

Connon RF, Quinton WL, Craig JR, Hayashi M. 2014. Changing hydrologic connectivity due to permafrost thaw in the lower Liard River valley, NWT, Canada. *Hydrological Processes* **28**: 4163–4178. DOI: 10.1002/hyp.10206

Constantz J .1998. Interaction between stream temperature, streamflow, and groundwater exchanges in Alpine streams. *Water Resources Research* **34**: 1609–1615.

Constantz, J. 2008. Heat as a tracer to determine streambed water exchanges. *Water Resources Research* **44**: W00D10. DOI: 10.1029/2008WR006996.

Constantz J, Stonestrom D. 2003. Heat as a tracer of water movement near streams, in: *Heat as a tool for studying the movement of ground water near streams*, edited by: Stonestrom D and Constantz J. US Geological Survey Circular 1260.

Cook SJ, Robinson ZP, Fairchild IJ, Knight PG, Waller RI, Boomer I. 2010. Role of glaciohydraulic supercooling in the formation of stratified facies basal ice: Svínafellsjökull and Skaftafellsjökull, southeast Iceland. Boreas **39**: 24-38. DOI: 10.1111/j.1502-3885.2009.00112.x.

Cook SJ, Swift DA. 2012. Subglacial basins: Their origin and importance in glacial systems and landscapes. *Earth Surface Reviews* **115**: 332-372. DOI: 10.1016/j.earscirev.2012.09.009

References

Cooper RJ, Wadham JL, Tranter M, Hodgkins R, Peters NE. 2002. Groundwater hydrochemistry in the active layer of the proglacial zone, Finsterwalderbreen, Svalbard. *Journal of Hydrology* **269**: 208-223. DOI: 10.1016/S0022-1694(02)00279-2

Cooper R, Hodgkins R, Wadham J, Tranter M. 2011. The hydrology of the proglacial zone of a high-Arctic glacier (Finsterwalderbreen, Svalbard): sub-surface water fluxes and complete water budgets. *Journal of Hydrology* **406**: 88-96. DOI: 10.1016/j.jhydrol.2011.06.008

Coudrain A, Francou B, Kundzewicz ZW. 2005. Glacier shrinkage in the Andes and consequences for water resources–Editorial. *Hydrological Sciences Journal* **50**: 4.

Council of the European Community (CEC), 2000. Directive 2000/60/EC of the European Parliament and of the Council of 23 October 2000 establishing a framework for Community action in the field of water policy. Official Journal of the European Communities, **L327/1, 23.10.2000**.

Cowton T, Nienow P, Sole A, Wadham J, Lis G, Bartholomew I, Mair D, Chandler D. 2013. Evolution of drainage system morphology at a land-terminating Greenlandic outlet glacier, *Journal of Geophysical Research Earth Surf*ace **118**: 29–41. DOI:10.1029/2012JF002540.

Cozzetto KD, Bencala KE, Gooseff MN, McKnight DM. 2013. The influence of stream thermal regimes and preferential flow paths on hyporheic exchange in a glacial meltwater stream. *Water Resources Research* **49**: 5552–5569 DOI:10.1002/wrcr.20410.

Craig H. 1961a. Standard for reporting concentrations of deuterium and oxygen-18 in natural waters. *Science* **133**: 1833-34.

Craig H. 1961b. Isotopic variations in meteoric waters. *Science* **133**: 1702–1703.

Crochet P. 2013. Sensitivity of Icelandic river basins to recent climate variations. Jökull **63**: 71-90.

Crossman J, Boomer I, Bradley C, Milner AM. 2011. Water flow dynamics of groundwater-fed streams and their ecological significance in a glacierized catchment. *Arctic, Antarctic and Alpine Research* **43**: 364-379. DOI: 10.1657/1938-4246-43.3.364

Crossman J, Bradley C, David JNW, Milner AM. 2012. Use of remote sensing to identify areas of groundwater upwelling on active glacial floodplains; their frequency, extent and significance on a landscape scale. *Remote Sensing of the Environment.* **123**: 116-126. DOI: 10.1016/j.rse.2012.03.023

Crossman, J., Bradley, C., Milner, A. and Pinay, G. 2013. Influence of environmental instability of groundwater-fed streams on hyporheic fauna, on a glacial floodplain, Denali National Park, Alaska. *River Research and Applications*. **29**: 548-559. DOI: 10.1002/rra.1619

Cuthbert MO, Mackay R, Tellam JH, Thatcher KE. 2010. Combining unsaturated and saturated hydraulic observations to understand and estimate groundwater recharge through glacial till. *Journal of Hydrology* **391**: 263–276.

Dahlke HE, Lyon SW, Jansson P, Karlin T, Rosqvist G. 2014. Isotopic investigation of runoff generation in a glacierized catchment in northern Sweden. *Hydrological Processes*, **28**: 1383–1398. DOI: 10.1002/hyp.9668

Dansgaard, W. 1964. Stable isotopes in precipitation. *Tellus* **16**: 436–468.

References

Darcy, H. 1856. *Les fontaines publiques de la ville Dijon*. Victor Dalmont, Paris.

Darling WG. 2004. Hydrological factors in the precipitation of stable isotopic proxy data present and past: a European perspective. *Quaternary Science Reviews* **23**: 743–770.

Datry T, Larned ST, Scarsbrook MR. 2007. Responses of hyporheic invertebrate assemblages to large-scale variation in flow permanence and surface–subsurface exchange. *Freshwater Biology* **52**: 1452–1462. DOI: 10.1111/j.1365-2427.2007.01775.x

de Woul M, Hock R , Braun M, Thorsteinsson T, Johannesson T, Halldorsdottir S. 2006. Firn layer impact on glacial runoff: a case study at Hofsjöekull, Iceland. *Hydrological Processes* **20**: 2171-2185.

Déry SJ, Stahl K, Moore RD, Whitfield PH, Menounos B, Burford JE . 2009. Detection of runoff timing changes in pluvial, nival, and glacial rivers of western Canada. *Water Resources Research* **45**: W04426, DOI:10.1029/2008WR006975.

Döll P, Hoffmann-Dobrev H, Portmann FT, Siebert S, Eicker A, Rodell M, Strassberg G, Scanlon BR. 2012. Impact of water withdrawals from groundwater and surface water on continental water storage variations. *Journal of Geodynamics*: **59–60**: 143-156, DOI 10.1016/j.jog.2011.05.001.

Domenico PA, Schwartz FW. 1998. *Physical and Chemical Hydrogeology*, John Wiley, New York.

Dragon K, Marciniak M. 2010. Chemical composition of groundwater and surface water in the Arctic environment (Petuniabukta region, central Spitsbergen). *Journal of Hydrology* **386**: 160-172. DOI: 10.1016/j.jhydrol.2010.03.017

Drexler JZ, Bedford BL, Scognamiglio R, Siegel DI. 1999. Fine-scale characteristics of groundwater flow in a peatland. *Hydrological Processes* **13**: 1341-1359.

Drexler JZ, Knifong D, Tuil JL, Flint LE, Flint AL. 2013. Fens as whole-ecosystem gauges of groundwater recharge under climate change. *Journal of Hydrology* **481:** 22-34. DOI: 10.1016/j.jhydrol.2012.11.056

Dugan HA, Gleeson T, Lamoureux SF, Novakowski K. 2012. Tracing groundwater discharge in a High Arctic lake using radon-222. *Environmental Earth Sciences* **66**: 1385-1392. 10.1007/s12665-011-1348-6

Earman S, Campbell AR, Newman BD, Phillips FM. 2006. Isotopic exchange between snow and atmospheric water vapour: estimation of the snowmelt component of groundwater recharge in the southwestern United States. *Journal of Geophysical Research* **111** D09302 DOI:10.1029/2005JD006470.

Edwards TWD, Wolfe BB, Gibson JJ, Hammarlund D. 2004. Use of water isotope tracers in high-latitude hydrology and paleohydrology. In: Pienitz, R., Douglas, M.S.V., Smol, J.P. (Eds.), Long-term Environmental Change in Arctic and Antarctic Lakes. Springer, Dordretch, The Netherlands, pp. 187–207

Egozi R, Lekach J. 2014.Stream catchment dynamics. *Geomorphology* **212**: Pages 1-3. DOI:dx.doi.org/10.1016/j.geomorph.2013.12.003.

Einarsson B, Jónsdóttir J. F. 2008. Runoff modelling in Iceland with the hydrological model, WASIM. In O. G. B. Sveinsson, S. M. Garðarsson and S. Gunnlaugsdóttir (Eds.), Northern hydrology and its global role: XXV Nordic hydrological conference, Nordic Association for Hydrology, Reykjavík, Iceland August 11-13, 2008, pp 630-637. Reykjavík: Icelandic Hydrological Committee.

References

Einarsson B, Jónsson S. 2010a. The effect of climate change on runoff from two watersheds in Iceland. Icelandic Meteorological Office, Rep. 2010-016. Available at http://www.vedur.is/-media/ces/2010_016.pdf

Einarsson B, Jónsson S. 2010b. Improving groundwater representation and the parameterization of glacial melting and evapotranspiration in applications of the WaSiM hydrological model within Iceland. Iceland Meteorological Office Report VI 2010-017.

Eiriksdóttir ES, Louvat P, Gíslason SR, Óskarsson N, Hardardóttir J. 2008. Temporal variation of chemical and mechanical weathering in NE Iceland: evaluation of a steady-state model of erosion. *Earth Planetary Science Letters* **272**: 78–88. DOI: 10.1016/j.epsl.2008.04.005

Emmer A, Vilímek V. 2013. Review Article: Lake and breach hazard assessment for moraine-dammed lakes: an example from the Cordillera Blanca (Peru), *Natural Hazards and Earth System Sciences* **13**: 1551-1565, DOI:10.5194/nhess-13-1551-2013.

Environment Agency (EA). 2009. *The Hyporheic Handbook: A Handbook on the groundwater-surfacewater interface and hyporheic zone for environmental managers.* Bristol, UK, Environment Agency, 280pp. (Science Report, SC0500).

Evans DJA, Twigg DR. 2002. The active temperate glacial landsystem: a model based on Breiðamerkurjökull and Fjallsjökull, Iceland. *Quaternary Science Reviews* **21**: 2143–2177. DOI: 10.1016/S0277-3791(02)00019-7

Evans DJA, Phillips ER, Hiemstra JF, Auton CA. 2006. Subglacial till: Formation, sedimentary characteristics and classification. *Earth-Science Reviews* **78**: 115-176. DOI: 10.1016/j.earscirev.2006.04.001

Everest J, Bradwell T. 2003. Buried glacier ice in southern Iceland and its wider significance. *Geomorphology* **52**: 347–358. DOI: 10.1016/S0169-555X(02)00277-5

Eyles N. 2006. The role of meltwaters in glacial processes. *Sedimentary Geology* **190**: 257-268.

Faeh AO. 1997. Understanding the Processes of Discharge Formation Under Extreme Precipitation: A Study Based on the Numerical Simulation of Hillslope Experiments, Mitteilungen 150, 197 pp., Vers. f€ur Wasserbau, Hydrol. und Glaziol. der Eidg. Tech. Hochsch., Zurich, Switzerland.

Fairchild, IJ, Bradby L, Sharp M, Tison J-L. 1994. Hydrochemistry of carbonate terrains in alpine glacial settings. *Earth Surface Processes and Landforms* **19**: 33-54.

Fairchild IJ, Tooth AF, Russell AJ. 1999a. Chemical weathering of volcanogenic sediments, Skeiðarársandur. *In:* Ármansson, H. (Ed.) *Proceedings of the 5th International Conference on Geochemistry of the Earth's Surface*, Reykjavík, Iceland, 91-94.

Fairchild IJ, Killawee JA, Sharp MJ, Spiro B, Hubbard B, Lorrain RD, Tison J-L. 1999b. Solute generation and transfer from a chemically reactive alpine glacial–proglacial system. *Earth Surface Processes and Landforms* **24**: 1189–1211.

Favier V, Coudrain A, Cadier E, Francou B, Ayabaca E, Maisincho L, Praderio E, Villacis M, Wagnon P. 2008. Evidence of groundwater flow on Antizana ice-covered volcano, Ecuador. *Hydrological Sciences Journal* **53**: 278 — 291. DOI 10.1623/hysj.53.1.278.

Fay H. 2002. The formation of ice-block obstacle marks during the November 1996 glacier outburst flood (jökulhlaup), Skeiðarársandur, southern Iceland. In *Flood and Megaflood*

References

Deposits: Recent and Ancient., Special Publication, Martini, IP, Baker, R, Garzón, G (eds.). International Association of Sedimentologists. **32**: 85–97.

Ferone JM, Devito KJ. 2004. Shallow groundwater–surface water interactions in pond–peatland complexes along a Boreal Plains topographic gradient. *Journal of Hydrology* **292**: 75-95. DOI: 10.1016/j.jhydrol.2003.12.032

Finger D*,* Heinrich G*,* Gobiet A*,* Bauder A. 2012*.,* Projections of future water resources and their uncertainty in a glacierized catchment in the Swiss Alps and the subsequent effects on hydropower production during the 21st century. *Water Resources Research* **48***: W02521, doi:*10.1029/2011WR010733*.*

Finger D, Hugentobler A, Huss M, Voinesco A, Wernli H, Fischer D, Weber E, Jeannin P-Y, Kauzlaric M, Wirz A, Vennemann T, Hüsler F, Schädler B, Weingartner R. 2013. Identification of glacial meltwater runoff in a karstic environment and its implication for present and future water availability. *Hydrology and Earth System Sciences* **17**: 3261-3277. DOI: 10.5194/hess-17-3261-2013

Finn DS, Räsänen K, Robinson CT. 2010. Physical and biological changes to a lengthening stream gradient following a decade of rapid glacial recession. *Global Change Biology* **16**: 3314–3326. DOI: 10.1111/j.1365-2486.2009.02160.x

Finn DS, Khamis K, Milner AM. 2013. Loss of small glaciers will diminish beta diversity in Pyrenean streams at two levels of biological organization. *Global Ecology and Biogeography* **22**: 40-51. DOI: 10.1111/j.1466-8238.2012.00766.x

Finn DS, Zamora-Muñoz C, Múrria C, Sáinz-Bariáin M, Alba-Tercedor J. 2014. Evidence from recently deglaciated mountain ranges that *Baetis alpinus* (Ephemeroptera) could lose significant genetic diversity as alpine glaciers disappear. *Freshwater Science* **33**: 207-216.

Fischer UH, Clarke GKC. 2001. Review of subglacial-mechanical coupling: Trapridge Glacier, Yukon Territory, Canada. *Quaternary International* **86**: 29-43.

Fisher DA. 1991. Remarks on the deuterium excess in precipitation in cold regions, *Tellus*, Series B **43**: 401– 407.

Flaathen TK, Gíslason SR. 2007. The effect of volcanic eruptions on the chemistry of surface waters: the 1991 and 2000 eruptions of Mt. Hekla, Iceland. *Journal of Volcanology and Geothermal Research* **164**: 293–316.

Flaathen TK, Gíslason SR, Oelkers EH, Sveinbjörnsdóttir ÁE. 2009. Chemical evolution of the Mt. Hekla, Iceland, groundwaters: a natural analogue for CO_2 sequestration in basaltic rocks. *Applied Geochemistry* **24**: 463–474.

Flaim G, Camin F, Tonon A, Obertegger U. 2013. Stable isotopes of lakes and precipitation along an altitudinal gradient in the Eastern Alps. *Biogeochemistry* **116**: 187-198. DOI 10.1007/s10533-013-9855-z

Fleckenstein JH, Krause S, Hannah DM, Boano F. 2010. Groundwater-surface water interactions: New methods and models to improve understanding of processes and dynamics. *Advances in Water Resources.* **33**: 1291-1295.

Flowers GE, Björnsson H, Pálsson F. 2003. New insights into the subglacial and periglacial hydrology of Vatnajökull, Iceland, from a distributed physical model. *Journal of Glaciology*, **49:** 257-270.

References

Flowers GE, Marshall SJ, Björnsson H, Clarke GKC. 2005. Sensitivity of Vatnajökull ice cap hydrology and dynamics to climate warming over the next 2 centuries. *Journal of Geophysical Research*, **110**: F02011, DOI:10.1029/2004JF000200.

Folk RI. 1966. A review of grain-size parameters. *Sedimentology* **6**: 73-93. doi: 10.1111/j.1365-3091.1966.tb01572.x

Fortner SK, Lyons WB, Fountain AG, Welch KA, Kehrwald NM. 2009. Trace element and major ion concentrations and dynamics in glacier snow and melt: Eliot Glacier, Oregon Cascades. *Hydrological Processes* **23**: 2987–2996. doi: 10.1002/hyp.7418

Fortner SK, Mark BG, McKenzie JM, Bury J, Trierweiler A, Baraer M, Burns PJ, Munk L. 2011. Elevated stream trace and minor element concentrations in the foreland of receding tropical glaciers. *Applied Geochemistry* **26:** 1792-1801. DOI: 10.1016/j.apgeochem.2011.06.003

Foster S, Chilton J, Nijsten G-J, and Richts A. 2013. Gronundwater- a global focus on the 'local resource'. *Current Opinion in Environmental Sustainability* 2013, 5:685–695. http://dx.doi.org/10.1016/j.cosust.2013.10.010

Fountain AG, Walder JS. 1998. Water flow through temperate glaciers. R*eviews of geophysics* **36**: 299-328.

Francis BA, Francis LK, Cardenas MB. 2010. Water table dynamics and groundwater–surface water interaction during filling and draining of a large fluvial island due to dam-induced river stage fluctuations. *Water Resources Research* **46**: W07513, DOI:10.1029/2009WR008694.

Freeze RA, Cherry JA. 1979. Groundwater. Prentice Hall, New Jersey.

Frezzotti M, Orombelli G. 2014. Glaciers and ice sheets: current status and trends. *Rendiconti Lincei* **25**: 59-70. DOI: 10.1007/s12210-013-0255-z

Fritz BG, Arntzen EV. 2007. Effect of rapidly changing river stage on uranium flux through the hyporheic zone. *Ground Water* **45**: 753–760.

Froehlich K, Gibson JJ, Aggarwal PK. 2002. Deuterium excess in precipitation and its climatological significance. *Study of environmental change using isotope techniques*. C&S Papers Series 13/P. 54–65. International Atomic Energy Agency: Vienna, Austria.

Füreder L, Schütz C, Wallinger M, Burger R. 2001. Physico-chemistry and aquatic insects of a glacier-fed and a spring-fed alpine stream. *Freshwater Biology* **46**: 1673–1690. DOI: 10.1046/j.1365-2427.2001.00862.x

Gabet EJ, Wolff-Boenisch D, Langner H, Burbank DW, Putkonen J. 2010. Geomorphic and climatic controls on chemical weathering in the High Himalayas of Nepal, *Geomorphology* **122**: 205-210. DOI: 10.1016/j.geomorph.2010.06.016

Galeczka I, Oelkers EH, Gislason SR. 2014. The chemistry and element fluxes of the July 2011 Múlakvísl and Kaldakvísl glacial floods, Iceland. *Journal of Volcanology and Geothermal Research* **273**: 41-57.

Gao J, Tandong Y, Joswiak D. 2014. Variations of water stable isotopes ($\delta^{18}O$) in two lake basins, southern Tibet Plateau. A*nnals of Glaciology* **55**: 97-104. DOI: 10.3189/2014AoG66A109 97

References

Gariglio FP, Tonina D, Luce CH. 2013. Spatiotemporal variability of hyporheic exchange through a pool-riffle-pool sequence. *Water Resources Research* **49**: 7185–7204 DOI:10.1002/wrcr.20419.

Gat JR. 1996. Oxygen and hydrogen isotopes in the hydrologic cycle. *Annual Review of Earth & Planetary Sciences* **24**: 225–262.

Gat JR, Mook WG, Meijer HAJ. 2001. *Environmental Isotopes in the Hydrological Cycle. Volume 2: Atmospheric Water.* Water Resources Research Program, IAEA Vienna.

Geyh MA, d'Amore F, Darling G, Paces T, Pang Z, Silar J. 2000. In: E*nvironmental isotopes in the hydrological cycle*. Principles and applications. Vol. 4 Groundwater saturated and unsaturated zone. International Atomic Energy Agency (IAEA), Vienna.

Gibert J, Culver DC. 2009. Assessing and conserving groundwater biodiversity: an introduction. *Freshwater Biology* **54**: 639–648. DOI: 10.1111/j.1365-2427.2009.02202.x

Gíslason SR. 2005. Chemical weathering, chemical denudation and the CO2 budget for Iceland. In: Caselding C, Russell A, Hardardottir J, Knudsen O. (Eds.), *Developments in Quaternary Sciences. Iceland Modern Processes and Past Environments*. Elsevier B, Amsterdam, pp. 289–307.

Gíslason SR. 2008. Weathering rates in Iceland. Jökull **58**: 387–408.

Gíslason SR, Eugster HP. 1987. Meteoric water-basalt interactions. II: A field study in N.E. Iceland. *Geochemica et Cosmochimica Acta,* 51, 2841-2855.

Gíslason SR, Arnórsson S. 1993. Dissolution of primary basaltic minerals in natural waters: saturation state and kinetics. *Chemical Geology* **105**: 117–135.

Gíslason SR, Torssander P. 2006. The response of Icelandic river sulphate concentration and isotope composition to the decline in global atmospheric SO2 emission to the North Atlantic region. *Environmental Science and Technology* **40**: 680–686.

Gíslason SR, Arnórsson S, Ármansson H. 1996. Chemical weathering of basalt in southwest Iceland: Effects of runoff, age of rocks, and vegetative /glacial cover. *American Journal of Science*, 296, 837-907.

Gíslason GM, Olafsson JS, Adalsteinsson H. 2000. Life in glacial and alpine rivers in central Iceland in relation to physical and chemical parameters. Nordic Hydrology **32**: 411-422.

Gíslason SR, Snorrason A, Ingvarsson GB, Camargo LGQ, Eiriksdottir ES, Elefsen SO, Hardardottir J, Thorlaksdottir SB, Torssander P. 2006. Chemical Composition, Discharge and Suspended Load in Rivers in South Iceland IX. Report RH-05-2006. Database of the Science Institute and the Hydrological Service of the National Energy Authority. 46 pp.

Glaser PH, Siegel DI, Reeve AS, Janssens JA, Janecky DR. 2004. Tectonic drivers for vegetation patterning and landscape evolution in the Albany River region of the Hudson Bay Lowlands. *Journal of Ecology* **92:** 1054-1070. DOI: 10.1111/j.0022-0477.2004.00930.x

Gonfiantini R. 1986 Environmental isotopes in lake studies. *Handbook of Environmental Isotope Geochemistry* (P. Fritz, J.-Ch. Fontes, Eds) Elsevier, Amsterdam, 113–168.

Goodman, J. 1999. Aquifer parameter characterisation for the hydrogeological impact assessment of sand and gravel workings. PhD thesis. University of Birmingham

References

Google Earth. Online. Accessed 2013.

Gooseff MN, McKnight DM, Runkel RL, Vaughn BH. 2003. Determining long time-scale hyporheic zone flow paths in Antarctic streams. *Hydrological Processes* **17**: 1691–1710. doi: 10.1002/hyp.1210

Gooseff MN, Lyons W, McKnight DM, Vaughn BH, Fountain AG, Dowling C. 2006. A stable isotopic investigation of a polar desert hydrologic system, McMurdo dry valleys, Antarctica. *Arctic, Antarctic, And Alpine Research* **38**: 60-71.

Gooseff MN, Barrett JE, Levy JS. 2013. Shallow groundwater systems in a polar desert, McMurdo Dry Valleys, Antarctica. *Hydrogeology Journal* **21**:171-183. DOI 10.1007/s10040-012-0926-3

Green TR, Taniguchi M, Kooi H, Gurdak JJ, Allen DM, Hiscock KM, Treidel H, Aureli A. 2011. Beneath the surface of global change: Impacts of climate change on groundwater. *Journal of Hydrology* **405**: 532-560. doi.org/10.1016/j.jhydrol.2011.05.002.

Gremaud V, Goldscheider N, Savoy L, Favre G, Masson H. 2009. Geological structure, recharge processes and underground drainage of a glacierized karst aquifer system, Tsanfleuron-Sanetsch, Swiss Alps. *Hydrogeology Journal* **17**: 1833-1848. DOI: 10.1007/s10040-009-0485-4

Gremaud V, Goldscheider N. 2010. Geometry and drainage of a retreating glacier overlying and recharging a karst aquifer, Tsanfleuron-Sanetsch, Swiss Alps. *Acta Carsologica* **39**: 289-300.

Grundl T, Magnusson N, Brennwald MS, Kipfer R. 2013. Mechanisms of subglacial groundwater recharge as derived from noble gas, 14C, and stable isotopic data. *Earth and Planetary Science Letters* **369-370**: 78-85. DOI: 10.1016/j.epsl.2013.03.012

Guðmundsson MT, Björnsson H, Pálsson F. 1995. Changes in jökulhlaup sizes in Grímsvötn, Vatnajökull, Iceland, 1934–91, deduced from in-situ measurements of subglacial lake volume. *Journal of Glaciology* **41:** 263– 272.

Guðmundsson MT, Bonnell A, Gunnarsson K. 2002. Seismic soundings of sediment thickness on Skeiðarársandur, SE-Iceland. *Jökull* **51**: 53-64.

Guðmundsson S, Björnsson H, Jóhannesson T, Aðalgeirsdóttir G, Pálsson F, Sigurðsson O. 2009. Similarities and differences in the response to climate warming of two ice caps in Iceland. *Hydrology Research* **40**: 495-502.

Guðmundsson MT, Höskuldsson ÁČ, Larsen G, Thordarson T, Óladóttir B, Oddsson B, Gudnason J, Högnadóttir T, Stevenson JA, Houghton B, McGarvie DW, Sigurdardottir G. 2012. The May 2011 eruption of Grímsvötn. *Geophysical Research Abstracts*, EGU2012–EGU12:**119**.

Gulley JD, Benn DI, Screaton E, Martin J. 2009. Mechanisms of englacial conduit formation and their implications for subglacial recharge. *Quaternary Science Reviews* **28**: 1984-1999.

Gurnell AM, Edwards PJ, Petts GE, Ward JV. 1999. A conceptual model for alpine proglacial river channel evolution under changing climatic conditions. *Catena* **38**: 223-242.

Gurrieri JT, Furniss G. 2004. Estimation of groundwater exchange in alpine lakes using non-steady mass-balance methods. Journal of Hydrology **297:** 187– 208. DOI: 10.1016/j.jhydrol.2004.04.021.

References

Hagen JO, Korsen OM, Vatne G. 1991. Drainage pattern in a subpolar glacier: Broggerbreen, Svalbard. In: Y. Gjessing, J.O. Hagen, K.A. Hassel, K. Sand and B. Weld, Editors, *Arctic Hydrology. Present and Future Tasks*, *Norwegian National Committee for Hydrology Report No. 23* (1991), pp. 121–131.

Hagg W, Braun LN, Kuhn M, Nesgaard TI. 2007. Modelling of hydrological response to climate change in glacierized Central Asian catchments. *Journal of Hydrology* **332**: 40–53.

Haldorsen S, Heim M. 1999. An Arctic groundwater system and its dependence upon climatic change: An Arctic example from Svalbard. *Permafrost and Periglacial Processes* **10**: 137-149.

Haldorsen S, Heim M, Dale B, Landvik JY, van der Ploeg M, Leijnse A, Salvigsen O, Hagen JO, Banks D. 2010. Sensitivity to long-term climate change of subpermafrost groundwater systems in Svalbard. *Quaternary Research* **73**: 393-402. DOI: 10.1016/j.yqres.2009.11.002

Haldorsen S, Heim M, van der Ploeg M. 2012. Impacts of climate change on groundwater in permafrost areas: case study from Svalbard, Norway. In: Treidel H, Martin-Bordes JL, Gurdak JJ (eds). *Climate Change Effects on Groundwater Resources: A Global Synthesis of Findings and Recommendations*. Edition: IAH - International Contributions to Hydrogeology, Chapter: 18, Publisher: CRC Press, Taylor & Francis Group, Editors:, pp.323 - 338

Hallet B, Hunter L, Bogen J. 1996. Rates of erosion and sediment evacuation by glaciers: A review of field data and their implications. *Global and Planetary Change* **12**: 213–235.

Hammarlund D, Barnekow L, Birks HJB, Buchardt B, Edwards TWD. 2002. Holocene changes in atmospheric circulation recorded in the oxygen-isotope stratigraphy of lacustrine carbonates from northern Sweden. *The Holocene* **12**, 339–351.

Hannah DM, Gurnell AM. 2001. A conceptual linear reservoir runoff model to investigate melt season changes in cirque glacier hydrology. *Journal of Hydrology* **246**: 123–141.

Hannah DM, Gurnell AM, McGregor GR. 1999. Identifying links between large-scale atmospheric circulation and local glacier ablation climates in the French Pyrénées, IAHS Publication **256**: 155–164.

Hannah DM, Gurnell AM, McGregor GR. 2000. Spatio-temporal variation in micro-climate, the energy balance and ablation over a cirque glacier. *International Journal of Climatology* **20**: 733-758.

Hannah DM, Brown LE, Milner AM, Gurnell AM, McGregor GR, Petts GE, Smith BPG, Snook DL. 2007. Integrating climate–hydrology–ecology for alpine river systems. *Aquatic Conservation: Marine and Freshwater Ecosystems* **17**: 636–656. DOI: 10.1002/aqc.800

Hannah DM, Malcolm IA, Bradley C. 2009. Seasonal hyporheic temperature dynamics over riffle bedforms, *Hydrological Processes* **23**: 2178-2194 DOI: 10.1002/hyp.7256

Harris KJ, Carey AE, Lyons WB, Welch KA, Fountain AG. 2007. Solute and isotope geochemistry of subsurface ice melt seeps in Taylor Valley, Antarctica. *Geological Society of America Bulletin* **119**: 548–555 doi:10.1130/B25913.1.

Hartley L, Joyce S. 2013. Approaches and algorithms for groundwater flow modelling in support of site investigations and safety assessment of the Forsmark site, Sweden. *Journal of Hydrology* **500**: 200-216. DOI: 10.1016/j.jhydrol.2013.07.031

References

Harvey JW, Bencala KE. 1993. The effect of stream bed topography on surface–subsurface water exchange in mountain catchments. *Water Resources Research* **29**: 89–98.

Hatch CE, Fisher AT, Revenaugh JS, Constantz J, Ruehl C. 2006. Quantifying surface water–groundwater interactions using time series analysis of streambed thermal records: Method development. Water Resources Research **42**: W10410. DOI:10.1029/2005WR004787.

Hatch CE, Fisher AT, Ruehl CR, Stemler G. 2010. Spatial and temporal variations in streambed hydraulic conductivity quantified with time series thermal methods. Journal of Hydrology **389**:276-288. DOI: 10.1016/j.jhydrol.2010.05.046.

Hayashi M. 2004. Temperature-Electrical Conductivity relation of water for environmental monitoring and geophysical data inversion. *Environmental Monitoring and Assessment* **96**: 119-128.

Hayashi M, Vogt T, Mächler L, Schirmer M. 2012. Diurnal fluctuations of electrical conductivity in a pre-alpine river: Effects of photosynthesis and groundwater exchange, *Journal of Hydrology* **450–451**: 93-104 DOI: 10.1016/j.jhydrol.2012.05.020

Hazen A. 1892. Physical properties of sands and gravels with reference to their use in filtration. *Report to the Massachusetts State Board of Health,* 24th Annual report, 539-556.

Henderson AK, Shuman BN. 2009. Hydrogen and oxygen isotopic composition of lake-water in the western US. *Geological Society of America Bulletin* **121**:1179–1189.

Henderson AK, Shuman BN. 2010. Differing controls on riverand lake-water hydrogen and oxygen isotopic values in the western United States. *Hydrological Processes* **24**: 3894–3906

Hendry MJ. 1982. Hydrogeology of clay till in a prairie region of Canada. *Ground Water* **20**: 162-169.

Hendry MJ. 1988. Hydrogeology of clay till in a prairie region of Canada, *Ground Water* **26**: 607-614.

Hendry MJ., Barbour SL, Novakowski K, Wassenaar LI. 2013. Paleohydrogeology of the Cretaceous sediments of the Williston Basin using stable isotopes of water. *Water Resources Research* **49**: 4580–4592, doi:10.1002/wrcr.20321.

Hieber M, Robinson CT, Rushforth SR, Uehlinger U. 2001. Algal communities associated with different alpine stream types. Arctic, Antarctic and Alpine Research **33**: 447-456. DOI: 10.2307/1552555

Hillel D. 2004. *Introduction to Environmental Soil Physics*. London: Elsevier, pp. 220-232.

Hindshaw RS, Tipper ET, Reynolds BC, Lemarchand E, Wiederhold JG, Magnusson J, Bernasconi SM, Kretzschmar R, Bourdon B. 2011. Hydrological control of stream water chemistry in a glacial catchment (Damma Glacier, Switzerland). *Chemical Geology* **285**: 215-230. DOI: 10.1016/j.chemgeo.2011.04.012

Hindshaw RS, Bourdon B, Pogge von Strandmann P, Vigier N, Burton K. 2013. The stable calcium isotopic composition of rivers draining basaltic catchments in Iceland. *Earth and Planetary Science Letters* **374**: 173–184. DOI: 10.1016/j.epsl.2013.05.038

References

Hiscock KM, Tabatabi Najafi M. 2011. Aquitard characteristics of clay-rich till deposits in East Anglia, Eastern England. *journal of Hydrology* **405**: 288-306.

Hjartarson Á. 1994. *Vatnsveitur og vatnsból, Samantekt um vatnsveitumál.* Reykjavík: Orkustofnun. OS-93061/VOD-04. (In Icelandic).

Hjulström F. 1955. The groundwater of the Hoffelsandur – a glacial outwash plain. *Geografiska Annaler* **37**: 234-245.

Hodgkins R. 1997. Glacier hydrology in Svalbard, Norwegian high arctic. *Quaternary Science Reviews* **16**: 957-973.

Hodgkins R, Tranter M, Dowdeswell JA. 1997. Solute provenance, transport and denudation in a high arctic glacierized catchment. *Hydrological Processes* **11**: 1813–1832. DOI: 10.1002/(SICI)1099-1085(199711)11:14<1813::AID-HYP498>3.0.CO;2-C

Hodgkins R, Tranter M, Dowdeswell JA. 1998. The hydrochemistry of runoff from a cold-based glacier in the High Arctic (Scott Turnerbreen, Svalbard). *Hydrological Processes* **12**: 87-103.

Hodgkins R, Tranter M, Dowdeswell JA. 2004. The characteristics and formation of a high-Arctic proglacial icing. *Geografiska Annaler: Series A, Physical Geography* **86**: 265–275. DOI: 10.1111/j.0435-3676.2004.00230.x

Hodgkins R, Cooper R, Tranter T, Wadham J. 2013. Drainage-system development in consecutive melt seasons at a polythermal, Arctic glacier, evaluated by flow-recession analysis and linear-reservoir simulation. *Water Resources Research* **49***:* 4230–4243. *doi:*10.1002/wrcr.20257*.*

Hodson A, Tranter M, Gurnell A, Clark M, Hagen JO. 2002. The hydrochemistry of Bayelva, a high Arctic proglacial stream in Svalbard. *Journal of Hydrology* **257**: 91-114, ISSN 0022-1694, http://dx.doi.org/10.1016/S0022-1694(01)00543-1.

Hoehn E, Meylan B. 2009. Measures to protect drinking-water wells near rivers from hydraulic engineering operations in peri-alpine flood-plains. *Grundwasser* **14**: 255-263. DOI: 10.1007/s00767-009-0111-3

Hoffman MJ, Price S. 2014. Feedbacks between coupled subglacial hydrology and glacier dynamics. *Journal of Geophysical Research Earth Surf*ace **119**: 414–436. DOI:10.1002/2013JF002943.

Hood E, Scott DT. 2008. Riverine organic matter and nutrients in southeast Alaska affected by glacial coverage. *Nature Geoscience* **1**: 583-587, doi:10.1038/ngeo280.

Hood E, Berner L. 2009. Effects of changing glacial coverage on the physical and biogeochemical properties of coastal streams in southeastern Alaska. *Journal of Geophysical Research* **114**: G03001, DOI:10.1029/2009JG000971.

Hood JL, Roy JW, Hayashi M. 2006. Importance of groundwater in the water balance of an alpine headwater lake. Geophysical Research Letters. **33:** L13405, DOI:10.1029/2006GL026611.

Hubbard B, Nienow P. 1997. Alpine subglacial hydrology. *Quaternary Science Review* **16**: 939-955.

Hubbard B, Sharp MJ, Willis IC, Nielsen MK, Smart CC. 1995. Borehole water-level variations and the structure of the subglacial hydrological system of Haut Glacier d'Arolla, Valais, Switzerland. *Journal of Glaciology* **41**: 572-583.

References

Hubbert MK. 1940. The theory of groundwater motion. The *Journal of Geology* **48**: 785-944.

Hublart P, Ruelland D, Dezetter A, Jourde H. 2013. Modeling current and future trends in water availability for agriculture on a semi-arid and mountainous Chilean catchment. *Cold and mountain region hydrological systems under climate change: towards improved projections* (Proc. of Symp. H02 held during IAHS/IAPSO/IASPEI Assembly in Gothenburg, Sweden. IAHS Publ. **360:** 26-33.

Hunt RJ*,* Krabbenhoft DP*,* Anderson MP. 1996. Groundwater Inflow Measurements in Wetland Systems*. Water Resources Research* **32**: 495–507*, DOI:*10.1029/95WR03724*.*

Huss M, Farinotti D, Bauder A, Funk M. 2008. Modelling runoff from highly glacierized drainage basins in a changing climate. *Hydrological Processes* **22**: 3888-3902.

Huss M, Jouvet G, Farinott D, Bauder A. 2010. Future high-mountain hydrology: a new parametrization of glacier retreat. *Hydrology and Earth System Science* **14**: 815-829.

Hvorslev MJ. 1951. Time lag and soil permeability in groundwater observations. *US Army Corps of Engineers Waterway Experts State Bulletin* **36**, Vicksburg, Mississippi.

Hylander S, Jephson T, Lebret K, von Einem J, Fagerberg T, Balseiro E, Modenutti B, Souza MS, Laspoumaderes C, Jönsson M, Ljungberg P, Nicolle A, Nilsson PA, Ranåker L Hansson L-A. 2011. Climate-induced input of turbid glacial meltwater affects vertical distribution and community composition of phyto-and zooplankton. *Journal of Plankton Research* **33**: 1239–1248. 10.1093/plankt/fbr025

Hyun Y, Kim H, Lee S-S,Lee K-K. 2011. Characterizing streambed water fluxes using temperature and head data on multiple spatial scales in Munsan stream, South Korea. *Journal of Hydrology*, **402**: 377-387. DOI: 10.1016/j.jhydrol.2011.03.032

International Atomic Energy Agency/ World Meteorological Organisation. 2014. Global Network of Isotopes in Precipitation. The GNIP Database. Accessible at: http://www.iaea.org/water.

Irvine-Fynn TDL*,* Hodson AJ*,* Moorman BJ*,* Vatne G, Hubbard AL*. 2011.* Polythermal Glacier Hydrology: A review. *A Review of Geophysics* **49***: RG4002, doi:*10.1029/2010RG000350.

Iverson N, Person M. 2012. Glacier-bed geomorphic processes and hydrologic conditions relevant to nuclear waste disposal. *Geofluids* **12**: 38–57. DOI: 10.1111/j.1468-8123.2011.00355.x

Jacobsen D, Dangles O, Andino P, Espinosa R, Hamerlik L, Cadier E. 2010. Longitudinal zonation of macroinvertebrates in an Ecuadorian glacier-fed stream: do tropical glacial systems fit the temperate model? *Freshwater Biology* **55**: 1234–1248.

Jacobsen D, Milner AM, Brown LE, Dangles O. 2012. Biodiversity under threat in glacier-fed river systems. *Nature Climate Change* **2**: 361-364. DOI: 10.1038/NCLIMATE1435

Jacobsen D, Andino P, Calvez R, Cauvy-Fraunié S, Espinosa R, Dangles O. 2014. Temporal variability in discharge and benthic macroinvertebrate assemblages in a tropical glacier-fed stream. *Freshwater Science* **33**: 32-45. DOI: 10.1086/674745

Jansson P, Hock R, Schneider T. 2003. The concept of glacier storage: a review. *Journal of Hydrology* **282**: 116-129.

References

Janszen A, Spaak M, Moscariello A. 2012. Effects of the substratum on the formation of glacial tunnel valleys: an example from the Middle Pleistocene of the southern North Sea Basin. *Boreas* **41**: 629-643 DOI 10.1111/j.1502-3885.2012.00260.x.

Jeelani Gh., Nadeem AB, Shivanna K. 2010. Use of δ18O tracer to identify stream and spring origins of a mountainous catchment: A case study from Liddar watershed, Western Himalaya, India. *Journal of Hydrology* **393**: 257-264. DOI: 10.1016/j.jhydrol.2010.08.021

Jefferson A, Nolin A, Lewis S, Tague C. 2008. Hydrogeologic controls on streamflow sensitivity to climate variation. *Hydrological Processes* **22**: 4371–4385. DOI: 10.1002/hyp.7041.

Jerome JH, Bukata RP, Whitfield PH, Rousseau N. 1994a. Colours of natural waters 1: Factors controlling the dominant wavelength. *Northwest Science* **68**: 43-52.

Jerome JH, Bukata RP, Whitfield PH, Rousseau N. 1994b. Colours of natural waters 2: Observations of spectral variations in British Columbia Rivers. *Northwest Science* **68**: 53–64.

Jóhannesson T, Aðalgeirsdóttir G, Ahlstrøm A, Andreassen LM, Björnsson H, de Woul M, Elvehøy H, Flowers GE, Guðmundsson S, Hock R, Holmlund P, Pálsson F, Radić V, Sigurðsson O,Thorsteinsson Th. 2006. The impact of climate change on glaciers and glacial runoff in the Nordic countries. In: Árnadóttir S (ed.) Proc. European Conference on Impacts of Climate Change on Renewable Energy Sources) pp. 31–34. (Reykjavik, Iceland). CE-2, Hydrological Service, National Energy Authority, Reykjavík, Iceland. ISBN 9979-68-189-6.

Jónsdóttir JF. 2008. A runoff map based on numerically simulated precipitation and a projection of future runoff in Iceland, *Hydrological Sciences Journal* **53**: 100-111.

Jonsson CE, Leng MJ, Rosqvist GC, Seibert J, Arrowsmith C. 2009. Stable oxygen and hydrogen isotopes in sub-Arctic lake waters from northern Sweden. *Journal of Hydrology* 376:143–151.

Jönsson M, Ranåker L, Nicolle A, Ljungberg R, Fagerberg T, Hylander S, Jephson T, Lebret K, von Einem J, Hansson L, Nilsson PA, Balseiro E,Modenutti B. 2011. Glacial clay affects foraging performance in a Patagonian fish and cladoceran. *Hydrobiologia* **663**: 101–108. 10.1007/s10750-010-0557-4

Jude-Eton TC, Thordarson T, Guðmundsson MT, Oddson B. 2012. Dynamics, stratigraphy and proximal dispersal of supraglacial tephra during the ice-confined 2004 eruption at Grímsvötn Volcano, Iceland. *Bulletin of Volcanology* **74**: 1057-1082. DOI: 10.1007/s00445-012-0583-3

Juen I, Käser G, Georges C. 2007. Modelling observed and future runoff from a glacierized tropical catchment (Cordillera Blanca, Peru). *Global and Planetary Change* **59**: 37-48. DOI: 10.1016/j.gloplacha.2006.11.038

Jumpponen A., Väre H, Mattson KG, Ohtonen R, Trappe JM. 1999. Characterization of 'safe sites' for pioneers in primary succession on recently deglaciated terrain. *Journal of Ecology* **87**: 98-105. DOI: 10.1046/j.1365-2745.1999.00328.x

Jung MT, Burt P, Bates PD. 2004. Toward a conceptual model of floodplain water table response. *Water Resources Research* **40** *W12409, DOI:*10.1029/2003WR002619.

Kalbus E, Reinstorf F, Schirmer M. 2006. Measuring methods for groundwater-surface water interactions: a review. *Hydrology and Earth System Sciences* **10**:873-887.

References

Kalbus E, Schmidt C, Bayer-Raich M, Leschik S, Reinstorf F, Balcke GU, Schirmer M. 2007. New methodology to investigate potential contaminant mass fluxes at the stream–aquifer interface by combining integral pumping tests and streambed temperatures. Environmental Pollution **148**: 808–816.

Kamb B. 1987. Glacier surge mechanism based on linked cavity configuration of the basal water conduit system, *Journal of Geophysical Research* **92**: 9083–9100

Kamb B, Raymond CF, Harrison WD, Engelhardt H, Echelmeyer KA, Humphrey N, Brugman MM, Pfeffer T. 1985. Glacier surge mechanism: 1982–1983 surge of Variegated Glacier, Alaska. *Science* **227**: 469–479. DOI: 10.1126/science.227.4686.469

Karan S, Engesgaard P, Rasmussen J. 2014. Dynamic streambed fluxes during rainfall-runoff events. *Water Resources Research* **50**: 2293–2311, DOI:10.1002/2013WR014155.

Käser DH, Binley A, Heathwaite AL, Krause S. 2009. Spatio-temporal variations of hyporheic flow in a riffle-step-pool sequence. *Hydrological Processes* **23**: 2138–2149. doi: 10.1002/hyp.7317

Kattlemann R, Elder K. 1991. Hydrologic characteristics and water balance of an alpine basin in the Sierra Nevada. *Water Resources Research* **27**: 1553–1562.

Keery J, Binley A, Crook N, Smith JWN. 2007. Temporal and spatial variability of groundwater-surface water fluxes: Development and application of an analytical method using temperature time series. *Journal of Hydrology* **336**:1-16. DOI: 10.1016/j.jhydrol.2006.12.003.

Kehew AE, Piotrowski JA, Jørgensen F. 2012. Tunnel valleys: Concepts and controversies — A review. *Earth-Science Reviews* **113**: 33-58.

Kennedy CD, Murdoch LC, Genereux DP, Corbett DR, Stone K, Pham P, and Mitasova H. 2010. Comparison of Darcian flux calculations and seepage meter measurements in a sandy streambed in North Carolina, United States. *Water Resources Research* **46**: W09501, doi:10.1029/2009WR008342.

Kidmose J, Engesgaard P, Nilsson B, Laier T, Looms MC. 2011. Spatial distribution of seepage to a flow through lake: Lake Hampen, Western Denmark. *Vadose Zone Journal* **10**: 110-124.

Kidmose J, Nilsson B, Engesgaard P, Frandsen M, Karan S, Landkildehus F, Søndergaard M, Jeppesen E. 2013. Focused groundwater discharge of phosphorus to a eutrophic seepage lake (Lake Væng, Denmark): implications for lake ecological state and restoration. *Hydrogeology Journal* **21**: 1787-1802. DOI 10.1007/s10040-013-1043-7

Kirillin G, Phillip W, Engelhardt C, Nützmann G. 2013. Net groundwater inflow in an enclosed lake: from synoptic variations to climatic projections. *Hydrological Processes* **27**: 347–359. doi: 10.1002/hyp.9227

Kjartansson G. 1945. Íslenzkar vatnsfallategundir (Icelandic river types) *Náttúrufræðingurinn* 15, 113–126 (in Icelandic).

Klaus J, McDonnell JJ. 2013. Hydrograph separation using stable isotopes: Review and evaluation, *Journal of Hydrology* **505**: 47-64. DOI: 10.1016/j.jhydrol.2013.09.006

Kløve B., Ala-aho P, Bertrand G, Boukalova Z, Ertürk A, Goldscheider N, Ilmonen J, Karakaya N, Kupfersberger H, Kvœrner J, Lundberg A, Mileusnić M, Moszczynska A, Muotka T, Preda E, Rossi P, Siergieiev D, Šimek J, Wachniew P, Angheluta V, Widerlund

References

A. 2011a. Groundwater dependent ecosystems. Part I: Hydroecological status and trends. *Environmental Science & Policy* **14**: 770-781, doi 10.1016/j.envsci.2011.04.002.

Kløve B., Allan A, Bertrand G, Druzynska E, Ertürk A, Goldscheider N, Henry S, Karakaya N, Karjalainen TP, Koundouri P, Kupfersberger H, Kvœrner J, Lundberg A, Muotka T, Preda E, Pulido-Velazquez M, Schipper P. 2011b. Groundwater dependent ecosystems. Part II. Ecosystem services and management in Europe under risk of climate change and land use intensification, *Environmental Science & Policy* **14:** 782-793. DOI 10.1016/j.envsci.2011.04.005.

Koch JC, Ewing SA, Striegl R, McKnight DM. 2013. Rapid runoff via shallow throughflow and deeper preferential flow in a boreal catchment underlain by frozen silt (Alaska, USA). *Hydrogeology Journal* **21**: 93–106.

Kong YL, Pang ZH, Li J, Huang TM. 2014. Seasonal variations of water isotopes in the Kumalak River catchments, western Tianshan mountains, Central Asia. *Fresenius Environmental Bulletin*. **23**: 169-174.

Kortelainen NM, Karhu JA. 2004. Regional and seasonal trends in the oxygen and hydrogen isotope ratios of Finnish groundwaters: a key for mean annual precipitation. *Journal of Hydrology* **285**: 143-157.

Krause S, Blume T. 2013. Impact of seasonal variability and monitoring mode on the adequacy of fiber-optic distributed temperature sensing at aquifer-river interfaces. *Water Resources Research* **49:**2408–2423. DOI: 10.1002/wrcr20232.

Krause S, Bronstert A, Zehe E. 2007. Groundwater-surface water interactions in a North German lowland floodplain- implications for the river discharge dynamics and riparian water balance. *Journal of Hydrology* **347**: 404-417.

Krause S, Hannah DM, Fleckenstein JH. 2009a. Hyporheic hydrology: interactions at the groundwater-surface water interface. *Hydrological Processes* **23**: 2103–2107. DOI: 10.1002/hyp.7366

Krause S, Heathwaite L, Binley A, Keenan P. 2009b. Nitrate concentration changes at the groundwater-surface water interface of a small Cumbrian river. *Hydrological Processes*, **23**: 2195–2211. DOI: 10.1002/hyp.7213

Krause S, Hannah DM, Sadler JP, Wood PJ. 2011a. Ecohydrology on the edge: interactions across the interfaces of wetland, riparian and groundwater-based ecosystems. *Ecohydrology* **4**: 477–480. doi: 10.1002/eco.240

Krause S, Hannah DM, Blume T. 2011b. Interstitial pore-water temperature dynamics across a pool-riffle-pool sequence. Ecohydrology **4:**549-563. DOI: 10.1002/eco.199.

Krause S, Blume T, Cassidy NJ. 2012. Investigating patterns and controls of groundwater up-welling in a lowland river by combining Fibre-optic Distributed Temperature Sensing with observations of vertical hydraulic gradients. *Hydrology and Earth System Sciences* **16**: 1775-1792. DOI: 10.5194/hess-16-1775-2012

Krause S, Boano F, Cuthbert MO, Fleckenstein JH, Lewandowski J. 2014. Understanding process dynamics at aquifer-surface water interfaces: An introduction to the special section on new modelling approaches and novel experimental technologies. *Water Resources Research* **50**: 1847–1855. DOI 10.1002/2013WR014755.

References

Kristiansen SM, Yde JC, Gómez Bárcena T, Jakobsen BH, Olsen J, Knudsen NT. 2013. Geochemistry of groundwater in front of a warm-based glacier in Southeast Greenland. *Geografiska Annaler: Series A Physical Geography* **95**: 97–108. doi:*10.1111/geoa.12003*

Kristmannsdóttir H, Ármannsson H. 2004. Groundwater in the Lake Myvatn area, North Iceland: Chemistry, origin and interaction. *Aquatic Ecology* **38**: 115–128.

Krumbein WC, Monk GD. 1943. permeability as a function of the size parametrs of unconsolidated sand. American Institute of Mining Engineering, Littleton, CO, Technical Publication pp. 153-163.

Krupa SL, Belanger TV, Heck HH, Brock JT, Jones BJ. 1998. Krupaseep-the next generation seepage meter. International Coastal Symposium (ICS 98) Special Issue **26**: 210-213.

Kumar K, Miral MS, Joshi S, Pant N, Joshi V, Joshi LM. 2009. Solute dynamics of meltwater of Gangotri glacier, Garhwal Himalaya, India. *Environmental Geology* **58**: 1151–1159. DOI 10.1007/s00254-008-1592-6

Kurylyk BL, MacQuarrie KTB, Voss CI. 2014a. Climate change impacts on the temperature and magnitude of groundwater discharge from shallow, unconfined aquifers, *Water Resources Research* **50**: *3253–3274 DOI:10.1002/2013WR014588.*

Kurylyk BL, MacQuarrie KTB, McKenzie JM. 2014b. Climate change impacts on groundwater and soil temperatures in cold and temperate regions: Implications, mathematical theory, and emerging simulation tools. *Earth-Science Reviews*, in press. DOI: 10.1016/j.earscirev.2014.06.006

La Frenierre J, Mark BG. 2014. A review of methods for estimating the contribution of glacial meltwater to total watershed discharge. *Progress in Physical Geography* **38**: 173-200. DOI: 10.1177/0309133313516161

LaBaugh JW, Winter TC, Rosenberry DO, Schuster PF, Reddy MM, Aiken GR. 1997. Hydrological and chemical estimates of the water balance of a closed-basin lake in north central Minnesota. *Water Resources Research* **33**: 2799–2812, *DOI:*10.1029/97WR02427.

Lafont M. Malard F. 2001. Oligochaete communities in the hyporheic zone of a glacial river, the Roseg River, Switzerland. *Hydrobiologia* **463**: 75-81.

Lambs L. 2004. Interactions between groundwater and surface water at river banks and the confluence of rivers. *Journal of Hydrology* **288**: 312-326.

Landmælinger Íslands [LMÍ], the Icelandic Geodetic Service 1978, 1997.

Langston G, Bentley LR, Hayashi M, McClymont A, Pidlisecky A. 2011. Internal structure and hydrological functions of an alpine proglacial moraine. *Hydrological Processes* **25**: 2967-2982. DOI: 10.1002/hyp.8144

Langston G, Hayashi M, Roy JW. 2013. Quantifying groundwater-surface water interactions in a proglacial moraine using heat and solute tracers. *Water Resources Research* **49**: 5411-5426. DOI: 10.1002/wrcr.20372

Lapham WW. 1989. Use of temperature profiles beneath streams to determine rates of vertical ground-water flow and vertical hydraulic conductivity. U.S. Geological Survey Water Supply Paper, 2337.

References

Lautz LK. 2010. Impacts of nonideal field conditions on vertical water velocity estimates from streambed temperature time series. *Water Resources Research* **46:** W01509. DOI: 10.1029/2009WR007917.

Lee DR. 1977. Device for Measuring Seepage Flux in Lakes and Estuaries. *Limnology and Oceanography* **22**: 140–147.

Lee JY, Lee KK. 2000. Use of hydrologic time series data for identification of recharge mechanism in a fractured bedrock aquifer system. *Journal of Hydrology* **229**:190–201

Leica TPS1200. *user manual 2004.*

Lemieux JM, Sudicky EA, Peltier WR, Tarasov L. 2008a. Dynamics of groundwater recharge and seepage over the Canadian landscape during the Wisconsinian glaciation. *Journal of Geophysical Research* **113**: F01011.

Lemieux JM, Sudicky EA, Peltier WR, Tarasov L. 2008b. Simulating the impact of glaciations on continental groundwater flow systems: 2. Model application to the Wisconsinian glaciation over the Canadian landscape. *Journal of Geophysical Research* **113**: F03018, 18 PP.

Lemieux JM, Sudicky EA. 2010. Simulation of groundwater age evolution during the Wisconsian glaciation over the Canadian landscape. *Environmental fluid Mechanisms* **10**: 91-102.

Lemke P, Ren J, Alley RB, Allison I, Carrasco J, Flato G, Fujii Y, Kaser G, Mote P, Thomas RH, Zhang T. 2007. Observations: changes in snow, ice and frozen ground. *In:* Solomon S, Qin D, Manning M, Chen Z, Marquis M, Averyt KB, Tignor M, Miller HL *(eds).* Climate Change 2007—The Physical Science Basis, *Contribution of Working Group I to the Fourth Assessment Report of the International Panel on Climate Change, Cambridge University Press:* Cambridge. *pages* 337-383.

León JG, Pedrozo FL. 2014. Lithological and hydrological controls on water composition: evaporite dissolution and glacial weathering in the south central Andes of Argentina (33°–34° S). *Hydrological Processes*. DOI: 10.1002/hyp.10226

Levy JS, Fountain AG, Gooseff MN, Welch KA, Lyons WB. 2011. Water tracks and permafrost in Taylor Valley, Antarctica: Extensive and shallow groundwater connectivity in a cold desert ecosystem. *Geological Society of America Bulletin* **123**: 2295-2311. DOI: 10.1130/B30436.1

Levy A, Robinson ZP, Krause S, Waller RI, Weatherill JJ. 2015. Long-term variability of proglacial groundwater-fed systems in an area of glacial retreat, Skeiðarársandur, SE Iceland. *Earth Surface Processes and Landforms*. DOI: 10.1002/esp.3696

Lewandowski J, Lischeid G, Nützmann G. 2009. Drivers of water level fluctuations and hydrological exchange between groundwater and surface water at the lowland River Spree (Germany): field study and statistical analyses. *Hydrological Processes* **23**: 2117–2128. DOI: 10.1002/hyp.7277

Li ZX, He YQ, Yang XM, Theakstone WH, Jia WX, Pu T, Liu Q, He XZ, Song B, Zhang NN, Wang SJ, Du JK. 2010. Changes of the Hailuogou glacier, Mt. Gongga, China, against the background of climate change during the Holocene. *Quaternary International* **218**: 166-175.

References

Liu F, Williams MW, Caine N. 2004. Source waters and flow paths in an alpine catchment, Colorado Front Range, United States, *Water Resources Research* **40**: W09401, DOI:10.1029/2004WR003076.

Liu QA, Liu SY, Zhang Y, Wang X, Zhang YS, Guo WQ, Xu JL. 2010. Recent shrinkage and hydrological response of Hailuogou glacier, a monsoon temperate glacier on the east slope of Mount Gongga, China. *Journal of Glaciology* **56**: 215-224.

Loheide SP II Lundquist JD. 2009. Snowmelt-induced diel fluxes through the hyporheic zone, *Water Resources Research* **45**: W07404, DOI:10.1029/2008WR007329.

Louvat P, Gíslason SR, Allegre CJ. 2008. Chemical and mechanical erosion rats in Iceland as deduced from river dissolved and solid material. *American Journal of Science* **308**: 679–726. DOI 10.2475/05.2008.02]

Lowry CS, Walker JF, Hunt RJ, Anderson MP. 2007. Identifying spatial variability of groundwater discharge in a wetland stream using a distributed temperature sensor. *Water Resources Research* **43**: W10408 DOI:10.1029/2007WR006145.

MacDonald AM, Maurice L, Dobbs MR, Reeves HJ, Auton CA. 2012. Relating *in situ* hydraulic conductivity, particle size and relative density of superficial deposits in a heterogeneous catchment. *Journal of Hydrology* **434-435**: 130-141.

Magilligan FJ, Gomez B, Mertes LAK, Smith LC, Smith ND, Finnegan D, Garvin JB. 2002. Geomorphic effectiveness, sandur development, and the pattern of landscape response during jökulhlaups: Skeiðarársandur, south eastern Iceland. *Geomorphology* **44:** 95–113. http://dx.doi.org/10.1016/S0169-555X(01)00147-7.

Magnusson J, Kobierska F, Huxol S, Hayashi M, Jonas T, Kirchner JW. 2014. Melt water driven stream and groundwater stage fluctuations on a glacier forefield (Dammagletscher, Switzerland). *Hydrological Processes* **28**: 826-836. DOI: 10.1002/hyp.9633

Mäkinen R, Orvomaa M, Veijalainen N, Huttunen I. 2008. The climate change and groundwater regimes in Finland. Proceedings 11th International Specialized Conference on watershed & River Basin Management, Budapest, Hungary, ISBN 978-963-06-5689-4.

Makridakis S., Wheelwright SC, Hyndman RJ. 1998. Forecasting, methods and applications. John Wiley and Sons: Hoboken, New Jersey. 3rd edition.

Malard F, Tockner K, Ward J. 1999. Shifting dominance of subcatchment water sources and flow paths in a glacial floodplain, Val Roseg, Switzerland. *Arctic, Antarctic and Alpine Research* **31:** 135-150. DOI: 10.2307/1552602

Malard F, Mangin A, Uehlinger U, Ward JV. 2001. Thermal heterogeneity in the hyporheic zone of a glacial floodplain. *Canadian Journal of Fish and Aquatic Sciences* **58**: 1319–1335. DOI:10.1139/cjfas-58-7-1319

Malard F, Uehlinger U, Tockner K. 2006. Flood-pulse and riverscape dynamics in a braided glacial river. *Ecology* **87**: 704–716.

Malcolm IA, Soulsby C, Youngson AF. 2002. Thermal regime in the hyporheic zone of two contrasting salmonid spawning streams. Fisheries Management and *Ecology* **9**: 1-10.

Marciniak M, Dragon K, Chudziak L. 2014. Water circulation within a high-Arctic glaciated valley (Petunia Bay, Central Spitsbergen): Recharge of a glacial river. *Journal of Hydrology* **513**: 91-100 DOI: 10.1016/j.jhydrol.2014.03.023

References

Mark BG, Seltzer GO. 2003. Tropical glacier meltwater contribution to stream discharge: a case study in the Cordillera Blanca, Peru. *Journal of Glaciology* **49**: 271-281.

Mark BG, McKenzie JM, Gomez J. 2005. Hydrochemical evaluation of changing glacier meltwater contribution to stream discharge: Callejon de Huaylas, Peru. *Hydrological Sciences–Journal–des Sciences Hydrologiques* **50**: 975-987.

Marren PM. 2002a. Fluvial–lacustrine interaction on Skeiðarársandur, Iceland: implications for sandur evolution. *Sedimentary Geology* **149**: 43-58. http://dx.doi.org/10.1016/S0037-0738(01)00243-3.

Marren PM. 2002b. Glacier margin fluctuations, Skaftafellsjökull, Iceland: implications for sandur evolution. *Boreas*, vol. 31, pp. 75-81.

Marren PM. 2005. Magnitude and frequency in proglacial rivers: a geomorphological and sedimentological perspective. *Earth-Science Reviews* **70**: 203-251. DOI: 10.1016/j.earscirev.2004.12.002

Marren PM, Toomath SC. 2013*:* Fluvial adjustments in response to glacier retreat: Skaftafellsjökull, Iceland*. Boreas* **42**: 57-70. DOI: 10.1111/j.1502-3885.2012.00275.x

Marteinsdóttir B, Svavarsdóttir K, Thórhallsdóttir TE. 2010. Development of vegetation patterns in early primary succession. *Journal of Vegetation Science* **21**: 531-540. DOI: 10.1111/j.1654-1103.2009.01161.x

Marteinsdóttir B, Thórhallsdóttir TE, Svavarsdóttir K. 2013. An experimental test of the relationship between small scale topography and seedling establishment in primary succession. *Plant Ecology* **214**: 1007-1015. DOI: 10.1007/s11258-013-0226-6

Mayr C, Lücke A, Stichler W, Trimborn P, Ercolano B, Oliva G, Ohlendorf C, Soto J, Fey M, Haberzettl T, Janssen S, Schäbitz F, Schleser GH, Wille M, Zolitschka B. 2007. Precipitation origin and evaporation of lakes in semi-arid Patagonia (Argentina) inferred from stable isotopes ($\delta^{18}O$, $\delta^{2}H$). *Journal of Hydrology* **334**: 53–63. DOI: 10.1016/j.jhydrol.2006.09.025

McCallum AM, Andersen MS, Rau GC, Larsen JR, Acworth RI. 2014. River-aquifer interactions in a semiarid environment investigated using point and reach measurements. *Water Resources Research* **50**: 2815–2829, doi:10.1002/2012WR012922.

McClymont AF, Hayashi M, Bentley LR, Liard J. 2012. Locating and characterising groundwater storage areas within an alpine watershed using time-lapse gravity, GPR and seismic refraction methods. *Hydrological Processes* **26**: 1792-1804.

Meierbachtol T, Harper J, Humphrey N. 2013. Basal drainage system response to increasing surface melt on the Greenland Ice Sheet. *Science* **341**: 777-779. *DOI: 10.1126/science.1235905*

Meinikmann K, Lewandowski J, Nützmann G. 2013. Lacustrine groundwater discharge: Combined determination of volumes and spatial patterns. *Journal of Hydrology*, Volume **502**: 202-211. http://dx.doi.org/10.1016/j.jhydrol.2013.08.021.

Melvold K, Schuler T, Lappegard G. 2003. Ground-water intrusions in a mine beneath Høganesbreen, Svalbard: assessing the possibility of evacuating water subglacially. *Annals of Glaciology* **37**: 269-274.

Meriano M, Eyles N. 2003. Groundwater flow through Pleistocene glacial deposits in the rapidly urbanizing Rouge River–Highland Creek watershed, City of Scarborough, southern Ontario, Canada. H*ydrogeology Journal* **11**: 288-303. DOI 10.1007/s10040-002-0226-4

References

Meriano M, Eyles N. 2009. Quantitative assessment of the hydraulic role of subglaciofluvial interbeds in promoting deposition of deformation till (Northern Till, Ontario). *Quaternary Science Reviews* **28**: 608-620.

Merlivat L, Jouzel J. 1979. Global climatic interpretation of the deuterium-oxygen 18 relationship for precipitation. *Journal of Geophysical Research* **84**: 5029 - 5033

Michel RL, Turk JT, Campbell DH, Mast MA. 2002. Use of natural 35S to trace sulphate cycling in small lakes, Flattops Wilderness Area, Colorado, U.S.A. *Water Air Soil Pollution Focus* **2**: 5–18.

Milner AM, Petts GE. 1994. Glacial rivers: physical habitat and ecology. *Freshwater Biology* **32:** 295–307. DOI: 10.1111/j.1365-2427.1994.tb01127.x

Milner AM, Brittain JE, Castella E, Petts GE. 2001. Trends of macroinvertebrate community structure in glacier-fed rivers in relation to environmental conditions: a synthesis. Freshwater Biology **46**: 1833–1847. doi: 10.1046/j.1365-2427.2001.00861.x

Milner AM, Brown LE, Hannah DM. 2009. Hydroecological response of river systems to shrinking glaciers. *Hydrological Processes* **23**: 62-77. DOI: 10.1002/hyp.7197

Moeller CA, Mickelson DM, Anderson MP, Winguth C. 2007. Groundwater flow beneath Late Wichselian glacier ice in Nordfjord, Norway. *Journal of Glaciology* **53**: 84-90.

Mohanty BP, Kanwar RS, Everts CJ. 1994. Comparison of saturated hydraulic conductivity measurement methods for a glacial-till soil. *Soil Science Society of America Journal* **58**: 672-677.

Moore RD. 2006. Stream temperature patterns in British Columbia, Canada, based on routine spot measurements. *Canadian Water Resources Journal* **31**:41-56.

Moore RD, Fleming SW, Menounos B, Wheate R, Fountain A, Stahl K, Holm K, Jakob M. 2009. Glacier change in western North America: influences on hydrology, geomorphic hazards and water quality. *Hydrological Processes* **23**: 42–61 DOI: 10.1002/hyp.7575

Moss B. 2012. Cogs in the endless machine: Lakes, climate change and nutrient cycles: a review. *Science of The Total Environment* **434:** 130–142.

Mountney NP, Russell AJ. 2009. Aeolian dune-field development in a water Table-controlled system: Skeiðarársandur, Southern Iceland. *Sedimentology* **56** : 2107-2131.

Muellegger C Weilhartner A, Battin TJ, Hofmann T. 2013. Positive and negative impacts of five Austrian gravel pit lakes on groundwater quality. *Science of the Total Environment* **443**: 14-23. DOI: 10.1016/j.scitotenv.2012.10.097

Muir DL, Hayashi M, McClymont AF. 2011. Hydrological storage and transmission characteristics of an alpine talus. *Hydrological Processes* **25**: 2954-2966. DOI: 10.1002/hyp.8060

Murdoch LC, Kelly SE. 2003. Factors affecting the performance of conventional seepage meters. W*ater Resources Research* **39**: 1163, DOI:10.1029/2002WR001347

Murray T, Dowdeswell JA .1992. Water throughflow and the physical effects of deformation on sedimentary glacier beds*. Journal of Geophysical Research: Solid Earth* **97**: 8993–9002. DOI: 10.1029/92JB00409*.*

References

Nawri N, Björnsson H. 2010. Surface air temperature and precipitation trends for Iceland in the 21st century. Icelandic Meteorological Office, report 2010-005. http://www.vedur.is/media/ces/2010_005.pdf. Viewed online, April 2011.

Nelitz, MA, Moore RD, Parkinson E. 2008. Developing a Framework to Designate Temperature Sensitive Streams in the B. C. Interior. Report prepared by ESSA Technologies Ltd., the University of British Columbia, and B. C.Ministry of Environment, Vancouver, B. C. for B. C. Forest Science Program, PricewaterhouseCoopers, Vancouver,

Neumann C, Beer J, Blodau C, Peiffer S, Fleckenstein JH. 2013. Spatial patterns of groundwater-lake exchange – implications for acid neutralization processes in an acid mine lake. *Hydrological Processes* **27**: 3240–3253. DOI: 10.1002/hyp.9656

Nield JM, Chiverrell RC, Darby SE, Leyland J, Vircavs LH, Jacobs B. 2013. Complex spatial feedbacks of tephra redistribution, ice melt and surface roughness modulate ablation on tephra covered glaciers. *Earth Surface Processes and Landforms* **38:** 95-102. DOI:10.1002/esp.3352

Nienow P, Sharp M, Willis I. 1998. Seasonal changes in the morphology of the subglacial drainage system, Haut Glacier d'Arolla, Switzerland. *Earth Surface Processes and Landforms* **23**: 825–843. DOI: 10.1002/(SICI)1096-9837(199809)23:9<825::AID-ESP893>3.0.CO;2-2

Nolin AW, Phillippe J, Jefferson A, Lewis SL. 2010. Present-day and future contributions of glacier runoff to summertime flows in a Pacific Northwest watershed: Implications for water resources. *Water Resources Research* **46**:W12509. DOI:10.1029/2009WR008968.

Norman FA, Cardenas MB. 2014. Heat transport in hyporheic zones due to bedforms: An experimental study*, Water Resources Research* **50***:* 3568–3582*, doi:*10.1002/2013WR014673*.*

Normani SD, Sykes JF. 2012. Paleohydrogeologic simulations of Laurentide ice-sheet history on groundwater at the eastern flank of the Michigan Basin. *Geofluids* **12**: 97–122. DOI: 10.1111/j.1468-8123.2012.00362.x

Ó Dochartaigh BÉ. 2012. Personal communication

Ogmundsson, G. personal communication, May 2013.

Ohlanders N, Rodriguez M, McPhee J. Stable water isotope variation in a Central Andean watershed dominated by glacier and snowmelt. 2013. *Hydrology and Earth System Sciences* **17**: 1035-1050. DOI:10.5194/hess-17-1035-2013.

Okkonen J, Kløve B. 2010. A conceptual and statistical approach for the analysis of climate impact on ground water table fluctuation patterns in cold conditions. Journal of Hydrology **388**: 1-12. DOI: 10.1016/j.jhydrol.2010.02.015.

Okkonen J, Kløve B. 2012. Assessment of temporal and spatial variation in chemical composition of groundwater in an unconfined esker aquifer in the cold temperate climate of Northern Finland. *Cold Regions Science and Technology* **71**:118-128. DOI: 10.1016/j.coldregions.2011.10.003

Okkonen J, Jyrkama M, Kløve B. 2009. A conceptual approach for assessing the impact of climate change on groundwater and related surface waters in cold regions (Finland). *Hydrogeology Journal* **18**: 429-439.

References

Óladóttir BA, Larsen G, Sigmarsson O. 2011. Holocene volcanic activity at Grímsvötn, Bárdarbunga and Kverkfjöll subglacial centres beneath Vatnajökull, Iceland. *Bulletin of Volcanology* **73**: 1187-1208. DOI 10.1007/s00445-011-0461-4.

Olichwer T, Tarka R, Modelska M. 2013. Chemical composition of groundwaters in the Hornsund region, southern Spitsbergen. *Hydrology Research* **44**: 117-130.

Olsson J, Stipp SLS, Dalby KN, Gíslason SR. 2013. Rapid release of metal salts and nutrients from the 2011 Grímsvötn, Iceland volcanic ash. G*eochimica et Cosmochimica Acta* **123**: 134-149. http://dx.doi.org/10.1016/j.gca.2013.09.009.

Óskarsdóttir SM, Gíslason SR, Snorasson A, Halldorsdottir SG, Gisladottir G. 2011. Spatial distribution of dissolved constituents in Icelandic river waters. *Journal of Hydrology* **397:** 175-190. 10.1016/j.jhydrol.2010.11.028.

Oskarsson N, Sigvaldason GE, Steinthórsson S. 1982. A dynamic model of rift zone petrogenesis and the regional petrology of Iceland. Journal of Petrology **23**: 28–74.

Pagli C, Sigmundsson F, Lund B, Sturkell E, Geirsson H, Einarsson P, Árnadóttir T, Hreinsdóttir S. 2007. Glacio-isostatic deformation around the Vatnajökull ice cap, Iceland, induced by recent climate warming: GPS observations and finite element modelling. *Journal of Geophysical Research* **112:** B08405. DOI: 10.1029/2006JB004421.

Pálsson S, Zóphóniasson S, Sigurðsson O, Kristmannsdóttir H, Aðalsteinsson H. 1992. Skeiðarárhlaup og framlaup Skeiðarárjökull 1991. Report OS-92035/VOD-09 B. Orkustofnun (National Energy Authorities), Reykjavík, Iceland, 33

Panagopoulos G, Lambrakis N. 2006. The contribution of time series analysis to the study of the hydrodynamic characteristics of the karst systems: Application on two typical karst aquifers of Greece (Trifilia, Almyros Crete). *Journal of Hydrology* **329**: 368-376 DOI: 10.1016/j.jhydrol.2006.02.023

Paulsen RJ, Smith CF, O'Rourke D, Wong TF. 2001. Development and evaluation of an ultrasonic ground water seepage meter. *Ground Water* **39**: 904–911.

Penna D, Stenni B, Sanda M, Wrede S, Bogaard TA, Gobbi A, Borga M, Fischer BMC, Bonazza M, Chárová Z. 2010. On the reproducibility and repeatability of laser absorption spectroscopy measurements for δ^2H and $\delta^{18}O$ isotopic analysis. *Hydrology and Earth System Sciences* **14**: 1551–1566. DOI:10.5194/hess-14-1551-2010.

Person M, McIntosh J, Bense V, Remenda VH. 2007a. Pleistocene hydrology of North America: The role of ice sheets in reorganizing groundwater flow systems. *Reviews of Geophysics* **45** RG3007. *DOI:10.1029/2006RG000206.*

Person M. 2007b. Pleistocene Hydrogeology of the Atlantic continental shelf, New England. In: Knight PG (ed.)*Glacier Science and Environmental Change*, Blackwell Publishing, Malden, MA, USA.

Person M, Bense V, Cohen D, Banerjee A. 2012. Models of ice-sheet hydrogeologic interactions: a review. *Geofluids* **12**: 58–78. DOI: 10.1111/j.1468-8123.2011.00360.x

Picarro, Inc. 2008. Picarro L1102- i Isotopic Water Liquid Analyzer.

Piotrowski JA. 1994. Tunnel-Valley formation in northwest Germany- geology, mechanisms of formation and subglacial bed conditions for the Bornhöved tunnel valley. *Sedimentary Geology* **89**: 107-141.

References

Piotrowski JA. 1997a. Subglacial hydrology in northwestern Germany during the last glaciation: groundwater flow, tunnel valleys, and hydrological cycles. *Quaternary Science Reviews* **16**: 169-185.

Piotrowski JA. 1997b. Subglacial groundwater flow during the last glaciation in northwestern Germany. *Sedimentary Geology* **111**: 217-224.

Piotrowski JA. 2007. Groundwater under ice sheets and glaciers. In: Knight PG (ed.) *Glacier Science and Environmental Change*, Blackwell Publishing, Malden, MA, USA.

Piotrowski JA and Kraus A. 1997. Response of sediment to ice sheet loading in northwestern Germany. *Journal of Glaciology* **43**: 495-502.

Pogge von Strandmann PAE, Burton KW, James RH, van Calsteren P, Gíslason SR, Sigfusson B. 2008. The influence of weathering processes on riverine magnesium isotopes in a basaltic terrain. *Earth Planetary Science Letters* **276**: 187–197.

Pringle C. 2003. What is hydrologic connectivity and why is it ecologically important?. *Hydrological Processes* **17**: 2685–2689. DOI: 10.1002/hyp.5145

Provost AM, Voss CI, Neuzil CE. 2012. Glaciation and regional groundwater flow in the Fennoscandian shield. *Geofluids* **12**: 79–96. DOI: 10.1111/j.1468-8123.2012.00361.x

Puckett WE, Dane JH, Hajek BF. 1985. Physical and mineralogical data to determine soil hydraulic properties. *Soil Science Society of America Journal* **49**: 831–836.

Quincey DJ, Braun M, Glasser NF, Bishop MP, Hewitt K, Luckman A. 2011. Karakoram glacier surge dynamics. *Geophysical Research Letters* **38**: L18504.

Radić V, Hock R. 2014. Glaciers in the Earth's Hydrological Cycle: Assessments of Glacier Mass and Runoff Changes on Global and Regional Scales. *Surveys in Geophysics* **35**: 813-837. DOI 10.1007/s10712-013-9262-y

Radić V, Bliss A Beedlow AC, Hock R, Miles E, Cogley JG. 2013. Regional and global projections of twenty-first century glacier mass changes in response to climate scenarios from global climate models. *Climate Dynamics* **42**: 37-58. DOI: 10.1007/s00382-013-1719-7

Raiswell R, Thomas AG. 1984. Solute acquisition in glacial melt water. I. Fjallsjökull (south-east Iceland): Bulk melt waters with closed-system characteristics. *Journal of Glaciology* **30**: 35-43.

Rau GC, Andersen MS, McCallum AM, Roshan H, Acworth RI. 2014. Heat as a tracer to quantify water flow in near-surface sediments. *Earth-Science Reviews* **129**: 40-58. DOI: 10.1016/j.earscirev.2013.10.015

Rautio A, Korkka-Niemi K. 2011. Characterization of groundwater-lake water interactions at Pyhäjärvi, a lake in SW Finland. *Boreal Environment Research* **16**: 363-380.

Rawls WJ, Brakensiek DL. 1989. Estimation of soil water retention and hydraulic properties. In: HJ Morel-Seytoux (Ed.) *Unsaturated Flow in Hydrologic Modelling Theory and Practice*: pages 275-300. Dordrecht, the Netherlands: Kluwer Academic Publishers.

Richards K, Sharp M, Arnold N, Gurnell A, Clark M, Tranter M, Nienow P, Brown G, Willis I, Lawson W. 1996. An integrated approach to modelling hydrology and water quality in glacierized catchments. *Hydrological Processes* **10**: 479–508. doi: 10.1002/(SICI)1099-1085(199604)10:4<479::AID-HYP406>3.0.CO;2-D

References

Roberts MJ, Pálsson F, Guðmundsson MT, Björnsson H, Tweed FS. 2005. Ice-water interactions during floods from Grænalón glacier-dammed lake, Iceland. *Annals of Glaciology* **40:** 133-138.

Robinson ZP. 2003. The geochemistry and behaviour of shallow groundwater in an Icelandic sandur. PhD thesis, Keele University.

Robinson CT, Kawecka B. 2005. Benthic diatoms of an Alpine stream/lake network in Switzerland. *Aquatic Sciences* **67**: 492-506.

Robinson ZP, Fairchild IJ, Russell AJ. 2008. Hydrogeological implications of glacial landscape evolution at Skeiðarársandur, SE Iceland. *Geomorphology* **97**: 218-236. DOI: 10.1016/j.geomorph.2007.02.044

Robinson ZP, Fairchild IJ, Spiro B. 2009a. The sulphur isotope and hydrochemical characteristics of Skeiðarársandur, Iceland: identification of solute sources and implications for weathering processes. *Hydrological Processes* **23:** 2212–2224. DOI: 10.1002/hyp.7368. DOI: 10.1002/hyp.7368

Robinson ZP, Fairchild IJ, Arrowsmith C. 2009b. Stable isotopes tracers of shallow groundwater recharge dynamics and mixing within an Icelandic sandur, Skeiðarársandur. In: Marks D, Hock R, Lehning M, Hayashi M, Gurney R (eds.). *Hydrology in Mountain Regions*, International Association of Hydrological Sciences publication no. 326.

Ronayne MJ, Houghton TB, Stednick JD. 2012. Field characterization of hydraulic conductivity in a heterogeneous alpine glacial till. *Journal of Hydrology* **458-459**: 103-109. http://dx.doi.org/10.1016/j.jhydrol.2012.06.036

Rosenberry DO, LaBaugh JW. 2008. Field techniques for estimating water fluxes between surface water and ground water: U.S. Geological Survey Techniques and Methods 4–D2, 128 pages.

Rosenberry DO, Toran L, Nyquist JE. 2010. Effect of surficial disturbance on exchange between groundwater and surface water in nearshore margins. *Water Resources Research* **46**: W06518, DOI:10.1029/2009WR008755.

Rosenberry DO, Sheibley RW, Cox SE, Simonds FW, Naftz DL. 2013. Temporal variability of exchange between groundwater and surface water based on high-frequency direct measurements of seepage at the sediment-water interface. *Water Resources Research* **49**: 2975–2986. doi:10.1002/wrcr.20198.

Rossaro B, Lencioni V, Boggero A,Marziali L. 2006. Chironomids from southern Alpine running waters: ecology, biogeography. *Hydrobiologia* **562**: 231–246.

Rossi PM, Ala-aho P, Ronkanen A, Kløve B. 2012. Groundwater-surface water interaction between an esker aquifer and a drained fen. *Journal of Hydrology* **432-433**: 52-60. DOI: 10.1016/j.jhydrol.2012.02.026

Röthlisberger H, Lang H. 1987. Glacial hydrology. In: Gurnell AM, Clark MJ (Eds). *Glacio-Fluvial Sediment Transfer: An Alpine Perspective* pages: 207–284. John Wiley, Chichester, UK.

Roy JW, Hayashi M. 2008. Groundwater exchange with two small alpine lakes in the Canadian Rockies. *Hydrological Processes* **22**: 2838-2846. DOI: 10.1002/hyp.6995

Roy JW, Hayashi M. 2009. Multiple, distinct groundwater flow systems of a single moraine-talus feature in an alpine watershed. *Journal of Hydrology* **373**: 139-150. DOI: 10.1016/j.jhydrol.2009.04.018

References

Roy JW, Zaitlin B, Hayashi M, Watson SB. 2011. Influence of groundwater spring discharge on small-scale spatial variation of an alpine stream ecosystem. *Ecohydrology* **4**: 661-670. DOI: 10.1002/eco.156.

Rozanski K, Araguás-Araguás L, Gonfiantini R. 1993. Isotopic patterns in modern global precipitation. In: Swart PK, Lohmann KC, Mckenzie J, Savin S (eds.) *Climate Change in Continental Isotopic Records*. American Geophysical Union, Geophysical Monograph vol. 78, pages1–36.

Ruelland D, Brisset N, Jourde H, Oyarzun R. 2011. Modelling the impact of climatic variability on groundwater and surface flows from a mountainous catchment in the Chilean Andes. *Cold Region Hydrology in a Changing Climate* (Proceedings of symposium H02 held during IUGG2011 in Melbourne, Australia, July 2011) (IAHS Publ. **346**:171-179).

Russell AJ, Knight PG, van Dijk TAGP. 2001. Glacier surging as a control on the development of proglacial fluvial landforms and deposits, Skeiðarársandur, Iceland. *Global and Planetary Change* **28**: 163–174. DOI: 10.1016/S0921-8181(00)00071-0

Russell AJ, Roberts MJ, Fay H, Marren PM, Cassidy NJ, Tweed FS, Harris T. 2006. Icelandic jökulhlaup impacts: implications for ice-sheet hydrology, sediment transfer and geomorphology. *Geomorphology* **75:** 33–64. DOI: 10.1016/j.geomorph.2005.05.018

Rutter N, Hodson A, Irvine-Fynn T, Kristensen Solås. 2011 Hydrology and hydrochemistry of a deglaciating high-Arctic catchment, Svalbard. *Journal of Hydrology* **410**: 39-50. DOI: 10.1016/j.jhydrol.2011.09.001

Saulnier-Talbot E, Leng MJ, Pienitz R. 2007. Recent climate and stable isotopes in modern surface waters of northernmost Ungava Peninsula, Canada. *Canadian Journal of Earth Sciences* **44**: 171–180.

Sawyer AH, Cardenas MB. 2009. Hyporheic flow and residence time distributions in heterogeneous cross-bedded sediment. *Water Resources Research* **45**: W08406, DOI:10.1029/2008WR007632,

Sawyer AH, Cardenas MB, Bomar A, Mackey M. 2009. Impact of dam operations on hyporheic exchange in the riparian zone of a regulated river. *Hydrological Processes* **23**: 2129–2137. DOI: 10.1002/hyp.7324

Scheidegger JM*,* Bense VF. 2014. Impacts of glacially recharged groundwater flow systems on talik evolution. *Journal of Geophysical Research Earth Surface* **119***:* 758–778*, doi:*10.1002/2013JF002894

Scheidegger JM*,* Bense VF, Grasby SE. 2012. Transient nature of Arctic spring systems driven by subglacial meltwater. *Geophysical Research Letters* **39***: L12405, doi:*10.1029/2012GL051445*.*

Schmidt C, Bayer-Raich M, Schirmer M. 2006. Characterization of spatial heterogeneity of groundwater–stream water interactions using multiple depth streambed temperature measurements at the reach scale. *Hydrology and Earth System Sciences* **10**: 849–859.

Schmidt C, Brewster C, Bayer-Raich M, Schirmer M. 2007. Evaluation and field-scale application of an analytical method to quantify groundwater discharge using mapped streambed temperatures. *Journal of Hydrology* **347**: 292-307. DOI: 10.1016/j.jhydrol.2007.08.022

Schmidt A, Gibson JJ, Santos IR, Schubert M, Tattrie K, Weiss H. 2010. The contribution of groundwater discharge to the overall water budget of two typical Boreal lakes in

References

Alberta/Canada estimated from a radon mass balance. *Hydrology and Earth System Sciences* **14**: 79-89, DOI:10.5194/hess-14-79-2010.

Schmidt C, Musolff A, Trauth N, Vieweg M, Fleckenstein JH. 2012. Transient analysis of fluctuations of electrical conductivity as tracer in the stream bed. *Hydrology and Earth System Sciences* **16:** 3689-3697. DOI:10.5194/hess-16-3689-2012

Schneider P, Vogt T, Schirmer M, Doetsch J, Linde N, Pasquale N, Perona P, Cirpka OA. 2011. Towards improved instrumentation for assessing river–groundwater interactions in a restored river corridor. *Hydrology and Earth System Sciences* **15**: 2531–2549. DOI: 10.5194/hess-15-2531-2011

Schornberg C, Schmidt C, Kalbus E, Fleckenstein JH. 2010., Simulating the effects of geologic heterogeneity and transient boundary conditions on streambed temperatures — Implications for temperature-based water flux calculations. *Advances in Water Resources* **33**: 1309-1319, ISSN 0309-1708, http://dx.doi.org/10.1016/j.advwatres.2010.04.007.

Sebok E, Duque C, Kazmierczak J, Engesgaard P, Nilsson B, Karan S, Frandsen M. 2013. High-resolution distributed temperature sensing to detect seasonal groundwater discharge into Lake Væng, Denmark. *Water Resources Research* **49**: 5355-5368. DOI:10.1002/wrcr.20436.

Selbekk RS, Tronnes RG. 2007. The 1362 AD Öræfajökull eruption, Iceland: petrology and geochemistry of large-volume homogeneous rhyolite. *Journal of Volcanology and Geothermal Research* **160**: 42–58. DOI: 10.1016/j.jvolgeores.2006.08.005

Selker JS, Thévenaz L, Huwald H, Mallet A, Luxemburg W, van de Giesen N, Stejskal M, Zeman J, Westhoff M, Parlange MB. 2006a. Distributed fiber-optic temperature sensing for hydrologic systems. *Water Resources Research* **42**: W12202. DOI: 10.1029/2006WR005326.

Selker JS, van de Giesen N, Westhoff M, Luxemburg W, Parlange MB. 2006b. Fiber optics opens window on stream dynamics. *Geophysical Research Letters* **33**: L24401. DOI: 10.1029/2006GL027979.

Sensornet. 2009. Online. http://www.sensornet.co.uk/images/technology/halo/download8a2d.cfm.pdf. Accessed on August 2013.

Shaw J. 1985. Subglacial and ice marginal environments. In: Ashley GM, Shaw J, Smith ND (eds.) *Glacial sedimentary environments*: Society of Economic Paleontologists and Mineralogists Short Course No. 16, 246 p.

Shaw GD, White ES, Gammons CH. 2013. Characterizing groundwater-lake interactions and its impact on lake water quality. *Journal of Hydrology* **492**: 69-78. DOI: 10.1016/j.jhydrol.2013.04.018.

Sholkovitz E, Herbold C, Charette M. 2003. An automated dye dilution based seepage meter for the time-series measurement of submarine groundwater discharge. *Limnology and Oceanography Methods* **1**: 16–28, 2003.

Sigfusson B, Gíslason SR, Paton GI. 2008. Pedogenesis and weathering rates of a Histic Andosol in Iceland: field and experimental soil solution study. *Geoderma* **144**: 572–592.

Sigurðsson F. 1990. Groundwater from glacial areas in Iceland. *Jökull* **40**: 119-145.

Sigurðsson F. 1993. Groundwater chemistry and aquifer classification in Iceland. *Memoires of the XXIVth Congress of IAH*, ÅS, Oslo.

References

Sigurðsson O. 1998: Glacier variations in Iceland 1930–1995 – from the database of the Icelandic Glaciological Society. *Jökull* **45**: 3–25.

Sigurðsson F, Einarsson K. 1988. Groundwater resources of Iceland – availability and demand. *Jökull* **38**: 35-53.

Simpkins WS, Mickleson DM. 1990. Groundwater flow systems and geochemistry near the margin of the Burroughs Glacier. *Proceedings of the Second Glacier Bay Science Symposium,* National Park Service, Anchorage, Alaska.

Skaftafell Sérkort 5 hiking map . 2009. Published by Mál og menning/Forlagið

Slemmons, KEH, Saros JE. 2012. Implications of nitrogen-rich glacial meltwater for phytoplankton diversity and productivity in alpine lakes. *Limnology & Oceanography* **57**: 1651-1663. DOI: 10.4319/lo.2012.57.6.1651

Slemmons KEH, Saros JE, Simon K. 2013. The influence of glacial meltwater on alpine aquatic ecosystems: a review. *Environmental Science Processes and Impacts.* **15**: 1794-1806. DOI: 10.1039/c3em00243h.

Smerdon BD, Devito KJ, Mendoza CA. 2005. Interaction of groundwater and shallow lakes on outwash sediments in the sub-humid Boreal Plains of Canada. *Journal of Hydrology* **314**: 246-262. DOI: 10.1016/j.jhydrol.2005.04.001

Smerdon, BD, Mendoza CA, Devito KJ. 2012. The impact of gravel extraction on groundwater dependent wetlands and lakes in the Boreal Plains, Canada. *Environmental Earth Sciences*. **67**: 1249-1259. DOI 10.1007/s12665-012-1568-4

Smith BPG, Hannah DM, Gurnell AM, Petts GE. 2001. A hydrogeomorphological context for ecological research on alpine glacial rivers. *Freshwater Biology* **46**: 1579–1596.

Solberg IL, Hansen L, Rokoengen K, Sveian H, Olsen L. 2008. Deglaciation history and landscape development of fjord-valley deposits in Buvika, Mid-Norway. *Boreas* **37**: 297-315. DOI: 10.1111/j.1502-3885.2007.00020.x

Song J, Chen X, Cheng C, Wang D, Lackey S, Xu Z. 2009. Feasibility of grain-size analysis methods for determination of vertical hydraulic conductivity of streambeds. *Journal of Hydrology* **375**:428-437. DOI: 10.1016/j.jhydrol.2009.06.043

Soulsby C, Tetzlaff D, Van Den Bedem D, Malcolm IA, Bacon PJ, Youngson AF. 2007. Inferring groundwater influences on surface water in montane catchments from hydrochemical surveys of springs and streamwaters. *Journal of Hydrology* **333**: 199-213. DOI: 10.1016/J.JHYDROL.2006.08.016

St. Jacques JM, Lapp SL, Zhao Y, Barrow EM, Sauchyn DJ. 2013. Twenty-first century central Rocky Mountain river discharge scenarios under greenhouse forcing, *Quaternary International* **310**: 34-46 DOI: 10.1016/j.quaint.2012.06.023

Stephenson DA, Fleming AH, Mickelson DM. 1988. The hydrogeology of glacial deposits: *The Decade of North American Geology*. The Geological Society of America.

Stewart IT. 2009. Changes in snowpack and snowmelt runoff for key mountain regions. *Hydrological Processes* **23**: 78-94 DOI: 10.1002/hyp.7128.

Stonedahl SH, Harvey JW, Wörman A, Salehin M, Packman A I. 2010. A multiscale model for integrating hyporheic exchange from ripples to meanders. *Water Resources Research* **46**: W12539, DOI:10.1029/2009WR008865, 2010.

References

Stonestrom DA, Constantz J. 2003. Heat as a tool for studying the movement of ground water near streams. US Geological Survey Circular 1260.

Storey RG, Howard KWF, Williams DD. 2003. Factors controlling riffle-scale hyporheic exchange flows and their seasonal changes in a gaining stream: A three-dimensional groundwater flow model, *Water Resources Research*, **39**: 1034, DOI:10.1029/2002WR001367,.

Stotler RL, Frape SK, El Mugammar HT, Johnston C, Judd-Henry I, Harvey FE, Drimmie R, Jones JP. 2010. Geochemical heterogeneity in a small, stratigraphically complex moraine aquifer system (Ontario, Canada): interpretation of flow and recharge using multiple geochemical parameters. *Hydrogeology Journal* **19**: 101–115. 10.1007/s10040-010-0628-7

Stott T, Mount N. 2007. Alpine proglacial suspended sediment dynamics in warm and cool ablation seasons: Implications for global warming. *Journal of Hydrology* **332**: 259–270.

Sutton RJ, Deas ML, Tanaka SK, Soto T, Corum RA. 2007. Salmonid observations at a Klamath River thermal refuge under various hydrological and meteorological conditions. *River Research and Applications* **23**: 775-785. DOI: 10.1002/rra.1026

Tague C, Grant GE. 2009. Groundwater dynamics mediate low-flow response to global warming in snow-dominated alpine regions. *Water Resources Research* **45**: *W0742.* DOI: 10.1029/2008WR007179

Tague C, Farrell M, Grant G, Lewis S, Rey S. 2007. Hydrogeologic controls on summer stream temperature in the McKenzie River basin, Oregon. *Hydrological Processes* **21**: 3288-3300.

Tague C, Grant G, Farrell M, Choate J, Jefferson A. 2008. Deep groundwater mediates streamflow response to climate warming in the Oregon Cascades. *Climatic Change* **86**: 189-210. DOI: 10.1007/s10584-007-9294-8

Taylor RG, Scanlon B, Döll P, Rodell M, van Beek R Wada Y, Longuevergne L, Leblanc M, Famiglietti JS, Edmunds M, Konikow L, Green TR, Chen JY, Taniguchi M, Bierkens MFP, MacDonald A, Fan Y, Maxwell RM, Yechieli Y, Gurdak JJ, Allen DM, Shamsudduha M, Hiscock K, Yeh PJF, Holman I, Treidel H. 2013. Ground water and climate change. *Nature Climate Change* **3**: 322-329. DOI: 10.1038/NCLIMATE1744

The Icelandic Geodetic Survey, Landmælingar Íslands (LMÍ).

The Icelandic Glaciological Society (IGS) database. 2013.

The Icelandic Meteorological Office (IMO) [Veðurstofa Íslands] (2013).

Theakstone WH, Knudsen NT. 1996. Isotopic and ionic variations in glacier river water during three contrasting ablation seasons. *Hydrological Processes* **10**: 523-539. doi: 10.1002/(SICI)1099-1085(199604)10:4<523::AID-HYP390>3.0.CO;2-8.

Thomas DSG and Goudie A. 2000. *The Dictionary of Physical Geography*. 3rd edition. Blackwell publishing.

Thompson A. 1988. Historical development of the proglacial landforms of Svínafellsjökull and Skaftafellsjökull, southeast Iceland. *Jökull* **38**: 17–31.

Thompson A, Jones A. 1986. Rates and causes of proglacial river terrace formation in southeast Iceland: an application of lichenometric dating techniques. *Boreas* **15**: 231–246.

References

Thorarinsson S. 1943. Oscillations of the Icelandic glaciers in the last 250 years. *Geografiska Annaler* **25**: 1–54.

Thorarinsson S. 1956. On the variations of Svínafellsjökull, Skaftafellsjökull and Kvíárjökull in Öræfi. *Jökull* **6**: 1–15.

Thordarson T, Larsen G. 2007. Volcanism in Iceland in historical time: volcano types, eruption styles and eruptive history. *Journal of Geodynamics* **43**: 118-152. DOI: 10.1016/j.jog.2006.09.005

Thornthwaite, CW. 1948. An approach toward a rational classification of climate. *Geographical Review* **38**: 55-94.

Thorsteinsson T, Björnsson H. 2011. Climate change and energy systems. Impacts, risks and adaptation in the Nordic and Baltic countries. In: Thorsteinsson, Th, Björnsson H (eds.). TemaNord 2011:502. Available at http://www.norden.org/en/publications/publikationer/2011-502/at_download/publicationfile

Thorsteinsson T, Johannesson T, Snorrason A. 2013. Glaciers and ice caps: vulnerable water resoucres in a warming climate. *Current opinion in environmental sustainability* **5**: 590-598. http://dx.doi.org/10.1016/j.cosust.2013.11.003

Tockner K, Malard F, Burgherr P, Robinson CT, Uehlinger U, Zah R, Ward JV. 1997. Physico-chemical characterization of channel types in a glacial floodplain ecosystem (Val Roseg, Switzerland). *Archive für Hydrobiologie* **140**: 433–463.

Tockner K, Malard F, Uehlinger U, Ward JV. 2002. Nutrients and organic matter in a glacial river-floodplain system (Val Roseg, Switzerland). *Limnology and Oceanography* **47**: 226–277.

Tómasson H. 1981. Vatnsafl Íslands, mat á stærð orkulindar. In: Orkuþing 81. Erindi flutt á Orkuþingi 9, 10–11 júní, 1981, vol. 2 (in Icelandic).

Tómasson H. 1982. Vattenkraft i Island och dess hydrologiska förutsätningar. Den nordiske hydrologiske konferense, NHK-82, Förde 28–30 juni 1982. Orkustofnun OS-82059/VOD-10 (in Swedish).

Tóth, J. 1963. A theoretical analysis of groundwater flow in small drainage basins. *Journal of Geophysical Research* **68**: 4795-4812.

Tóth, J. 1999. Groundwater as a geologic agent: an overview of the causes, processes, and manifestations. *Hydrogeology Journal* **7**: 1-14. DOI: 10.1007/s100400050176

Tóth, J. 2009. *Gravitational systems of groundwater flow*. Cambridge University Press, Cambridge, the UK.

Tranter M. 1982. Controls on the chemical composition of Alpine glacial meltwaters. PhD Thesis, University of East Anglia.

Tranter M. 2003. Geochemical Weathering in Glacial and Proglacial Environments. In: Holland HD, Turekian KK. (Eds.) *Treatise on Geochemistry*. Pergamon, Oxford, pp. 189–205.

Tranter M, Brown GH, Raiswell R, Sharp MJ, Gurnell AM. 1993. A conceptual model of solute acquisition by Alpine glacial meltwaters. *Journal of Glaciology* **39**: 573–581.

Tranter M, Brown GH, Hodson AJ, Gurnell AM. 1996. Hydrochemistry as an indicator of subglacial drainage system structure: a comparison of Alpine and sub-polar environments.

References

Hydrological Processes **10**: 541–556. DOI: 10.1002/(SICI)1099-1085(199604)10:4<541::AID-HYP391>3.0.CO;2-9

Tranter M, Sharp MJ, Brown GH, Willis IC, Hubbard BP, Nielsen MK, Smart CC, Gordon S, Tulley M, Lamb HR. 1997. Variability in the chemical composition of in situ subglacial meltwaters. *Hydrological Processes* **11**: 59–77. DOI: 10.1002/(SICI)1099-1085(199701)11:1<59::AID-HYP403>3.0.CO;2-S

Tranter M, Huybrechts P, Munhoven G, Sharp MJ, Brown GH, Jones IW, Hodson AJ, Hodgkins R, Wadham JL. 2002a. Glacial bicarbonate, sulphate and base cation fluxes during the last glacial cycle, and their potential impact on atmospheric CO_2 . *Chemical Geology* **190**: 33-44.

Tranter M, Sharp MJ, Lamb HR, Brown GH, Hubbard BP, Willis IC. 2002b. Geochemical weathering at the bed of Haut Glacier d'Arolla, Switzerland-a new model. *Hydrological Processes* **16**: 959-993.

Tristram DA, Krause S, Levy A, Robinson ZP, Waller RI, Weatherill JJ. Tracing spatial and temporal dynamics of proglacial groundwater-surface water exchange using combined temperature tracing methods. *Freshwater Sciences*. In revision.

Tweed FS, Roberts MJ, Russell AJ. 2005. Hydrologic monitoring of supercooled discharge from Icelandic glaciers. *Quaternary Science Reviews* **24**: 2308-2318. http://dx.doi.org/10.1016/j.quascirev.2004.11.020.

Tyler SW, Selker JS, Hausner MB, Hatch CE, Torgersen T, Thodal CE, Schladow SG. 2009. Environmental temperature sensing using Raman spectra DTS fiber-optic methods. *Water Resources Research* **45**:W00D23. DOI: 10.1029/2008WR007052.

Uchida T, Kosugi KI, Mizuyama T. 2001. Effects of pipeflow on hydrological process and its relation to landslide: A review of pipeflow studies in forested headwater catchments. *Hydrological Processes* **15**: 2151–2174.

Uehlinger U, Robinson CT, Hieber M, Zah R .2010. The physico-chemical habitat template for periphyton in Alpine glacial streams under a changing climate. Hydrobiologia **657**: 107–121.

Ullah S, Zhang H, Heathwaite AL, Heppell CM, Lansdown K, Binley A, Trimmer M. 2014. Influence of emergent vegetation on nitrate cycling in sediments of a groundwater-fed river. *Biogeochemistry: an international journal* **118**: 121-134. DOI 10.1007/s10533-013-9909-2.

Uma KO, Egboka BCE, Onuoha KM. 1989. New statistical grain-size method for evaluating the hydraulic conductivity of sandy aquifers. *Journal of Hydrology* **108**: 343-366.

Van Dijk TAGP, Sigurðsson O. 2002. Surge-related floods at Skeiðarárjökull Glacier, Iceland: implications for ice-marginal outwash development. In: Snorasson A, Finnsdóttir HP, Moss M. (eds.) *The Extremes of the Extremes: Extraordinary Floods.* International Association of Hydrological Sciences Publication. **271**: 193–198.

van Overmeeren RA. 1994. Georadar for hydrogeology. *First Break* **12**: 401-408.

Varian Inc. 2014. Online. http://www.speciation.net/Database/Instruments/Varian-Inc-Part-A/Vista-MPX-Simultaneous-ICPOES-;i210. Accessed 2014.

References

Vatnajökull National Park. 2007. From the Icelandic Geodetic Survey (LMI). http://www.loftmyndir.is/k/kortasja.asp?client=vatnajokull# online. Accessed May 2012.

Vaughan DG, Comiso JC, Allison I, Carrasco J, Kaser G, Kwok R, Mote P, Murray T, Paul F, Ren J, Rignot E, Solomina O, Steffen K, Zhang T. 2013. Observations: Cryosphere. In: Stocker TF, Qin D, Plattner GK, Tignor M, Allen SK, Boschung J, Nauels A, Xia Y, Bex V, Midgley PM (eds).*Climate Change 2013: The Physical Science Basis*. Contribution of Working Group I to the Fifth Assessment Report of the Intergovernmental Panel on Climate Change. Cambridge University Press, Cambridge, United Kingdom and New York, NY, USA.

Vicuña S, McPhee J, Garreaud R. 2012. Agriculture vulnerability to climate change in a snowmelt-driven basin in semiarid Chile. *Journal of Water Resources Plan and Management*. **138**: 431-441. DOI: 10.1061/(ASCE)WR.1943-5452.0000202

Vidstrand P, Follin S, Selroos JO, Naslund JO, Rhen I. 2013. Modelling of groundwater flow at depth in crystalline rock beneath a moving ice-sheet margin, exemplified by the Fennoscandian Shield, Sweden. *Hydrogeology Journal* **21**: 239-255.

Vitvar T, Balderer W. 1997. Estimation of mean water residence times and runoff generation by 18O measurements in a Pre-Alpine catchment (Rietholzbach, Eastern Switzerland). *Applied Geochemistry* **12**: 787–796.

Vogt T, Hoehn E, Schneider P, Freund A, Schirmer M, Cirpka OA. 2010. Fluctuations of electrical conductivity as a natural tracer for bank filtration in a losing stream. *Advances in Water Resources* **33**: 1296–1308

Wadham JL, Cooper RJ, Tranter M, Hodgkins R. 2001. Enhancement of glacial solute fluxes in the proglacial zone of a polythermal glacier. *Journal of Glaciology* **47**: 378-386.

Wadham JL, Cooper RJ, Tranter M, Bottrell S. 2007. Evidence for widespread anoxia in the proglacial zone of an Arctic glacier. *Chemical Geology* **243**: 1–15.

Walder JS, Fowler A. 1994. A Channelized subglacial drainage over a deformable bed, *Journal of Glaciology* **40**: 3–15.

Waller RI, van Dijk TAGP, Knudsen Ó. 2008. Subglacial bedforms and conditions associated with the 1991 surge of Skeiðarárjökull, Iceland. *Boreas* **37**: 179–194. 10.1111/j.1502-3885.2007.00017.x.

Wang Lin, Zhongqin Li, Wang Feiteng, Edwards Ross. 2014. Glacier shrinkage in the Ebinur lake basin, Tien Shan, China, during the past 40 years. *Journal of Glaciology* **60**: 245-254. **DOI:** http://dx.doi.org/10.3189/2014JoG13J023

Ward JV, Stanford JA. 1982. Thermal Responses in the Evolutionary Ecology of Aquatic Insects. *Annual Review of Entomology* **27**: 97-117 DOI: 10.1146/annurev.en.27.010182.000525

Ward JV, Stanford JA. 1989. The four-dimensional nature of lotic ecosystems. *Journal of the North American Benthological Society* **8**: 2–8.

Ward JV, Malard F, Tockner K, Uehlinger U. 1999. Influence of groundwater on surface water conditions in a glacial flood plain of the Swiss Alps. *Hydrological Processes* **13:** 277–293. DOI: 10.1002/(SICI)1099-1085(19990228)13:3<277::AID-HYP738>3.0.CO;2-N

Ward AS, Gooseff MN*,* Voltz TJ*,* Fitzgerald M*,* Singha K*,* Zarnetske JP. 2013. How does rapidly changing discharge during storm events affect transient storage and channel water

References

balance in a headwater mountain stream? *Water Resources Res*earch **49***:* 5473–5486 *doi:*10.1002/wrcr.20434*.*

Weatherill JJ, Krause S, Voyce K, Drijfhout F, Levy A, Cassidy NJ. 2014. Nested monitoring approaches to delineate groundwater trichloroethene discharge to a UK lowland stream at multiple spatial scales. *Journal of Contaminant Hydrology* **158**: 38-54.

Webb BW, Zhang Y. 1999. Water temperatures and heat budgets in Dorset chalk water courses. *Hydrological Processes* **13**: 309–321.

Welch C, Cook PG, Harrington GA, Robinson NI. 2013. Propagation of solutes and pressure into aquifers following river stage rise, *Water Resources Research* **49**: 5246–5259, doi:10.1002/wrcr.20408.

Welch C, Harrington GA, Leblanc M, Batlle-Aguilar J, Cook PG. 2014. Relative rates of solute and pressure propagation into heterogeneous alluvial aquifers following river flow events. *Journal of Hydrology* **511**: 891-903. DOI: 10.1016/j.jhydrol.2014.02.032

Westhoff MC, Savenije HHG, Luxemburg WMJ, Stelling GS, van de Giesen NC, Selker J, Pfister L, Uhlenbrook S. 2007. A distributed stream temperature model using high resolution temperature observations. *Hydrology and Earth System Sciences* **11**:1469–1480. DOI: 10.5194/hess-11-1469-2007.

Westhoff MC, Bogaard TA, Savenije HHG. 2011. Quantifying spatial and temporal discharge dynamics of an event in a first order stream, using distributed temperature sensing. *Hydrology and Earth System Sciences* **15**: 1945-1957. DOI: 10.5194/hess-15-1945-2011.

Williams MW, Knauf M, Caine N, Liu F, Verplanck PL. 2006. Geochemistry and source waters of rock glacier outflow, Colorado Front Range. *Permafrost and Periglacial Processes* **17**: 13–33. doi: 10.1002/ppp.535

Wimpenny J, James RH, Burton KW, Gannoun A, Mokadem F, Gíslason SR. 2010. Glacial effects on weathering processes: new insights from the elemental and lithium isotopic composition of West Greenland rivers. *Earth Planetary Science Letters* **290**: 427–437.

Wimpenny J, Burton KW, James RH, Gannoun A, Mokadem F, Gíslason SR. 2011. The behaviour of magnesium and its isotopes during glacial weathering in an ancient shield terrain in West Greenland. *Earth and Planetary Science Letters* **304**: 260–269.

Winter TC. 1999. Relation of streams, lakes, and wetlands to groundwater flow systems. *Hydrogeology Journal* **7**: 28–45

Winter TC. 2003. The hydrology of lakes. In: O'Sullivan PE, Reynolds CS (eds.). *The Lakes Handbook*, *Limnology and Limnetic Ecology* **1**: 61– 78. Blackwell Science, Oxford, UK.

Winter TC, Rosenberry DO. 1995. The interaction of groundwater with prairie pothole wetlands in the Cottonwood Lake area, east-central North Dakota, 1979–1990. *Wetlands* **15**: 193–211

Winter TC, Harvey JW, Franke OL, Alley WM. 1998. Groundwater and surface water – a single resource. US Geological Survey Circular 1139.

Wiśniewski E, Andrzejewski EL, Molewski P. 1997. Fluctuations of the snout of Skeiðarárjökull in Iceland in the last 100 years and some of their consequences in the central part of its forefield. *Landform Analysis* **1:** 73–78.

References

Wolfe PM, English MC. 1995. Hydrometeorological relationships in a glacierized catchment in the Canadian high Arctic. *Hydrological Processes* **9**: 911-921. DOI: 10.1002/hyp.3360090807

Wolff-Boenisch D, Gabet EJ, Burbank DW, Langner H, Putkonen J. 2009. Spatial variations in chemical weathering and CO2 consumption in Nepalese High Himalayan catchments during the monsoon season, Geochimica et Cosmochimica Acta **73**: 3148-3170, ISSN 0016-7037, http://dx.doi.org/10.1016/j.gca.2009.03.012.

Wongfun N, Götze J, Furrer G, Brandl H, Plötze M. 2013. Effect of water regime and vegetation on initial granite weathering in a glacier forefield: Evidences from CL, SEM, and Nomarski DIC microscopy. *Geoderma* **211–212**: 116-127. DOI: 10.1016/j.geoderma.2013.07.009

Yang Y, Xiao H, Qin Z, Zou S. 2013. Hydrogen and oxygen isotopic records in monthly scales variations of hydrological characteristics in the different landscape zones of alpine cold regions. *Journal of Hydrology* **499**: 124-131 DOI: 10.1016/j.jhydrol.2013.06.025

Yde JC, Knudsen NT, Nielsen OB. 2005. Glacier hydrochemistry, solute provenance,and chemical denudation at a surge-type glacier in Kuannersuit Kuussuat, Disko Island, West Greenland. *Journal of Hydrology* **300**: 172–187.

Yde JC, Riger-kusk M, Christiansen HH, Knudsen NT, Humlum O. 2008. Hydrochemical characteristics of bulk meltwater from an entire ablation season, Longyearbreen, Svalbard. *Journal of Glaciology* **54**: 259-272.

Yong N, Zhang Y, Lui L, Zhang J. 2010. Glacial change in the vicinity of Mt. Qomolangma (Everest), central high Himalayas since 1976. *Journal of Geographical Sciences* **20**: 667-686. DOI: 10.1007/s11442-010-0803-8

Young KL, Assini J, Abnizova A, De Miranda N. 2010. Hydrology of hillslope-wetland streams, Polar Bear Pass, Nunavut, Canada. *Hydrological Processes* **24**: 3345–3358. doi: 10.1002/hyp.7751

Zah R, Uehlinger U. 2001. Particulate organic matter inputs to a glacial stream ecosystem in the Swiss Alps. *Freshwater Biology* **46**: 1597-1608.

Zemp M, Roer I, Kaeaeb A, Hoelzle M, Paul F, Haeberli W. 2008. Global Glacier Changes: Facts and Figures. UNEP and WGMS, Nairobi and Zurich.

Zemp M, Hoelzle M, Haeberli W . 2009. Six decades of glacier mass-balance observations: a review of the worldwide monitoring network. *Annals of Glaciology* **50**: 101-111.

Zhang Z, Chen X, Chen X, Shi P. 2013. Quantifying time lag of epikarst-spring hydrograph response to rainfall using correlation and spectral analyses. *Hydrogeology Journal* **21:** 1619-1631. DOI 10.1007/s10040-013-1041-9

Zhou S, Nakawo M, Hashimoto S, Sakai A. 2008. The effect of refreezing on the isotopic composition of melting snowpack. Hydrological Processes **22**: 873–882. DOI: 10.1002/hyp.6662.

Zhou SQ, Wang Z, Joswiak DR. 2013. From precipitation to runoff: stable isotopic fractionation effect of glacier melting on a catchment scale. *Hydrological Processes* **28**: 3341-3349. 10.1002/hyp.9911

Appendices

Western Skeiðarársandur	**Elevation (mAD)**		
datum 1-ZR P3 1m west		Skaftafellsjökull	Elevation (mAD)
datum 1-ZR P32m east	82.62	T3	100.08
datum 1-ZR P4 1st pipe	82.78	P11	99.92
datum1-ZR P4 2nd pipe	86.14	L8	100.52
datum- GW1	86.26	GW8	100.39
datum1 AL P3100	80.14	L1	100.18
datum1-AL P3150	79.56	L2	99.99
datum1- P8	79.99	L3	100.14
datum1-datum 2 (nr. GW2 lake) foresight	81.20	L4	100.15
datum 2 -datum 1 (backsight)	95.36	L5	100.46
datum2-GW2	94.17	L6	99.99
datum3-GW2	76.61	L7	100.28
datum3- P13 (western pipe)	76.94	Sand50	100.28
datum3- P13 central pipe)	77.53	Sand100	100.26
datum3-GW3	77.53	sand150old	100.37
datum4-GW7	76.88	sand150new	100.29
Skaftafellsjökull foreland	76.64	clay50	100.31
GW10		clay100	100.45
GW11	101.27	clay150	100.26
P10	100.70	river	99.18
P12	101.06		
GW12	101.11		
GW9	100.45		
GW5	100.07		
T1	100.23		
T2	100.61		
	100.48		

Appendix 1. List of piezometers in western Skeiðarársandur and the Skaftafellsjökull foreland.

Appendices

Grain size distribution N. Oasis					
%< (mm)	dead bird lake	dry lake nr. Lake lupin	L. Lupin	Muddy lake (N Oasis)	Nort. Outlet Lake
0.00	0.07	0.03	0.04	0.02	0.04
0.00	1.42	0.64	0.96	0.42	0.91
0.00	4.50	2.16	3.23	1.37	3.03
0.00	9.00	4.71	7.10	2.88	6.46
0.00	14.90	8.45	13.10	5.01	11.50
0.00	32.83	17.33	30.40	10.43	25.50
0.06	99.99	87.77	95.30	55.97	92.60
0.13	100.00	94.13	98.57	73.23	95.83
0.25	100.00	97.90	100.00	91.37	99.92
0.50	100.00	99.40	100.00	98.97	100.00
1.00	100.00	100.00	100.00	100.00	100.00
2.00	100.00	100.00	100.00	100.00	100.00

Grain size distribution S. Oasis								
%< (mm)	SKF3 (Island Lake)	SKF1 (head GWFR)	Swan Lake stage board	Heart Lake	Thin Lake	Island Lake	GW8	L8
0.00			0.02				0.01	0.00
0.00			0.38				0.23	0.06
0.00			1.26				0.76	0.21
0.00			2.60				1.55	0.44
0.00			4.33				2.57	0.74
0.00			8.01				4.60	1.40
0.06	7.60	8.95	70.10	10.00	7.20	10.20	55.43	12.03
0.13	10.77	17.30	79.67	16.60	14.89	20.58	81.87	20.83
0.25	21.69	38.37	85.63	35.20	29.29	35.35	97.33	37.77
0.50	50.66	65.21	90.73	63.60	52.17	59.70	99.73	53.50
1.00	77.64	82.31	97.13	82.80	74.85	82.46	99.97	74.87
2.00	100.00	100.00	100.06	99.62	97.73	98.65	100.00	100.00

Grain size distribution Instrumented Lake						
%< (mm)	claynest_100	clay_nest_150	clay_nest	CN_10 cm	L4	instrumented_lake
0.00	0.02	0.02	0.02	0.00	0.00	0.02
0.00	0.47	0.47	0.43	0.00	0.00	0.51
0.00	1.53	1.55	1.41	0.00	0.00	1.65
0.00	3.14	3.24	2.92	0.27	0.25	3.39
0.00	5.22	5.41	4.87	2.60	2.41	5.54

0.00	9.69	9.78	8.69	5.47	5.23	9.67
0.06	87.30	89.87	87.73	92.90	92.70	93.20
0.13	94.67	96.70	96.97	98.90	100.00	98.77
0.25	97.50	99.53	99.99	100.00	100.00	100.00
0.50	98.60	99.90	100.00	100.00	100.00	100.00
1.00	100.00	100.00	100.00	100.00	100.00	100.00
2.00	100.00	100.00	100.00	100.00	100.00	100.00

Grain size distribution outwash										
%< (mm)	S.N. 100	S.N. 50	S.N. 150	SED2	SED3	SED4	SED5	SED6	SED7	SED8
0.00	0.0	0.0	0.0							
0.00	0.0	0.0	0.0							
0.00	0.1	0.1	0.1							
0.00	0.2	0.1	0.1							
0.00	0.2	0.2	0.2							
0.00	0.5	0.5	0.4							
0.06	2.3	3.3	1.5	3.6	6.4	2.0	2.8	24.0	9.8	5.8
0.13	4.7	5.3	2.4	8.8	7.2	2.0	4.4	33.0	13.6	8.0
0.25	10.6	7.9	7.2	25.2	11.2	4.4	9.9	42.0	20.4	14.1
0.50	23.4	13.8	19.2	57.4	24.1	17.1	27.3	55.0	33.6	30.3
1.00	57.9	34.8	47.6	82.4	49.5	44.4	57.0	73.0	64.2	60.4
2.00	100.0	100.0	100.1	98.3	96.1	96.3	99.0	96.0	99.0	99.6

Appendix 2. Results of PSA for the different hydrological environments.

	sorting Folk, 1986	sorting Folk, 1986
claynest_100	0.034	V.W
clay_nest_150	0.028	V.W
clay_nest_1	0.029	V.W
CN (VTP1 location)	0.022	V.W
L4 (VTP 3)	0.022	V.W
dead bird lake_3	0.011	V.W
dry lake nr. Lake lupin_1	0.035	V.W
GW8_1	0.063	V.W
instrumented_lake_1	0.021	V.W
L8_1	0.538	M.W
lake_lupin	0.023	V.W
muddy_lake_n_oasis_1	0.106	V.W
n_outlet_lake_3	0.028	V.W
sand_nest_100	0.541	M.W
sand_nest_50_1	0.591	M.W
sand_nest_150	0.596	M.W
swan_lake_sb_1	0.145	M.W

Heart Lake	0.509	M.W
Island Lake	0.516	M.W
SED2	0.495	well sorted
SED 3	0.607	M.W
SED4	0.582	M.W
SED5	0.618	M.W
SED6	0.655	M.W
SED7	0.617	M.W
SED8	0.606	M.W
Skf1	0.507	M.W
SkF3	0.523	M.W

Appendix 3. Sorting coefficient and description

Hydraulic conductivity (m/day)							
		Hazen	**extremes (C=1)**	**C=1300**	**Puckett**	**Alyamani &Sen**	**porosity**
N. Oasis (5)	**Dead Bird Lake**	0.000114	3.26E-07	0.000424	0.005752	0.008885	0.280972
	Dry Lake nr. Lake lupin	0.000555	1.59E-06	0.002063	0.122819	4.733348	0.258015
	Lake Lupin	0.000184	5.26E-07	0.000683	0.0093	0.011268	0.274515
	Muddy Lake N. Oasis	**0.002746**	**7.85E-06**	**0.010199**	**0.479844**	**0.579627**	**0.257422**
	N Outlet Lake	0.000245	7E-07	0.00091	0.024478	0.01316	0.262228
S. Oasis (8)	**Island Lake**	22.5	0.0225	29.25		190.4966	0.313117
	Swan Lake SB	0.006655	1.9E-05	0.02472	0.773876	0.14789	0.305277
	Heart Lake		3.969E-03				0.322379
	Thin Lake	3.969	0.003969	5.1597		216.1911	
	GW8	0.100601	0.000101	0.130781	1.517602	8.552657	0.338649
	L8	2.383392	0.002383	3.09841	2.85517	482.8388	0.280823
	SKF1 (head GWFR)	3.969	0.003969	5.1597		123.1631	0.322379
	SKF3 (Island Lake)	7.225	0.007225	9.3925		334.4933	0.314267
IL (6)	**clay nest 50**	0.00536	1.53E-05	0.019908	0.677513	1.209398	0.298796
	clay 100	0.003536	1.01E-05	0.013135	0.555723	1.206488	0.296433
	clay 150	0.003422	9.78E-06	0.012712	0.545573	1.205006	0.295208
	VTP1 (CN)	0.024275		0.032	0.773876	0.333823	
	VTP3 (L4)	0.026235		0.034	1.34	0.334162	
	Instr. Lake (clay end)	0.003615	1.03E-05	0.013426	0.55829	5.233988	0.30529
Outwash (11)							
		61.00625	0.061006	79.30813		1148.722	
	SED2	40	0.04	52		272.8421	0.383774
	SED3	140.625	0.140625	182.8125		1352.52	0.33837
	SED4	62.5	0.0625	81.25		1936.903	0.388663
	SED5	0.9	0.0009	1.17		1032.625	0.367327
	SED6	3.969	0.003969	5.1597		191.3186	0.258299
	SED7	15.625	0.015625	20.3125		765.1247	0.272804

	SED8	15.625	0.015625	20.3125		764.5264	0.312433
	VTP2 (river)	0.236237	0.00024	0.31	2.66	30.8341	
	Sand Nest 50	123.5757	0.123576	160.6484	3.424074	1105.936	0.376413
	Sand Nest 100	56.43792	0.056438	73.3693	3.403847	866.2724	0.36474
	Sand Nest 150	97.71876	0.097719	127.0344	3.494672	775.4718	0.379709

Appendix 4. Results of K using different PSA equations

					Concentration (µeq/l)			
			Temp (°C)	**EC**	**Cl^-**	**SO_4^{2-}**	**Ca^{2+}+ Mg^{2+}**	**K^++ Na^+**
AL011	08/07	GW8	8.7	115	136	107	1049	376

AL158	29/08	GW8	10.1	153	119	213	1497	610
AL018	10/07	L1 piez	9.9	153	146	168	1493	539
AL091	25/07	L1 piez	10.4	159	144	185	1522	601
AL142	25/08	L1 piez	9.9	158	126	223	1274	845
AL020	10/07	L2	10.3	182	141	161	1504	973
AL143	25/08	L2	9.2	181	123	134	1258	1087
AL021	10/07	L3	8.2	114	136	135	1105	319
AL093	25/07	L3	8.4	117	135	126	1129	385
AL144	25/08	L3	9.2	124	120	142	1237	649
AL022	11/07	L8	12.1	130	141	126	1221	582
AL092	25/07	L8	9.2	150	137	145	1283	740
AL029	12/07	L4 piez	12.5	120	135	122	1138	342
AL080	24/07	L4 piez	12.3	118	133	134	1163	361
AL145	25/08	L4 piez	8	126	121	151	929	665
AL024	11/07	L5	13.9	126	138	133	1266	356
AL081	24/07	L5 piez	11	127	132	136	1291	373
AL146	25/08	L5	9.5	128	116	146	1109	670
AL015	10/07	L6 piez	12.4	115	140	125	1105	318
AL094	25/07	L6 piez	6.5	118	134	140	1172	333
AL147	25/08	L6 piez	8.3	105	94	110	931	744
AL019	10/07	L7	13.1	139	155	129	1417	527
AL082	24/07	L7 piez			137	146	1548	743
AL025	11/07	sand50	14.1	193	143	181	2115	544
AL141	25/08	sand nest50	9.8	135	111	125	923	757
AL014	10/07	clay150 pipe	11.5	113	134	120	1005	355
AL017	10/07	clay100	14.2	114	136	118	1132	384
AL148	25/08	clay nest150	7.3	123	118	146	964	761
AL111	28/07	spring at instr. Lake	4.7	118	134	146	1205	344
AL112	28/07	spring at instr. Lake	5.3	119	135	137	1241	371
AL003	08/07	T1	10.5	155	135	375	1526	433
AL088	24/07	T1	8.9	155	136	258	1594	462
AL153	28/08	T1	10.7	181	148	415	1923	497
AL004	08/07	T2	11.6	132	137	141	1317	361
AL089	24/07	T2	8.8	156	153	219	1649	415
AL152	28/08	T2	10.9	179	136	318	1935	506
AL005	08/07	T3	9.1	150	138	164	1461	525
AL090	24/07	T3	8.5	161	137	158	1595	552
AL151	28/08	T3	10.1	153	137	201	1555	551
AL001	08/07	GW10	9.9	123	136	133	1184	353
AL087	24/07	GW10	9	143	141	217	1497	421
AL155	29/08	GW10	12.6	149	145	277	1540	443
	09/07	GW11	7.7	120	135	145	1157	334
AL086	24/07	GW11	7.1	126	134	164	1263	359

AL150	28/08	GW11	7.7	132	127	192	1345	421
	09/07	GW12 (barlogger pipe)	9.4	121	135	140	1187	397
AL085	24/07	GW12 (barlogger pipe)	7.9	124	132	154	1236	392
AL154	28/08	GW12 (barlogger pipe)	9.4	135	130	187	1384	421
AL095	26/07	P12	9.1	144	137	177	1487	439
AL149	25/08	P12	8.3	152	121	189	1471	682
AL026	11/07	P10	12.7	133	81	131	1307	411
AL007	08/07	GW5	7.7	92	69	72	836	384
AL084	24/07	GW5	9.4	138	69	145	1472	449
AL157	29/08	GW5	11.5	209	123	405	2304	561
AL008	08/07	GW9	4.7	49	50	23	424	179
AL083	24/07	GW9	5.1	55	49	30	486	204
AL156	29/08	GW9	10.3	91	63	88	898	312
AL006	08/07	instr. lake, nr. Sand nest	17.4	115	145	66	816	337
AL016	10/07	instr, lake nr. Clay nest		114	145	68	816	348
AL052	21/07	instr. Lake, nr. T3	14.6	114	62	6	873	398
AL053		N. side instr. Lake	14.5	114	58	5	872	355
AL054		inst. Lake, nr. Clay nest	14.8	111	61	6	869	377
AL055		inst. Lake, nr. L4	14.4	114	62	6	857	353
AL108	28/07	Instrumented lake	14.4	112	146	81	948	399
AL109		Instrumented lake	15.2	112	146	82	958	399
AL110		Instrumented lake	14.5	111	146	82	963	371
AL113		Instrumented lake	16.1	112	149	85	967	394
AL164	29/08	instrumented lake, by staging board	7.9	80	61	53	788	180
AL165		instrumented lake, nr. L5, l6	11.3	80	64	52	778	184
AL030	12/07	Swan Lake w. shore		110	152	45	786	290
AL037	13/07	Swan Lake, E. shore	18	110	154	61	824	335
AL057	21/07	Swan lake, nw shore	14.5	106	151	46	798	323
AL058	21/07	swan lake, s. shore	14.9	108	152	42	612	523
AL059	21/07	swan lake, centre	13.9	107	153	46	794	321
AL060	21/07	swan lake, N. shore	14.4	105	150	47	814	315
AL114	28/07	Swan Lake	17.6	105	156	51	833	347
AL115	28/07	Swan Lake	17.8	107	155	46	799	331
AL116	28/07	Swan Lake	17.6	109	126	40	821	338
AL117	28/07	Swan Lake	16.3	104	154	52	841	345

AL166	29/08	Swan Lake, nr. Stage board	9.1	68	62	38	593	150
AL167	29/08	swan lake, NE corner	9.1	67	61	36	598	157
AL033	12/07	Island Lake, S. section	18.9	130	152	42	1087	363
AL034	12/07	Island Lake, N. section	20.7	136	161	60	1159	353
AL063	23/07	Island lake, NE shore	13.4	118	144	74	1192	372
AL064	23/07	Island Lake, N. shore	13.8	119	142	59	1496	455
AL065	23/07	Island Lake, S. section	14.9	121	146	36	1057	379
AL066	23/07	Island Lake, W. shore	14.8	118	144	43	1074	396
AL135	30/07	Island Lake	14.3	127	145	60	1137	354
AL136	30/07	Island Lake	14.2	130	149	44	1081	376
AL137	30/07	Island Lake	15.1	126	149	49	1104	390
AL170	31/08	Island Lake, opposite end to stage board	9.5	126	150	78	1118	354
AL171	31/08	Island lake, s. end, nr. Stage board, but deep water	9.9	124	150	76	1224	368
AL035	12/07	Thin Lake E. side	15	118	136	106	1136	329
AL036	12/07	Thin Lake W. side	23.2	125	138	122	1178	356
AL061	21/07	Thin Lake, E. shore	11.4	113	132	104	1081	348
AL062	21/07	thin Lake, W. shore	13.6	118	130	110	1098	337
AL132	30/07	Thin Lake	11.5	115	133	111	1175	360
AL133	30/07	Thin Lake	15	120	134	113	1161	367
AL134	30/07	Thin Lake	12.5	116	134	111	1143	360
AL168	31/08	Thin Lake, nr. Stage board	8.9	112	120	100	1092	344
AL169	31/08	Thin Lake, shallow end	10.3	107	119	102	1103	344
AL067	23/07	Heart Lake, W. shore	15	142	166	44	1505	437
AL068	23/07	heart Lake, s. shore	14	142	166	46	1483	445
AL069	23/07	Heart Lake, N. end	14.1	141	169	43	1486	460
AL138	30/07	Heart Lake	15.5	144	170	46	1542	469
AL139	30/07	Heart Lake	15.2	144	168	45	873	924
AL172	31/08	Heart Lake (NE corner)	10.1	135	150	58	1442	387
AL173	31/08	Heart Lake, southernmost tip	10.4	138	152	57	1460	401
AL002	08/07	river Skaftafellsá (at stilling well)	1.7	27	56	18	88	130
AL070	23/07	river Skaftafellsá	1.1	24	36	13	121	119
AL071	23/07	river Skaftafellsá	1	24	37	13	129	128

AL072	23/07	river Skaftafellsá	1	24	36	15	112	133
AL073	23/07	River Skaftafellsá	0.8	22	24	13	107	120
AL162	29/08	Skaftafellsá, nr. Staging well	1.2	20	26	15	42	80
AL163	29/08	Skaftafellsá, n. of moraine, nr. GW10	1.2	20	26	16	40	81
AL038	14/07	Dead Bird Lake	14.7	71	60	21	379	674
AL096	27/07	Dead Bird Lake	17.5	66	188	44	389	273
AL097	27/07	Dead Bird Lake	15.4	56	170	41	344	222
AL098	27/07	Dead Bird Lake	14.4	47	151	37	300	196
AL099	27/07	Dead Bird Lake	14.7	47	151	38	298	198
AL039	14/07	Little island lake	16.7	49	169	17	175	247
AL100	27/07	Little island lake	17.7	48	194	28	192	240
AL101	27/07	Little island lake	16.9	48	193	25	202	250
AL042	14/07	Lake Lupin	16.6	46	126	10	44	206
AL105	27/07	Lupin Lake	16.8	55	175	25	217	206
AL106	27/07	Lupin Lake	16.4	50	175	26	233	199
AL107	27/07	Lupin Lake	16.4	47	174	25	234	214
AL040	14/07	Twin Lake	16.4	57	139	12	361	225
AL041	14/07	small lake nr. Twin Lake		81	85	10	487	263
AL102	27/07	Twin Lake	15.4	58	149	42	380	218
AL103	27/07	Twin Lake	15.4	58	151	44	302	710
AL104	27/07	Twin Lake	15	58	151	45	310	527
AL159	29/08	head of GWFR			193	2448	4698	821
AL160	29/08	GWFR, 150 downstream of AL159			144	128	1420	394
AL161	29/08	GWFR. Towards the river			145	114	1439	372

Appendix 5. water quality and solute concentrations

Hydrological environment	Location	$\delta^{18}O$	δD	GMWL	Det. Excess
meltwater	Skaftafellsá	-11.12	-78.92	-79.00	10.08
	Skaftafellsá	-11.11	-78.64	-78.86	10.22
	Skaftafellsá	-11.03	-77.99	-78.21	10.22
	Skaftafellsá	-11.13	-78.40	-79.00	10.60
	Skaftafellsá	-10.98	-78.35	-77.84	9.49

	Skaftafellsá	-11.03	-77.67	-78.22	10.56
groundwater	SKF T1	-7.42	-53.22	-49.37	6.15
	SKF T2	-7.98	-56.49	-53.84	7.35
	SKF T3	-7.50	-54.45	-49.96	5.52
	SKF GW5	-8.97	-64.54	-61.78	7.24
	SKF GW9	-10.00	-71.13	-69.98	8.85
	SKF GW11	-8.00	-56.76	-53.98	7.21
	SKF GW12	-7.89	-57.11	-53.15	6.04
	SKF P12	-7.83	-56.48	-52.63	6.15
	SKF L1	-7.52	-55.01	-50.17	5.16
	SKF L2	-8.44	-61.70	-57.49	5.80
	SKF L3	-7.80	-55.59	-52.43	6.84
	SKF L4	-7.91	-56.10	-53.27	7.17
	SKF L5	-7.75	-56.94	-52.01	5.07
	SKF sand nest 50	-7.67	-55.05	-51.36	6.31
	SKF sand nest 150	-7.80	-56.78	-52.41	5.63
GWFR	SKF Head GW FR	-5.95	-47.97	-37.57	-0.39
	SKF Mid GW FR	-7.76	-55.50	-52.08	6.57
	SKF GW-Creek	-7.67	-55.54	-51.38	5.84
	*SKF GW-Creek (PS)	-7.64	-55.44	-51.13	5.69
lakes	SKF island Lake	-6.28	-49.30	-40.28	0.98
	SKF thin lake east	-7.68	-56.10	-51.46	5.36
	SKF thin lake west	-7.65	-56.65	-51.23	4.58
	SKF swan lake, w-shore	-8.47	-63.35	-57.79	4.43
	SKF lake nr., clay nest	-8.64	-63.79	-59.12	5.33
	SKF lake nr., sand nest	-8.59	-64.08	-58.70	4.62

Appendix 6. Stable isotope composition of groundwater and surface water at the Skaftafellsjökull margin.